

The Physiology of Dementia

Network reorganisation in progressive non-fluent aphasia as a
model of neurodegeneration



Thomas Edmund Cope

Gonville and Caius College, University of Cambridge
Department of Clinical Neuroscience

This dissertation is submitted for the degree of
Doctor of Philosophy

January 2018

Declaration

This dissertation is the result of my own work and includes nothing which is the outcome of work done in collaboration except where specifically indicated in the text. Several of the chapters have been accepted for publication with co-authors. In each case a preface to the chapter sets out my personal contribution to the work:

Chapter 1 forms the basis of Chapter 25 of the upcoming *Oxford Textbook of Neuropsychiatry*.

Chapter 2 forms the basis of a paper that has been published in *Brain* (Cope et al., 2018).

Chapter 3 forms the basis of a paper that has been published in *Nature Communications* (Cope et al., 2017a).

Chapter 4 forms the basis of a paper that has been published in *Neuropsychologia* (Cope et al., 2017b).

This dissertation is within the word limit requirements set by the Clinical Medicine Degree Committee and the Board of Graduate Studies.

I confirm that no part of this dissertation has previously been submitted for any other qualification.

Acknowledgements

I am, and always will be, grateful to my supervisor, Professor James Rowe, for his support of my research and personal development. He has provided me with the perfect balance of guidance and freedom to allow me to make impactful and meaningful discoveries while acquiring my own investigative skills and analytical approach. His influence has extended far beyond the scientific, being a fantastic clinical mentor, pastoral support, inspirational role model, and good friend.

I am grateful to my advisor, Dr Matt Davis, who has been generous with his time, collaborative in his approach, and constructive in his criticism.

I am grateful to my former supervisor, Prof Tim Griffiths, who has always been willing to discuss my projects and never fails to provide insight when I lack clarity. I hope that our productive collaboration continues for many years to come.

I am grateful to Prof Karalyn Patterson, from whom I have learned everything I now know about aphasia. I have been extremely privileged to work next to you scientifically, and to share my consultations with you clinically.

I am grateful to the many others with whom I have worked during my PhD. While the mandatory declaration begins by stating that this work is entirely my own, in truth none of it could have been accomplished without the collaborations that are described in the preface to each chapter. I am especially indebted to Dr Ediz Sohoglu, who was generous in his time and computer code getting me up to speed with his experiments, on which chapter 3 builds; Dr Laura Hughes and Mr Maarten van Casteren for teaching me the practicalities of MEG acquisition; Prof Chris Petkov, whose boundless enthusiasm kept chapter 4 on the road; and Mr P Simon Jones, who taught me MRI analysis with unfailing patience.

Most of all, I am grateful to my wife, Wei, whose support and understanding knows no bounds. I don't know how she puts up with me.

This work was primarily supported by the Patrick Berthoud Charitable Trust and the Association of British Neurologists, with additional support from the NIHR Biomedical Research Centre and the Medical Research Council.

Dedication

I dedicate this dissertation to my daughters Ellie and Catherine, who bring sunshine wherever they go.

Table of Contents

Declaration	ii
Acknowledgements	iii
Dedication	iv
Table of Contents	v
Table of Figures	x
Table of Tables	xii
General Introduction.....	1
Chapter 1: The current clinical context of dementia	4
1.1 Preface	4
1.2 Introduction.....	5
1.3 Core Progressive Dementias	6
1.3.1 Alzheimer’s Disease – Amnestic	6
1.3.2 Alzheimer’s Disease – Posterior Cortical Atrophy – Benson’s Syndrome	10
1.3.3 Alzheimer’s Disease – Logopenic and Mixed Primary Progressive Aphasia	12
1.3.4 Alzheimer’s Disease – Dysexecutive/Behavioural Variant	14
1.3.5 Frontotemporal Dementia – Behavioural Variant – bvFTD.....	15
1.3.6 Frontotemporal Dementia – Semantic Dementia - SD	19
1.3.7 Frontotemporal Dementia – non-fluent variant Primary Progressive Aphasia – nfvPPA/PNFA.....	22
1.4 Dementias associated with Movement Disorders.....	26
1.4.1 Lewy Body related – Dementia with Lewy Bodies – DLB	26
1.4.2 Lewy Body related – Parkinson’s Disease Dementia - PDD	27
1.4.3 Progressive Supranuclear Palsy - PSP	28
1.4.4 Corticobasal Syndrome.....	30
1.4.5 Multiple System Atrophy - MSA.....	33
1.4.6 Huntington’s Disease - HD	34
1.4.7 Normal Pressure Hydrocephalus - NPH	35
1.4.8 Niemann-Pick type C.....	36
1.4.9 Spinocerebellar Ataxia - SCA.....	37

1.5 Cognitive impairments that may or may not progress.....	38
1.5.1 Mild Cognitive Impairment.....	38
1.5.2 Subjective Cognitive Impairment.....	40
1.5.3 Transient Global Amnesia - TGA.....	41
1.5.4 Transient Epileptic Amnesia - TEA.....	41
1.6 Challenges and opportunities	42
1.7 Chapter Summary:	44
Chapter 2: Tau burden and the functional connectome in Alzheimer's disease and progressive supranuclear palsy.....	45
2.1 Preface	45
2.2 Introduction.....	46
2.3 Methods.....	48
2.3.1 Participants.....	48
2.3.2 Study Procedures.....	51
2.3.3 MRI data acquisition and pre-processing	51
2.3.4 Functional Connectivity Assessment.....	53
2.3.5 Tau Burden Assessment.....	55
2.3.6 Statistical Approach	56
2.4 Results	58
2.4.1 Resting state connectivity differences exist between groups	58
2.4.2 Findings in AD but not PSP are consistent with trans-neuronal spread of tau	59
2.4.3 Findings in PSP but not AD are consistent with hub vulnerability due to metabolic demand and lack of trophic support.	66
2.4.4 Alzheimer's disease and PSP have opposite effects on the strength of <i>cortical</i> functional connectivity.....	70
2.4.5 Reorganisation of cortical functional connectivity reflects cortical vs subcortical pathology.....	74
2.4.6 Local functional connectivity reorganisation is related to local [¹⁸ F]AV-1451 binding potential in Alzheimer's disease	83
2.5 Discussion.....	84
2.5.1 Insights into the mechanisms of disease progression in humans.....	85
2.5.2 Is the difference between AD and PSP mediated by tau isoform or intrinsic connectivity?.....	87

2.5.3 Cross-sectional data reveal patterns less visible at the group level	88
2.5.4 Re-organisation of brain networks.....	89
2.5.5 Study limitations.....	90
2.6 Conclusion	91
2.7 Chapter Summary:.....	92
Chapter 3: Top-down frontal contributions to predictive processes in speech perception	94
3.1 Preface.....	94
3.2 Introduction.....	97
3.3 Methods:	100
3.3.1 Participants	100
3.3.2 Voxel Based Morphometry	101
3.3.3 Modifications to Sohoglu MEG paradigm	103
3.3.4 Behavioural data stimuli and procedure.....	104
3.3.5 Behavioural data modelling	105
3.3.6 Alternative data models	107
3.3.7 MEG and EEG data acquisition and analysis.....	108
3.3.8 Sensor-space evoked analysis	110
3.3.9 Evoked data source reconstruction	110
3.3.10 Sensor-space induced analysis.....	111
3.3.11 Induced data source reconstruction.....	112
3.3.12 Coherence and Connectivity Analyses.....	112
3.4 Results:.....	113
3.4.1 Structural consequences of nfvPPA	113
3.4.2 Subjective speech perception symptoms in nfvPPA.....	114
3.4.3 Evoked neural responses during the reconciliation of predictions, and their cortical origins.....	115
3.4.4 Behavioural Experiment 1: Vcoded Word Clarity Rating.....	125
3.4.5 Behavioural Experiment 2: Vcoded Word Identification	126
3.4.6 Bayesian modelling of experiments 1 and 2	127
3.4.7 Induced oscillatory dynamics	130
3.4.8 Coherence and Connectivity during the reconciliation of predictions	135

3.5 Discussion:	137
3.5.1 Fronto-temporal dissociations in nfvPPA	139
3.5.2 Frontotemporal hierarchy and predictive coding	140
3.5.3 Study limitations	142
3.6 Conclusion:	143
3.7 Chapter Summary:	144
Chapter 4: Artificial grammar learning in vascular and progressive non-fluent aphasia	
.....	145
4.1 Preface	145
4.2 Introduction	147
4.3 Methods.....	150
4.3.1 Participants	150
4.3.2 Stimuli	155
4.3.3 Procedure.....	158
4.3.4 Stroke lesion mapping.....	160
4.3.5 nfvPPA atrophy mapping	161
4.3.6 Analysis	161
4.4 Results	165
4.4.1 Discriminability of sequencing rules.....	165
4.4.2 Bias towards permissibility.....	168
4.4.3 Implicit learning through repeated exposure-test cycles	169
4.4.4 Separation of rule learning between linguistic and non-linguistic sequences	
.....	170
4.4.5 Relationship to diagnostic category and disease severity.....	171
4.4.6 Relationship to structural anatomy	171
4.5 Discussion	172
4.5.1 Rule acquisition differs when structurally identical sequences are comprised	
of linguistic or non-linguistic stimuli.	172
4.5.2 Artificial grammar learning in aphasia is similar across aetiologies.....	174
4.5.3 Agrammatic aphasic patients are similarly impaired for both complex and	
simple sequencing operations.	175
4.5.4 Patients with aphasia show improved performance over repeated cycles. .	176
4.5.5 Brain behaviour relationships.....	178

4.5.6 Study limitations.....	179
4.6 Conclusion	179
4.7 Appendix: Supplementary tables	181
4.8 Chapter Summary:.....	182
Chapter 5: Review and Synthesis.....	183
5.1 Network organisation and reorganisation in neurodegeneration	183
5.2 Clinical implications of inflexible predictions in nfvPPA	187
5.2.1 Inflexible predictions can explain speech comprehension symptoms in nfvPPA	187
5.2.2 Inflexible predictions can explain auditory processing abnormalities in nfvPPA	189
5.2.3 Inflexible predictions can explain receptive agrammatism in frontal aphasia	194
Summary.....	196
References.....	199
Appendix: Published work resulting from this thesis	232

Table of Figures

Figure 1-1 MRI images for the amnesic Alzheimer’s disease vignette.	6
Figure 1-2 MRI images for the Posterior Cortical Atrophy vignette.	11
Figure 1-3 MRI images for the logopenic Primary Progressive Aphasia vignette.....	13
Figure 1-4 MRI images for the Semantic Dementia vignette.....	20
Figure 1-5 MRI images for the non-fluent variant Primary Progressive Aphasia vignette.....	22
Figure 1-6 MRI images for the Dementia with Lewy Bodies vignette.	27
Figure 1-7 Serial structural MRI sections through the midbrain of a patient with PSP	30
Figure 1-8 MRI and SPECT images for the Corticobasal Syndrome vignette.....	32
Figure 1-9 DaT scan summary image for the Corticobasal Syndrome vignette.	32
Figure 2-1 Movement parameters.	52
Figure 2-2 The relationship between tau burden and age for each group.....	57
Figure 2-3 Connectivity matrices.	58
Figure 2-4 Weighted degree.	61
Figure 2-5 Alzheimer’s disease comparison of the three graph metrics representing the three principal hypotheses of hub vulnerability.....	63
Figure 2-6 PSP comparison of the three graph metrics representing the three principal hypotheses of hub vulnerability.	64
Figure 2-7 Unthresholded nodal connectivity strength.	65
Figure 2-8 Weighted participation coefficient.	67
Figure 2-9 Clustering coefficient.	69
Figure 2-10 Between-subjects analysis of the relationship between global tau burden and each graph metric at a network density of 6%, with the effect of age on tau burden partialled out.....	73
Figure 2-11 Betweenness centrality.	76
Figure 2-12 Closeness centrality (1/path length from each node to all other nodes)....	78
Figure 2-13 Local efficiency.....	80
Figure 2-14 Eigenvector centrality.	82
Figure 3-1 An illustration of the experimental motivation.....	98
Figure 3-2 Auditory symptoms in nfvPPA.....	115
Figure 3-3 Behavioural results	117

Figure 3-4 Total evoked power.	118
Figure 3-5 The effect of clarity.	120
Figure 3-6 The evoked effect of cue congruency.	121
Figure 3-7 Evoked source space analysis.	123
Figure 3-8 Replication of experiment 1 with additional, neutral cues.	126
Figure 3-9 Example Bayesian model fits for a single subject in a single condition.	129
Figure 3-10 Induced analysis after the written but before spoken word.	131
Figure 3-11 Induced analysis after the spoken word.	132
Figure 3-12 Scalp distribution and source reconstructions of induced effects.	134
Figure 3-13 Coherence and connectivity analysis.	136
Figure 4-1 Group characteristics	152
Figure 4-2 A plot for nfvPPA of difficulty ‘Understanding speech in a quiet room’ against ‘Grammatical form’ from the BDAE.	153
Figure 4-3 Composite pure tone audiograms for each group.	155
Figure 4-4 Artificial grammar structure and stimuli.	156
Figure 4-5 Distribution of decision variables.	163
Figure 4-6 Group performance on sequence identification.	166
Figure 4-7 Bias metrics by group for each language type	169
Figure 4-8 Correlation and clustering analysis.	170
Figure 5-1 Systems identification framework.	186
Figure 5-2 Basic auditory processing in nfvPPA, after Grube et al. (2016).	190
Figure 5-3 Overall average adaptive tracks by group.	191
Figure 5-4 Individual nfvPPA performance profiles.	192

Table of Tables

Table 2-1 Participant demographics summary	49
Table 2-2 Detailed neuropsychological profiles of individual study participants.	50
Table 2-3 Sign tests	83
Table 3-1 Demographic details of the experimental groups.....	101
Table 3-2 Voxel-based morphometry regions of significant atrophy in nfvPPA.....	114
Table 3-3 Repeated measures ANOVA of evoked source power in frontal and temporal voxels of interest over the whole post auditory epoch.	124
Table 3-4 Repeated Measures ANOVA of behavioural data from experiment 1.	125
Table 3-5 Repeated measures ANOVA of behavioural data from experiment 2.....	127
Table 4-1 Participant demographics.....	150
Table 4-2 Exposure and testing sequences.	157
Table 4-3 Single subject lesion percentages by region for the stroke group.....	161
Table 4-4 Statistical tests corresponding to Figure 4-6 and Figure 4-7.	167
Table 4-5 Supplementary analysis of d' discriminability.....	181
Table 4-6 Supplementary analysis of d' learning	181

General Introduction

I undertook the work that comprises this thesis with three general aims in mind. The first was to demonstrate that systems neuroscience provides an effective and necessary translational bridge between the molecular biology of dementia and clinical trials of therapies and medications. The second was to demonstrate that studies of patients with neurodegenerative disease can further our understanding of normative brain function. In other words, I wanted to show that there is still a role for the ‘lesion study’ in experimental psychology. In chapters 3-5, I show that the application of modern imaging techniques and carefully designed psychophysics in patients with relatively selective but incomplete damage to part of the language processing network provides stronger evidence for causal interactions than associative studies in healthy individuals. The third aim was that this thesis should represent a formative training in a comprehensive suite of computational, neuroimaging and psychophysical techniques. To this end, it intentionally comprises a diverse set of studies and investigations that employ a wide range of methods. Therefore, as well as making a meaningful contribution to scientific knowledge, this research I describe here is the philosophical foundation upon which I intend to build towards an independent research programme in the short timescales afforded by integrated clinical academic career pathways.

Although different in methods and approach, the chapters of this thesis provide complementary insights into the neurophysiology of dementia.

I begin with an introductory, clinically-focussed review (Chapter 1) that sets out the features, aetiology, management, epidemiology and prognosis of the dementias. This sets the scene for the experimental chapters of my thesis by placing the model diseases on which I place special emphasis within the context of the broader clinical challenge posed by dementia.

In the first experimental chapter (Chapter 2) I combine graph theoretical analyses of resting state functional MR imaging and PET imaging using the ligand AV-1451. This work followed from a number of ligand validation studies on which I was a co-author but that were not primarily my own work, and are therefore not reported here, which

together demonstrate AV-1451 to be effective at recapitulating the distribution of molecular pathology *in vivo* (Bevan-Jones *et al.*, 2016, Bevan-Jones *et al.*, 2017a, Passamonti *et al.*, 2017). For this chapter I evaluated Alzheimer's disease (AD) and progressive supranuclear palsy (PSP) as they represent prototypical neurodegenerative tauopathies with predominantly cortical and subcortical disease burdens respectively. I begin by considering how the connectivity of the brain might predispose to the contrasting patterns of neurodegeneration seen in these disorders, and empirically assess the hypotheses that have been proposed by cellular biologists and computational neuroscientists. Then, by taking a cross sectional approach, I go on to demonstrate those brain connectivity changes that occur with increasing tau burden. In this way, I am able to dissociate the *causes* of tau accumulation from its *consequences*.

The remainder of my thesis relies on the in-depth study of a disease called non-fluent variant Primary Progressive Aphasia (nfvPPA). This disease has a clear clinical phenotype of speech apraxia and agrammatism, associated with a focal pattern of mild atrophy in frontal lobes. The combination of relatively preserved cortical volume and well-preserved general cognition in early disease makes this an ideal model in which to study the neurophysiological consequences of neurodegeneration for connectivity and cognition.

The second, and largest, experimental chapter (Chapter 3) comprises an experiment in which patients with nfvPPA and matched controls performed a receptive language task while having their brain activity recorded with magnetoencephalography. I manipulated expectations and sensory detail to assess the role of top-down frontal contributions in predictive processes in speech perception. I am able to account for the behavioural psychophysics in a Bayesian perceptual inference framework, and to directly relate the outputs of these simulations to measured neural data. By relating evoked, induced and connectivity data, I demonstrate distant neural effects of the degeneration of frontal lobes that are not simply related to disconnection, and their associated behavioural consequences.

The final experimental chapter (Chapter 4) uses behavioural psychophysics to precisely define the ability of patients with nfvPPA to learn a novel, mixed-complexity artificial grammar designed to assess processing of increasingly complex sequencing relationships. I compare these abilities to patients with non-fluent aphasia due to stroke

and neurological controls. In this way I am able to directly evaluate the impact of sequence modality and complexity on learning in agrammatic aphasics of two different aetiologies.

I conclude with a clinical synthesis chapter (Chapter 5), in which I explain how abnormal frontal lobe function and the consequential inflexible perceptual predictions can account for the subjective speech comprehension difficulties, auditory processing abnormalities and agrammatism of nfvPPA.

Finally, I summarise the way in which the thesis as a whole provides a translational bridge; relating cellular biology to molecular chemistry, molecular chemistry to neural circuits, neural circuits to core cognitive systems, and core cognitive systems to complex behaviours.

Chapter 1: The current clinical context of dementia

1.1 Preface

The aim of this narrative and introductory chapter is to present the current clinical context of dementia and neurodegenerative aphasia. I do this by describing the primary neurodegenerative conditions that impair cognition in terms of their clinical features, aetiology, management, epidemiology and prognosis. This sets the scene for the experimental chapters of my thesis by outlining how the diseases on which I place special emphasis relate to the broader clinical challenge posed by the dementias.

An extended version of this chapter, with additional material covering non-neurodegenerative memory disorders, has been accepted for publication as Chapter 25 of the upcoming Oxford Textbook of Neuropsychiatry, entitled *Memory disorders and Dementias*. The published version includes contributions from Dr Jeremy Isaacs of St George's Hospital, London and Prof Michael Kopelman of King's College London, but what I present here precedes their input and is entirely my own work. All of the figures in this chapter represent the clinical neuroimaging of patients whose care I have managed while conducting my PhD (with their consent).

1.2 Introduction

Dementia is a persistent disorder of the mental processes affecting more than one cognitive domain, which is generally but not universally progressive. It must be of sufficient severity to interfere with an individual's adaptive function, and represent a decline from a previous level of function (McKhann *et al.*, 2011). The clinical dementias can be classified either by their cognitive phenotype or by their aetiological origin, and there is not necessarily a linear mapping between the two.

This chapter is concerned with those disorders of mind or brain that result either in a primary dementia or a disorder of declarative memory. There are a large number of other conditions that result in secondary cognitive impairment or impair sensory or working memory that will not be discussed in detail. These include vascular insults and insufficiency, prion diseases, functional illness, traumatic brain injury, infections of the central nervous system, tumours, inflammatory and autoimmune disorders, demyelinating disorders, mitochondrial disorders, alcohol related disorders, side effects of drugs and toxins, obstructive sleep apnoea, nutritional deficiencies, and delirium.

The assessment of dementia is a multi-disciplinary pursuit, with clinical and diagnostic assessments undertaken by psychiatrists, psychologists, neurologists, geriatricians and, increasingly, specialist nurses, occupational therapists and other allied health professionals. A detailed history of the cognitive impairment is key, and is complemented by appropriate neurological examination and focussed investigation. For illustrative purposes the structural investigations presented will usually be magnetic resonance images (MRI), which are generally clinically preferred in the UK (NICE and SCIE, 2006 (updated March 2016)), but in many cases computed tomography (CT) would be clinically sufficient as the primary purpose of the scan is usually to exclude structural causes of the clinical syndrome (i.e. tumours, bleeds, infarcts and abscesses) (Cole, 1978). Similarly, case vignettes will include screening neuropsychology with the Addenbrooke's Cognitive Examination third edition (ACE-III) (Hsieh *et al.*, 2013) due to its simplicity of administration and favourable sensitivity and specificity (Larner,

2007, Larner, 2015), but similar clinical tools are available that might be more appropriate in particular practice settings.

1.3 Core Progressive Dementias

1.3.1 Alzheimer's Disease – Amnestic

Vignette

A 70 year old gentleman presents to clinic, accompanied by his wife and daughter. His relatives tell you that over the past two years he has been becoming increasingly forgetful, especially for recent events. He has missed a number of appointments and recently became lost while driving an unfamiliar route. The gentleman himself feels that his relatives are over-emphasising his difficulties, but does admit to his memory not being as good as it once was. He is still able to manage all of his activities of daily living, but was unable to recall what he had for dinner yesterday. There are no abnormalities detected on physical or neurological examination. He scores 72 on an ACE-III (attention 12/18, memory 14/26, fluency 10/14, language 24/26, visuospatial 12/16). His MRI scan demonstrated mild global atrophy with disproportionate and symmetrical atrophy of the hippocampi relative to the rest of cortex (Figure 1-1)

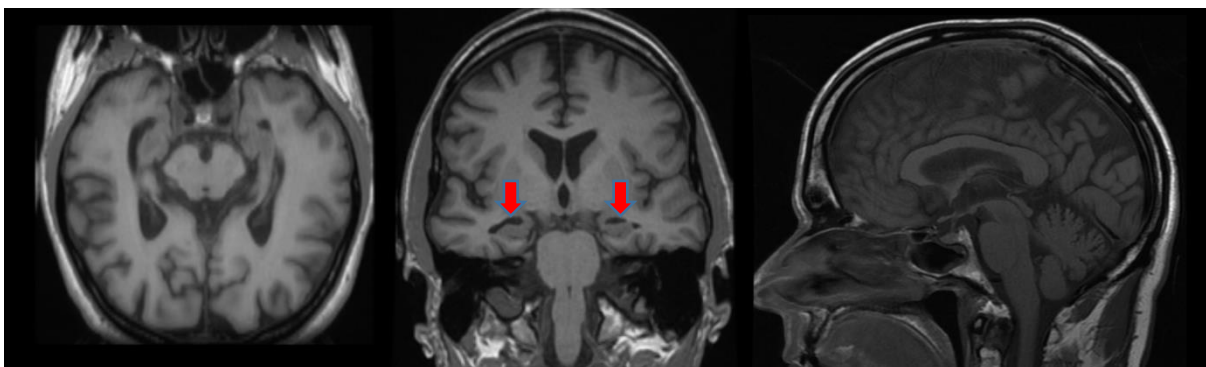


Figure 1-1 MRI images for the amnestic Alzheimer's disease vignette.
Radiological convention; T1 weighted axial, coronal and sagittal projections. Bilateral, disproportionate atrophy of the hippocampi can be seen (arrows).

Clinical Features

A number of diagnostic criteria are available for the diagnosis of Alzheimer's disease, but the most commonly used is that jointly proposed by the National Institute of Neurological and Communicative Disorders and Stroke and the Alzheimer's Disease and Related Disorders Association (now known as the Alzheimer's Association) in 1984 (McKhann *et al.*, 1984). These have stood the test of time, but there have been attempts to update them with more modern imaging techniques for both research (Dubois *et al.*, 2007) and clinical (McKhann *et al.*, 2011) purposes. The condition is characterised by an amnesic syndrome with insidious onset over months or years, without the core features of another of the conditions discussed later in this chapter.

Aetiology

In its 'typical' form, Alzheimer's disease is a progressive disorder of episodic memory, reflecting the typical early involvement of the hippocampal formation. The first microscopically observable abnormalities are tau lesions (non-argyrophilic pretangle material, argyrophilic neuropil threads, neurofibrillary tangles), and later by amyloid- β deposition (Braak and Braak, 1995, Braak and Del Tredici, 2015). Accumulating evidence suggests that this pathological process begins decades before clinical onset (Braak and Del Tredici, 2015), but progresses extremely slowly; usually only crossing a threshold for clinically detectable abnormality many decades after it began. As the disease progresses, the accumulation of pathology accelerates and spreads to involve other cortical areas and therefore cognitive domains. Relatively rarely, the predominant burden of tau and amyloid pathology is outside of the hippocampal formation, resulting in the rarer presentations of Alzheimer's disease discussed below.

Alzheimer's disease is predominantly a sporadic disease, but risk and age of onset are influenced by a number of genetic polymorphisms (Harold *et al.*, 2009). The strongest association is with the apolipoprotein E allele epsilon 4 (Saunders *et al.*, 1993), the presence of which leads to a younger age of onset (Meyer *et al.*, 1998). It is unclear whether this risk is primarily mediated by congenital alterations in brain activity and connectivity (Filippini *et al.*, 2009) or a direct effect on beta amyloid (Bales *et al.*, 1997). Around 2% of cases result from autosomal dominant mutations in genes coding for either the amyloid precursor protein (APP), or the gamma-secretase complex

components presenilin 1 (PSEN1) and two (PSEN2) (Brouwers *et al.*, 2008). Duplication of APP due to trisomy 21, and consequent overexpression of amyloid precursor protein, is the cause of early onset Alzheimer's disease in Down's syndrome (Rumble *et al.*, 1989).

Management

At the time of writing, no effective disease modifying therapies are available for Alzheimer's disease. By 2013, more than 200 drug candidates had been evaluated unsuccessfully (Becker and Greig, 2013). It is not clear whether these drugs were all ineffective because their mechanism of action was a flawed therapeutic strategy, or whether other factors were at play. Certainly, by the time disease is clinically evident underlying neuropathological abnormalities are advanced and progressing rapidly. It has been proposed that one or more of these candidates might still prove efficacious in pre-symptomatic disease, but clinical trials in this group are difficult because high-risk case selection is complex and measurement of progression in the absence of validated biomarkers requires long and expensive clinical trials (Fitzgerald, 2014). As well as drugs that specifically target Alzheimer-type pathology, novel agents are in development that target more general cellular stress response pathways to prevent toxic protein accumulation (Moreno *et al.*, 2013, Halliday and Mallucci, 2014).

Therefore, at present, the aim of treatment is to manage symptoms. The mainstay of management for all of the diseases discussed in this chapter is to provide information and guidance to patients and their family about support available and the likely course of the disease to enable future planning. Assessment and information exchange should be holistic, and as a minimum should cover: advanced planning of decision making arrangements for health and finances (lasting power of attorney); financial matters and available benefits; housing and social arrangements and future plans; cognitive stimulation; carer support; and opportunities for pharmacological intervention.

Initial symptomatic treatment in mild to moderate disease is usually with a cholinesterase inhibitor (and, if possible, the cessation of anti-cholinergic medications (Lu and Tune, 2003)). On average these result in small improvements in cognitive test scores and measures of activities of daily living and behaviour (Birks, 2006). The three drugs in this class (donepezil, rivastigmine and galantamine) have similar efficacy

(Bullock *et al.*, 2005). Which to initiate is therefore a clinical judgment based on practical concerns, side effect profile and cost. Donepezil has once daily dosing; while Rivastigmine has a patch preparation that can be useful in late disease if swallowing is impaired (this can be particularly useful in the Lewy body disorders). Donepezil seems to have a more tolerable side effect profile than rivastigmine (Bullock *et al.*, 2005), but there is no difference in serious adverse effects. Common side effects include nausea, vomiting and diarrhoea – these effects can be dose dependent and it is therefore common practice to begin at a low dose, and slowly titrate upwards to the highest tolerable level. Serious adverse events are very rare, but caution should be exercised in the presence of cardiac rhythm abnormalities and patients with peptic ulcer disease (Schachter and Davis, 1999). In the absence of side-effects, it would be usual to continue these medications lifelong because of the risk of cognitive relapse on their cessation (Rainer *et al.*, 2001).

Where dementia is moderate to severe (or in more mild disease where cholinesterase inhibitors cannot be tolerated), the addition of the NMDA receptor antagonist memantine should be considered (Raina *et al.*, 2008). This has a small but robustly demonstrable benefit to measures of cognition, activities of daily living, behaviour and overall performance status (Tariot *et al.*, 2004).

Pharmacological intervention for other specific neuropsychiatric symptoms should be addressed with caution. For example, while there is sometimes a role for low doses of antipsychotics in managing difficult behaviours that might have significant negative sequelae (such as jeopardising an otherwise successful residential placement), the side effect profile of these drugs means that it is normally preferable to address these issues with social interventions and targeted carer support.

Low mood is a frequent complaint in dementia. Unfortunately there is converging evidence that commonly used anti-depressant medications are broadly ineffective at treating low mood in Alzheimer's disease, while carrying a side effect burden (Banerjee *et al.*, 2011). Mirtazapine has been shown to improve carer quality of life, primarily by improving appetite and sleep, while high-dose citalopram was effective for agitation (Porsteinsson *et al.*, 2014). The specific indication for treatment should therefore be carefully considered.

Epidemiology

Alzheimer's disease is the most common dementia in the western world, representing approximately 70% of the 4.6 million global annual incident cases (Ferri *et al.*, 2005). Prevalence is felt to be rising especially rapidly in the developing world, as life expectancy increases (Reitz *et al.*, 2011). While age-for-age dementia incidence is falling in the UK (Matthews *et al.*, 2013, Matthews *et al.*, 2016), the ageing population means that dementia continues to rise in both prevalence and incidence. Prevalence increases rapidly with age, from <5% of those below age 75, to 10% at age 80-84, 20% at 85-89 and 30% over 90.

Prognosis

Alzheimer's disease is a relentlessly progressive condition that alters behaviour (Reisberg *et al.*, 1996), induces dependency and shortens life expectancy. The most powerful predictors of life expectancy from diagnosis are age, sex, degree of cognitive impairment at diagnosis, and magnitude of cognitive decline over the first year (Larson *et al.*, 2004). Median life expectancy for 70 year old women with Alzheimer's disease is 8 years, compared to 16 years for those without. For men at 70, it is 4.4 years compared to 12.4 years without. Diagnosis at an older age has less impact on survival – prognosis for Alzheimer's sufferers at age 90 is 2-3 years, compared to 3-4 years without. Mini-mental state exam scores below 24/30 at diagnosis predict poorer prognosis, with those below 17 having a particularly high hazard ratio for death (2.6x that of an MMSE > 24). A decline of more than 5 points in the MMSE over the first year results in a hazard ratio of 1.6. Recent suggestions of multimodal prognostication using quantitative neuroimaging and CSF analysis have not yet found clinical utility, but hold promise for research applications (Perrin *et al.*, 2009).

1.3.2 Alzheimer's Disease – Posterior Cortical Atrophy – Benson's Syndrome

Vignette

A 58 year old man presents to clinic with his wife. Two years ago he noticed difficulty with using money, being unable to easily distinguish between coins without feeling them. A year later he began to have problems with not noticing hazards while driving.

His wife describes him, “looking but not seeing.” He has been assessed by an optician and an ophthalmologist, both of whom said that his visual acuity was normal, but suggested that there might be a neurological cause for his problems. On examination you note simultagnosia, bilateral dyspraxia, dyscalculia, dysarithmetria and visual working memory difficulties. His speech is also slightly hesitant, and he displays some anomia with preserved semantic knowledge during confrontational naming. There are no abnormalities on neurological examination, and specifically there is no movement disorder. ACE-III is 82/100 (attention 18/18, memory 22/26, fluency 12/14, language 22/26, visuospatial 8/16). His MRI scan demonstrated global atrophy especially severe in the parietal lobes (*Figure 1-2*).

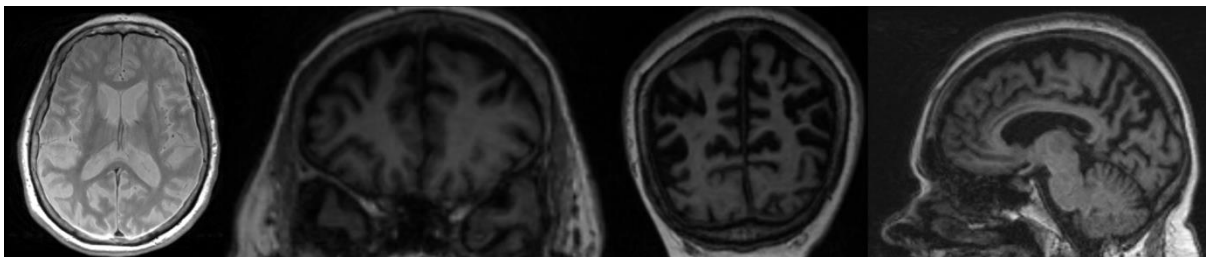


Figure 1-2 MRI images for the Posterior Cortical Atrophy vignette.
Radiological convention. Proton density weighted axial projection; T1 weighted coronal projections through frontal and then parietal regions; T1 weighted sagittal projection. Disproportionate, bilateral parietal lobe atrophy can be seen.

Clinical Features

Reflecting the biparietal predominance of pathological damage (Ossenkoppele *et al.*, 2015), posterior cortical atrophy is a primary disorder of the dorsal ‘where’ visual stream (Ungerleider and Mishkin, 1982, McMonagle *et al.*, 2006), leading to visuospatial disorientation with or without a broader biparietal syndrome of ideomotor and gesture copy apraxia, Gerstmann syndrome (dysgraphia, dyscalculia, finger agnosia and left-right confusion) and Bálint’s syndrome (optic ataxia, ocular apraxia and simultagnosia). An associated occipitotemporal syndrome of alexia and apperceptive agnosia (including prosopagnosia) is also common, as is the later emergence of a parietal, Alzheimer-type language deficit (see next section on logopenic and mixed primary progressive aphasia).

Prognosis

Although there is a clinical perception that the prognosis of posterior cortical atrophy is better than that of amnesic Alzheimer's disease, this seems to be a result of the generally younger age of presentation and the often shorter duration of symptoms before coming to medical attention. When age matched groups are studied, there is no significant difference between typical and focal Alzheimer's disease in time from first symptoms to death (mean 9.7 years) (Alladi *et al.*, 2007).

Epidemiology and Management

There have been no robust epidemiological or prevalence studies of focal presentations of Alzheimer's disease. The clinical perception is that even if all of the focal subtypes are combined, they are still far less common than typical Alzheimer's disease. Focal presentations tend to present at an earlier age than typical AD, but it is not clear whether this represents a referral or case selection bias. Medical management is generally similar to typical Alzheimer's disease, as the symptoms become more phenotypically similar as disease progresses. The additional consideration in posterior cortical atrophy is management of the visual symptoms, which can be very disabling. Driving should cease at an early stage. Some patients have found it beneficial to become registered as legally blind, as in the UK this facilitates access to a number of benefits and concessions, as well as practical support from charitable bodies. This application can require careful wording, as patients with cortical blindness of this type will have good visual acuity and the visual field might appear normal to single-target confrontation. An ophthalmologist's report will be required, and the criterion that can usually be applied is that which states: "If you have a good visual acuity, you will usually have had to have lost a large part of your visual field to be certified as severely sight impaired (blind) or sight impaired (partially sighted)." It should be stressed that, while the detection of single targets can be in-tact, analysis of the visual field as a whole is catastrophically impaired.

1.3.3 Alzheimer's Disease – Logopenic and Mixed Primary Progressive Aphasia

Vignette

A 59 year old right-handed gentleman presents to clinic with an 18 month history of subjective speech disturbance. He describes difficulty in finding words, such that he

becomes derailed half way through a sentence. He is clear that he can bring to mind the object or concept and give a description of it, but feels as if the word itself is stuck ‘at the tip of his tongue’. He has given up work as a local government planning officer because of this difficulty, although his managers had not felt that his performance had deteriorated. Conversationally he is fluent and his speech is full of content, but there are pauses as he gropes for words, and sometimes the train of thought is lost. There are some problems with confrontational naming, but he is able to give a semantically detailed description of these items. He finds it difficult to repeat long sentences, giving close approximations that carry the gist and are grammatically correct. He scores 89/100 on the ACE-III (Attention 18/18, Memory 19/26, Fluency 10/14, Language 26/26, Visuospatial 16/16); note that the language testing on ACE-III is relatively simple, with no long sentence repetitions, and so the symptomatic deficits in this domain were not evident on bedside cognitive testing. His MRI demonstrates mild global atrophy, with a parietal predominance (Figure 1-3).

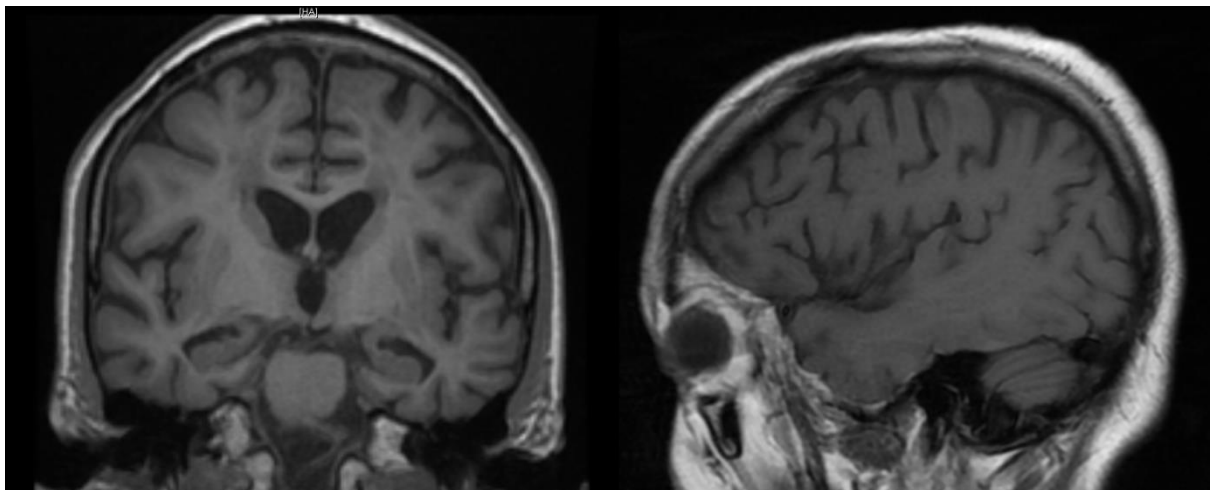


Figure 1-3 MRI images for the logopenic Primary Progressive Aphasia vignette. *Radiological convention. T1 weighted coronal and sagittal projections. Subtle atrophy of hippocampi and parietal lobe can be seen, with a left sided predominance.*

Clinical Features

Aphasia is very common in typical Alzheimer’s disease (Cummings *et al.*, 1985), but in rare cases it can be the leading or only clinical feature. The core clinical feature of this condition is a deficit in responsive and confrontational naming with preserved semantic knowledge. This can often be subtle at presentation, as patients notice the problem early, frustrated by pauses in their speech as they find themselves groping for words.

The diagnostic criteria for logopenic variant primary progressive aphasia are the presence of impaired single-word retrieval in both spontaneous speech and naming together with impaired repetition of sentences and phrases in a length dependent manner, as well as three out of the following: phonological errors, spared single word comprehension and object knowledge, spared motor speech, and absence of agrammatism (Gorno-Tempini *et al.*, 2011). These features are strongly supportive of Alzheimer's pathology involving left parietal lobe (Gorno-Tempini *et al.*, 2004). In recent years, it has been suggested that these diagnostic criteria are too narrow. There is converging evidence that any primary progressive aphasia that does not meet diagnostic criteria for semantic dementia or progressive non-fluent aphasia (i.e. a mixed aphasia), is also likely to represent Alzheimer's pathology in left parietal lobe (Sajjadi *et al.*, 2012, Sajjadi *et al.*, 2014), especially if confrontational anomia or amnesia is present (Alladi *et al.*, 2007).

1.3.4 Alzheimer's Disease – Dysexecutive/Behavioural Variant

Clinical Features

It can be very difficult to clinically distinguish between a behavioural variant of Alzheimer's disease and the behavioural variant of frontotemporal dementia (bvFTD). Presentations can be very similar (see vignette and clinical features of bvFTD below) (Woodward *et al.*, 2010). The clinical syndrome reflects the distribution of neuronal loss rather than its aetiology, with distinct regional atrophy patterns found in syndromes characterised by disinhibition, apathy or aberrant motor behaviours (Rosen *et al.*, 2005). The presence of significantly impaired episodic memory is not sufficient evidence that one is dealing with a dementia of the Alzheimer's type, as there is now converging evidence for memory involvement in a significant proportion of bvFTD (Hornberger *et al.*, 2010, Hornberger and Piguet, 2012), but should prompt the clinician to consider further investigation with detailed neuropsychological, neuroimaging and/or neuropathological assessment (Larner, 2006). While an educated guess as to the likely aetiology can be made, it should be borne in mind that without pathological or biomarker confirmation at least 5-10% of seemingly typical cases are misclassified (Graham *et al.*, 2005, Alladi *et al.*, 2007, Rascovsky *et al.*, 2011).

Management

While cholinesterase inhibitors have some efficacy in managing the neuropsychiatric manifestations of Alzheimer's disease (Wynn and Cummings, 2004), they have been reported to worsen behavioural symptoms in frontotemporal dementia (Mendez *et al.*, 2007, Kimura and Takamatsu, 2013). Similarly, while Memantine had promising initial anecdotal reports of efficacy in bvFTD (Swanberg, 2007), two randomised controlled clinical trials proved negative (Vercelletto *et al.*, 2011, Boxer *et al.*, 2013). Given the practical difficulties in distinguishing these two syndromes, circumspection and careful assessment of response should be employed in prescribing. Strategies for the management of bvFTD are discussed in the next section.

1.3.5 Frontotemporal Dementia – Behavioural Variant – bvFTD

Vignette

A 77 year old right handed lady is referred to clinic by her family. They report that she has become progressively more 'childish' over the past two years. She is inappropriately familiar with strangers, and displays total disregard for etiquette such as table manners. You notice that her clothes are dirty and that she is wearing three scarves, two pairs of trousers and two bras. Her husband, who is well kempt, reports that she insists on re-wearing dirty clothes and that he is unable to intervene. The patient tells you that there is a man living in her attic; she has never seen him, but knows that he is there. On examination you note the presence of primitive reflexes (grasp, palmomental, pout), as well as deltoid fasciculations, thinning of the first dorsal interosseous and thenar eminence bilaterally, slow tongue movements and hyperreflexia. ACE-III is 85/100 (Attention 16/18, Memory 21/26, Fluency 10/14, Language 21/26, Visuospatial 16/16). Her language deficits are in naming, and you note that she has some mild semantic impairment for these items.

Clinical Features

The most recent diagnostic criteria allow for the diagnosis of 'possible' bvFTD on clinical grounds in the presence of three of the following six features: disinhibition, apathy, loss of empathy, perseverative behaviours, hyperorality (an excessively sweet

tooth) and dysexecutive neuropsychological profile (Rascovsky *et al.*, 2011). The level of certainty is increased to ‘probable’ in the presence of functional disability and characteristic neuroimaging, while ‘definite’ diagnosis requires either histopathological confirmation or a pathogenic mutation. It is especially important to assess for progression of symptoms and neuroimaging changes, as a significant proportion of cases diagnosed on clinical features alone fail to progress in terms of clinical syndrome or atrophy (Hornberger *et al.*, 2009, Kipps *et al.*, 2010). It is unclear whether these cases represent atypical, late-onset neuropsychiatric disease (Belin *et al.*, 2015) or are simply retiring males spending more time with, often new, life partners. When progression is established (Mioshi and Hodges, 2009), these criteria have a sensitivity of 72-95% and specificity of 82-95% (Harris *et al.*, 2013), with the majority of misclassifications being with frontal Alzheimer-type pathology as discussed above.

Over time, the evolution of the syndrome to include semantic deficits is common, reflecting a shared aetiology with semantic dementia. A proportion of patients with bvFTD will go on to develop progressive supranuclear palsy (Kaat *et al.*, 2007) or, as here, motor neurone disease.

Aetiology

The clinical syndrome of FTD represents several histopathological patterns of frontotemporal lobar degeneration. 40%-50% of cases display inclusions of the microtubule-binding protein tau (Mackenzie *et al.*, 2010) with either three or four microtubule-binding repeats (Cairns *et al.*, 2007). Approximately 40-50% of cases have inclusions of TDP-43 (43 kDa TAR DNA-binding protein) (Piguet *et al.*, 2011) and 5% inclusions of FUS (fused in sarcoma) (Seelaar *et al.*, 2010a). These proteins are both involved in RNA-processing, but their pathogenic mechanisms are not yet known. The remaining 5% of cases with typical phenotype and distribution of neuronal loss (and without Alzheimer-type or Lewy body pathology) are negative for tau, TDP-43 and FUS, suggesting an as-yet unknown pathogenic mechanism (Mackenzie *et al.*, 2008).

bvFTD is highly heritable, with up to 50% of patients having a family history of the disorder (a far higher proportion than the other FTD syndromes, which do not generally run in families) (Rosso *et al.*, 2003). A single causative gene can be

demonstrated in approximately half of these cases, with the proportion rising in clear autosomal dominant inheritance patterns with multiple family members affected (Rohrer *et al.*, 2009). It is now possible to test for most of the common exon mutations on a single chip; *MAPT* and *GRN* each account for 5-11% of FTD, while *TARDBP*, *FUS*, *CHMP2B*, *TBK1*, *VCP*, *SQSTM1* and *hnRMP1a* account for progressively fewer cases and tend to be associated with additional clinical features (Seelaar *et al.*, 2010b). At least as common as any of these is a hexanucleotide repeat expansion in the intron *C9ORF72*. This must be separately tested, and is particularly suggested by the presence of motor neurone disease (DeJesus-Hernandez *et al.*, 2011, Renton *et al.*, 2011) or prominent psychiatric features in the proband or family members (Arighi *et al.*, 2012, Snowden *et al.*, 2012). While *C9ORF72* has autosomal dominant inheritance, it is incompletely penetrant and manifests differently within a family, as motor neurone disease, psychiatric disorders and bvFTD alone or in combination. In the vignette, the combination of bvFTD, motor neurone disease and delusions would strongly suggest *C9ORF72*, even in the absence of a family history.

Management

In contrast to AD, there is no role for cholinesterase inhibitors in bvFTD (Mendez *et al.*, 2007, Kimura and Takamatsu, 2013). Similarly, while Memantine had promising initial anecdotal reports of efficacy (Swanberg, 2007), two randomised controlled clinical trials proved negative (Vercelletto *et al.*, 2011, Boxer *et al.*, 2013).

One medication with evidence for efficacy in relieving the behavioural symptoms of bvFTD is trazodone (Lebert *et al.*, 2004), from which sustained benefit can often be obtained (Lebert, 2006). These benefits are not always observed, and the decision to continue with this medication should be made by the prescriber based on a comprehensive assessment of both patient and carer experience. A possible disease-modifying mechanism for trazodone has been proposed through actions on the cellular unfolded protein response (Halliday *et al.*, 2017), however any conclusions about clinical efficacy would be premature without carefully conducted clinical trials (Halliday and Mallucci, 2017).

The mainstay of treatment is non-pharmacological. Abnormal behaviours can be challenging, especially for members of the public. It is important to consider whether

any community stakeholders would benefit from being aware of the diagnosis, and suggesting this to patients and their families. It is often appropriate for families to inform local law enforcement services and frequently visited shops.

Driving can be a particularly thorny issue – patients with bvFTD, more than any other group in the dementia clinic, lack insight into their symptoms and the problems they cause in judgment. While it is usual practice in the UK to tell patients that they must inform the DVLA of their diagnosis, in bvFTD it is often necessary to firmly advise against driving and directly inform the DVLA of this advice. Family members can be a useful guide towards the necessity of taking such action.

Hyperorality and dietary changes are often a significant issue. Overeating can represent a simple utilisation behaviour, in which case it can be fairly easily addressed by selective purchasing and locking cupboards. In some individuals, however, obtaining sweet foods becomes an overarching goal-directed behaviour, and weight gain can be dramatic (Ikeda *et al.*, 2002, Seeley *et al.*, 2005). Social interventions are often insufficient in these cases, and pharmacological intervention required. Diabetes is often comorbid, and metformin can be a useful suppressor of appetite. Similarly if myoclonus, tremor or seizures are present, topiramate can be considered. Limited or repetitive diets can be similarly damaging, and in such cases potential vitamin deficiencies should be addressed lest a diet of biscuits and fizzy drinks lead to scurvy. In advanced disease, weight gain gives way to weight loss as more than 80% of patients become unable to eat independently (Diehl-Schmid *et al.*, 2017).

Epidemiology

The behavioural variant of FTD has a significantly younger age of onset than the other disorders in the FTLD spectrum (Coyle-Gilchrist *et al.*, 2016), with the majority of both genetic and sporadic cases presenting before the age of 65 (peak incidence across FTLD as a whole is between age 65 and 80). Incidence of FTLD in the UK is about 10/100,000 person-years, with bvFTD representing approximately a quarter of these cases (SD and nfvPPA together represent another quarter, with the other half being CBS or PSP). When adjusted for higher female life expectancy, there is no significant gender bias in bvFTD or in FTLD as a whole.

Prognosis

Mean survival from symptom onset is approximately 8 years (in the absence of signs of motor-neurone disease). The clinical syndrome evolves significantly through this period, as the over-activity, social inappropriateness and hypersexuality that can be so distressing in early disease frequently give way to a syndrome of apathy and semantic impairment after the first few years. This should be recognised by dynamic symptom management, with the cessation of no-longer-necessary medications and pro-active interventions given equal priority.

1.3.6 Frontotemporal Dementia – Semantic Dementia - SD

Vignette

A 70 year old right-handed man is brought to clinic by his wife. He has not noticed any problems, and is unsure why he has been brought to clinic. His wife says that she first noticed something wrong a year ago, when they were perusing a restaurant menu and her husband asked her what asparagus was. Since then, his understanding of words and concepts, both written and spoken, has gradually declined. She relates that some activities are completely unchanged, for example her husband is still able to drive and route find, and still enjoys playing bridge to a relatively high standard. The patient's conversational speech is fluent and grammatical but empty of content words. He is unable to name lower frequency animals, and nor is he able to tell you which of several model animals is dangerous or edible. When asked to draw animals he produces images that lack distinctive features – for example a camel without a hump and an elephant without a trunk (Bozeat *et al.*, 2003). Similarly, he cannot name or demonstrate the use of some kitchen implements. He is able to repeat long words and sentences without difficulty, but has poor understanding. When reading aloud he pronounces irregular words phonetically (surface dyslexia) (Woollams *et al.*, 2007). ACE-III is 70/100 (attention 18/18, memory 22/26, fluency 2/14, language 12/26, visuospatial 16/16). His MRI scan demonstrates severe, selective atrophy of the left temporal lobe (Figure 1-4).

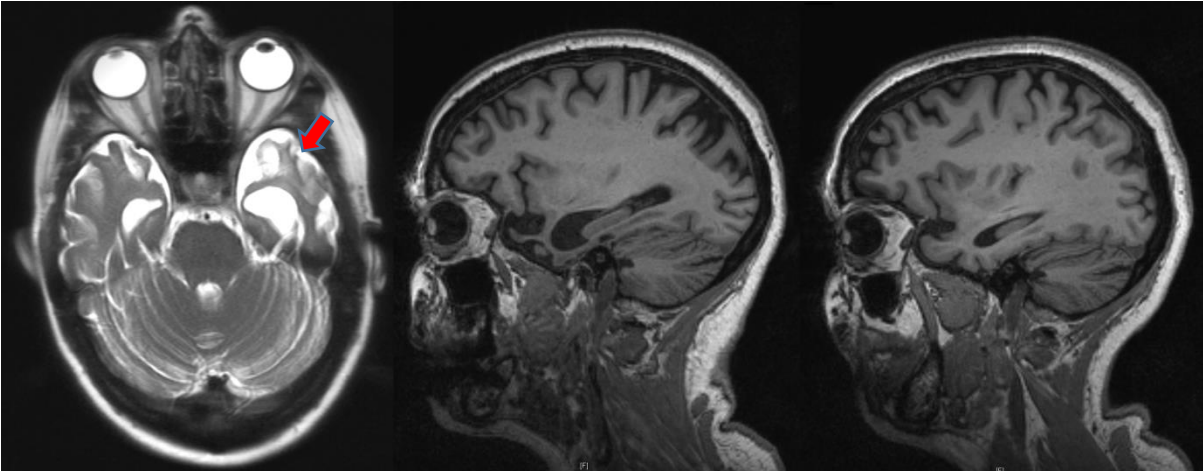


Figure 1-4 MRI images for the Semantic Dementia vignette.

Radiological convention. T2 weighted axial projection; T1 weighted sagittal projections through the left and right temporal lobes at roughly the same eccentricity. Severe, selective atrophy of the temporal poles can be seen, with a significant left sided predominance (arrow).

Clinical features

SD is a stereotyped syndrome of progressive loss of semantic knowledge associated with left sided temporal lobe atrophy (Warrington, 1975, Basso *et al.*, 1988, Snowden *et al.*, 1989, Hodges *et al.*, 1992). It is often classified together with the other neurodegenerative aphasia (nfvPPA and logopenic Alzheimer's disease), as fluent, content-less speech is a leading symptom; in this context it is named the semantic variant of primary progressive aphasia, svPPA. The aphasia is, however, a consequence of a broader loss of semantic knowledge for objects. This can be best conceptualised by an example: if a patient with logopenic Alzheimer's disease is presented with a model lion, they might not be able to tell you that it is a lion (displaying anomia), but they would be able to give semantic detail about lions, for example that they are dangerous and live in Africa. A patient with SD might similarly lack the word 'lion', but they would also lack all knowledge about lions. Therefore, although they do indeed have an agnosia for words, this amodal deficit extends to all semantic domains and is not, primarily, an aphasia (Bozeat *et al.*, 2000, Fairhall and Caramazza, 2013).

In fact, it is possible that a patient with SD will tell you that what they are looking at is a cat, and that they have one at home. This reflects the postulated mechanism for semantic memory, whereby knowledge about objects is stored as a commonly observed 'template', with specific differentiating flags. For example, an elephant might be stored

as a commonly observed large quadruped such as an horse, with the additional flags ‘has a trunk’, ‘lives in Africa or Asia’, ‘ has big ears’, ‘is very large’ etc. (Snowden *et al.*, 2001). This can be clinically observed by asking patients with SD to draw animals with distinguishing features. The more unique the feature, the more likely it is to be omitted – for example a patient with SD might draw an elephant without a trunk, a camel without a hump, or a duck with four legs (Bozeat *et al.*, 2003).

Behavioural features are common (Seeley *et al.*, 2005, Coyle-Gilchrist *et al.*, 2016, Lansdall *et al.*, 2017), especially later in the disease course when the right temporal lobe becomes involved. These overlap with bvFTD, but are more likely to comprise compulsive, repetitive behaviours and disinhibition than apathy and indiscriminate eating, reflecting a temporal rather than frontal predominance of atrophy (Snowden *et al.*, 2001). The syndrome of predominant right sided temporal atrophy is dominated by this behavioural phenotype (Chan *et al.*, 2009), often in combination with prosopagnosia (loss of semantic knowledge of familiar people) (Evans *et al.*, 1995). Similarly, as temporal lobe atrophy becomes bilateral, an additional SD phenotype often develops.

Overall, there can be striking preservation of ability outside of semantic and behavioural domains. It is not uncommon for a patient to demonstrate catastrophic loss of object knowledge, but retain complex procedural skills and navigational ability. Schemata can be well preserved, but sometimes break down with object substitution – for example proficiently making a cup of tea but then putting the milk in the cupboard and tea bags in the fridge.

Aetiology

Semantic dementia is almost always associated with TDP-43 related histopathology affecting the temporal lobes, with a left sided predominance. In contrast to bvFTD it does not show significant heritability, and indeed at least three patients seen in the Cambridge clinic are known to have had SD and an unaffected monozygotic twin (personal communication from Prof Karalyn Patterson).

1.3.7 Frontotemporal Dementia – non-fluent variant Primary Progressive Aphasia – nfvPPA/PNFA

Vignette

A 63 year old right-handed lady presents to clinic with a one year history of a progressively worsening difficulty in getting her words out. She finds this extremely frustrating. She is very clear that she knows what the word is that she wants to say, but she is unable to articulate it. She has not noticed any other problems. Her conversational speech is effortful, with phonological paraphasias being especially noticeable with words requiring articulatory agility. It is also telegraphic, lacking connecting words and some grammatical form. She performs poorly at parsing grammatically complex sentences, but demonstrates flawless confrontational naming and semantic knowledge. You ask for a sample of her writing, and note that this too contains grammatical errors. She scores 96/100 on the ACE-III (Attention 18/18, Memory 25/26, Fluency 12/14, Language 25/26, Visuospatial 16/16). Her MRI scan appeared normal (Figure 1-5).

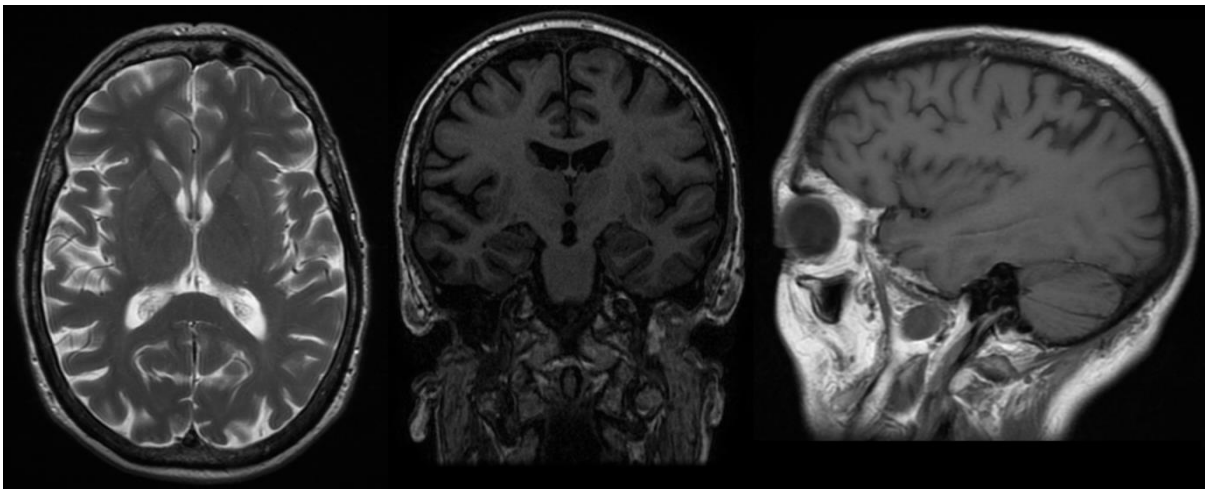


Figure 1-5 MRI images for the non-fluent variant Primary Progressive Aphasia vignette.

Radiological convention. T2 weighted axial projection; T1 weighted coronal and sagittal projections. Normal appearances for age can be seen, with good hippocampal bulk.

Clinical Features

Non-fluent variant Primary Progressive Aphasia (nfvPPA), formerly known as Progressive Non-Fluent Aphasia (PNFA), is an adult onset neurodegenerative aphasia

characterised by apraxia of speech and/or agrammatism (Gorno-Tempini *et al.*, 2011). Importantly, patients should not have word finding difficulties (anomia) or a general cognitive impairment in the early stages of disease; if this is present, a diagnosis of mixed primary progressive aphasia should be made and the underlying neuropathology is almost always of the Alzheimer's type (Sajjadi *et al.*, 2012, Sajjadi *et al.*, 2014). Sentence repetition is impaired where articulatory agility is required or the grammatical structure is complex. Semantic deficits should not be present in early disease, but these and/or behavioural features can evolve later. Yes/no confusion is a common feature in relatively early disease, and digit span can be markedly shortened due to impairment of the phonological loop (Baddeley and Hitch, 1974). Neuroimaging changes can be very subtle in early disease, often appearing normal in the single subject, but predominant atrophy is in left frontal lobe (Rogalski *et al.*, 2011, Grube *et al.*, 2016).

Although nfvPPA is commonly thought of as an expressive aphasia, the neurodegenerative equivalent of Broca's syndrome, patients also frequently complain that perceiving speech is effortful, even in optimal listening environments. Many have sought hearing aids, but been told that they do not have a peripheral deficit. It is thought that this reflects a double-hit to auditory processing, with impairments in basic auditory processing (Goll *et al.*, 2010, Grube *et al.*, 2016) compounded by damage to frontal regions making predictions to 'fill-in' unclear speech (see Chapter 5).

The diagnostic criteria require the presence of only one of apraxia of speech and agrammatism. This has led some authors to propose that nfvPPA should be clinically subdivided into an agrammatic variant (agPPA) and an apraxic variant (primary progressive apraxia of speech, PPAOS) (Josephs *et al.*, 2012, Josephs *et al.*, 2013). The justification for this division has been the observation that those presenting with PPAOS are more likely to develop a motor syndrome consistent with PSP or CBS later in their illness (Josephs *et al.*, 2005) and have a neuropathological diagnosis of tau rather than TDP-43 pathology (Josephs *et al.*, 2006). However, this subdivision has not gained widespread acceptance in the aphasia community, and the new research diagnostic criteria for PSP acknowledge that apraxic speech and agrammatism either individually or in combination can be associated with underlying PSP pathology (Höglinger *et al.*, 2017). There are several reasons for this:

- 1) There is a clear spectrum to nfvPPA, with some patients displaying predominant apraxia of speech, and others having marked difficulties with both expressive and receptive grammar, but all patients displaying deficits in both domains on careful testing.
- 2) Fewer than half of patients with PPAOS will develop a movement disorder, and even if this does occur this transformation often emerges five or more years into the illness (Josephs *et al.*, 2012, Josephs *et al.*, 2014). Similarly, movement disorders sometimes occur later in the illness of those who present with agrammatism.
- 3) While there is a statistical trend for symptom type at onset to predict progression and pathology, even in the presence of a movement disorder, predominant TDP-43 pathology in the absence of tau has been observed. I have encountered one such case in my own practice, through donation to the Cambridge Brain Bank.
- 4) Although there are differences in patterns of atrophy between PPAOS and agPPA at the group level (Josephs *et al.*, 2013), these are relatively subtle. Changes in cortical thickness in left inferior frontal gyrus correlate with grammatical processing, while those in inferior frontal sulcus correlate with fluency (Rogalski *et al.*, 2011). These are neighbouring regions, and the differences are certainly less marked than those between PPAOS and PSP (Whitwell *et al.*, 2013). Regardless of diagnostic subgroup, progression of aphasic symptoms is associated with neurodegeneration in the language network, while progression of motor symptoms is associated with neurodegeneration outside of the language network, in motor cortex and brainstem (Tetzloff *et al.*, 2017).
- 5) nfvPPA is already a very rare syndrome, and further subdivision would make clinician education and meaningful research more difficult.

Aetiology

The syndrome of nfvPPA predicts atrophy centred on left frontal lobe, but not the nature of the causative pathology. The majority of cases represent tauopathies, but a significant minority have TDP-43 related disease (Kertesz *et al.*, 2005, Josephs *et al.*, 2006, Knibb *et al.*, 2006a, Knibb *et al.*, 2006b, Mesulam *et al.*, 2014). Neuropathological series vary markedly (from 0-40%) in the proportion of nfvPPA found to have Alzheimer's neuropathology. This likely represents differences in local diagnostic practice, perhaps in terms of the stringency with which anomic patients are excluded from nfvPPA diagnosis.

Management and prognosis

Patients with nfvPPA are intensely frustrated by their symptoms, and present early in their disease course (Coyle-Gilchrist *et al.*, 2016). The cornerstone of therapy is explanation of symptoms and practical management of the aphasia; there is no role for medications unless additional motor or behavioural features emerge later in the disease. It is often fruitful to approach nfvPPA in the same way as Broca's aphasia, with the provision of communication aids and explanation cards. Some patients even find it simpler to tell shopkeepers and acquaintances that they have had a stroke, as this encapsulates their problems more quickly than an explanation of an unusual neurodegeneration. Speech therapy can be helpful in teaching strategies to avoid words with challenging articulation or sentences with ambiguous grammar, but attempts at rehabilitation are rarely fruitful.

Yes/no confusion can be challenging and perplexing to carers, and should be explicitly acknowledged and explained. Strategies for dealing with this include asking patients to include a gesture as well as a verbal response (for example thumbs up and saying yes together so that discordance can be more easily recognised), and training carers to present non-binary choices.

Survival from symptom onset averages 9 years (similar to bvFTD), but as symptoms are troublesome presentation is often earlier. Age of onset is also older than bvFTD, with peak rates observed between age 65 and 80 (Coyle-Gilchrist *et al.*, 2016). Even when patients present at a young age, a genetic cause is rarely found; while patients with *GRN* mutations often have non-fluent speech, they also have anomia and single

word comprehension problems not consistent with a diagnosis of nfvPPA (Rohrer *et al.*, 2010).

1.4 Dementias associated with Movement Disorders

The neuropsychiatry of movement disorders could form a thesis in itself (see, for example, (Ghosh, 2011), leading to (Ghosh *et al.*, 2012)). The discussion here will therefore be restricted to those clinical features that aid the differential diagnosis of these disorders in the cognitive clinic.

1.4.1 Lewy Body related – Dementia with Lewy Bodies – DLB

Vignette

A 73 year old lady is referred by her family doctor because of a three year history of hallucinations. These occur daily, primarily when she is tired or the lighting is poor. The most common manifestation is that she will make three or four coffees for people sitting on the sofa, and her husband will have to remind her that it is only the two of them in the house. She also frequently hallucinates individuals in the garden, and on one occasion thought that they were stealing her furniture. This caused some minor distress. She has good retrospective insight into the fact that these people are not real, but finds it very confusing at the time. If her husband reassures her that they are just hallucinations, she is able to understand this. Her cognition is fluctuant, with good days and bad days. She has REM sleep behaviour disorder. On examination you elicit a mild Parkinsonian motor syndrome, which is not symptomatic, and her sense of smell is poor. Despite only scoring 53/100 on an ACE-III (attention 11/18, memory 12/26, fluency 7/14, language 14/26, visuospatial 9/16), she is still able to travel to and from town alone on the bus once a week, where she follows a fixed routine of going to Marks and Spencer's and coming home again. Her MRI scan demonstrated mild global atrophy (Figure 1-6).

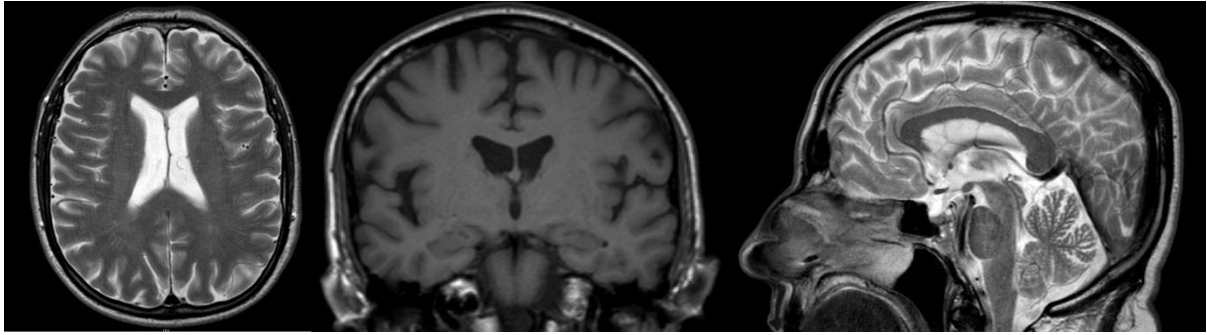


Figure 1-6 MRI images for the Dementia with Lewy Bodies vignette.

Radiological convention. T2 weighted axial projection; T1 weighted coronal projection; T2 weighted sagittal projection. Mild generalised atrophy can be seen, with good hippocampal bulk and normal brainstem appearances.

Clinical features

DLB is a dementia characterised by fluctuating cognition, attention and alertness and/or recurrent visual hallucinations. The diagnosis is upgraded from ‘possible’ to ‘probable’ by the presence of REM sleep behaviour disorder, severe neuroleptic sensitivity or abnormal dopamine transporter activity on nuclear imaging (McKeith *et al.*, 2005). Impairments of visuospatial, executive and attentional function can be particularly prominent. Other supportive features include repeated falls and syncope, transient unexplained losses of consciousness, autonomic dysfunction, delusions, depression, and the absence of hippocampal atrophy on structural imaging. DLB is diagnosed when this characteristic cognitive syndrome develops either in the absence of, or within one year of the presentation of a movement disorder typical of idiopathic Parkinson’s disease. The evolution of a movement disorder is not inevitable, as a proportion of patients dying with DLB have relative preservation of nigral dopaminergic neurones and consequently normal dopamine transporter imaging (Colloby *et al.*, 2012). It is hypothesised, but not demonstrated, that this group might show less severe adverse neuroleptic reactions.

1.4.2 Lewy Body related – Parkinson’s Disease Dementia - PDD

Parkinson’s disease dementia is diagnosed when the syndrome of dementia with Lewy Bodies described above evolves more than one year into typical idiopathic Parkinson’s disease (McKeith *et al.*, 2005). There is evolving consensus that DLB and PDD represent the same underlying disease, with the phenotypic presentation reflecting a

spectrum of relative predominance of Lewy body pathology in cortex and brainstem (McKeith and Burn, 2000, McKeith, 2009). Patients with Parkinson's disease have quadruple the relative risk of incident dementia of age matched controls (Hobson and Meara, 2004). Although severity and duration of Parkinsonian symptoms are risk factors in development of dementia, the strongest risk factor is the patient's current age, with these factors having a multiplicative effect (Levy *et al.*, 2002). Not all dementia developing in Parkinson's disease is PDD – Alzheimer's pathology is found in up to two thirds of patients with Lewy body disease (Barker *et al.*, 2002), and it is therefore perfectly reasonable to make concomitant diagnoses of idiopathic Parkinson's disease and either Alzheimer's disease or mixed dementia in the presence of a characteristic amnesic syndrome.

1.4.3 Progressive Supranuclear Palsy - PSP

Vignette

A 58 year old man is referred because he has begun to struggle at work. He is a maintenance engineer, and over the past year has been purchasing an increasing number of unnecessary instruments and gadgets. More recently he has made some inappropriate sexual comments and, when challenged, he has become aggressive. In clinic you note that he is inappropriately familiar and labile in his mood, quickly alternating between jocular and confrontation. His speech is adynamic, with palilogia at times (repetition of a single word with no words in between). The conversation is slow. He has some insight into his changed personality, describing himself as previously being a reserved individual but acknowledging that he now says whatever is on his mind even if it hurts others. He also admits to a sweet tooth, stating that he is eating more cakes and would eat a whole packet given the chance. On neurological examination the only abnormality is slowed saccades, especially in the vertical plane, but with no restriction in the extent of eye movements. He scores 70/100 on ACE-III, with predominant deficits in attention and verbal fluency (attention 9/18, memory 20/26, fluency 3/14, language 24/26, visuospatial 14/16). His MRI scan demonstrated mild global atrophy, with disproportionate volume loss in the midbrain (see Figure 1-7 for longitudinal imaging from a different patient). You follow him up, and by one year he has begun to suffer frequent unprovoked falls characterised by

postural instability and an inability to correct in time. A supranuclear gaze palsy has now emerged, with almost complete restriction of voluntary eye movements in the vertical plane. By two years, he is confined to a wheelchair and beginning to have significant difficulties with chewing and swallowing. He has severe axial rigidity, but tone in his limbs remains relatively normal.

Clinical Features

PSP is a highly protean disease, with only around a quarter of pathologically confirmed cases presenting initially with the classic Richardson's syndrome of falls, postural instability, cognitive dysfunction and abnormal eye movements (Respondek *et al.*, 2014). Previous diagnostic criteria (Litvan *et al.*, 1996) did not reflect this, and consequently suffered from limited sensitivity (Hughes *et al.*, 2002, Osaki *et al.*, 2004) at first presentation. To address this, the Movement Disorder Society have recently published new diagnostic criteria recognising early forms of the disease (Höglinger *et al.*, 2017). These criteria split 'variant' PSP into a new classification based on predominant symptomatology, recognising onsets with movement disorders, cerebellar disorders, primary lateral sclerosis, behavioural features and abnormal speech (Respondek and Höglinger, 2016). As illustrated in the vignette, it is important to remember that up to 20% of PSP initially presents with a frontal cognitive syndrome that is sometimes indistinguishable from bvFTD until the evolution of the characteristic movement disorder (Kaat *et al.*, 2007). A striking lack of verbal fluency is a frequent finding in PSP, and can be especially helpful in distinguishing PSP from idiopathic Parkinson's disease (Rittman *et al.*, 2013). Structural imaging can be helpful in the appropriate clinical context, with the characteristic findings of the 'Mickey Mouse' and 'Morning Glory' signs on axial section (Stamelou *et al.*, 2011) and 'Hummingbird' or 'Penguin' sign on sagittal section (Kato *et al.*, 2003, Massey *et al.*, 2012) (Figure 1-7) being formalised in measurement of the midbrain to pons ratio (Massey *et al.*, 2013).

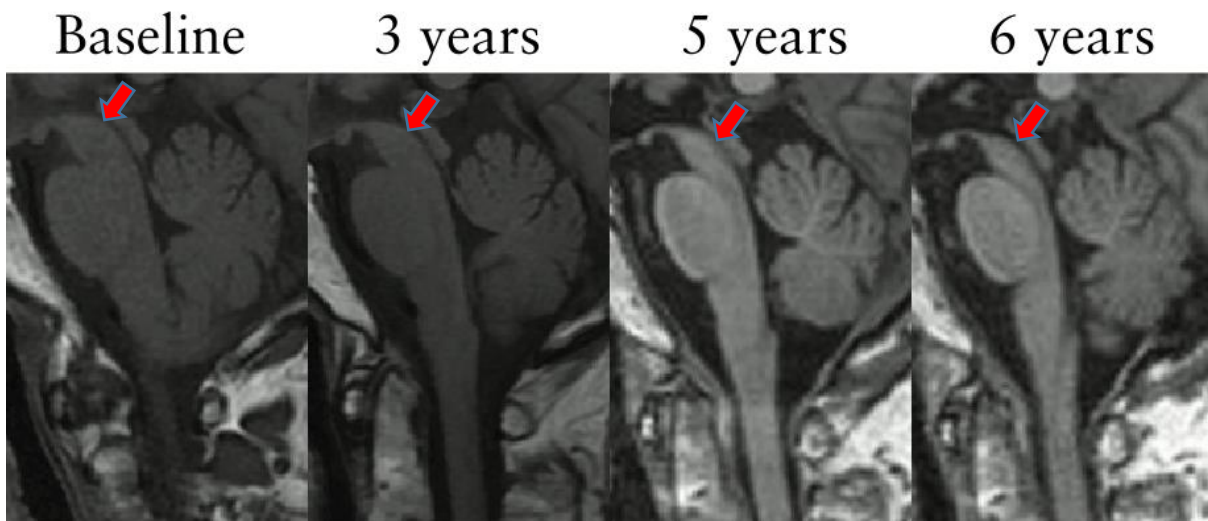


Figure 1-7 Serial structural MRI sections through the midbrain of a patient with PSP T1 weighted midline sagittal projection, whole brain aligned across scanning sessions. Progressive volume loss in the midbrain can be seen (arrows) resulting in a change from the normal ‘chaffinch’ appearance to the abnormal ‘hummingbird’ sign.

Aetiology

PSP is caused by an accumulation of tau in midbrain structures (periaqueductal grey matter, red nucleus, colliculi, substantia nigra), dentate nucleus of the cerebellum and basal ganglia (Ellison *et al.*, 2012). In the Richardson’s syndrome, Tau spreads to cortical brain regions only in advanced stages of the disease (Williams *et al.*, 2007). In contrast to Alzheimer’s disease, the pathological tau deposits are composed of straight filaments of predominantly 4R tau (Taniguchi-Watanabe *et al.*, 2016). The clinical variants of PSP share similar cellular and molecular features, but with differential distributions: i.e. presentation with focal cortical syndromes generally reflects greater cortical tau pathology, and with levodopa-responsive Parkinsonism reflects greater basal ganglia tau pathology (Dickson *et al.*, 2010). Even within the Richardson syndrome, the distribution of disease burden predicts the severity of separable symptom domains (Ghosh *et al.*, 2012).

1.4.4 Corticobasal Syndrome

Vignette

A 69 year-old professional organist attends clinic with a friend. For a year or more he has noticed difficulties with left sided coordination, which are especially noticeable when playing the organ. He finds that his left hand is less confident and his left foot is hesitant when trying to find the pedals. He has also had some difficulties with walking, and generally feels that his left leg is less responsive, but he has never fallen and has no true mobility problems. While he can still sight read 3 staves of music, he complains of difficulty integrating this into a single percept. In fact, he initially thought that his difficulties were with his eyes, but has now realised there is more going on. Despite this, he is still functioning at an extremely high level and even the choir master at his church has not noticed a problem with his playing. Outside of these domains he has very few problems. He has no REM sleep behaviour disorder. He has been hyposmic since a sinus washout 15 years ago but there has been no particular change. He describes normal forgetting such as going into rooms and forgetting the purpose, but also admits that he is a bit more reliant on his wife to remember appointments. On examination he has some left sided difficulties with both ideomotor and gesture copy praxis, and struggles with graphesthesia. Foot tapping is normal and there is no Parkinsonism. He scores 95/100 on ACE-III (attention 18/18, memory 23/26, fluency 13/14, language 25/26, visuospatial 16/16). Given the subtlety of his presentation, detailed neuropsychological assessment was requested, which revealed impairment across all cognitive domains, dominated by moderate memory and hand-sequencing deficits, with patchy performance across language, visuo-spatial and executive functioning tasks. His MRI demonstrated subtle biparietal atrophy, and a SPECT scan demonstrated neuronal hypometabolism in these areas (Figure 1-8). His dopamine transporter scan (DaT) demonstrated asymmetrically reduced tracer uptake (Figure 1-9).

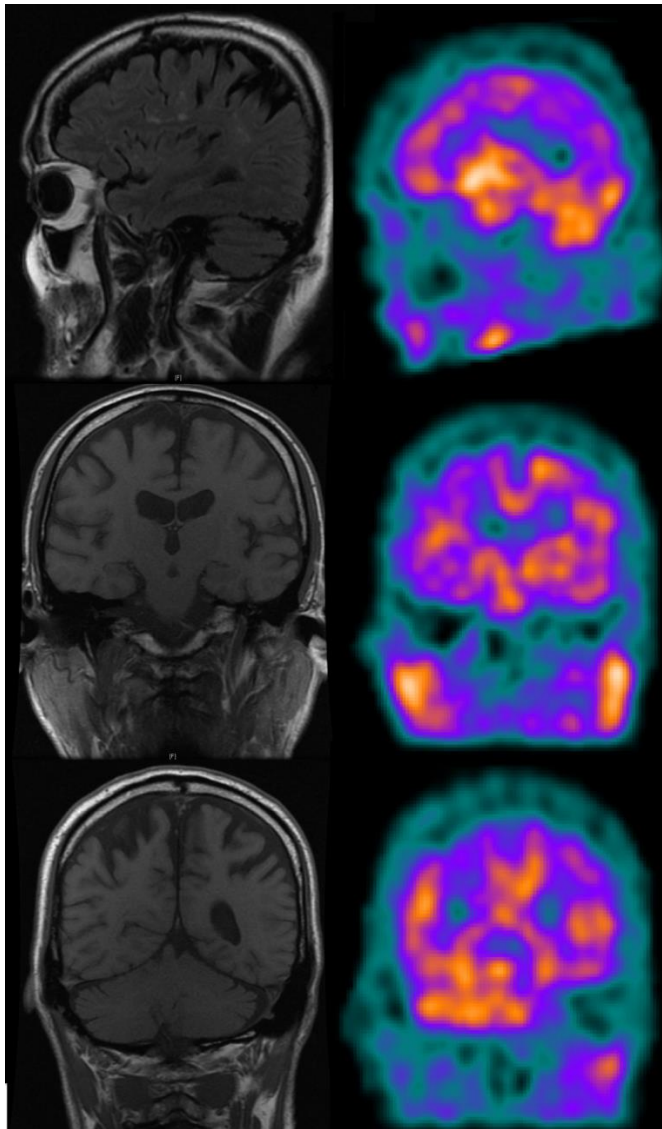


Figure 1-8 MRI and SPECT images for the Corticobasal Syndrome vignette.
Radiological convention. T1 weighted sagittal and coronal projections are shown, next to SPECT images from roughly the same projection. Moderate selective atrophy of parietal lobes can be seen, with a matching reduction in SPECT activity.

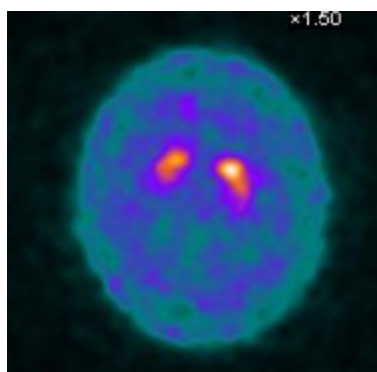


Figure 1-9 DaT scan summary image for the Corticobasal Syndrome vignette.
Radiological convention. Reduced transporter activity can be seen, more marked on the right (in keeping with his predominantly left sided symptoms).

Clinical features and aetiology

It is important to distinguish corticobasal syndrome (CBS), which is a clinical diagnosis based on the criteria below, and corticobasal degeneration (CBD), which is a histopathological diagnosis based on a cortical distribution of tau lesions together with ballooned achromatic neurones and astrocytic plaques (Dickson *et al.*, 2002). There are similarities between the histopathological appearances of CBD and PSP, and some regard them as being opposite ends of a spectrum of cortical vs brainstem involvement (Armstrong *et al.*, 2013). The predictive value of CBS for a post-mortem diagnosis of CBD is poor (Shelley *et al.*, 2009, Ling *et al.*, 2010), and only a small proportion of pathologically confirmed CBD displayed CBS in life (Ling *et al.*, 2010).

A ‘possible’ diagnosis of corticobasal syndrome can be made in the presence of at least one of the following: limb rigidity or akinesia; limb dystonia; limb myoclonus; and at least one of: orobuccal or limb apraxia; cortical sensory deficit; alien limb phenomena beyond simple levitation. The diagnosis is upgraded to ‘probable’ if the presentation is asymmetrical and at least two features from each category are present (Armstrong *et al.*, 2013).

1.4.5 Multiple System Atrophy - MSA

Dementia is rarer in MSA than in the other neurodegenerative movement disorders, perhaps reflecting a younger age of onset; severe cognitive decline at presentation should prompt a reconsideration of the diagnosis. Addenbrooke’s Cognitive Examination score is usually in the normal range, especially if verbal fluency is excluded (Cope *et al.*, 2014a). Characteristic cognitive deficits can, however, be revealed by detailed neuropsychological testing. Performance is impaired on tests of visuospatial and constructive function (Kawai *et al.*, 2008), executive function (Robbins *et al.*, 1992) and time perception (Cope *et al.*, 2014a), especially in the Parkinsonian phenotype (MSA-P). Focussed intervention for these cognitive deficits can be helpful, for example the impairment of ability to internally generate a regular beat (Grahn and Rowe, 2012) means that patients with MSA have particularly significant benefits from the use of a metronome to pace their gait (Thaut *et al.*, 1996) and prevent freezing (Okuma, 2006).

1.4.6 Huntington's Disease - HD

Vignette

A 56 year old lady presents to clinic with progressively worsening slurred speech and difficulty with co-ordinating fine hand movements. Tasks like doing buttons, combing her hair and doing up her bra have become very difficult. Her balance has become poorer, but she has not fallen. Her husband mentions that she has begun to cram food into her mouth, earning the nickname 'hamster' from family members. You notice choreiform movements, but the patient says that these are not bothersome. Her mood is low, she is visibly anxious, and she becomes tearful while discussing her difficulties. Her maternal grandmother was said to have died from an aggressive form of Parkinson's disease with dementia, while her mother died of cancer in her 40s. On examination you elicit a 'milkmaid grip', an unstable tandem gait, dysdiadochokinesis, symmetrical difficulties with Luria hand movements and finger tapping, impersistence of tongue protrusion and the initiation of saccades with a head thrust. ACE-III is 82/100 (attention 16/18, memory 19/26, fluency 7/14, language 24/26, visuospatial 14/16).

Clinical Features

While the chorea that characterises Huntington's disease is immediately obvious to the observer, it is usually the least disabling of the symptoms. The neuropsychiatric features of HD are significant, and can be broadly separated into dementia, executive dysfunction, and affective disorder.

It is a fallacy that the motor disorder develops in advance of the dementia in HD. Even in cohorts with early disease specifically selected for seemingly normal cognition, significant cognitive deficits are revealed even by screening neuropsychology (Cope *et al.*, 2014a). Detailed neuropsychological testing reveals difficulty on tests of executive function, planning, cognitive flexibility, abstract thought, action selection and time perception (Montoya *et al.*, 2006, Tabrizi *et al.*, 2009, Cope *et al.*, 2014a). The affective disorder in HD is heterogeneous. Anxiety and irritability are the most common features at presentation often in conjunction with depression, but aggression, compulsive or addictive behaviours and sometimes inappropriate happiness are observed (Montoya *et al.*, 2006, Klöppel *et al.*, 2010). Psychosis does occur but, in the

absence of genetic confirmation of HD, its presence should prompt consideration of the HD mimics DRPLA (dentatorubral-pallidoluysian atrophy) (Adachi *et al.*, 2001) and *C9ORF72* related neurodegeneration (Moss *et al.*, 2014). An autosomal dominant family history of a movement disorder or dementia is usually present but, as here, misdiagnosis in earlier generations is common. At the single subject level structural imaging can appear normal in early HD, with the most commonly observed abnormality being flattening of the caudate head (Lang, 1985). The diagnostic genetic test is for an expansion of CAG triplet repeats in the gene encoding developmental protein Huntingtin, which lies on the short arm of chromosome 4. Fewer than 26 repeats is normal, and more than 40 predicts full penetrance of HD (Walker, 2007).

1.4.7 Normal Pressure Hydrocephalus - NPH

NPH is characterised by an insidious onset of dementia with psychomotor retardation and an apraxic gait, often associated with urinary incontinence, in the presence of ventricular enlargement and normal CSF pressure (Adams *et al.*, 1965). It is a rare condition in younger individuals, but prevalence rises rapidly after the age of 80 (Jaraj *et al.*, 2014). Ventricular enlargement has classically been defined as a ratio of greater than 0.3 between the maximum axial width of the frontal horns of the lateral ventricles and maximal internal diameter of skull at the same level (the so-called Evans' index). This is a sensitive measure that lacks specificity, being present in 20% of elderly individuals (Jaraj *et al.*, 2014) and an even greater proportion of those with neurodegenerative disease (Missori *et al.*, 2016). Novel metrics such as the ratio between ventricular and intracranial volume (Toma *et al.*, 2011) and a reduction in the angle of the corpus callosum on coronal section (Ishii *et al.*, 2008) have increased specificity, and might have a role in case selection for neurosurgical management (Virhammar *et al.*, 2014). NPH is, in many cases, treatable by one of a number of neurosurgical procedures that provide constant drainage of CSF, but case selection remains difficult (Anderson, 1986, Freimann *et al.*, 2012). The gait disturbance commonly responds better than the cognitive impairment. At *post mortem*, NPH is strongly associated with demyelination of frontal regions in a pattern typical for small vessel disease (Akai *et al.*, 1987). It remains unclear whether this white matter

pathology causes the altered CSF dynamics or is a consequence of altered periventricular metabolism (Jeppsson *et al.*, 2013).

1.4.8 Niemann-Pick type C

Niemann-Pick disease types A and B are caused by autosomal recessive mutations in *SMPD1* (Schuchman *et al.*, 1992), which cause deficiency or absence of the lysosomal enzyme acid sphingomyelinase (Brady *et al.*, 1966). This leads to a lipid storage disorder characterised by an accumulation of sphingomyelin (Klenk, 1935). Niemann-Pick type A is a severe, neurodegenerative disease of infancy that leads to death in the first few years of life, while type B is milder, causing hepatosplenomegaly, growth retardation and lung dysfunction, but generally exhibiting no neurological features.

Niemann-Pick type C is caused by autosomal recessive mutations in *NPC1* (95% of cases) or *NPC2*, which respectively encode a large endosomal glycoprotein and a small, cholesterol-binding lysosomal protein (Ioannou, 2000). This leads to dysfunctional intracellular transport of cholesterol, leading to its sequestration in lysosomes and/or late endosomes. Age of onset is variable and, while approximately 50% of cases manifest by age 5, adult onset cases make up at least 20% of the total (Vanier and Millat, 2003). Mean age of onset in this subgroup is approximately 25 years, with the oldest reported case presenting at 54 (Vanier *et al.*, 1991). Presentation is protean, but a progressive dementia is present in approximately 60% of cases. Other clinical features include cerebellar ataxia (76%), vertical supranuclear ophthalmoplegia (75%), dysarthria, (63%), movement disorders (58%), splenomegaly (54%), psychiatric disorders (45%) and dysphagia (37%) (Sevin *et al.*, 2007). Epilepsy and cataplexy are more rarely reported, but the presence of gelastic cataplexy in the absence of a sleep disorder is highly suggestive of Niemann-Pick type C.

Psychiatric disturbance is the presenting feature in more than a third of cases, and can be manifest for a number of years before visceral or deep brain signs appear. Psychosis is the most common manifestation, but bipolar disorder, isolated depression and obsessive compulsive disorder have been reported (Sullivan *et al.*, 2005). While onset can be progressive, most patients present acutely and have relapsing and remitting disease, leading to an initial diagnosis of schizophrenia before additional clinical

features emerge. It is rare but recognised for psychiatric disturbance to complicate later disease in patients initially presenting with motor features.

About a quarter of patients present with isolated cognitive dysfunction. Again, the phenotype is variable, from mild dysexecutive features to aggressive global dementia. Interestingly, neurofibrillary tangles and beta amyloid plaques have been observed in relatively young patients with Niemann-Pick type C (Saito *et al.*, 2002), but their presence is the exception not the rule.

Diagnostic testing for Niemann-Pick type C is complex. Classically, the diagnostic cornerstone has been skin biopsy with fibroblast culture and the demonstration of impaired intracellular cholesterol transport with filipin staining (Patterson *et al.*, 2012). This test is strongly positive in about 80% of cases, and can also give a clear negative result, but about 20% of patients show only intermediate staining. In recent years this has been complemented by next generation sequencing of the NPC1 and NPC2 genes, but novel mutations of uncertain significance are commonly found and interpretation can be difficult. Simpler tests, based on mass spectroscopy of plasma biomarkers, have recently become available; validation studies are ongoing, but initial evidence suggests that these tests might prove sensitive but not specific (Vanier *et al.*, 2016).

Disease modification can be achieved with Miglustat, a small molecule inhibitor of glucosylceramide synthase (Patterson *et al.*, 2007) that has been demonstrated to reduce the rate of disease progression. Current clinical consensus is that all patients with neurological, psychiatric or cognitive manifestations should be offered this medication. The primary side effects are gastrointestinal, and can be partially ameliorated with dietary and anti-propulsive strategies (Belmatoug *et al.*, 2011). There is also a significant role for symptomatic therapy to treat seizures, cataplexy, dystonia, psychiatric disturbance and sleep disorders.

1.4.9 Spinocerebellar Ataxia - SCA

SCA is a collection of more than 60 genetic neurodegenerative diseases that are united by their primary manifestation with ataxia and (usually) cerebellar degeneration, but with different associated features. Most are autosomal dominant with adult onset, but X-linked and childhood onset forms are recognised (Stephen *et al.*, 2016). The SCAs

are assigned a number according to the date of discovery of the associated gene, and the classification is consequently confusing and difficult to remember (see Worth, 2004 for a clinically focussed review). While even those disorders such as SCA-6 thought to result in ‘pure’ cerebellar dysfunction display a subtle ‘cerebellar cognitive phenotype’ of impairments in cognitive flexibility, response inhibition, verbal reasoning (Cooper *et al.*, 2010) and time interval perception (Grube *et al.*, 2010), many of the SCAs display a broader cognitive phenotype. Cognitive impairment, hallucinations or depression are especially common as an early or presenting feature in SCA-17, which is caused by a triplet repeat expansion in *TBP* (Rolfs *et al.*, 2003).

1.5 Cognitive impairments that may or may not progress

In this section I introduce the concepts of mild cognitive impairment and subjective cognitive impairment. These diagnostic labels are agnostic as to the underlying aetiology of the impairment, and as such they may or may not progress. I then conclude the chapter with brief descriptions of two conditions that can present to the cognitive clinic but that do not reflect neurodegenerative disease; transient epileptic amnesia and transient global amnesia.

1.5.1 Mild Cognitive Impairment

Vignette

A 62 year old mathematics teacher presents to clinic alone. She complains that her memory is generally poorer than it was, and she is finding it especially difficult to learn the names of children in her class. She is not struggling with the mathematical aspect of their work, but has found it difficult to adapt to curriculum changes and new information technology. Her mood is stable, and she denies any significant stressors. ACE-III is 89 (attention 16/18, memory 20/26, fluency 13/14, language 26/26, visuospatial 16/16).

Clinical Features

The primary differentiation between dementia and mild cognitive impairment (MCI) is one of degree. Generally speaking, a diagnosis of MCI is made when deficits are

insufficiently severe to interfere with function at work or in daily activities, but this is not a firm criterion. The distinction is a sensitive clinical judgment that requires a skilled clinician to make an holistic assessment of the patient from primary and secondary sources. In the vignette above, the patient's work function was affected, but a similar level of difficulty might not have had such a noticeable effect on a different profession or in one retired. Clearly it is not intellectually satisfying for the same constellation of symptoms and signs to lead to different diagnoses dependent solely on work status. Another factor that must weigh on this decision is the level of certainty that one is dealing with a progressive condition. A diagnosis of dementia carries with it the inevitable long-term implications of a neurodegenerative condition; the same is not necessarily true of MCI, from which only a proportion of individuals will progress. Some clinicians might find it appropriate in mild cases to make an initial diagnosis of MCI pending imaging and longitudinal neuropsychological assessment, while others prefer to refrain from making any diagnosis until progression has been assessed – neither approach is incorrect, and this decision should be made on an individual basis in a patient-centred manner.

Management

Once structural and significant vascular pathology has been excluded with structural imaging, the most important management step in MCI is to closely monitor for the emergence of a dementia requiring medical or social intervention. It is possible to subclassify mild cognitive impairment by the cognitive domain or domains affected. It has been proposed by some that those with a predominantly amnesic phenotype are more likely to progress to Alzheimer's disease, and that this group should be further investigated with biomarkers of amyloid deposition and neuronal injury such as CSF tau/phosphorylated tau and A β 42, PET amyloid imaging (PiB or Florbetapir), or perfusion imaging with FDG-PET or SPECT (Albert *et al.*, 2011). Others have gone further, suggesting that amnesic MCI with supportive biomarkers should be termed prodromal Alzheimer's disease (Dubois and Albert, 2004). While of undoubted utility in research, where the current focus of therapeutic trials is in early disease, this approach is clinically available in a limited number of centres and is not generally advocated by the UK National Institute for Clinical Excellence (NICE and SCIE, 2006

(updated March 2016)). Clearly the emergence of disease modifying therapeutics will change the balance of this decision.

1.5.2 Subjective Cognitive Impairment

Vignette

A 52 year old gentleman attends clinic alone. He left school at 16 with three CSEs, and became a planning officer at a telecoms company, where he undertook an apprenticeship and several postgraduate qualifications. He describes several years of poor anterograde memory. He has developed elaborate coping mechanisms such as littering his house with post-it notes and 'quick guides' for new computer programs. He reports poor day-to-day memory, but is unable to give concrete examples of this. He presents due to a perceived worsening in symptoms. There have been no concerns from his partner or employer about performance. He reports anxiety at work, but ascribes this to his perceived performance difficulties; there is no overt mood disorder. Neurological examination is normal. ACE-III is 96 (attention 18/18, memory 23/26, fluency 13/14, language 26/26, visuospatial 16/16). Detailed neuropsychological assessment is undertaken, which reveals normal performance on tests of verbal comprehension, perceptual reasoning, executive function, processing speed and language, but catastrophic failure on tests of memory. The pattern of failure is a lack of immediate recall of both a story and the Rey complex figure, with consequent impairment of delayed recall. The neuropsychologist reports that he displayed significant anxiety during testing. Screening blood tests were normal, as was structural brain scanning.

Clinical Features

A subjective cognitive impairment is defined as the presence of cognitive symptoms in the absence of objective evidence of cognitive impairment or psychopathy (Reisberg *et al.*, 2010, Stewart, 2012). It is characterised by a seeming inconsistency between disability and measureable deficit. While it has traditionally been viewed as a syndrome of hyper-vigilance, there is now converging evidence that at the population level it is a predictor of risk of future decline. Those with subjective cognitive impairment do show small differences from controls on neuropsychology and imaging at the group level

(Hohman *et al.*, 2011), and subjective cognitive impairment sufferers over the age of 65 have a hazard ratio of 2.3 for acquiring dementia within four years (Waldorff *et al.*, 2012). Nonetheless, the appropriate clinical management is usually reassurance and practical suggestions such as list keeping and sleep hygiene. Where it is evident, anxiety should be addressed.

1.5.3 Transient Global Amnesia - TGA

TGA is a syndrome characterised by an isolated temporary amnesia for a period of a few hours (Fisher, 1958). During an attack autobiographical memory is intact, but patients are frequently disoriented in time, place and person, and ask repetitive questions on these topics (Bolwig, 1968). After an attack, there is a total loss of episodic memory for the period of confusion and, usually, a period of time beforehand. The aetiology is unknown. It has been observed that vascular risk factors are over-represented in patients with TGA compared to controls (Shuping *et al.*, 1980a), but under-represented compared to patients with TIA (Melo *et al.*, 1992). Some individuals display diffusion-weighted imaging changes in medial temporal regions during and after an attack, but the evidence for an ischaemic cause is somewhat conflicted (see (Huber *et al.*, 2002) for a review). The syndrome is usually monophasic, with approximately 6% of patients experiencing a second attack (Melo *et al.*, 1992). Recurrent attacks should prompt a search for a structural (Shuping *et al.*, 1980b) or embolic (Shuping *et al.*, 1980a) cause.

1.5.4 Transient Epileptic Amnesia - TEA

TEA is a syndrome of recurrent, brief attacks of amnesia due to focal temporal lobe seizures. It characteristically occurs on waking, and is most common in middle-age (Zeman and Butler, 2010). Like TGA, repetitive questioning is common, but recurrent attacks are characteristic and amnesia for the attack is sometimes less dense (Zeman *et al.*, 1998). Important distinguishing symptoms are a loss of remote autobiographical knowledge (Butler *et al.*, 2007) and accelerated long-term forgetting (Muhlert *et al.*, 2010). The latter is a fascinating symptom, in which memories are initially well encoded but fade more rapidly than normal over subsequent days. The wonderfully

eccentric defining study of this phenomenon involved patients and their spouses or friends visiting the stately homes of Britain while wearing video cameras. When quizzed on the same day about what they had seen, patients performed as well as controls, but recall across a number of modalities (images, thoughts, events and sensory information) was much poorer after a delay of days to weeks. While the seizures, and consequently the discrete amnesic attacks, often respond well to small doses of anticonvulsant medication, accelerated long-term forgetting frequently persists (Butler, 2006).

1.6 Challenges and opportunities

The ultimate goal of dementia research is to prevent or reverse deteriorations in cognitive function, early in the evolution of disease. The diverse array of clinical syndromes that comprise the dementias, and their differing underlying causative pathologies, represent a significant challenge to this goal. Therefore, the original research I outline in this thesis assesses specific neurodegenerative diseases as demonstrator conditions, informing us not only about the conditions themselves but allowing a more general insight into what might be the ultimate similarities and differences in approach between successful treatments for the conditions reviewed in this introductory chapter.

Neurodegenerative diseases are united by early effects in synaptic loss, reduced plasticity and aberrant connectivity that precede cell death and atrophy. However, patterns of connectivity in the healthy brain have strong influences on the vulnerability of brain regions to the accrual of neuropathology. It is therefore often difficult to dissociate the *causes* of neurodegeneration from its *consequences*. In Chapter 2, I address this question in two diseases both characterised by abnormal intracellular deposits of hyper-phosphorylated filamentous tau inclusions but with very different distributions. I assess three competing hypotheses of neuronal vulnerability to explain why tau in Alzheimer's disease impacts large-scale cortical connectivity networks but, by contrast, tau in PSP is confined to midbrain and deep brain nuclei in early to mid-stage disease. Understanding the variation in tau expression is an essential step to

developing appropriate treatments to prevent its accrual, and hopefully reduce its harmful effects, in differing clinical syndromes.

As well as understanding the pathogenesis of neurodegeneration, the development and evaluation of therapeutic interventions at economically viable timescales will require validated models of the neurocognitive code and the tools to assess it in patients. In chapter 2 I assess the effects of regional neurodegeneration on the observable functional connectivity of the brain in terms of correlated activity. In chapter 3, I go beyond this by directly observing the consequences of regional neurodegeneration on brain activity in unaffected regions. To do this I use the frontal aphasic form of frontotemporal dementia (nfvPPA) as demonstrator condition, because of its stereotyped pattern of neurodegeneration, the psychophysical precision of language as a probe, and the fragility of human language networks to synaptic disruption. By characterising the neurophysiology of this disease using magnetoencephalography (MEG), and explaining patients' behaviour with Bayesian computational models, I provide causal evidence about the mechanisms of normal human higher cognitive functioning and neural information coding. This leads on to chapter 4, in which I undertake a detailed psychophysical examination of the brain basis of agrammatism in nfvPPA, as a model of higher order cognitive disruption in neurodegeneration, and discuss the potential utility of therapeutic approaches to symptom rehabilitation.

Overall, this use of demonstrator conditions within the broader clinical context of dementia allows for the use of systems neuroscience as a translational bridge between the molecular biology of dementia and targeted clinical trials. Further, it improves our understanding of normative brain networks through the study of focal forms of neurodegeneration, as the basis for new frameworks for cognitive deficits in neurodegenerative disease. Together, this approach holds the promise of translating recent fantastic progress in understanding the cellular mechanisms of neurodegeneration, and success in rescuing animal models, to the development of effective disease modifying therapies for dementia in humans.

1.7 Chapter Summary:

The dementias are persistent or progressive disorders affecting more than one cognitive domain that interfere with an individual's ability to function at work or home, and represent a decline from a previous level of function. The assessment of dementias is a multi-disciplinary pursuit, with clinical and diagnostic assessments undertaken by psychiatrists, psychologists, neurologists, geriatricians and, increasingly, specialist nurses, occupational therapists and other allied health professionals.

The dementias can be classified either by their cognitive phenotype, or by their aetiological origin, and there is not necessarily a linear mapping between the two. This chapter outlines the neurodegenerative causes of cognitive impairment in terms of their clinical features, epidemiology and aetiology. For each I provide a brief discussion of management and prognosis, focussing on the differences between the syndromes rather than providing a general approach to the patient with a memory complaint or neurodegenerative cognitive impairment.

The intention of this introductory chapter is to set the scene for the experimental chapters that follow, in which I undertake in-depth studies of particular aspects of the physiology of dementia. For this, I will use model diseases that allow controlled experiment and robust comparison. These diseases serve as examples of how cellular and molecular pathologies give rise to aberrant physiological function across widespread brain networks, which in turn leads to deficits in core cognitive systems, resulting in the complex symptomatology of individual dementia syndromes.

Chapter 2: Tau burden and the functional connectome in Alzheimer's disease and progressive supranuclear palsy

2.1 Preface

In this experimental chapter I assess the relationship between functional connectivity and *in vivo* tau burden by combining graph theoretical analyses of resting state functional MR imaging and PET imaging using the ligand AV-1451. I do this in two model diseases, Alzheimer's disease and Progressive Supranuclear Palsy, which represent a contrast between predominantly 'cortical' and 'subcortical' burdens of tau neuropathology.

A paper based on this chapter has been published in *Brain* with myself as first author (Cope *et al.*, 2018). The original data on which the analyses in this chapter were based were collected by Ms Patricia Vazquez-Rodriguez, Dr Richard Bevan-Jones and Mr Robert Arnold; patients were scanned and assessed as part of the NIMROD study (Bevan-Jones *et al.*, 2017b), which was conceptualised by Prof John O'Brien and Prof James Rowe. The neuroimaging data were pre-processed by Mr Robin Borchert and Mr P Simon Jones. I am particularly grateful to Dr Tim Rittman for introducing me to graph metrics, and for using the software he developed during his own PhD to derive the graph theoretical measures from the functional connectivity data (Maybrain: github.com/rittman/maybrain). I am grateful to Dr Luca Passamonti and Dr Deniz Vatansever for helpful comments on interpretation, and to Dr Kieren Allinson for his expertise on *post mortem* neuropathological distribution. Finally, I am grateful to three anonymous reviewers at *Brain*, who suggested the useful addition of several additional graph measures. I designed the analysis strategy, performed the analyses, constructed all of the figures, and wrote the text with comments from all of those listed above.

2.2 Introduction

Alzheimer's disease and Progressive Supranuclear Palsy (PSP) are both characterised by intracellular neurofibrillary lesions containing hyper-phosphorylated filamentous tau inclusions (Goedert and Spillantini, 2006). However, the diseases differ in: 1) the distribution of these tau inclusions; 2) the balance of expression of tau isoforms; and 3) the ultrastructure of tau filaments. Here, I test the impact of these differences in tau pathology on the reorganisation of large-scale functional brain connectivity architecture.

Alzheimer's disease is characterised by widespread extracellular deposition of amyloid- β and paired helical filaments of tau with three (3R) and four (4R) repeats in the microtubule-binding domain (Sisodia *et al.*, 1990, Liu *et al.*, 2001). In Alzheimer's disease, these pathological proteins arise early in the transentorhinal cortex, from where they spread to limbic regions, followed by inferior frontal and parietal cortex (Braak and Braak, 1991, Braak and Braak, 1995). Although tau and amyloid- β have complex and synergistic effects (Nisbet *et al.*, 2015), there is converging evidence that tau mediates direct toxic effects on neurons and synaptic plasticity (Ballatore *et al.*, 2007, Roberson *et al.*, 2007, Ittner and Götz, 2011, Myeku *et al.*, 2016) and correlates with hypo-metabolism and symptomatology in Alzheimer's disease (Lehmann *et al.*, 2013, Ossenkoppele *et al.*, 2015, Ossenkoppele *et al.*, 2016). By contrast, pathological tau deposits in PSP are composed of straight filaments of predominantly 4R tau (Taniguchi-Watanabe *et al.*, 2016). This is most prominent in midbrain and deep brain nuclei early in the course of the Richardson's syndrome variant of PSP, spreading to cortical regions in advanced stages of the disease (Williams *et al.*, 2007).

To estimate the burden of tau pathology *in vivo*, PET ligands have been developed, including [^{18}F]AV-1451 (Chien *et al.*, 2013, Xia *et al.*, 2013, Ossenkoppele *et al.*, 2015, Ossenkoppele *et al.*, 2016). While there has been significant debate about the specificity of this ligand for tau, especially in the non-Alzheimer's dementias (Bevan-Jones *et al.*, 2017a, Xia and Dickerson, 2017), the distribution of [^{18}F]AV-1451

binding recapitulates Braak staging in Alzheimer's disease (Schwarz *et al.*, 2016) and correlates with *post-mortem* neuropathology in primary tauopathies (Smith *et al.*, 2016). [¹⁸F]AV-1451 binding has been shown to correlate with cognitive performance in Alzheimer's disease (Johnson *et al.*, 2016) and healthy older adults (Schöll *et al.*, 2016) more robustly than quantitative beta amyloid imaging (Brier *et al.*, 2016). The [¹⁸F]AV-1451 ligand also effectively distinguishes between AD and PSP cases on the basis of both the intensity and regional distribution of its binding potential (BP_{ND}) (Passamonti *et al.*, 2017).

In many neurodegenerative disorders, neuropathology and atrophy are most marked in those brain regions that are densely connected, both at the structural (Crossley *et al.*, 2014) and functional level (Dai *et al.*, 2014). In graph-theoretical terms, these densely connected regions are usually referred as 'hubs' (Buckner *et al.*, 2009). There are a number of hypotheses as to why hubs are vulnerable to neurodegeneration. First, pathological proteins may propagate trans-neuronally, in a prion-like manner (Prusiner, 1984, Baker *et al.*, 1994, Goedert, 2015) such that highly connected regions are more likely to receive pathology from 'seed' regions affected in early stages of the disease (Zhou *et al.*, 2012), leading to neurodegeneration that mirrors structural and functional brain connectivity (Raj *et al.*, 2012, Abdelnour *et al.*, 2014, Raj *et al.*, 2015). Alternatively, hubs might be selectively vulnerable to a given level of pathology, due to a lack of local trophic factors (Appel, 1981), higher metabolic demands (Saxena and Caroni, 2011, de Haan *et al.*, 2012), or differential gene expression (Rittman *et al.*, 2016).

These alternate hypotheses lead to different predictions about the relationship between tau burden and connectivity. The trans-neuronal spread hypothesis predicts that regions that are more strongly interconnected would accrue more tau pathology. This would manifest as higher tau burden in nodes with larger weighted degree, which is a measure of the number and strength of functional connections involving each node. In contrast, if hubs are vulnerable to tau accumulation because of increased metabolic demand this might manifest as a positive relationship between tau burden and

participation coefficient, which is a measure of the proportion of a node's connections that are with other neural communities, and is the graph metric that is most closely correlated with metabolic activity (Chennu *et al.*, 2017). Finally, if trophic support is an important factor in tau accumulation, this might manifest as a negative relationship between tau burden and clustering coefficient; nodes with less tightly clustered connectivity patterns might have more vulnerable trophic supply.

Here I go beyond previous associative studies to examine, in the same subjects, the relationship between *in vivo* tau burden, as measured by the PET ligand [¹⁸F]AV-1451 BP_{ND}, and functional connectivity, as summarised by graph theoretic measures based on resting state (task-free) functional magnetic resonance imaging (fMRI) (Sporns *et al.*, 2004, Bullmore and Sporns, 2009, Rubinov and Sporns, 2010). I test the following linked hypotheses:

- 1) Brain regions that are normally more densely interconnected accrue more tau pathology.
- 2) In Alzheimer's disease, where tau accumulation is predominantly cortical, the functional consequence is that affected nodes become more weakly connected and local efficiency of information transfer is reduced.
- 3) In PSP-Richardson's syndrome, where neurodegeneration associated with tau accumulation is most severe in midbrain and basal ganglia, the functional consequence of disrupted cortico-subcortical and cortico-brainstem interactions (Gardner *et al.*, 2013) is that indirect cortico-cortical connections become stronger.

2.3 Methods

2.3.1 Participants

All patients had mental capacity to take part in the study and provided informed consent. Study procedures were approved by the National Research Ethics Service. I recruited 17 patients with Alzheimer's disease, as evidenced by either a clinical diagnosis of probable Alzheimer's dementia according to consensus criteria ($n = 10$)

(McKhann *et al.*, 2011), or a clinical diagnosis of mild cognitive impairment (MCI) and a positive amyloid PET scan ($n = 7$) (Klunk *et al.*, 2004, Okello *et al.*, 2009). Patients with MCI and evidence of beta amyloid were included to ensure the largest possible spread in tau burden within the Alzheimer’s disease group. I also recruited 17 patients with PSP-Richardson’s syndrome by 1996 criteria (Litvan *et al.*, 1996). Retrospective case review confirmed that all PSP subjects also met the revised 2017 criteria for PSP-RS (Höglinger *et al.*, 2017). 12 age matched controls were also examined. Participant demographics are shown in Table 2-1 and detailed neuropsychological test results for each subject are shown in Table 2-2.

Group	Number	Age	Years of Education	MMSE	ACE-R	PSP-RS
AD	17	71 (9)	14 (3)	25 (4)	72 (14)	-
PSP	17	69 (6)	12 (2)	27 (4)	83 (14)	41 (14)
Controls	12	67 (8)	16 (2)	29 (1)	96 (3)	-

Table 2-1 Participant demographics summary

Mean (s.d.). MMSE – Mini-mental state examination. ACE-R – Addenbrooke’s Cognitive Examination, Revised Edition. PSP-RS – Progressive Supranuclear Palsy Rating Scale.

Group	ACE-R	MMSE	BADLS	CAF	CBI-R	GDS	HADS	INECO	NPI	PAL	PPT	RAVLT	SRT	UPDRS
AD	73	24	6	2	25	0	3	16	12	49	43	25	374	4
AD	57	21	3	2	38	0	6	19	5	7	49	11	311	0
AD	50	17	11	2	94	2	3	12	51	71	50	11	499	1
AD	41	15	16	1	59	5	6	2	22	N/A	N/A	14	748	0
AD	82	26	5	0	38	1	4	18	11	11	50	33	236	0
AD	75	25	10	7	66	9	15	9	26	14	48	8	335	0
AD	69	22	1	N/A	20	2	4	9	10	64	44	19	241	0
AD	70	27	17	5	93	1	1	9	32	40	48	15	305	13
AD	53	19	18	3	52	6	11	9	21	75	42	29	472	2
AD	60	22	10	0	39	0	4	12	6	49	49	19	417	27
AD	80	27	8	0	28	3	10	21	14	45	51	26	343	0
AD	85	28	2	2	18	1	2	15	0	48	50	30	216	0
AD	84	26	0	0	7	3	17	18.5	0	46	51	26	235	0
AD	83	26	0	0	10	0	0	25	0	3	51	35	346	1
AD	72	26	0	0	50	2	6	15	4	13	42	20	365	1
AD	77	23	2	4	18	0	8	5	0	45	47	18	363	2

AD	87	29	0	0	7	1	2	15	0	26	52	31	278	0
PSP	96	30	2	0	16	12	10	16	13	16	51	N/A	359	46
PSP	95	27	22	1	24	4	8	17.5	8	1	51	N/A	326	33
PSP	88	28	28	1	43	3	7	18	6	N/A	N/A	N/A	500	69
PSP	70	24	15	0	18	7	17	12	0	N/A	N/A	N/A	546	21
PSP	75	27	24	6	38	2	5	16	0	N/A	48	N/A	517	N/A
PSP	83	27	8	3	32	7	18	18	8	24	46	N/A	297	32
PSP	36	16	51	5	81	3	13	N/A	48	N/A	N/A	N/A	N/A	69
PSP	83	27	36	4	83	14	16	18	19	N/A	50	N/A	702	29
PSP	93	30	3	2	7	3	4	15	0	8	50	N/A	594	22
PSP	72	24	26	8	86	5	15	9	32	2	48	N/A	323	39
PSP	80	26	31	2	48	10	11	12	19	12	41	N/A	499	23
PSP	88	30	12	2	41	4	3	20.5	25	3	52	N/A	270	35
PSP	89	27	9	7	32	1	5	17	15	1	49	N/A	244	31
PSP	87	27	25	3	81	6	7	20	44	19	49	N/A	487	54
PSP	77	25	12	3	103	3	13	15	28	32	52	N/A	430	43
PSP	93	29	5	0	1	1	9	22	5	20	50	N/A	361	29
PSP	92	29	14	1	46	11	9	16	37	5	52	N/A	477	35
Control	97	30	N/A	N/A	N/A	0	5	26.5	N/A	0	52	58	236	0
Control	89	29	N/A	N/A	N/A	0	3	21.5	N/A	5	50	44	228	0
Control	98	30	N/A	N/A	N/A	1	6	24	N/A	2	52	45	322	0
Control	97	30	N/A	N/A	N/A	1	9	27	N/A	11	50	35	259	0
Control	98	30	N/A	N/A	N/A	3	4	21	N/A	4	52	33	233	0
Control	93	30	N/A	N/A	N/A	10	28	23.5	N/A	2	52	43	254	0
Control	98	28	N/A	N/A	N/A	5	21	27	N/A	6	50	50	256	N/A
Control	96	29	N/A	N/A	N/A	1	3	29	N/A	0	52	42	207	0
Control	99	30	N/A	N/A	N/A	2	8	26	N/A	6	51	56	232	0
Control	97	30	N/A	N/A	N/A	0	4	22.5	N/A	0	51	45	237	N/A
Control	95	29	N/A	N/A	N/A	0	2	23	N/A	4	52	45	238	N/A
Control	90	28	N/A	N/A	N/A	3	11	21.5	N/A	3	52	39	252	N/A

Table 2-2 Detailed neuropsychological profiles of individual study participants.

N/A = data not available. ACE-R: Addenbrooke's Cognitive Examination, Revised; MMSE: Mini Mental State Examination; BADLS: Bristol Activities of Daily Living; CAF: Clinical Assessment of Fluctuation; CBI-R: Cambridge Behavioural Inventory Revised; GDR: Geriatric Depression Scale; HADS: Hospital Anxiety and Depression Scale Combined Score; INECO: Institute of Cognitive Neurology Frontal Screening; NPI: Neuropsychiatric Inventory; PAL: Paired Associates Learning; PPT: Pyramids and Palm Trees; RAVLT: Rey Auditory Verbal Learning; SRT: Simple Reaction Time (mean); UPDRS: Unified Parkinson's Disease Rating Scale.

2.3.2 Study Procedures

This study formed part of the NIMROD (Neuroimaging of Inflammation in Memory and Related Other Disorders) project, for which the trial protocol containing general methods has been previously published (Bevan-Jones *et al.*, 2017b).

All participants underwent the Addenbrooke's Cognitive Examination-Revised (ACE-R), eleven minutes of resting state functional MRI at 3 Tesla, and [¹⁸F]AV-1451 PET imaging. Participants with PSP were also examined according to the PSP-Rating Scale (Golbe and Ohman-Strickland, 2007). Those with a clinical diagnosis of MCI had [¹¹C] PiB PET imaging on a separate visit – only those with increased uptake indicative of underlying Alzheimer's pathology are reported here.

2.3.3 MRI data acquisition and pre-processing

MR imaging was performed at the Wolfson Brain Imaging Centre, University of Cambridge, UK using a 3T Siemens Magnetom Tim Trio scanner with a Siemens 32-channel phased-array head coil (Siemens Healthcare, Erlangen, Germany).

A T1-weighted magnetization-prepared rapid gradient-echo (MPRAGE) image was acquired with repetition time (TR) = 2300ms, echo time (TE) = 2.98ms, matrix = 256x240, in-plane resolution of 1x1mm, 176 slices of 1mm thickness, inversion time = 900ms and flip angle = 9°.

Eyes-closed resting state (task-free) multi-echo functional imaging was carried out for eleven minutes. A total of 269 EPI image volumes were acquired with TR = 2430ms, TEs = 13.00, 30.55, and 48.10ms, matrix = 64x64, in-plane resolution of 3.75x3.75mm, 34 slices of 3.8mm thickness with an interslice gap of 0.38mm, GRAPPA parallel imaging with an acceleration factor of 2 and bandwidth = 2368 Hz/pixel. The first six volumes were discarded to eliminate saturation effects and achieve steady state magnetization. Preprocessing employed the ME-ICA pipeline

(<https://wiki.cam.ac.uk/bmuwiki/MEICA>) (Kundu *et al.*, 2012, Kundu *et al.*, 2013), which uses independent component analysis to classify BOLD and non-BOLD signals based on the identification of linearly dependent and independent echo time (TE) dependent components. This provides an optimal approach to correct for movement-related and non-neuronal signals, and is therefore particularly well suited to our study, in which systematic differences in movement or head position might reasonably have been expected between patient groups. In fact, perhaps surprisingly, such differences were not observed (Figure 2-1) – between group ANOVAs demonstrated no significant differences between groups in terms of frame displacement before ($p = 0.88$) or after ($p = 0.42$) ME-ICA pre-processing, nor in terms of DVARS (Power *et al.*, 2012) before ($p = 0.89$) or after ($p = 0.67$) ME-ICA pre-processing. Note that both movement parameters were approximately an order of magnitude lower after ME-ICA pre-processing.

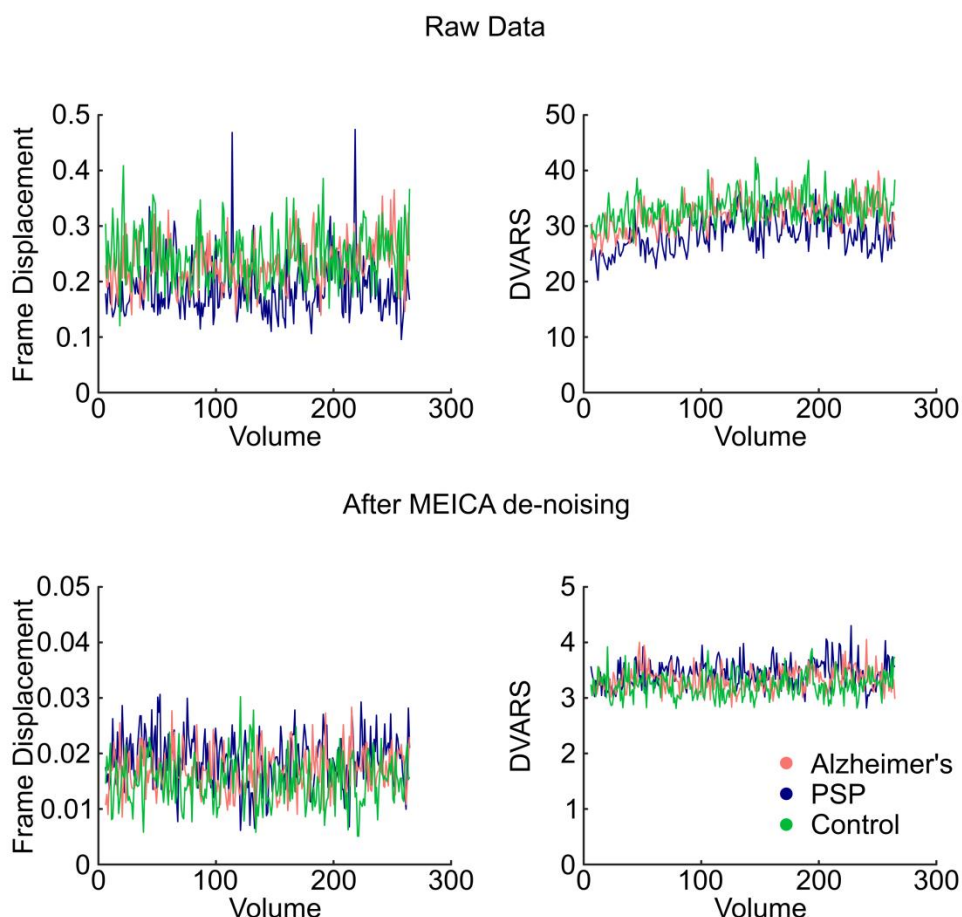


Figure 2-1 Movement parameters.

Movement quantified by frame displacement and DVARS (D referring to temporal derivative of timecourses, VARS referring to RMS variance over voxels), before and

after MEICA de-noising. No significant differences were demonstrated between groups.

The MPRAGE images were processed into the standard space using DARTEL (Ashburner, 2007), producing a study specific template in stereotactic space. Each fMRI series mean image was co-registered to the corresponding MPRAGE image. The whole fMRI series was warped to the template space using the DARTEL flow fields.

In order to perform a whole brain graph-theoretical analysis that included the brainstem, cerebellum and subcortical structures, the Harvard-Oxford Cortical atlas and Harvard-Oxford subcortical atlas, each thresholded at 25%, were combined. Additionally, a Freesurfer 6 brainstem parcellation of the MNI152 (2009 asymmetric) brain together with remaining Ventral DC completed the whole brain labelling. This atlas was sub-parcellated into 598 regions of approximately equal volume (mean 1.995, SD 0.323ml) such that each sub-parcel could be uniquely identified with an atlas region. The MNI-space parcellation was matched to the group standard space using inverse deformations following application of the 'Population to ICBM Registration' SPM function to the group template, with nearest neighbour interpolation.

The BOLD time series for each node was extracted using the CONN functional connectivity toolbox (Whitfield-Gabrieli and Nieto-Castanon, 2012). Between-node association matrices were generated, and then z-transformed for further analysis.

2.3.4 Functional Connectivity Assessment

Graph theoretical analysis was used to investigate the global and local characteristics of brain networks. These metrics were calculated in python using the Maybrain software (github.com/ritman/maybrain) and networkx (version 1.11). Reported metrics were calculated in each subject at absolute network density thresholds of 1-10% in 1% increments using a minimum spanning tree to ensure complete connectivity of the graph (Alexander-Bloch *et al.*, 2010). Primary statistical analysis was performed at an intermediate density of 6%, with confirmatory analyses separately performed at all other densities. Weighted degree and participation coefficient were analysed in their

raw forms, and all other metrics were dissociated from variation in degree by binarisation after thresholding and normalisation against 1000 random graphs with the same number of connections at each node.

The graph metrics assessed were:

- i) **Weighted degree:** the number and strength of functional connections involving each node.
- ii) **Weighted participation coefficient:** the proportion of a node's functional connectivity that involves other nodes that are not part of its own community structure, as defined by the Louvain community detection algorithm. Nodes with high degree and low participation coefficient are 'provincial hubs' (i.e. display strong connectivity only within their own community), while those with high participation coefficient are connector nodes (Joyce *et al.*, 2010).
- iii) **Betweenness centrality:** the number of shortest paths between any other two nodes that pass through the node of interest. Nodes that are important for the transfer of information between other nodes have high betweenness centrality.
- iv) **Closeness centrality:** the inverse of the path length between a node and all other nodes in the graph. This is the node-wise equivalent of global efficiency, which is the inverse sum of all the shortest path lengths in the graph.
- v) **Local efficiency:** the number of strong connections a node has with its neighbouring nodes. This reflects the robustness of local networks to disruption.
- vi) **Eigenvector centrality:** this measure quantifies the functional influence of a node on every other node in the graph, by weighting the importance of each nodal connection based on the influence of the nodes with which they connect.
- vii) **Clustering coefficient:** the fraction of triangular connections formed by a node with other nodes. In other words, a node is strongly clustered if a large proportion of its neighbours are neighbours of each other.

Nodal connectivity strength was assessed for comparison to weighted degree, to ensure that our results did not result from bias introduced by proportionate thresholding. This metric is related to weighted degree, but includes information from all strengths of

connection between every pair of nodes. As such, it is more subject to fMRI signal to noise ratio limitations, and it is not a suitable metric for whole-brain, cross-sectional analysis across individuals, but it can be used to make a node-wise, group average assessment analogous to that for weighted degree.

2.3.5 Tau Burden Assessment

Other than the atlas used to define regions of interest, all AV-1451 and PiB data acquisition and pre-processing steps were identical to those reported by Passamonti *et al.* (2017). Ligand preparation was carried out at the Wolfson Brain Imaging Centre, University of Cambridge, with high radiochemical purity. [¹⁸F]AV-1451 was produced with a specific activity of 216±60 GBq/μmol at the end of synthesis (60min); [¹¹C] PiB specific activity was >150GBq/μmol. PET imaging was performed on a GE Advance PET scanner with a 15min ⁶⁸Ge transmission scan used for attenuation correction acquiring 58 frames of increasing duration. PET scanning was performed in 3D mode (63 image planes; 15.2cm axial field of view; 5.6mm transaxial resolution and 2.4mm slice interval) 80-100 minutes after a 9.0 to 11.0 mCi bolus injection in frames of 4x5 minutes. Each [¹¹C] PiB scan was acquired using an 8.5 to 15 mCi bolus injection immediately followed by a 60-minute dynamic acquisition in 69 frames (12x15 seconds, 57x60 seconds). Scans were reconstructed on the GE Advance scanner using the PROMIS 3D filtered back projection algorithm, correcting for randoms, dead time, normalisation, sensitivity and scatter attenuation.

The cerebellar grey matter was used as a reference tissue to express the distribution volume ratio (DVR) for the [¹¹C] PiB PET data for each MCI participant. PiB scans were classified as positive if the average SUVR values across the cortex were more than 1.5 times that of the cerebellar ROIs. Seven MCI participants met this criterion and were included in the study.

The non-displaceable binding potential of [¹⁸F]AV-1451 was assessed at each ROI in the sub-parcellated atlas after rigid registration of each subject's dynamic PET image series to their T1-weighted MRI scan. This was normalised against the superior cerebellum, a reference region considered to have no tau pathology in either PSP or Alzheimer's disease (Williams *et al.*, 2007, Schöll *et al.*, 2016, Passamonti *et al.*, 2017).

These data were corrected for white matter and CSF partial volumes by calculating the ordinary least squared solution for the BP map voxel-wise in each region for grey plus white matter segments, each smoothed to PET resolution.

2.3.6 Statistical Approach

A stereotyped statistical approach was taken to the analysis of graph metrics of theoretical interest. All statistical analyses were performed in Matlab 2015b (The Mathworks Inc., 2015), with the exception of moderation analysis, which was performed in R (R Core Team, 2016).

A group-averaged analysis assessed hypothesis 1 by examining the node-wise relationships between [¹⁸F]AV-1451 binding potential and weighted degree, weighted participation coefficient, and clustering coefficient. These analyses were performed across the whole brain and within ten intrinsic connectivity networks. To avoid circularity, where the regions of interest are defined by the test data, the intrinsic connectivity networks were independently derived from a publically available dataset (Smith *et al.*, 2009). A binary mask was constructed for each resting state network by thresholding at $Z \geq 2.6$ ($p < 0.005$ uncorrected). Nodes were defined as belonging to a network if their centre of mass was within 5mm of any positive voxel.

A between-subject analysis assessed hypotheses 2 and 3. This was undertaken at a variety of spatial scales. I first looked across the whole brain. For each individual I first calculated a measure of disease-related tau burden. For participants with AD, in whom tau deposition increases in both magnitude and distribution as disease progresses (Braak and Braak, 1995), tau burden was calculated as average [¹⁸F]AV-1451 binding potential across the whole brain. In PSP, tau deposition remains confined to brainstem and deep nuclei even in late disease (Williams *et al.*, 2007); tau burden was therefore calculated as average [¹⁸F]AV-1451 binding potential across the left and right thalamus, caudate, putamen, pallidum, accumbens, ventral diencephalon, midbrain, pons and medulla.. Both methods were separately assessed for controls. These measures of individual tau burden were then correlated with whole-brain averaged graph metrics to assess the relationship between the metric in question and disease

burden in each group separately. Moderation analysis was performed for each metric to assess whether the relationships differed between AD and PSP. It has recently been reported that patients with early onset AD have a higher tau burden than those with later onset, especially in later Braak stage regions (Schöll *et al.*, 2017). Non-significant trend relationships between overall tau burden and age were observed in our cohort (AD $r = -0.27$, PSP $r = -0.02$, Control $r = -0.38$; Figure 2-2). Cross-sectional analyses were therefore performed twice, with and without partialling out the effect of age on tau burden.

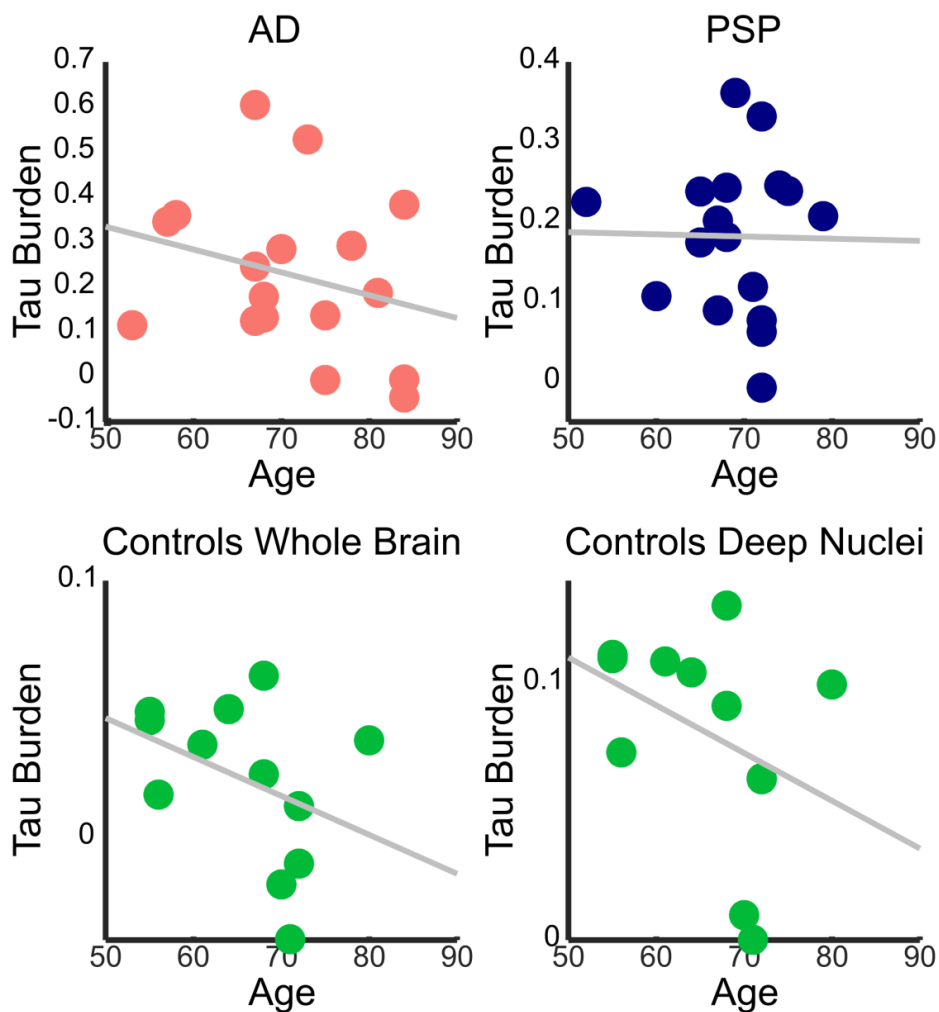


Figure 2-2 The relationship between tau burden and age for each group. Both methods of calculating tau burden are shown for the control group. As previously reported, there was a negative trend in AD, although this was not statistically significant. No such relationship was demonstrated for PSP. Controls also displayed a negative relationship, although this was across a much smaller range of AV-1451 binding.

Regionality of the demonstrated effects was assessed within groups by correlating tau burden with the single subject graph metric values at each node; the gradient of the best fit linear regression within each group was the outcome measure. The nodal gradients in cerebellar regions were discarded (as this was the reference region for PET imaging), and the remaining regional maps were then collapsed into a vector. This was correlated with a matching vector of local tau burden at each node, calculated as the group-averaged increase in [¹⁸F]AV-1451 binding potential. This resulted in a measure of the relationship between the distribution of disease-related change in each graph metric and regional deposition of tau.

2.4 Results

2.4.1 Resting state connectivity differences exist between groups

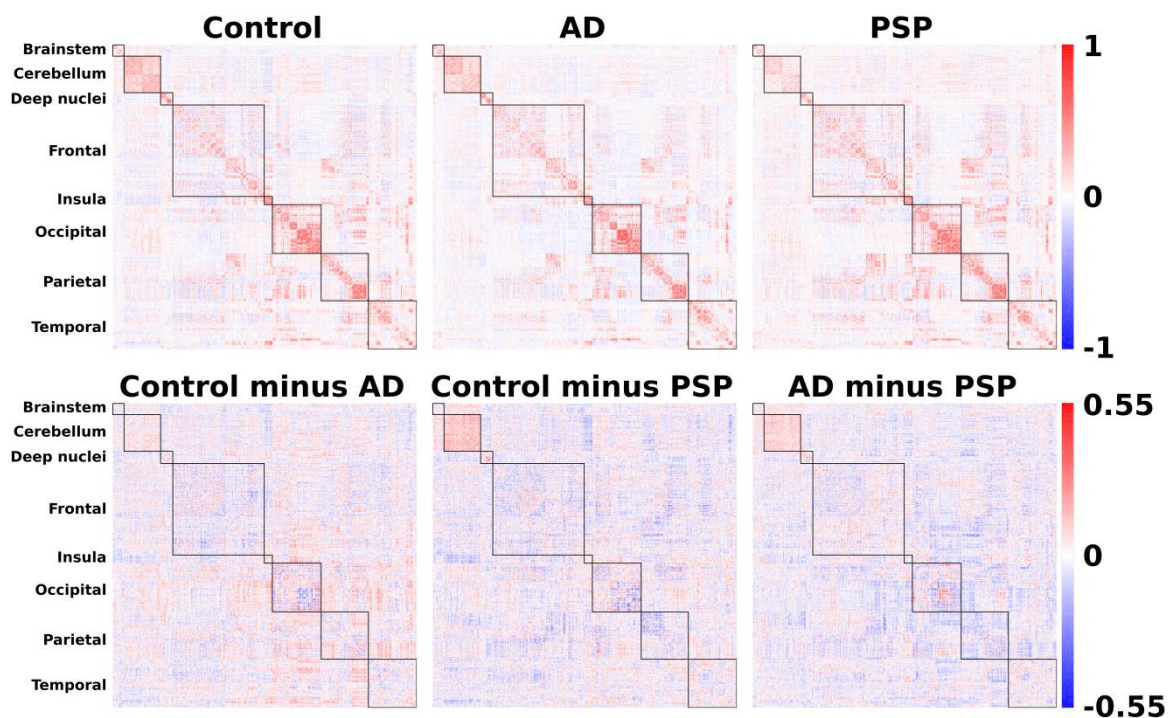


Figure 2-3 Connectivity matrices.

Upper: Association matrices derived from resting state (task-free) fMRI. Lower: Pairwise subtractions of the Fisher-z transformed association matrices to illustrate the large scale within and between-region disease related changes in functional connectivity.

As a prelude to the detailed analysis of network features, I first confirmed that our groups differed in their resting state connectivity, by testing for differences between the group averaged association matrices (Figure 2-3, upper). Jennrich tests confirmed highly significant statistical differences between controls and Alzheimer's disease ($\chi^2 = 1.15 \times 10^8$, $n_1 = 12$, $n_2 = 17$, $P < 0.0001$); controls and PSP ($\chi^2 = 975547$, $n_1 = 12$, $n_2 = 17$, $P < 0.0001$); and Alzheimer's disease and PSP ($\chi^2 = 733030$, $n_1 = 17$, $n_2 = 17$, $P < 0.0001$).

The nature of these differences would be opaque without abstraction techniques. Pairwise subtraction of the Fisher transformed association matrices (Figure 2-3, lower) revealed the presence of structure within the data, with both within-lobe and between-lobe group differences. While one can make general observations from these raw data, such as a prominent reduction in cerebello-cerebellar and brainstem-cerebellar connectivity in PSP, and a general reduction in between-region connectivity in Alzheimer's disease, the insights would be limited. Instead, graph theoretic measures allow one to examine which specific properties of the network underpin disease-related differences. For this approach each region in the brain becomes a node in a graph, which is functionally connected to all other nodes with a finite strength that is given by their pairwise correlation over time. Each individual's graph is then thresholded so that the highest 'x' percentage of connections survives. Effects are sought that are consistently present at a variety of network thresholds. Here I examine network thresholds from $1 < x < 10\%$, representing a range of graphs from sparse to dense. Very sparse graphs contain less information and can miss important relationships. Conversely, very dense graphs are more subject to noise and, when binarised, begin to provide less meaningful information. Therefore, in what follows, I present the primary statistical analyses at an intermediate density of 6%, with statistical detail given for this density. To assess the robustness of effects to different thresholding decisions I note separately the range of network densities exhibiting statistical significance.

2.4.2 Findings in AD but not PSP are consistent with trans-neuronal spread of tau

I hypothesised that trans-neuronal spread of tau would manifest as a positive relationship between [^{18}F]AV-1451 and weighted degree. As I have parcellated the brain into nodes of equal size, weighted degree is a measure of the volume of cortex to

which a node is connected, and the strength of these connections. In Alzheimer's disease, a strong positive correlation was observed at all network thresholds, such that the most strongly connected nodes had higher [¹⁸F]AV-1451 BP_{ND} (Pearson's $r = 0.48$, $P < 0.0001$, Spearman's $\rho = 0.48$, $P < 0.0001$) (Figure 2-4 A). A consistent relationship was not present in PSP (Pearson's $r = -0.09$, Spearman's $\rho = 0.12$) (Figure 2-4 B) or controls (Pearson's $r = 0.03$, Spearman's $\rho = 0.11$) (Figure 2-4 C). These patterns were present at all examined network density thresholds.

Weighted Degree

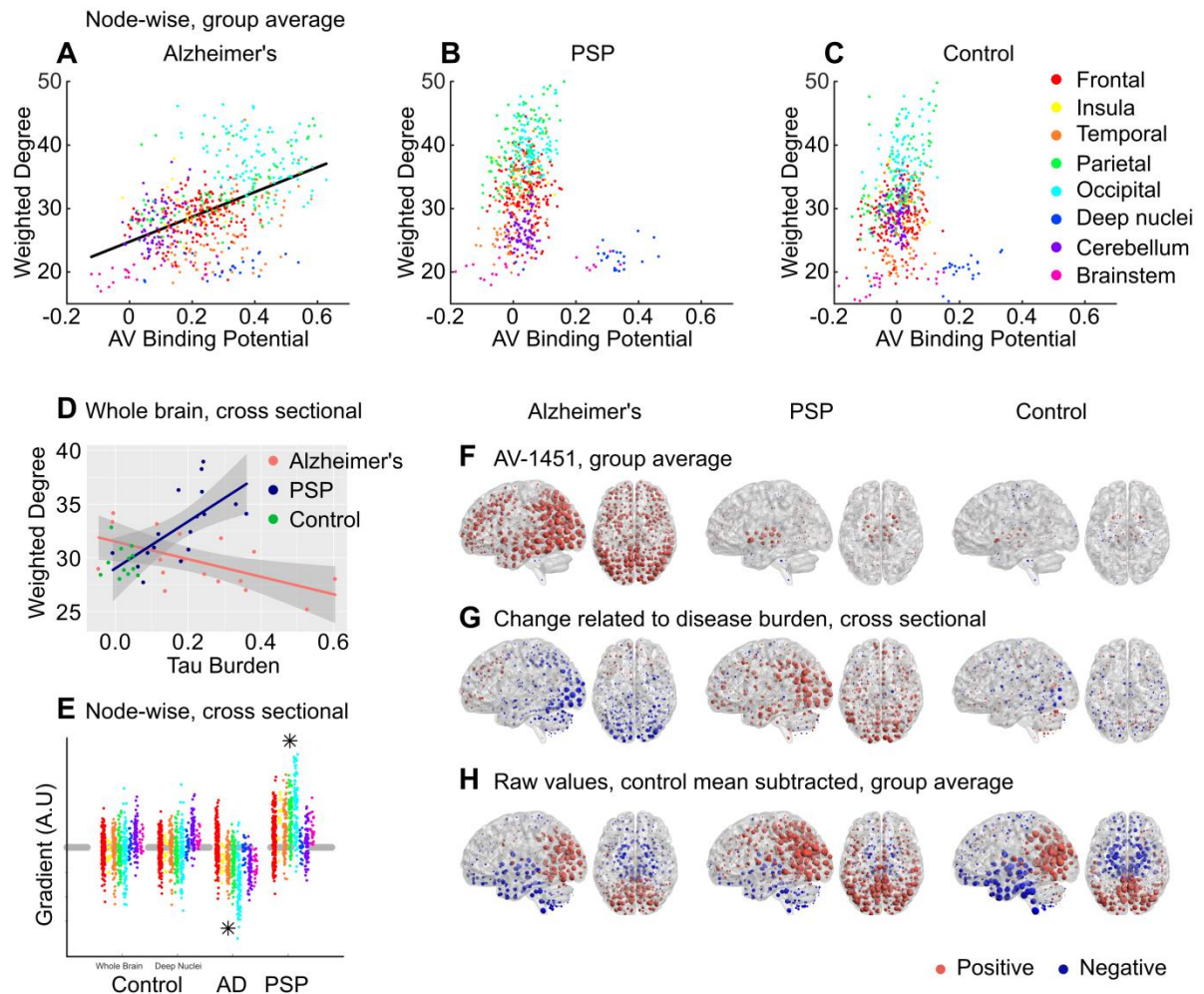


Figure 2-4 Weighted degree.

A-C: Group-averaged connection strength at each node, quantified by weighted degree, plotted against $[^{18}\text{F}]\text{AV-1451}$ binding potential at that node. A statistically significant linear relationship was demonstrated only in AD (Pearson's $r = 0.48$, $p < 0.0001$, Spearman's $\rho = 0.48$, $p < 0.0001$), and the corresponding regression line is plotted for this group. D: Between-subjects analysis of the relationship between global tau burden and each weighted degree at a network density of 6%. No significant relationship was found for the control subjects with either method of assessing tau burden – for simplicity only their whole-brain average points are illustrated here. Moderation analysis for a differential relationship between graph metric and tau burden in the two disease groups (AD and PSP) was statistically significant. E: The magnitude of disease related change at each node is plotted as a single point, grouped by lobe. Control data are shown for both methods of assessing tau burden. Stars represent statistically significant excesses of positive or negative gradients in the disease groups. F: Average $[^{18}\text{F}]\text{AV-1451}$ binding potential at each node. Red spheres represent increases compared to the cerebellar reference region. Blue spheres represent decreases. The centre of the sphere is placed at the centre of the region of interest. The radius of

each sphere is linearly related to the magnitude of binding at that node. All groups are scaled identically. G: The local tau burden-related change in weighted degree is plotted for each group at each node. Red spheres represent local increases as a result of greater overall tau burden; blue spheres represent local decreases. The radius of each sphere is linearly related to the magnitude of disease-related change at that node across the whole range of disease burden observed in each group. All groups are scaled identically. Control images are based on the whole-brain method of assessing tau burden. H: Average raw values of each graph metric within each group. The control mean for each metric is subtracted at every node. Red spheres represent increases compared to the control mean value. Blue spheres represent decreases. The centre of the sphere is placed at the centre of the region of interest. The radius of each sphere is linearly related to the difference from the control mean at that node. All groups are scaled identically.

It is important to acknowledge that the degree of a node as defined by correlated activity is impacted by the size of the connectivity network to which it belongs (Power *et al.*, 2013). Therefore, one concern might be that correlations between [¹⁸F]AV-1451 and degree are driven by the coincidence that AD happens to affect the default mode network (DMN), which happens to be a large intrinsic connectivity network. To exclude this possibility, I undertook two additional analyses. Firstly, I re-examined [¹⁸F]AV-1451 and degree when nodes belonging to the DMN were excluded; this did not abolish the strong relationship (Pearson's $r = 0.43$, $P < 0.0001$). Secondly, I examined the relationship within each intrinsic connectivity network (Figure 2-5). A strong positive relationship between [¹⁸F]AV-1451 and degree was seen in nine out of the ten networks examined (Pearson's $r \geq 0.4$, $P < 0.0001$).

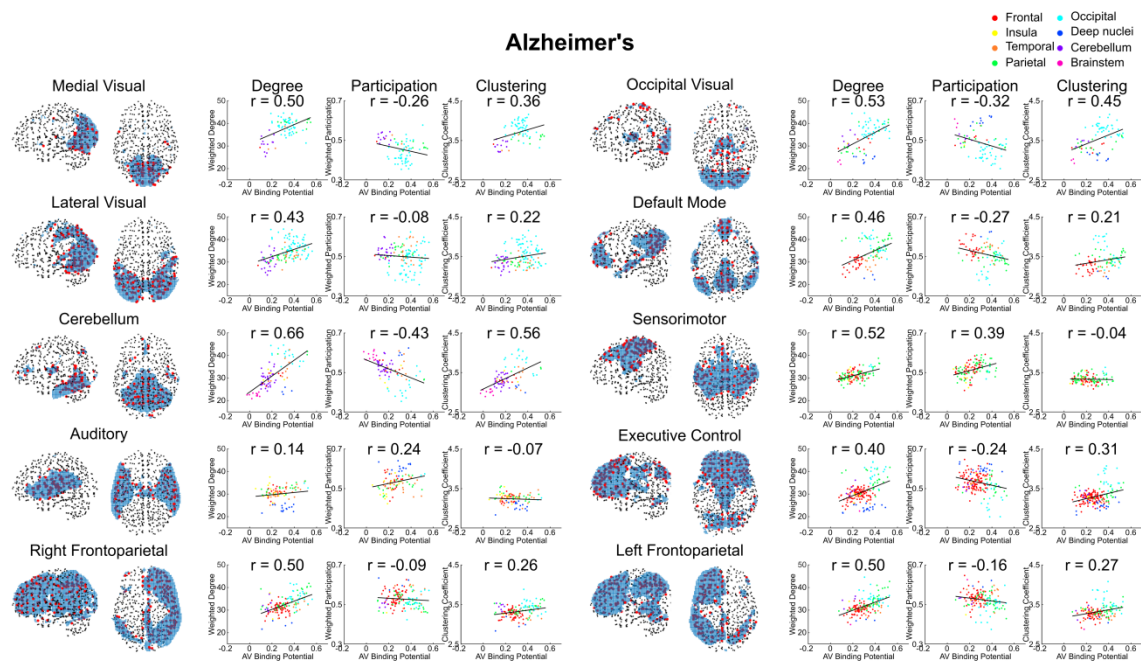


Figure 2-5 Alzheimer's disease comparison of the three graph metrics representing the three principal hypotheses of hub vulnerability. Broken down by intrinsic connectivity network defined from (Smith et al., 2009). The group-averaged graph metric at each node within a network is plotted against [¹⁸F]AV-1451 binding potential at that node. The Pearson correlation coefficient is noted in each case. Only weighted degree demonstrated a consistent relationship across all networks in keeping with its related hypothesis.

In contrast, no strong positive correlations were observed in any network in PSP (Figure 2-6).

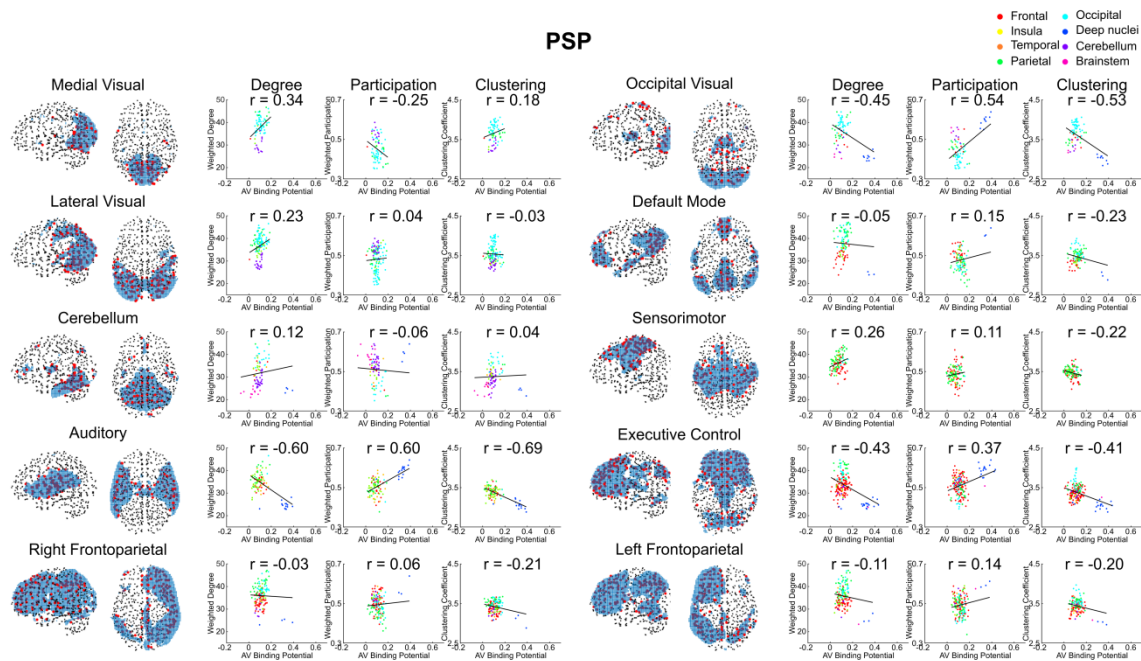


Figure 2-6 PSP comparison of the three graph metrics representing the three principal hypotheses of hub vulnerability.

Broken down by intrinsic connectivity network defined from (Smith et al., 2009). The group-averaged graph metric at each node within a network is plotted against $[^{18}\text{F}]$ AV-1451 binding potential at that node. The Pearson correlation coefficient is noted in each case.

Finally, in each group I examined the relationship between each node's unthresholded connectivity strength and $[^{18}\text{F}]$ AV-1451 BP_{ND} (Figure 2-7). This is a local measure of the strength of functional connectivity that does not rely on thresholding the graph and therefore takes into account both strong and weak connections. The pattern of results observed in weighted degree was replicated; in Alzheimer's disease, a positive correlation was observed ($r = 0.28$, $P < 0.0001$), but no significant relationship was observed in PSP ($r = -0.05$, $P = 0.22$) or controls ($r = 0.04$, $P = 0.31$).

Nodal Connectivity Strength

Node-wise, group average

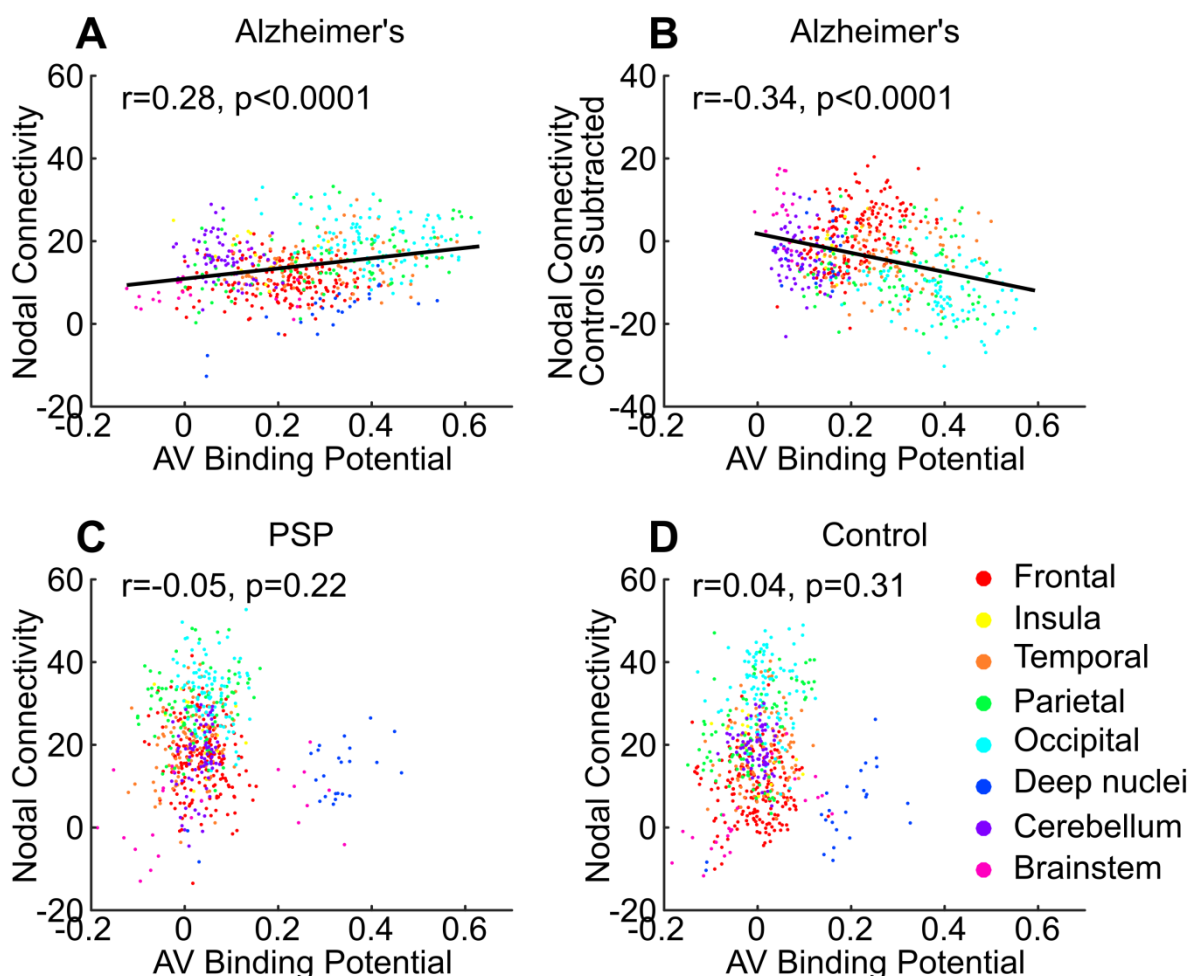


Figure 2-7 Unthresholded nodal connectivity strength.

A: Group average for Alzheimer's disease. A statistically significant positive relationship was observed ($r = 0.28, p < 0.0001$). B: The disease-related change in nodal connectivity strength at each node in the Alzheimer's disease group. A statistically significant negative relationship was observed ($r = -0.34, p < 0.0001$). Therefore nodes that were more strongly connected accrued more tau, but the consequence of tau accrual was that those same nodes then lost connectivity. C: Group average for PSP. No statistical relationship was observed ($r = -0.05, p = 0.22$). D: Group average for controls. No statistical relationship was observed ($r = 0.04, p = 0.31$).

2.4.3 Findings in PSP but not AD are consistent with hub vulnerability due to metabolic demand and lack of trophic support.

I hypothesised that tau accumulation due to metabolic demand would manifest as a positive relationship between [18F]AV-1451 and weighted participation coefficient. This was not observed in AD; in fact there was a weak negative correlation (Pearson's $r = -0.18$) (Figure 2-8 A).

In PSP, however, those nodes that displayed elevated [18F]AV-1451 were those that had the highest participation coefficient (Figure 2-8 B).

Weighted Participation Coefficient

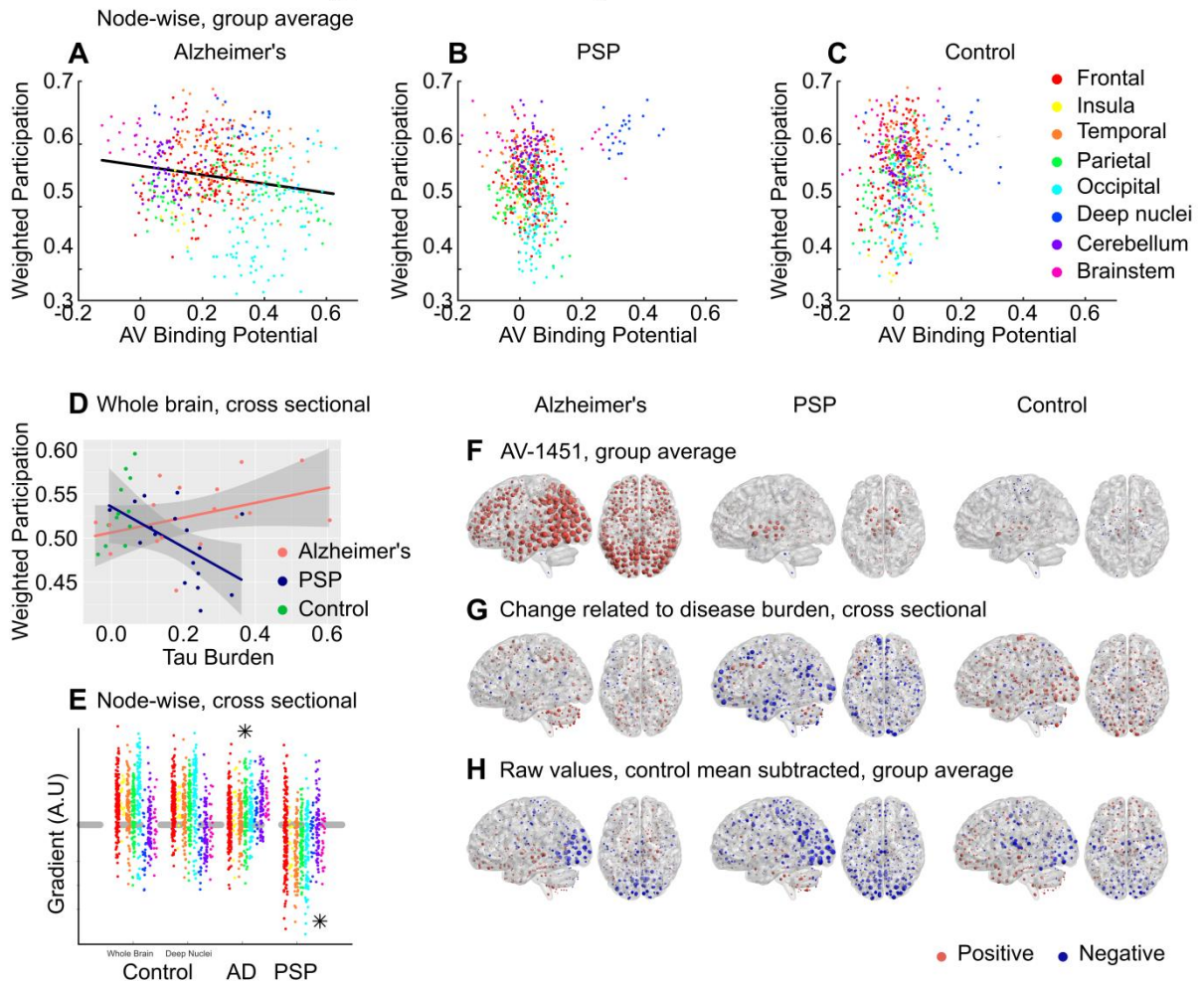


Figure 2-8 Weighted participation coefficient.

A-C: Group-averaged weighted participation coefficient at each node, plotted against $[18F]AV-1451$ binding potential at that node. A negative relationship was observed in Alzheimer's disease, in violation of the metabolic demand hypothesis. D: Between-subjects analysis of the relationship between global tau burden and participation coefficient at a network density of 6%. No significant relationship was found for the control subjects with either method of assessing tau burden. Moderation analysis for a differential relationship between graph metric and tau burden in the two disease groups (AD and PSP) was statistically significant. E: The magnitude of disease related change at each node is plotted as a single point, grouped by lobe. Control data are shown for both methods of assessing tau burden. Stars represent statistically significant excesses of positive or negative gradients in the disease groups. F: Average $[18F]AV-1451$ binding potential at each node. Red spheres represent increases compared to the cerebellar reference region. Blue spheres represent decreases. The centre of the sphere is placed at the centre of the region of interest. The radius of each sphere is linearly related to the magnitude of binding at that node. All groups are scaled identically. G: The local tau burden-related change in participation coefficient is plotted for each group at each node. Red spheres represent local increases as a result of greater overall tau burden; blue spheres represent local decreases. The radius of each sphere is linearly related to the magnitude of disease-related change at that node across the whole range

of disease burden observed in each group. All groups are scaled identically. Control images are based on the whole-brain method of assessing tau burden. H: Average raw values for participation coefficient within each group. The control mean for each metric is subtracted at every node. Red spheres represent increases compared to the control mean value. Blue spheres represent decreases. The centre of the sphere is placed at the centre of the region of interest. The radius of each sphere is linearly related to the difference from the control mean at that node. All groups are scaled identically.

Similarly, I hypothesised that tau accumulation due to a lack of trophic support would manifest as a negative relationship between [18F]AV-1451 and clustering coefficient. In AD, the opposite relationship was observed; strongly clustered nodes were more likely to display elevated [18F]AV-1451 binding (Pearson's $r = 0.33$) (Figure 2-9 A).

Again, by contrast, in PSP those nodes that displayed elevated [18F]AV-1451 were those that had the lowest clustering coefficient (Figure 2-9 B).

Clustering Coefficient

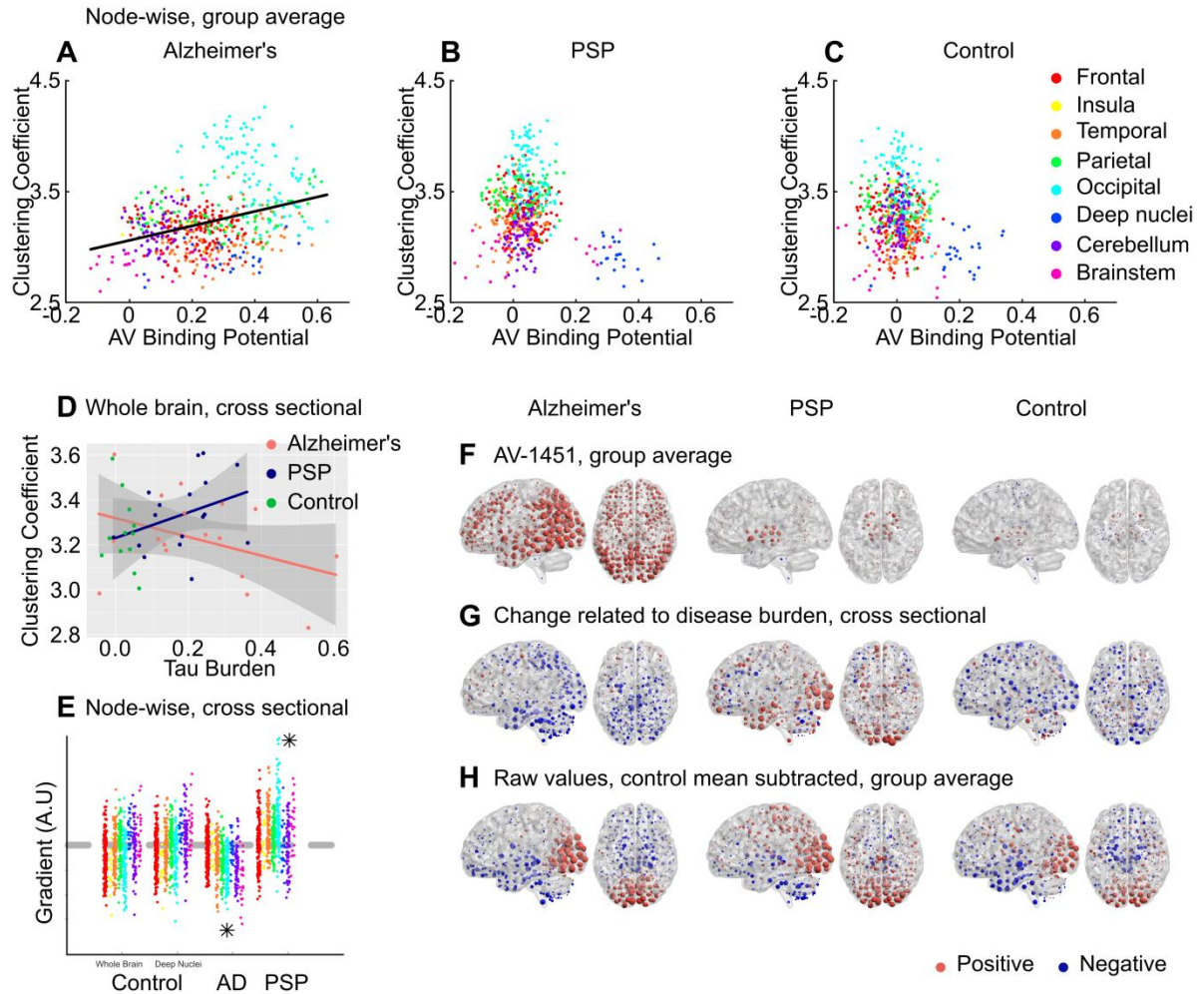


Figure 2-9 Clustering coefficient.

A-C: Group-averaged clustering coefficient at each node, plotted against $[18F]AV-1451$ binding potential at that node. A positive relationship was observed in Alzheimer's disease, in violation of the trophic support hypothesis. D: Between-subjects analysis of the relationship between global tau burden and clustering coefficient at a network density of 6%. No significant relationship was found for the control subjects with either method of assessing tau burden. Moderation analysis for a differential relationship between graph metric and tau burden in the two disease groups (AD and PSP) was statistically significant. E: The magnitude of disease related change at each node is plotted as a single point, grouped by lobe. Control data are shown for both methods of assessing tau burden. Stars represent statistically significant excesses of positive or negative gradients in the disease groups. F: Average $[18F]AV-1451$ binding potential at each node. Red spheres represent increases compared to the cerebellar reference region. Blue spheres represent decreases. The centre of the sphere is placed at the centre of the region of interest. The radius of each sphere is linearly related to the magnitude of binding at that node. All groups are scaled identically. G: The local tau burden-related change in clustering coefficient is plotted for each group at each node. Red spheres represent local increases as a result of greater overall tau burden; blue spheres represent local decreases. The radius of each sphere is linearly related to the magnitude of disease-related change at that node across the whole range of disease

burden observed in each group. All groups are scaled identically. Control images are based on the whole-brain method of assessing tau burden. H: Average raw values for clustering coefficient within each group. The control mean for each metric is subtracted at every node. Red spheres represent increases compared to the control mean value. Blue spheres represent decreases. The centre of the sphere is placed at the centre of the region of interest. The radius of each sphere is linearly related to the difference from the control mean at that node. All groups are scaled identically.

2.4.4 Alzheimer's disease and PSP have opposite effects on the strength of *cortical* functional connectivity

I assessed the impact of the presence of tau on connection strength at a variety of spatial scales. Firstly, I averaged weighted degree across the whole brain, resulting in a single measure for each individual. As the overall number of connections in each individual's graph was thresholded at an identical network density, this measure represented the average strength of the strongest X% of connections. To assess global disease burden in Alzheimer's disease I averaged [¹⁸F]AV-1451 BP_{ND} across the whole brain. In PSP, I averaged [¹⁸F]AV-1451 BP_{ND} across midbrain and basal ganglia, reflecting the more focal distribution of disease and our hypotheses about dissociated functional effects of cortical and subcortical tau (Passamonti *et al.*, 2017). Confirmatory tests demonstrated that the pattern of the moderation analyses below were unchanged if whole-brain average [¹⁸F]AV-1451 BP_{ND} was used to assess tau burden in PSP. Both methods of assessing tau burden were independently assessed in the control group, with no significant effects demonstrated in either case.

In AD, I found a negative correlation between average connection strength and tau burden (Pearson's $r = -0.58$, $p = 0.015$) (Figure 2-4 D). In PSP this relationship was reversed, with average connection strength increasing in line with tau burden ($r = 0.65$, $p = 0.004$). No relationship was observed in controls ($r = -0.10$, $p = 0.75$). Moderation analysis confirmed a dissociated relationship between tau and connection strength in Alzheimer's disease and PSP at all network densities ($\Delta r^2 = 0.29$, $F(1,30) = 19.0$, $p = 0.0001$; after partialling out age (Figure 2-10 A) $\Delta r^2 = 0.28$, $F(1,30) = 17.9$, $p = 0.0002$). Therefore, while in Alzheimer's disease the presence of tau pathology causes the strongest functional connections to weaken, in PSP, the presence of tau had the opposite effect, i.e., to strengthen functional connections.

Secondly, I assessed the distribution of change by repeating the correlation of disease burden against weighted degree at every individual node. I hypothesised that this effect would be greatest in those regions that display the strongest functional connectivity in the healthy brain, and which I have demonstrated to accrue most tau in Alzheimer's disease. The gradient of this nodewise relationship reflects a measure of local change in weighted degree with disease burden (Figure 2-4 E). Firstly, I examined whether the whole-brain average relationship could be replicated in these individual gradients, by performing sign tests. For Alzheimer's disease, a negative relationship was confirmed ($Z = -13.0$, $P < 0.0001$); for PSP there was a positive relationship ($Z = 14.8$, $P < 0.0001$); while for controls no relationship was demonstrated using either whole brain ($Z = -1.1$, $P = 0.27$) or deep brain ($Z = 1.1$, $P = 0.27$) tau burden.

Next, I assessed whether the functional connectivity change at each node related to local tau burden, by correlating the gradient of the disease-related change in weighted degree with the disease-associated increase in [^{18}F]AV-1451 binding potential at each node (i.e. correlating each column of Figure 2-4 F with the corresponding column of Figure 2-4 G). A negative correlation between these measures was demonstrated in Alzheimer's disease (Pearson's $r = -0.30$, $P < 0.0001$, Spearman's $\rho = -0.24$, $P < 0.0001$). This relationship was absent in PSP (Pearson's $r = -0.07$, $P = 0.11$, Spearman's $\rho = -0.00$, $P = 0.98$) and in controls (Pearson's $r = -0.01$, $P = 0.75$, Spearman's $\rho = -0.01$, $P = 0.80$). As well as being present at all examined network densities, the negative correlation between disease-related change in functional connectivity strength and tau burden in Alzheimer's disease was replicated in nodal connectivity strength, the equivalent unthresholded measure ($r = -0.34$, $p < 0.0001$, Figure 2-7 B).

Finally, I assessed whether the functional connectivity change at each node related to the strength of its connections in the healthy control brain (i.e. correlating each patient panel of Figure 2-4 G with the control panel in Figure 2-4 H). As would be expected from the propensity of highly connected nodes to accrue tau, a negative relationship was demonstrated in Alzheimer's disease (Pearson's $r = -0.23$, $P < 0.0001$, Spearman's $\rho = -0.24$, $P < 0.0001$). Importantly, however, this relationship explained less variance than AV binding, with which I have demonstrated it to be correlated. In PSP,

a positive relationship was demonstrated (Pearson's $r = 0.27$, $P < 0.0001$, Spearman's $\rho = 0.26$, $P < 0.0001$).

In summary, nodes that are constitutionally more strongly connected to a larger volume of cortex are more likely to accrue tau pathology in Alzheimer's disease but not PSP. This relationship is independent of the connectivity network to which a node belongs. Once present, the tau pathology appears to cause local functional connectivity strength to fall. By contrast, in PSP tau selectively accumulates in midbrain and deep nuclei, which has the consequence of increasing the strength of cortico-cortical functional connectivity, especially in those nodes that are constitutionally highly connected.

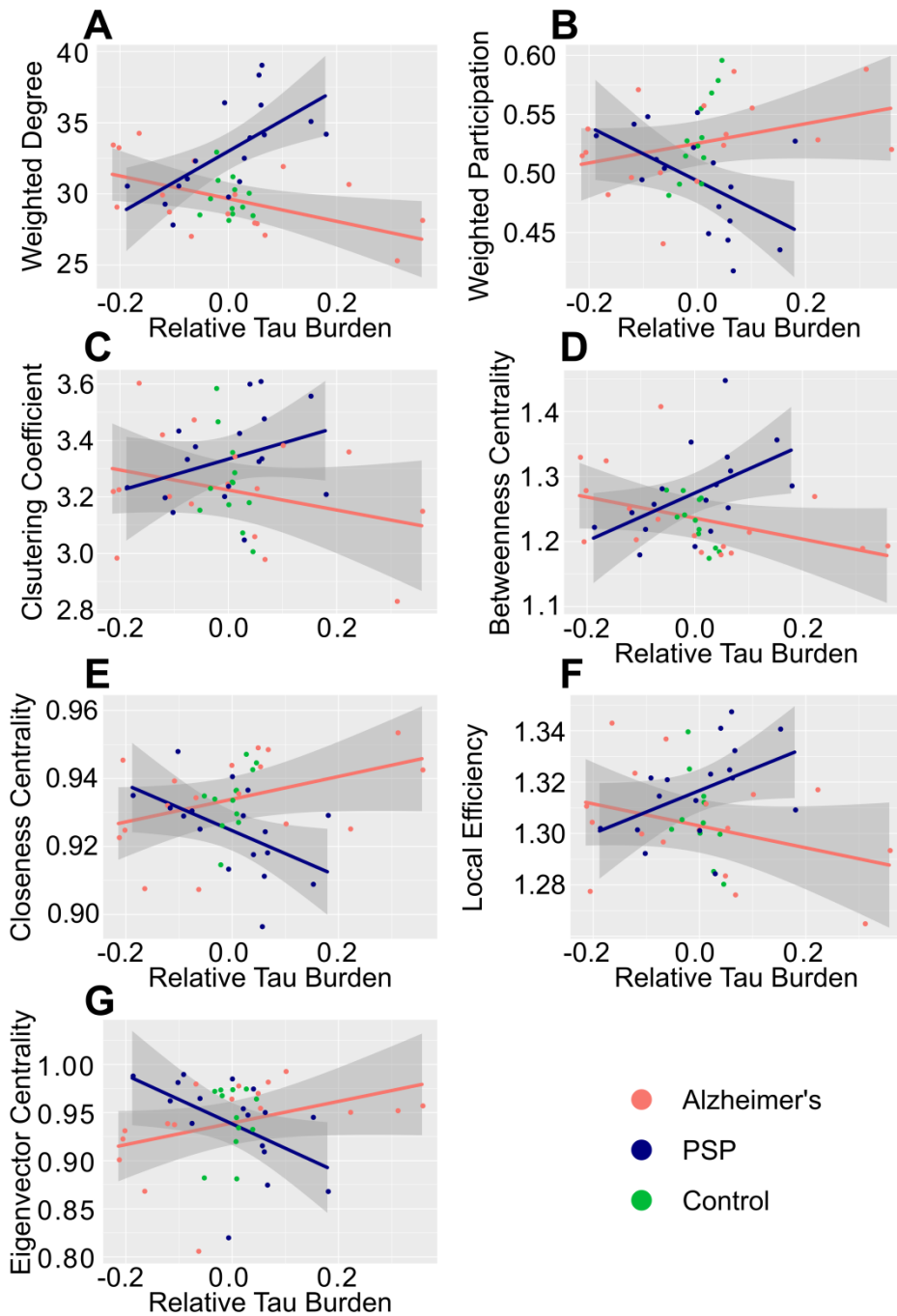


Figure 2-10 Between-subjects analysis of the relationship between global tau burden and each graph metric at a network density of 6%, with the effect of age on tau burden partialled out.

A Relative tau burden of 0 is the age-expected tau burden within each disease group (i.e. lying on the group trend line in Figure 2-2). Individuals with lower-than-average tau burden within their disease group have negative Relative tau burdens, while those with higher-than-average tau burden have positive Relative tau burdens. Moderation

analysis for a differential relationship between graph metric and tau burden in the two disease groups (AD and PSP) was statistically significant for all metrics.

2.4.5 Reorganisation of cortical functional connectivity reflects cortical vs subcortical pathology

I hypothesised that the presence of subcortical pathology in PSP might be causing an increase in weighted degree by necessitating an increase in the relative strength of short-range cortico-cortical connections as longer range connections are disrupted. This view is supported by the observation that a consequence of increasing tau burden in PSP is a marked reduction in participation coefficient (Figure 2-8 D). This relationship was not observed in AD, where increasing tau burden caused increasing participation. Moderation analysis confirmed this differential relationship at all network densities from 1-10% ($\Delta r^2 = 0.21$, $F(1,30) = 7.6$, $p = 0.002$; after partialling out age (Figure 2-10 B) $\Delta r^2 = 0.17$, $F(1,30) = 8.3$, $p = 0.007$).

I further examined this hypothesis by examining the effect of tau on other measures of graph structure in each individual, dissociated from variation in degree by binarisation after thresholding and normalisation against 1000 random graphs with the same number of connections at each node.

The clustering coefficient quantifies how many of a node's neighbours are neighbours of each other. All individuals in all groups displayed clustering to at least 2.8x that of random graphs of the same degree (Figure 2-9 D), consistent with a small-world connectivity distribution. While in AD a non-significant trend was observed towards reduced clustering with increasing tau burden, in line with previous reports (Stam *et al.*, 2006, Sanz-Arigita *et al.*, 2010), in PSP the opposite relationship was observed. Moderation analysis trended towards significance at the density of primary interest ($\Delta r^2 = 0.08$, $F(1,30) = 3.8$, $p = 0.06$; after partialling out age (Figure 2-10 C) $\Delta r^2 = 0.07$, $F(1,30) = 2.5$, $p = 0.09$), and was significant from 7-10% density. The betweenness centrality of a node is a measure of the number of shortest paths between any other two nodes that pass through it. If the presence of subcortical pathology in PSP means that long-range information transfer must occur through a trans-cortical route, average betweenness centrality should increase. Conversely, predominantly cortical pathology in AD might increase reliance on cortico-subcortical connections,

reducing average betweenness centrality. This prediction was verified (Figure 2-11 A), with a differential relationship between tau burden and betweenness centrality confirmed by moderation analysis at all network densities from 1-10% ($\Delta r^2 = 0.21$, $F(1,30) = 9.3$, $p = 0.005$; after partialling out age (Figure 2-10 D) $\Delta r^2 = 0.20$, $F(1,30) = 8.9$, $p = 0.006$).

Betweenness Centrality

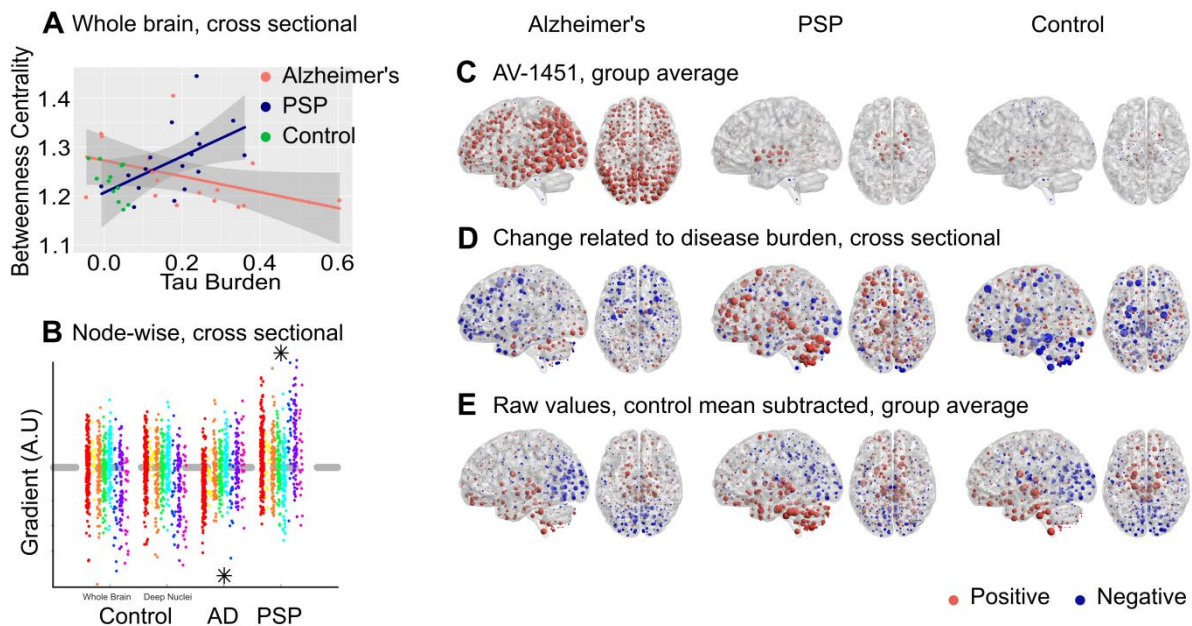


Figure 2-11 Betweenness centrality.

A: Between-subjects analysis of the relationship between global tau burden and betweenness centrality at a network density of 6%. No significant relationship was found for the control subjects with either method of assessing tau burden. Moderation analysis for a differential relationship between graph metric and tau burden in the two disease groups (AD and PSP) was statistically significant. B: The magnitude of disease related change at each node is plotted as a single point, grouped by lobe. Control data are shown for both methods of assessing tau burden. Stars represent statistically significant excesses of positive or negative gradients in the disease groups (supplementary table 2). C: Average [18F]AV-1451 binding potential at each node. Red spheres represent increases compared to the cerebellar reference region. Blue spheres represent decreases. The centre of the sphere is placed at the centre of the region of interest. The radius of each sphere is linearly related to the magnitude of binding at that node. All groups are scaled identically. D: The local tau burden-related change in betweenness centrality is plotted for each group at each node. Red spheres represent local increases as a result of greater overall tau burden; blue spheres represent local decreases. The radius of each sphere is linearly related to the magnitude of disease-related change at that node across the whole range of disease burden observed in each group. All groups are scaled identically. Control images are based on the whole-brain method of assessing tau burden. E: Average raw values for betweenness centrality within each group. The control mean for each metric is subtracted at every node. Red spheres represent increases compared to the control mean value. Blue spheres represent decreases. The centre of the sphere is placed at the centre of the region of interest. The radius of each sphere is linearly related to the difference from the control mean at that node. All groups are scaled identically.

Long-range information transfer by a cortico-cortical route implies an inefficient, indirect process, perhaps accounting for the cognitive slowing characteristic of neurodegenerative disorders with predominant sub-cortical pathology. I tested for this by examining closeness centrality, which is the inverse of the path length between a node and all other nodes in the graph. As would be predicted by this account, increasing disease burden resulted in a higher average path length (lower closeness centrality) in PSP but a lower average path length in Alzheimer's disease (higher closeness centrality) at network densities from 2-10% (Figure 2-12 A, moderation $\Delta r^2 = 0.20$, $F(1,30) = 9.1$, $p = 0.005$; after partialling out age (Figure 2-10 E) $\Delta r^2 = 0.16$, $F(1,30) = 8.0$, $p = 0.008$). Averaged across the whole brain, this measure is equivalent to the global efficiency of the graph, and indeed the same statistical results were obtained from a moderation analysis of that metric; increasing disease burden resulted in reduced global efficiency in PSP.

Closeness Centrality (1/Path Length)

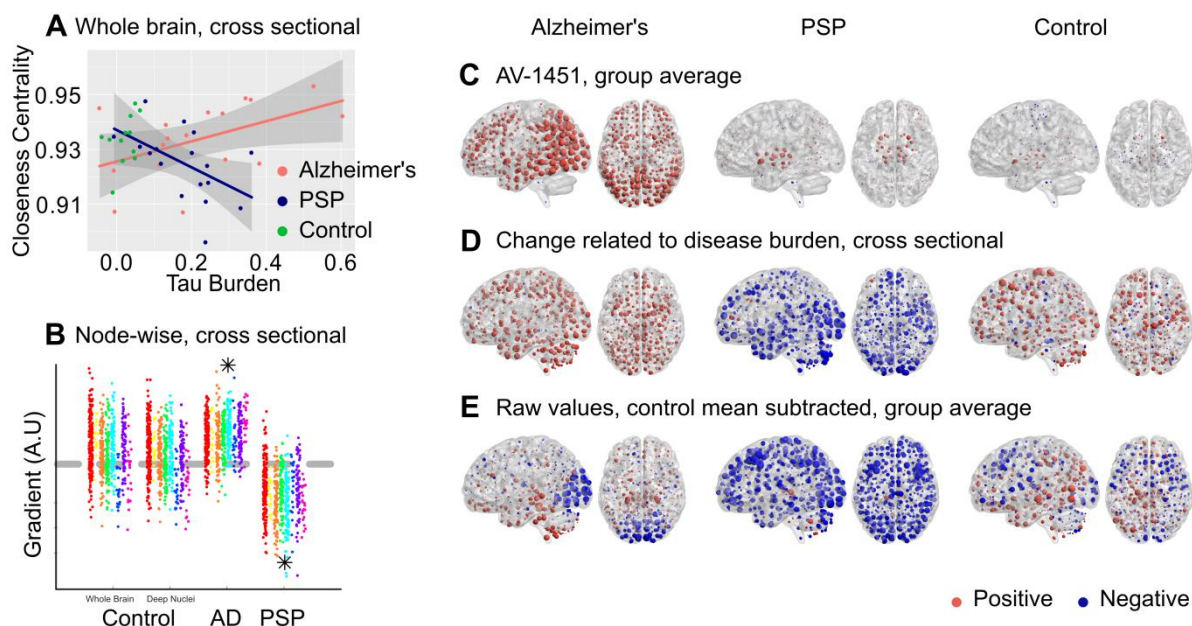


Figure 2-12 Closeness centrality (1/path length from each node to all other nodes).

A: Between-subjects analysis of the relationship between global tau burden and closeness centrality at a network density of 6%. No significant relationship was found for the control subjects with either method of assessing tau burden. Moderation analysis for a differential relationship between graph metric and tau burden in the two disease groups (AD and PSP) was statistically significant. B: The magnitude of disease related change at each node is plotted as a single point, grouped by lobe. Control data are shown for both methods of assessing tau burden. Stars represent statistically significant excesses of positive or negative gradients in the disease groups (supplementary table 2). C: Average [18F]AV-1451 binding potential at each node. Red spheres represent increases compared to the cerebellar reference region. Blue spheres represent decreases. The centre of the sphere is placed at the centre of the region of interest. The radius of each sphere is linearly related to the magnitude of binding at that node. All groups are scaled identically. D: The local tau burden-related change in closeness centrality is plotted for each group at each node. Red spheres represent local increases as a result of greater overall tau burden; blue spheres represent local decreases. The radius of each sphere is linearly related to the magnitude of disease-related change at that node across the whole range of disease burden observed in each group. All groups are scaled identically. Control images are based on the whole-brain method of assessing tau burden. E: Average raw values for closeness centrality within each group. The control mean for each metric is subtracted at every node. Red spheres represent increases compared to the control mean value. Blue spheres represent decreases. The centre of the sphere is placed at the centre of the region of interest. The radius of each sphere is linearly related to the difference from the control mean at that node. All groups are scaled identically.

While tau-mediated re-organisation of connectivity in PSP results in slower and less efficient long-range information transfer, in Alzheimer's disease one might suppose it to be a beneficial consequence of the loss of overall connection strength as those connections that remain are more globally efficient. However, I hypothesised this would be at the cost of local efficiency, which is a measure of the number of strong connections between neighbouring nodes and the robustness of local networks to disruption. Indeed this was found to be the case at network densities from 4-10% (Figure 2-13 A, $\Delta r^2 = 0.15$, $F(1,30) = 6.5$, moderation $p = 0.016$; after partialling out age (Figure 2-10 F) $\Delta r^2 = 0.12$, $F(1,30) = 5.5$, $p = 0.026$).

Local Efficiency

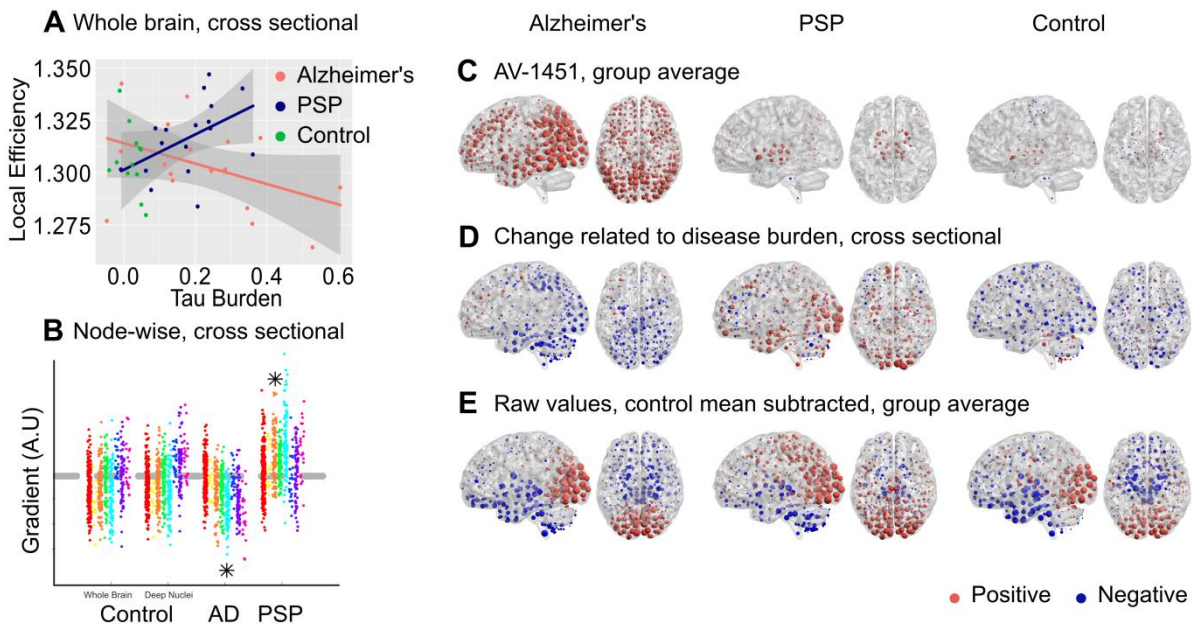


Figure 2-13 Local efficiency.

A: Between-subjects analysis of the relationship between global tau burden and local efficiency at a network density of 6%. No significant relationship was found for the control subjects with either method of assessing tau burden. Moderation analysis for a differential relationship between graph metric and tau burden in the two disease groups (AD and PSP) was statistically significant. B: The magnitude of disease related change at each node is plotted as a single point, grouped by lobe. Control data are shown for both methods of assessing tau burden. Stars represent statistically significant excesses of positive or negative gradients in the disease groups (supplementary table 2). C: Average [18F]AV-1451 binding potential at each node. Red spheres represent increases compared to the cerebellar reference region. Blue spheres represent decreases. The centre of the sphere is placed at the centre of the region of interest. The radius of each sphere is linearly related to the magnitude of binding at that node. All groups are scaled identically. D: The local tau burden-related change in local efficiency is plotted for each group at each node. Red spheres represent local increases as a result of greater overall tau burden; blue spheres represent local decreases. The radius of each sphere is linearly related to the magnitude of disease-related change at that node across the whole range of disease burden observed in each group. All groups are scaled identically. Control images are based on the whole-brain method of assessing tau burden. E: Average raw values for local efficiency within each group. The control mean for each metric is subtracted at every node. Red spheres represent increases compared to the control mean value. Blue spheres represent decreases. The centre of the sphere is placed at the centre of the region of interest. The radius of each sphere is linearly related to the difference from the control mean at that node. All groups are scaled identically.

Finally, I assessed the functional influence of each node on the other nodes in the network by examining the eigenvector centrality. Again, an opposite effect of disease burden was observed in AD and PSP at network densities from 3-10% (Figure 2-14 A, $\Delta r^2 = 0.22$, $F(1,30) = 8.5$, $p = 0.007$; after partialling out age (Figure 2-10 G) $\Delta r^2 = 0.20$, $F(1,30) = 8.3$, $p = 0.007$) such that, on average, as PSP progressed each node had less functional influence on every other node in the graph.

Eigenvector Centrality

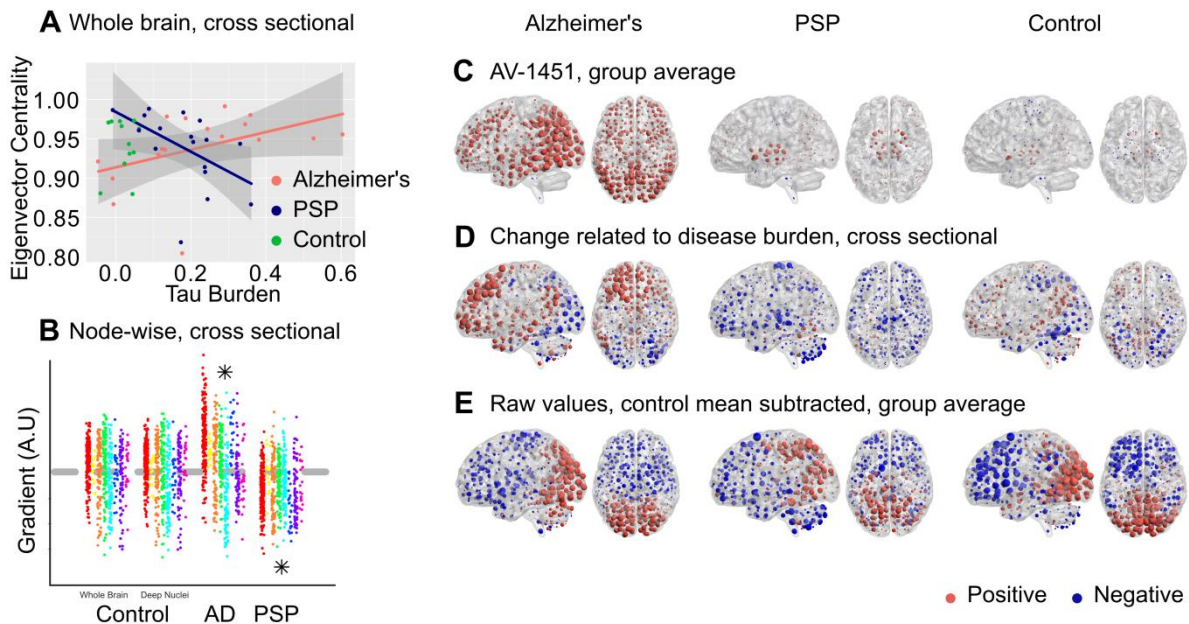


Figure 2-14 Eigenvector centrality.

A: Between-subjects analysis of the relationship between global tau burden and eigenvector efficiency at a network density of 6%. No significant relationship was found for the control subjects with either method of assessing tau burden. Moderation analysis for a differential relationship between graph metric and tau burden in the two disease groups (AD and PSP) was statistically significant. B: The magnitude of disease related change at each node is plotted as a single point, grouped by lobe. Control data are shown for both methods of assessing tau burden. Stars represent statistically significant excesses of positive or negative gradients in the disease groups (supplementary table 2). C: Average [18F]AV-1451 binding potential at each node. Red spheres represent increases compared to the cerebellar reference region. Blue spheres represent decreases. The centre of the sphere is placed at the centre of the region of interest. The radius of each sphere is linearly related to the magnitude of binding at that node. All groups are scaled identically. D: The local tau burden-related change in eigenvector efficiency is plotted for each group at each node. Red spheres represent local increases as a result of greater overall tau burden; blue spheres represent local decreases. The radius of each sphere is linearly related to the magnitude of disease-related change at that node across the whole range of disease burden observed in each group. All groups are scaled identically. Control images are based on the whole-brain method of assessing tau burden. E: Average raw values for eigenvector efficiency within each group. The control mean for each metric is subtracted at every node. Red spheres represent increases compared to the control mean value. Blue spheres represent decreases. The centre of the sphere is placed at the centre of the region of interest. The radius of each sphere is linearly related to the difference from the control mean at that node. All groups are scaled identically.

2.4.6 Local functional connectivity reorganisation is related to local [¹⁸F]AV-1451 binding potential in Alzheimer’s disease

To understand the differential reorganisation of functional connectivity in Alzheimer’s disease and PSP, I replicated the approach taken for weighted degree; correlating the gradient of the disease-related change at every individual node with local change in [¹⁸F]AV-1451 binding potential. For all metrics, the differential group effects demonstrated by moderation analysis could be replicated by statistical significance of opposite directionality in sign tests performed on the individual gradients at each node (Table 2-3, Figure 2-4, Figure 2-8, Figure 2-9, Figure 2-11, Figure 2-12, Figure 2-13, Figure 2-14). In all cases, controls showed either no relationship or a weaker effect in the same direction as patients with Alzheimer’s disease.

Group	Betweenness Centrality	Closeness Centrality	Local Efficiency	Eigenvector Centrality
AD	Z = - 5.4, p<0.0001	Z = 19.8, p<0.0001	Z = - 11.2, p<0.0001	Z = 6.3, p<0.0001
PSP	Z = 5.0, p<0.0001	Z = - 17.9, p<0.0001	Z = 9.3, p<0.0001	Z = - 10.8, p<0.0001
Control (tau burden averaged across brain as for AD)	Z = - 0.45, p=0.65	Z = 5.8, p<0.0001	Z = - 6.9, p<0.0001	Z = 3.9, p<0.0001
Control (tau burden assessed in brainstem and deep nuclei as for PSP)	Z = 0, p=1	Z = 9.7, p<0.0001	Z = - 4.2, p<0.0001	Z = 3.6, p=0.0002

Table 2-3 Sign tests

Performed on the best fit linear gradients at each of 598 nodes, comparing tau burden and graph metric across individuals. Analysis was performed twice in controls, independently assessing the measures of tau burden used in AD and PSP.

The reorganisation of graph metrics followed two distinct patterns. Closeness centrality (Figure 2-12) displayed a global effect, with most nodes increasing in Alzheimer’s disease and decreasing in PSP. This was not strongly related to local [¹⁸F]AV-1451 binding potential in AD (Pearson’s $r = 0.05$, $p = 0.25$, Spearman’s $\rho = 0.06$, $p = 0.18$) or PSP (Pearson’s $r = 0.08$, $p = 0.06$, Spearman’s $\rho = 0.11$, $p = 0.01$). Similarly,

participation coefficient displayed global changes in both diseases (Figure 2-8) (AD Pearson's $r = 0.09$, Spearman's $\rho = 0.07$, PSP Pearson's $r = 0.08$, Spearman's $\rho = 0.06$).

By contrast, eigenvector centrality (Figure 2-14) was more strongly related to local [^{18}F]AV-1451 binding potential in Alzheimer's disease (Pearson's $r = -0.28$, $P < 0.0001$, Spearman's $\rho = -0.25$, $P < 0.0001$). Strikingly, the positive relationship I demonstrated across the whole brain masked opposing regional effects. As global tau burden increased, the functional influence of frontal regions on all other regions increased, while that of occipital regions decreased. In PSP no consistent relationship with AV was observed (Pearson's $r = -0.10$, $p = 0.02$, Spearman's $\rho = -0.04$, $p = 0.38$), with almost all regions having less functional influence on all other regions as tau burden increased.

Clustering coefficient (Figure 2-9), local efficiency (Figure 2-13) and betweenness centrality (Figure 2-11) displayed an intermediate degree of regional specificity, being weakly but significantly correlated with change in [^{18}F]AV-1451 binding potential in AD (clustering coefficient Pearson's $r = -0.12$, $p < 0.0001$, Spearman's $\rho = -0.14$, $p < 0.0001$, local efficiency Pearson's $r = -0.16$, $p < 0.0001$, Spearman's $\rho = -0.19$, $p < 0.0001$, betweenness centrality Pearson's $r = 0.19$, $p < 0.0001$, Spearman's $\rho = 0.19$, $p < 0.0001$) and PSP (clustering coefficient Pearson's $r = -0.14$, $p < 0.0001$, Spearman's $\rho = -0.12$, $p < 0.0001$, local efficiency Pearson's $r = -0.14$, $p = 0.001$, Spearman's $\rho = -0.11$, $p = 0.02$, betweenness centrality Pearson's $r = 0.17$, $P < 0.0001$, Spearman's $\rho = 0.08$, $P = 0.08$).

2.5 Discussion

I have demonstrated that in Alzheimer's disease a strong relationship exists between the propensity of a node to display elevated [^{18}F]AV-1451 binding and the volume of cortex to which it is strongly connected (Figure 2-4 A). Further, I have demonstrated that this effect exists both within and between intrinsic connectivity networks (Figure 2-5). This is consistent with the theory of trans-neuronal spread. The predictions of the competing hypotheses that highly active brain regions are vulnerable to tau accumulation due to a positive relationship with metabolic demand (Figure 2-8 A) or

negative relationship with clustering due to a lack of trophic support (Figure 2-9 A) were not supported by the data.

In contrast, in PSP, I have demonstrated the opposite findings. Those brain regions that accrue most tau display weak connectivity (Figure 2-4 B), but are predicted to have high metabolic demand (Figure 2-8 B) and a lack of trophic support (Figure 2-9 B).

Further, I have explored the consequences of tau accumulation with cross sectional analyses at a variety of spatial scales. In Alzheimer's disease, I have demonstrated that with greater levels of tau pathology the strongest inter-nodal connections are weakened (Figure 2-4 G). This reorganisation of the brain network leads to more direct long-range connections passing through fewer nodes (Figure 2-12 A, Figure 2-11 A), at the cost of lower local efficiency (Figure 2-13 A).

In PSP, where tau accumulation is predominantly subcortical, I demonstrate the opposite re-organisation of the connectivity graph. With greater levels of tau in midbrain and deep nuclei (Figure 2-4 F), the strongest functional connections are strengthened; these are predominantly cortical (Figure 2-4 G, H). Information transfer therefore takes a less direct path (Figure 2-12 D), passing through a larger number of cortical nodes en-route (Figure 2-11 A), as deep structures can no longer sustain long range connectivity. This is accompanied by a decrease in participation coefficient (Figure 2-8 D) and an increase in clustering (Figure 2-9 D) as connectivity becomes increasingly modular.

2.5.1 Insights into the mechanisms of disease progression in humans

It has been proposed that the pathological mechanisms underlying Alzheimer's disease begin in a single, vulnerable location and spread from cell to cell, rather than occurring independently in a large number of vulnerable cell populations (Guo and Lee, 2014, Goedert, 2015). The primary direct evidence for such propagation of tau comes from rodent studies. For example, the injection of brain extract from transgenic mice expressing mutant tau into mice expressing wild-type human tau caused wild-type tau to form filaments and spread to neighbouring brain regions (Clavaguera *et al.*, 2009). Further, pathological tau from human brains causes disease in wild-type mice, in whom the pathological human tau species becomes self-propagating (Clavaguera *et al.*, 2013).

This tau propagation is mediated by the presence and strength of synaptic connectivity rather than spatial proximity (Liu *et al.*, 2012, Iba *et al.*, 2013, Ahmed *et al.*, 2014).

Associative studies of the healthy brain have demonstrated that large-scale, functionally connected neural networks strongly resemble the known patterns of atrophy in distinct neurodegenerative syndromes mediated by tau and TDP-43 (Zhou *et al.*, 2012). Further human evidence comes from the observation that patterns of atrophy in the rare disease non-fluent variant primary progressive aphasia (nfvPPA) strongly correspond to structural and functional connectivity in the healthy speech production network (Mandelli *et al.*, 2016). This is an important observation, because clinically and radiologically indistinguishable cases of nfvPPA can be caused either by tau or by the unrelated protein TDP-43, which has been demonstrated to propagate trans-neuronally (Braak *et al.*, 2013).

Here, I go beyond these associative studies to measure tau burden and functional connectivity in the same individuals at both the whole-brain and regional level. Our observation that those brain areas that are more strongly functionally connected have accrued more tau pathology in Alzheimer's disease (Figure 2-4 A), independent of which connectivity network they belong to (Figure 2-5), is consistent with trans-neuronal spread. I demonstrate that the presence of tau is not, in itself, inducing stronger regional connectivity by our cross sectional analysis of the AD group, in which I demonstrate that as cortical tau accumulates the overall functional connectivity of cortex falls (Figure 2-4 D), and this between-subjects effect is strongest in those brain regions with most tau accumulation (Figure 2-4 F, G). Crucially, I demonstrate that [¹⁸F]AV-1451 binding potential at each node is better than the connectivity of that node in the healthy brain at accounting for regional variance in connectivity change, arguing against the presence of tau being a secondary marker of neurodegeneration in vulnerable hubs. In other words it is not coincidence that AD tends to impact large networks; it is a predictable consequence of trans-neuronal spread of a disease-causing protein. Graph theoretic models of transmissible disease epidemics are in agreement that the likelihood of an individual becoming infected (and the dose of the infectious agent received) is directly proportional to its number of infected neighbours and their infectivity (Durrett, 2010). As our nodes represent brain regions of equal volume, the binary portion of degree represents a surrogate measure of the number of neurons to

which a brain region is connected, and the weighted portion of degree is a measure of the strength of these connections. By the time Alzheimer's Disease is sufficiently advanced to cause the symptoms of mild cognitive impairment, tau is generally already present to some degree throughout neocortex (Markesbery, 2010), and therefore reaching a disease stage at which the number of neighbours more closely approximates the number of infected neighbours, and the connection strength between infected neighbours (here the weighted portion of degree) becomes a strong driver of infectivity.

Conversely, our analyses do not provide support for models of hub vulnerability due to metabolic demand or lack of trophic support in Alzheimer's disease. It is important to acknowledge that this does not mean that these mechanisms are unimportant, but rather that they are a downstream event of tau accumulation. In other words, while I demonstrate that the propensity of a node to accrue tau is not related to metabolic demand or trophic support, these factors might still contribute to determining the vulnerability of brain regions to the presence of a given amount of tau. This hypothesis could be addressed in future studies by relating the information content of tau ligand binding to other measures of neurodegeneration such as longitudinal changes in grey matter volume.

In PSP, I do find support for models of hub vulnerability due to metabolic demand and lack of trophic support, but not for models of trans-neuronal spread. This is in line with other recent studies, demonstrating that neurodegeneration in PSP is related to local gene expression patterns (Rittman *et al.*, 2016).

2.5.2 Is the difference between AD and PSP mediated by tau isoform or intrinsic connectivity?

A striking feature of our results is that I demonstrate a strong relationship between [¹⁸F]AV-1451 binding potential and the strength of functional connectivity in AD but not PSP. There are at least two potential (and not mutually exclusive) explanations for this dissociation.

The first possibility is that trans-neuronal tau propagation might occur more slowly in PSP. Cellular models have demonstrated that the propensity of tau to propagate intracellularly depends on its ability to form aggregates (Falcon *et al.*, 2015). Once

present in a new cell, the ability of tau fibrils to induce the aggregation of constitutionally present tau depends on the conformation of the fibril structure (Nonaka *et al.*, 2010, Fitzpatrick *et al.*, 2017). It might be that the straight filaments of predominantly 4R tau that characterise PSP are simply less able to propagate or need to be present in higher concentrations before they can induce a chain reaction of local tau aggregation (Guo *et al.*, 2016). This view is supported by our demonstration that tau is restricted to brainstem and deep nuclei in PSP despite these nodes being highly promiscuous between networks, displaying a high participation coefficient (Figure 2-8 B) and low clustering (Figure 2-9 B).

Secondly, it is possible that tau propagation does occur, but that it is limited in range to a subcortical intrinsic connectivity network (Raj *et al.*, 2012) (perhaps network 5 in (Laird *et al.*, 2011)). Such a subcortical network may be poorly visualised by multi-echo fMRI, and is less frequently observed at rest than the default mode network (Greicius *et al.*, 2003), which has been implicated in Alzheimer's disease (Greicius *et al.*, 2004). Together, therefore, our findings of weak functional connectivity in deep nuclei and brainstem nodes (Figure 2-4 B) might mask meaningful functional connectivity within and between these regions, accounting for the restricted and stereotyped pattern of tau accumulation in early PSP (Ellison *et al.*, 2012) and cortical escape in advanced PSP (Schofield *et al.*, 2012a).

2.5.3 Cross-sectional data reveal patterns less visible at the group level

Computational modelling of connectivity-dependent cell death predicts a dissociation between changes in functional connectivity in early and late Alzheimer's disease (de Haan *et al.*, 2012). It has been proposed that, in early disease, hubs compensate for declines in structural connectivity by increasing their firing rate, manifesting as stronger functional connectivity (Maestú *et al.*, 2015). As disease progresses, this mechanism breaks down as neural damage prevents the maintenance of this metabolically demanding compensation (Jones *et al.*, 2015). This dissociation is thought to underlie some of the seemingly inconsistent findings in the analysis of graph properties in neurodegenerative disease. By using a cross-sectional approach across a range of disease severity, I demonstrate relationships consistent with this hypothesis. In Alzheimer's disease, weighted degree (Figure 2-4 D) and betweenness centrality (Figure

2-11 A) consistently fall as tau burden increases. However, in early disease where tau burden is low (our sample includes a range of severity, including PiB positive mild cognitive impairment), the regression line for these metrics is above the control average. Similarly, examining the regional changes related to disease burden reveals striking patterns that are obscured at the group level. This underlines the more general principle that one should be cautious in interpreting a main effect of group in the presence of an interaction, or correlation with severity.

2.5.4 Re-organisation of brain networks

Our examination of two distinct tau-mediated neurodegenerative pathologies with different distributions of pathology has enabled us to distinguish their consequences. I demonstrate strongly opposing effects in a range of metrics resulting from the presence of predominantly cortical (AD) or subcortical (PSP) tau. The direction of these effects in Alzheimer's disease is consistent with the previously recognised impact of neurodegeneration, leading to increasingly random cortical connectivity (Sanz-Arigita *et al.*, 2010, Stam, 2014) and a reduction in small-world properties (Stam *et al.*, 2006). Eigenvector centrality showed particularly strong regional effects in Alzheimer's disease, with a negative correlation observed between disease-related changes in this metric and local tau burden at each node – i.e. those brain regions that displayed less tau pathology had greater functional influence on other brain regions.

In contrast, cortico-subcortical functional connectivity is preferentially impaired in PSP-Richardson's syndrome, resulting in cerebral information transfer taking a less direct path through a larger number of cortical nodes, reducing closeness centrality and eigenvector centrality, but increasing cortical degree, betweenness centrality and local efficiency. This results in an excessively modular connectivity arrangement, with decreasing participation coefficient and increasing clustering. These findings tie together classical observations of the 'subcortical dementia' phenotype of PSP (Albert *et al.*, 1974) with more modern observations that behavioural change and cognitive impairment in PSP correlates with frontal cortical hypometabolism (D'Antona *et al.*, 1985, Foster *et al.*, 1988) and atrophy (Cordato *et al.*, 2002, Cordato *et al.*, 2005). I propose that increases in cortical functional connectivity can compensate for subcortical tau burden in PSP. Increasingly indirect information transfer accounts for

the cognitive slowing that is the hallmark of the ‘subcortical dementias’, but performance on untimed tests is preserved until cortical regions become atrophic in late disease.

2.5.5 Study limitations

The main limitation of our analysis is that it is cross-sectional, and I use [¹⁸F]AV-1451 binding as a surrogate marker of tau burden. By making observations about the relationship between tau burden and functional connectivity in this way, I assume a uniformity of effect within our disease groups. As novel PET ligands such as [¹⁸F]AV-1451 gain maturity, longitudinal assessment of tau burden and functional connectivity in the same individuals will be an important and powerful validation of our results. Definite evidence of the causal relationship between tau and connectivity will require the combination of longitudinal assessment and interventional studies targeting tau pathology. It should also be noted that [¹⁸F]AV-1451 binding identifies predominantly aggregated tau in tangles, and does not directly measure oligomeric tau, which may be more toxic to the cell and synaptic plasticity, nor extracellular forms of tau that may mediate spread of pathology. The molecular binding target of [¹⁸F]AV-1451 in non-AD tauopathies is disputed; elevated ‘off-target’ binding has been demonstrated in the basal ganglia of healthy controls (Johnson *et al.*, 2016), albeit to a lesser degree than that observed in PSP (Figure 2-4 F, (Passamonti *et al.*, 2017)), and in TDP-43 associated disorders without evident tau pathology (Bevan-Jones *et al.*, 2017a). Nonetheless, [¹⁸F]AV-1451 is able to recapitulate the distribution of *post-mortem* neuropathology in these disorders, making it appropriate for use here (Smith *et al.*, 2016).

Our analysis is focussed towards cortico-cortical functional connectivity. In particular, multi-echo MRI might have a poor signal to noise ratio in deep brain structures, although the main advantage of using this sequence is that it enables robust de-noising of movement related artefacts pipeline (Kundu *et al.*, 2012, Kundu *et al.*, 2013). This is critical in clinical populations, in which fMRI data may differentially suffer from quality degradation due to head movements.

Finally, by examining proportionately thresholded graphs with 1-10% density, our analysis focusses on the strongest inter-regional functional connections. However, it is

possible that I am missing additional effects of neurodegeneration on weak or medium-strength connections. Tract-tracing studies indicate that there are weak anatomical connections, equivalent to a few axons, between some cortical areas (Ypma and Bullmore, 2016). Such weak links may have functional importance in complex networks (Granovetter, 1983). However, weak connections are difficult to evaluate with functional MRI, as it is not possible to disentangle them from correlation arising from signal noise. Future evaluation of these weaker connections with *in vivo* tractography, neuropathology or novel methods might reveal additional effects not evident in our dataset. In the interim, the thresholding procedure exhibits several advantages; by retaining only the most strongly correlated edges one is less likely to include false positive correlations and topologically random edges. It also allows the computationally intense process of normalisation of metrics against random graphs of equal density. The consistency between the results using thresholded nodal weighted degree and unthresholded nodal connectivity strength provides reassurance in the choice of thresholding of connections.

2.6 Conclusion

This study reveals the differential relationship between tau burden and functional connectivity in two distinct human neurodegenerative tauopathies. Our results enable us to disentangle the *causes* of tau accumulation from their *consequences*. They have wide-ranging implications, from the validation of models of tau trafficking in humans to corroborating computational models of hub compensation in Alzheimer's disease, while accounting for the contrasting cognitive phenotype of these two conditions. These insights into the relationship between tau burden and brain connectivity changes will inform translational models and clinical trials of disease-modifying therapies.

2.7 Chapter Summary:

Alzheimer's Disease (AD) and Progressive Supranuclear Palsy (PSP) represent neurodegenerative tauopathies with predominantly cortical vs subcortical disease burden. In AD, neuropathology and atrophy preferentially affect 'hub' brain regions that are densely connected. It was unclear whether hubs are differentially affected by neurodegeneration because they are more likely to receive pathological proteins that propagate trans-neuronally, in a prion-like manner, or whether they are selectively vulnerable due to a lack of local trophic factors, higher metabolic demands, or differential gene expression.

I assessed the relationship between tau burden and brain functional connectivity, by combining *in vivo* PET imaging using the ligand AV-1451, and graph theoretic measures of resting-state fMRI in 17 patients with AD, 17 patients with PSP, and 12 controls. Strongly connected nodes displayed more tau pathology in AD, independently of intrinsic connectivity network, validating the predictions of theories of trans-neuronal spread but not supporting a role for metabolic demands or deficient trophic support in tau accumulation. This was not a compensatory phenomenon, as the functional consequence of increasing tau burden in AD was a progressive weakening of the connectivity of these same nodes, reducing weighted degree and local efficiency and resulting in weaker 'small-world' properties.

Conversely, in PSP, unlike in AD, those nodes that accrued pathological tau were those that displayed graph metric properties associated with increased metabolic demand and a lack of trophic support rather than strong functional connectivity. Together, these findings go some way towards explaining why AD affects large scale connectivity networks throughout cortex while neuropathology in PSP is concentrated in a small number of subcortical structures. Further, I demonstrate that in PSP increasing tau burden in midbrain and deep nuclei was associated with strengthened cortico-cortical functional connectivity. Disrupted cortico-subcortical and cortico-brainstem interactions meant that information transfer took less direct paths, passing through a larger number of cortical nodes, reducing closeness centrality and eigenvector centrality in PSP, while increasing weighted degree, clustering, betweenness centrality and local efficiency.

Our results have wide-ranging implications, from the validation of models of tau trafficking in humans to understanding the relationship between regional tau burden and brain functional reorganization.

Chapter 3: Top-down frontal contributions to predictive processes in speech perception

3.1 Preface

Chapter 2 provided a link between the molecular pathology of neurodegeneration and the physiology of dementia in terms of functional connectivity. In this experimental chapter I explore how disruption of neural circuits gives rise to changes in core cognitive systems. To do this, I turn to a new model disease, non-fluent variant Primary Progressive Aphasia (nfvPPA). This disease is an ideal model for behavioural studies as it has a clinical phenotype that is restricted to the speech domain in early disease, allowing for precisely controlled auditory psychophysical assessment supported by well-preserved general cognition in early disease. Additionally, the focal pattern of mild atrophy in frontal lobes with relatively preserved cortical volume elsewhere greatly simplifies the analysis of neurophysiological data.

The concept for this study arose from the clinical observation that our patients with nfvPPA, who have classically been thought to have an output aphasia, were complaining of deafness unrelieved by hearing aids. This symptom had previously been validated by the observation that patients with nfvPPA perform surprisingly poorly at some tasks of basic auditory processing (Goll *et al.*, 2010, Grube *et al.*, 2016). However, the reasons for these deficits were poorly explained. Separately, for his PhD Ediz Sohoglu (supervised by my advisor, Dr Matt Davis) conducted a series of experiments in young healthy individuals in which he assessed the perceptual and neurophysiological impacts of manipulating prior expectations for word identity (Sohoglu *et al.*, 2012, Sohoglu *et al.*, 2014). He demonstrated that this manipulation modulated activity in the same frontal brain regions in which patients with nfvPPA have significant neurodegeneration, and activity in temporal brain regions, where patients do not have significant neurodegeneration. The question therefore arose as to whether abnormal, network-level neural processing of prior expectations might account for the perceptual symptoms in nfvPPA, and whether the demonstration of a diaschisis in temporal lobe activity caused by frontal neurodegeneration might provide

evidence for causal top-down frontal contributions to predictive processes in speech perception. In this chapter I primarily address the latter question, examining normative language functioning using nfvPPA as a model of abnormal network function. In chapter 5, I discuss the implications of this work for our understanding of receptive auditory difficulties in nfvPPA.

A paper based on this chapter has been published in *Nature Communications* with myself as first author (Cope *et al.*, 2017a). The study was conceptualised by my supervisor Prof James Rowe and my advisor Dr Matt Davis. Experiment one is based on a paradigm developed by Dr Ediz Sohoglu, and I am very grateful to him for allowing me to use his stimulus presentation materials. I modified these materials to ensure suitability for our participants with advice and guidance from Prof Karalyn Patterson and Mrs Kate Dawson (research nurse). I developed experiment two together with my advisor. I am grateful to Dr Helen Blank for the stimuli used in that experiment (Blank and Davis, 2016). I developed the subjective symptom rating scales with advice from Dr Bob Carlyon. I am grateful to Dr Manon Grube for allowing me to exactly replicate a subset of the experiments from her *Brain* paper (Grube *et al.*, 2016), using her computer code. I collected all of the behavioural and MEG data. I am grateful to Mrs Julie Wiggins (research nurse) for accompanying the patients to their structural MRI scans. The Bayesian perceptual modelling is based on work previously published by Dr Sohoglu (Sohoglu and Davis, 2016), developed by myself to allow for the assessment of perceptual clarity and derivation of quantitative parameters (https://github.com/thomascope/Bayesian_Model_Code). I undertook all MEG analyses, but I was afforded a head-start by the kind sharing of computer code and detailed advice from Dr Ediz Sohoglu, Prof Richard Henson and Dr William Sedley. I updated this code for SPM12, and integrated it into a standardised pre-processing pipeline that is publically available and has now been used by others (<https://github.com/thomascope/VESPA/tree/master/SPM12version/Standalone%20preprocessing%20pipeline/seconddistrib>). I analysed the structural MRI data with guidance from Mr P Simon Jones. I am grateful to Dr Bob Carlyon, Prof Richard Henson, Prof Tim Griffiths and Dr Dennis Norris for productive external perspectives about data interpretation, and to Dr Kieren Allinson for neuropathological opinion. Finally, I am indebted to six anonymous reviewers (two at *Science* and four at *Nature*

Communications) for helpful suggestions of refinements to the Bayesian modelling and additional MEG analyses of single subject timecourses, coherence and connectivity. I constructed all of the figures, and wrote the text with comments from all of those listed above.

3.2 Introduction

It has long been recognised that perception relies on the integration of sensory input with expectations based on prior knowledge or experience (von Helmholtz, 1925 translation of 1868 original). This can be instantiated in hierarchical generative models, which contain both top-down connections for priors or beliefs about sensory evidence, and bottom-up connections for recognition or prediction error. The layers of these hierarchical models represent progressively more abstract descriptions of the underlying sensory data (Hinton, 2007, Friston, 2008). An influential implementation of hierarchical generative models is known as predictive coding (Rao and Ballard, 1999, Friston, 2005), in which the top-down generative connections express predictions for expected sensory signals while bottom-up processes pass forward prediction errors to update the model (Figure 3-1 A). This method of information transfer is highly efficient (Musmann, 1979). Neural models of predictive coding are well formalised, and I set our results into this framework throughout the manuscript, but it should be emphasised that the results I present are equally applicable to all hierarchical generative frameworks involving top-down and bottom-up influences at each processing stage.

There is empirical evidence for predictive coding in health, for vision (Murray *et al.*, 2002, Alink *et al.*, 2010), hearing (Arnal *et al.*, 2009, Grahn and Rowe, 2009, Phillips *et al.*, 2016) and the link between perception and action in motor control (Kilner *et al.*, 2007, Shipp *et al.*, 2013, Wolpe *et al.*, 2016). Furthermore, dysfunctional predictive coding mechanisms can explain a range of neurological and psychiatric phenomena, in schizophrenia (Brown *et al.*, 2013), functional movement disorders (Edwards *et al.*, 2012, Pareés *et al.*, 2014), alien limb syndrome (Wolpe *et al.*, 2014), tinnitus (Sedley *et al.*, 2016) and hallucinations (Kumar *et al.*, 2014). Although these disorders have been explained in terms of aberrant predictive coding, the functional consequences of degradation of the neural architecture responsible for generating top-down predictions are unknown. This is a critical and novel test for hierarchical models of perception, which motivates the following hypothesis: degeneration of top-down prediction mechanisms in frontal lobe should have a substantial impact on lower-level sensory responses in temporal lobe, and should impair perceptual function when prior knowledge and sensory input must be combined.

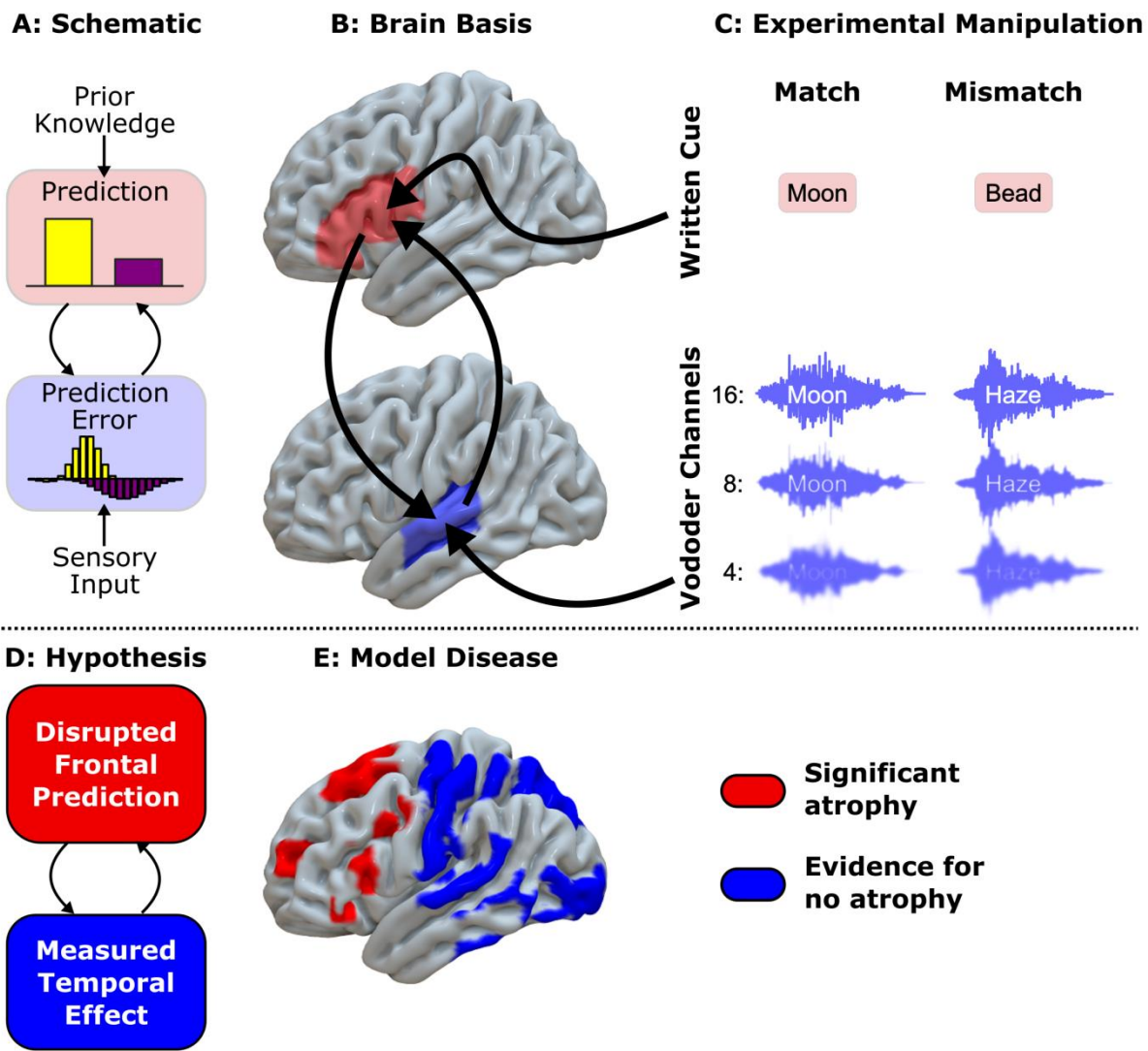


Figure 3-1 An illustration of the experimental motivation.

A: A schematic Bayesian framework for predictive coding in speech perception. B: The putative brain basis of this framework (Park et al., 2015). Predictions are generated in inferior frontal gyrus and/or frontal motor speech regions (pink), and instantiated in auditory regions of superior temporal lobe (pale blue). C: The two dimensional experimental manipulation employed here to detect a dissociation between normal temporal lobe responses to sensory detail (number of vocoder channels) and abnormal frontal lobe responses to prior congruency. D: Our experiment relies on detecting the consequences of degraded predictions in abnormal frontal brain regions by measuring their effects in normal temporal regions. E: Voxel-based morphometry in our patient group. Regions coloured in red displayed consistent reductions in grey matter volume (FWE $p < 0.05$). Regions coloured blue had strong evidence for normal cortical volume in nfvPPA (Bayesian probability of the null > 0.7 , cluster volume $> 1\text{cm}^3$). Uncoloured (grey) areas had no strong evidence for or against atrophy.

I test this hypothesis in the context of neurodegeneration of the language network from nfvPPA. Speech is a natural domain in which to study predictive coding, as humans are

able to exploit a wide variety of visual, contextual and semantic cues to improve perception, especially in difficult listening environments (Sumbly and Pollack, 1954, Miller and Isard, 1963). Indeed, contradictory beliefs established by mismatching visual and auditory speech can lead to false perception (McGurk and MacDonald, 1976, Van Wassenhove *et al.*, 2005). It is important to note that such multi-modal integration can be modelled in terms of predictive coding regardless of whether or not visual information occurs before auditory information (Schwartz and Savariaux, 2014); what is important is that auditory sensory predictions are set up based on information from prior experience, sentential context or sensory information from another domain. I exploited the importance of written text in supporting perception of degraded speech (Remez *et al.*, 1981, Sohoglu *et al.*, 2014) (Figure 3-1 C). There is evidence for left lateralised top-down information transfer (Park *et al.*, 2015) from frontal language (Abdelnour *et al.*, 2014) and motor speech (Raj *et al.*, 2012, Raj *et al.*, 2015) regions to auditory cortex during speech perception (Figure 3-1 B); in predictive coding theory this top-down transfer generates prior expectations for speech content and explains how listeners combine prior knowledge and sensory signals during perception and perceptual learning (Blank and Davis, 2016, Sohoglu and Davis, 2016).

To assess the effects of disrupted predictions (Figure 3-1 D) I studied patients with early non-fluent primary progressive aphasia (nfvPPA), which is associated with selective neurodegeneration of the frontal lobe language and motor speech areas (Murray *et al.*, 2005), but preservation of temporal lobe auditory regions (Figure 3-1 E). Disordered speech output in nfvPPA is characterised by apraxia of speech and/or agrammatism (Gorno-Tempini *et al.*, 2011). In contrast to stroke aphasia the neural damage in frontal regions is partial (Mackenzie *et al.*, 2006, Sampathu *et al.*, 2006, Mohandas and Rajmohan, 2009, Mackenzie *et al.*, 2011) enabling us to study a disruption of predictive mechanisms, rather than a system reorganised following their complete absence. Additionally, this patient cohort presents fewer problems for the modelling and interpretation of magnetoencephalography (MEG) or electroencephalography (EEG), as atrophy is subtle in early nfvPPA (Gorno-Tempini *et al.*, 2004, Rogalski *et al.*, 2011).

For patients and matched control participants I recorded behavioural and neural data showing the influence of top-down and bottom-up manipulations on speech perception

using a well-understood paradigm involving presentation of written text that matches or mismatches with degraded spoken words (Sohoglu *et al.*, 2012, Sohoglu *et al.*, 2014, Blank and Davis, 2016) (Figure 3-1 C). With this paradigm, I can determine whether and how frontal cortical neurodegeneration impairs speech perception. The presence and function of top-down influences on speech perception is controversial (see (Norris *et al.*, 2000, McClelland *et al.*, 2006, McQueen *et al.*, 2006, Norris *et al.*, 2016)), as is the question of whether frontal cortical regions make a critical contribution to speech perception, through predictive coding or alternative mechanisms. Some authors suggest that these contributions are task-specific and not a core component of speech perception systems (Lotto *et al.*, 2009). The present study provides causal neural evidence with which to assess both of these claims.

I hypothesised that, if the frontal lobes play a central role in the reconciliation of predictions with sensory evidence, frontal neurodegeneration would result in a disrupted neural effect of prior context in temporal lobe speech regions. Further, if predictive coding is a core mechanism for speech perception, then I hypothesised that frontal neurodegeneration would disrupt the application of prior knowledge, leading to aberrant speech perception in nfvPPA patients.

3.3 Methods:

All study procedures were approved by the UK National Research Ethics Service. Protocols for magnetoencephalography and magnetic resonance imaging were reviewed by the Suffolk Research Ethics Committee, and for neuropsychological tests outside of the scanner environments by the County Durham & Tees Valley Ethics Committee. All participants had mental capacity and gave informed consent to participation in the study.

3.3.1 Participants

Eleven patients with early nfvPPA were identified according to consensus diagnostic criteria (Gorno-Tempini *et al.*, 2011). Particular care was taken to exclude patients with yes/no confusion that would confound behavioural analysis, and to include only those who lacked the lexical difficulties of logopenic and mixed aphasias, in order to

select patients most likely to have underlying tau or TDP-43 related pathology preferentially involving frontal lobes (rather than Alzheimer-type pathology of parietal lobes) (Rogalski *et al.*, 2011, Rohrer *et al.*, 2012, Sajjadi *et al.*, 2012, Sajjadi *et al.*, 2014, Mandelli *et al.*, 2016). On the short form of the Boston Diagnostic Aphasia Examination all patients scored 10/10 for responsive naming, 12/12 for special categories, at least 15/16 for basic word discrimination and at least 9/10 for following complex commands. One patient was unable to tolerate the MEG scanner environment so, for that case, results contribute only to the behavioural analysis.

I obtained standardised volumetric T1 MRI scans on nine of the patients within two months of their MEG session, for co-registration and voxel-based morphometry.

Eleven age-, gender- and education-matched controls were recruited for behavioural and physiological studies (demographic information in Table 3-1). Thirty-six healthy age-matched control MRI datasets were selected for voxel-based morphometry.

	Number	Age	Gender	Age leaving Education	MMSE	ACE-R	Raven's Matrices
nfvPPA	11	72 (9)	8F, 3M	18 (3)	28 (2)	84 (12)	36 (9)
MEG Controls	11	72 (8)	7F, 4M	17 (2)	29 (1)	95 (2)	46 (7)
MRI Controls	36	73 (7)	17F, 19M	-	-	-	-

Table 3-1 Demographic details of the experimental groups.

Mean (standard deviation). There were no statistically significant differences in age, gender or education between nfvPPA patients and MEG controls. nfvPPA patients scored more poorly than controls on the Addenbrooke's Cognitive Examination (Revised) and Raven's Progressive Matrices, but were still within the population normal range. Most of the difference between nfvPPA and controls on the ACE-R was accounted for by verbal fluency. Audiometric thresholds are available in Figure 3-2 B. One patient was unable to tolerate the MEG scanner environment so, for that case, results contribute only to the behavioural analysis.

3.3.2 Voxel Based Morphometry

Nine patients with nfvPPA underwent structural MR imaging at the Wolfson Brain Imaging Centre, University of Cambridge, UK using a 3T Siemens Magnetom Tim Trio scanner with a Siemens 32-channel phased-array head coil (Siemens Healthcare,

Erlangen, Germany). A T1-weighted magnetization-prepared rapid gradient-echo (MPRAGE) image was acquired with repetition time (TR)=2300ms, echo time (TE)=2.86ms, matrix=192x192, in-plane resolution of 1.25x1.25mm, 144 slices of 1.25mm thickness, inversion time=900ms and flip angle=9°. These images were compared to 36 healthy control scans with identical parameters.

All analysis was performed using SPM12 (<http://www.fil.ion.ucl.ac.uk/spm>). Images were first approximately aligned by coregistration to an average image in MNI space, before segmentation and calculation of total intracranial volume (TIV). After segmentation, a study-specific DARTEL template was created from the patient scans and the 9 closest age-matched controls using default parameters. The remaining controls were then warped to this template. The templates were affine aligned to the SPM standard space using 'Normalise to MNI space' and the transformation applied to all individual grey-matter segments together with an 8mm FWHM Gaussian smoothing kernel. The resulting images were entered into a full factorial general linear model with a single factor having two levels, and age and TIV as covariates of no interest. This model was estimated in two ways. Firstly, a classical estimation based on the restricted maximum likelihood was performed to assess for group difference. Voxels were defined as atrophic if they were statistically significant at the peak FWE $p < 0.05$ level. Secondly, a Bayesian estimation was performed on the same model, and a Bayesian contrast between patients and controls specified. The resulting Bayesian map was subjected to hypothesis testing for the null in SPM12, resulting in a map of the posterior probability of the null at each voxel. For visualisation in Figure 3-1 E, this map was thresholded for posterior probabilities for the null above 0.7 and cluster volumes of greater than 1cm³.

To assess for the dissociation between atrophic and preserved cortical regions, both model estimations were assessed at voxels of interest. Atrophic regions were assessed with classical statistical parametric mapping across the whole brain. This identified highly significant peaks centred in left (MNI -37, 17, 7) and right (MNI 37, 20, 6) inferior frontal regions but no peaks in superior temporal regions (supplementary table 1). Superior temporal voxels of interest were therefore defined from the Neuromorphometrics atlas, at locations corresponding to left primary auditory cortex (MNI -59, -24, 9) and superior temporal gyrus (MNI -67, -17, 3). Frequentist

probability of atrophy and Bayesian probability of no atrophy are reported at each of these four locations in results.

To create Figure 3-1 E, a rendering of the significant regions in each analysis, the DARTEL template images were further warped using the 'Population to ICBM Registration' function with the transformation parameters applied to all thresholded statistical maps.

To extract grey matter volume for correlation with the latency of MEG responses (Figure 3-11 E, F), a full factorial general linear model was constructed with the 9 patients alone, with age and TIV as covariates of no interest. Each subject's age and TIV adjusted grey matter density was extracted at the voxel closest to the MEG regions of interest (left frontal [-46 2 28]; left temporal [-56 -34 12]). A secondary SPM analysis with neural latency entered as a covariate into the model and small volume correction of 8mm (to match the FWHM Gaussian smoothing kernel) at each location confirmed the results of the primary analysis – correlations below $p < 0.05$ were observed at the frontal but not the temporal location.

3.3.3 Modifications to Sohoglu MEG paradigm

Stimuli and experimental procedures during neuroimaging were closely modelled on a task previously performed to evaluate influences of prior knowledge and sensory degradation in young, healthy listeners (Sohoglu *et al.*, 2012) (Figure 3-3 A). In this task, individuals are presented with a written word, followed 1050 (+/-50) ms later by a spoken word, which is acoustically degraded using a noise vocoder (Shannon *et al.*, 1995). After a further delay of 1050 (+/-50) ms, participants are asked to rate the perceptual clarity of the vocoded word. This allows for a factorial manipulation of two stimulus dimensions that in previous studies have been shown to affect speech perception: (1) the degree of correspondence between the written and spoken words can be modified by presenting text that either matches or mismatches with the speech, (2) the amount of sensory detail can be manipulated by varying the number of channels in the noise vocoder. 108 trials of each condition were presented across six blocks. Each block contained 18 trials of each combination of vocoder channel number and cue congruency in one of two fixed random orders counterbalanced across groups. To

avoid predictability, each subject observed 216 words twice in written form and twice in spoken form (once as part of a match pair and once as part of a mismatch pair) and 108 words only once (in either a match or mismatch pair). The following modifications were made to the Sohoglu *et al.* paradigm in order to simplify procedures for patients and elderly controls. The number of channels used in the vocoder was doubled to 4/8/16, the range expected to cover the steepest portion of the psychometric response function in older adults (Sheldon *et al.*, 2008). The duration of the visual prime was increased from 200ms to 500ms. The resolution of the clarity rating scale was reduced from 1-8 to 1-4, so that a four-button box could be used to indicate responses. Finally, the neutral priming condition was removed to reduce the overall number of trials inside the scanner by a third, while minimising the reduction in the power with which I could test for an effect of prime congruency. 108 trials of each condition were presented across six presentation blocks. A fully crossed 2x3 factorial design was employed, with two levels of prime congruency (matching/mismatching) and three levels of sensory detail (4/8/16 vocoder channels). Each spoken word was presented no more than twice to each participant, once with a congruent prime and once with an incongruent prime.

3.3.4 Behavioural data stimuli and procedure

To ensure that I was observing an effect of prediction and that patients were not simply being confused by mismatching written words, experiment 1 was repeated outside the scanner with identical parameters but an additional, neutral, cue condition (Figure 3-8), mirroring that of Sohoglu *et al.* (2012). 18 trials of each condition were presented in a single block.

A second experiment was undertaken to assess participants' ability to identify vocoded words. In this task, (Figure 3-3 C), no prior written text was provided. Participants simply heard a noise vocoded word and, 1050 +/- 50 ms after word onset, were presented with four alternatives, from which they selected the word that they had heard. I used this forced choice response format to ensure that performance was not confounded by speech production difficulties. As in experiment 1, the clarity of the spoken word was varied between 4, 8 and 16 noise vocoder channels. The closeness of the three distractor items to the correct response was also varied by manipulating the number of neighbours between the spoken word and the alternatives. In the example

shown in Figure 3-3 C, the spoken word is ‘Gaze’. The alternatives presented to the participant comprised ‘Daze’ (an offset neighbour), ‘Gaze’ (the target), ‘Game’ (an onset neighbour), and ‘Then’ (not a neighbour). This set of four response alternatives occurred in trials where the spoken word was either: (1) “Gaze” (such that there were two word neighbours, “Daze” and “Game” in the response array), (2) “Daze” (only one onset neighbour, “Gaze”), (3) “Game” (one offset neighbour “Gaze”), or (4) “Then” (no neighbours in the response array). This achieved a factorial experimental design with a 3-level manipulation of sensory detail fully crossed with a 4-level manipulation of distractor difficulty. There were 90 trials in a single block; at each of the 3 levels of sensory detail there were 10 spoken words in each of cases (1) and (4) above, and 5 each in (2) and (3). This resulted in 30 sets of four response options each being presented three times and having 3 of its 4 members heard during the experiment. Word presentation orders were randomised across participants, but the sensory detail and written neighbour difficulty order was fixed.

Auditory stimuli were presented in a quiet room through Sennheiser HD250 linear 2 headphones, driven by a Behringer UCA 202 external sound card, and visual stimuli were displayed on a laptop computer screen. Participants indicated responses either by pressing a number on a keyboard (clarity rating outside of MEG) or a button on a custom made response box (all other experiments).

3.3.5 Behavioural data modelling

Subjective ratings of clarity were modelled using an hierarchical Bayesian inference approach previously described for data of this type (Sohoglu and Davis, 2016) (Figure 3-9). This model exploits the principles of predictive coding, in which perception arises from a combined representation of sensory input and prior beliefs (Rao and Ballard, 1999, Friston, 2005, Hickok, 2012). It is able to explain both the perceptual benefit of matching prior information, as the precision of the ‘posterior’ (or subjective experience) is increased by congruency between the prior and the sensory input, as well as the previously observed dissociated modulations in superior temporal gyrus activity by cue congruency and sensory detail (Sohoglu *et al.*, 2012, Sohoglu and Davis, 2016).

The model is able to predict subjective clarity as a function of the precision of the posterior distribution, which is estimated as the precision of the sensory input multiplied by a weighted function of the precision of the prior. The weighting given to the prior information depends on its congruency. In the case of a mismatching prior, the precision of the posterior simply matches the precision of the sensory input, while for matching priors it increases as a function of the precision of prior expectation. Finally, the precision of the posterior is compared against a perceptual threshold (below which degraded speech is deemed completely unclear and given a rating of 1), and the height above this threshold is mapped to the rest of the rating scale (subjects were instructed to use the full range of the rating scale, and undertook practice trials to familiarise themselves with the range of experimental stimuli – all subjects were able to do this).

The precision of the sensory input was individually pre-defined for each subject at each level of sensory detail, based on their measured ability to correctly report words with that number of vocoder channels (Figure 3-3 D). The weighting of matching prior information was defined as 0.5, reflecting the experimental context in which 50% of written words were congruent with (i.e. matched) the degraded spoken words. In ‘open set’ listening situations like those used in the present experiment, the weighting of prior expectation for the occurrence of any uncued word is the inverse of the number of nouns in the participant’s lexicon. I therefore approximated the weighting to zero for both mismatching and neutral prior expectations (Blank and Davis, 2016). This accounts for the observation that clarity ratings in this and previous experiments were almost identical following mismatching and neutral (uninformative) written words (Sohoglu *et al.*, 2012, Sohoglu *et al.*, 2014).

It is possible that the patients might have an inappropriately high ‘weighting’ for the written cue. In other words, they apply their prior expectations ‘inflexibly’, being unable to account for the fact that they will only be correct half the time. As we have a binary situation (the text was either fully matching or fully mismatching) I am unable to assess this possibility directly – in my model allowing the weighting of matching prior information to vary would be mathematically equivalent to allowing the precision of the prior to vary. Accordingly, I use the terms ‘excessively precise priors’ and ‘inflexible priors’ interchangeably.

The precision of the prior expectation and the level of the perceptual threshold were then individually optimised to provide the best-fit to each subject's clarity ratings by global minimisation of squared residuals (using the Global Optimisation Toolbox in MATLAB).

3.3.6 Alternative data models

It was observed that model fits were less good for the mismatch condition in some controls, with the model systematically under-predicting slope. The primary driver of this effect seemed to be a 'washing out' of the effect of prior knowledge in the face of very clear speech for some individuals (i.e. there is less perceptual clarity benefit to prior knowledge if the auditory token is itself very clear). This has been previously observed in young healthy individuals (Sohoglu *et al.*, 2012, Sohoglu *et al.*, 2014) and seems to result from participants nearing the upper end of their psychometric response functions and entering a region of non-linear response. That is, doubling from 8 to vocoder 16 channels results in more benefit in terms of perceptual clarity than doubling from 16 to 32 channels. Indeed, as can be observed from Figure 3-3 D many controls are reaching ceiling performance at reporting 16 channel vocoded speech in the absence of prior information. While we know that humans are able to detect sensory detail changes even in the face of unimpaired word identification (think, for example, of hi-fi reviews), it is not unreasonable to assume that these changes in perceptual clarity might result in smaller rating changes than those that meaningfully improve word identification performance.

The model as originally formulated does not account for non-linearities of this type because the relative increase in the precision of the posterior distribution resulting from congruent prior expectations is modelled as being a constant function of sensory detail. In reality, congruent prior expectations are shifting the position on the psychometric response function (see (Sohoglu *et al.*, 2014)). As I do not have experimental data for higher degrees of sensory detail (for example unprimed 24 or 32 channel speech) I cannot account for this directly. If, however, I allow the weighting of prior expectations to vary in the Match case for 16 channel speech this would simulate the effect of entering a flatter portion of the psychometric response function. Doing this did improve the model fits overall by reducing the under-prediction of slope in the

controls. Although this resulted in small changes in the optimised values of the other model parameters it did not affect any of the statistical results or relationships reported in the chapter (the priors are still more precise in the patients at $p < 0.01$, and their precision still significantly correlates with beta power during the instantiation of predictions with $r = -0.51$).

I compared the performance of the original model and the new model with the Akaike information criterion (corrected for small samples, AICc), which assesses whether additional model parameters sufficiently improve the information provided to account for reductions in parsimony. The simpler (original) model was favoured for 10 of the 11 patients, and 8 of the 11 controls. On average, the simpler model had an AICc 4.02 points lower than the more complex model (lower AICc scores are better).

Therefore, I retain the original model in the results section. Overall, however, I take reassurance from the fact that both models result in the same statistical relationships between the precision of prior expectations and beta power during the instantiation of predictions.

3.3.7 MEG and EEG data acquisition and analysis

An *Elekta Neuromag Vectorview System* was used to simultaneously acquire magnetic fields from 102 magnetometers and 204 paired planar gradiometers, and electrical potentials from 70 Ag-AgCl scalp electrodes in an *Easycap* extended 10-10% system, with additional electrodes providing a nasal reference, a forehead ground, and paired horizontal and vertical electrooculography. All data were digitally sampled at 1kHz and high-pass filtered above 0.01Hz. Head shape, EEG electrode locations, and the position of three anatomical fiducial points (nasion, left and right pre-auricular) were measured before scanning with a 3D digitiser (Fastrak Polhemus). The initial impedance of all EEG electrodes was optimised to below 5 kiloOhms, and if this could not be achieved in a particular channel, or if it appeared noisy to visual inspection, it was excluded from further analysis.

During data acquisition, the 3D position of five evenly distributed head position indicator coils was monitored relative to the MEG sensors (magnetometers and gradiometers). These data were used by Neuromag Maxfilter 2.2, to perform Signal

Source Separation (Taulu *et al.*, 2005) for motion compensation, and environmental noise suppression.

Subsequent pre-processing and analysis was undertaken in SPM12 (Wellcome Trust Centre for Neuroimaging, London, UK), FieldTrip (Donders Institute for Brain, Cognition, and Behavior, Radboud University, Nijmegen, The Netherlands) and EEG lab (Swartz Center for Computational Neuroscience, University of California San Diego), implemented in MATLAB 2013a. Artefact rejection for eye movements and blinks was undertaken by separate independent component analysis decomposition for the three sensor types. For MEG data, components were automatically identified that were both significantly temporally correlated with contemporaneous electrooculography data and spatially correlated with separately acquired template data for blinks and eye movements. For EEG data, components spatially and temporally consistent with eye blinks were automatically identified with ADJUST (Mognon *et al.*, 2011). These components were then projected out from the dataset with a translation matrix. Due to a technical difficulty during acquisition, one control subject had no signal recorded from two thirds of their EEG sensors, and one patient had seven sensors that failed quality control – these individuals were excluded from the EEG analysis, but included in MEG and behavioural analyses.

For evoked analysis, the data were then sequentially epoched from -500 to 1500ms relative to speech onset, downsampled to 250Hz, EEG data referenced to the average of all sensors, baseline corrected to the 100ms before speech onset, lowpass filtered below 40Hz, robustly averaged across epochs, refiltered below 40Hz (to remove any high frequency components introduced by the robust averaging procedure), planar gradiometer data were root-mean-square combined, all data were smoothed with a 10mm spatial kernel and 25ms temporal kernel before conversion to images in a window from -100 to 900ms for statistical analysis.

For induced analysis, the de-artefacted continuous data were downsampled, re-referenced, baseline corrected as above, lowpass filtered below 100Hz, notch filtered to exclude line noise between 48 and 52Hz, then epoched, before being submitted to four separate time frequency decompositions by the Morlet wavelet method: two separate time windows of -500 to 1500ms relative to written word and speech onsets were examined, with and without pre-subtraction of the condition-averaged waveform from

every trial. These were robustly averaged and log rescaled compared to pre-visual baseline power in each frequency band. Morlet decomposition parameters were focused for sensitivity to low-mid frequencies, with 7 wavelet cycles in a range from 4 to 80Hz in steps of 2Hz.

3.3.8 Sensor-space evoked analysis

For each sensor type separately, a flexible factorial design was specified in SPM12, and interrogated across all participants for main effects of prime congruency and clarity. For all sensor types, a scalp position of peak effect was defined where peak FWE $p < 0.01$. The sensor data at this scalp position was then compared across groups at every time point. A significant group x condition interaction was defined as at least 7 consecutive timepoints of $p < 0.05$, exceeding the temporal smoothing induced by lowpass filtering at 40Hz. This approach does not represent double-dipping as the location of interest was defined by an orthogonal contrast (Friston and Henson, 2006, Kriegeskorte *et al.*, 2009, Kilner, 2013), and in any case for the effect of congruency (where group x condition interactions were observed with this method), for both the planar gradiometers and the magnetometers the location of peak effect for patients alone was within 2mm of the conjoint peak effect.

3.3.9 Evoked data source reconstruction

Source inversion methods by the sLORETA algorithm were identical to those employed by Sohoglu *et al.* (2012), except that they were undertaken in SPM12 rather than SPM8. It was observed that the time windows of interest defined in healthy young controls were slightly earlier than the main data features in my cohort of more elderly controls, who displayed similar overall profiles to patients with nvPPA (Figure 3-4). The time windows of interest were therefore slightly lengthened and delayed, to ensure that the main data variance was captured.

The aim of the source data analysis was to localise and explore the brain basis of the group by congruency interaction statistically demonstrated in the sensor space data. While localisation of the main effect of clarity was undertaken across all individuals,

and is shown in Figure 3-7, in the absence of a group by clarity interaction in sensor space, no further analysis was performed on this condition.

From the previous studies in healthy young controls, it was anticipated that significant main effects of congruency would be observed in opposite directions in left frontal regions and left superior temporal gyrus. This was indeed the case, with a small left frontal region being significantly more active across the whole time window with Matching prior information, and a larger region centred on left superior temporal gyrus being significantly more active with Mismatching prior information. These peak locations were defined as voxels of interest, and the source power averaged for each condition at each location within every time window of interest for every individual. Independent, repeated measures ANOVAs were then performed in each time window. Those that demonstrated a statistically significant main effect of group or a group by congruency interaction are illustrated in Figure 3-7 C (the main effect of congruency was not examined, as this would represent double dipping at these voxels).

3.3.10 Sensor-space induced analysis

The primary analysis of induced data was undertaken in the planar gradiometers because of their superior signal to noise ratio for data of this kind (Muthukumaraswamy and Singh, 2013). Other sensor types were examined secondarily to check for consistency of effect, which was confirmed in all cases. Visual inspection of the time x frequency data at a variety of scalp positions revealed no clear difference in the pattern of effect (although its strength differed, as shown in Figure 3-12), so data were collapsed across all sensors for statistical comparison. A flexible factorial design was specified in SPM12 for time x frequency data across a time window of -100 to 1000ms, and interrogated across all participants for all contrasts of interest (main effects of group, prime congruency and sensory detail, all pairwise and the three-way interaction). A second, confirmatory, analysis was performed with the condition-averaged waveform subtracted from every trial with identical statistical results, demonstrating that the effects were induced rather than evoked (I make no claims as to whether they are dynamic or structural (David *et al.*, 2006)).

3.3.11 Induced data source reconstruction

The significant group by condition interactions observed in alpha and beta frequency bands were localised with the ‘Data Analysis in Sensor Space’ toolbox in SPM12. sLORETA was not available in this toolbox, so for closest comparability with the evoked reconstructions, the eLORETA algorithm was used. Reconstructions used time frequency data at the frequency of maximum group x congruency interaction, +/-6Hz. Data were truncated at 50 principal components, to avoid any problems with beamforming after Signal Source Separation, which reduces the number of independent components in the data to around 70 (Taulu *et al.*, 2005). Lead fields were calculated over a window of interest from 350ms to 900ms, and sources reconstructed in three separate time windows of equal duration defined by the sensor space group x congruency interaction: 300-450ms, where controls had a greater main effect of congruency; 450-600ms, where there was no group x congruency interaction; and 600-750ms, where patients had a greater main effect of congruency. A flexible factorial design was specified in SPM12, and the group by congruency interaction (already statistically demonstrated across the whole brain) thresholded for visualisation at uncorrected $p < 0.01$.

3.3.12 Coherence and Connectivity Analyses

The timeseries of the frontal ([-46,2,28]) and temporal ([-56,-34,12]) sources of interest (see Figure 3-7 B) were extracted between 0 and 912ms after every spoken word using the function `spm_eeg_inv_extract`. The condition-averaged waveform (i.e. the evoked response) in each source was then subtracted from every trial to result in data with zero-mean and approximate stationarity within the time window of interest. The Fourier spectra were then computed in FieldTrip using multitapers with a +/- 4Hz smoothing box. This decomposition was then subjected to separate FieldTrip connectivity analyses with either imaginary coherence or Granger causality (based on an optimised multivariate auto-regressive model of maximum order 10 (Harrison *et al.*, 2003, Schnitzler and Gross, 2005)). This same procedure was repeated 1000 times with the trial labels in each region shuffled to create a null distribution. Statistical assessment of the presence of coherence or connectivity at each frequency involved the

comparison of the observed data against the null distribution (Figure 3-13 A, C). Between-group comparisons of imaginary coherence employed unpaired t-tests with unequal variance (the normality assumption was not violated), cluster corrected for multiple comparisons (Figure 3-13 B). To compare the strength of Granger causal relationships between regions, I first corrected for differences in signal to noise ratio between subjects and regions by dividing the magnitude of each frequency value by the across-frequency mean for that individual-region pair. This created a profile of relative influence for each region at each frequency, corrected for overall differences in signal strength. At each frequency, the significance of ‘directionality’ (i.e. temporal to frontal vs frontal to temporal) was assessed with a repeated measures general linear model, and the output corrected for multiple comparisons (Figure 3-13 D).

3.4 Results:

3.4.1 Structural consequences of nfvPPA

To confirm the dissociation between frontal atrophy and intact temporal cortex, upon which my experiment relies, I used voxel-based morphometry to compare grey matter volume in my patients with nfvPPA to 36 age-matched healthy individuals. As anticipated, brain regions of interest displayed a localised pattern of atrophy in nfvPPA (Figure 3-1 E), with grey matter volume loss in left inferior frontal regions (whole brain peak FWE $p = 0.001$ at MNI [-37, 17, 7]; Bayes posterior probability of no difference <0.00001), but not in left primary auditory cortex (FWE $p = 1$; Bayes posterior probability of no difference 0.75 at MNI [-59, -24, 9]) or superior temporal gyrus (FWE $p = 1$; Bayes posterior probability of no difference 0.91 at MNI [-67, -17, 3]). Significant atrophy was also observed in right inferior frontal regions (FWE $p = 0.004$; peak MNI [37, 20, 6]) but not right primary auditory cortex (FWE $p=1$ at MNI [59, -24, 9]) or superior temporal gyrus (FWE $p = 1$ at MNI [67 -17 3]). Significant atrophy in left inferior frontal regions lay within pars triangularis, pars opercularis and anterior insula in the Desikan-Killiany Atlas (see Table 3-2 for significantly atrophic clusters and their probabilistic centre of mass based on the Neuromorphometrics atlas).

cluster	cluster	peak	peak	MNI Co-ordinates			Neuromorphometrics region
p (FWE)	voxels	p (FWE)	t-score	x	y	z	
0.001	751	0	6.95	-14	25	53	Left Superior Frontal Gyrus
0	1675	0	6.92	11	8	58	Right Supplementary Motor Cortex
		0.001	6.52	5	-1	49	Right Supplementary Motor Cortex
		0.001	6.5	4	0	62	Right Supplementary Motor Cortex
0.001	879	0.001	6.65	-35	17	7	Left Frontal Operculum
		0.021	5.46	-49	19	12	Left Opercular Part of Inferior Frontal Gyrus
0.002	638	0.001	6.49	31	-4	56	Right Precentral Gyrus
		0.018	5.53	28	2	49	Right Middle Frontal Gyrus
		0.018	5.52	19	0	58	Right Superior Frontal Gyrus
0	1069	0.002	6.27	40	5	9	Right Central Operculum
		0.004	6.05	37	20	6	Right Frontal Operculum

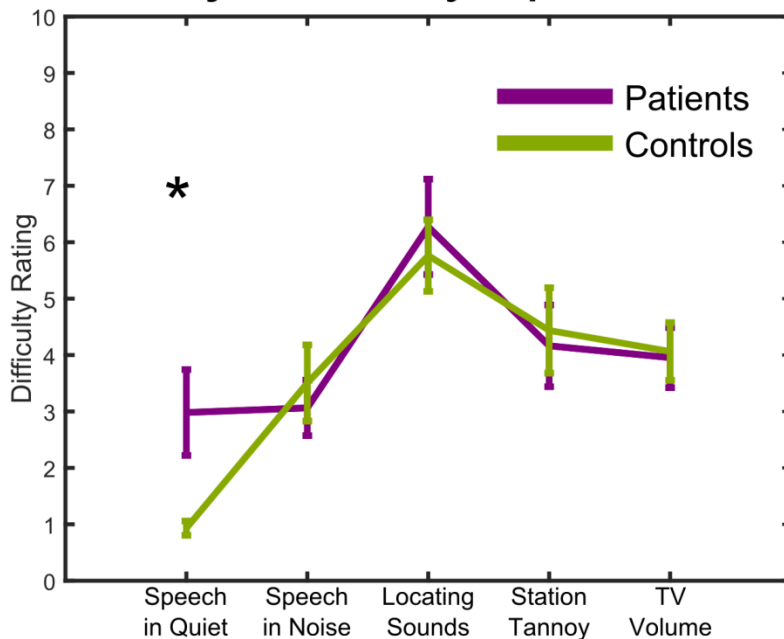
Table 3-2 Voxel-based morphometry regions of significant atrophy in nfvPPA. Corresponding to Figure 3-1 E. Output of an SPM thresholded at peak FWE $p < 0.05$. To avoid an over-long table, only clusters of ≥ 500 voxels are listed here.

3.4.2 Subjective speech perception symptoms in nfvPPA

While the core symptoms in nfvPPA relate to apraxia of speech and agrammatism, patients often complain of a feeling of ‘speech deafness’. To test for this symptom in my cohort, I asked patients and controls to rate their subjective difficulty with five listening scenarios, by placing a mark on a line from ‘very easy’ to ‘very difficult’. Patients could respond appropriately to such rating scales. Patients and controls displayed very similar mean and standard deviation of the subjective difficulty ratings for ‘speech in noise’, ‘localising sounds’, ‘understanding station announcements’ and ‘how loud others say their television is’ (all $p > 0.3$, Figure 3-2 A). However, there was a difference in their assessments of difficulty in understanding speech in quiet environments ($t(20) = 2.66$, $p = 0.015$): controls universally rated this as very easy, while patients rated it almost as difficult as understanding speech in noise (interaction

$F(1,20)=8.21, p=0.010$). Patients and controls had similar, age-appropriate, hearing as measured by pure tone audiometry (Figure 3-2 B).

A: Subjective Symptom Rating



B: Audiograms

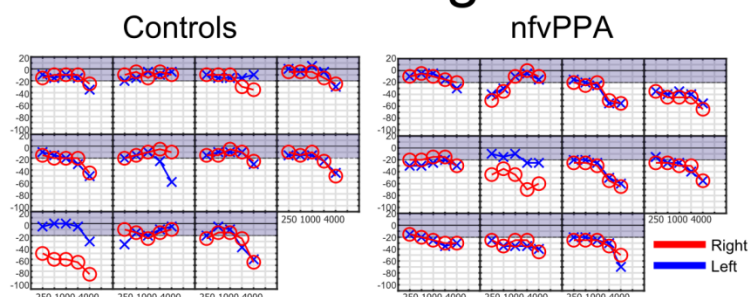


Figure 3-2 Auditory symptoms in nfvPPA

A: Self-rated listening difficulty for patients and controls for four different listening scenarios, and the related question: “how loud do people tell you your TV is?” B: Pure tone audiograms for each individual participant.

3.4.3 Evoked neural responses during the reconciliation of predictions, and their cortical origins

My hypothesis that nfvPPA patients would display aberrant effects of prior knowledge during speech perception reflects an hierarchical generative model for speech perception in which frontal brain regions both instantiate and reconcile predictions

that act top-down on temporal lobe regions (Abdelnour *et al.*, 2014, Park *et al.*, 2015, Raj *et al.*, 2015). Neural responses evoked by speech presentation reflect the operation of bottom-up prediction errors in response to speech signals (Figure 3-1 A). In this framework, frontal lobe neurodegeneration in nfvPPA would be expected to alter the way that neural activity in (anatomically and functionally intact) temporal lobe is modulated by the fulfillment or violation of sensory predictions.

To assess the neural correlates of degraded predictive mechanisms in nfvPPA (Figure 3-1 D), I recorded simultaneous MEG and EEG during a speech perception task, in which I manipulated prior expectations using matching or mismatching text cues, before subjects heard spoken words that were varied in sensory detail by manipulating the number of vocoder channels (Figure 3-3 A) (Shannon *et al.*, 1995). Overall evoked power in the planar gradiometers was similar for the two groups of participants, with the magnetometers displaying slightly lower overall power in patients and the EEG electrodes displaying the opposite pattern (Figure 3-4). Thus, frontal neurodegeneration does not lead to any large difference in the magnitude of the neural response evoked by single spoken words that could manifest as spurious group by condition interactions in neural activity.

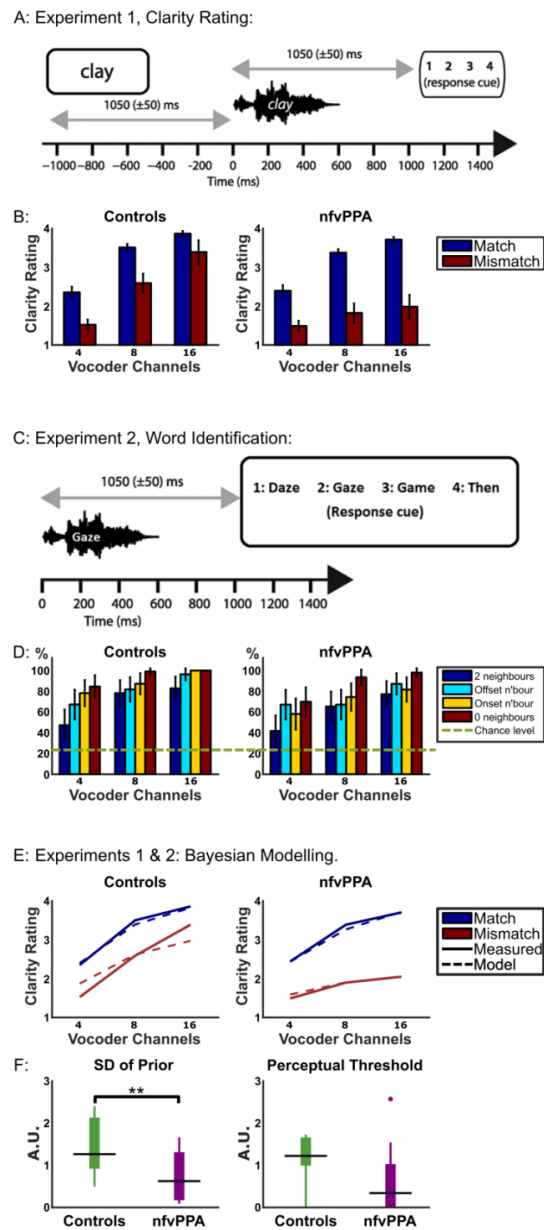


Figure 3-3 Behavioural results

A: Experiment 1 design. A Match trial is shown. In a mismatch trial, the written and vocoded words would share no phonology (for example the written cue 'clay' might be paired with the vocoded word 'sing'). B: Group averaged clarity ratings for each condition. Error bars represent standard error across individuals within each group. C: 4 alternative forced choice vocoded word identification task. D: Group averaged percent correct report for each condition. Chance performance at 25%. Error bars represent standard error across individuals within each group. E: Overall group fits for single subject Bayesian data modelling of the data from panel B. F: Derived parameters from the Bayesian data modelling. A.U.: Arbitrary units. Patients with nfvPPA displayed significantly more precise prior expectations than controls (Wilcoxon $U(11,11)$ $p < 0.01$). They also displayed a trend towards a reduction in perceptual thresholds (Wilcoxon $U(11,11)$ $p = 0.075$).

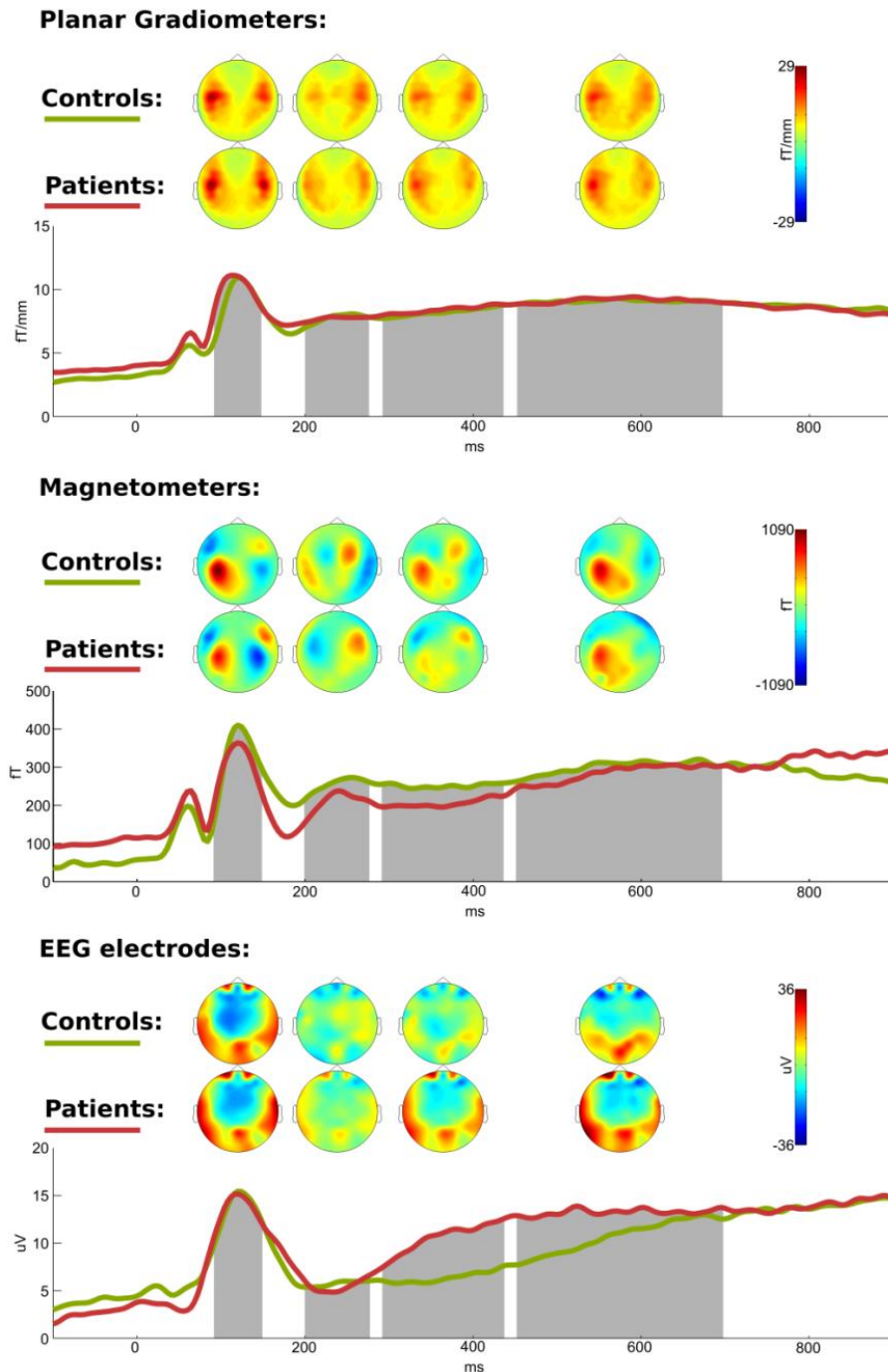


Figure 3-4 Total evoked power.

Root mean square averaged evoked response across all sensors for each modality, after averaging across conditions and participants. The time windows over which the evoked brain sources were reconstructed are depicted by the areas shaded in grey (90-150ms, 200-280ms, 290-440ms, and 450-700ms). Scalp topographic plots display the average evoked response within each window.

To confirm whether patients have normal responses to manipulations of sensory detail independent of predictions (as expected given preserved cortical volume in auditory cortex and superior temporal gyrus, Figure 3-1 E), I first assessed the neural effect of the number of vocoder channels (Figure 3-5). Across all individuals, a peak effect was observed in the planar gradiometers at 96ms (FWE $p < 0.001$), in magnetometers at 188ms (FWE $p < 0.001$) and again at 380ms (FWE $p < 0.001$), and in EEG at 392ms (FWE $p < 0.001$). These findings are consistent with previous studies in young individuals (Sohoglu *et al.*, 2012). Neither at the scalp locations of the peak main effect, nor with a secondary SPM analysis of all scalp-time locations, nor with time-frequency analysis, were reliable group by sensory detail interactions demonstrated at any timepoint. Together, these results are consistent with the idea that patients and controls produce similar neural responses to manipulations of sensory detail in degraded speech. Crucially for what follows, the latency of these responses was also the same in both groups. In magnetometers, where the late effects of vocoder channel number were most clearly seen, control peaks occurred at 196ms and 340ms, and patient peaks at 172ms and 372ms, with very close agreement of waveform morphology at the scalp location of peak conjoint effect (Figure 3-5).

Main Effect of Vocoder Channels

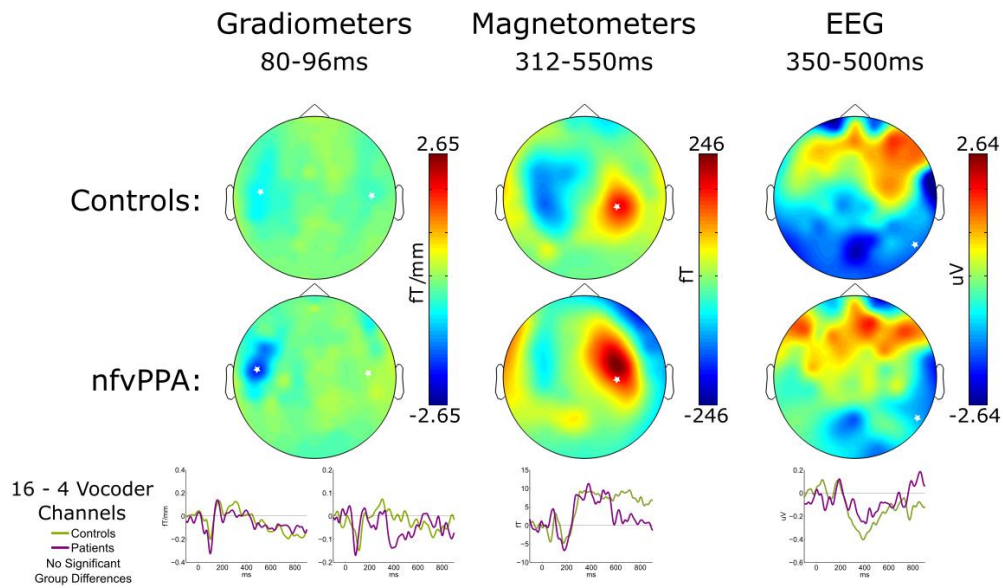


Figure 3-5 The effect of clarity.

Illustrative topographic plots are shown of the main effect of vocoder channels across all participants. No group by sensory detail interactions were observed either at the peak location or in a confirmatory SPM analysis.

Having performed these control analyses, I tested my primary hypothesis by examining the neural effect of manipulating whether prior expectations matched sensory input. During the reconciliation of predictions there were significant main effects of cue congruency in all sensor types (Figure 3-6 A).

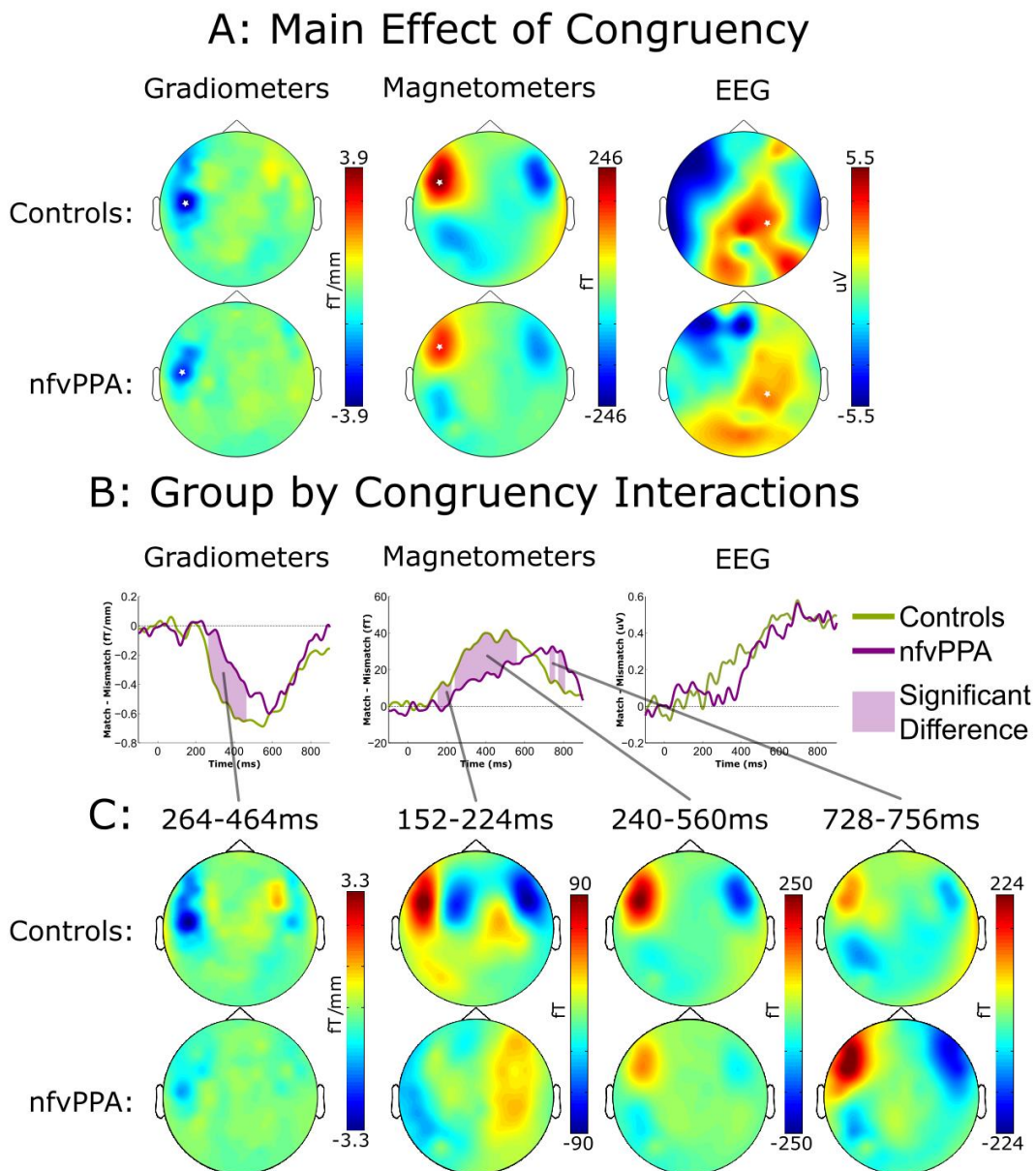


Figure 3-6 The evoked effect of cue congruency.

A: Illustrative scalp topographic plots of the main effect of cue congruency for each group from 400ms to 700ms, a period of where both groups showed a large statistical effect of congruency with similar topography. White stars indicate the scalp location of the peak congruency effect across both groups between -100ms and 900ms (FWE $p < 0.001$ for all sensor types). B: Significant group by congruency interactions ($p < 0.05$ sustained for more than 25ms at the scalp locations marked by white stars in the upper panel) were observed in planar gradiometers and magnetometers, and are shaded in lilac. C: Topographic plots for each group are shown averaged across each significant cluster of group by congruency interaction.

Across all individuals (controls and nfvPPA), the peak effect was observed in the planar gradiometers at 464ms (FWE $p < 0.001$), in magnetometers at 400ms (FWE $p < 0.001$), and in EEG at 700ms (FWE $p < 0.001$). At these scalp locations, significant group by

congruency interactions were observed in the planar gradiometers and in the magnetometers, but not in the EEG electrodes. In the planar gradiometers, between 264ms and 464ms controls had a significantly larger effect of congruency than patients (Figure 3-6 B). The scalp topography averaged across this time window resembled that observed during the peak of the main effect, but with the pattern being stronger in controls (Figure 3-6 C). In the magnetometers, a cluster with similar timing and scalp topography was observed between 240 and 560ms (Figure 3-6 B). Two additional clusters were also observed. In later time windows, from 728 to 808ms, group by congruency interactions were observed in the opposite direction, with patients showing a significantly greater effect than controls. Again, the scalp topographies in this cluster resembled those during the main effect (Figure 3-6 C). This indicates that the effect of congruency was present in both groups, but that the effect was significantly delayed in nfvPPA. Finally, an early cluster was observed between 152ms and 224ms, with the controls displaying a significantly greater effect of congruency than patients. Intriguingly, the scalp topography in this time window was different to that observed during the conjoint main effect, with dipoles having a much more anterior centre of mass (Figure 3-6 C). This anterior topography is consistent with a frontal source, expected to appear in this earlier time window as shown in similar previous studies with young healthy listeners (Sohoglu *et al.*, 2012, Sohoglu and Davis, 2016).

To assess the underlying neural sources of these effects, multimodal sensor data were combined (Henson *et al.*, 2009) and inverted into source space with sLORETA (Pascual-Marqui, 2002). For the main effect of vocoder channel number, reconstructions were performed across all individuals combined, because no group difference or group by clarity interaction was demonstrated in sensor space. The main effect of sensory detail shown in MEG sensors and EEG electrodes is explained by significantly more activity for 16 channel speech in temporal lobe auditory areas in mid-latency time windows (Figure 3-7 A), replicating previous findings in younger individuals (Sohoglu *et al.*, 2012, Sohoglu and Davis, 2016).

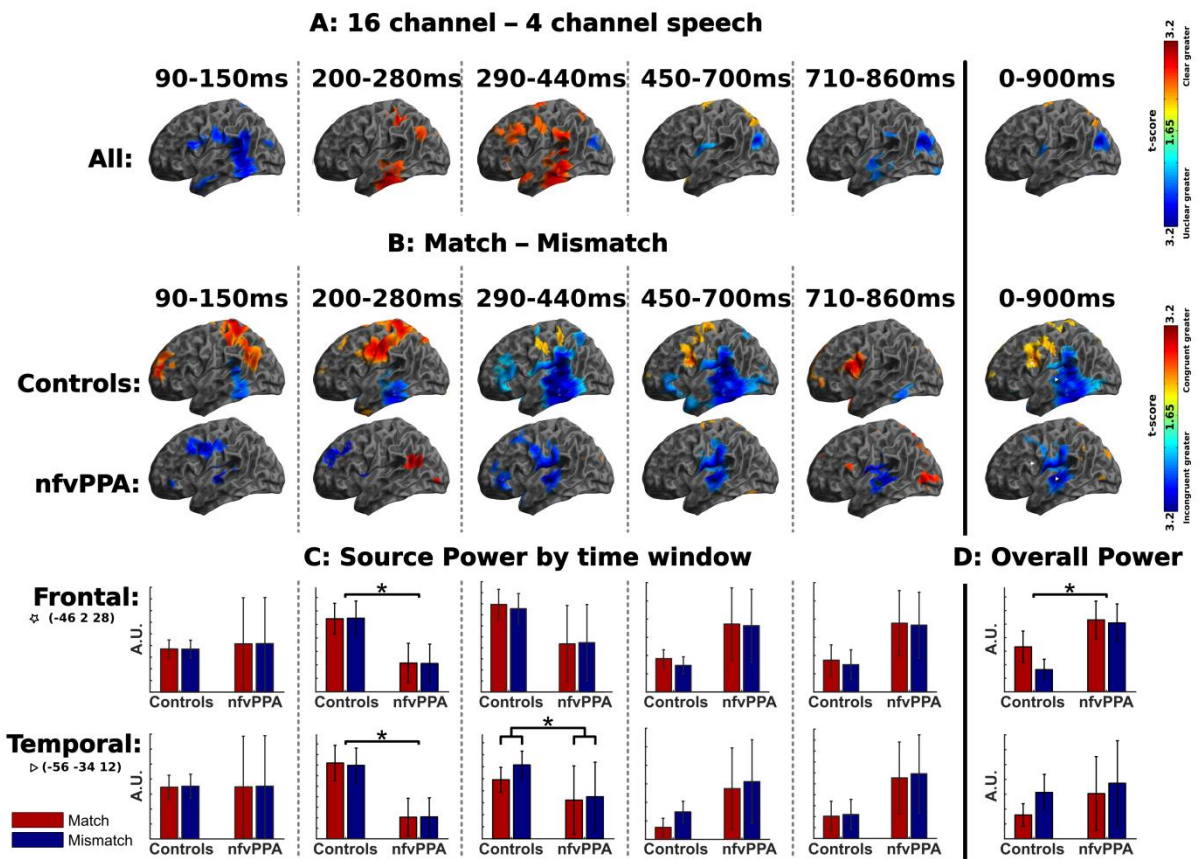


Figure 3-7 Evoked source space analysis.

A: Evoked source reconstructions (sLORETA) for the main effect of clarity for all participants combined. B: Source reconstructions for the main effect of congruency for each group individually. C: Illustrative bar charts are plotted at the bottom for source power by group and condition in the frontal (IFG) and temporal (STG) regions of interest for the each time window. A.U.: Arbitrary units. Statistically significant differences are marked by asterisks (detail in results section of text). Error bars represent the between-subject standard error of the mean (not the between condition standard error, which is much lower due to the repeated measures design). D: Overall power in each source by group and condition across the whole time window of interest.

To localise the group by cue congruency interaction, I first display source reconstructions for the main effect of cue congruency in each group (Figure 3-7 B) for time windows defined by the main data features in overall sensor power averaged over conditions and participants replicating the methods of Sohoglu *et al.* (2012) (Figure 3-4). Given my findings of delayed congruency effects in patients, an additional, late, time window (710-850ms) was also examined *post hoc*. I focus on the two principal sources observed in young healthy individuals for this task (Sohoglu *et al.*, 2012, Sohoglu and Davis, 2016), extracting average power in each condition at frontal and

superior temporal voxels of interest defined by the main effect of congruency averaged across the whole epoch (Figure 3-7 D). No group differences were demonstrated in the earliest (90-150ms) or latest (450-700ms) time windows. Between 200 and 280ms, there were significant main effects of group in both frontal and temporal voxels, with greater responses in controls than patients. Between 290 and 440ms, this main effect had dissipated, but there was a group by condition interaction, with controls showing a greater effect of cue congruency in the superior temporal but not the frontal voxel.

The analysis across the whole epoch is of particular interest. Across all individuals, a repeated-measures ANOVA (Table 3-3) confirmed the pattern of opposing effects of prior knowledge in frontal and superior temporal regions seen in a previous study (Sohoglu *et al.*, 2012) ($F(1,134)=60.1$, $p<0.001$). However, there was a group by source by congruency interaction ($F(1,134)=11.9$, $p=0.001$), primarily driven by the absence of a significant effect of congruency in frontal regions in nfvPPA (Figure 3-7 B). When the total power in the frontal region was examined, a main effect of group was observed such that patients had significantly *more* frontal power than controls, but their modulation of frontal power by congruency was absent (Figure 3-7 D).

Test	df	F	p
Group	1,134	1.1	0.317
Source	1,134	2003.1	<0.001
Condition	1,134	5.1	0.037
Vocoder Channels	2,134	0.0	0.970
Individual (Group)	18,134	1.1	0.383
Group*Source	1,134	0.1	0.816
Group*Condition	1,134	0.4	0.550
Group*Vocoder Channels	2,134	0.8	0.433
Source*Condition	1,134	60.1	<0.001
Source*Vocoder Channels	2,134	0.1	0.884
Condition*Vocoder Channels	2,134	1.8	0.165
Group*Source*Condition	1,134	11.8	0.001
Source* Individual (Group)	18,134	76.6	<0.001
Condition * Individual (Group)	18,134	4.9	<0.001
Vocoder Channels * Individual (Group)	36,134	1.2	0.227

Table 3-3 Repeated measures ANOVA of evoked source power in frontal and temporal voxels of interest over the whole post auditory epoch. *Bold, red rows indicate statistically significant results.*

3.4.4 Behavioural Experiment 1: Vcoded Word Clarity Rating

Given these neural differences, I sought to understand the perceptual correlates of neural delay in the reconciliation of predictions by examining the behavioural consequences of manipulations of prior knowledge in my two groups. All individuals reported that the perceptual clarity of vocoded words was significantly increased by matching text cues (Figure 3-3 B), but this effect was greater in patients with nvPPA than in controls. A repeated-measures ANOVA (Table 3-4) revealed that Group, Number of Vocoder Channels and Cue Congruency were significant either as main effects or as part of two-way or three-way interactions.

Test	df	F	p (Greenhouse-Geisser)
Group	1,40	7.7	0.011
Clarity	2,40	69.3	<0.001
Group * Clarity	2,40	17.1	<0.001
Congruency	1,40	1.2	0.287
Group * Congruency	1,40	13.2	0.002
Clarity * Congruency	2,40	2.3	0.140
Group * Clarity * Congruency	2,40	8.2	0.007

Table 3-4 Repeated Measures ANOVA of behavioural data from experiment 1.

A replication experiment outside the MEG scanner confirmed that the difference between match and mismatch trials was due to a facilitatory effect of matching prior knowledge and not simply increased confusion in the face of mismatching priors: ratings of perceptual clarity after a mismatching text cue were not statistically different from those after a ‘neutral’ or uninformative cue. Furthermore, patients with nvPPA had a much larger difference in clarity rating between ‘neutral’ and ‘match’ trials than controls (Figure 3-8).

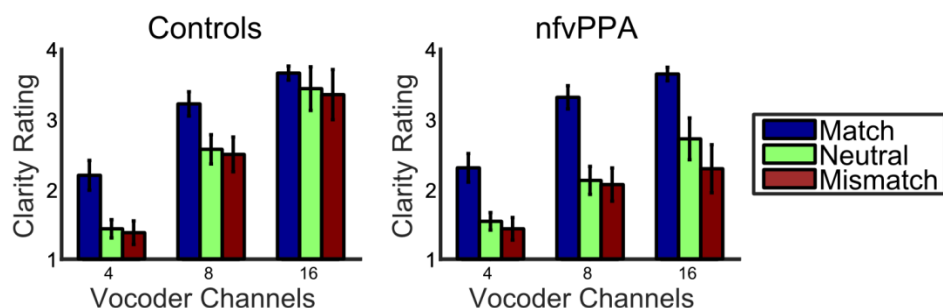


Figure 3-8 Replication of experiment 1 with additional, neutral cues.

Group averaged clarity ratings from the repetition of experiment 1 (Figure 3-3 A) with the addition of a neutral written cue (a row of “XXXX”).

It is important to note that participants were explicitly instructed to rate clarity across their own range of perceptual experience within the experiment, and were given training until they were able to do this. Comparing clarity ratings across groups is not, therefore, a direct measure of comparative listening difficulty as a rating of ‘1’ simply means ‘one of the least clear words I heard in the experiment’, while a ‘4’ means ‘one of the clearest words I heard’. To fully assess the perceptual basis of my findings, with a further experiment and Bayesian modelling I assessed the elements contributing to perceptual clarity: 1) patients’ and controls’ ability to identify degraded spoken words and 2) participants’ introspective ability to perform higher level estimation of the global precision of sensory input.

3.4.5 Behavioural Experiment 2: Vcoded Word Identification

To ensure that my finding was not a consequence of impaired word identification in patients leading to a group difference in reliance on prior knowledge (Shankweiler *et al.*, 2008), I performed a second experiment in which participants identified noise vocoded words in the absence of prior expectations (Figure 3-3 C). To reduce response demands for patients with non-fluent speech I used a 4-alternative forced-choice identification task. All individuals with nfvPPA were above chance at identifying even the most degraded vocoded speech however, as a group, they did not perform quite as well as controls (Figure 3-3 D, Table 3-5). Both groups were influenced in the same way by the number of noise vocoder channels and the number of close distractor items presented as alternatives in the forced choice (Table 3-5). As expected, it was easier for

all individuals to identify words with more vocoder channels and if there were fewer close distractor items. This effect was strongest for the most degraded speech, manifesting as an interaction between vocoder channels and distractor difficulty.

Test	df	F	p (Greenhouse-Geisser)
Group	1,120	10.9	0.003
Vocoder Channels	2,120	5.79	0.015
Distractor Difficulty	3,120	0.839	0.457
Group * Clarity	2,120	0.169	0.765
Group * Distractor Difficulty	3,120	1.14	0.334
Vocoder Channels * Distractor Difficulty	6,120	4.23	0.004
Group * Vocoder Channels * Distractor Difficulty	6,120	1.76	0.149

Table 3-5 Repeated measures ANOVA of behavioural data from experiment 2.

Crucially, these data show that a lower-level impairment in perceiving vocoded speech cannot be the sole explanation of my finding of an increased congruency effect in nfvPPA patients. Although they did not perform as well at identifying speech of equivalent sensory detail, these patients performed better at identifying speech with 8 channels than controls did with 4 channels. Yet, patients still display a much larger congruency effect for 8-channel vocoded words than controls do for 4-channel speech. Hence, the magnitude of congruency effects in clarity rating is not simply related to objective abilities at word identification, but rather reflects a difference in the mechanisms by which prior knowledge influences lower-level perceptual processing. I investigate the nature of this effect with a Bayesian perceptual model combining word report and clarity rating data.

3.4.6 Bayesian modelling of experiments 1 and 2

To dissociate changes in the precision of predictions from difficulties with higher level estimation of the precision of sensory input, I performed hierarchical Bayesian inference simulations (c.f. (Sohoglu and Davis, 2016); Figure 3-9).

Individual differences in word discriminability were accounted for by defining the precision of sensory input for each subject as the percentage above chance for word identification at each vocoder channel number in experiment 2. This allowed us to

individually optimise two free parameters against the clarity ratings measured in experiment 1. These parameters were the precision of prior expectations (as measured by their standard deviation), and a perceptual threshold below which the observer rated speech as unclear (Figure 3-9). The model explained more than 99% of the variance in the group-averaged clarity ratings (Figure 3-3 E). Even better fits could be obtained for the controls by accounting for non-linearities in the effect of the increasing sensory detail on perceptual clarity beyond 16 vocoder channels, but analysis of the Akaike information criterion suggested that this increase in variance explained did not outweigh the loss of parsimony compared to the simpler model (see methods section 3.4.6). The simpler model was therefore retained, but all of the group differences and associations between model outputs and neurophysiology reported below remained significant if the complex model was used.

Example fit: Control 10, Matching Prime, 4 Channels

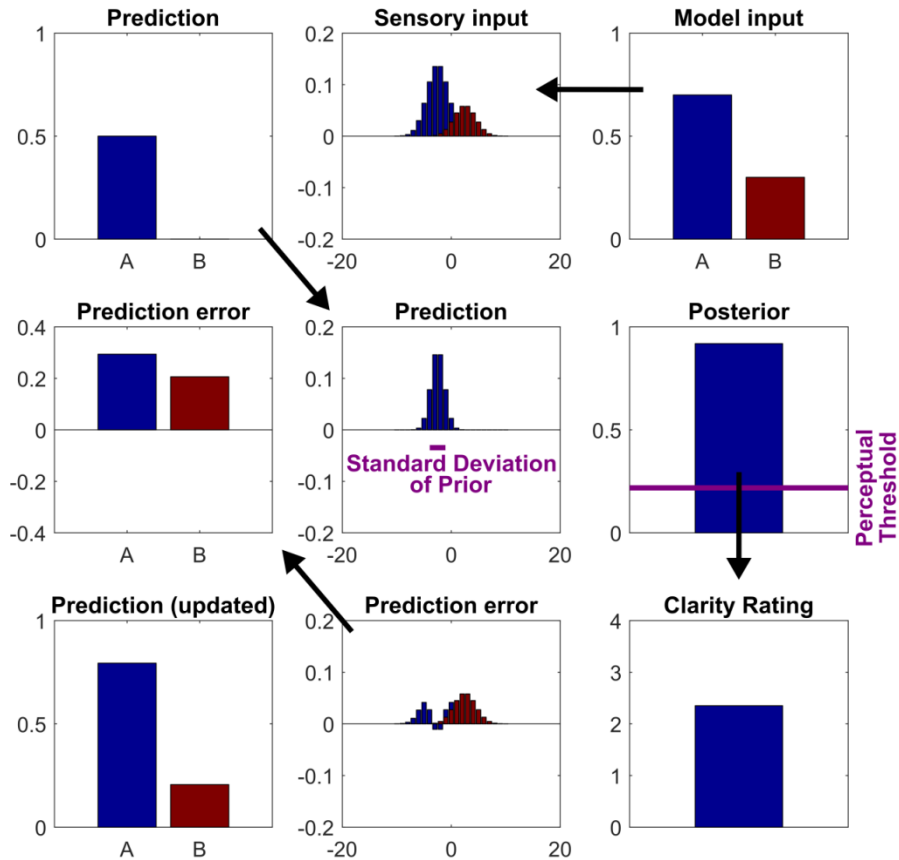


Figure 3-9 Example Bayesian model fits for a single subject in a single condition.

In this case control 10 for 4 channel vocoded speech and matching written cue and vocoded word. The standard deviation of the prior and the perceptual threshold were individually optimised to best model the clarity ratings from experiment 1. Upper left: the prediction, in this case a 50% chance of the cued word (A) and an approximately zero chance of any other given word (B). Middle left: the total area under the curve of the prediction error fed back to frontal regions from temporal regions. Bottom left: the updated prediction, from which an A vs B discrimination might be performed. Upper centre: the modelled activity in a set of 21 neural units representing phonological feature categories; a weighted function of the upper right panel. Middle centre: the modelled prediction for activity in the set of 21 neural units representing phonological feature categories; a weighted function of the upper left panel. Bottom centre: The prediction error in each of the 21 modelled neural units, calculated by subtracting the prediction from the sensory input. Upper right: the probability density for the sensory identification of the cued word (A) vs any other word (B); this was defined for each subject individually as the percentage above chance in experiment 2 at the number of vocoder channels being modelled. Middle right: the area under the curve of the posterior distribution, calculated as the sum of the area under the curve of the sensory input and a weighted product of the sensory input and prior precision, with the weighting determined by the congruency of the written cue. Bottom right: the modelled clarity rating, calculated as the height of the posterior above perceptual threshold, individually normalised to a 1-4 rating scale.

Parametric and non-parametric tests indicated that patients had significantly more precise prior expectations than did controls (both $p < 0.01$; Figure 3-3 F). There was a trend towards patients having lower perceptual thresholds (Wilcoxon $p = 0.08$); patients required less sensory detail to give a clarity rating of 2 or higher, reflecting an appropriate downwards extension of the subjective clarity scale rather than a higher level introspective deficit resulting in patients not being ideal observers of their sensory experience (see discussion). The model results confirm that the consequence of degraded neural mechanisms for sensory predictions is not that the brain is unable to use prior knowledge (written cues) to modulate perception, but rather that patients with nvfPPA apply their prior knowledge with greater precision and inflexibility.

3.4.7 Induced oscillatory dynamics

To examine the effects of nvfPPA and task manipulations on induced oscillatory activity, I performed a time-frequency analysis of the planar gradiometer data, averaged across sensors (Figure 3-10). First, I inspected the neural instantiation of predictions by exploring induced activity during the period following presentation of the written word but before the onset of the auditory stimulus. Based on recent studies in the auditory domain I expected this updating of predictions to manifest as an increase in beta frequency oscillations preceding the onset of the spoken word (Sedley *et al.*, 2016). This was confirmed in my cohort, with a significant increase in beta power (10 to 28 Hz) for both groups of participants beginning around 800ms after the onset of the written word, i.e. approximately 250ms before the onset of the spoken word (cluster FWE $p = 0.001$, Figure 3-10). At the time (992ms) and frequency (24Hz) of the peak effect for both groups overall, the single subject magnitude of the induced response correlated significantly with their precision of prior expectations as simulated by my behavioural Bayesian model (Pearson's $r(19) = -0.52$, $p = 0.017$; Spearman's $\rho = -0.54$, $p = 0.012$). A confirmatory SPM across the whole time window confirmed the group difference implied by this relationship, with patients displaying a single cluster of greater induced beta (20 to 34Hz) power from 868ms (cluster FWE $p = 0.010$). There were no induced effects that were greater in controls than in patients.

Written Word Response

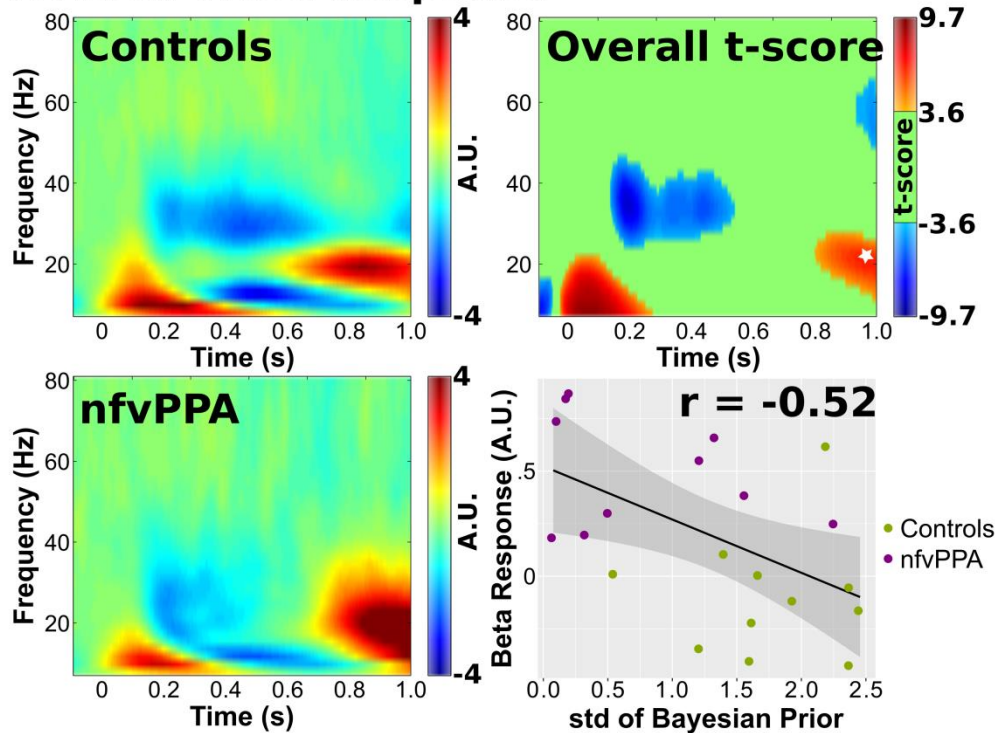


Figure 3-10 Induced analysis after the written but before spoken word.

Total induced power after written word onset by group, the overall t -score for difference from baseline for both groups combined, and the relationship between single subject response at the late beta peak and precision of their prior expectations in the Bayesian behavioural model. A.U.: Arbitrary units. The grey shaded area in the bottom right plot indicates the 95% confidence band for the regression line, marked in black.

Second, I complemented my evoked analysis by assessing oscillatory power during the reconciliation of predictions, i.e. after the onset of the spoken word, averaged across sensors. The results described below were not altered by subtraction of the condition-averaged evoked waveform subtracted from every trial, confirming that these are true induced responses rather than high-frequency contamination from the evoked responses described previously. Figure 3-11 A illustrates the oscillatory power induced by hearing noise vocoded speech for each group, normalised to the pre-visual stimulus baseline and averaged across the whole brain. Across all conditions, the general pattern was for increased alpha and beta power for the first ~200ms, followed by a desynchronisation from ~200ms onwards.

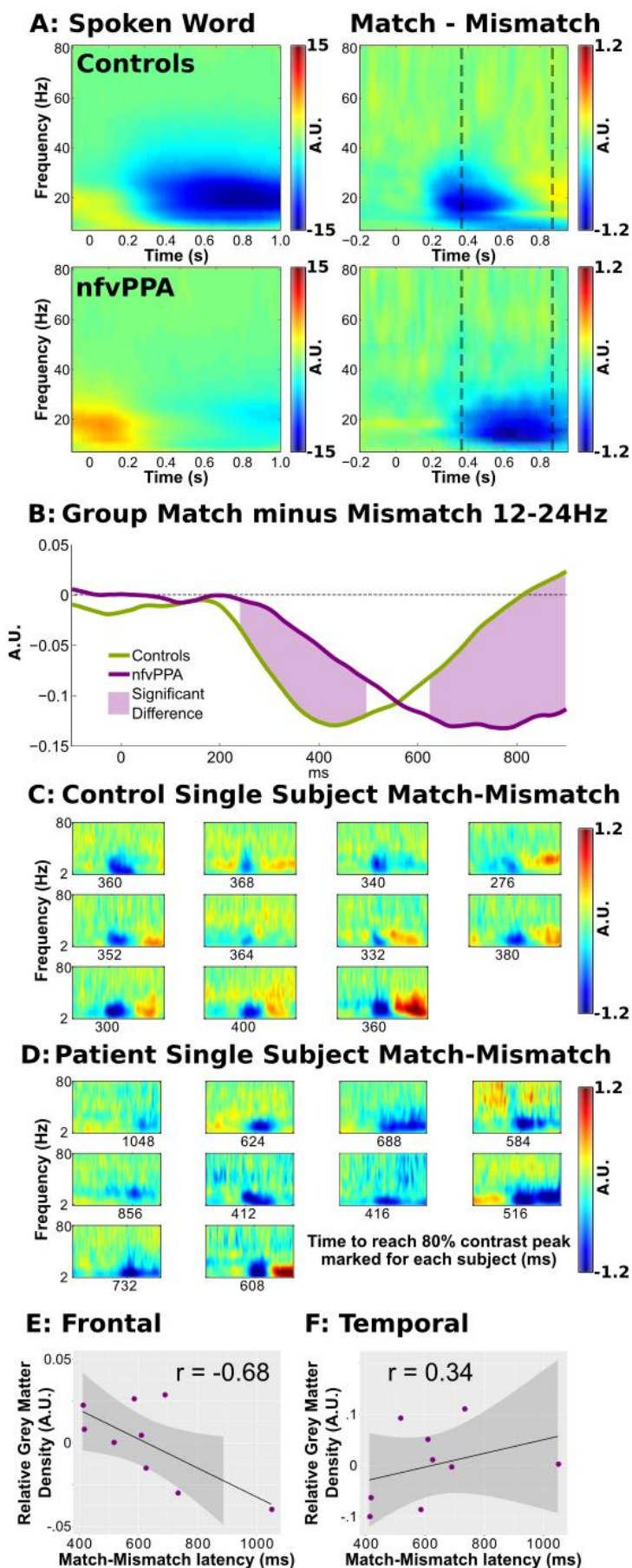


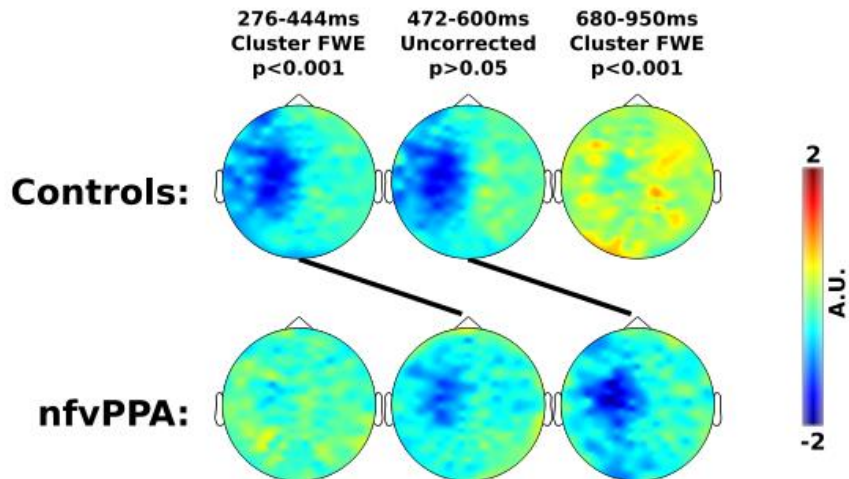
Figure 3-11 Induced analysis after the spoken word.

A: Total induced power after spoken word onset and main effect of cue congruency by group. B: Overall induced power difference between Match and Mismatch conditions in the alpha/beta overlap range. C: Single subject time-frequency profiles for each control. The time taken to reach 80% of the peak power contrast between Match and Mismatch trials is indicated for each individual by the number below the corresponding abscissa. D: Single subject time-frequency profiles for each patient. E: Significant negative correlation between frontal grey matter volume (adjusted for age and total-intracranial volume at the co-ordinates in Figure 3-7 C) and the time taken to express a congruency contrast (panel D). The grey shaded area indicates the 95% confidence band for the regression line, marked in black. F: No significant correlation between similarly adjusted superior temporal grey matter volume and effect latency.

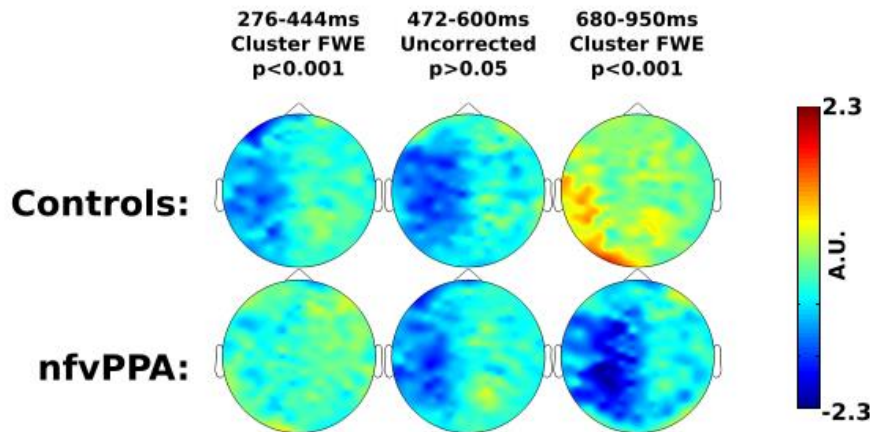
A significant main effect of congruency was observed in both groups (Figure 3-11 A). In controls, this effect peaked at 436ms at a frequency of 12Hz (FWE $p < 0.001$), with greater suppression of this response for spoken words that matched prior written text. In patients, a similar effect was observed, also at 12Hz, but with a later peak at 824ms (FWE $p < 0.001$).

There were two time/frequency clusters that showed a group by congruency interaction. In the first, extending from 276-444ms between 4-24Hz (peak 300ms, 16Hz), controls displayed a greater effect of congruency than did patients (cluster FWE $p < 0.001$). In the second, beginning at 680ms and extending beyond the end of the analysis from 6-34Hz (peak 888ms, 20Hz), the interaction was reversed, with patients showing a greater effect of congruency than did controls (cluster FWE $p < 0.001$). The scalp distribution and source localisations of this effect are illustrated in Figure 3-12: effects were restricted to the left hemisphere and localised to areas around superior temporal gyrus. Both interaction clusters remained significant (FWE $p \leq 0.002$) in a confirmatory analysis in which power was normalised to the pre-auditory stimulus baseline. To illustrate the time-course of this oscillatory dissociation, the data from all three sensor types were restricted to 12-24Hz, encompassing the interactions in both directions, and the total effect of congruency on power in this band across the whole brain was plotted in Figure 3-11 B.

A: Beta band (14-30Hz) topography:



B: Alpha band (8-14Hz) topography:



C: Source Reconstructions 12-24Hz:

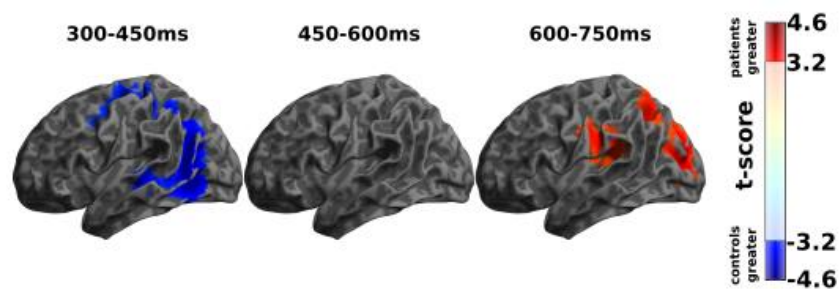


Figure 3-12 Scalp distribution and source reconstructions of induced effects.

A: Scalp topographies for the group by congruency interaction in the beta frequency band. B: Scalp topographies for the group by congruency interaction in the alpha frequency band. C: eLORETA source reconstructions for 300-450ms, 450-600ms and 600-750ms, corresponding to time windows displaying a greater effect of congruency in controls, no group by congruency interaction, and a greater effect of congruency in nfvPPA. Only left hemispheres are shown, as no significant right sided sources were demonstrated.

To investigate this delay in this beta response in individual patients, single subject time-frequency decompositions were performed and the time taken to reach 80% of the peak overall power contrast between matching and mismatching prior knowledge was defined for each subject. The effect latencies for controls were all tightly clustered between 275 and 400ms (Figure 3-11 C). Every single patient was delayed compared to every single control, with a range of 412-1048ms (Figure 3-11 D). In the patient group neural response latency was negatively correlated with grey matter density in my left frontal region of interest ($r=-0.68$, $p=0.042$; Figure 3-11 E) but not in my left temporal region of interest ($r=0.34$, $p=0.36$; Figure 3-11 F). There was a trend towards a negative relationship between latency and the standard deviation of prior expectations, though this did not reach significance ($r=-0.37$, $p=0.1$).

To summarise, all participants show the same congruency-induced reduction in activity in the STG, but nfvPPA patients are delayed in showing this response compared to controls. Thus, the differential response of patients and controls reflects a top-down effect of frontal neurodegeneration on brain responses in posterior regions that remain structurally intact (compare, Figure 3-7 B and Figure 3-12 C with Figure 3-1 E) and that respond normally to bottom-up manipulations of speech clarity (Figure 3-5, Figure 3-7 A).

3.4.8 Coherence and Connectivity during the reconciliation of predictions

To determine whether these effects are due to frontal degeneration or fronto-temporal disconnection, I examined coherence and connectivity between the frontal and temporal lobe sources of interest (Figure 3-7 C) during the 900ms immediately following the onset of each spoken word. I employed two MEG connectivity analysis methods that give complementary information concerning fronto-temporal dynamics during the reconciliation of predictions. First, Imaginary Coherence, which is immune to volume conduction effects and source spread (Nolte *et al.*, 2004) as well as differences in power (Bowyer, 2016), allowing us to be confident that relationships I describe are true reflections of the underlying brain dynamics. Both groups had significant fronto-temporal coherence up to around 25 Hz (Figure 3-13 A). Coherence in the beta band (13-23Hz) was significantly stronger in patients than controls (Figure

3-13 B). This suggests that an overall reduction of fronto-temporal connectivity cannot explain my observed differences between nfvPPA patients and controls.

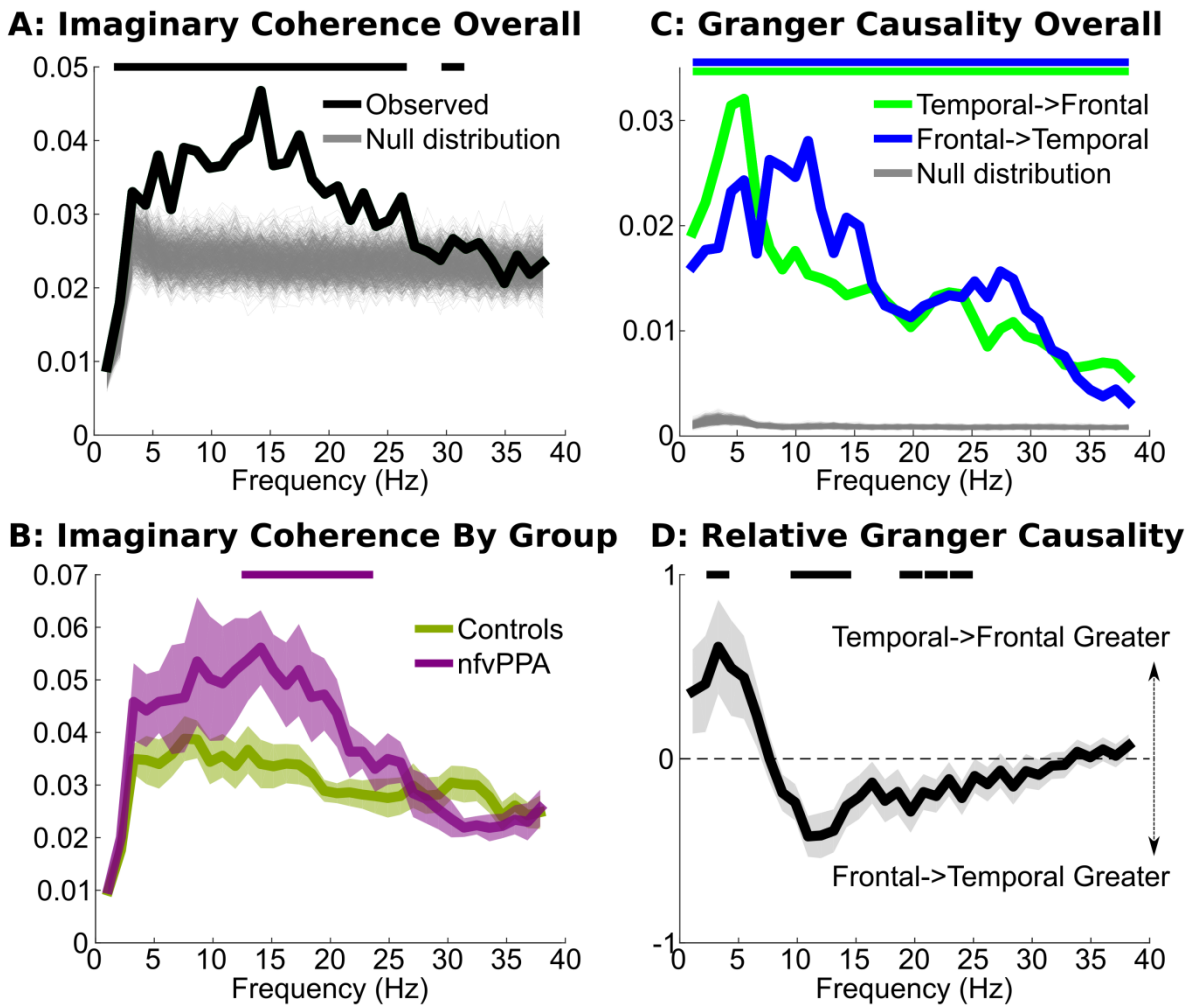


Figure 3-13 Coherence and connectivity analysis.

For the time series of frontal and temporal sources of interest between 0 and 900ms after every spoken word onset. The evoked waveform was subtracted from the time series of frontal and temporal source activity between 0 and 900ms after every spoken word onset before analysis. Horizontal lines at the top of each plot denote frequencies at which the line of matching colour statistically exceeds either the null distribution (A and C), its counterpart group (B) or differs from zero (D). A: Imaginary coherence. The median of the observed inter-source coherence is shown in black. 1000 randomisations of the null distribution are shown in grey. B: Imaginary coherence by group. Shading represents standard error of the mean. C: Granger causality. Median influences from temporal to frontal sources are shown in green and frontal to temporal sources in blue. 1000 randomisations of the null distribution are shown in grey. D: Relative normalised Granger causal relationships between temporal and frontal sources by frequency. Grey shading represents the standard error of the directionality contrast in a repeated measures general linear model.

Imaginary coherence does not provide robust indices of directionality, because inter-regional interactions potentially occur over more than one oscillatory cycle. I therefore also examined Granger causal relationships between my sources of interest (Granger, 1969, Gow *et al.*, 2008). This metric allows us to look at the directionality of non-zero-lag fronto-temporal interactions while still being relatively robust to volume conduction. Granger causality tests whether information from the past activity of one region can predict future activity in another better than its own past. Highly significant bi-directional Granger causal relationships were observed between temporal and frontal sources (Figure 3-13 C). To compare these, while avoiding confounds due to differences in signal to noise ratio between regions and between individuals (which can alter the magnitude of Granger Causal relationships (Nolte *et al.*, 2004)), I divided the magnitude of each frequency value by the across-frequency mean for each individual and region to create a profile of relative influence for each region at each frequency. This demonstrated significantly stronger temporal to frontal Granger Causal relationships at low frequencies, while frontal to temporal influences were stronger at higher, beta band, frequencies (Figure 3-13 D). These findings are in agreement with a recent study of MEG connectivity during written language comprehension (Schoffelen *et al.*, 2017).

Overall, my finding of increased imaginary coherence in the patient group in a frequency band where frontal to temporal Granger causal influences predominate demonstrates that frontal neurodegeneration has increased rather than reduced top-down connectivity from frontal to temporal regions.

3.5 Discussion:

The principal finding of this study is that neurodegeneration of the frontal language network results in the delayed neural resolution of predictions in temporal lobe. Conversely, the temporal lobe neural responses to bottom-up manipulations of sensory detail were not delayed. This is evidence that the resolution of sensory predictions is mediated by frontal regions in humans. My source-space analysis demonstrates that frontal regions are working harder overall in nfvPPA patients. My demonstration of increased coherence in the patient group, in a frequency band where frontal to

temporal influences predominate, is consistent with degraded neural mechanisms in frontal regions requiring increased fronto-temporal interaction to reconcile excessively precise predictions. This view is supported by recent observations that left inferior frontal imaginary coherence is decreased in nfvPPA during the resting state (Ranasinghe *et al.*, 2017), confirming that the increased fronto-temporal coherence I observe here reflects specific engagement of these mechanisms during language perception and not simply a global upregulation. Together, these findings resolve a key controversy in speech perception, by demonstrating that frontal regions are playing a core role in reconciling predictions with sensory input during the perception of speech (Abdelnour *et al.*, 2014, Park *et al.*, 2015, Raj *et al.*, 2015).

This impairment of predictive processing has significant perceptual consequences. Most strikingly, frontal neurodegeneration does not reduce the degree to which the brain employs contextual prior knowledge to guide lower-level speech perception. Rather, through Bayesian modelling, I show that prior knowledge of expected speech content is applied in an overly precise or inflexible fashion, thereby producing a larger-than-normal behavioural effect of prior knowledge on nfvPPA patients' ratings of speech clarity. This is not an effect specific to my experimental manipulation; it can explain why patients with nfvPPA complain of difficulties with understanding speech, out of keeping with their auditory sensitivity (see section 5.2.1), why they perform poorly on tasks requiring the comparison of two auditory stimuli (Goll *et al.*, 2010, Grube *et al.*, 2016) (section 5.2.2) despite being able to perform other forced choice tasks well, and why they display receptive agrammatism (section 5.2.3). In validation of computational and theoretical models of predictive coding (Arnal and Giraud, 2012, Bastos *et al.*, 2012, Sedley *et al.*, 2016), I demonstrate that the precision of subjects' predictions correlates with the magnitude of induced beta-frequency oscillations, which have recently been shown to correspond temporally and quantitatively to the updating of predictions (Sedley *et al.*, 2016).

Previous neuro-imaging evidence has suggested that frontally-mediated top-down predictions during speech perception are able to explain MEG response magnitudes (Sohoglu *et al.*, 2012, Sohoglu and Davis, 2016) and fMRI pattern information in the superior temporal gyrus (Blank and Davis, 2016). Here, I go beyond these associations and provide causal evidence for a functional contribution of frontal networks in

supporting top-down predictions by demonstrating that disruption of these networks has the remote effect of delaying the reconciliation of predictions in temporal lobe regions that are anatomically intact, with striking behavioural consequences.

The behavioural data, Bayesian modelling and neurophysiological results all support the proposal that perceptual predictions operate within an hierarchical generative network, which for speech perceptions spans auditory, superior temporal, and inferior frontal cortices.

3.5.1 Fronto-temporal dissociations in nvfPPA

Patients with nvfPPA lacked normal modulation of frontal neural activity by cue congruency, were delayed in engaging frontal regions, and showed greater frontal activity than control participants overall. This is analogous to the observation that elderly controls globally upregulate cognitive control networks that are selectively engaged by younger listeners only when speech is degraded, and thus appear to lack difficulty-related modulation of activity (Erb and Obleser, 2013). My work goes significantly beyond these previous findings, however, in showing that this frontal deficit also affects neural responses in (anatomically unaffected) posterior regions.

In contrast to these impairments, patients displayed normal power of evoked neural responses for analyses combined over sensors and had normal neural responses to changes in sensory detail shown here and in previous work to localise to temporal regions (Sohoglu *et al.*, 2012) (Figure 3-7 A). These observations provide reassurance that the lack of atrophy in auditory regions of temporal lobe does not mask a microscopic abnormality in auditory neural function. Similarly, it is reassuring that in both groups clarity ratings were similar for mismatching and neutral cues, and the response to questionnaires suggested similar ecological perception of speech in most conditions. This excludes trivial explanations for my behavioural results such as patients becoming confused by mismatches or having an altered approach to subjective rating scales. The group difference in uncued identification of vocoded speech was small, and was accounted for in my Bayesian modelling, by using the results of experiment 2 to individually define the precision of the sensory input for each subject and number of noise vocoder channels. Thus, my observation of abnormal effects of

cue congruency in nfvPPA cannot easily be explained by basic auditory processing deficits, or by higher signal detection thresholds.

Most strikingly, patients displayed a significant delay in the effects of cue congruency in temporal lobe in my sensor space, source space and induced analyses. Under the predictive coding framework, these effects arise because the integration of prediction error is an iterative process, whereby predictions are recursively updated in the light of sensory input to minimise error (Blank and Davis, 2016). For the patients with nfvPPA, the degraded neural architecture and aberrantly precise predictions might mean that this updating requires more iterations and/or that each iteration takes more time. As a consequence, more neural activity is observed and reconciliation of predictions with sensory signals is delayed.

3.5.2 Frontotemporal hierarchy and predictive coding

My experiments have demonstrated that frontal lobes have top-down causal influences on neural activity in temporal lobe. This requires hierarchical sensory processing, with feed-back and feed-forward of information between levels. Predictive coding is one framework to understand such processing, and makes a number of specific claims about the nature of top-down and bottom-up signals. Here I discuss the evidence for predictive coding, and the inability of alternative frameworks to explain my findings.

Firstly, the spatial and temporal pattern of neurophysiological responses in elderly control participants replicated those previously demonstrated in young people (Sohoglu *et al.*, 2012), which have been successfully modelled in a predictive coding framework (Sohoglu and Davis, 2016), and which cannot be effectively modelled by sharpening theories of neural representation (Blank and Davis, 2016). Current instantiations of predictive coding models state that each stage of the processing hierarchy passes forwards to the next stage only prediction errors and backwards only predictions (Hinton, 2007, Friston, 2008). An alternative hypothesis – which might explain some of the present data – is that prior expectations are set up in frontal regions but not fed back to superior temporal regions (Norris *et al.*, 2000, Norris *et al.*, 2016). When auditory input is received, a process of sensory analysis begins in temporal lobe, with the output fed forwards to frontal regions in real-time, where a matching process

occurs. If frontal regions detect that the auditory information matches expectations, they indicate that further processing is unnecessary by feeding back a stop signal to temporal regions. Such a mechanism could also account for my observation of a delayed reduction in superior temporal activity when the text cue is matching. This alternative hypothesis would also predict that total superior temporal lobe activity over the whole epoch would be greater in patients than in controls, as their stop signal is delayed. The present data showed a non-significant trend in this direction. However, this stop-signal hypothesis is unable to account for fMRI evidence demonstrating an interaction of prior knowledge and sensory detail in superior temporal representations of degraded speech (Blank and Davis, 2016). These fMRI findings can only be simulated by a computational model in which superior temporal regions represent the discrepancy between predicted and heard speech (i.e. prediction error). In the predictive coding model, the delayed neural effects of cue congruency observed here reflect an iterative process whereby predictions are recursively updated to minimise error; this process operates more slowly in my patient group.

Most models of prediction and perception, including my own Bayesian modelling, make the assumption that perceptual outcomes represent an ideal observation of peripheral sensation. This might not be the case if individuals hold aberrant beliefs about the fidelity of their sensory input based on differences in previous experience (Orhan and Jacobs, 2014). The results of my Bayesian modelling are inconsistent with the view that my patients are not ideal observers of their sensory experience. If patients with nvPPA had learnt that their auditory input were unreliable, this could only explain the present data by proposing a dissociation between an underestimation of the precision of their sensory input when reporting perceptual clarity (experiment 1) and an intact ability to discriminate sensory features when distinguishing alternative vocoded words (experiment 2) (Norris *et al.*, 2016). This would manifest in my Bayesian modelling as an increase in perceptual threshold, as any given distribution of sensory input would be reported as less clear. In fact, I found that patients did not statistically differ from controls in terms of their perceptual thresholds. Indeed, the trend was towards lower thresholds, which might reflect an appropriate downwards extension of the bottom-end of their perceptual clarity rating scale to reflect the fact that they were slightly less good at identifying vocoded speech than controls

(experiment 2), indicating that they had access to slightly less sensory detail during the experiment. Therefore, my behavioural results cannot be accounted for by patients with nfvPPA not being ideal observers of vocoded speech.

The hypothesis that beta oscillations represent the instantiation of predictions has existed for some time (see (Arnal and Giraud, 2012) for review). It has been supported by evidence including computational simulations (Bastos *et al.*, 2012), and empirical observations of backward beta connectivity in speech processing (Fontolan *et al.*, 2014). More recently, direct recordings from human auditory cortex have directly linked beta frequency oscillations to the updating of predictions (Sedley *et al.*, 2016), based on correlations between observed brain activity and Bayes-optimal predictions generated from presented stimuli. In my cohort, I not only replicate the finding of beta oscillations as a correlate of prediction instantiation, but go further in demonstrating that, irrespective of disease status, the strength of this beta activity across subjects relates to the precision of their predictions, as determined by my Bayesian behavioural modelling.

3.5.3 Study limitations

This experiment relies on a dissociation in neurodegeneration between affected frontal brain regions and unaffected superior temporal regions. In section 3.4.1 I have demonstrated this to be true in terms of grey matter volume, however neurodegeneration caused by tau and TDP-43 pathology manifests in synaptic dysfunction before volume loss becomes evident. While I cannot exclude such early changes in my cohort, in section 3.4.3 I demonstrate that measured physiological responses to bottom-up manipulations of sensory detail are normal, and that it is only through the manipulation of prior expectations that a group difference in the timecourse of neuronal is evident.

In section 3.4.5 I demonstrated that patients with nfvPPA do not perform as well as controls at identifying vocoded speech. It is therefore possible that an overall difference in task difficulty affected the degree to which participants relied on priming information. However, the group performance difference was small, and was accounted for on an individual basis in the Bayesian modelling of section 3.4.6 .

Additionally, patients performed better at identifying speech with 8 channels than controls did with 4 channels, but still displayed a much larger congruency effect for 8-channel vocoded words than controls do for 4-channel speech.

Finally, as nfvPPA is a very rare disease and only early-stage patients were assessed, the number of individuals in this study is relatively small. The principal finding of a neuronal processing delay dependent on prior expectations was manifest in every patient individually (Figure 3-11), and is therefore not in doubt. However, while statistically significant, the correlation analyses between induced beta power and prediction strength (Figure 3-10), and between processing latency and frontal grey matter volume (Figure 3-11) would be strengthened by replication.

3.6 Conclusion:

I demonstrate distant neural effects of the degeneration of top-down signals from frontal lobes, during speech perception. Patients with neural damage in these frontal regions displayed significantly delayed activity in temporal regions that I have demonstrated to function normally in response to bottom-up manipulations of speech clarity. This did not result in an inability to utilise contextual information, but was rather associated with inflexible and overly precise prior expectations. I provide evidence of a direct relationship between the degree of frontal lobe degeneration and a delay in the neural mechanism for the reconciliation of predictions, which results in their inflexible application. In turn, this results in the formation of aberrantly precise prior expectations, perhaps in order to maximise their benefit in the more challenging states of a dynamic environment. These aberrantly precise priors manifest as increased beta power during the instantiation of predictions, in agreement with theoretical frameworks of predictive coding. Together, my results provide causal evidence for a critical role of frontal regions for the reconciliation of predictions during the perception and comprehension of speech.

3.7 Chapter Summary:

Perception relies on the integration of sensory information and prior expectations. Studies of speech perception provide evidence for left-lateralised top-down influences of frontal activity on temporal brain regions, which might support hierarchical generative models of sensory input such as predictive coding. However, the role of top-down predictions in supporting higher level perception remains controversial. Here I show that selective neurodegeneration of human frontal speech regions results in significantly delayed reconciliation of predictions in temporal cortex. These temporal regions were not atrophic, displayed normal evoked magnetic and electrical power, and preserved neural sensitivity to (bottom-up) manipulations of sensory detail. Frontal neurodegeneration did not prevent the use of contextual information: instead, prior expectations were applied inflexibly. The precision of predictions correlated with beta power during the instantiation of predictions, in line with theoretical models of the neural instantiation of predictive coding. My results provide evidence that fronto-temporal interactions play a causal role in reconciling prior predictions with degraded sensory signals, thereby demonstrating that top-down frontal mechanisms are necessary for effective use of prior knowledge during the perception of speech. This work demonstrates that higher level frontal mechanisms for cognitive and behavioural flexibility make a critical functional contribution to the hierarchical generative models underlying speech perception.

Chapter 4: Artificial grammar learning in vascular and progressive non-fluent aphasia

4.1 Preface

Chapter 3 provided a link between the network-level physiological changes that occur in neurodegeneration and the deficits they cause in core cognitive systems, by providing evidence for diaschisis; abnormalities in top-down influences from frontal brain regions caused changes in neural processing in temporal brain regions that were functionally and anatomically intact in isolation. In this chapter I further explore deficits in core cognitive systems by using psychophysical methods to investigate the nature of grammatical impairment in frontal aphasia. To do this I used an artificial grammar learning paradigm to define the abilities of patients with agrammatism due to nfvPPA, in comparison to controls and patients with agrammatic aphasia due to frontal stroke. This chapter concentrates specifically on the nature of grammatical processing as a core cognitive system, but lays the groundwork for chapter 5, section 5.2.3 in which I integrate the results of chapters 3 and 4 to directly relate abnormal neurophysiological connections in the language network to the complex behavioural abnormalities observed in nfvPPA.

This chapter is based on a paper I have recently published in *Neuropsychologia* (Cope *et al.*, 2017b). It represents a multi-site study, requiring the help of many hands. I designed and piloted the artificial grammar in conjunction with Dr Benjamin Wilson and Prof Christopher Petkov, as it flows naturally from their studies of the grammatical abilities of non-human primates. I collected the data for all of the patients with nfvPPA, all of the controls, and one of the stroke patients; the rest of the stroke patients were tested in Reading by Ms Rebecca Drinkall under supervision of Dr Holly Robson, who followed my protocol and used computer programmes written by me for stimulus delivery. Stereotyped speech samples were recorded for each participant, and were triple-rated according to the Boston Diagnostic Aphasia Examination scales by myself, Dr Holly Robson and Prof Karalyn Patterson. Ms Julie Wiggins (research nurse) very kindly helped me to obtain structural MRI scans for the nfvPPA group. I

performed the voxel based morphometry analysis of these scans with assistance from Mr P Simon Jones. Lesion mapping of the stroke group was performed by Dr Lauren Dean (because many had only clinical MRI scans unsuitable for voxel based morphometry). I am grateful to Prof Timothy Griffiths (Newcastle) for initial discussions about study design, and for allowing me to recruit one of his patients with nfvPPA, one of his patients with frontal stroke aphasia, and several of the neurological controls to the final study. I am also indebted to Professor Matthew Lambon-Ralph (Manchester) for allowing me access to some of his well characterised patients with aphasia due to frontal stroke for the purposes of sequence development and piloting (these pilots do not form part of the final study reported here, but were invaluable in ensuring that the stimuli and paradigms would be accessible to my clinical cohorts). I performed all of the analyses, made all of the figures except the lower half of panel B of Figure 4-1 (which was made by Dr Lauren Dean) and Figure 4-4 (which was made by Dr Benjamin Wilson). I wrote the manuscript on which this chapter is based with the aid of insightful comments from the collaborators listed above, especially Dr Wilson and Prof Petkov, as well as Dr Manon Grube and my supervisor, Prof James Rowe.

4.2 Introduction

Aphasia is an impairment of speech and language that often leaves other cognitive and intellectual capacities preserved. Patients with non-fluent aphasias due to frontal lobe damage exhibit significant impairments in grammar (Caramazza and Zurif, 1976, Caplan *et al.*, 1985, Berndt *et al.*, 1996). The grammatical impairments in comprehension and production are separable, but tend to be highly correlated (Berndt *et al.*, 1983), suggesting that they stem from disruption of core syntactic processes rather than processes such as memory, executive function or motor function (Wilson *et al.*, 2011). The deficits are phenomenologically similar in patients with damage due to neurodegeneration (non-fluent variant Primary Progressive Aphasia, nfvPPA) and stroke ('Broca's aphasia'); however detailed analysis of speech *output* has revealed somewhat differential impairments (Patterson *et al.*, 2006, Thompson *et al.*, 2013). Impairments of *receptive* abilities have not previously been compared in similar detail.

Beyond these linguistic deficits, patients with aphasia also display auditory domain general processing deficits that are not specifically related to language (Caramazza and Zurif, 1976, Dominey *et al.*, 2003, Patel *et al.*, 2008, Christiansen *et al.*, 2010, Goll *et al.*, 2010, Grube *et al.*, 2012, Geranmayeh *et al.*, 2014a, Zimmerer *et al.*, 2014a, Zimmerer and Varley, 2015, Grube *et al.*, 2016). Such studies have raised the possibility that deficits in structured sound processing may play a prominent role in language disorders, but the nature and extent of these deficits remain unclear. It also remains unclear whether impairments in aphasia are specific to the speech domain (Conway and Pisoni, 2008), or also apply to non-linguistic auditory sequences (Christiansen *et al.*, 2010). One study identified impairments in implicit musical sequence learning in vascular aphasia (Patel *et al.*, 2008), but direct comparisons outside of a musical framework are lacking. If artificial grammar learning tasks tap into domain general (rather than language specific) processes, one would expect rule acquisition to generalise from sequences of nonsense words to identically structured sequences of other sounds, such as tones.

It has been commonly held that grammatical impairments are specific to complex linguistic constructs such as hierarchical relationships and the passive voice (Goodman and Bates, 1997, Grodzinsky, 2000), but there is limited evidence for such dissociations

(Zimmerer *et al.*, 2014b). By contrast, some studies suggest that the processing of adjacent relationships may be disproportionately impaired by frontal lesions involving motor association cortex (Opitz and Kotz, 2012). Recent studies examining artificial grammar learning in agrammatic aphasia secondary to stroke have focussed on linear sentential structures with varying transitional probabilities (Schuchard and Thompson, 2017). A key outstanding question, therefore, is whether agrammatic aphasia is characterised specifically by deficits for more complex linguistic structures or rather by a more global impairment in processing structured auditory sequences (Berndt, 2000).

Artificial grammar learning tasks are particularly well suited for delineating competence in structured sequence processing, as they focus on ordering relationships in the absence of other cues (e.g., semantics, phonology or pragmatics). They test learning of the rules governing the order in which stimuli occur in a sequence (Reber, 1967). Participants are typically exposed to sequences of stimuli that follow certain rules, so that the ordering relationships between the sequence elements can be learned implicitly. They are then tested with novel sequences that are either consistent with these rules or that violate them in some way, to assess learning. The implicit nature of these tasks allows the testing of a wide range of participants, including patients with aphasia. Unlike natural language tasks, it is possible to present structurally identical sequences comprised of different tokens, for example nonsense words or non-linguistic tone stimuli, to assess the contribution of phonological processing. Finally, artificial grammars with multiple levels of complexity can be used to quantify how well participants are able to learn increasingly complex rules, which may more closely reflect those in natural language grammars (Romberg and Saffran, 2013, Wilson *et al.*, 2015).

The ability to process auditory sequences, even when stimuli are meaningless, is strongly linked with linguistic proficiency (Gómez and Gerken, 2000, Conway and Pisoni, 2008, Conway *et al.*, 2010, Frost *et al.*, 2015). Neuroimaging studies have demonstrated that artificial grammar processing engages a left-lateralised network of frontal, temporal and parietal brain areas similar to the set of regions involved in syntactic operations during natural language tasks (Friederici *et al.*, 2000, Ni *et al.*, 2000, Friederici and Kotz, 2003, Petersson *et al.*, 2004, Forkstam *et al.*, 2006, Friederici *et al.*, 2006, Hickok and Poeppel, 2007, Bahlmann *et al.*, 2008, Makuuchi *et*

al., 2009, Folia *et al.*, 2011, Friederici, 2011, Fedorenko *et al.*, 2012, Petersson *et al.*, 2012) and are associated with developmental language impairment (Evans *et al.*, 2009).

The sequence processing ability of patients with non-fluent aphasia patient groups has not been systematically compared across aetiologies. Non-fluent variant Primary Progressive Aphasia (nfvPPA) is in many ways the neurodegenerative equivalent of Broca's aphasia, being an adult onset neurodegenerative aphasia characterised by agrammatism and speech apraxia (Gorno-Tempini *et al.*, 2011), although some differences do exist in the pattern of speech output impairment (Patterson *et al.*, 2006). The majority of cases are associated with primary tau pathology but a significant minority have TDP-43 related disease (Kertesz *et al.*, 2005, Josephs *et al.*, 2006, Knibb *et al.*, 2006ab, Knibb *et al.*, 2006ba, Mesulam *et al.*, 2014). nfvPPA typically leads to subtle neuroimaging changes in left inferior frontal and insular cortex (Gorno-Tempini *et al.*, 2004), which correlate with clinical severity (Rogalski *et al.*, 2011). Chronic non-fluent aphasia due to stroke (Broca's aphasia) results in a similar clinical phenotype of agrammatism and apraxia of speech. The left frontal tissue damage is stable, with partial clinical improvement over time (Kertesz and McCabe, 1977). The extent and pace of this improvement is variable and depends strongly on the integrity of the underlying white matter (Price *et al.*, 2010, Seghier *et al.*, 2016). Better understanding of the abilities of participants with similar symptoms arising from very different aetiologies could provide valuable insights into the neurobiological underpinnings of domain-general and language-related processes, and inform treatment strategies (Brownsett *et al.*, 2014, Geranmayeh *et al.*, 2014a).

In the present study, patients with nfvPPA, non-fluent aphasia due to stroke, and matched controls were tested on their implicit learning of a mixed-complexity artificial grammar, combining sequencing relationships of increasing complexity using nonsense words or tones. I aimed to test the following linked hypotheses:

- 1) Rule acquisition differs when structurally identical sequences are comprised of nonsense words rather than non-linguistic tones.
- 2) Artificial grammar learning ability is similar in patients with vascular and neurodegenerative aphasia.

- 3) Grammatical impairments in aphasic patients are disproportionately greater for complex, configurational or hierarchical, sequencing operations.
- 4) Patients with aphasia can improve their ability to detect grammatical disruptions with repeated implicit training.

4.3 Methods

4.3.1 Participants

Three groups of participants were recruited. The nfvPPA group overlapped with, but was not identical to, that recruited for the work described in chapter 3. Demographics of the groups are outlined in Table 4-1.

	Control	nfvPPA	Stroke
Number	11	10	12
Age	69 (8, 54-79)	73 (7, 63-82)	60 (11, 33-74)
Age leaving education	18 (2, 15-22)	18 (3, 15-25)	20 (4, 15-26)
Years of musical training	2 (3, 0-10)	1 (1, 0-3)	3 (5, 0-13)

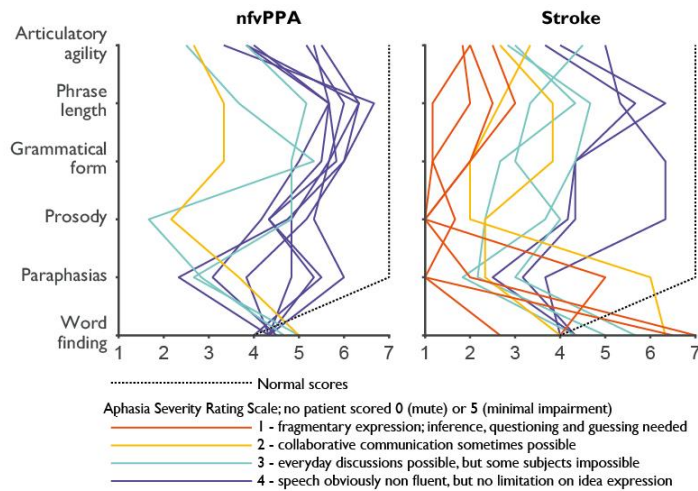
Table 4-1 Participant demographics

Mean (s.d., range). Age leaving education is reported as it is a better measure of highest scholastic attainment than number of years in study. No individuals were mature students.

All patients were right handed. One control was left handed. Thirteen patients with mild to moderate nfvPPA were identified from specialist cognitive clinics according to consensus diagnostic criteria (Gorno-Tempini *et al.*, 2011). These criteria were strictly applied; particular care was taken to exclude non-fluent patients who had lexical difficulties, in order to select patients most likely to have underlying tau or TDP-43 related pathology preferentially involving left frontal lobes, rather than Alzheimer-type pathology of parietal lobes (Rogalski *et al.*, 2011, Rohrer *et al.*, 2012, Sajjadi *et al.*, 2012, Sajjadi *et al.*, 2014, Mandelli *et al.*, 2016). Three patients were excluded on the basis of yes/no response confusion (a common early symptom in nfvPPA that might otherwise have reduced my power to detect language specific effects), resulting in 10

complete nfvPPA datasets. On the short form of the Boston Diagnostic Aphasia Examination (BDAE) (Goodglass *et al.*, 1983) all patients scored 10/10 for responsive naming, 12/12 for special categories, at least 15/16 for basic word discrimination and at least 9/10 for following complex commands. While nfvPPA exists on a spectrum, with differing ratios of speech apraxia and agrammatism, all of my patients displayed some degree of impairment of expressive grammar in free speech, and all but two displayed impairment of receptive grammar as measured by the sentence comprehension task on the ‘verb and sentences test’ (VAST) (Bastiaanse *et al.*, 2003) (mean 87.5%, range 70-100%). Similarly, the patients varied in their degree of expressive agrammatism, but none was completely unimpaired. Speech profiles are shown in Figure 4-1 A. I determined BDAE profiles as the average of three independent ratings of free speech and picture description undertaken by Dr Holly Robson, Prof Karalyn Patterson, and myself. Inter-rater reliability for grammatical form was good, with pairwise Pearson correlations of 0.87, 0.85 and 0.85. Areas of significant grey or white matter loss are shown in Figure 4-1 B, upper panel.

A) Boston Diagnostic Aphasia Examination Profiles



B) Patient Lesion Mapping

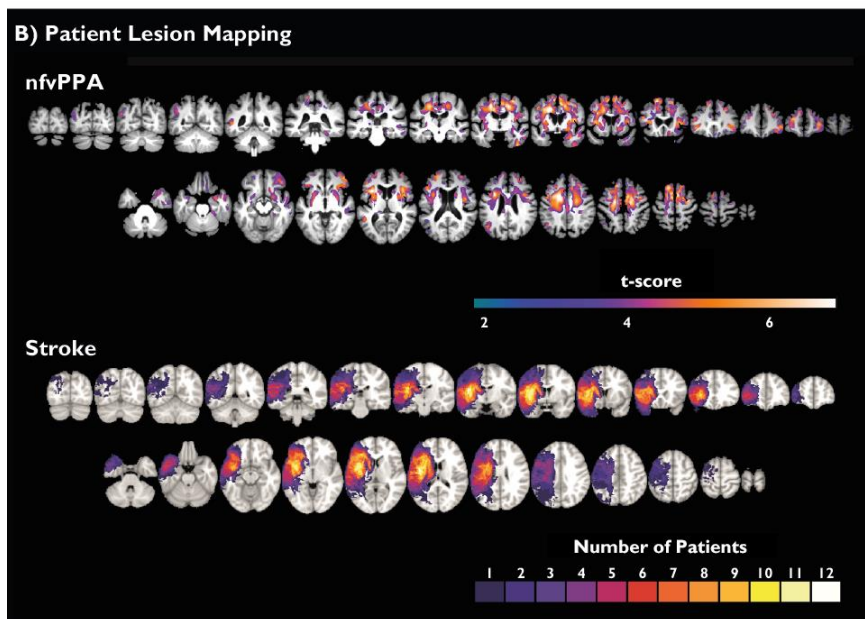


Figure 4-1 Group characteristics

A) Boston Diagnostic Aphasia Examination Profiles for *nfvPPA* and stroke groups. Normal values illustrated as a broken black line. Colour coding of individual profiles based on Aphasias Severity Rating Scale; 1 = red, 2 = magenta, 3 = yellow, 4 = blue. No patients had an ASRS of 0 (no usable speech or auditory comprehension) or 5 (minimal discernible handicap). B) Upper: Voxel based morphometry of *nfvPPA* vs age-matched healthy controls. Coloured regions demonstrate cluster-wise significance at $FWE < 0.05$ with a cluster defining threshold of 0.001 for either grey or white matter volume. Lower: lesion overlap map for the stroke group.

It is widely recognised that patients with nfvPPA report difficulties with understanding speech (Goll *et al.*, 2010, Cope *et al.*, 2014b, Grube *et al.*, 2016). I asked the patients in this study to complete Likert scales assessing their difficulty with ‘Understanding speech in a quiet room’, ‘Telling the direction a sound is coming from’, ‘Understanding speech in a noisy restaurant’, ‘Hearing announcements at a bus or rail station’ as well as ‘How loud do people tell you your TV is?’ Compared to a matched group of controls, patients differed only in reporting more difficulty with ‘Understanding speech in a quiet room’ ($p=0.02$). Of the Boston Diagnostic Aphasia Examination (BDAE) sub-scores, this difficulty was strongly correlated only with ‘Grammatical form’ ($r^2=0.778$, $p<0.001$, Figure 4-2).

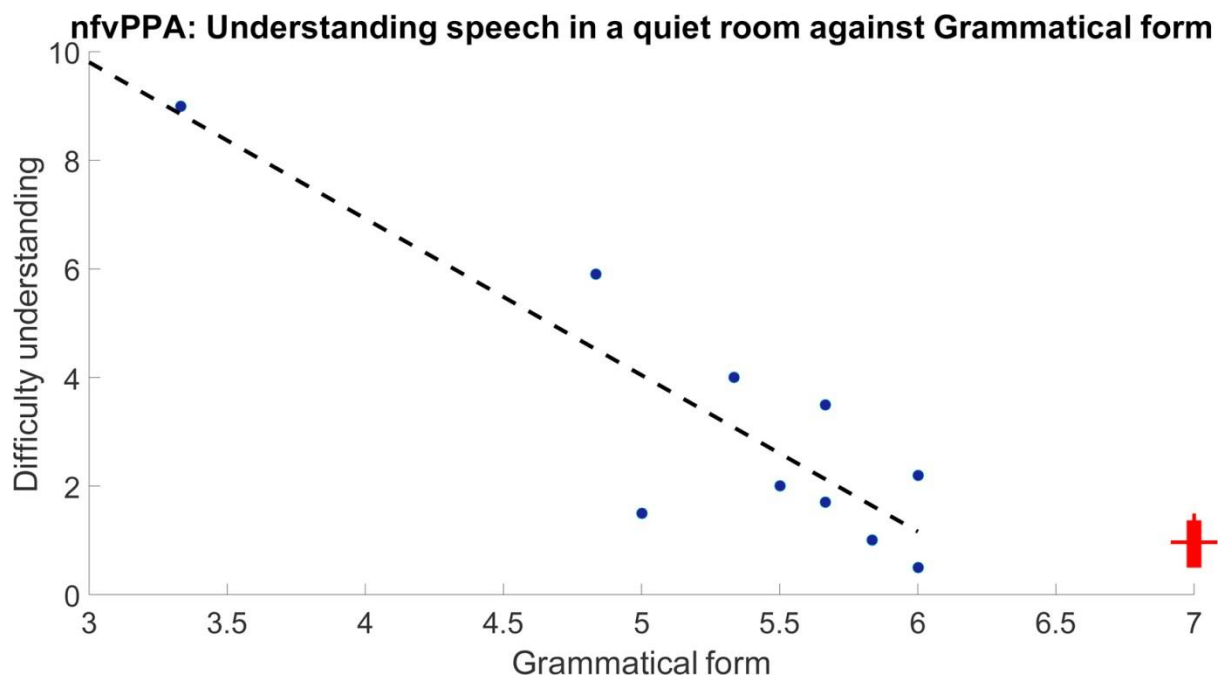


Figure 4-2 A plot for nfvPPA of difficulty ‘Understanding speech in a quiet room’ against ‘Grammatical form’ from the BDAE. Individual patients are shown as blue circles. A boxplot of control ratings is shown in red. The dashed trend line had an r^2 of 0.778 ($p<0.001$).

Patients with non-fluent aphasia due to left sided stroke were recruited from a volunteer database, supplemented by the identification of incident cases by regional research networks. Recruitment criteria were: a single stroke of at least six months chronicity resulting in at least one month of non-fluent aphasia, with MRI evidence of

involvement of either left inferior trigone or operculum. Samples of speech from the participants are available in supplementary materials, and speech profiles (again triple marked) are shown in Figure 4-1 A. On the whole, the stroke group had more severe language impairments than the nfvPPA group. All had some degree of impairment of grammatical form in free speech, and all but two had impairment of receptive grammar on the VAST (mean 70%, range 40-100%). Lesion overlap maps are shown in Figure 4-2 B, lower panel.

Care was taken to recruit an appropriate control group. During development of the artificial grammar, extensive piloting developed structures for which learning was least influenced by years of education or performance on global cognitive tests. Nonetheless, it is important to minimise this potential confound by avoiding the use of biased volunteer panels, which tend to preferentially recruit highly educated individuals with supra-normal motivation in research tasks. Therefore, I recruited 8 neurological controls with either chronic inflammatory demyelinating polyneuropathy or multifocal motor neuropathy with conduction block, and three spouses of patients with nfvPPA, resulting in 11 control datasets. These individuals were chosen to represent a cohort of age-matched individuals with healthy brains and similar levels of habitual neurological contact to the patient groups. All scored normally on the Addenbrooke's Cognitive Examination – Revised (ACE-R) (mean 96/100, range 92-99) and Raven's progressive matrices (mean 47/60, range 37-60).

It was possible to perform pure tone audiometry in all patients with nfvPPA, 9 of the 12 patients with stroke aphasia and 8 of the 11 neurological controls. This demonstrated that the groups had well matched and age-appropriate auditory acuity (Figure 4-3).

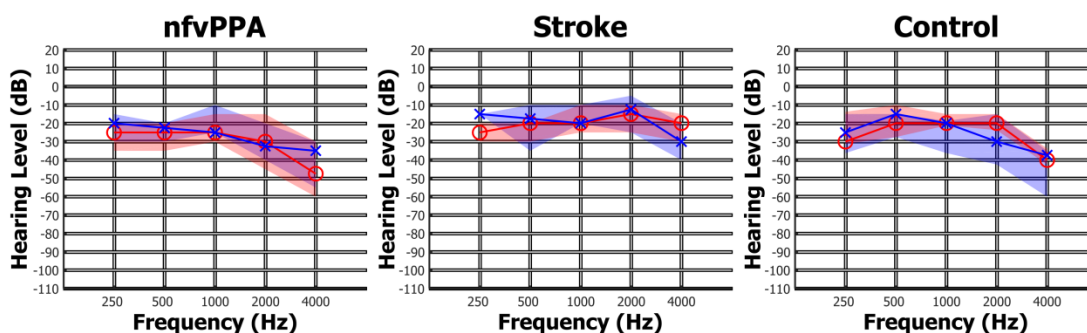
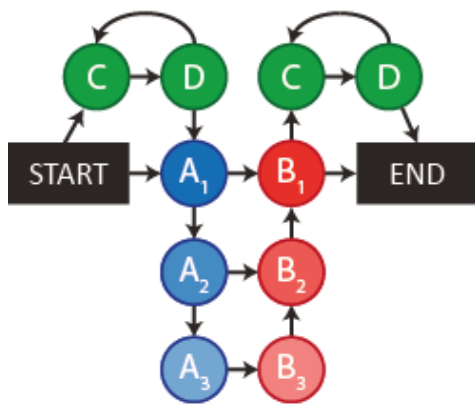


Figure 4-3 Composite pure tone audiograms for each group.

Red circles joined by lines denote the median auditory threshold in the right ear; blue crosses joined by lines the median auditory threshold in the left ear. Shaded areas represent the inter-quartile range of auditory acuity in the right (red) and left (blue) ears.

4.3.2 Stimuli

The Artificial Grammar (AG) used here generates sequences of stimuli from 8 unique elements (Figure 4-4). These sequences are governed by a number of rules of increasing complexity. Rule 1) if a ‘C’ element occurs it must be immediately followed by a ‘D’ element. This represents a simple, invariant linear relationship between two adjacent sequence elements, and will henceforth be referred to as the ‘linear’ rule. Rule 2) all of the ‘A’ elements in the sequence must occur before all of the ‘B’ elements. This is a more complex rule, requiring the participants to recognise a general property of the sequences, and will henceforth be referred to as the ‘configurational’ rule (Zimmerer and Varley, 2015). Rule 3) each ‘A’ element type must be paired with the appropriate ‘B’ elements in embedded relationships (e.g., $A_1[A_2[A_3B_3]B_2]B_1$). This complex operation requires tracking both the number and the order of the ‘A’ elements and matching these to the subsequent ‘B’ elements, and is referred to as the ‘hierarchical’ rule.



Nonsense Words **Tones**

A ₁	'saf'	Mid up sweep
A ₂	'sef'	Low up sweep
A ₃	'sif'	High up sweep
B ₁	'gak'	Mid down sweep
B ₂	'gek'	Low down sweep
B ₃	'gik'	High down sweep
C	'pob'	Low tone
D	'jat'	High tone

Three Tasks

- Task 1: Nonsense word task
- Task 2: Tone sweep task
- Task 3: Oddball deviance detection task

Three levels of Sequence Complexity

- Level 1: **Linear** - C is followed by D
- Level 2: **Configurational** - all A elements occur before B elements
- Level 3: **Hierarchical** - each A element must be paired with the correct B

Example sequences

	Consistent	Violation
<i>Linear</i>	CDCDA ₁ B ₁	CCDDA ₁ B ₁
<i>Configurational</i>	A ₁ A ₂ B ₂ B ₁ CD	A ₁ B ₁ A ₂ B ₂ CD
<i>Hierarchical</i>	A ₁ A ₂ A ₃ B ₃ B ₂ B ₁	A ₁ A ₂ A ₃ B ₂ B ₃ B ₁

Figure 4-4 Artificial grammar structure and stimuli.

Sequences consistent with the AG are generated by following any path of arrows from start to end in the illustrated state transition graph (Figure 4-4). Ten consistent sequences were used for the exposure phase of the experiment (Table 4-2). These sequences were of variable length and contained all of the legal transitions possible with the AG. The remaining subset of consistent sequences generated by the AG were kept for the subsequent testing phase, to allow us to present novel, previously unheard sequences (Table 4-2). During the testing phase, the participants were presented with 4 repetitions each of 6 consistent and 6 violation sequences, in a pseudo-random order. All test sequences were six elements long, meaning that sequence duration could not be used as a cue by participants. The six violation sequences contained two sequences with violations of each of the three AG rules (Table 4-2). This design allowed us to identify the specific features of the sequences to which the participants were sensitive.

Exposure Sequences	Testing Sequences		
A ₁ A ₂ A ₃ B ₃ B ₂ B ₁	A ₁ A ₂ A ₃ B ₃ B ₂ B ₁	Consistent	Familiar
CDA ₁ B ₁ CD	A ₁ B ₁ CD	Consistent	Familiar
A ₁ B ₁ CD	CDA ₁ B ₁ CD	Consistent	Familiar
A ₁ A ₂ B ₂ B ₁	CDA ₁ A ₂ B ₂ B ₁	Consistent	Novel
CDA ₁ B ₁	A ₁ A ₂ B ₂ B ₁ CD	Consistent	Novel
A ₁ B ₁ CD	CDCDA ₁ B ₁	Consistent	Novel
CDCDA ₁ B ₁ CD	CCDD A ₁ B ₁	Violation	Violates Rule 1
CDA ₁ A ₂ A ₃ B ₃ B ₂ B ₁	DCA ₁ B ₁ DC	Violation	Violates Rule 1
A ₁ A ₂ A ₃ B ₃ B ₂ B ₁ CD	C D ₁ A ₁ CD	Violation	Violates Rule 2
A ₁ A ₂ A ₃ B ₃ B ₂ B ₁	A ₁ B ₁ A ₂ B ₂ CD	Violation	Violates Rule 2
	A ₁ A ₂ B ₁ B ₂ CD	Violation	Violates Rule 3
	A ₁ A ₂ A ₃ B ₂ B ₃ B ₁	Violation	Violates Rule 3

Table 4-2 Exposure and testing sequences.

I tested participants with identically structured sequences of both naturally spoken consonant-vowel-consonant (CVC) nonsense words and non-linguistic tone stimuli. The stimuli were designed to provide acoustic cues to highlight the relationships between some of the key sequencing relationships, as follows. In both the CVC and tone experiments, the ‘A’ and ‘B’ elements fell into distinct acoustic categories. In the CVC experiment the ‘A’ elements all took the form “s-vowel-f” (e.g., “sif”) while the ‘B’ elements were “g-vowel-k” (e.g., “gik”). In the tone experiment the ‘A’ elements were all upwards pitch sweeps while the ‘B’ elements were downward sweeps. Furthermore, the A_X-B_X relationships that are critical to Rule 3 were highlighted by the presence of the same vowel sounds in the nonsense word experiment (i.e., A₁ and B₁ both contain the central vowel ‘a’) or the tone height in the tone experiment (i.e., both the A₁ and B₁ pitch sweeps are centred on the same frequency). To ensure that the participants learned aspects of the AG during the exposure phase, rather than simply responding to acoustical properties of the stimuli, I designed the tone stimuli to avoid linearly increasing or decreasing in pitch in the A₁A₂A₃ or B₃B₂B₁ parts of the sequences. Instead, the centre frequencies of the tone sweeps in such a sequence would be ‘mid-low-high-high-low-mid’. The ‘C’ and ‘D’ elements in the nonsense word experiment were designed to be clearly phonetically distinct from the ‘A’ and ‘B’ stimuli, and in the tone experiments they were continuous pure tones of high or low pitch.

The nonsense words were produced by a female speaker, recorded with an Edirol R-09HR (Roland Corp.) sound recorder, and combined into exposure and testing sequences using Matlab (100ms inter-stimulus intervals, ISI). The average duration of the nonsense words was 477ms (standard deviation = 7ms). The tone stimuli were generated using Matlab. The low tone sweeps were linear sweeps between 100 and 150Hz (i.e., A₂ began at 100Hz and increased to 150Hz, B₂ began at 150Hz and decreased to 100Hz). The middle tone sweeps ranged between 200 and 300Hz and the high tone sweeps ranged between 400 and 600Hz. The C and D stimuli were pure tones at 350 and 800Hz respectively. The duration of all tones was 450ms, and these were combined into sequences with ISIs of 100ms. Stimuli were presented through Sennheiser HD250 linear 2 headphones, driven by either an Edirol UA-4X or Behringer UCA 202 external sound card. The amplitudes of all stimuli were root-mean-square (RMS) balanced, and sequences were initially presented to participants at ~75 dB SPL (calibrated with an XL2 sound level meter, NTI Audio). At the start of the exposure phase, participants were asked if this volume was comfortable and clearly audible and, if not, were allowed to freely adjust the volume to their preference.

Exposure sequences and test sequences for the CVC and tone languages were presented in exactly the same fixed pseudo-random order. There were no differences between the orders of sequences in the CVC and tone runs; only the sound tokens used to represent each element in the artificial grammar differed.

4.3.3 Procedure

The experimental procedure and instructions given to participants were tightly constrained, to ensure that explicit learning strategies and receptive language difficulties were minimised. The exact wording of the instruction is included in supplementary materials.

Participants were exposed to the CVC language for five minutes. During this time they were simply instructed to listen to the language and to pay attention to the order of the words (the exact script for the instructions is available as supplementary material). They were then tested by being asked to decide whether 48 individual sequences (Table 4-2) were correct (i.e. consistent with the artificial grammar) or incorrect (i.e. violated

the artificial grammar in some way). Participants were able to express their decision either by pressing a button on a keyboard or custom made response box, or by pointing to yes or no on a piece of paper; whichever they found easier. At the end of a run, general overall feedback was provided with smiley to sad faces (Wong and Baker, 1988) according to overall percentage correct, along with the performance descriptor 'Great!' (>60%), 'Well' (55-60%), 'OK' (45-55%), or 'Badly' (<45%). This exposure-test cycle was then repeated in an identical fashion for the tone language. Again, they were explicitly instructed that the important thing was the order of the sounds.

After a short break, participants were then re-exposed to the CVC language for three minutes, before being re-tested. Sequences for both exposure and testing were presented in a different fixed pseudo-random order on each repetition. At the end of this run, feedback was provided relative to the previous CVC run with faces paired with the descriptors 'Much Better' (>110% of previous score), 'Better' (105-110%), 'Same' (90-105%), or 'Worse' (<90%). This procedure was then repeated for the tone language.

After a longer break, during which tea and biscuits were provided, participants completed a personal details questionnaire, which included questions about musical training and handedness (all patients were right handed). Patients then undertook the short form of the Boston Diagnostic Aphasia Examination (Kaplan, 1983) and the first half of the sentence comprehension section of the Verbs and Sentences Test to assess receptive grammar (Bastiaanse *et al.*, 2003); controls completed an ACE-R and were tested on matrix reasoning (Raven, 1960); similarly demanding tasks of similar duration. Participants then completed another three minute exposure and test session on the CVC and tone languages, for a total of three testing sessions for each language.

Finally, each participant was re-exposed to the CVC language for three minutes, but the testing session that followed was replaced with an 'oddball' task. Participants were told that in this final test the 'incorrect' sequences were wrong in a different way, but were not explicitly instructed that they were looking for novel tokens. Where an ordering violation would first have occurred in an 'incorrect' sequence, the CVC token was replaced by a novel, previously unheard, oddball element ('fen', 'muz', 'rol', 'dut', 'boz' or 'cav'). In this way, I was able to assess whether differential performance on the

three grammatical rule types was related to other undesired effects such as stimulus ordering.

All individuals undertook all study procedures on a single day, to ensure that differential patterns of performance consolidation during sleep did not confound my findings. The study procedures took up to four hours, including breaks.

Patients also undertook the short form of the Boston Diagnostic Aphasia Examination (Kaplan, 1983) and the first half of the sentence comprehension section of the Verbs and Sentences Test to assess receptive grammar; (Bastiaanse *et al.*, 2003).

4.3.4 Stroke lesion mapping

The lesioned area of each brain was manually defined on every slice of each patient's 3T T1-weighted MRI scan in FSL, resulting in a 3D lesion mask. The resulting image was then registered to the standard MNI152 brain using FLIRT (FMRIB's Linear Image Registration Tool (Jenkinson and Smith, 2001); affine transformation model, 12 degrees of freedom). This registration matrix was used to register the patient's lesion mask to the standard space, from which a standardised lesion volume was computed in Matlab. Regions of interest in the left hemisphere (frontal inferior trigone, frontal inferior operculum, rolandic operculum, putamen and caudate) were identified using the aal atlas in SPM12, and the percentage of each sub-region that was lesioned was extracted for analysis (Table 4-3).

Subject Number	Broca WM	Broca GM	FOP WM	FOP GM	Frontal Inferior Trigone	Frontal Inferior Operculum	Rolandic Operculum	Putamen	Caudate
1	99	98	99	97	98	98	92	74	28
2	32	33	30	19	33	22	46	77	17
3	0	0	8	45	0	34	83	3	0
4	77	86	77	89	84	86	89	70	42
5	77	54	88	84	60	85	89	10	47
6	100	96	94	61	97	70	71	12	59
7	89	91	85	89	91	88	100	16	0
8	0	0	21	3	0	8	26	51	36
9	54	32	97	73	38	80	99	76	10
10	16	1	35	8	5	16	0	59	30
11	79	59	92	62	65	70	48	48	46
12	32	5	30	16	20	13	21	0	0

Table 4-3 Single subject lesion percentages by region for the stroke group.

4.3.5 nfvPPA atrophy mapping

Nine of the patients in the nfvPPA group underwent a 3T volumetric T1 MRI scan. From a database of healthy control scans from the same scanner, an age-matched normative sample of 36 individuals was selected by finding the four nearest-neighbours to each patient in terms of age, excluding duplication (mean age of these controls was 73 years). After segmentation, the nine nfvPPA scans and nine nearest-neighbour controls were used to create a DARTEL template. This was then applied to the remaining 27 controls. Resultant images were normalised to MNI space in SPM12 with an 8mm smoothing kernel, and separate statistical comparisons were performed for grey and white matter, with total intracranial volume and age as covariates.

As for the stroke lesion mapping, regions of interest in the nfvPPA patients were then identified using the aal atlas, normalised to MNI space. As distinct from the lesion analysis in the stroke cases, these regions were defined bilaterally. The grey matter volume in each region was then extracted by applying these regions to each individual's modulated, warped grey matter segmentation and correcting for total intracranial volume.

4.3.6 Analysis

Performance metrics for analysis were based on signal detection theory (Stanislaw and Todorov, 1999). Standard signal detection measures of discriminability and bias rely

on the underlying trial difficulty within a run being constant. In my artificial grammar, it was expected that violations of the linear relationship (complexity level 1) would be easier to detect than configurational violations (complexity level 2), which in turn might be easier to detect than violations of the hierarchical structure (complexity level 3) (Figure 4-5). To accommodate this, I separately calculated d' and the non-parametric equivalent A' , based on a comparison of performance on each of the three types of violation sequence to all of the consistent sequences. A single value for bias measures was also calculated based on the combined distribution of violation sequences (Figure 4-5). Hit and false alarm rates of 1 were replaced with $(n-0.5)/n$ (where n is the number of trials), and those of 0 with $0.5/n$ (Macmillan and Kaplan, 1985, Stanislaw and Todorov, 1999). The non-parametric analogues of these signal detection metrics, A' for discriminability and β'' for bias, were used for the primary analysis.

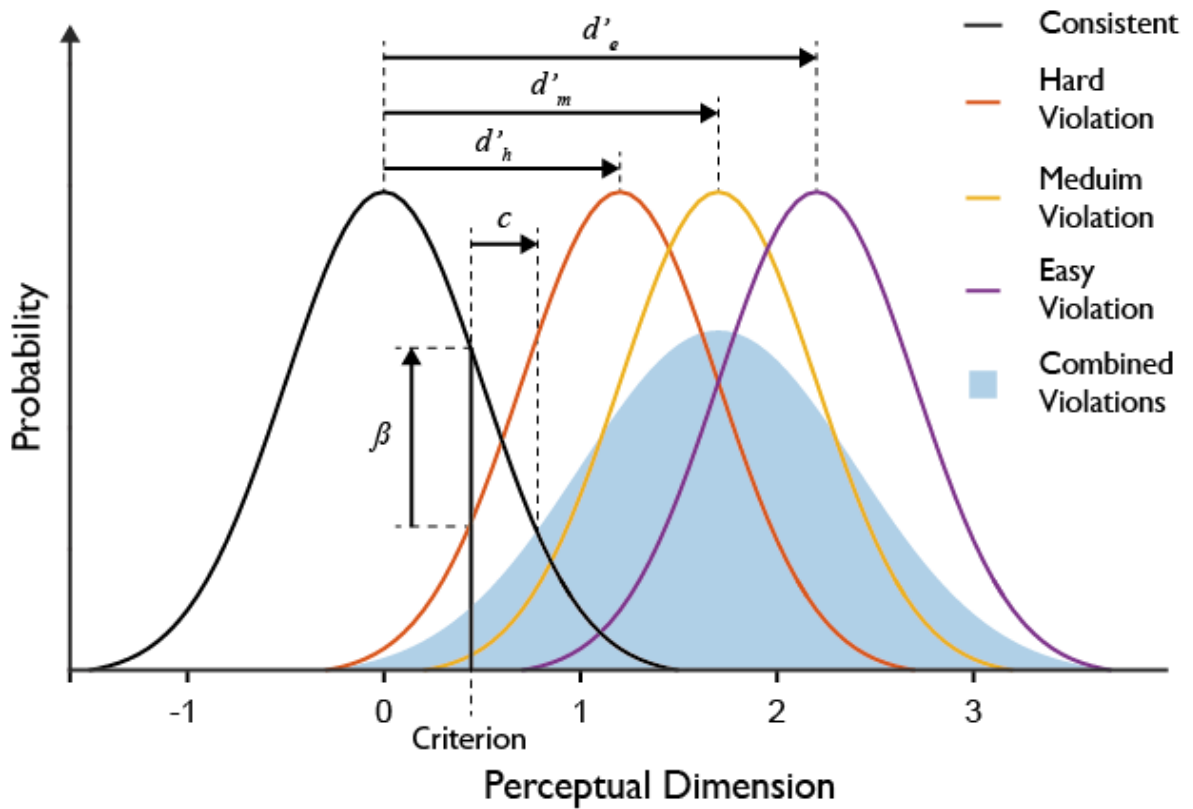


Figure 4-5 Distribution of decision variables.

Cartoon illustrating the distribution of parametric decision variables for an hypothetical experiment with easy, medium and hard to detect rule violations. d' represents the single subject discriminability of each rule violation, while c and β represent different measures of bias (i.e. in this case the tendency to say that a sequence is grammatical if there is no evidence to the contrary). Each rule violation has its own d' measure, reflecting its respective discrimination difficulty, while the bias measures apply to the experimental context as a whole.

All statistical analyses were performed in Matlab R2015b with the Statistics and Machine Learning Toolbox unless otherwise specified. Differences from chance performance in both discriminability measures (A' and d') and measures of bias ($\ln(\beta)$, c and β'') were assessed for each group and condition separately using one-sample Wilcoxon signed rank tests (the non-parametric equivalent of the one sample t-test).

The effects of group and rule complexity on discriminability were assessed with three separate repeated measures ANOVA tests (one for each test type; CVC, tones and oddball), with the factor 'participant number' nested within 'group'. This parametric statistical test was employed because there is no appropriate non-parametric test for repeated measures designs of the kind employed here; the Friedman test does not allow multiple groups to be compared. Significant results were explored with post-hoc comparisons of population marginal means.

The degree of learning across exposure-test pairs was assessed by fitting a general linear model in Minitab 17 for the CVC and tone languages. The response variable was discriminability (A') and the factors were 'participant number' (nested within 'group'), 'rule type', and 'run number'. Significant results were explored with post-hoc Tukey's range tests.

To assess whether the same rules were learned by participants between task types (CVC vs tones vs oddball), and by extension whether learning of the same artificial grammar was transferrable across token types (for CVC vs tones), Spearman correlation matrices were constructed based on performance patterns by sequence for each group. From these, hierarchical cluster analysis was performed to construct dendrograms representing the similarity of performance pattern across test and group, using a 'farthest neighbour' linkage method with a data-driven inconsistency coefficient (The Mathworks Inc., 2015).

Exploratory regression analyses were performed in Minitab 17. As I measured a large number of variables for each subject, I performed stepwise regression to determine those variables that best predicted artificial grammar learning. This is an automated process to identify a useful subset of predictors by sequentially adding and removing predictors until an optimal model is obtained. Software default alpha-to-enter and alpha-to-remove values of 0.15 were used, with confirmatory analyses at 0.1/0.15 and

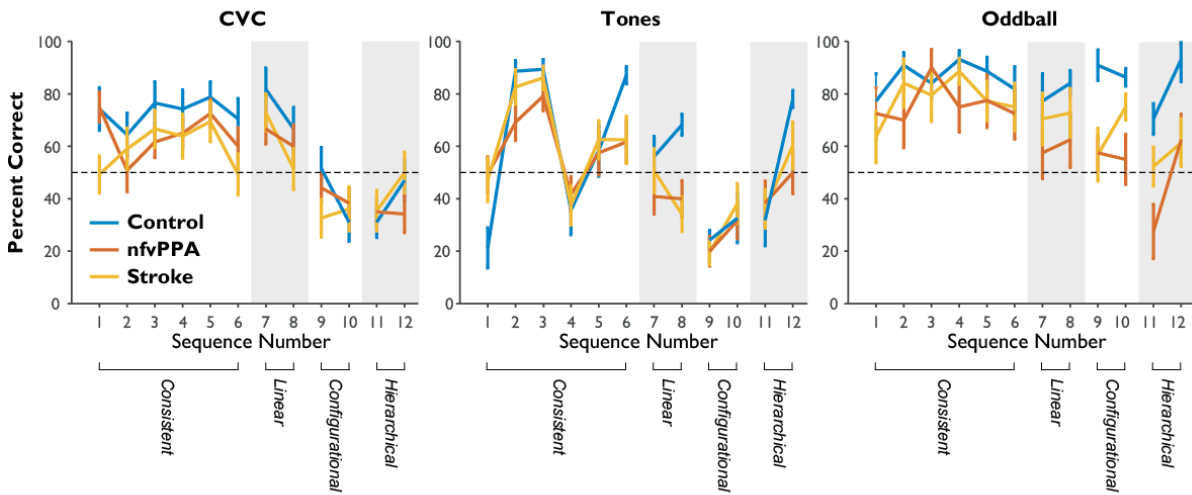
0.1/0.1 yielding identical results. Three separate sets of stepwise regressions were performed; one to explore possible correlations between rule discriminability and neuropsychological and language measures, a second to explore correlations between rule discriminability and stroke lesion site, and a third to explore correlations between rule discriminability and grey matter volume in nfvPPA. The potential continuous predictors included in the first model set were Age, Raven's Progressive Matrix score, years of musical training (which I hypothesised might impact tone language difficulty), sentence comprehension (from the Verbs and Sentences Test), and overall aphasia severity (Aphasia Severity Rating Score). For the second set, the potential continuous predictors were age, the proportion of each region of interest lesioned, total lesion volume, and the number of years since stroke. For the third, potential predictors were age, grey matter volume summed across regions of interest in each hemisphere, and corrected whole brain grey matter volume.

4.4 Results

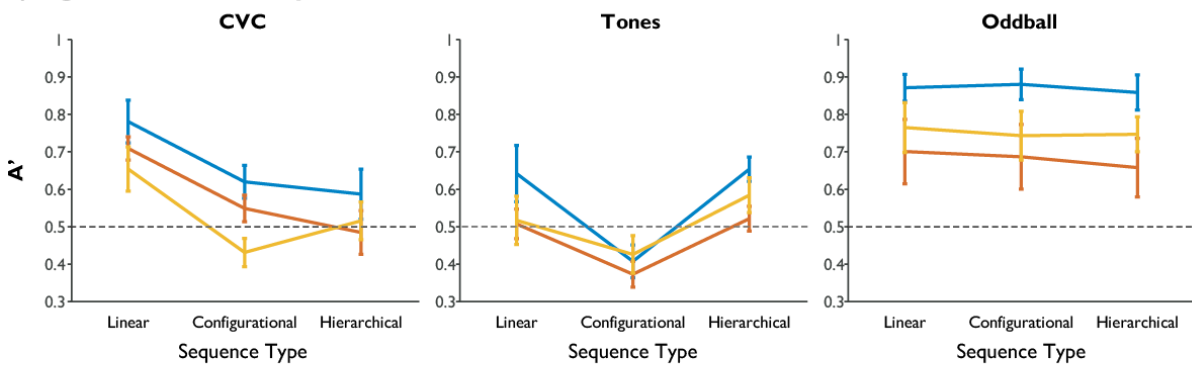
4.4.1 Discriminability of sequencing rules

Raw performance for each individual sequence is shown in Figure 4-6 A, and the results of the signal detection theory analysis are illustrated in Figure 4-6 B. The hierarchical cluster analysis is illustrated in Figure 4-8. Performance did not differ between sequences heard during exposure and test phases (Figure 4-6 A sequences 1-3) and those that were novel during the test phase (Figure 4-6 A sequences 4-6), so these were collapsed. Results are presented for the non-parametric discrimination measure A' , but the same pattern of findings was present for the parametric equivalent d' (see appendix Table 4-5, Table 4-6).

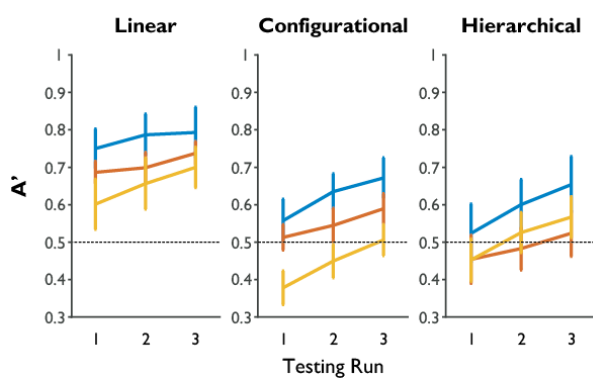
A) Performance on all sequences



B) Signal Detection Analyses



C) Performance over repeated testing - CVC



D) Performance over repeated testing - Tones

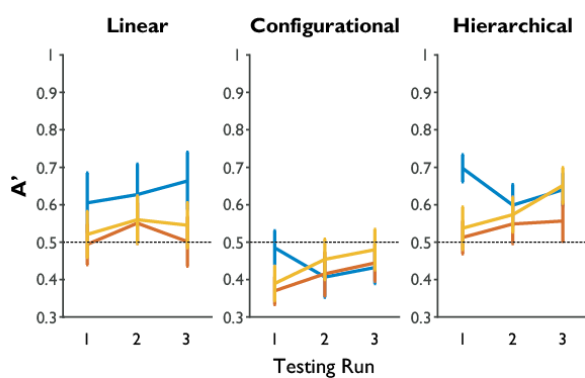


Figure 4-6 Group performance on sequence identification.

Dashed lines represent chance performance. Error bars represent group-wise standard error of the mean. Controls are in blue, *nfvPPA* in red and stroke in orange. A) Proportion of correct responses for each testing sequence by group and task. Sequences 1-3 were consistent with the grammar and familiar from the exposure phase, while 4-6 were consistent and novel. Sequences 7-12 contained violations of the types indicated (see table 2). B) Discriminability of each rule type by group for each language type. C) Overall discriminability by group and run number for the CVC language (improving performance by run represents learning over time). D) Overall discriminability by group and run number for the tone language.

A Figure 4-6 B	Rule complexity	Group	Group x complexity	Participant	
CVC	F(2,60) = 14.8 p<0.0001	F(2,60) = 4.1 p=0.0264	F(4,60) = 0.7 p=0.5933	F(30,60) = 1.4 p=0.1246	
Tones	F(2,60) = 9.1 p=0.0004	F(2,60) = 7.1 p=0.0029	F(4,60) = 0.5 p=0.7421	F(30,60) = 0.3 p=0.9995	
Oddball	F(2,60) = 0.5 p=0.6018	F(2,60) = 2.6 p=0.0916	F(4,60) = 0.2 p=0.9575	F(30,60) = 11.9 p<0.0001	
B Figure 4-7	Bias metric	Group	Group x metric	Participant	
CVC	F(2,60) = 6.7 p=0.0024	F(2,60) = 2.3 p=0.1150	F(4,60) = 0.5 p=0.7721	F(30,60) = 4.0 p<0.0001	
Tones	F(2,60) = 19.1 p<0.0001	F(2,60) = 0.1 p=0.9445	F(4,60) = 1.0 p=0.4184	F(30,60) = 1.7 p=0.0371	
Oddball	F(2,60) = 3.6 p=0.033	F(2,60) = 0.2 p=0.8344	F(4,60) = 0.6 p=0.6516	F(30,60) = 8.2 p<0.0001	
C	Rule	Run	Group	Run x Complexity	Run x Group
CVC Figure 4-6 C	F(2,890) = 141.2 p<0.001	F(2,890) = 28.5 p<0.001	F(30,890) = 14.4 p=0.029	F(4,890) = 0.9 p=0.626	F(4,890) = 0.7 p=0.479
Tones Figure 4-6 D	F(2,890) = 73.8 p<0.001	F(2,890) = 2.9 p=0.055	F(30,890) = 4.3 p=0.026	F(4,890) = 0.7 p=0.572	F(4,890) = 3.3 p=0.010

Table 4-4 Statistical tests corresponding to Figure 4-6 and Figure 4-7.

A and B: Repeated measures ANOVAs of group against rule for the non-parametric discriminability measure A' (panel A; corresponding to Figure 4-6 B) and bias (panel B; corresponding to Figure 4-7), with participant number as a nested factor within group. C: The general linear model assessing learning across runs for the non-parametric discriminability measure A' (corresponding to Figure 4-6 C (CVC) and Figure 4-6 D (Tones)).

For the CVC language, discriminability as measured by A' showed significant main effects of rule complexity and group, but no group x rule interaction or consistent inter-individual differences (Figure 4-6 B, Table 4-4 A). Post-hoc comparison of marginal means indicated that the group difference is driven by the control participants performing significantly better than participants in the stroke group (p=0.0058). Participants with nfvPPA performed at an intermediate level, and were not statistically different from either controls (p=0.14) or stroke (p=0.50). Further, all groups performed better at detecting violations of linear grammatical rules than configurational (p=0.0001) or hierarchical (p=0.0001), which in turn did not differ (p=0.99).

The tone language discriminability measured by A' showed significant main effects of rule complexity and group, but no group x rule interaction or consistent inter-individual differences (Figure 4-6 B, Table 4-4 A). For this language, post-hoc

comparison of marginal means indicated that the group difference is driven by the control participants performing significantly better than participants in the nfvPPA group ($p=0.048$). Participants with stroke performed at an intermediate level, and were not statistically different from either controls ($p=0.31$) or nfvPPA ($p=0.57$). Rather than showing lower performance with increasingly complex rule violations, all groups performed significantly more poorly at detecting violations of the configurational rules than both the linear ($p=0.0009$) and hierarchical ($p=0.0001$), which in turn did not differ ($p=0.73$). Possible reasons for this unexpected pattern are discussed below.

All groups performed well at discriminating the oddball stimuli. For all groups, mean and median discriminability was better than for the CVC or Tone languages. Crucially, there was no effect of rule type for the oddball language (Figure 4-6 B, Table 4-4 A). This is because violations were no longer based on detection of grammatical rules, but on the detection of novel CVC tokens in various positions within the sequence. This observation reassures us that the effect of rule complexity in the CVC language cannot be explained by the position of the violation within a sequence. There was no significant group difference in performance or group x rule interaction, but there was a strongly significant effect of participant, indicating that individuals within each group differed in their ability to detect the novel non-word tokens. Post-hoc comparison of marginal means was not performed, as there was no rationale from the ANOVA to proceed to this.

4.4.2 Bias towards permissibility

From Figure 4-6 A it can be seen that for some sequences, particularly those that violate the more complex rules, participants in all groups performed at a level below chance (50% correct). This would not be expected if participants were simply guessing for these sequences, but would be expected if the grammatical violation was sufficiently subtle that participants made an active decision that the sequence is not inconsistent with the grammar. In other words, participants would display bias towards stating that a sequence was consistent with the artificial grammar unless they had evidence otherwise, but it was not known whether this tendency would differ between groups (Haendiges *et al.*, 1996, Dickey *et al.*, 2008). A bias towards yes was demonstrated,

but there was no group difference in bias or group x metric interaction (Figure 4-7, Table 4-4 B).

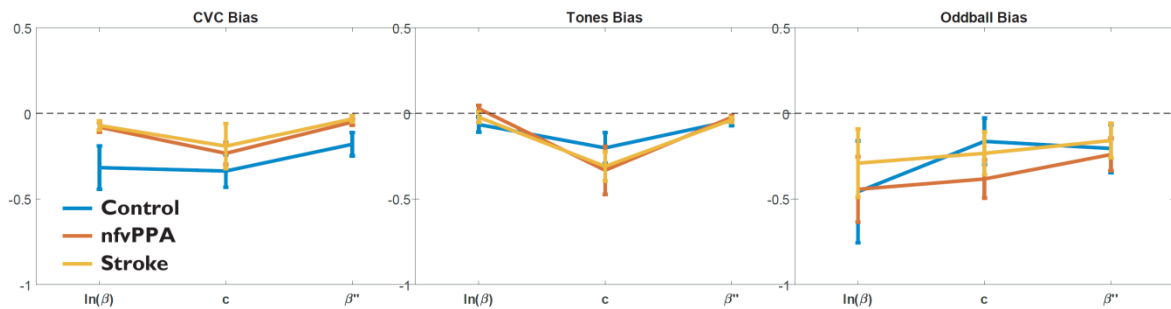


Figure 4-7 Bias metrics by group for each language type
Values less than zero indicate a bias towards classifying sequences as correct.

4.4.3 Implicit learning through repeated exposure-test cycles

Participants, including patients, improved with practice. Results of the general linear model analysis including run number are illustrated in Figure 4-6 C, Figure 4-6 D, and Table 4-4 C. For the CVC language, there were main effects of rule type, run number and group, but no interactions between run number and either rule complexity or group. This suggests, (a) that all groups were learning across repeated exposure-test cycles, (b) that the amount of learning over time was not different between the three rule types, and (c) that the group difference in overall discriminability described above was driven by differences in initial grammatical learning, not by a reduced ability to refine the internal grammatical model through feedback and repeated exposure. Tukey tests confirmed that participants improved on each set of exposure and testing ($p < 0.05$ in all cases). Mean A' across groups for run 1 was 0.55, for run 2 was 0.60, and for run 3 was 0.64 (chance performance is 0.5). Control performance was significantly superior to nfvPPA performance, which was in turn significantly superior to performance in the stroke group.

For the tone language, there were main effects of rule type and group, but only a trend towards a main effect of run number. There was an interaction between run number and group, but not run number and rule complexity. Tukey tests demonstrated that control participants performed significantly better than those with stroke, who in turn performed significantly better than those with nfvPPA. Performance on run 3 was significantly better than on run 1, while run 2 did not differ from either run 1 or 3.

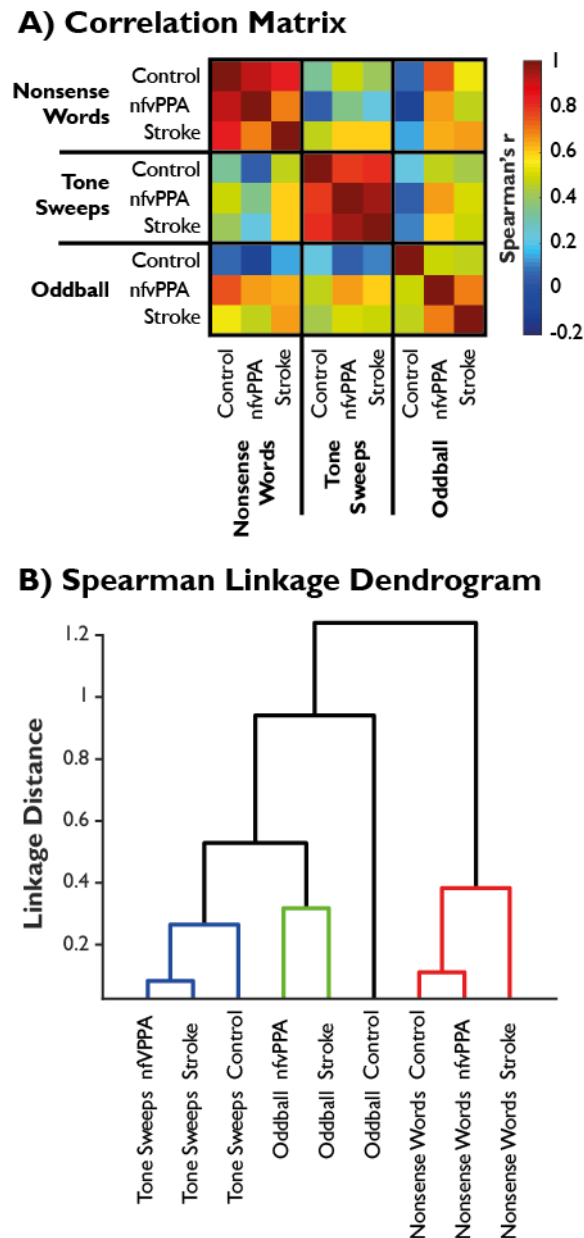


Figure 4-8 Correlation and clustering analysis.

A) Spearman rank-order correlation matrices. B) Linkage based on hierarchical cluster analysis of Spearman correlations. Three clusters emerge with a linkage distance cut-off of 0.5, and are indicated in colour groupings (blue, green and red).

4.4.4 Separation of rule learning between linguistic and non-linguistic sequences

Spearman rank-order correlograms are shown in Figure 4-8 A, and the resultant hierarchical cluster analysis is visualised in Figure 4-8 B. Rule acquisition patterns are highly correlated between groups within each task, but not between tasks within each group. This is confirmed by the cluster analysis. Performance on CVC and Tone languages represent strongly distinct clusters, while Oddball performance profiles are

less distinct (as expected if sequence ordering is unimportant for novel token detection). The difference in profiles between CVC and Tone languages across group was further assessed by a two-sample t-test with unequal variance based on the similarities shown in Figure 4-8 A. In sample 1 were the six within-language similarities (excluding the diagonal) and in sample 2 were the 9 between-language similarities. This confirmed a highly significant group difference in language similarity; $t(12.5)=5.2$, $p=0.0002$. Identical pair-wise tests between groups across language (blinded to overall ability by non-parametric Spearman rank-order correlation) confirmed that performance profiles did not differ between groups (control vs nfvPPA $t(12.3)=-0.12$, $p=0.90$; control vs stroke $t(10.2)=-0.76$, $p=0.46$; nfvPPA vs stroke $t(12.2)=-0.01$, $p=0.99$).

4.4.5 Relationship to diagnostic category and disease severity

Stepwise regression analysis between overall measures of discriminability and the behavioural measures listed in the methods yielded no statistically significant predictors for CVC or oddball language performance. If performance on CVC linear rules (where performance was highest) is considered in isolation, overall aphasia severity ($\alpha=0.002$) was the only significant predictor. The only significant predictor for tone language performance was diagnosis ($\alpha=0.035$), confirming that patients with nfvPPA performed more poorly than those with stroke, independent of aphasia severity.

4.4.6 Relationship to structural anatomy

Lesion volume and site affected performance in the stroke group. Stepwise regression analysis between overall measures of discriminability for each language and the lesion metrics listed in methods yielded a model for the CVC language including only left putamen ($\alpha=0.06$); in other words, the ability to detect sequencing violations decreased with more severe putaminal lesions. For the oddball language, total lesion volume ($\alpha=0.016$) and involvement of the left ventral frontal operculum ($\alpha=0.076$) were included in the model (overall $p=0.023$), but in opposite directions: participants with larger lesions were less able to detect oddball CVCs, but this deficit was ameliorated if

their lesion had a more anterior distribution. The model yielded no statistically significant predictors for the tones language.

Grey matter volume affected performance in the nfvPPA group. The best model for nfvPPA performance on the CVC language included age ($\alpha=0.002$) and total grey matter volume in the left frontal lobe regions of interest ($\alpha=0.016$), but not in their right sided equivalents or total grey matter volume. These acted such that performance improved with higher left frontal grey matter volume, and also with age. While it might initially seem counter intuitive that older patients performed better, this is likely to reflect the natural loss of grey matter with age. The model is therefore improved by accounting for the fact that any given value of grey matter volume is relatively more atrophic in a younger individual. There were no statistically significant predictors with grey matter volume in the nfvPPA group for performance on the tone or oddball languages.

4.5 Discussion

This study successfully used a mixed-complexity artificial grammar learning task with speech sounds and tone stimuli to test aphasic patients with two different aetiologies. The principal observations were that: 1) both healthy individuals and patients with aphasia apply strongly contrasting strategies to assess structured sequences depending on whether the sequences consist of linguistic or non-linguistic auditory tokens; 2) patients with vascular aphasia and nfvPPA show similar patterns of auditory sequence processing impairment compared to controls; 3) aphasic patients are not disproportionately impaired on more complex auditory sequencing tasks, instead displaying a general impairment in processing structured auditory input; 4) patients with aphasia are capable of implicit learning of this kind through repeated exposure/test cycles. I discuss these results in turn in the following sections.

4.5.1 Rule acquisition differs when structurally identical sequences are comprised of linguistic or non-linguistic stimuli.

In all groups, performance profiles on the CVC language followed the expected pattern of linear relationships being more discriminable than configurational or hierarchical

structures. By contrast, participants' judgments about the tone language did not seem to be based on the abstraction of the intended grammatical rules (Figure 4-6 A, panel 2). This impression was confirmed by correlation and cluster analyses (Figure 4-8). Hierarchical clustering based on non-parametric correlations of single subject performance profiles was clearly able to recover the language learned, but not the group structure. This demonstrates that all groups acquired the same set of rules when making decisions about the CVC language; all that differed between groups was their overall performance. Further, a completely different set of rules were acquired for the tone language, but again this learning profile was almost identical across groups. Therefore, rule acquisition was not transferred between the two languages, and the separation of approach to linguistic and non-linguistic structured sequences was strongly maintained despite agrammatic aphasia of either type. This is despite the two languages having an identical structure, and being presented and tested in the same order. This finding cannot be trivially explained by a lower level deficit such as the tone language simply being more difficult, more affected by a reduced fidelity of auditory processing or subject to a higher 'lapse rate', which would affect discriminability but could not produce the complete dissociation of response patterns shown here across all groups.

Despite extensive exposure, all groups performed poorly at classifying tone sequence number 1 as consistent with the artificial grammar, and indeed seemed to actively reject it, with control performance for this sequence well below chance. This sequence was comprised entirely of tone sweeps, embedded within a recursive structure. The participants also correctly classified sequence 12, which has similar properties, as inconsistent with the artificial grammar. In this case, good performance on this tone sequence does not reflect an ability to extract the hierarchical rule, but rather a consistent tendency to reject the embedded pattern of tone sweep sequences. Overall, therefore, it does not seem that the tone sequences were assessed for the specific violations of the grammatical rules inherent in the artificial language. Instead, they were judged on the overall 'feel' of the sequence in a manner very different to the CVC language but entirely consistent across groups.

I therefore infer that, while both patient groups are impaired in their ability to learn and discriminate sequencing rules for both CVC and tone languages, they maintain the

same separation of processing of these languages seen in control participants. Taken together, these results imply that domain specific processes exist for linguistic and non-linguistic structured sequence learning, which are preserved even in the presence of acquired grammatical deficits. These processes might therefore engage different brain networks (Geranmayeh *et al.*, 2014b). It is possible that this separation is instantiated by an assessment of phonological ‘well-formedness’ in auditory temporal regions (Obrig *et al.*, 2016).

4.5.2 Artificial grammar learning in aphasia is similar across aetiologies.

A second key observation was that patients with nfvPPA and stroke showed similar patterns of performance for the CVC language. All groups were able to correctly classify the grammatical testing sequences as consistent with the exemplary sequences heard during exposure, and this ability fully generalised from the exposure set to the novel sequences not heard during exposure (Table 4-2; Figure 4-6 A). While there was a group difference, with performance in the stroke group being poorer on the CVC task, this effect disappeared when overall aphasia severity was accounted for. This novel result in agrammatic patients with primary progressive aphasia provides the evidence to suggest that existing findings on stroke patients should prove applicable to the progressive aphasias.

The lack of an effect of rule type for the oddball task confirms that the pattern of performance for the CVC language cannot be explained by stimulus-level differences such as the position of the violation within the sequence. The lack of a statistical group difference in the ability to detect oddball CVCs, a task performed at the end of the testing session, suggests that the patients’ impairments in this study are not solely due to generic difficulties with performing psychophysical sequence processing tasks, latent yes/no confusion, difficulties with basic auditory processing or differential effects of fatigue between groups.

The only consistent group difference not accounted for by severity was that patients with nfvPPA performed more poorly than those with stroke on the tone based language. There are a number of possible reasons for this. It might be a consequence of the tone language being more affected by the basic auditory processing deficits

previously demonstrated in nvfPPA (Goll *et al.*, 2010, Grube *et al.*, 2016). Alternatively, it might reflect involvement of the right IFC, which was spared in the stroke group (Figure 4-1 B), and is posited to have a role in prosodic and tonality based judgments. Nonetheless, patients with nvfPPA maintained the same pattern of learning as the other groups (Figure 4-8), demonstrating that this deficit is a specific difficulty with processing tonal input rather than a breakdown of the separation of phonological vs tonal structured sequence processing.

4.5.3 Agrammatic aphasic patients are similarly impaired for both complex and simple sequencing operations.

As expected, patients did not perform as well as controls, but the magnitude of this performance deficit did not differ by rule complexity, counter to my initial hypothesis. The results demonstrate that aphasic patients showed a global deficit in sequence processing, and were not selectively impaired on complex sequences. Clinically, patients in both groups make errors in the parsing of more complex syntax, and tend to stick to active, subject-relative structures in their expressive language (Grossman and Moore, 2005). I suggest that this does not reflect a specific deficit in the processing of more complex linguistic structures, but rather that these constructions are simply more difficult and therefore more vulnerable to a global deficit. As well as explaining a clinical symptom, this conclusion is consistent with the functional imaging finding that, in nvfPPA, left inferior frontal cortex activity lacks the normal relationship with syntactic complexity (Wilson *et al.*, 2010); it suggests that the efficiency of IFC is so degraded that even the least complex grammatical structures require maximal neural recruitment. This is analogous to the finding that older adults are no longer able to selectively modulate anterior cingulate cortex in response to increasingly difficult listening environments as they have already fully engaged this region in easy listening conditions (Erb and Obleser, 2013).

It is possible that patients attempt to compensate for this deficit by engaging a wider syntactic processing network involving temporo-parietal regions (Schofield *et al.*, 2012b, Blank *et al.*, 2016), but that this is insufficient to compensate for lost language function (Wilson *et al.*, 2016). In stroke, where the IFC is lost entirely, the presence of residual ability could be due to complete reliance on this wider network (Thompson *et*

al., 2010), or the involvement of contralateral IFC. Future functional imaging studies of implicit grammar learning will inform this debate. In any case, my findings of a general impact on sequence processing suggest that the grammatical deficits observed in aphasia, and the recovery from these, might reflect higher level, domain general processes (Caramazza and Zurif, 1976, Dominey *et al.*, 2003, Patel *et al.*, 2008, Brownsett *et al.*, 2014, Geranmayeh *et al.*, 2014a, Geranmayeh *et al.*, 2017).

The lack of group by rule complexity interactions is unlikely to be explained by limitations in sample size, as in no case was there even a trend in this direction (all interactions with complexity in Table 4-4 have p-values > 0.5). Therefore, these results appear to represent a genuine null effect, rather than sub-threshold effects that might become significant with a greater sample size. Moreover, the lack of interaction is also consistent in the tone and CVC experiments, although the response patterns between the two are vastly different. Nor can the results be trivially explained by floor effects in processing the more complex relationships for the following reasons: 1) the nfvPPA group show strikingly parallel behaviour in relation to the control group, consistent with a proportional impairment even on the linear sequencing operation (Figure 4-6 B, panel 1); 2) the stroke patients may well have reached a floor in performance on the complex sequences in the nonsense word task, but even excluding this group did not cause the group by complexity interaction to approach significance; 3) all groups improved over the three testing runs, and performance improvement was parallel in relation to sequencing complexity (i.e. there was a main effect of run but no run-by-complexity interaction, Figure 4-6 C); and 4) the tone language showed a very different pattern of results to that for the nonsense words yet, again, there was no evidence of a group-by-complexity interaction.

4.5.4 Patients with aphasia show improved performance over repeated cycles.

All three groups demonstrated the same amount of learning across repeated exposure/test cycles of the CVC language; the only difference was in their initial levels of performance (Figure 4-6 C; Table 4-4 C). This suggests that patients with aphasia were able to update their internal model of the artificial grammar based on feedback

and implicit comparison with short periods of exposure. It also suggests that patients did not suffer greater effects of fatigue than controls. By contrast, learning did not occur to the same degree for the tone language (Figure 4-6 D; Table 4-4 C). It is therefore clear that learning was not transferrable between the CVC and tone languages, despite them sharing the same underlying artificial grammar structure.

Together, these findings provide a theoretical basis upon which an exposure-based speech therapy for grammar could be built with the aim of improving subjective difficulty with speech comprehension (Figure 4-2). The results imply that there is potential for improvement from an intensive paradigm based on repeated exposure-test cycles. This could in principle be made home-deliverable and patient-led, an approach that has demonstrable efficacy for improving speech production in similar patient groups (Varley *et al.*, 2016); the tasks employed in this study were automated and computer based. The finding that learning did not generalise across modalities implies that such a therapy would need to use linguistic material, as it would be unlikely to be so well learnt with non-linguistic material or to transfer across domains. In contrast, the finding that patients were able to generalise perfectly from sequences heard during exposure (Figure 4-6 A, sequences 1-3), to those that were novel during the test phase (Figure 4-6 A, sequences 4-6), to the extent that performance did not differ, suggests that such a therapy might not need to be comprehensive with regards to specific sentence structures. Instead, it is envisaged that a graded programme could be designed, such that training focusses initially on those structures that are having most frequent impact on speech comprehension. Clearly my study does not provide evidence that such a therapy would be more efficacious than existing methods for addressing asyntactic deficits after stroke, nor do I have any evidence of how well these strategies would work within an already-learned but now-impaired natural language. Indeed, a recent small study of nine patients who had chronic agrammatic aphasia secondary to stroke suggests that implicit learning alone (on a visuo-motor serial reaction time task) does not necessarily translate into improved real-world performance (Schuchard *et al.*, 2017). Larger scale trials and assessment with other tasks are clearly required in more acute disease cohorts. As my method relies on exposure-based implicit learning rather than explicit instruction, future therapeutic trials could follow recent trends for patient-led practice in the home environment, increasingly with support from internet-based

resources (Rogalski *et al.*, 2016). This has the potential for providing the benefits of an intensive approach (Bhagal *et al.*, 2003, Brady *et al.*, 2016, Breitenstein *et al.*, 2017) without the resource constraints that limit the frequency and therefore efficacy of traditional irregular, face-to-face instruction (Sarno *et al.*, 1970, Lincoln *et al.*, 1984).

4.5.5 Brain behaviour relationships

My use of stepwise regression, to assess associations between brain structure and function, should be seen as exploratory, since the study was powered only to detect strong effect sizes. Nonetheless, significant associations between brain structure and behavioural performance within the patient groups were observed. The nfvPPA group demonstrated significant grey and white matter loss in frontal regions bilaterally. In keeping with previous studies of expressive grammar (Rogalski *et al.*, 2011), the discriminability of grammatical structure in the CVC language correlated with age-corrected loss of volume only in left frontal regions (but not similar right-sided regions or total corrected grey matter volume). No such association was found for the tone language or the oddball task.

In the stroke group there was catastrophic loss of fronto-temporal regions in the dominant hemisphere, but complete contralateral preservation. For the CVC language, the model included only the putamen. The putamen is known from the functional imaging literature to be important in implicit sequence detection and learning in healthy individuals (Grafton *et al.*, 1995, Rauch *et al.*, 1995, Rauch *et al.*, 1997, Grahn and Rowe, 2009). No such relationships were significant for the tone task. Performance on the oddball sound detection task was predicted by overall lesion volume and a weaker, opposite, effect of the extent of involvement of the most frontal region analysed. This suggests that more anterior lesion locations were less deleterious to CVC Oddball detection than those located closer to auditory temporal cortex.

Similar performance in a relatively bilateral disease (nfvPPA) and one so clearly unilateral (stroke) immediately poses the question of which components of a broader language network are recruited to underpin the demonstrated learning over repeated exposure-test cycles (Crinion and Price, 2005). Thus, there is clear scope for a

functional imaging study to be conducted in these patient groups, the results of which could complement the development of grammar-based speech therapy.

4.5.6 Study limitations

The main limitation of this study is the relatively small number of patients in each group, which renders the correlation analyses exploratory, and more subtle voxel-based lesion-symptom mapping analyses impossible. Future work in larger and more heterogeneous cohorts would complement functional neuroimaging in exploring the brain basis of implicit sequence learning.

The stroke group all had left-hemisphere lesions, while the nfvPPA group had relatively bilateral disease that involved a more distributed language network. I have demonstrated a preserved separation of rule learning between the CVC and tone languages in both disease groups, confirming the domain specificity of structured sequence learning. However, overall performance on the tone language was poorer in nfvPPA, and the reasons for this are not clear. The lack of a cohort of stroke patients with right-hemisphere lesions, auditory psychophysical examination of all groups, or detailed neuropsychological testing including an assessment of working memory, means that discussion of the potential brain basis for this difference is speculation that must be confirmed or refuted in future work.

4.6 Conclusion

In this chapter I reconcile a controversy in the literature regarding the effects of structural complexity on receptive grammar in the frontal aphasias. I demonstrate that, while the patients found complex, non-adjacent structuring relationships more difficult to acquire, this did not represent a disproportionate impairment; aphasia resulted in a similar performance penalty for adjacent relationships. I also provide insights into the language-specificity of artificial grammar learning by demonstrating that humans learn otherwise identical linguistic and non-linguistic structured sequences entirely separately, even if the neural architecture underlying this learning is disrupted. My direct comparison of two patient groups suggests that previous findings regarding implicit sequence learning in stroke aphasia are likely to prove transferrable to nfvPPA.

Finally, the ability of both patient groups to learn an artificial grammar as demonstrated here provides a rationale and approach for future trials of implicit, exposure-based approaches to rehabilitation of agrammatism in non-fluent aphasia.

4.7 Appendix: Supplementary tables

A	Rule complexity	Group	Group x Rule	Participant
CVC	<0.0001	0.0311	0.6445	0.0006
Tones	0.0006	0.0027	0.6069	0.9994
Oddball	0.1383	0.0611	0.7245	<0.0001

Table 4-5 Supplementary analysis of d' discriminability

P-values for a repeated measures ANOVA of group against rule for the parametric discriminability measure d' , with participant number as a nested factor within group.

	Rule	Run	Group	Rule x Run	Run x Group
CVC	<0.001	<0.001	0.020	1	0.054
Tones	0.070	<0.001	0.010	0.333	0.019

Table 4-6 Supplementary analysis of d' learning

P-values for the general linear model assessing learning across runs for the parametric discriminability measure d' .

4.8 Chapter Summary:

Patients with non-fluent aphasia display impairments of expressive and receptive grammar. This has been attributed to deficits in processing configurational and hierarchical sequencing relationships. This hypothesis had not been formally tested. It was also controversial whether impairments are specific to language, or reflect domain general deficits in processing structured auditory sequences.

Here I used an artificial grammar learning paradigm to compare the abilities of controls to participants with agrammatic aphasia of two different aetiologies: stroke and frontotemporal dementia.

Patients with non-fluent variant primary progressive aphasia (nfvPPA), non-fluent aphasia due to stroke, and controls implicitly learned a novel mixed-complexity artificial grammar designed to assess processing of increasingly complex sequencing relationships. I compared response profiles for otherwise identical sequences of speech tokens (nonsense words) and tone sweeps.

In all three groups the ability to detect grammatical violations varied with sequence complexity, with performance improving over time and better for adjacent than non-adjacent phonological relationships. Patients performed less well than controls overall, and this was related more strongly to aphasia severity than to aetiology. All groups improved with practice and performed well at a control task of detecting oddball nonwords. Crucially, group differences did not interact with sequence complexity, demonstrating that aphasic patients were not disproportionately impaired on complex structures. Hierarchical cluster analysis revealed that response patterns were very similar across all three groups, but very different in the nonsense word and tone tasks, despite identical artificial grammar structures.

Overall, I demonstrate that agrammatic aphasics of two different aetiologies are not disproportionately impaired on complex sequencing relationships, and that the learning of phonological and non-linguistic sequences occurs independently. The similarity of profiles of discriminatory abilities and rule learning across groups suggests that insights from previous studies of implicit sequence learning in vascular aphasia are likely to prove applicable in nfvPPA.

Chapter 5: Review and Synthesis

5.1 Network organisation and reorganisation in neurodegeneration

Neurons within the human brain are functionally and structurally connected at a number of scales. With neuroimaging it is possible to assess this connectivity at the mesoscopic scale, visualising the way in which groups of neurons interact with each other across brain regions. In chapter 2, I observed such connectivity in terms of shared temporal dynamics in fMRI signals (Hampson *et al.*, 2002). In chapter 3, I went beyond this by taking direct measurements of neuronally-derived magnetic and electrical signals at high temporal resolution, with simultaneous magnetoencephalography and electroencephalography. This allowed me to test for the presence of consistent phase relationships between distant brain regions, manifesting as signal coherence (Nolte *et al.*, 2004). Having thus demonstrated functional connectivity (statistical dependency), I assessed effective connectivity (causal interaction) by fitting a frequency-resolved multivariate autoregressive model to these same data, which then allowed me to directly evaluate the Granger-causal relationships between regions (Granger, 1969, Gow *et al.*, 2008).

By combining measurements of functional connectivity with experimental psychology in chapter 3, I robustly demonstrated one way in which the connectivity of the healthy brain underpins perception and higher cognitive function by allowing the rapid and flexible integration of predictions with sensory input. By taking a cross-sectional approach to multimodal imaging data in chapter 2, I have also demonstrated the way in which connectivity contributes to the progression of neurodegeneration through trans-neuronal spread of tau pathology in Alzheimer's disease and regional vulnerability factors in progressive supranuclear palsy, settling a key debate about reasons for differential network vulnerability in Alzheimer's disease and fronto-temporal lobar degeneration (Zhou and Seeley, 2014). Therefore, while the methods employed in chapters 2 and 3 are different, they provide complementary insights into the interplay between brain network organisation, function and degeneration.

As well as exploring the nature, purpose and effects of healthy brain network organisation, I have precisely defined the consequences of regional neurodegenerative burden for brain networks at the local and global scale. In chapter 2, by employing a cross-sectional approach, I was able to reconcile previous literature that seemed to provide contradictory evidence about the consequences of Alzheimer's disease pathology for functional connectivity. Although based on a relatively small number of individuals ($n=17$), my data were consistent with computational models that predict a dissociation between changes in functional connectivity in early and late Alzheimer's disease (de Haan *et al.*, 2012). In this framework, neurons initially compensate for synaptic loss by increasing their firing rate, manifesting as stronger functional connectivity (Maestú *et al.*, 2015). As neurodegeneration progresses, this mechanism breaks down, and functional connectivity weakens (Jones *et al.*, 2015). This state of affairs can account for group-average results demonstrating either weakened or strengthened connectivity depending on the stage of illness (and hence position on the 'inverted U' shaped curve) at which patients were assessed.

In PSP, I demonstrated diaschisis, whereby the focal presence of tau pathology in midbrain and basal ganglia led to widespread dysfunction in the functional connectivity across cortical networks. This is a generalisation of previous demonstrations of disruption of spatially distant connectivity networks resulting from damage to computational hubs within that network. For example, semantic dementia (semantic variant primary progressive aphasia) results from focal neurodegeneration of anterior temporal lobe. Anterior temporal lobe is proposed to perform a binding function for multi-modal semantic knowledge, which is itself distributed throughout cortex. Disruption of anterior temporal lobe function therefore leads to widespread abnormalities in functional connectivity, not only with temporal lobe itself but also between its neighbours (Guo *et al.*, 2013). In PSP, I have demonstrated that the loss of inter-regional connectivity through subcortical structures results in greater cortico-cortical connectivity. This was at the cost of reduced network participation, eigenvector centrality and closeness centrality and increased betweenness centrality, together indicating that connectivity patterns were becoming more modular and information transfer was taking a less direct route. This goes some way towards

accounting for the phenotypic characteristics of subcortical cognitive impairment, including apathy and bradyphrenia.

Computational analyses are not without their pitfalls and the potential for misinterpretation. I minimised such risks by directly assessing focussed scientific hypotheses within a systems identification framework (Figure 5-1) (Goodwin and Payne, 1977, Ljung, 1998, Stokes and Purdon, 2017). Such a framework is equally applicable to the assessment of behavioural and neurophysiological data, and was at the core of my analysis strategies in chapters 2, 3 and 4. In this process it is vital to explicitly consider the assumptions made at every step, and to design the experiment in such a way that these assumptions can either be directly tested or rendered inconsequential. For example, in chapter 3 I formulated my candidate behavioural Bayesian inference models within a predictive coding framework, but they were equally applicable to any hierarchical generative model set in which top-down predictions are fed back to lower-order processing levels. I was then able to directly test this hypothesis (of bi-directional communication between higher and lower-order processing levels) with a second systems identification process based on neuronal coherence and Granger causality between left frontal and temporal regions of interest. In this way, I was able to provide direct evidence for causal top-down prediction signals, and to go on to precisely define the neural correlates and behavioural consequences of their disruption.

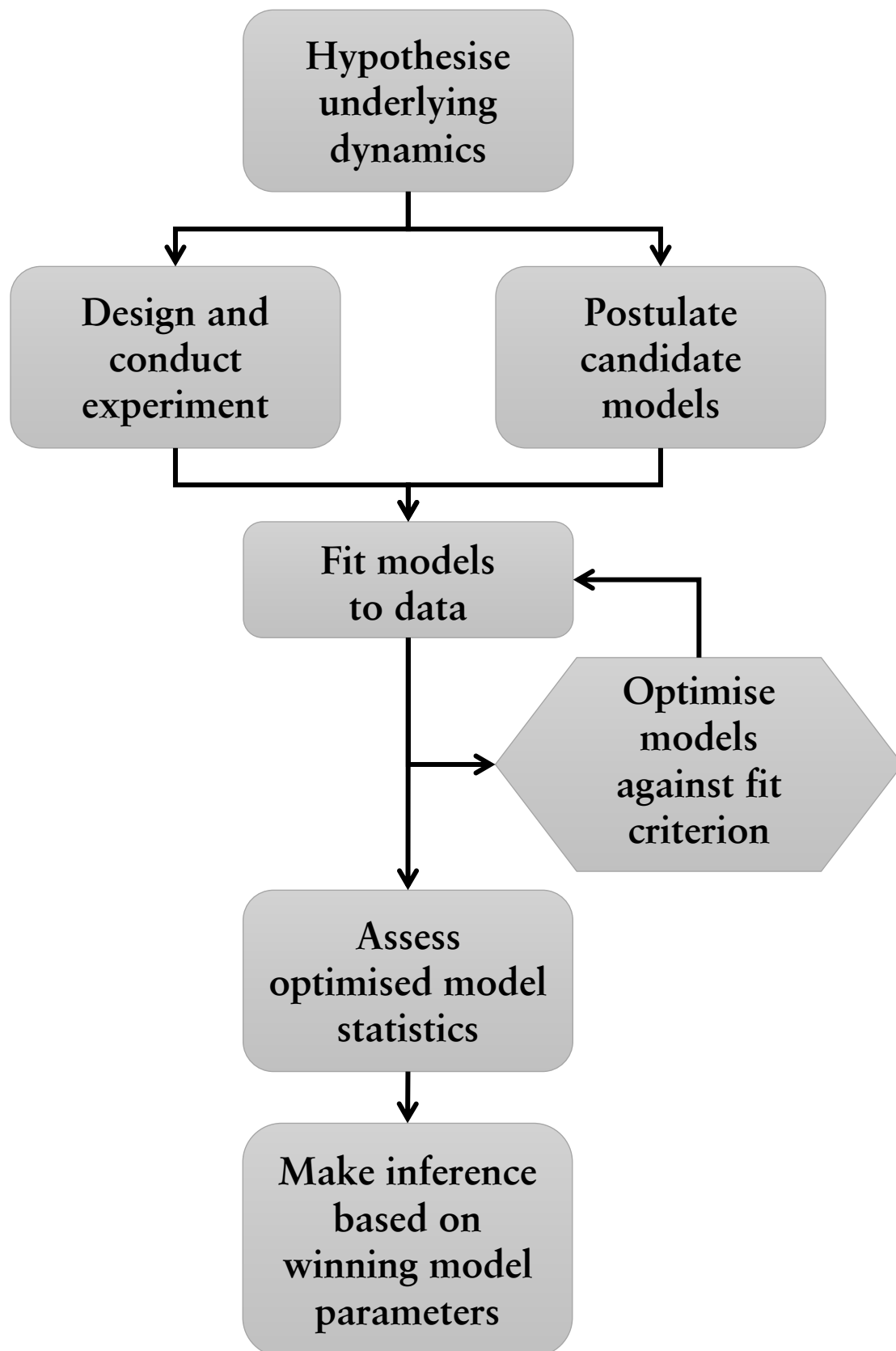


Figure 5-1 Systems identification framework
After Stokes and Purdon (2017). The process of making inference about brain function from computational modelling of behavioural and neurophysiological data.

5.2 Clinical implications of inflexible predictions in nfvPPA

The discussion in Chapter 3 was focussed on how investigations of the neurophysiological abnormalities of nfvPPA can provide insight into how the healthy brain processes language. In this section I change the focus, to address the question of how the neurophysiological abnormalities of nfvPPA that I have demonstrated can account for the clinical symptoms and signs of this disease. I begin (5.2.1) by considering the subjective speech comprehension symptoms that led to the initial conceptualisation of the study. I then go on (5.2.2) to address the basic auditory processing deficits that have previously been observed in nfvPPA, by first demonstrating these abnormalities in my cohort and then providing an explanation in terms of inflexible predictions. Finally (5.2.3), I place my results in the wider context of theories of grammatical comprehension. I explain how a synthesis of the results of chapters 3 and 4 can provide a perspective in which inflexible predictions can account for receptive agrammatism in nfvPPA.

5.2.1 Inflexible predictions can explain speech comprehension symptoms in nfvPPA

Chapter 3 was motivated by the observation that, in clinic, patients with nfvPPA frequently complain of difficulties in hearing speech that are disproportionate to any measured deficits and resistant to hearing aids. In some cases, this can be a presenting or prodromal feature of the illness, developing in advance of the output aphasia (Iizuka *et al.*, 2007). Similarly, patients not meeting diagnostic criteria for nfvPPA but with a demonstrable metabolic or structural abnormality of inferior frontal brain regions have been reported to suffer from apperceptive auditory agnosias leading to amusia (Confavreux *et al.*, 1992) or pure word deafness (Otsuki *et al.*, 1998). Patients frequently describe using cross-modal cues such as lip reading or reading to support speech comprehension, even in quiet environments (Jörgens *et al.*, 2008).

The symptom rating scales in my patient cohort (Figure 3-2) demonstrated a dissociation in subjective assessment between understanding speech in noise (which was rated as equally difficult by both patients and controls), and speech in quiet (which only patients rated as difficult). Greater difficulty in quiet environments may seem counterintuitive at first, but it is consistent with the primary abnormality being one of

inflexible predictions. Successful perception and comprehension of speech requires continuous updating of predictions based on sentential context and other cues. In a noisy environment, it is beneficial for listeners to rely heavily on these prior predictions as the patients do, because the sensory signal to noise ratio is poor. In a quiet environment, however, this is a suboptimal strategy as greater reliance can and should be placed on more precise or informative sensory inputs. If patients are unable to flexibly adapt the precision of their predictions to quiet listening environments, speech-in-quiet will remain difficult. It might be that globally strong predictions in nfvPPA are an adaptation to their inflexibility, as dysfunctioning networks are forced to choose one prediction strength for all scenarios. If, instead, predictions were globally weakened, this would be beneficial to the perception of speech-in-quiet but detrimental to speech-in-noise, perhaps having a greater overall cost to intelligibility in a dynamic environment (see (Wolpe *et al.*, 2016) for similar arguments in motor control).

In the main experiment in chapter 3, I probed for subjective clarity ratings around 1050ms after the onset of the spoken word. It could be argued that the abnormal precision of prior expectations in patients might be adaptive to the experimental context. Delayed processing might mean that they have less time for predictions to be enacted before a decision must be made, and therefore stronger predictions are required if they are to have meaningful effects. In this experiment, I demonstrated that the neural processing of perceptual predictions was delayed in every patient compared to controls (Figure 3-11), and that in some individuals this processing continued beyond the analysis window. It could therefore be argued that my finding of increased prior precision in patients might have been attenuated if clarity ratings were requested after a longer delay. However, predictions on this slower timescale would be of limited real-world consequence for speech perception and comprehension, because content-containing words such as nouns and verbs are separated by similarly short intervals in typical sentences (Altmann and Kamide, 1999), the temporal range in which human perception is optimal (Cope *et al.*, 2011, Cope *et al.*, 2014a). Visual cues from lip reading also operate over millisecond timescales and are mediated by similar increases in fronto-temporal functional connectivity to those I demonstrate here (Giordano *et al.*, 2017). Similarly, I included a delay of around 1050ms between the written word and the onset of the spoken word. For control participants and patients alike, this was

sufficient time to instantiate an appropriate prediction for upcoming speech signals (Figure 3-10).

5.2.2 Inflexible predictions can explain auditory processing abnormalities in nfvPPA

Goll *et al.* (2010) demonstrated that patients with nfvPPA were more impaired than those with Semantic Dementia at tasks assessing auditory perceptual function, despite similar disease duration and non-verbal cognitive impairment. The 12 nfvPPA patients in that study were rather more advanced than those I assessed in chapters 3 and 4, having an average Mini-Mental Status Examination (MMSE) score of 21/30, compared to an average MMSE of 28/30 in my cohort. The tasks at which patients with nfvPPA were most impaired compared to controls were a same/different judgment of two spectrally shaped harmonic series (essentially a test of timbre discrimination) and a same/different judgment of the semantic identity of two auditory stimuli. These deficits were less severe in analogous tasks undertaken in the visual domain. In a subsequent study containing 5 patients with nfvPPA, (Goll *et al.*, 2011) demonstrated that the magnitude of impairment was similar across a range of auditory tasks in which the acoustic judgment was same/different or up/down, but that they performed better when asked to assess a property of the stimulus source such as big/small or tool/animal.

Grube *et al.* (2016) sought to quantify this impairment by using adaptive psychophysical methods to assess a comprehensive auditory processing battery in 18 consecutive patients with Primary Progressive Aphasia. This battery comprised 16 tasks, assessing sensitivity to changes in stimulus pitch, rhythm and temporal dynamics. All of the tasks required two-alternative forced choice same/different (either as AB or AxB comparisons), or change-detection judgments. They demonstrated that, on average, the six patients in their cohort with nfvPPA were more than 1 standard deviation poorer than control participants at all tasks, with an overall mean Z-score of approximately -1.9. This impairment was not present to the same extent in groups with semantic dementia (mean Z-score -0.7) or logopenic aphasia (mean Z-score -0.1). Performance was particularly poor where a comparison of prolonged stimulus sequences was required.

In my, larger, cohort of 11 nfvPPA patients described in chapter 3 I exactly replicated a subset of the tasks used by Grube *et al.* (2016). I selected a cross section of tasks on which the patients with nfvPPA had displayed particular difficulties, covering a range of auditory processing from simple to complex. These comprised pitch change detection (Grube task P1), 2Hz and 40Hz frequency modulation detection (Grube tasks M1 and M2), and dynamic ripple discrimination (Grube task M4).

Basic Auditory Processing

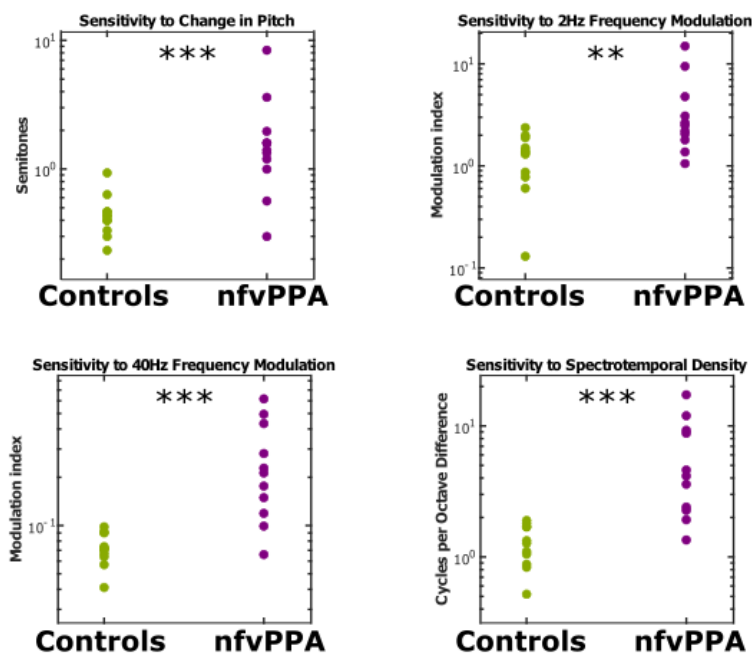


Figure 5-2 Basic auditory processing in nfvPPA, after Grube *et al.* (2016).

*The tasks employed were pitch change detection, 2Hz FM detection, 40Hz FM detection, and dynamic ripple density discrimination. Statistical group differences were assessed with unpaired t-tests with unequal variance, and are indicated by * $p < 0.05$, ** $p < 0.01$, *** $p < 0.001$.*

My results replicated the primary finding of Grube *et al.* (2016), that patients with nfvPPA perform very poorly at some tasks of basic auditory processing (Figure 5-2). This did not seem to have a trivial explanation like an inability to sustain attention or yes/no confusion, as the individual adaptive tracks had a similar shape in patients and controls, with consistent correct responses in ‘easy’ trials and, once threshold is reached, flat profiles maintained for the remainder of a run (Figure 5-3).

Average Adaptive Tracks by Group

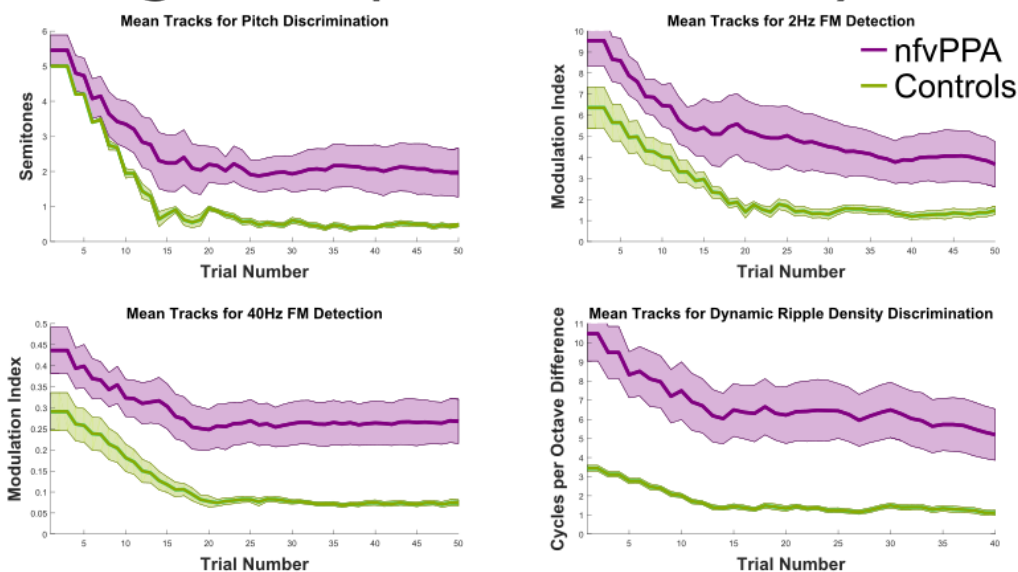


Figure 5-3 Overall average adaptive tracks by group

The pattern of performance was highly variable between individuals, but highly consistent within individuals. As can be seen in the individual Z-scores for each task, some patients were able to consistently perform some discrimination tasks in the normal range, while being dozens of standard deviations poorer than the mean in other tasks. Patients who performed well on a particular task continued to perform well if it was repeated but, even after repeated practice, they remained unable to perform well on tasks that they had previously found difficult.

On the face of it, these consistent demonstrations of impaired basic auditory function in nfvPPA seem surprising as the Bayesian VBM provides evidence for no atrophy in primary auditory regions (Figure 3-1 E), and at post mortem patients with nfvPPA do not display disproportionate pathology in either primary auditory cortex or auditory brainstem nuclei. Further, it is known that patients with progressive supranuclear palsy, who do have severe brain stem atrophy and focal pathology that involves the inferior colliculi, continue to display complex auditory psychophysical effects late in disease (Hughes *et al.*, 2014). Similarly, my patients with nfvPPA demonstrated good performance at identifying vocoded words, performing almost as well as controls (Figure 3-3 D). Finally, the pattern of psychophysical deficits was observed to be highly variable between individuals (Figure 5-4), but highly consistent within individuals;

impairment of a bottom-up perceptual process would predict a consistent profile of performance that might vary in severity, while what I observe is that all individuals perform very poorly on some tasks, but the relative difficulty of the tasks varies between individuals. This is fundamentally different from the performance profile seen in conditions where abnormal auditory processing could in itself be a sufficient explanation for patients' symptomatology. For example, patients with Wernicke's aphasia due to lesions of left temporo-parietal junction display normal low-level processing of pitch and timbre information, but impaired ability to detect or process spectral flux (those changes in the frequency domain that occur over time) (Robson *et al.*, 2013). This is explicable as higher stages of the auditory system process progressively longer temporal windows (Cope *et al.*, 2011). Further, it can potentially account for the receptive symptomatology in Wernicke's aphasia by accounting for impaired mapping of auditory objects to phonemes as the neural architecture of planum temporale is disrupted (Griffiths and Warren, 2004).

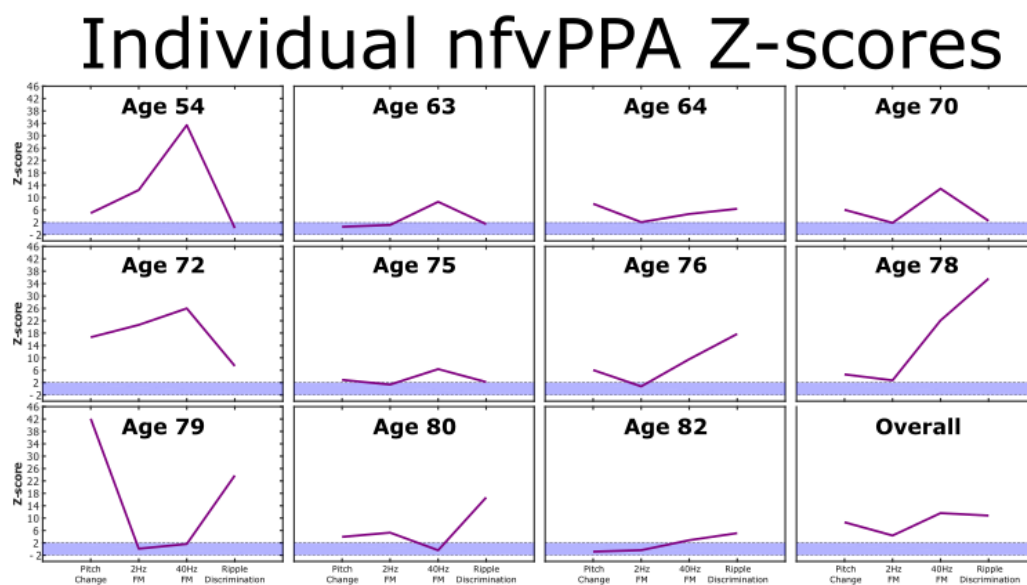


Figure 5-4 Individual nfVPPA performance profiles.

Overall, therefore, a higher level, cortical explanation must be invoked to account for these psychophysical findings. This effect has previously been understood in terms of impaired working memory (Grube *et al.*, 2016), but it is worth considering whether it might also be explained by the abnormalities of predictive coding demonstrated here,

and indeed whether the two explanations might in fact reflect the same underlying cognitive process.

Basic auditory processing is traditionally assessed with two- or three-alternative forced choice psychophysical paradigms, with the difference between exemplars adaptively modified to track a given performance percentile (Levitt, 1971). A predictive coding model can also be applied to this experimental context, in which subjects make a decision based on the location of the peak of their posterior in the perceptual dimension of interest. The distribution of this posterior is based on a prediction that is modified by prediction error induced by sensory input. For example, in a task where one is asked to detect the presence of a pitch change the subject might listen to the first pitch and then set up a prediction that the second pitch would be unchanged. A decision would be made by performing two-point discrimination on the peak locations of prior and posterior distributions. If all subjects establish similar predictions, the accuracy of this decision process is dependent only on the precision of the sensory input, as is the intent of adaptive measures in psychoacoustics (Levitt, 1971). If, however, subjects with nfvPPA make more precise predictions, the perceptual distance between prior and posterior would be reduced, leading to poor discriminatory performance even though the sensory input is unchanged. This also explains the lack of a hierarchical relationship in performance profiles (Figure 5-4); for example to discriminate the density of dynamic ripples it is necessary to be able to process frequency modulations, and yet some patients were able to perform within the normal range at discriminating ripples whilst seemingly unable to detect its building blocks (i.e. frequency modulation).

This explanation in terms of abnormally precise predictions is not exclusive of that in terms of impaired working memory (which could be modelled here as a drift in the location of the prior distribution over time), and indeed both processes could be occurring simultaneously. The argument I make is simply that it is possible that inflexible perceptual predictions, of themselves, are a sufficient explanation for measured impairments in basic sound discrimination in nfvPPA.

5.2.3 Inflexible predictions can explain receptive agrammatism in frontal aphasia

Agrammatism is a prominent symptom in both nfvPPA and its vascular analogue Broca-type aphasia. In ecological contexts, patients are observed to have particular difficulties understanding complex grammatical structures containing hierarchical structures or the passive voice (Goodman and Bates, 1997, Grodzinsky, 2000). At first glance this observation seems at odds with the empirical findings I presented in chapter 4, where I demonstrated patients to be equally impaired at the acquisition of grammatical rules based on linear transition probabilities, configurational position or hierarchical structure. However, these observations can be unified by inflexible perceptual predictions for sentential structure.

In most European languages, clauses are only disambiguated after the presentation of at least one noun. For example, when hearing one of the two sentences “The boy pushed the girl,” or “The boy was pushed by the girl,” the listener must either wait to hear the tensed verb before undertaking any sentential processing, or make a prediction about the likely relationship of ‘the boy’ to what follows. Sub-clausal descriptions are subject to similar constraints: the subject-relative sub-clause in, “The doctor that annoyed the nurse ran a clinic,” is more easily and quickly parsed than the object-relative sentence, “The doctor that the nurse annoyed ran a clinic,” (Ford, 1983). Linear, subject-relative sentences are much more frequently encountered across a range of European languages (Mak *et al.*, 2002). It would therefore be reasonable to hold a prior expectation for these more frequent, subject-oriented linear word orders. Indeed, frequent exposure to non-linear sentence structures has been shown to increase their processing speed through statistical learning (Wells *et al.*, 2009). There are a number of mechanistic explanations for this effect, but one view is formalised in the *perspective-shifting* account of syntactic processing, in which the listener must re-orient their mental imagery to an unexpected agent to parse a sentence or sub-clause (for a review, see (Traxler *et al.*, 2002)). If patients with frontal aphasia are less able to flexibly modify their prior expectations and shift perspective on the basis of grammatical cues, it could account for their selective behavioural impairment.

Support for this view comes from the observation that sentence predictability modulates the difficulty of syntactic comprehension in healthy individuals. Inanimate

objects are more frequently the subject of object-relative descriptions across a range of languages (Mak *et al.*, 2002). Consequently, when readers or listeners encounter inanimate objects as the first noun in a sentence, their perceptual prediction that the sentence will follow a linear progression will be less strong. This leads to the observation that non-linear structures are processed more quickly and require less re-reading (so-called '*first-pass regressions*') when the first noun is inanimate, rather than animate (Traxler *et al.*, 2002). Similarly, manipulating semantic predictability can reduce or eliminate syntactic complexity effects by ensuring that the sentence could only be legitimately interpreted in one way (Traxler *et al.*, 2005). These two effects (animacy and semantic content) interact, such that higher-order understanding of the topic combines with implicit statistical learning to produce optimal perceptual predictions (Mak *et al.*, 2006). When these predictions are violated during reading, electrophysiological correlates are observed with a peak at around 400ms (the N400 response) (Dambacher *et al.*, 2006, Van Petten and Luka, 2012), a strikingly similar latency to that observed in my control participants in chapter 3 (Figure 3-11).

Thus, the inflexible predictions that I demonstrate in chapter 3 are able to reconcile the seeming inconsistency between the findings of chapter 4 and the observed symptomatology of agrammatic aphasia, by proposing that the core perceptual deficit occurs downstream of the syntactic cue. In other words, although the patients have not lost the ability to implicitly learn and understand more complex sequencing relationships, they are unable to use these subtle word-ordering or tense cues to *perspective-shift* and modify their initial prediction for a linear presentation. This view is consistent with emerging perspectives of linguistic processing as a specialised function of a more general cognitive computational system for complex and flexible thought, based on dynamic functional interactions between inferior frontal and superior temporal cortex (Friederici *et al.*, 2017, Milne *et al.*, 2018).

Summary

The dementias are persistent or progressive disorders affecting more than one cognitive domain that interfere with an individual's ability to function at work or home, and represent a decline from a previous level of function. In this thesis I consider the neurophysiology of dementia at a number of levels. I investigate the ways in which the connectivity and function of the brain predisposes to the specific focal patterns of neurodegeneration seen in the various dementias. I aim to identify the mesoscopic changes that occur in individuals with neurodegeneration and how these relate to their cognitive difficulties. I show how, by assessing patients in whom there is focal disruption of brain networks and observing the outcomes in comparison to controls, I can gain insight into the mechanisms by which the normal brain makes predictions and processes language.

In Chapter 1, I set the scene for the focussed experimental investigations of model diseases by beginning with an introductory, clinically-focussed review that sets out the features, aetiology, management, epidemiology and prognosis of the dementias. This places these model diseases in the context of the broader clinical challenge posed by the dementias.

In Chapter 2, I turn to 'prototypical' model diseases that represent neurodegenerative tauopathies with predominantly cortical (Alzheimer's disease, AD) and subcortical (Progressive Supranuclear Palsy, PSP) disease burdens. I investigate the neurophysiological causes and consequences of Tau accumulation by combining graph theoretical analyses of resting state functional MR imaging and *in vivo* 'Tau' PET imaging using the ligand AV-1451. By relating Tau distribution to the functional connectome I provide *in vivo* evidence consistent with 'prion-like' trans-neuronal spread of Tau in AD but not PSP. This provides important validation of disease modification strategies that aim to halt or slow down the progression of AD by sequestration of pathological Tau in the synapse. In contrast, I demonstrate associations consistent with regional vulnerability to Tau accumulation due to metabolic demand and a lack of trophic support in PSP but not AD. With a cross-sectional approach, using Tau burden as a surrogate marker of disease severity, I then go on to show how the changes in functional connectivity that occur as disease

progresses account for the contrasting cognitive phenotypes in AD and PSP. In advancing AD, functional connectivity across the whole brain becomes increasingly random and disorganised, accounting for symptomatology across multiple cognitive domains. In advancing PSP, by contrast, disrupted cortico-subcortical and cortico-brainstem interactions meant that information transfer passed through a larger number of cortical nodes, reducing closeness centrality and eigenvector centrality, while increasing weighted degree, clustering, betweenness centrality and local efficiency. Together, this resulted in increasingly modular processing with inter-network communication taking less direct paths, accounting for the bradyphrenia characteristic of the ‘subcortical dementias’.

From chapter 3 onwards, I turn to the in-depth study of a model disease called non-fluent variant Primary Progressive Aphasia (nfvPPA). This disease has a clear clinical phenotype of speech apraxia and agrammatism, associated with a focal pattern of mild atrophy in frontal lobes. Importantly, general cognition is usually well preserved until late disease.

In chapter 3 itself, I relate an experiment in which patients with nfvPPA and matched controls performed a receptive language task while having their brain activity recorded with magnetoencephalography. I manipulated expectations and sensory detail to explore the role of top-down frontal contributions to predictive processes in speech perception. I demonstrate that frontal neurodegeneration led to inflexible and excessively precise predictions, and that fronto-temporal interactions play a causal role in reconciling prior predictions with degraded sensory signals. The discussion here concentrates on the insights provided by neurodegenerative disease into the normal function of the brain in processing language. Overall, I demonstrate that higher level frontal mechanisms for cognitive and behavioural flexibility make a critical functional contribution to the hierarchical generative models underlying speech perception

In chapter 4, I precisely define the sequence processing and statistical learning abilities of patients with nfvPPA in comparison to patients with non-fluent aphasia due to stroke and neurological controls. I do this by exposing participants to a novel, mixed-complexity artificial grammar designed to assess processing of increasingly complex sequencing relationships, and then assessing the degree of implicit rule learning. I demonstrate that agrammatic aphasics of two different aetiologies are not

disproportionately impaired on complex sequencing relationships, and that the learning of phonological and non-linguistic sequences occurs independently in health and disease.

In chapter 5, I summarise the synergies between the experimental chapters, and explain how I have applied a systems identification framework to a diverse set of experimental methods, with the common goal of defining the physiology of dementia. I then return to the results of chapter 3 with a clinical focus to explain how inflexible predictions can account for subjective speech comprehension difficulties, auditory processing abnormalities and (in synthesis with chapter 4) receptive agrammatism in nfvPPA.

Overall, this body of work has contributed to knowledge in several ways. It has achieved its tripartite aims by:

- 1) Providing *in vivo* evidence consistent with theoretical models of trans-neuronal Tau spread (chapter 2), and a comprehensive clinical account of the previously poorly-understood receptive symptomatology of nfvPPA (chapter 5), thus demonstrating that systems neuroscience can provide a translational bridge between the molecular biology of dementia and clinical trials of therapies and medications. In this way, I begin to disentangle the network-level *causes* of neurodegeneration from its *consequences*.
- 2) Providing evidence for a causal role for fronto-temporal interactions in language processing (chapter 3), and demonstrating domain separation of statistical learning between linguistic and non-linguistic sequences (chapter 4), thus demonstrating that studies of patients with neurodegenerative disease can further our understanding of normative brain function.
- 3) Successfully integrating neuropsychology, behavioural psychophysics, functional MRI, structural MRI, magnetoencephalography and computational modelling to provide comprehensive research training, as the platform for a future research programme in the physiology of dementia.

References

- Abdelnour F, Voss HU, Raj A. Network diffusion accurately models the relationship between structural and functional brain connectivity networks. *Neuroimage*. 2014;90:335-47.
- Adachi N, Arima K, Asada T, Kato M, Minami N, Goto Y-i, Onuma T, Ikeuchi T, Tsuji S, Hayashi M. Dentatorubral-pallidoluyian atrophy (DRPLA) presenting with psychosis. *The Journal of neuropsychiatry and clinical neurosciences*. 2001.
- Adams R, Fisher C, Hakim S, Ojemann R, Sweet W. Symptomatic occult hydrocephalus with normal cerebrospinal-fluid pressure: a treatable syndrome. *N Engl J Med*. 1965;273(3):117-26.
- Ahmed Z, Cooper J, Murray TK, Garn K, McNaughton E, Clarke H, Parhizkar S, Ward MA, Cavallini A, Jackson S. A novel in vivo model of tau propagation with rapid and progressive neurofibrillary tangle pathology: the pattern of spread is determined by connectivity, not proximity. *Acta Neuropathol*. 2014;127(5):667-83.
- Akai K, Uchigasaki S, Tanaka U, Komatsu A. Normal pressure hydrocephalus. *Pathol Int*. 1987;37(1):97-110.
- Albert ML, Feldman RG, Willis AL. The 'subcortical dementia' of progressive supranuclear palsy. *J Neurol Neurosurg Psychiatry*. 1974 Feb;37(2):121-30.
- Albert MS, DeKosky ST, Dickson D, Dubois B, Feldman HH, Fox NC, Gamst A, Holtzman DM, Jagust WJ, Petersen RC. The diagnosis of mild cognitive impairment due to Alzheimer's disease: Recommendations from the National Institute on Aging-Alzheimer's Association workgroups on diagnostic guidelines for Alzheimer's disease. *Alzheimer's & dementia*. 2011;7(3):270-9.
- Alexander-Bloch AF, Gogtay N, Meunier D, Birn R, Clasen L, Lalonde F, Lenroot R, Giedd J, Bullmore ET. Disrupted modularity and local connectivity of brain functional networks in childhood-onset schizophrenia. *Front Syst Neurosci*. 2010;4:147.
- Alink A, Schwiedrzik CM, Kohler A, Singer W, Muckli L. Stimulus predictability reduces responses in primary visual cortex. *The Journal of Neuroscience*. 2010;30(8):2960-6.
- Alladi S, Xuereb J, Bak T, Nestor P, Knibb J, Patterson K, Hodges JR. Focal cortical presentations of Alzheimer's disease. *Brain*. 2007 Oct;130(Pt 10):2636-45.
- Altmann GT, Kamide Y. Incremental interpretation at verbs: Restricting the domain of subsequent reference. *Cognition*. 1999;73(3):247-64.
- Anderson M. Normal pressure hydrocephalus. *Br Med J (Clin Res Ed)*. 1986;293(6551):837.
- Appel SH. A unifying hypothesis for the cause of amyotrophic lateral sclerosis, parkinsonism, and Alzheimer disease. *Ann Neurol*. 1981;10(6):499-505.

- Arighi A, Fumagalli GG, Jacini F, Fenoglio C, Ghezzi L, Pietroboni AM, De Riz M, Serpente M, Ridolfi E, Bonsi R. Early onset behavioral variant frontotemporal dementia due to the C9ORF72 hexanucleotide repeat expansion: psychiatric clinical presentations. *J Alzheimers Dis.* 2012;31(2):447-52.
- Armstrong MJ, Litvan I, Lang AE, Bak TH, Bhatia KP, Borroni B, Boxer AL, Dickson DW, Grossman M, Hallett M. Criteria for the diagnosis of corticobasal degeneration. *Neurology.* 2013;80(5):496-503.
- Arnal LH, Giraud A-L. Cortical oscillations and sensory predictions. *Trends in cognitive sciences.* 2012;16(7):390-8.
- Arnal LH, Morillon B, Kell CA, Giraud A-L. Dual neural routing of visual facilitation in speech processing. *The Journal of neuroscience.* 2009;29(43):13445-53.
- Ashburner J. A fast diffeomorphic image registration algorithm. *Neuroimage.* 2007;38(1):95-113.
- Baddeley AD, Hitch G. Working memory. *Psychology of learning and motivation.* 1974;8:47-89.
- Bahlmann J, Schubotz RI, Friederici AD. Hierarchical artificial grammar processing engages Broca's area. *Neuroimage.* 2008 Aug 15;42(2):525-34.
- Baker H, Ridley R, Duchen L, Crow T, Bruton C. Induction of β (A4)-amyloid in primates by injection of Alzheimer's disease brain homogenate. *Mol Neurobiol.* 1994;8(1):25-39.
- Bales KR, Verina T, Dodel RC, Du Y, Altstiel L, Bender M, Hyslop P, Johnstone EM, Little SP, Cummins DJ, Piccardo P, Ghetti B, Paul SM. Lack of apolipoprotein E dramatically reduces amyloid beta-peptide deposition. *Nat Genet.* 1997 Nov;17(3):263-4.
- Ballatore C, Lee VM-Y, Trojanowski JQ. Tau-mediated neurodegeneration in Alzheimer's disease and related disorders. *Nature reviews Neuroscience.* 2007;8(9):663.
- Banerjee S, Hellier J, Dewey M, Romeo R, Ballard C, Baldwin R, Bentham P, Fox C, Holmes C, Katona C. Sertraline or mirtazapine for depression in dementia (HTA-SADD): a randomised, multicentre, double-blind, placebo-controlled trial. *The Lancet.* 2011;378(9789):403-11.
- Barker WW, Luis CA, Kashuba A, Luis M, Harwood DG, Loewenstein D, Waters C, Jimison P, Shepherd E, Sevush S, Graff-Radford N, Newland D, Todd M, Miller B, Gold M, Heilman K, Doty L, Goodman I, Robinson B, Pearl G, Dickson D, Duara R. Relative frequencies of Alzheimer disease, Lewy body, vascular and frontotemporal dementia, and hippocampal sclerosis in the State of Florida Brain Bank. *Alzheimer Dis Assoc Disord.* 2002 Oct-Dec;16(4):203-12.
- Basso A, Capitani E, Laiacona M. Progressive language impairment without dementia: a case with isolated category specific semantic defect. *J Neurol Neurosurg Psychiatry.* 1988;51(9):1201-7.

- Bastiaanse R, Edwards S, Mass E, Rispens J. Assessing comprehension and production of verbs and sentences: The Verb and Sentence Test (VAST). *Aphasiology*. 2003;17(1):49-73.
- Bastos AM, Usrey WM, Adams RA, Mangun GR, Fries P, Friston KJ. Canonical microcircuits for predictive coding. *Neuron*. 2012 Nov 21;76(4):695-711.
- Becker RE, Greig NH. Fire in the ashes: Can failed Alzheimer's disease drugs succeed with second chances? *Alzheimer's & Dementia*. 2013;9(1):50-7.
- Belin C, Maillet D, Pop G, Carpentier A. bvFTD phenocopy syndrome: Myth or reality?(P1. 215). *Neurology*. 2015;84(14 Supplement):P1. 215.
- Belmatoug N, Burlina A, Giraldo P, Hendriksz CJ, Kuter DJ, Mengel E, Pastores GM. Gastrointestinal disturbances and their management in miglustat-treated patients. *J Inherit Metab Dis*. 2011;34(5):991-1001.
- Berndt RS. Sentence comprehension in Broca's aphasia: A critique of the evidence. *Behav Brain Sci*. 2000;23(01):24-.
- Berndt RS, Caramazza A, Zurif E. *Language Functions: Syntax. Language functions and brain organization*. 1983:5.
- Berndt RS, Mitchum CC, Haendiges AN. Comprehension of reversible sentences in "agrammatism": A meta-analysis. *Cognition*. 1996;58(3):289-308.
- Bevan-Jones WR, Cope TE, Jones PS, Passamonti L, Hong YT, Fryer TD, Arnold R, Allinson KSJ, Coles JP, Aigbirhio FI, Patterson K, O'Brien JT, Rowe JB. [18F]AV-1451 binding in vivo mirrors the expected distribution of TDP-43 pathology in the semantic variant of primary progressive aphasia. *J Neurol Neurosurg Psychiatry*. 2017a Sep 14;*in press*.
- Bevan-Jones WR, Cope TE, Passamonti L, Fryer TD, Hong YT, Aigbirhio F, Kril JJ, Forrest SL, Allinson K, Coles JP, Simon Jones P, Spillantini MG, Hodges JR, O'Brien JT, Rowe JB. [18F]AV-1451 PET in behavioral variant frontotemporal dementia due to MAPT mutation. *Annals of Clinical and Translational Neurology*. 2016;3(12):940-7.
- Bevan-Jones WR, Surendranathan A, Passamonti L, Rodríguez PV, Arnold R, Mak E, Su L, Coles JP, Fryer TD, Hong YT. Neuroimaging of Inflammation in Memory and Related Other Disorders (NIMROD) study protocol: a deep phenotyping cohort study of the role of brain inflammation in dementia, depression and other neurological illnesses. *BMJ open*. 2017b;7(1):e013187.
- Bhagal SK, Teasell RW, Foley NC, Speechley MR. Rehabilitation of aphasia: more is better. *Top Stroke Rehabil*. 2003 Summer;10(2):66-76.
- Birks JS. *Cholinesterase inhibitors for Alzheimer's disease*. The Cochrane Library. 2006.
- Blank H, Davis MH. Prediction Errors but Not Sharpened Signals Simulate Multivoxel fMRI Patterns during Speech Perception. *PLoS Biol*. 2016;14(11):e1002577.

- Blank I, Balewski Z, Mahowald K, Fedorenko E. Syntactic processing is distributed across the language system. *Neuroimage*. 2016;127:307-23.
- Bolwig TG. Transient global amnesia. *Acta Neurol Scand*. 1968;44(1):101-6.
- Bowyer SM. Coherence a measure of the brain networks: past and present. *Neuropsychiatric Electrophysiology*. 2016;2(1):1.
- Boxer AL, Knopman DS, Kaufer DI, Grossman M, Onyike C, Graf-Radford N, Mendez M, Kerwin D, Lerner A, Wu C-K. Memantine in patients with frontotemporal lobar degeneration: a multicentre, randomised, double-blind, placebo-controlled trial. *The Lancet Neurology*. 2013;12(2):149-56.
- Bozeat S, Lambon-Ralph MA, Patterson K, Garrard P, Hodges J. Non-verbal semantic impairment in semantic dementia. *Neuropsychologia*. 2000;38:1207-15.
- Bozeat S, Lambon Ralph MA, Graham KS, Patterson K, Wilkin H, Rowland J, Rogers TT, Hodges JR. A duck with four legs: Investigating the structure of conceptual knowledge using picture drawing in semantic dementia. *Cogn Neuropsychol*. 2003;20(1):27-47.
- Braak H, Braak E. Neuropathological staging of Alzheimer-related changes. *Acta Neuropathol*. 1991;82(4):239-59.
- Braak H, Braak E. Staging of Alzheimer's disease-related neurofibrillary changes. *Neurobiol Aging*. 1995;16(3):271-8.
- Braak H, Brettschneider J, Ludolph AC, Lee VM, Trojanowski JQ, Del Tredici K. Amyotrophic lateral sclerosis—a model of corticofugal axonal spread. *Nature reviews Neurology*. 2013;9(12):708.
- Braak H, Del Tredici K. The preclinical phase of the pathological process underlying sporadic Alzheimer's disease. *Brain*. 2015;138(10):2814-33.
- Brady MC, Kelly H, Godwin J, Enderby P, Campbell P. Speech and language therapy for aphasia following stroke. *The Cochrane Library*. 2016.
- Brady RO, Kanfer JN, Mock MB, Fredrickson DS. The metabolism of sphingomyelin. II. Evidence of an enzymatic deficiency in Niemann-Pick disease. *Proceedings of the National Academy of Sciences*. 1966;55(2):366-9.
- Breitenstein C, Grewe T, Flöel A, Ziegler W, Springer L, Martus P, Huber W, Willmes K, Ringelstein EB, Haeusler KG. Intensive speech and language therapy in patients with chronic aphasia after stroke: a randomised, open-label, blinded-endpoint, controlled trial in a health-care setting. *The Lancet*. 2017;389(10078):1528-38.
- Brier MR, Gordon B, Friedrichsen K, McCarthy J, Stern A, Christensen J, Owen C, Aldea P, Su Y, Hassenstab J, Cairns NJ, Holtzman DM, Fagan AM, Morris JC, Benzinger TL, Ances BM. Tau and Aβ imaging, CSF measures, and cognition in Alzheimer's disease. *Sci Transl Med*. 2016 May 11;8(338):338ra66.

- Brouwers N, Slegers K, Van Broeckhoven C. Molecular genetics of Alzheimer's disease: an update. *Ann Med.* 2008;40(8):562-83.
- Brown H, Adams RA, Parees I, Edwards M, Friston K. Active inference, sensory attenuation and illusions. *Cognitive processing.* 2013;14(4):411-27.
- Brownsett SL, Warren JE, Geranmayeh F, Woodhead Z, Leech R, Wise RJ. Cognitive control and its impact on recovery from aphasic stroke. *Brain.* 2014;137(1):242-54.
- Buckner RL, Sepulcre J, Talukdar T, Krienen FM, Liu H, Hedden T, Andrews-Hanna JR, Sperling RA, Johnson KA. Cortical hubs revealed by intrinsic functional connectivity: mapping, assessment of stability, and relation to Alzheimer's disease. *J Neurosci.* 2009;29(6):1860-73.
- Bullmore E, Sporns O. Complex brain networks: graph theoretical analysis of structural and functional systems. *Nature Reviews Neuroscience.* 2009;10(3):186-98.
- Bullock R, Touchon J, Bergman H, Gambina G, He Y, Rapatz G, Nagel J, Lane R. Rivastigmine and donepezil treatment in moderate to moderately-severe Alzheimer's disease over a 2-year period. *Curr Med Res Opin.* 2005;21(8):1317-27.
- Butler CR. Transient epileptic amnesia. *Pract Neurol.* 2006;6(6):368-71.
- Butler CR, Graham KS, Hodges JR, Kapur N, Wardlaw JM, Zeman AZ. The syndrome of transient epileptic amnesia. *Ann Neurol.* 2007;61(6):587-98.
- Cairns NJ, Bigio EH, Mackenzie IR, Neumann M, Lee VM-Y, Hatanpaa KJ, White III CL, Schneider JA, Grinberg LT, Halliday G. Neuropathologic diagnostic and nosologic criteria for frontotemporal lobar degeneration: consensus of the Consortium for Frontotemporal Lobar Degeneration. *Acta Neuropathol.* 2007;114(1):5-22.
- Caplan D, Baker C, Dehaut F. Syntactic determinants of sentence comprehension in aphasia. *Cognition.* 1985;21(2):117-75.
- Caramazza A, Zurif EB. Dissociation of algorithmic and heuristic processes in language comprehension: Evidence from aphasia. *Brain Lang.* 1976;3(4):572-82.
- Chan D, Anderson V, Pijnenburg Y, Whitwell J, Barnes J, Scahill R, Stevens JM, Barkhof F, Scheltens P, Rossor MN. The clinical profile of right temporal lobe atrophy. *Brain.* 2009;132(5):1287-98.
- Chennu S, Annen J, Wannez S, Thibaut A, Chatelle C, Cassol H, Martens G, Schnakers C, Gosseries O, Menon D. Brain networks predict metabolism, diagnosis and prognosis at the bedside in disorders of consciousness. *Brain.* 2017;140(8):2120-32.
- Chien DT, Bahri S, Szardenings AK, Walsh JC, Mu F, Su M-Y, Shankle WR, Elizarov A, Kolb HC. Early clinical PET imaging results with the novel PHF-tau radioligand [F-18]-T807. *J Alzheimers Dis.* 2013;34(2):457-68.

- Christiansen MH, Kelly ML, Shillcock RC, Greenfield K. Impaired artificial grammar learning in agrammatism. *Cognition*. 2010;116(3):382-93.
- Clavaguera F, Akatsu H, Fraser G, Crowther RA, Frank S, Hench J, Probst A, Winkler DT, Reichwald J, Staufenbiel M. Brain homogenates from human tauopathies induce tau inclusions in mouse brain. *Proceedings of the National Academy of Sciences*. 2013;110(23):9535-40.
- Clavaguera F, Bolmont T, Crowther RA, Abramowski D, Frank S, Probst A, Fraser G, Stalder AK, Beibel M, Staufenbiel M. Transmission and spreading of tauopathy in transgenic mouse brain. *Nat Cell Biol*. 2009;11(7):909.
- Cole G. Intracranial space-occupying masses in mental hospital patients: necropsy study. *J Neurol Neurosurg Psychiatry*. 1978;41(8):730-6.
- Colloby SJ, McParland S, O'Brien JT, Attems J. Neuropathological correlates of dopaminergic imaging in Alzheimer's disease and Lewy body dementias. *Brain*. 2012 Sep;135(Pt 9):2798-808.
- Confavreux C, Croisile B, Garassus P, Aimard G, Trillet M. Progressive amusia and aprosody. *Arch Neurol*. 1992;49(9):971-6.
- Conway CM, Bauernschmidt A, Huang SS, Pisoni DB. Implicit statistical learning in language processing: Word predictability is the key. *Cognition*. 2010;114(3):356-71.
- Conway CM, Pisoni DB. Neurocognitive basis of implicit learning of sequential structure and its relation to language processing. *Ann N Y Acad Sci*. 2008;1145(1):113-31.
- Cooper FE, Grube M, Elsegood KJ, Welch JL, Kelly TP, Chinnery PF, Griffiths TD. The contribution of the cerebellum to cognition in spinocerebellar ataxia type 6. *Behav Neurol*. 2010;23(1-2):3-15.
- Cope TE, Grube M, Singh B, Burn DJ, Griffiths TD. The basal ganglia in perceptual timing: Timing performance in Multiple System Atrophy and Huntington's disease. *Neuropsychologia*. 2014a Jan;52:73-81.
- Cope TE, Patterson K, Sohoglu E, Dawson K, Grube M, Davis MH, Rowe JB. P67. Predictive Mechanisms and Speech Perception in Progressive Non-Fluent Aphasia. *Am J Neurodegener Dis*. 2014b;3(Suppl. 1):123.
- Cope TE, Rittman T, Borchert RJ, Jones PS, Vatansever D, Allinson K, Passamonti L, Vazquez Rodriguez P, Bevan-Jones WR, O'Brien JT, Rowe JB. Tau burden and the functional connectome in Alzheimer's disease and progressive supranuclear palsy. *Brain*. 2018 Feb 1;141(2):550-67.
- Cope TE, Sedley W, Griffiths TD. Timing and the Auditory Brain. *Adv Clin Neurosci Rehabil*. 2011;10(6):10-3.
- Cope TE, Sohoglu E, Sedley W, Patterson K, Jones PS, Wiggins J, Dawson C, Grube M, Carlyon R, Griffiths T, Davis MH, Rowe JB. Evidence for causal top-down frontal

- contributions to predictive processes in speech perception. *Nature Communications*. 2017a;8(1):2154.
- Cope TE, Wilson B, Robson H, Drinkall R, Dean L, Grube M, Jones PS, Patterson K, Griffiths TD, Rowe JB, Petkov CI. Artificial grammar learning in vascular and progressive non-fluent aphasia. *Neuropsychologia*. 2017b Sep;104:201-13.
- Cordato N, Duggins A, Halliday G, Morris J, Pantelis C. Clinical deficits correlate with regional cerebral atrophy in progressive supranuclear palsy. *Brain*. 2005;128(6):1259-66.
- Cordato N, Pantelis C, Halliday G, Velakoulis D, Wood S, Stuart G, Currie J, Soo M, Olivieri G, Broe G. Frontal atrophy correlates with behavioural changes in progressive supranuclear palsy. *Brain*. 2002;125(4):789-800.
- Coyle-Gilchrist IT, Dick KM, Patterson K, Rodríguez PV, Wehmann E, Wilcox A, Lansdall CJ, Dawson KE, Wiggins J, Mead S. Prevalence, characteristics, and survival of frontotemporal lobar degeneration syndromes. *Neurology*. 2016;86(18):1736-43.
- Crinion J, Price CJ. Right anterior superior temporal activation predicts auditory sentence comprehension following aphasic stroke. *Brain*. 2005 Dec;128(Pt 12):2858-71.
- Crossley NA, Mechelli A, Scott J, Carletti F, Fox PT, McGuire P, Bullmore ET. The hubs of the human connectome are generally implicated in the anatomy of brain disorders. *Brain*. 2014;137(8):2382-95.
- Cummings JL, Benson F, Hill MA, Read S. Aphasia in dementia of the Alzheimer type. *Neurology*. 1985 Mar;35(3):394-7.
- D'Antona R, Baron JC, Samson Y, Serdaru M, Viader F, Agid Y, Cambier J. Subcortical dementia. Frontal cortex hypometabolism detected by positron tomography in patients with progressive supranuclear palsy. *Brain*. 1985 Sep;108 (Pt 3):785-99.
- Dai Z, Yan C, Li K, Wang Z, Wang J, Cao M, Lin Q, Shu N, Xia M, Bi Y. Identifying and mapping connectivity patterns of brain network hubs in Alzheimer's disease. *Cereb Cortex*. 2014:bhu246.
- Dambacher M, Kliegl R, Hofmann M, Jacobs AM. Frequency and predictability effects on event-related potentials during reading. *Brain Res*. 2006;1084(1):89-103.
- David O, Kilner JM, Friston KJ. Mechanisms of evoked and induced responses in MEG/EEG. *Neuroimage*. 2006 Jul 15;31(4):1580-91.
- de Haan W, Mott K, van Straaten EC, Scheltens P, Stam CJ. Activity dependent degeneration explains hub vulnerability in Alzheimer's disease. *PLoS Comput Biol*. 2012;8(8):e1002582.
- DeJesus-Hernandez M, Mackenzie IR, Boeve BF, Boxer AL, Baker M, Rutherford NJ, Nicholson AM, Finch NA, Flynn H, Adamson J. Expanded GGGGCC hexanucleotide repeat in noncoding region of C9ORF72 causes chromosome 9p-linked FTD and ALS. *Neuron*. 2011;72(2):245-56.

- Dickey MW, Milman LH, Thompson CK. Judgment of functional morphology in agrammatic aphasia. *J Neurolinguistics*. 2008 Jan;21(1):35-65.
- Dickson DW, Ahmed Z, Algom AA, Tsuboi Y, Josephs KA. Neuropathology of variants of progressive supranuclear palsy. *Curr Opin Neurol*. 2010 Aug;23(4):394-400.
- Dickson DW, Bergeron C, Chin S, Duyckaerts C, Horoupian D, Ikeda K, Jellinger K, Lantos P, Lippa C, Mirra S. Office of Rare Diseases neuropathologic criteria for corticobasal degeneration. *J Neuropathol Exp Neurol*. 2002;61(11):935-46.
- Diehl-Schmid J, Richard-Devantoy S, Grimmer T, Förstl H, Jox R. Behavioral variant frontotemporal dementia: advanced disease stages and death. A step to palliative care. *Int J Geriatr Psychiatry*. 2017;32(8):876-81.
- Dominey PF, Hoen M, Blanc J-M, Lelekov-Boissard T. Neurological basis of language and sequential cognition: evidence from simulation, aphasia, and ERP studies. *Brain Lang*. 2003;86(2):207-25.
- Dubois B, Albert ML. Amnesic MCI or prodromal Alzheimer's disease? *The Lancet Neurology*. 2004;3(4):246-8.
- Dubois B, Feldman HH, Jacova C, DeKosky ST, Barberger-Gateau P, Cummings J, Delacourte A, Galasko D, Gauthier S, Jicha G. Research criteria for the diagnosis of Alzheimer's disease: revising the NINCDS-ADRDA criteria. *The Lancet Neurology*. 2007;6(8):734-46.
- Durrett R. Some features of the spread of epidemics and information on a random graph. *Proceedings of the National Academy of Sciences*. 2010;107(10):4491-8.
- Edwards MJ, Adams RA, Brown H, Pareés I, Friston KJ. A Bayesian account of 'hysteria'. *Brain*. 2012;135(11):3495-512.
- Ellison D, Love S, Chimelli LMC, Harding B, Lowe JS, Vinters HV, Brandner S, Yong WH. *Neuropathology: a reference text of CNS pathology: Elsevier Health Sciences; 2012.*
- Erb J, Obleser J. Upregulation of cognitive control networks in older adults' speech comprehension. *Front Syst Neurosci*. 2013;7:116.
- Evans JJ, Heggs A, Antoun N, Hodges JR. Progressive prosopagnosia associated with selective right temporal lobe atrophy. *Brain*. 1995;118(1):1-13.
- Evans JL, Saffran JR, Robe-Torres K. Statistical learning in children with specific language impairment. *J Speech Lang Hear Res*. 2009;52(2):321-35.
- Fairhall SL, Caramazza A. Brain regions that represent amodal conceptual knowledge. *The Journal of Neuroscience*. 2013;33(25):10552-8.
- Falcon B, Cavallini A, Angers R, Glover S, Murray TK, Barnham L, Jackson S, O'Neill MJ, Isaacs AM, Hutton ML. Conformation determines the seeding potencies of native and recombinant Tau aggregates. *J Biol Chem*. 2015;290(2):1049-65.

- Fedorenko E, Duncan J, Kanwisher N. Language-selective and domain-general regions lie side by side within Broca's area. *Curr Biol*. 2012 Nov 6;22(21):2059-62.
- Ferri CP, Prince M, Brayne C, Brodaty H, Fratiglioni L, Ganguli M, Hall K, Hasegawa K, Hendrie H, Huang Y, Jorm A, Mathers C, Menezes PR, Rimmer E, Sczufca M. Global prevalence of dementia: a Delphi consensus study. *Lancet*. 2005 Dec 17;366(9503):2112-7.
- Filippini N, MacIntosh BJ, Hough MG, Goodwin GM, Frisoni GB, Smith SM, Matthews PM, Beckmann CF, Mackay CE. Distinct patterns of brain activity in young carriers of the APOE-epsilon4 allele. *Proc Natl Acad Sci U S A*. 2009 Apr 28;106(17):7209-14.
- Fisher C. Transient global amnesia. *Trans Am Neurol Assoc*. 1958;83:143-6.
- Fitzgerald S. Two Large Alzheimer's Trials Fail to Meet Endpoints: What's Next? *Neurology Today*. 2014;14(5):12-5.
- Fitzpatrick AWP, Falcon B, He S, Murzin AG, Murshudov G, Garringer HJ, Crowther RA, Ghetti B, Goedert M, Scheres SHW. Cryo-EM structures of tau filaments from Alzheimer's disease. *Nature*. 2017 Jul 13;547(7662):185-90.
- Folia V, Forkstam C, Ingvar M, Hagoort P, Petersson KM. Implicit Artificial Syntax Processing: Genes, Preference, and Bounded Recursion. *Biolinguistics*. 2011;5:105-32.
- Fontolan L, Morillon B, Liegeois-Chauvel C, Giraud A-L. The contribution of frequency-specific activity to hierarchical information processing in the human auditory cortex. *Nature communications*. 2014;5.
- Ford M. A method for obtaining measures of local parsing complexity throughout sentences. *Journal of verbal learning and verbal behavior*. 1983;22(2):203-18.
- Forkstam C, Hagoort P, Fernandez G, Ingvar M, Petersson KM. Neural correlates of artificial syntactic structure classification. *Neuroimage*. 2006 Aug 15;32(2):956-67.
- Foster NL, Gilman S, Berent S, Morin EM, Brown MB, Koeppe RA. Cerebral hypometabolism in progressive supranuclear palsy studied with positron emission tomography. *Ann Neurol*. 1988;24(3):399-406.
- Freimann FB, Streitberger K-J, Klatt D, Lin K, McLaughlin J, Braun J, Sprung C, Sack I. Alteration of brain viscoelasticity after shunt treatment in normal pressure hydrocephalus. *Neuroradiology*. 2012;54(3):189-96.
- Friederici AD. The brain basis of language processing: from structure to function. *Physiol Rev*. 2011 Oct;91(4):1357-92.
- Friederici AD, Bahlmann J, Heim S, Schubotz RI, Anwander A. The brain differentiates human and non-human grammars: functional localization and structural connectivity. *Proc Natl Acad Sci U S A*. 2006 Feb 14;103(7):2458-63.

- Friederici AD, Chomsky N, Berwick RC, Moro A, Bolhuis JJ. Language, mind and brain. *Nature Human Behaviour*. 2017 2017/09/18.
- Friederici AD, Kotz SA. The brain basis of syntactic processes: functional imaging and lesion studies. *Neuroimage*. 2003 Nov;20 Suppl 1:S8-17.
- Friederici AD, Opitz B, von Cramon DY. Segregating semantic and syntactic aspects of processing in the human brain: an fMRI investigation of different word types. *Cereb Cortex*. 2000 Jul;10(7):698-705.
- Friston K. A theory of cortical responses. *Philosophical transactions of the Royal Society B: Biological sciences*. 2005;360(1456):815-36.
- Friston K. Hierarchical models in the brain. *PLoS Comput Biol*. 2008 Nov;4(11):e1000211.
- Friston K, Henson R. Commentary on: divide and conquer; a defence of functional localisers. *Neuroimage*. 2006;30(4):1097-9.
- Frost R, Armstrong BC, Siegelman N, Christiansen MH. Domain generality versus modality specificity: the paradox of statistical learning. *Trends in cognitive sciences*. 2015;19(3):117-25.
- Gardner RC, Boxer AL, Trujillo A, Mirsky JB, Guo CC, Gennatas ED, Heuer HW, Fine E, Zhou J, Kramer JH. Intrinsic connectivity network disruption in progressive supranuclear palsy. *Ann Neurol*. 2013;73(5):603-16.
- Geranmayeh F, Brownsett SL, Wise RJ. Task-induced brain activity in aphasic stroke patients: what is driving recovery? *Brain*. 2014a;137(10):2632-48.
- Geranmayeh F, Chau T, Wise R, Leech R, Hampshire A. Domain general sub-regions of the medial prefrontal cortex contribute to recovery of language after stroke. *Brain*. 2017;140(7):1947-58.
- Geranmayeh F, Wise RJ, Mehta A, Leech R. Overlapping networks engaged during spoken language production and its cognitive control. *J Neurosci*. 2014b Jun 25;34(26):8728-40.
- Ghosh B. *The neurobiology of cognition in progressive supranuclear palsy*: University of Cambridge; 2011.
- Ghosh BC, Calder AJ, Peers PV, Lawrence AD, Acosta-Cabronero J, Pereira JM, Hodges JR, Rowe JB. Social cognitive deficits and their neural correlates in progressive supranuclear palsy. *Brain*. 2012 Jul;135(Pt 7):2089-102.
- Giordano BL, Ince RA, Gross J, Schyns PG, Panzeri S, Kayser C. Contributions of local speech encoding and functional connectivity to audio-visual speech perception. *eLife*. 2017;6.
- Goedert M. Alzheimer's and Parkinson's diseases: The prion concept in relation to assembled A β , tau, and α -synuclein. *Science*. 2015;349(6248):1255555.

- Goedert M, Spillantini MG. A century of Alzheimer's disease. *Science*. 2006;314(5800):777-81.
- Golbe LI, Ohman-Strickland PA. A clinical rating scale for progressive supranuclear palsy. *Brain*. 2007;130(6):1552-65.
- Goll JC, Crutch SJ, Loo JHY, Rohrer JD, Frost C, Bamiou DE, Warren JD. Non-verbal sound processing in the primary progressive aphasia. *Brain*. 2010 Jan;133:272-85.
- Goll JC, Kim LG, Hailstone JC, Lehmann M, Buckley A, Crutch SJ, Warren JD. Auditory object cognition in dementia. *Neuropsychologia*. 2011;49(9):2755-65.
- Gómez RL, Gerken L. Infant artificial language learning and language acquisition. *Trends in cognitive sciences*. 2000;4(5):178-86.
- Goodglass H, Barresi B, Kaplan E. *The Boston diagnostic aphasia examination*: Lippincott Williams & Wilkins. A Wolters Kluwer Company; 1983.
- Goodman E, Bates JC. On the inseparability of grammar and the lexicon: Evidence from acquisition, aphasia and real-time processing. *Language and cognitive Processes*. 1997;12(5-6):507-84.
- Goodwin GC, Payne RL. *Dynamic system identification: experiment design and data analysis*: Academic press New York; 1977.
- Gorno-Tempini ML, Dronkers NF, Rankin KP, Ogar JM, Phengrasamy L, Rosen HJ, Johnson JK, Weiner MW, Miller BL. Cognition and anatomy in three variants of primary progressive aphasia. *Ann Neurol*. 2004 Mar;55(3):335-46.
- Gorno-Tempini ML, Hillis AE, Weintraub S, Kertesz A, Mendez M, Cappa SF, Ogar JM, Rohrer JD, Black S, Boeve BF, Manes F, Dronkers NF, Vandenberghe R, Rascovsky K, Patterson K, Miller BL, Knopman DS, Hodges JR, Mesulam MM, Grossman M. Classification of primary progressive aphasia and its variants. *Neurology*. 2011 Mar 15;76(11):1006-14.
- Gow DW, Segawa JA, Ahlfors SP, Lin F-H. Lexical influences on speech perception: a Granger causality analysis of MEG and EEG source estimates. *Neuroimage*. 2008;43(3):614-23.
- Grafton ST, Hazeltine E, Ivry R. Functional mapping of sequence learning in normal humans. *J Cogn Neurosci*. 1995 Fall;7(4):497-510.
- Graham A, Davies R, Xuereb J, Halliday G, Kril J, Creasey H, Graham K, Hodges J. Pathologically proven frontotemporal dementia presenting with severe amnesia. *Brain*. 2005;128(3):597-605.
- Grahn JA, Rowe JB. Feeling the Beat: Premotor and Striatal Interactions in Musicians and Nonmusicians during Beat Perception. *J Neurosci*. 2009 June 10, 2009;29(23):7540-8.

- Grahn JA, Rowe JB. Finding and Feeling the Musical Beat: Striatal Dissociations between Detection and Prediction of Regularity. *Cereb Cortex*. 2012 April 11, 2012.
- Granger CW. Investigating causal relations by econometric models and cross-spectral methods. *Econometrica: Journal of the Econometric Society*. 1969:424-38.
- Granovetter M. The strength of weak ties: A network theory revisited. *Soc Theory*. 1983:201-33.
- Greicius MD, Krasnow B, Reiss AL, Menon V. Functional connectivity in the resting brain: a network analysis of the default mode hypothesis. *Proceedings of the National Academy of Sciences*. 2003;100(1):253-8.
- Greicius MD, Srivastava G, Reiss AL, Menon V. Default-mode network activity distinguishes Alzheimer's disease from healthy aging: evidence from functional MRI. *Proc Natl Acad Sci U S A*. 2004 Mar 30;101(13):4637-42.
- Griffiths TD, Warren JD. What is an auditory object? *Nature Reviews Neuroscience*. 2004;5(11):887-92.
- Grodzinsky Y. The neurology of syntax: Language use without Broca's area. *Behav Brain Sci*. 2000;23(01):1-21.
- Grossman M, Moore P. A longitudinal study of sentence comprehension difficulty in primary progressive aphasia. *J Neurol Neurosurg Psychiatry*. 2005 May;76(5):644-9.
- Grube M, Bruffaerts R, Schaefferbeke J, Neyens V, De Weer AS, Seghers A, Bergmans B, Dries E, Griffiths TD, Vandenberghe R. Core auditory processing deficits in primary progressive aphasia. *Brain*. 2016 Apr 9;139(6):1817-29.
- Grube M, Cooper FE, Chinnery PF, Griffiths TD. Dissociation of duration-based and beat-based auditory timing in cerebellar degeneration. *Proc Natl Acad Sci U S A*. 2010 Jun 22;107(25):11597-601.
- Grube M, Kumar S, Cooper FE, Turton S, Griffiths TD. Auditory sequence analysis and phonological skill. *Proc Biol Sci*. 2012 Nov 7;279(1746):4496-504.
- Guo CC, Gorno-Tempini ML, Gesierich B, Henry M, Trujillo A, Shany-Ur T, Jovicich J, Robinson SD, Kramer JH, Rankin KP. Anterior temporal lobe degeneration produces widespread network-driven dysfunction. *Brain*. 2013;136(10):2979-91.
- Guo JL, Lee VM. Cell-to-cell transmission of pathogenic proteins in neurodegenerative diseases. *Nat Med*. 2014 Feb;20(2):130-8.
- Guo JL, Narasimhan S, Changolkar L, He Z, Stieber A, Zhang B, Gathagan RJ, Iba M, McBride JD, Trojanowski JQ. Unique pathological tau conformers from Alzheimer's brains transmit tau pathology in nontransgenic mice. *J Exp Med*. 2016;213(12):2635-54.
- Haendiges AN, Berndt RS, Mitchum CC. Assessing the elements contributing to a "mapping" deficit: a targeted treatment study. *Brain Lang*. 1996 Jan;52(1):276-302.

- Halliday M, Mallucci GR. Targeting the unfolded protein response in neurodegeneration: a new approach to therapy. *Neuropharmacology*. 2014;76:169-74.
- Halliday M, Mallucci GR. Reply: Trazodone to change the risk of neurodegeneration: bedside to bench. *Brain*. 2017;140(8):e48-e.
- Halliday M, Radford H, Zents KA, Molloy C, Moreno JA, Verity NC, Smith E, Ortori CA, Barrett DA, Bushell M. Repurposed drugs targeting eIF2 α -P-mediated translational repression prevent neurodegeneration in mice. *Brain*. 2017;140(6):1768-83.
- Hampson M, Peterson BS, Skudlarski P, Gatenby JC, Gore JC. Detection of functional connectivity using temporal correlations in MR images. *Hum Brain Mapp*. 2002;15(4):247-62.
- Harold D, Abraham R, Hollingworth P, Sims R, Gerrish A, Hamshere ML, Pahwa JS, Moskvina V, Dowzell K, Williams A. Genome-wide association study identifies variants at CLU and PICALM associated with Alzheimer's disease. *Nat Genet*. 2009;41(10):1088-93.
- Harris JM, Gall C, Thompson JC, Richardson AM, Neary D, du Plessis D, Pal P, Mann DM, Snowden JS, Jones M. Sensitivity and specificity of FTDC criteria for behavioral variant frontotemporal dementia. *Neurology*. 2013;80(20):1881-7.
- Harrison L, Penny WD, Friston K. Multivariate autoregressive modeling of fMRI time series. *Neuroimage*. 2003;19(4):1477-91.
- Henson RN, Mouchlianitis E, Friston KJ. MEG and EEG data fusion: simultaneous localisation of face-evoked responses. *Neuroimage*. 2009;47(2):581-9.
- Hickok G. The cortical organization of speech processing: Feedback control and predictive coding the context of a dual-stream model. *J Commun Disord*. 2012;45(6):393-402.
- Hickok G, Poeppel D. The cortical organization of speech processing. *Nat Rev Neurosci*. 2007 May;8(5):393-402.
- Hinton GE. Learning multiple layers of representation. *Trends in cognitive sciences*. 2007;11(10):428-34.
- Hobson P, Meara J. Risk and incidence of dementia in a cohort of older subjects with Parkinson's disease in the United Kingdom. *Mov Disord*. 2004 Sep;19(9):1043-9.
- Hodges JR, Patterson K, Oxbury S, Funnell E. Semantic dementia. *Brain*. 1992;115(6):1783-806.
- Höglinger GU, Respondek G, Stamelou M, Kurz C, Josephs KA, Lang AE, Mollenhauer B, Müller U, Nilsson C, Whitwell JL. Clinical diagnosis of progressive supranuclear palsy: the Movement Disorder Society Criteria. *Mov Disord*. 2017.

- Hohman TJ, Beason-Held LL, Lamar M, Resnick SM. Subjective cognitive complaints and longitudinal changes in memory and brain function. *Neuropsychology*. 2011;25(1):125.
- Hornberger M, Piguet O. Episodic memory in frontotemporal dementia: a critical review. *Brain*. 2012;135(3):678-92.
- Hornberger M, Piguet O, Graham A, Nestor P, Hodges J. How preserved is episodic memory in behavioral variant frontotemporal dementia? *Neurology*. 2010;74(6):472-9.
- Hornberger M, Shelley BP, Kipps CM, Piguet O, Hodges JR. Can progressive and non-progressive behavioural variant frontotemporal dementia be distinguished at presentation? *J Neurol Neurosurg Psychiatry*. 2009;80(6):591-3.
- Hsieh S, Schubert S, Hoon C, Mioshi E, Hodges JR. Validation of the Addenbrooke's Cognitive Examination III in frontotemporal dementia and Alzheimer's disease. *Dement Geriatr Cogn Disord*. 2013;36(3-4):242-50.
- Huber R, Aschoff A, Ludolph A, Riepe M. Transient global amnesia. *J Neurol*. 2002;249(11):1520-4.
- Hughes AJ, Daniel SE, Ben-Shlomo Y, Lees AJ. The accuracy of diagnosis of parkinsonian syndromes in a specialist movement disorder service. *Brain*. 2002;125(4):861-70.
- Hughes LE, Rowe JB, Ghosh BC, Carlyon RP, Plack CJ, Gockel HE. The binaural masking level difference: cortical correlates persist despite severe brain stem atrophy in progressive supranuclear palsy. *J Neurophysiol*. 2014 Sep 17;jn 00062 2014.
- Iba M, Guo JL, McBride JD, Zhang B, Trojanowski JQ, Lee VM. Synthetic tau fibrils mediate transmission of neurofibrillary tangles in a transgenic mouse model of Alzheimer's-like tauopathy. *J Neurosci*. 2013 Jan 16;33(3):1024-37.
- Iizuka O, Suzuki K, Endo K, Fujii T, Mori E. Pure word deafness and pure anarthria in a patient with frontotemporal dementia. *Eur J Neurol*. 2007;14(4):473-5.
- Ikeda M, Brown J, Holland AJ, Fukuhara R, Hodges J. Changes in appetite, food preference, and eating habits in frontotemporal dementia and Alzheimer's disease. *J Neurol Neurosurg Psychiatry*. 2002;73(4):371-6.
- Ioannou YA. The structure and function of the Niemann–Pick C1 protein. *Mol Genet Metab*. 2000;71(1):175-81.
- Ishii K, Kanda T, Harada A, Miyamoto N, Kawaguchi T, Shimada K, Ohkawa S, Uemura T, Yoshikawa T, Mori E. Clinical impact of the callosal angle in the diagnosis of idiopathic normal pressure hydrocephalus. *Eur Radiol*. 2008 Nov;18(11):2678-83.
- Ittner LM, Götz J. Amyloid- β and tau--a toxic pas de deux in Alzheimer's disease. *Nature Reviews Neuroscience*. 2011;12(2):65.
- Jaraj D, Rabiei K, Marlow T, Jensen C, Skoog I, Wikkelsø C. Prevalence of idiopathic normal-pressure hydrocephalus. *Neurology*. 2014;82(16):1449-54.

- Jenkinson M, Smith S. A global optimisation method for robust affine registration of brain images. *Med Image Anal.* 2001;5(2):143-56.
- Jeppsson A, Zetterberg H, Blennow K, Wikkelso C. Idiopathic normal-pressure hydrocephalus Pathophysiology and diagnosis by CSF biomarkers. *Neurology.* 2013;80(15):1385-92.
- Johnson KA, Schultz A, Betensky RA, Becker JA, Sepulcre J, Rentz D, Mormino E, Chhatwal J, Amariglio R, Papp K. Tau positron emission tomographic imaging in aging and early Alzheimer disease. *Ann Neurol.* 2016;79(1):110-9.
- Jones DT, Knopman DS, Gunter JL, Graff-Radford J, Vemuri P, Boeve BF, Petersen RC, Weiner MW, Jack Jr CR. Cascading network failure across the Alzheimer's disease spectrum. *Brain.* 2015;139(2):547-62.
- Jürgens S, Biermann-Ruben K, Kurz MW, Flügel C, Daehli Kurz K, Antke C, Hartung H-P, Seitz RJ, Schnitzler A. Word deafness as a cortical auditory processing deficit: a case report with MEG. *Neurocase.* 2008;14(4):307-16.
- Josephs KA, Boeve BF, Duffy JR, Smith GE, Knopman DS, Parisi JE, Petersen RC, Dickson DW. Atypical progressive supranuclear palsy underlying progressive apraxia of speech and nonfluent aphasia. *Neurocase.* 2005;11(4):283-96.
- Josephs KA, Duffy JR, Strand EA, Machulda MM, Senjem ML, Gunter JL, Schwarz CG, Reid RI, Sychalla AJ, Lowe VJ, Jack CR, Jr., Whitwell JL. The evolution of primary progressive apraxia of speech. *Brain.* 2014 Oct;137(Pt 10):2783-95.
- Josephs KA, Duffy JR, Strand EA, Machulda MM, Senjem ML, Lowe VJ, Jack CR, Whitwell JL. Syndromes dominated by apraxia of speech show distinct characteristics from agrammatic PPA. *Neurology.* 2013;81(4):337-45.
- Josephs KA, Duffy JR, Strand EA, Machulda MM, Senjem ML, Master AV, Lowe VJ, Jack CR, Whitwell JL. Characterizing a neurodegenerative syndrome: primary progressive apraxia of speech. *Brain.* 2012:aws032.
- Josephs KA, Duffy JR, Strand EA, Whitwell JL, Layton KF, Parisi JE, Hauser MF, Witte RJ, Boeve BF, Knopman DS, Dickson DW, Jack CR, Jr., Petersen RC. Clinicopathological and imaging correlates of progressive aphasia and apraxia of speech. *Brain.* 2006 Jun;129(Pt 6):1385-98.
- Joyce KE, Laurienti PJ, Burdette JH, Hayasaka S. A new measure of centrality for brain networks. *PLoS One.* 2010;5(8):e12200.
- Kaat LD, Boon A, Kamphorst W, Ravid R, Duivenvoorden H, Van Swieten J. Frontal presentation in progressive supranuclear palsy. *Neurology.* 2007;69(8):723-9.
- Kaplan E. *The assessment of aphasia and related disorders*: Lippincott Williams & Wilkins; 1983.

- Kato N, Arai K, Hattori T. Study of the rostral midbrain atrophy in progressive supranuclear palsy. *J Neurol Sci.* 2003;210(1):57-60.
- Kawai Y, Suenaga M, Takeda A, Ito M, Watanabe H, Tanaka F, Kato K, Fukatsu H, Naganawa S, Kato T. Cognitive impairments in multiple system atrophy MSA-C vs MSA-P. *Neurology.* 2008;70(16 Part 2):1390-6.
- Kertesz A, McCabe P. Recovery patterns and prognosis in aphasia. *Brain.* 1977 Mar;100 Pt 1:1-18.
- Kertesz A, McMonagle P, Blair M, Davidson W, Munoz DG. The evolution and pathology of frontotemporal dementia. *Brain.* 2005 Sep;128(Pt 9):1996-2005.
- Kilner J. Bias in a common EEG and MEG statistical analysis and how to avoid it. *Clin Neurophysiol.* 2013;124(10):2062-3.
- Kilner JM, Friston KJ, Frith CD. Predictive coding: an account of the mirror neuron system. *Cognitive processing.* 2007;8(3):159-66.
- Kimura T, Takamatsu J. Pilot study of pharmacological treatment for frontotemporal dementia: risk of donepezil treatment for behavioral and psychological symptoms. *Geriatrics & gerontology international.* 2013;13(2):506-7.
- Kipps CM, Hodges JR, Hornberger M. Nonprogressive behavioural frontotemporal dementia: recent developments and clinical implications of the 'bvFTD phenocopy syndrome'. *Curr Opin Neurol.* 2010;23(6):628-32.
- Klenk E. Über die Natur der Phosphatide und anderer Lipide des Gehirns und der Leber bei der Niemann-Pickschen Krankheit.[12. Mitteilung über Phosphatide.]. *Hoppe-Seyler's Zeitschrift für physiologische Chemie.* 1935;235(1-2):24-36.
- Klöppel S, Stonnington CM, Petrovic P, Mobbs D, Tüscher O, Craufurd D, Tabrizi SJ, Frackowiak RS. Irritability in pre-clinical Huntington's disease. *Neuropsychologia.* 2010;48(2):549-57.
- Klunk WE, Engler H, Nordberg A, Wang Y, Blomqvist G, Holt DP, Bergström M, Savitcheva I, Huang GF, Estrada S. Imaging brain amyloid in Alzheimer's disease with Pittsburgh Compound-B. *Ann Neurol.* 2004;55(3):306-19.
- Knibb JA, Kipps CM, Hodges JR. Frontotemporal dementia. *Curr Opin Neurol.* 2006a Dec;19(6):565-71.
- Knibb JA, Xuereb JH, Patterson K, Hodges JR. Clinical and pathological characterization of progressive aphasia. *Ann Neurol.* 2006b Jan;59(1):156-65.
- Kriegeskorte N, Simmons WK, Bellgowan PS, Baker CI. Circular analysis in systems neuroscience: the dangers of double dipping. *Nat Neurosci.* 2009;12(5):535-40.
- Kumar S, Sedley W, Barnes GR, Teki S, Friston KJ, Griffiths TD. A brain basis for musical hallucinations. *Cortex.* 2014 Mar;52:86-97.

- Kundu P, Brenowitz ND, Voon V, Worbe Y, Vértes PE, Inati SJ, Saad ZS, Bandettini PA, Bullmore ET. Integrated strategy for improving functional connectivity mapping using multiecho fMRI. *Proceedings of the National Academy of Sciences*. 2013;110(40):16187-92.
- Kundu P, Inati SJ, Evans JW, Luh W-M, Bandettini PA. Differentiating BOLD and non-BOLD signals in fMRI time series using multi-echo EPI. *Neuroimage*. 2012;60(3):1759-70.
- Laird AR, Fox PM, Eickhoff SB, Turner JA, Ray KL, McKay DR, Glahn DC, Beckmann CF, Smith SM, Fox PT. Behavioral interpretations of intrinsic connectivity networks. *J Cogn Neurosci*. 2011;23(12):4022-37.
- Lang C. Is direct CT caudatometry superior to indirect parameters in confirming Huntington's disease? *Neuroradiology*. 1985;27(2):161-3.
- Lansdall CJ, Coyle-Gilchrist IT, Jones PS, Vázquez Rodríguez P, Wilcox A, Wehmann E, Dick KM, Robbins TW, Rowe JB. Apathy and impulsivity in frontotemporal lobar degeneration syndromes. *Brain*. 2017;140(6):1792-807.
- Larner A. Addenbrooke's Cognitive Examination (ACE) for the diagnosis and differential diagnosis of dementia. *Clin Neurol Neurosurg*. 2007;109(6):491-4.
- Larner AJ. "Frontal variant Alzheimer's disease": A reappraisal. *Clin Neurol Neurosurg*. 2006;108(7):705-8.
- Larner AJ. *Diagnostic Test Accuracy Studies in Dementia : A Pragmatic Approach*. Cham: Springer International Publishing; 2015.
- Larson EB, Shadlen MF, Wang L, McCormick WC, Bowen JD, Teri L, Kukull WA. Survival after initial diagnosis of Alzheimer disease. *Ann Intern Med*. 2004 Apr 6;140(7):501-9.
- Lebert F. Behavioral benefits of trazodone are sustained for the long term in frontotemporal dementia. 2006.
- Lebert F, Stekke W, Hasenbroekx C, Pasquier F. Frontotemporal dementia: a randomised, controlled trial with trazodone. *Dement Geriatr Cogn Disord*. 2004;17(4):355-9.
- Lehmann M, Ghosh PM, Madison C, Laforce R, Corbetta-Rastelli C, Weiner MW, Greicius MD, Seeley WW, Gorno-Tempini ML, Rosen HJ. Diverging patterns of amyloid deposition and hypometabolism in clinical variants of probable Alzheimer's disease. *Brain*. 2013;136(3):844-58.
- Levitt H. Transformed up-down methods in psychoacoustics. *J Acoust Soc Am*. 1971 Feb;49(2):Suppl 2:467+.
- Levy G, Schupf N, Tang MX, Cote LJ, Louis ED, Mejia H, Stern Y, Marder K. Combined effect of age and severity on the risk of dementia in Parkinson's disease. *Ann Neurol*. 2002;51(6):722-9.

- Lincoln NB, McGuirk E, Mulley GP, Lendrem W, Jones AC, Mitchell JR. Effectiveness of speech therapy for aphasic stroke patients. A randomised controlled trial. *Lancet*. 1984 Jun 2;1(8388):1197-200.
- Ling H, O'Sullivan SS, Holton JL, Revesz T, Massey LA, Williams DR, Paviour DC, Lees AJ. Does corticobasal degeneration exist? A clinicopathological re-evaluation. *Brain*. 2010;133(7):2045-57.
- Litvan I, Agid Y, Calne D, Campbell G, Dubois B, Duvoisin R, Goetz C, Golbe LI, Grafman J, Growdon J. Clinical research criteria for the diagnosis of progressive supranuclear palsy (Steele-Richardson-Olszewski syndrome) Report of the NINDS-SPSP International Workshop*. *Neurology*. 1996;47(1):1-9.
- Liu L, Drouet V, Wu JW, Witter MP, Small SA, Clelland C, Duff K. Trans-synaptic spread of tau pathology in vivo. *PLoS One*. 2012;7(2):e31302.
- Liu WK, Le TV, Adamson J, Baker M, Cookson N, Hardy J, Hutton M, Yen SH, Dickson DW. Relationship of the extended tau haplotype to tau biochemistry and neuropathology in progressive supranuclear palsy. *Ann Neurol*. 2001;50(4):494-502.
- Ljung L. System identification. Signal analysis and prediction: Springer; 1998. p. 163-73.
- Lotto AJ, Hickok GS, Holt LL. Reflections on mirror neurons and speech perception. *Trends Cogn Sci*. 2009 Mar;13(3):110-4.
- Lu C-j, Tune LE. Chronic exposure to anticholinergic medications adversely affects the course of Alzheimer disease. *The American Journal of Geriatric Psychiatry*. 2003;11(4):458-61.
- Mackenzie IR, Baborie A, Pickering-Brown S, Du Plessis D, Jaros E, Perry RH, Neary D, Snowden JS, Mann DM. Heterogeneity of ubiquitin pathology in frontotemporal lobar degeneration: classification and relation to clinical phenotype. *Acta Neuropathol*. 2006 Nov;112(5):539-49.
- Mackenzie IR, Foti D, Woulfe J, Hurwitz TA. Atypical frontotemporal lobar degeneration with ubiquitin-positive, TDP-43-negative neuronal inclusions. *Brain*. 2008;131(5):1282-93.
- Mackenzie IR, Neumann M, Baborie A, Sampathu DM, Du Plessis D, Jaros E, Perry RH, Trojanowski JQ, Mann DM, Lee VM. A harmonized classification system for FTL-DTP pathology. *Acta Neuropathol*. 2011 Jul;122(1):111-3.
- Mackenzie IR, Neumann M, Bigio EH, Cairns NJ, Alafuzoff I, Kril J, Kovacs GG, Ghetti B, Halliday G, Holm IE. Nomenclature and nosology for neuropathologic subtypes of frontotemporal lobar degeneration: an update. *Acta Neuropathol*. 2010;119(1):1-4.
- Macmillan NA, Kaplan HL. Detection theory analysis of group data: estimating sensitivity from average hit and false-alarm rates. *Psychol Bull*. 1985;98(1):185.
- Maestú F, Peña J-M, Garcés P, González S, Bajo R, Bagic A, Cuesta P, Funke M, Mäkelä JP, Menasalvas E. A multicenter study of the early detection of synaptic dysfunction in Mild

Cognitive Impairment using Magnetoencephalography-derived functional connectivity. *NeuroImage: Clinical*. 2015;9:103-9.

Mak WM, Vonk W, Schriefers H. The influence of animacy on relative clause processing. *Journal of Memory and Language*. 2002;47(1):50-68.

Mak WM, Vonk W, Schriefers H. Animacy in processing relative clauses: The hikers that rocks crush. *Journal of Memory and Language*. 2006;54(4):466-90.

Makuuchi M, Bahlmann J, Anwender A, Friederici AD. Segregating the core computational faculty of human language from working memory. *Proc Natl Acad Sci U S A*. 2009 May 19;106(20):8362-7.

Mandelli ML, Vilaplana E, Brown JA, Hubbard HI, Binney RJ, Attygalle S, Santos-Santos MA, Miller ZA, Pakvasa M, Henry ML, Rosen HJ, Henry RG, Rabinovici GD, Miller BL, Seeley WW, Gorno-Tempini ML. Healthy brain connectivity predicts atrophy progression in non-fluent variant of primary progressive aphasia. *Brain*. 2016 Oct;139(Pt 10):2778-91.

Markesbery WR. Neuropathologic alterations in mild cognitive impairment: a review. *J Alzheimers Dis*. 2010;19(1):221-8.

Massey LA, Jäger HR, Paviour DC, O'Sullivan SS, Ling H, Williams DR, Kallis C, Holton J, Revesz T, Burn DJ. The midbrain to pons ratio A simple and specific MRI sign of progressive supranuclear palsy. *Neurology*. 2013;80(20):1856-61.

Massey LA, Micallef C, Paviour DC, O'Sullivan SS, Ling H, Williams DR, Kallis C, Holton JL, Revesz T, Burn DJ. Conventional magnetic resonance imaging in confirmed progressive supranuclear palsy and multiple system atrophy. *Mov Disord*. 2012;27(14):1754-62.

Matthews F, Stephan B, Robinson L, Jagger C, Barnes L, Arthur A, Brayne C, Collaboration ASC. A two decade dementia incidence comparison from the Cognitive Function and Ageing Studies I and II. *Nature communications*. 2016;7.

Matthews FE, Arthur A, Barnes LE, Bond J, Jagger C, Robinson L, Brayne C, Function MRCC, Collaboration A. A two-decade comparison of prevalence of dementia in individuals aged 65 years and older from three geographical areas of England: results of the Cognitive Function and Ageing Study I and II. *The Lancet*. 2013;382(9902):1405-12.

McClelland JL, Mirman D, Holt LL. Are there interactive processes in speech perception? *Trends in Cognitive Sciences*. 2006;10(8):363-9.

McGurk H, MacDonald J. Hearing lips and seeing voices. *Nature*. 1976;264:746-8.

McKeith I. Commentary: DLB and PDD: the same or different? Is there a debate? *Int Psychogeriatr*. 2009;21(02):220-4.

McKeith I, Dickson DW, Lowe J, Emre M, O'brien J, Feldman H, Cummings J, Duda J, Lippa C, Perry E. Diagnosis and management of dementia with Lewy bodies third report of the DLB consortium. *Neurology*. 2005;65(12):1863-72.

McKeith IG, Burn D. Spectrum of Parkinson's disease, Parkinson's dementia, and Lewy body dementia. *Neurol Clin.* 2000;18(4):865-83.

McKhann G, Drachman D, Folstein M, Katzman R, Price D, Stadlan EM. Clinical diagnosis of Alzheimer's disease Report of the NINCDS-ADRDA Work Group* under the auspices of Department of Health and Human Services Task Force on Alzheimer's Disease. *Neurology.* 1984;34(7):939-.

McKhann GM, Knopman DS, Chertkow H, Hyman BT, Jack CR, Kawas CH, Klunk WE, Koroshetz WJ, Manly JJ, Mayeux R. The diagnosis of dementia due to Alzheimer's disease: Recommendations from the National Institute on Aging-Alzheimer's Association workgroups on diagnostic guidelines for Alzheimer's disease. *Alzheimer's & dementia.* 2011;7(3):263-9.

McMonagle P, Deering F, Berliner Y, Kertesz A. The cognitive profile of posterior cortical atrophy. *Neurology.* 2006 Feb 14;66(3):331-8.

McQueen JM, Norris D, Cutler A. Are there really interactive processes in speech perception? *Trends in Cognitive Sciences.* 2006;10(12):533-.

Melo T, Ferro J, Ferro H. Transient global amnesia. *Brain.* 1992;115(1):261-70.

Mendez MF, Shapira JS, McMurtray A, Licht E. Preliminary findings: behavioral worsening on donepezil in patients with frontotemporal dementia. *The American Journal of Geriatric Psychiatry.* 2007;15(1):84-7.

Mesulam MM, Weintraub S, Rogalski EJ, Wieneke C, Geula C, Bigio EH. Asymmetry and heterogeneity of Alzheimer's and frontotemporal pathology in primary progressive aphasia. *Brain.* 2014 Apr;137(Pt 4):1176-92.

Meyer MR, Tschanz JT, Norton MC, Welsh-Bohmer KA, Steffens DC, Wyse BW, Breitner JC. APOE genotype predicts when—not whether—one is predisposed to develop Alzheimer disease. *Nat Genet.* 1998;19(4):321-2.

Miller GA, Isard S. Some perceptual consequences of linguistic rules. *Journal of Verbal Learning and Verbal Behavior.* 1963;2(3):217-28.

Milne A, Wilson B, Christiansen M. Structured sequence learning across sensory modalities in humans and nonhuman primates. *Current Opinion in Behavioral Sciences.* 2018;21:39-48.

Mioshi E, Hodges J. Rate of change of functional abilities in frontotemporal dementia. *Dement Geriatr Cogn Disord.* 2009;28(5):404-11.

Missori P, Rughetti A, Peschillo S, Gualdi G, Di Biasi C, Nofroni I, Marinelli L, Fattapposta F, Curra A. In normal aging ventricular system never attains pathological values of Evans' index. *Oncotarget.* 2016 Mar 15;7(11):11860-3.

Mognon A, Jovicich J, Bruzzone L, Buiatti M. ADJUST: An automatic EEG artifact detector based on the joint use of spatial and temporal features. *Psychophysiology.* 2011;48(2):229-40.

- Mohandas E, Rajmohan V. Frontotemporal dementia: An updated overview. *Indian J Psychiatry*. 2009 Jan;51 Suppl 1:S65-9.
- Montoya A, Price BH, Menear M, Lepage M. Brain imaging and cognitive dysfunctions in Huntington's disease. *Journal of psychiatry & neuroscience: JPN*. 2006;31(1):21.
- Moreno JA, Halliday M, Molloy C, Radford H, Verity N, Axten JM, Ortori CA, Willis AE, Fischer PM, Barrett DA. Oral treatment targeting the unfolded protein response prevents neurodegeneration and clinical disease in prion-infected mice. *Sci Transl Med*. 2013;5(206):206ra138-206ra138.
- Moss DJH, Poulter M, Beck J, Hehir J, Polke JM, Campbell T, Adamson G, Mudanohwo E, McColgan P, Haworth A. C9orf72 expansions are the most common genetic cause of Huntington disease phenocopies. *Neurology*. 2014;82(4):292-9.
- Muhlert N, Milton F, Butler CR, Kapur N, Zeman AZ. Accelerated forgetting of real-life events in Transient Epileptic Amnesia. *Neuropsychologia*. 2010;48(11):3235-44.
- Murray B, Lynch T, Farrell M. Clinicopathological features of the tauopathies. *Biochem Soc Trans*. 2005 Aug;33(Pt 4):595-9.
- Murray SO, Kersten D, Olshausen BA, Schrater P, Woods DL. Shape perception reduces activity in human primary visual cortex. *Proceedings of the National Academy of Sciences*. 2002;99(23):15164-9.
- Musmann H. Predictive image coding. *Image transmission techniques*. 1979;73:112.
- Muthukumaraswamy SD, Singh KD. Visual gamma oscillations: the effects of stimulus type, visual field coverage and stimulus motion on MEG and EEG recordings. *Neuroimage*. 2013;69:223-30.
- Myeku N, Clelland CL, Emrani S, Kukushkin NV, Yu WH, Goldberg AL, Duff KE. Tau-driven 26S proteasome impairment and cognitive dysfunction can be prevented early in disease by activating cAMP-PKA signaling. *Nat Med*. 2016;22(1):46.
- Ni W, Constable RT, Mencl WE, Pugh KR, Fulbright RK, Shaywitz SE, Shaywitz B, Gore JC, Shankweiler D. An event-related neuroimaging study distinguishing form and content in sentence processing. *Cognitive Neuroscience, Journal of*. 2000;12(1):120-33.
- NICE, SCIE. Dementia: Supporting People with Dementia and their Carers in Health and Social Care. NICE clinical guideline 42; 2006 (updated March 2016).
- Nisbet RM, Polanco J-C, Ittner LM, Götz J. Tau aggregation and its interplay with amyloid- β . *Acta Neuropathol*. 2015;129(2):207-20.
- Nolte G, Bai O, Wheaton L, Mari Z, Vorbach S, Hallett M. Identifying true brain interaction from EEG data using the imaginary part of coherency. *Clin Neurophysiol*. 2004;115(10):2292-307.

- Nonaka T, Watanabe ST, Iwatsubo T, Hasegawa M. Seeded Aggregation and Toxicity of α -Synuclein and Tau CELLULAR MODELS OF NEURODEGENERATIVE DISEASES. *J Biol Chem.* 2010;285(45):34885-98.
- Norris D, McQueen JM, Cutler A. Merging information in speech recognition: Feedback is never necessary. *Behav Brain Sci.* 2000;23(03):299-325.
- Norris D, McQueen JM, Cutler A. Prediction, Bayesian inference and feedback in speech recognition. *Language, cognition and neuroscience.* 2016;31(1):4-18.
- Obrig H, Mentzel J, Rossi S. Universal and language-specific sublexical cues in speech perception: a novel electroencephalography-lesion approach. *Brain.* 2016 Jun;139(Pt 6):1800-16.
- Okello A, Koivunen J, Edison P, Archer H, Turkheimer F, Någren Ku, Bullock R, Walker Z, Kennedy A, Fox N. Conversion of amyloid positive and negative MCI to AD over 3 years An 11C-PIB PET study. *Neurology.* 2009;73(10):754-60.
- Okuma Y. Freezing of gait in Parkinson's disease. *J Neurol.* 2006;253(7):vii27-vii32.
- Opitz B, Kotz SA. Ventral premotor cortex lesions disrupt learning of sequential grammatical structures. *Cortex.* 2012 Jun;48(6):664-73.
- Orhan AE, Jacobs RA. Are performance limitations in visual short-term memory tasks due to capacity limitations or model mismatch? *arXiv preprint arXiv:14070644.* 2014.
- Osaki Y, Ben-Shlomo Y, Lees AJ, Daniel SE, Colosimo C, Wenning G, Quinn N. Accuracy of clinical diagnosis of progressive supranuclear palsy. *Mov Disord.* 2004;19(2):181-9.
- Ossenkoppele R, Schonhaut DR, Baker SL, O'Neil JP, Janabi M, Ghosh PM, Santos M, Miller ZA, Bettcher BM, Gorno-Tempini ML, Miller BL, Jagust WJ, Rabinovici GD. Tau, amyloid, and hypometabolism in a patient with posterior cortical atrophy. *Ann Neurol.* 2015 Feb;77(2):338-42.
- Ossenkoppele R, Schonhaut DR, Schöll M, Lockhart SN, Ayakta N, Baker SL, O'Neil JP, Janabi M, Lazaris A, Cantwell A. Tau PET patterns mirror clinical and neuroanatomical variability in Alzheimer's disease. *Brain.* 2016:aww027.
- Otsuki M, Soma Y, Sato M, Homma A, Tsuji S. Slowly progressive pure word deafness. *Eur Neurol.* 1998;39(3):135-40.
- Pareés I, Brown H, Nuruki A, Adams RA, Davare M, Bhatia KP, Friston K, Edwards MJ. Loss of sensory attenuation in patients with functional (psychogenic) movement disorders. *Brain.* 2014;137(11):2916-21.
- Park H, Ince RA, Schyns PG, Thut G, Gross J. Frontal top-down signals increase coupling of auditory low-frequency oscillations to continuous speech in human listeners. *Curr Biol.* 2015 Jun 15;25(12):1649-53.

- Pascual-Marqui RD. Standardized low-resolution brain electromagnetic tomography (sLORETA): technical details. *Methods Find Exp Clin Pharmacol*. 2002;24(Suppl D):5-12.
- Passamonti L, Vazquez Rodriguez P, Hong YT, Allinson KS, Williamson D, Borchert RJ, Sami S, Cope TE, Bevan-Jones WR, Jones PS, Arnold R, Surendranathan A, Mak E, Su L, Fryer TD, Aigbirhio FI, O'Brien JT, Rowe JB. 18F-AV-1451 positron emission tomography in Alzheimer's disease and progressive supranuclear palsy. *Brain*. 2017 Mar 1;140(3):781-91.
- Patel AD, Iversen JR, Wassenaar M, Hagoort P. Musical syntactic processing in agrammatic Broca's aphasia. *Aphasiology*. 2008;22(7-8):776-89.
- Patterson K, Graham N, Ralph MAL, Hodges J. Progressive non-fluent aphasia is not a progressive form of non-fluent (post-stroke) aphasia. *Aphasiology*. 2006;20(9):1018-34.
- Patterson MC, Hendriksz CJ, Walterfang M, Sedel F, Vanier MT, Wijburg F. Recommendations for the diagnosis and management of Niemann-Pick disease type C: an update. *Mol Genet Metab*. 2012 Jul;106(3):330-44.
- Patterson MC, Vecchio D, Prady H, Abel L, Wraith JE. Miglustat for treatment of Niemann-Pick C disease: a randomised controlled study. *The Lancet Neurology*. 2007;6(9):765-72.
- Perrin RJ, Fagan AM, Holtzman DM. Multimodal techniques for diagnosis and prognosis of Alzheimer's disease. *Nature*. 2009 Oct 15;461(7266):916-22.
- Petersson K-M, Folia V, Hagoort P. What artificial grammar learning reveals about the neurobiology of syntax. *Brain Lang*. 2012;120(2):83-95.
- Petersson KM, Forkstam C, Ingvar M. Artificial syntactic violations activate Broca's region. *Cognitive Science*. 2004 May-Jun;28(3):383-407.
- Phillips HN, Blenkmann A, Hughes LE, Kochen S, Bekinschtein TA, Cam C, Rowe JB. Convergent evidence for hierarchical prediction networks from human electrocorticography and magnetoencephalography. *Cortex*. 2016 Sep;82:192-205.
- Piguet O, Hornberger M, Mioshi E, Hodges JR. Behavioural-variant frontotemporal dementia: diagnosis, clinical staging, and management. *The Lancet Neurology*. 2011;10(2):162-72.
- Porsteinsson AP, Drye LT, Pollock BG, Devanand DP, Frangakis C, Ismail Z, Marano C, Meinert CL, Mintzer JE, Munro CA, Pelton G, Rabins PV, Rosenberg PB, Schneider LS, Shade DM, Weintraub D, Yesavage J, Lyketsos CG. Effect of citalopram on agitation in Alzheimer disease: the CitAD randomized clinical trial. *JAMA*. 2014 Feb 19;311(7):682-91.
- Power JD, Barnes KA, Snyder AZ, Schlaggar BL, Petersen SE. Spurious but systematic correlations in functional connectivity MRI networks arise from subject motion. *Neuroimage*. 2012;59(3):2142-54.
- Power JD, Schlaggar BL, Lessov-Schlaggar CN, Petersen SE. Evidence for hubs in human functional brain networks. *Neuron*. 2013;79(4):798-813.

- Price CJ, Seghier ML, Leff AP. Predicting language outcome and recovery after stroke: the PLORAS system. *Nature Reviews Neurology*. 2010;6(4):202-10.
- Prusiner SB. Some speculations about prions, amyloid, and Alzheimer's disease. *Mass Medical Soc*; 1984.
- R Core Team. *R: A language and environment for statistical computing.*: R Foundation for Statistical Computing, Vienna, Austria.; 2016.
- Raina P, Santaguida P, Ismaila A, Patterson C, Cowan D, Levine M, Booker L, Oremus M. Effectiveness of cholinesterase inhibitors and memantine for treating dementia: evidence review for a clinical practice guideline. *Ann Intern Med*. 2008;148(5):379-97.
- Rainer M, Mucke H, Krüger-Rainer C, Kraxberger E, Haushofer M, Jellinger K. Cognitive relapse after discontinuation of drug therapy in Alzheimer's disease: cholinesterase inhibitors versus nootropics. *J Neural Transm*. 2001;108(11):1327-33.
- Raj A, Kuceyeski A, Weiner M. A network diffusion model of disease progression in dementia. *Neuron*. 2012;73(6):1204-15.
- Raj A, LoCastro E, Kuceyeski A, Tosun D, Relkin N, Weiner M, Initiative AsDN. Network diffusion model of progression predicts longitudinal patterns of atrophy and metabolism in Alzheimer's disease. *Cell reports*. 2015;10(3):359-69.
- Ranasinghe KG, Hinkley LB, Beagle AJ, Mizuiri D, Honma SM, Welch AE, Hubbard I, Mandelli ML, Miller ZA, Garrett C. Distinct spatiotemporal patterns of neuronal functional connectivity in primary progressive aphasia variants. *Brain*. 2017.
- Rao RP, Ballard DH. Predictive coding in the visual cortex: a functional interpretation of some extra-classical receptive-field effects. *Nat Neurosci*. 1999;2(1):79-87.
- Rascovsky K, Hodges JR, Knopman D, Mendez MF, Kramer JH, Neuhaus J, van Swieten JC, Seelaar H, Dopper EG, Onyike CU. Sensitivity of revised diagnostic criteria for the behavioural variant of frontotemporal dementia. *Brain*. 2011;134(9):2456-77.
- Rauch SL, Savage CR, Brown HD, Curran T, Alpert NM, Kendrick A, Fischman AJ, Kosslyn SM. A PET investigation of implicit and explicit sequence learning. *Hum Brain Mapp*. 1995;3(4):271-86.
- Rauch SL, Whalen PJ, Savage CR, Curran T, Kendrick A, Brown HD, Bush G, Breiter HC, Rosen BR. Striatal recruitment during an implicit sequence learning task as measured by functional magnetic resonance imaging. *Hum Brain Mapp*. 1997;5(2):124-32.
- Raven JC. *Guide to the standard progressive matrices: sets A, B, C, D and E*: HK Lewis; 1960.
- Reber AS. Implicit learning of artificial grammars. *Journal of verbal learning and verbal behavior*. 1967;6(6):855-63.

- Reisberg B, Auer SR, Monteiro IM. Behavioral pathology in Alzheimer's disease (BEHAVE-AD) rating scale. *Int Psychogeriatr*. 1996;8 Suppl 3:301-8; discussion 51-4.
- Reisberg B, Shulman MB, Torossian C, Leng L, Zhu W. Outcome over seven years of healthy adults with and without subjective cognitive impairment. *Alzheimer's & Dementia*. 2010;6(1):11-24.
- Reitz C, Brayne C, Mayeux R. Epidemiology of Alzheimer disease. *Nature Reviews Neurology*. 2011;7(3):137-52.
- Remez RE, Rubin PE, Pisoni DB, Carrell TD. Speech perception without traditional speech cues. *Science*. 1981;212(4497):947-9.
- Renton AE, Majounie E, Waite A, Simón-Sánchez J, Rollinson S, Gibbs JR, Schymick JC, Laaksovirta H, Van Swieten JC, Myllykangas L. A hexanucleotide repeat expansion in C9ORF72 is the cause of chromosome 9p21-linked ALS-FTD. *Neuron*. 2011;72(2):257-68.
- Respondek G, Höglinger G. The phenotypic spectrum of progressive supranuclear palsy. *Parkinsonism Relat Disord*. 2016;22:S34-S6.
- Respondek G, Stamelou M, Kurz C, Ferguson LW, Rajput A, Chiu WZ, van Swieten JC, Troakes C, al Sarraj S, Gelpi E. The phenotypic spectrum of progressive supranuclear palsy: a retrospective multicenter study of 100 definite cases. *Mov Disord*. 2014;29(14):1758-66.
- Rittman T, Ghosh BC, McColgan P, Breen DP, Evans J, Williams-Gray CH, Barker RA, Rowe JB. The Addenbrooke's Cognitive Examination for the differential diagnosis and longitudinal assessment of patients with parkinsonian disorders. *J Neurol Neurosurg Psychiatry*. 2013;jnnp-2012-303618.
- Rittman T, Rubinov M, Vértes PE, Patel AX, Ginestet CE, Ghosh BC, Barker RA, Spillantini MG, Bullmore ET, Rowe JB. Regional expression of the MAPT gene is associated with loss of hubs in brain networks and cognitive impairment in Parkinson disease and progressive supranuclear palsy. *Neurobiol Aging*. 2016;48:153-60.
- Robbins T, James M, Lange KW, Owen A, Quinn N, Marsden C. Cognitive performance in multiple system atrophy. *Brain*. 1992;115(1):271-91.
- Roberson ED, Scarce-Levie K, Palop JJ, Yan F, Cheng IH, Wu T, Gerstein H, Yu G-Q, Mucke L. Reducing endogenous tau ameliorates amyloid β -induced deficits in an Alzheimer's disease mouse model. *Science*. 2007;316(5825):750-4.
- Robson H, Grube M, Ralph MAL, Griffiths TD, Sage K. Fundamental deficits of auditory perception in Wernicke's aphasia. *Cortex*. 2013 Jul-Aug;49(7):1808-22.
- Rogalski E, Cobia D, Harrison TM, Wieneke C, Thompson CK, Weintraub S, Mesulam MM. Anatomy of language impairments in primary progressive aphasia. *J Neurosci*. 2011 Mar 2;31(9):3344-50.
- Rogalski EJ, Saxon M, McKenna H, Wieneke C, Rademaker A, Corden ME, Borio K, Mesulam M-M, Khayum B. Communication Bridge: A pilot feasibility study of Internet-

based speech–language therapy for individuals with progressive aphasia. *Alzheimer's & Dementia: Translational Research & Clinical Interventions*. 2016.

Rohrer J, Guerreiro R, Vandrovcova J, Uphill J, Reiman D, Beck J, Isaacs A, Authier A, Ferrari R, Fox N. The heritability and genetics of frontotemporal lobar degeneration. *Neurology*. 2009;73(18):1451-6.

Rohrer JD, Crutch SJ, Warrington EK, Warren JD. Progranulin-associated primary progressive aphasia: a distinct phenotype? *Neuropsychologia*. 2010 Jan;48(1):288-97.

Rohrer JD, Rossor MN, Warren JD. Alzheimer's pathology in primary progressive aphasia. *Neurobiol Aging*. 2012 Apr;33(4):744-52.

Rolfs A, Koeppen AH, Bauer I, Bauer P, Buhlmann S, Topka H, Schols L, Riess O. Clinical features and neuropathology of autosomal dominant spinocerebellar ataxia (SCA17). *Ann Neurol*. 2003 Sep;54(3):367-75.

Romberg AR, Saffran JR. All Together Now: Concurrent Learning of Multiple Structures in an Artificial Language. *Cognitive Science*. 2013;37(7):1290-320.

Rosen HJ, Allison SC, Schauer GF, Gorno-Tempini ML, Weiner MW, Miller BL. Neuroanatomical correlates of behavioural disorders in dementia. *Brain*. 2005;128(11):2612-25.

Rosso SM, Kaat LD, Baks T, Joosse M, de Koning I, Pijnenburg Y, de Jong D, Dooijes D, Kamphorst W, Ravid R. Frontotemporal dementia in The Netherlands: patient characteristics and prevalence estimates from a population-based study. *Brain*. 2003;126(9):2016-22.

Rubinov M, Sporns O. Complex network measures of brain connectivity: uses and interpretations. *Neuroimage*. 2010;52(3):1059-69.

Rumble B, Retallack R, Hilbich C, Simms G, Multhaup G, Martins R, Hockey A, Montgomery P, Beyreuther K, Masters CL. Amyloid A4 protein and its precursor in Down's syndrome and Alzheimer's disease. *N Engl J Med*. 1989 Jun 1;320(22):1446-52.

Saito Y, Suzuki K, Nanba E, Yamamoto T, Ohno K, Murayama S. Niemann–Pick type C disease: Accelerated neurofibrillary tangle formation and amyloid β deposition associated with apolipoprotein E ϵ 4 homozygosity. *Ann Neurol*. 2002;52(3):351-5.

Sajjadi SA, Patterson K, Arnold RJ, Watson PC, Nestor PJ. Primary progressive aphasia: a tale of two syndromes and the rest. *Neurology*. 2012 May 22;78(21):1670-7.

Sajjadi SA, Patterson K, Nestor PJ. Logopenic, mixed, or Alzheimer-related aphasia? *Neurology*. 2014;82(13):1127-31.

Sampathu DM, Neumann M, Kwong LK, Chou TT, Micsenyi M, Truax A, Bruce J, Grossman M, Trojanowski JQ, Lee VM. Pathological heterogeneity of frontotemporal lobar degeneration with ubiquitin-positive inclusions delineated by ubiquitin

immunohistochemistry and novel monoclonal antibodies. *Am J Pathol.* 2006 Oct;169(4):1343-52.

Sanz-Arigita EJ, Schoonheim MM, Damoiseaux JS, Rombouts SA, Maris E, Barkhof F, Scheltens P, Stam CJ. Loss of 'small-world' networks in Alzheimer's disease: graph analysis of fMRI resting-state functional connectivity. *PLoS One.* 2010;5(11):e13788.

Sarno MT, Silverman M, Sands E. Speech therapy and language recovery in severe aphasia. *J Speech Hear Res.* 1970 Sep;13(3):607-23.

Saunders AM, Strittmatter WJ, Schmechel D, George-Hyslop PH, Pericak-Vance MA, Joo SH, Rosi BL, Gusella JF, Crapper-MacLachlan DR, Alberts MJ, et al. Association of apolipoprotein E allele epsilon 4 with late-onset familial and sporadic Alzheimer's disease. *Neurology.* 1993 Aug;43(8):1467-72.

Saxena S, Caroni P. Selective neuronal vulnerability in neurodegenerative diseases: from stressor thresholds to degeneration. *Neuron.* 2011;71(1):35-48.

Schachter AS, Davis KL. Guidelines for the appropriate use of cholinesterase inhibitors in patients with Alzheimer's disease. *CNS Drugs.* 1999;11(4):281-8.

Schnitzler A, Gross J. Functional connectivity analysis in magnetoencephalography. *Int Rev Neurobiol.* 2005;68:173-95.

Schoffelen J-M, Hultén A, Lam N, Marquand AF, Uddén J, Hagoort P. Frequency-specific directed interactions in the human brain network for language. *Proceedings of the National Academy of Sciences.* 2017 July 25, 2017;114(30):8083-8.

Schofield EC, Hodges JR, Bak TH, Xuereb JH, Halliday GM. The relationship between clinical and pathological variables in Richardson's syndrome. *J Neurol.* 2012a;259(3):482-90.

Schofield TM, Penny WD, Stephan KE, Crinion JT, Thompson AJ, Price CJ, Leff AP. Changes in auditory feedback connections determine the severity of speech processing deficits after stroke. *J Neurosci.* 2012b Mar 21;32(12):4260-70.

Schöll M, Lockhart SN, Schonhaut DR, O'Neil JP, Janabi M, Ossenkoppele R, Baker SL, Vogel JW, Faria J, Schwimmer HD. PET imaging of tau deposition in the aging human brain. *Neuron.* 2016;89(5):971-82.

Schöll M, Ossenkoppele R, Strandberg O, Palmqvist S, Jögi J, Ohlsson T, Smith R, Hansson O. Distinct 18F-AV-1451 tau PET retention patterns in early- and late-onset Alzheimer's disease. *Brain.* 2017.

Schuchard J, Nerantzini M, Thompson CK. Implicit learning and implicit treatment outcomes in individuals with aphasia. *Aphasiology.* 2017 2017/01/02;31(1):25-48.

Schuchard J, Thompson CK. Sequential learning in individuals with agrammatic aphasia: evidence from artificial grammar learning. *Journal of Cognitive Psychology.* 2017:1-14.

- Schuchman EH, Levran O, Pereira LV, Desnick RJ. Structural organization and complete nucleotide sequence of the gene encoding human acid sphingomyelinase (SMPD1). *Genomics*. 1992;12(2):197-205.
- Schwartz J-L, Savariaux C. No, there is no 150 ms lead of visual speech on auditory speech, but a range of audiovisual asynchronies varying from small audio lead to large audio lag. *PLoS Comput Biol*. 2014;10(7):e1003743.
- Schwarz AJ, Yu P, Miller BB, Shcherbinin S, Dickson J, Navitsky M, Joshi AD, Devous MD, Mintun MS. Regional profiles of the candidate tau PET ligand 18F-AV-1451 recapitulate key features of Braak histopathological stages. *Brain*. 2016;139(5):1539-50.
- Sedley W, Gander PE, Kumar S, Kovach CK, Oya H, Kawasaki H, Howard MA, Griffiths TD. Neural Signatures of Perceptual Inference. *eLife*. 2016 2016/03/07;5:e11476.
- Seelaar H, Klijnsma KY, de Koning I, van der Lugt A, Chiu WZ, Azmani A, Rozemuller AJ, van Swieten JC. Frequency of ubiquitin and FUS-positive, TDP-43-negative frontotemporal lobar degeneration. *J Neurol*. 2010a;257(5):747-53.
- Seelaar H, Rohrer JD, Pijnenburg YA, Fox NC, Van Swieten JC. Clinical, genetic and pathological heterogeneity of frontotemporal dementia: a review. *J Neurol Neurosurg Psychiatry*. 2010b;jnnp. 2010.212225.
- Seeley W, Bauer A, Miller B, Gorno-Tempini M, Kramer J, Weiner M, Rosen H. The natural history of temporal variant frontotemporal dementia. *Neurology*. 2005;64(8):1384-90.
- Seghier ML, Patel E, Prejawa S, Ramsden S, Selmer A, Lim L, Browne R, Rae J, Haigh Z, Ezekiel D. The PLORAS Database: A data repository for predicting language outcome and recovery after stroke. *Neuroimage*. 2016;124:1208-12.
- Sevin M, Lesca G, Baumann N, Millat G, Lyon-Caen O, Vanier MT, Sedel F. The adult form of Niemann-Pick disease type C. *Brain*. 2007 Jan;130(Pt 1):120-33.
- Shankweiler D, Mencl WE, Braze D, Tabor W, Pugh KR, Fulbright RK. Reading differences and brain: Cortical integration of speech and print in sentence processing varies with reader skill. *Dev Neuropsychol*. 2008;33(6):745-75.
- Shannon RV, Zeng FG, Kamath V, Wygonski J, Ekelid M. Speech recognition with primarily temporal cues. *Science*. 1995 Oct 13;270(5234):303-4.
- Sheldon S, Pichora-Fuller MK, Schneider BA. Priming and sentence context support listening to noise-vocoded speech by younger and older adults. *The Journal of the Acoustical Society of America*. 2008;123(1):489-99.
- Shelley BP, Hodges JR, Kipps CM, Xuereb JH, Bak TH. Is the pathology of corticobasal syndrome predictable in life? *Mov Disord*. 2009;24(11):1593-9.
- Shipp S, Adams RA, Friston KJ. Reflections on agranular architecture: predictive coding in the motor cortex. *Trends Neurosci*. 2013;36(12):706-16.

- Shuping JR, Rollinson RD, Toole JF. Transient global amnesia. *Ann Neurol.* 1980a;7(3):281-5.
- Shuping JR, Toole JF, Alexander E. Transient global amnesia due to glioma in the dominant hemisphere. *Neurology.* 1980b;30(1):88-.
- Sisodia S, Koo E, Beyreuther K, Unterbeck A, Price D. Evidence that beta-amyloid protein in Alzheimer's disease is not derived by normal processing. *Science.* 1990;248(4954):492-6.
- Smith R, Puschmann A, Schöll M, Ohlsson T, Van Swieten J, Honer M, Englund E, Hansson O. 18F-AV-1451 tau PET imaging correlates strongly with tau neuropathology in MAPT mutation carriers. *Brain.* 2016:aww163.
- Smith SM, Fox PT, Miller KL, Glahn DC, Fox PM, Mackay CE, Filippini N, Watkins KE, Toro R, Laird AR. Correspondence of the brain's functional architecture during activation and rest. *Proceedings of the National Academy of Sciences.* 2009;106(31):13040-5.
- Snowden JS, Bathgate D, Varma A, Blackshaw A, Gibbons ZC, Neary D. Distinct behavioural profiles in frontotemporal dementia and semantic dementia. *J Neurol Neurosurg Psychiatry.* 2001 Mar;70(3):323-32.
- Snowden JS, Goulding P, Neary D. Semantic dementia: a form of circumscribed cerebral atrophy. *Behav Neurol.* 1989.
- Snowden JS, Rollinson S, Thompson JC, Harris JM, Stopford CL, Richardson AM, Jones M, Gerhard A, Davidson YS, Robinson A. Distinct clinical and pathological characteristics of frontotemporal dementia associated with C9ORF72 mutations. *Brain.* 2012;135(3):693-708.
- Sohoglu E, Davis MH. Perceptual learning of degraded speech by minimizing prediction error. *Proceedings of the National Academy of Sciences.* 2016;113(12):E1747-E56.
- Sohoglu E, Peelle JE, Carlyon RP, Davis MH. Predictive top-down integration of prior knowledge during speech perception. *J Neurosci.* 2012 Jun 20;32(25):8443-53.
- Sohoglu E, Peelle JE, Carlyon RP, Davis MH. Top-down influences of written text on perceived clarity of degraded speech. *J Exp Psychol Hum Percept Perform.* 2014 Feb;40(1):186-99.
- Sporns O, Chialvo DR, Kaiser M, Hilgetag CC. Organization, development and function of complex brain networks. *Trends in cognitive sciences.* 2004;8(9):418-25.
- Stam C, Jones B, Nolte G, Breakspear M, Scheltens P. Small-world networks and functional connectivity in Alzheimer's disease. *Cereb Cortex.* 2006;17(1):92-9.
- Stam CJ. Modern network science of neurological disorders. *Nature reviews Neuroscience.* 2014;15(10):683.
- Stamelou M, Knake S, Oertel W, Höglinger G. Magnetic resonance imaging in progressive supranuclear palsy. *J Neurol.* 2011;258(4):549-58.

- Stanislaw H, Todorov N. Calculation of signal detection theory measures. *Behav Res Methods Instrum Comput.* 1999;31(1):137-49.
- Stephen C, Sweadner K, Penniston J, Schmahmann J. X-linked spinocerebellar ataxia (SCA) type 1A: a novel late onset phenotype of the ATP2B3 mutation (P5. 392). *Neurology.* 2016;86(16 Supplement):P5. 392.
- Stewart R. Subjective cognitive impairment. *Current opinion in psychiatry.* 2012;25(6):445-50.
- Stokes PA, Purdon PL. A study of problems encountered in Granger causality analysis from a neuroscience perspective. *Proc Natl Acad Sci U S A.* 2017 Aug 22;114(34):E7063-E72.
- Sullivan D, Walterfang M, Velakoulis D. Bipolar disorder and Niemann-Pick disease type C. *Am J Psychiatry.* 2005;162(5):1021-a-2.
- Summy WH, Pollack I. Visual contribution to speech intelligibility in noise. *The journal of the acoustical society of america.* 1954;26(2):212-5.
- Swanberg MM. Memantine for behavioral disturbances in frontotemporal dementia: a case series. *Alzheimer Dis Assoc Disord.* 2007;21(2):164-6.
- Tabrizi SJ, Langbehn DR, Leavitt BR, Roos RA, Durr A, Craufurd D, Kennard C, Hicks SL, Fox NC, Scahill RI. Biological and clinical manifestations of Huntington's disease in the longitudinal TRACK-HD study: cross-sectional analysis of baseline data. *The Lancet Neurology.* 2009;8(9):791-801.
- Taniguchi-Watanabe S, Arai T, Kametani F, Nonaka T, Masuda-Suzukake M, Tarutani A, Murayama S, Saito Y, Arima K, Yoshida M. Biochemical classification of tauopathies by immunoblot, protein sequence and mass spectrometric analyses of sarkosyl-insoluble and trypsin-resistant tau. *Acta Neuropathol.* 2016;131(2):267-80.
- Tariot PN, Farlow MR, Grossberg GT, Graham SM, McDonald S, Gergel I, Group MS. Memantine treatment in patients with moderate to severe Alzheimer disease already receiving donepezil: a randomized controlled trial. *JAMA.* 2004;291(3):317-24.
- Taulu S, Simola J, Kajola M. Applications of the signal space separation method. *IEEE transactions on signal processing.* 2005;53(9):3359-72.
- Tetzloff KA, Duffy JR, Clark HM, Strand EA, Machulda MM, Schwarz CG, Senjem ML, Reid RI, Spsychalla AJ, Tosakulwong N, Lowe VJ, Jack CR, Jr., Josephs KA, Whitwell JL. Longitudinal structural and molecular neuroimaging in agrammatic primary progressive aphasia. *Brain.* 2017 Dec 8.
- Thaut M, McIntosh G, Rice R, Miller R, Rathbun J, Brault J. Rhythmic auditory stimulation in gait training for Parkinson's disease patients. *Mov Disord.* 1996;11(2):193-200.
- The Mathworks Inc. Matlab and Statistics and Machine Learning Toolbox. Release 2015b ed. Natick, Massachusetts; 2015.

- Thompson CK, den Ouden D-B, Bonakdarpour B, Garibaldi K, Parrish TB. Neural plasticity and treatment-induced recovery of sentence processing in agrammatism. *Neuropsychologia*. 2010;48(11):3211-27.
- Thompson CK, Meltzer-Asscher A, Cho S, Lee J, Wieneke C, Weintraub S, Mesulam M. Syntactic and morphosyntactic processing in stroke-induced and primary progressive aphasia. *Behav Neurol*. 2013;26(1, 2):35-54.
- Toma AK, Holl E, Kitchen ND, Watkins LD. Evans' index revisited: the need for an alternative in normal pressure hydrocephalus. *Neurosurgery*. 2011;68(4):939-44.
- Traxler MJ, Morris RK, Seely RE. Processing subject and object relative clauses: Evidence from eye movements. *Journal of Memory and Language*. 2002;47(1):69-90.
- Traxler MJ, Williams RS, Blozis SA, Morris RK. Working memory, animacy, and verb class in the processing of relative clauses. *Journal of Memory and Language*. 2005;53(2):204-24.
- Ungerleider LG, Mishkin M. Two cortical visual systems. In: Ingle DJ, Mansfield RJW, MD G, editors. *Analysis of visual behavior*; 1982. p. 549-86.
- Van Petten C, Luka BJ. Prediction during language comprehension: Benefits, costs, and ERP components. *Int J Psychophysiol*. 2012;83(2):176-90.
- Van Wassenhove V, Grant KW, Poeppel D. Visual speech speeds up the neural processing of auditory speech. *Proc Natl Acad Sci U S A*. 2005;102(4):1181-6.
- Vanier M, Millat G. Niemann–Pick disease type C. *Clin Genet*. 2003;64(4):269-81.
- Vanier MT, Gissen P, Bauer P, Coll MJ, Burlina A, Hendriksz CJ, Latour P, Goizet C, Welford RW, Marquardt T, Kolb SA. Diagnostic tests for Niemann–Pick disease type C (NP-C): A critical review. *Mol Genet Metab*. 2016 Jun 7.
- Vanier MT, Rodriguez-Lafrasse C, Rousson R, Duthel S, Harzer K, Pentchev PG, Revol A, Louisot P. Type C Niemann-Pick disease: biochemical aspects and phenotypic heterogeneity. *Dev Neurosci*. 1991;13(4-5):307-14.
- Varley R, Cowell PE, Dyson L, Inglis L, Roper A, Whiteside SP. Self-Administered Computer Therapy for Apraxia of Speech. *Stroke*. 2016;47(3):822-8.
- Vercelletto M, Boutoleau-Bretonnière C, Volteau C, Puel M, Auriacombe S, Sarazin M, Michel B-F, Couratier P, Thomas-Antérion C, Verpillat P. Memantine in behavioral variant frontotemporal dementia: negative results. *J Alzheimers Dis*. 2011;23(4):749-59.
- Virhammar J, Laurell K, Cesarini KG, Larsson EM. The callosal angle measured on MRI as a predictor of outcome in idiopathic normal-pressure hydrocephalus. *J Neurosurg*. 2014 Jan;120(1):178-84.
- von Helmholtz H. *Helmholtz's treatise on physiological optics*: Optical Society of America; 1925.

Waldorff FB, Siersma V, Vogel A, Waldemar G. Subjective memory complaints in general practice predicts future dementia: a 4-year follow-up study. *Int J Geriatr Psychiatry*. 2012;27(11):1180-8.

Walker FO. Huntington's disease. *The Lancet*. 2007;369(9557):218-28.

Warrington EK. The selective impairment of semantic memory. *Q J Exp Psychol*. 1975;27(4):635-57.

Wells JB, Christiansen MH, Race DS, Acheson DJ, MacDonald MC. Experience and sentence processing: Statistical learning and relative clause comprehension. *Cogn Psychol*. 2009;58(2):250-71.

Whitfield-Gabrieli S, Nieto-Castanon A. Conn: a functional connectivity toolbox for correlated and anticorrelated brain networks. *Brain connectivity*. 2012;2(3):125-41.

Whitwell JL, Duffy JR, Strand EA, Machulda MM, Senjem ML, Gunter JL, Kantarci K, Eggers SD, Jack CR, Jr., Josephs KA. Neuroimaging comparison of primary progressive apraxia of speech and progressive supranuclear palsy. *Eur J Neurol*. 2013 Apr;20(4):629-37.

Williams DR, Holton JL, Strand C, Pittman A, de Silva R, Lees AJ, Revesz T. Pathological tau burden and distribution distinguishes progressive supranuclear palsy-parkinsonism from Richardson's syndrome. *Brain*. 2007;130(6):1566-76.

Wilson B, Smith K, Petkov CI. Mixed-complexity artificial grammar learning in humans and macaque monkeys: evaluating learning strategies. *Eur J Neurosci*. 2015 MAR 2015;41(5):568-78.

Wilson SM, DeMarco AT, Henry ML, Gesierich B, Babiak M, Miller BL, Gorno-Tempini ML. Variable disruption of a syntactic processing network in primary progressive aphasia. *Brain*. 2016 Aug 23.

Wilson SM, Dronkers NF, Ogar JM, Jang J, Growdon ME, Agosta F, Henry ML, Miller BL, Gorno-Tempini ML. Neural correlates of syntactic processing in the nonfluent variant of primary progressive aphasia. *J Neurosci*. 2010 Dec 15;30(50):16845-54.

Wilson SM, Galantucci S, Tartaglia MC, Rising K, Patterson DK, Henry ML, Ogar JM, DeLeon J, Miller BL, Gorno-Tempini ML. Syntactic processing depends on dorsal language tracts. *Neuron*. 2011 Oct 20;72(2):397-403.

Wolpe N, Ingram JN, Tsvetanov KA, Geerligs L, Kievit RA, Henson RN, Wolpert DM, Rowe JB. Ageing increases reliance on sensorimotor prediction through structural and functional differences in frontostriatal circuits. *Nat Commun*. 2016 Oct 03;7:13034.

Wolpe N, Moore JW, Rae CL, Rittman T, Altena E, Haggard P, Rowe JB. The medial frontal-prefrontal network for altered awareness and control of action in corticobasal syndrome. *Brain*. 2014 Jan;137(Pt 1):208-20.

Wong DL, Baker CM. Pain in children: comparison of assessment scales. *Okla Nurse*. 1988 Mar;33(1):8.

- Woodward M, Jacova C, Black SE, Kertesz A, Mackenzie IR, Feldman H. Differentiating the frontal variant of Alzheimer's disease. *Int J Geriatr Psychiatry*. 2010;25(7):732-8.
- Woollams AM, Ralph MAL, Plaut DC, Patterson K. SD-squared: on the association between semantic dementia and surface dyslexia. *Psychol Rev*. 2007;114(2):316.
- Worth PF. Sorting out ataxia in adults. *Pract Neurol*. 2004;4(3):130-51.
- Wynn ZJ, Cummings JL. Cholinesterase inhibitor therapies and neuropsychiatric manifestations of Alzheimer's disease. *Dement Geriatr Cogn Disord*. 2004;17(1-2):100-8.
- Xia C-F, Arteaga J, Chen G, Gangadharmath U, Gomez LF, Kasi D, Lam C, Liang Q, Liu C, Mocharla VP. [18 F] T807, a novel tau positron emission tomography imaging agent for Alzheimer's disease. *Alzheimer's & Dementia*. 2013;9(6):666-76.
- Xia C, Dickerson BC. Multimodal PET Imaging of Amyloid and Tau Pathology in Alzheimer Disease and Non-Alzheimer Disease Dementias. *PET clinics*. 2017;12(3):351-9.
- Ypma RJ, Bullmore ET. Statistical analysis of tract-tracing experiments demonstrates a dense, complex cortical network in the mouse. *PLoS Comput Biol*. 2016;12(9):e1005104.
- Zeman A, Butler C. Transient epileptic amnesia. *Curr Opin Neurol*. 2010;23(6):610-6.
- Zeman AZ, Boniface SJ, Hodges JR. Transient epileptic amnesia: a description of the clinical and neuropsychological features in 10 cases and a review of the literature. *J Neurol Neurosurg Psychiatry*. 1998;64(4):435-43.
- Zhou J, Gennatas ED, Kramer JH, Miller BL, Seeley WW. Predicting regional neurodegeneration from the healthy brain functional connectome. *Neuron*. 2012;73(6):1216-27.
- Zhou J, Seeley WW. Network dysfunction in Alzheimer's disease and frontotemporal dementia: implications for psychiatry. *Biol Psychiatry*. 2014;75(7):565-73.
- Zimmerer VC, Cowell PE, Varley RA. Artificial grammar learning in individuals with severe aphasia. *Neuropsychologia*. 2014a;53:25-38.
- Zimmerer VC, Dąbrowska E, Romanowski CA, Blank C, Varley RA. Preservation of passive constructions in a patient with primary progressive aphasia. *Cortex*. 2014b;50:7-18.
- Zimmerer VC, Varley RA. A case of "order insensitivity"? Natural and artificial language processing in a man with primary progressive aphasia. *Cortex*. 2015;69:212-9.

Appendix: Published work resulting from this thesis

At the time of binding, chapters 2, 3 and 4 have resulted in journal publications. These publications now follow in their final forms as appendices to this thesis.

Chapter 2 forms the basis of a paper that has been published in *Brain* (Cope et al., 2018).

Chapter 3 forms the basis of a paper that has been published in *Nature Communications* (Cope et al., 2017a).

Chapter 4 forms the basis of a paper that has been published in *Neuropsychologia* (Cope et al., 2017b).

Tau burden and the functional connectome in Alzheimer's disease and progressive supranuclear palsy

Thomas E. Cope,¹ Timothy Rittman,¹ Robin J. Borchert,¹ P. Simon Jones,¹ Deniz Vatansever,^{1,2,3,4} Kieren Allinson,⁵ Luca Passamonti,¹ Patricia Vazquez Rodriguez,¹ W. Richard Bevan-Jones,^{1,4} John T. O'Brien^{4,*} and James B. Rowe^{1,6,*}

*These authors contributed equally to this work.

Alzheimer's disease and progressive supranuclear palsy (PSP) represent neurodegenerative tauopathies with predominantly cortical versus subcortical disease burden. In Alzheimer's disease, neuropathology and atrophy preferentially affect 'hub' brain regions that are densely connected. It was unclear whether hubs are differentially affected by neurodegeneration because they are more likely to receive pathological proteins that propagate trans-neuronally, in a prion-like manner, or whether they are selectively vulnerable due to a lack of local trophic factors, higher metabolic demands, or differential gene expression. We assessed the relationship between tau burden and brain functional connectivity, by combining *in vivo* PET imaging using the ligand AV-1451, and graph theoretic measures of resting state functional MRI in 17 patients with Alzheimer's disease, 17 patients with PSP, and 12 controls. Strongly connected nodes displayed more tau pathology in Alzheimer's disease, independently of intrinsic connectivity network, validating the predictions of theories of trans-neuronal spread but not supporting a role for metabolic demands or deficient trophic support in tau accumulation. This was not a compensatory phenomenon, as the functional consequence of increasing tau burden in Alzheimer's disease was a progressive weakening of the connectivity of these same nodes, reducing weighted degree and local efficiency and resulting in weaker 'small-world' properties. Conversely, in PSP, unlike in Alzheimer's disease, those nodes that accrued pathological tau were those that displayed graph metric properties associated with increased metabolic demand and a lack of trophic support rather than strong functional connectivity. Together, these findings go some way towards explaining why Alzheimer's disease affects large scale connectivity networks throughout cortex while neuropathology in PSP is concentrated in a small number of subcortical structures. Further, we demonstrate that in PSP increasing tau burden in midbrain and deep nuclei was associated with strengthened cortico-cortical functional connectivity. Disrupted cortico-subcortical and cortico-brainstem interactions meant that information transfer took less direct paths, passing through a larger number of cortical nodes, reducing closeness centrality and eigenvector centrality in PSP, while increasing weighted degree, clustering, betweenness centrality and local efficiency. Our results have wide-ranging implications, from the validation of models of tau trafficking in humans to understanding the relationship between regional tau burden and brain functional reorganization.

1 Department of Clinical Neurosciences, University of Cambridge, Cambridge, UK

2 Department of Psychology, University of York, York, UK

3 Division of Anaesthesia, Department of Medicine, University of Cambridge, Cambridge, UK

4 Department of Psychiatry, University of Cambridge, Cambridge, UK

5 Department of Pathology, Cambridge University Hospitals NHS Foundation Trust, Cambridge, UK

6 Medical Research Council Cognition and Brain Sciences Unit, Cambridge, UK

Received July 24, 2017. Revised October 25, 2017. Accepted October 29, 2017. Advance Access publication January 5, 2018

© The Author(s) (2018). Published by Oxford University Press on behalf of the Guarantors of Brain.

This is an Open Access article distributed under the terms of the Creative Commons Attribution License (<http://creativecommons.org/licenses/by/4.0/>), which permits unrestricted reuse, distribution, and reproduction in any medium, provided the original work is properly cited.

Correspondence to: Dr Thomas E. Cope,
Herchel Smith Building, Department of Clinical Neurosciences, University of Cambridge, Cambridge, UK
E-mail: thomascope@gmail.com

Keywords: Alzheimer's disease; progressive supranuclear palsy; tau; functional connectivity; graph theory

Abbreviations: BP_{ND} = binding potential of PET ligand; MCI = mild cognitive impairment; PSP = progressive supranuclear palsy

Introduction

Alzheimer's disease and progressive supranuclear palsy (PSP) are both characterized by intracellular neurofibrillary lesions containing hyper-phosphorylated filamentous tau inclusions (Goedert and Spillantini, 2006). However, the diseases differ in: (i) the distribution of these tau inclusions; (ii) the balance of expression of tau isoforms; and (iii) the ultrastructure of tau filaments. Here, we test the impact of these differences in tau pathology on the reorganization of large-scale functional brain connectivity architecture.

Alzheimer's disease is characterized by widespread extracellular deposition of amyloid- β and paired helical filaments of tau with three (3R) and four (4R) repeats in the microtubule-binding domain (Sisodia *et al.*, 1990; Liu *et al.*, 2001). In Alzheimer's disease, these pathological proteins arise early in the transentorhinal cortex, from where they spread to limbic regions, followed by inferior frontal and parietal cortex (Braak and Braak, 1991, 1995). Although tau and amyloid- β have complex and synergistic effects (Nisbet *et al.*, 2015), there is converging evidence that tau mediates direct toxic effects on neurons and synaptic plasticity (Ballatore *et al.*, 2007; Roberson *et al.*, 2007; Ittner and Götz, 2011; Myeku *et al.*, 2016) and correlates with hypometabolism and symptomatology in Alzheimer's disease (Lehmann *et al.*, 2013; Ossenkoppele *et al.*, 2015, 2016). By contrast, pathological tau deposits in PSP are composed of straight filaments of predominantly 4R tau (Taniguchi-Watanabe *et al.*, 2016). This is most prominent in midbrain and deep brain nuclei early in the course of the Richardson's syndrome variant of PSP, spreading to cortical regions in advanced stages of the disease (Williams *et al.*, 2007).

To estimate the burden of tau pathology *in vivo*, PET ligands have been developed, including ^{18}F -AV-1451 (Chien *et al.*, 2013; Xia *et al.*, 2013; Ossenkoppele *et al.*, 2015, 2016). While there has been significant debate about the specificity of this ligand for tau, especially in the non-Alzheimer's dementias (Bevan-Jones *et al.*, 2017a; Xia and Dickerson, 2017), the distribution of ^{18}F -AV-1451 binding recapitulates Braak staging in Alzheimer's disease (Schwarz *et al.*, 2016) and correlates with post-mortem neuropathology in primary tauopathies (Smith *et al.*, 2016; Passamonti *et al.*, 2017). ^{18}F -AV-1451 binding has been shown to correlate with cognitive performance in Alzheimer's disease (Johnson *et al.*, 2016) and healthy older adults (Schöll *et al.*, 2016) more robustly than quantitative amyloid- β

imaging (Brier *et al.*, 2016). The ^{18}F -AV-1451 ligand also effectively distinguishes between Alzheimer's disease and PSP cases based on both the intensity and regional distribution of its binding potential (BP_{ND}) (Passamonti *et al.*, 2017).

In many neurodegenerative disorders, neuropathology and atrophy are most marked in those brain regions that are densely connected, both at the structural (Crossley *et al.*, 2014) and functional level (Dai *et al.*, 2014). In graph-theoretical terms, these densely connected regions are usually referred to as 'hubs' (Buckner *et al.*, 2009). There are a number of hypotheses as to why hubs are vulnerable to neurodegeneration. First, pathological proteins may propagate trans-neuronally, in a prion-like manner (Prusiner, 1984; Baker *et al.*, 1994; Goedert, 2015) such that highly connected regions are more likely to receive pathology from 'seed' regions affected in early stages of the disease (Zhou *et al.*, 2012), leading to neurodegeneration that mirrors structural and functional brain connectivity (Raj *et al.*, 2012, 2015; Abdelnour *et al.*, 2014). Alternatively, hubs might be selectively vulnerable to a given level of pathology, due to a lack of local trophic factors (Appel, 1981), higher metabolic demands (Saxena and Caroni, 2011; de Haan *et al.*, 2012), or differential gene expression (Rittman *et al.*, 2016).

These alternate hypotheses lead to different predictions about the relationship between tau burden and connectivity. The trans-neuronal spread hypothesis predicts that regions that are more strongly interconnected would accrue more tau pathology. This would manifest as higher tau burden in nodes with larger weighted degree, which is a measure of the number and strength of functional connections involving each node. In contrast, if hubs are vulnerable to tau accumulation because of increased metabolic demand this might manifest as a positive relationship between tau burden and participation coefficient, which is a measure of the proportion of a node's connections that are with other neural communities, and is the graph metric that is most closely correlated with metabolic activity (Chennu *et al.*, 2017). Finally, if trophic support is an important factor in tau accumulation, this might manifest as a negative relationship between tau burden and clustering coefficient; nodes with less tightly clustered connectivity patterns might have more vulnerable trophic supply.

Here we go beyond previous associative studies to examine, in the same subjects, the relationship between *in vivo* tau burden, as measured by the PET ligand ^{18}F -AV-1451

BP_{ND}, and functional connectivity, as summarized by graph theoretic measures based on resting state (task-free) functional MRI. We test the following linked hypotheses:

- (i) Brain regions that are normally more densely interconnected accrue more tau pathology.
- (ii) In Alzheimer's disease, where tau accumulation is predominantly cortical, the functional consequence is that affected nodes become more weakly connected and local efficiency of information transfer is reduced.
- (iii) In PSP-Richardson's syndrome, where neurodegeneration associated with tau accumulation is most severe in midbrain and basal ganglia, the functional consequence of disrupted cortico-subcortical and cortico-brainstem interactions (Gardner *et al.*, 2013) is that indirect cortico-cortical connections become stronger.

Materials and methods

Participants

All patients had mental capacity to take part in the study and provided informed consent. Study procedures were approved by the National Research Ethics Service. We recruited 17 patients with Alzheimer's disease, as evidenced by a either clinical diagnosis of probable Alzheimer's dementia according to consensus criteria ($n = 10$) (McKhann *et al.*, 2011), or a clinical diagnosis of mild cognitive impairment (MCI) and a positive amyloid PET scan ($n = 7$) (Klunk *et al.*, 2004; Okello *et al.*, 2009). Patients with MCI and evidence of amyloid- β were included to ensure the largest possible variability in tau burden within the Alzheimer's disease group. We also recruited 17 patients with PSP-Richardson's syndrome by 1996 criteria (Litvan *et al.*, 1996). Retrospective case review confirmed that all PSP subjects also met the revised 2017 criteria for PSP-RS (Höglinger *et al.*, 2017). Twelve age-matched controls were also examined. Participant demographics are given in Table 1 and detailed neuropsychological test results for each subject are shown in Supplementary Table 1.

Study procedures

This study formed part of the NIMROD (Neuroimaging of Inflammation in Memory and Related Other Disorders) project, for which the trial protocol containing general methods has been previously published (Bevan-Jones *et al.*, 2017b).

All participants underwent the Addenbrooke's Cognitive Examination-Revised (ACE-R), 11 min of resting state

functional MRI at 3 T, and ¹⁸F-AV-1451 PET imaging. Participants with PSP were also examined according to the PSP Rating Scale (Golbe and Ohman-Strickland, 2007). Those with a clinical diagnosis of MCI had ¹¹C-PiB PET imaging on a separate occasion—only those with increased uptake indicative of underlying Alzheimer's pathology are reported here.

MRI data acquisition and preprocessing

MRI was performed at the Wolfson Brain Imaging Centre, University of Cambridge, UK using a 3 T Siemens Magnetom Tim Trio scanner with a Siemens 32-channel phased-array head coil (Siemens Healthcare).

A T₁-weighted magnetization-prepared rapid gradient-echo (MPRAGE) image was acquired with repetition time = 2300 ms, echo time = 2.98 ms, matrix = 256 × 240, in-plane resolution of 1 × 1 mm, 176 slices of 1 mm thickness, inversion time = 900 ms and flip angle = 9°.

Eyes-closed resting state (task-free) multi-echo functional imaging was carried out for 11 min. A total of 269 EPI image volumes were acquired with repetition time = 2430 ms, echo times = 13.00, 30.55 and 48.10 ms, matrix = 64 × 64, in-plane resolution of 3.75 × 3.75 mm, 34 slices of 3.8 mm thickness with an interslice gap of 0.38 mm, GRAPPA parallel imaging with an acceleration factor of 2 and bandwidth = 2368 Hz/pixel. The first six volumes were discarded to eliminate saturation effects and achieve steady state magnetization. Preprocessing employed the ME-ICA pipeline (<https://wiki.cam.ac.uk/bmuwiki/MEICA>) (Kundu *et al.*, 2012, 2013), which uses independent component analysis to classify BOLD and non-BOLD signals based on the identification of linearly dependent and independent echo time dependent components. This provides an optimal approach to correct for movement-related and non-neuronal signals, and is therefore particularly well suited to our study, in which systematic differences in movement or head position might reasonably have been expected between patient groups. In fact, perhaps surprisingly, such differences were not observed (Supplementary Fig. 1)—between group ANOVAs demonstrated no significant differences between groups in terms of frame displacement before ($P = 0.88$) or after ($P = 0.42$) ME-ICA preprocessing, nor in terms of DVARS (Power *et al.*, 2012) before ($P = 0.89$) or after ($P = 0.67$) ME-ICA preprocessing. Note that both movement parameters were approximately an order of magnitude lower after ME-ICA preprocessing.

The MPRAGE images were processed into the standard space using DARTEL (Ashburner, 2007), producing a study-specific template in stereotactic space. Each functional MRI

Table 1 Participant demographics

Group	Number	Age, years	Years of education	MMSE	ACE-R	PSP-RS
Alzheimer's disease	17	71 (9)	14 (3)	25 (4)	72 (14)	-
PSP	17	69 (6)	12 (2)	27 (4)	83 (14)	41 (14)
Controls	12	67 (8)	16 (2)	29 (1)	96 (3)	-

Values are mean (SD). ACE-R = Addenbrooke's Cognitive Examination, Revised Edition; MMSE = Mini-Mental State Examination; PSP-RS = Progressive Supranuclear Palsy Rating Scale.

series mean image was co-registered to the corresponding MPRAGE image. The whole functional MRI series was warped to the template space using the DARTEL flow fields.

To perform a whole brain graph-theoretical analysis that included the brainstem, cerebellum and subcortical structures, the Harvard-Oxford Cortical atlas and Harvard-Oxford Subcortical atlas, each thresholded at 25%, were combined. Additionally, a Freesurfer 6 brainstem parcellation of the MNI152 (2009 asymmetric) brain together with remaining Ventral DC completed the whole brain labelling. This atlas was sub-parcellated into 598 regions of approximately equal volume [mean 1.995, standard deviation (SD) 0.323 ml] such that each sub-parcel could be uniquely identified with an atlas region. The MNI-space parcellation was matched to the group standard space using inverse deformations following application of the 'Population to ICBM Registration' SPM function to the group template, with nearest neighbour interpolation.

The blood oxygen level-dependent (BOLD) time series for each node was extracted using the CONN functional connectivity toolbox (Whitfield-Gabrieli and Nieto-Castanon, 2012). Between-node association matrices were generated, and then z-transformed for further analysis.

Functional connectivity assessment

Graph theoretical analysis was used to investigate the global and local characteristics of brain networks. These metrics were calculated in python using the Maybrain software (github.com/rittmann/maybrain) and networkx (version 1.11). Reported metrics were calculated in each subject at absolute network density thresholds of 1–10% in 1% increments using a minimum spanning tree to ensure complete connectivity of the graph (Alexander-Bloch *et al.*, 2010). Primary statistical analysis was performed at an intermediate density of 6%, with confirmatory analyses separately performed at all other densities. Weighted degree and participation coefficient were analysed in their raw forms, and all other metrics were dissociated from variation in degree by binarization after thresholding and normalization against 1000 random graphs with the same number of connections at each node.

The graph metrics assessed were:

- (i) Weighted degree: the number and strength of functional connections involving each node.
- (ii) Weighted participation coefficient: the proportion of a node's functional connectivity that involves other nodes that are not part of its own community structure, as defined by the Louvain community detection algorithm. Nodes with high degree and low participation coefficient are 'provincial hubs' (i.e. display strong connectivity only within their own community), while those with high participation coefficient are connector nodes (Joyce *et al.*, 2010).
- (iii) Betweenness centrality: the number of shortest paths between any other two nodes that pass through the node of interest. Nodes that are important for the transfer of information between other nodes have high betweenness centrality.
- (iv) Closeness centrality: the inverse of the path length between a node and all other nodes in the graph. This is the node-wise equivalent of global efficiency, which is the inverse sum of all the shortest path lengths in the graph.

- (v) Local efficiency: the number of strong connections a node has with its neighbouring nodes. This reflects the robustness of local networks to disruption.
- (vi) Eigenvector centrality: this measure quantifies the functional influence of a node on every other node in the graph, by weighting the importance of each nodal connection based on the influence of the nodes with which they connect.
- (vii) Clustering coefficient: the fraction of triangular connections formed by a node with other nodes. In other words, a node is strongly clustered if a large proportion of its neighbours are neighbours of each other.

Nodal connectivity strength was assessed for comparison to weighted degree, to ensure that our results did not result from bias introduced by proportionate thresholding. This metric is related to weighted degree, but includes information from all strengths of connection between every pair of nodes. As such, it is more subject to functional MRI signal-to-noise ratio limitations, and it is not a suitable metric for whole-brain, cross-sectional analysis across individuals, but it can be used to make a node-wise, group average assessment analogous to that for weighted degree.

Tau burden assessment

Other than the atlas used to define regions of interest, all AV-1451 and PiB data acquisition and preprocessing steps were identical to those reported by Passamonti *et al.* (2017). Ligand preparation was carried out at the Wolfson Brain Imaging Centre, University of Cambridge, with high radiochemical purity. ^{18}F -AV-1451 was produced with a specific activity of 216 ± 60 GBq/ μmol at the end of synthesis (60 min); ^{11}C -PiB specific activity was >150 GBq/ μmol . PET imaging was performed on a GE Advance PET scanner with a 15 min ^{68}Ge transmission scan used for attenuation correction acquiring 58 frames of increasing duration. PET scanning was performed in 3D mode (63 image planes; 15.2 cm axial field of view; 5.6 mm transaxial resolution and 2.4 mm slice interval) 80–100 min after a 9.0 to 11.0 mCi bolus injection in frames of 4×5 min. Each ^{11}C -PiB scan was acquired using a 8.5 to 15 mCi bolus injection immediately followed by a 60-min dynamic acquisition in 69 frames (12×15 s, 57×60 s). Scans were reconstructed on the GE Advance scanner using the PROMIS 3D filtered back projection algorithm, correcting for randoms, dead time, normalization, sensitivity and scatter attenuation.

The cerebellar grey matter was used as a reference tissue to express the distribution volume ratio (DVR) for the ^{11}C -PiB PET data for each MCI participant. PiB scans were classified as positive if the average SUVR values across the cortex were more than 1.5 times that of the cerebellar regions of interest. Seven MCI participants met this criterion and were included in the study.

The non-displaceable binding potential of ^{18}F -AV-1451 was assessed at each region of interest in the sub-parcellated atlas after rigid registration of each subject's dynamic PET image series to their T_1 -weighted MRI scan. This was normalized against the superior cerebellum, a reference region considered to have no tau pathology in either PSP or Alzheimer's disease (Williams *et al.*, 2007; Schöll *et al.*, 2016; Passamonti *et al.*, 2017). These data were corrected for white matter and CSF partial volumes by calculating the ordinary least squared

solution for the binding potential map voxel-wise in each region for grey plus white matter segments, each smoothed to PET resolution.

Statistical approach

A stereotyped statistical approach was taken to the analysis of graph metrics of theoretical interest. All statistical analyses were performed in MATLAB 2015b (The Mathworks Inc., 2015), with the exception of moderation analysis, which was performed in R (R Core Team, 2016).

A group-averaged analysis assessed the first hypothesis by examining the node-wise relationships between ^{18}F -AV-1451 binding potential and weighted degree, weighted participation coefficient, and clustering coefficient. These analyses were performed across the whole brain and within 10 intrinsic connectivity networks. To avoid circularity, where the regions of interest are defined by the test data, the intrinsic connectivity networks were independently derived from a publicly available dataset (Smith *et al.*, 2009). A binary mask was constructed for each resting state network by thresholding at $Z \geq 2.6$ ($P < 0.005$ uncorrected). Nodes were defined as belonging to a network if their centre of mass was within 5 mm of any positive voxel.

A between-subject analysis assessed the second and third hypotheses. This was undertaken at a variety of spatial scales. We first looked across the whole brain. For each individual, we first calculated a measure of disease-related tau burden. For participants with Alzheimer's disease, in whom tau deposition increases in both magnitude and distribution as disease progresses (Braak and Braak, 1995), tau burden was calculated as average ^{18}F -AV-1451 binding potential across the whole brain. In PSP tau deposition remains confined to brainstem and deep nuclei even in late disease (Williams *et al.*, 2007); tau burden was therefore calculated as average ^{18}F -AV-1451 binding potential across the left and right thalamus, caudate, putamen, pallidum, accumbens, ventral diencephalon, midbrain, pons and medulla. Both methods were separately assessed for controls. These measures of individual tau burden were then correlated with whole-brain averaged graph metrics to assess the relationship between the metric in question and disease burden in each group separately. Moderation analysis was performed for each metric to assess whether the relationships differed between Alzheimer's disease and PSP. It has recently been reported that patients with early onset Alzheimer's disease have a higher tau burden than those with later onset, especially in later Braak stage regions (Schöll *et al.*, 2017). Non-significant trend relationships between overall tau burden and age were observed in our cohort (Alzheimer's disease $r = -0.27$, PSP $r = -0.02$, Control $r = -0.38$; Supplementary Fig. 2). Cross-sectional analyses were therefore performed twice, with and without partialling out the effect of age on tau burden.

Regionality of the demonstrated effects was assessed within groups by correlating tau burden with the single subject graph metric values at each node; the gradient of the best fit linear regression within each group was the outcome measure. The nodal gradients in cerebellar regions were discarded (as this was the reference region for PET imaging), and the remaining regional maps were then collapsed into a vector. This was correlated with a matching vector of local tau burden at each node, calculated as the group-averaged increase in ^{18}F -AV-1451 binding potential. This resulted in a measure of

the relationship between the distribution of disease-related change in each graph metric and regional deposition of tau.

Results

Resting state connectivity differences exist between groups

As a prelude to the detailed analysis of network features, we first confirmed that our groups differed in their resting state connectivity, by testing for differences between the group averaged association matrices (Fig. 1, top). Jennrich tests confirmed highly significant statistical differences between controls and Alzheimer's disease ($\chi^2 = 1.15 \times 10^8$, $n_1 = 12$, $n_2 = 17$, $P < 0.0001$); controls and PSP ($\chi^2 = 975\,547$, $n_1 = 12$, $n_2 = 17$, $P < 0.0001$); and Alzheimer's disease and PSP ($\chi^2 = 733\,030$, $n_1 = 17$, $n_2 = 17$, $P < 0.0001$).

The nature of these differences would be opaque without abstraction techniques. Pairwise subtraction of the Fisher transformed association matrices (Fig. 1, bottom) revealed the presence of structure within the data, with both within-lobe and between-lobe group differences. While one can make general observations from these raw data, such as a prominent reduction in cerebello-cerebellar and brainstem-cerebellar connectivity in PSP, and a general reduction in between-region connectivity in Alzheimer's disease, the insights would be limited. Instead, graph theoretic measures allow one to examine which specific properties of the network underpin disease-related differences. For this approach each region in the brain becomes a node in a graph, which is functionally connected to all other nodes with a finite strength that is given by their pairwise correlation over time. Each individual's graph is then thresholded so that the highest 'x' percentage of connections survive. Effects are sought that are consistently present at a variety of network thresholds. Here we examine network thresholds from $1 < x < 10\%$, representing a range of graphs from sparse to dense. Very sparse graphs contain less information and can miss important relationships. Conversely, very dense graphs are more subject to noise and, when binarized, begin to provide less meaningful information. Therefore, in what follows, we present the primary statistical analyses at an intermediate density of 6%, with statistical detail given for this density. To assess the robustness of effects to different thresholding decisions we note separately the range of network densities exhibiting statistical significance.

Findings in Alzheimer's disease but not PSP are consistent with trans-neuronal spread of tau

We hypothesized that trans-neuronal spread of tau would manifest as a positive relationship between ^{18}F -AV-1451 and weighted degree. As we have parcellated the brain into nodes of equal size, weighted degree is a measure of the

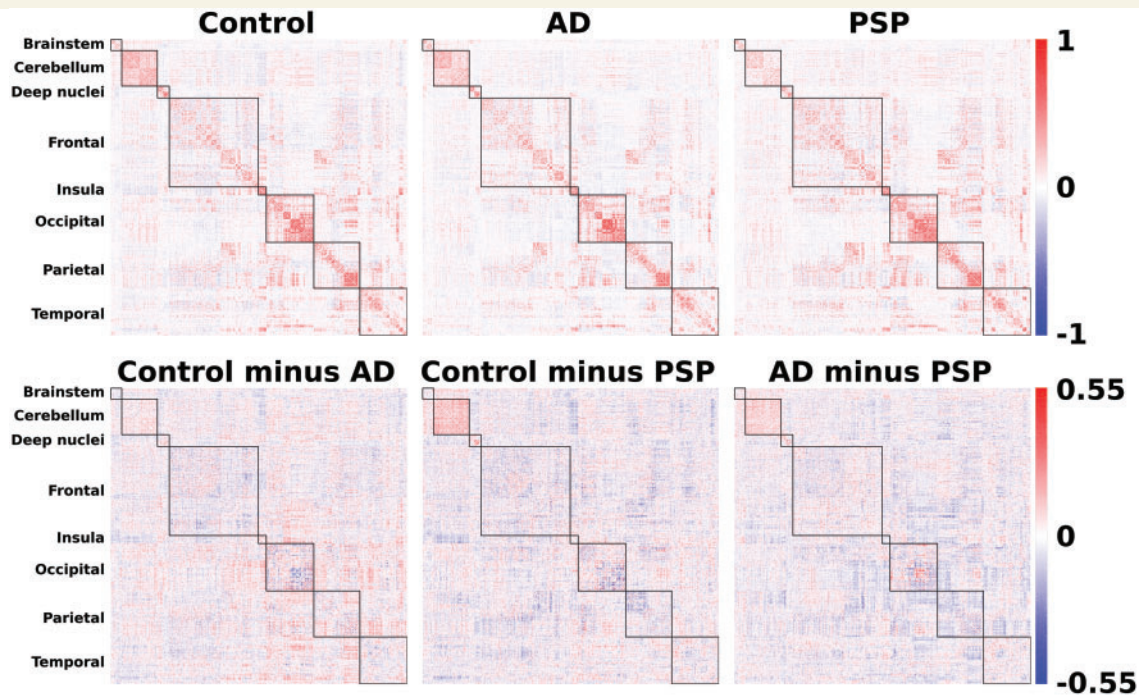


Figure 1 Connectivity matrices. *Top:* Association matrices derived from resting state (task-free) functional MRI. *Bottom:* Pairwise subtractions of the Fisher-z transformed association matrices to illustrate the large scale within and between-region disease-related changes in functional connectivity. AD = Alzheimer's disease.

volume of cortex to which a node is connected, and the strength of these connections. In Alzheimer's disease, a strong positive correlation was observed at all network thresholds, such that the most strongly connected nodes had higher $^{18}\text{F-AV-1451}$ BP_{ND} (Pearson's $r = 0.48$, $P < 0.0001$, Spearman's $\rho = 0.48$, $P < 0.0001$) (Fig. 2A). A consistent relationship was not present in PSP (Pearson's $r = -0.09$, Spearman's $\rho = 0.12$) (Fig. 2B) or controls (Pearson's $r = 0.03$, Spearman's $\rho = 0.11$) (Fig. 2C). These patterns were present at all examined network density thresholds.

It is important to acknowledge that the degree of a node as defined by correlated activity is impacted by the size of the connectivity network to which it belongs (Power *et al.*, 2013). Therefore, one concern might be that correlations between $^{18}\text{F-AV-1451}$ and degree are driven by the coincidence that Alzheimer's disease happens to affect the default mode network (DMN), which happens to be a large intrinsic connectivity network. To exclude this possibility, we undertook two additional analyses. First, we re-examined $^{18}\text{F-AV-1451}$ and degree when nodes belonging to the DMN were excluded; this did not abolish the strong relationship (Pearson's $r = 0.43$, $P < 0.0001$). Second, we examined the relationship within each intrinsic connectivity network (Fig. 3). A strong positive relationship between $^{18}\text{F-AV-1451}$ and degree was seen in 9 of 10 networks examined (Pearson's $r \geq 0.4$, $P < 0.0001$). In contrast, no

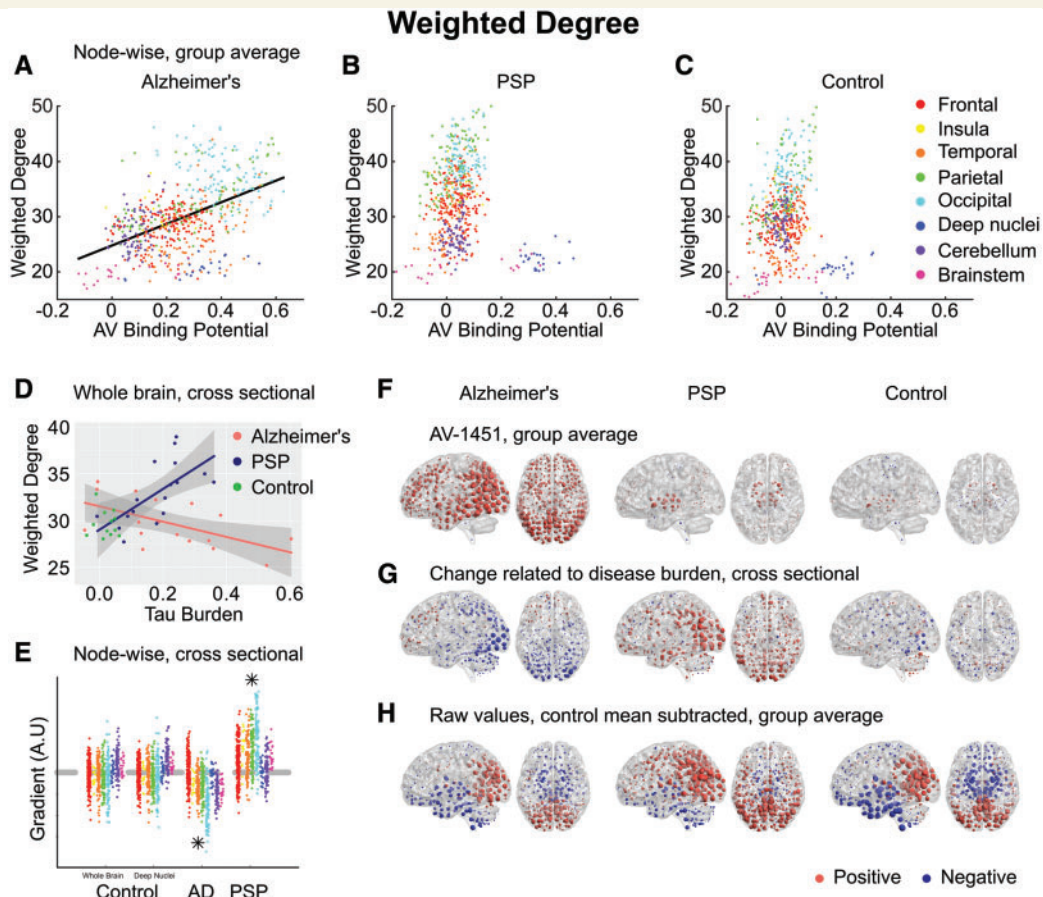
strong positive correlations were observed in any network in PSP (Supplementary Fig. 3).

Finally, in each group we examined the relationship between each node's unthresholded connectivity strength and $^{18}\text{F-AV-1451}$ BP_{ND} (Supplementary Fig. 4). This is a local measure of the strength of functional connectivity that does not rely on thresholding the graph and therefore takes into account both strong and weak connections. The pattern of results observed in weighted degree was replicated; in Alzheimer's disease, a positive correlation was observed ($r = 0.28$, $P < 0.0001$), but no significant relationship was observed in PSP ($r = -0.05$, $P = 0.22$) or controls ($r = 0.04$, $P = 0.31$).

Findings in PSP but not Alzheimer's disease are consistent with selective vulnerability

We hypothesized that tau accumulation due to metabolic demand would manifest as a positive relationship between $^{18}\text{F-AV-1451}$ and weighted participation coefficient. This was not observed in Alzheimer's disease; in fact there was a weak negative correlation (Pearson's $r = -0.18$) (Fig. 4A).

In PSP, however, those nodes that displayed elevated $^{18}\text{F-AV-1451}$ were those that had the highest participation coefficient (Fig. 4B).



Similarly, we hypothesized that tau accumulation due to a lack of trophic support would manifest as a negative relationship between ^{18}F -AV-1451 and clustering coefficient. In Alzheimer's disease, the opposite relationship was observed; strongly clustered nodes were more likely to display elevated ^{18}F -AV-1451 binding (Pearson's $r = 0.33$) (Fig. 5A).

Again, by contrast, in PSP those nodes that displayed elevated ^{18}F -AV-1451 were those that had the lowest clustering coefficient (Fig. 5B).

Alzheimer's disease and PSP have opposite effects on the strength of cortical functional connectivity

We assessed the impact of the presence of tau on connection strength at a variety of spatial scales. First, we averaged weighted degree across the whole brain, resulting in a single measure for each individual. As the overall number of connections in each individual's graph was thresholded

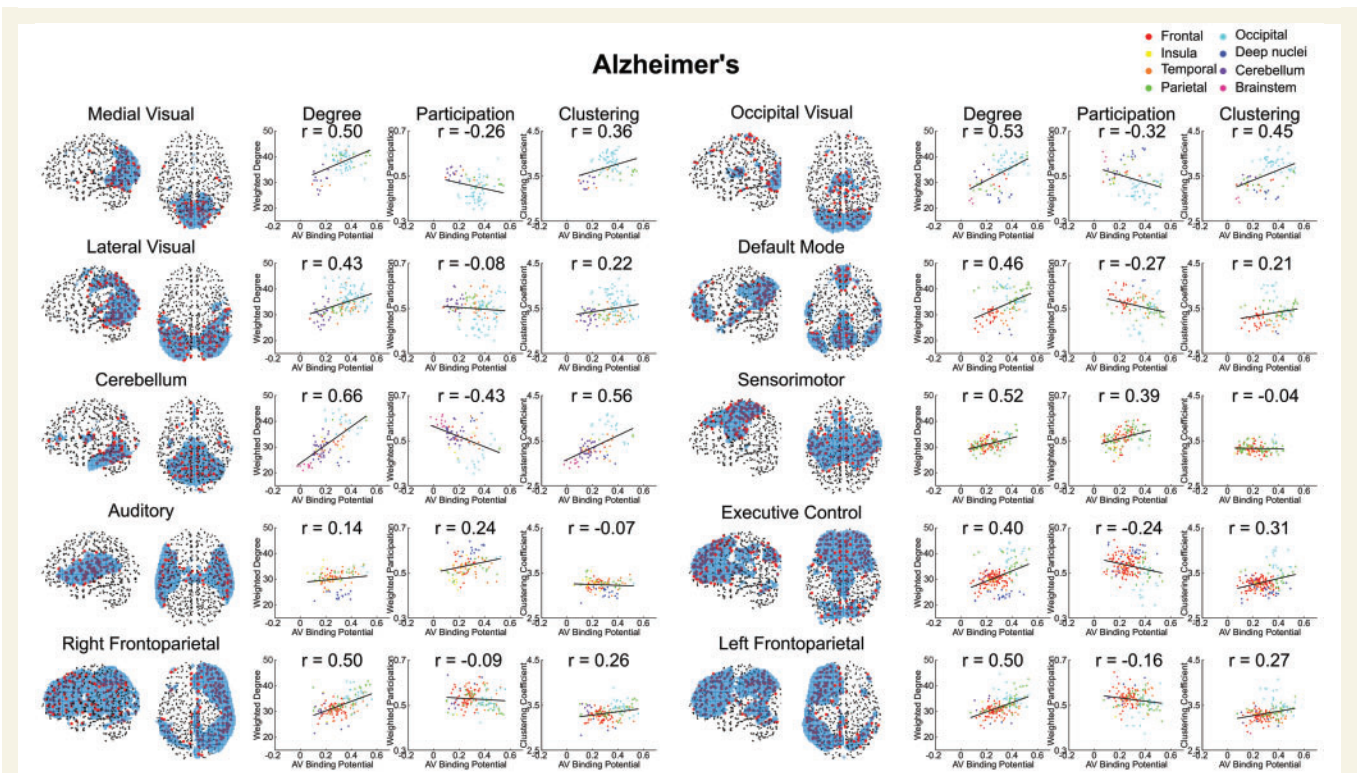


Figure 3 Alzheimer's disease comparison of the three graph metrics representing the three principal hypotheses of hub vulnerability. Broken down by intrinsic connectivity network defined from Smith *et al.* (2009). The group-averaged graph metric at each node within a network is plotted against $^{18}\text{F-AV-1451}$ binding potential at that node. The Pearson correlation coefficient is noted in each case. Only weighted degree demonstrated a consistent relationship across all networks in keeping with its related hypothesis.

at an identical network density, this measure represented the average strength of the strongest $x\%$ of connections. To assess global disease burden in Alzheimer's disease we averaged $^{18}\text{F-AV-1451}$ BP_{ND} across the whole brain. In PSP, we averaged $^{18}\text{F-AV-1451}$ BP_{ND} across midbrain and basal ganglia, reflecting the more focal distribution of disease and our hypotheses about dissociated functional effects of cortical and subcortical tau (Passamonti *et al.*, 2017). Confirmatory tests demonstrated that the pattern of the moderation analyses below were unchanged if whole-brain average $^{18}\text{F-AV-1451}$ BP_{ND} was used to assess tau burden in PSP. Both methods of assessing tau burden were independently assessed in the control group, with no significant effects demonstrated in either case.

In Alzheimer's disease, we found a negative correlation between average connection strength and tau burden (Pearson's $r = -0.58$, $P = 0.015$) (Fig. 2D). In PSP this relationship was reversed, with average connection strength increasing in line with tau burden ($r = 0.65$, $P = 0.004$). No relationship was observed in controls ($r = -0.10$, $P = 0.75$). Moderation analysis confirmed a dissociated relationship between tau and connection strength in Alzheimer's disease and PSP at all network densities [$\Delta r^2 = 0.29$, $F(1,30) = 19.0$, $P = 0.0001$; after partialling out age (Supplementary Fig. 5A) $\Delta r^2 = 0.28$, $F(1,30) = 17.9$, $P = 0.0002$]. Therefore, while in Alzheimer's disease the presence of tau pathology causes the strongest functional

connections to weaken, in PSP, the presence of tau had the opposite effect, i.e. to strengthen functional connections.

Second, we assessed the distribution of change by repeating the correlation of disease burden against weighted degree at every individual node. We hypothesized that this effect would be greatest in those regions that display the strongest functional connectivity in the healthy brain, and which we have demonstrated to accrue most tau in Alzheimer's disease. The gradient of this nodewise relationship reflects a measure of local change in weighted degree with disease burden (Fig. 2E). First, we examined whether the whole-brain average relationship could be replicated in these individual gradients, by performing sign tests. For Alzheimer's disease, a negative relationship was confirmed ($Z = -13.0$, $P < 0.0001$); for PSP there was a positive relationship ($Z = 14.8$, $P < 0.0001$); while for controls no relationship was demonstrated using either whole brain ($Z = -1.1$, $P = 0.27$) or deep brain ($Z = 1.1$, $P = 0.27$) tau burden.

Next, we assessed whether the functional connectivity change at each node related to local tau burden, by correlating the gradient of the disease-related change in weighted degree with the disease-associated increase in $^{18}\text{F-AV-1451}$ binding potential at each node (i.e. correlating each column of Fig. 2F with the corresponding column of Fig. 2G). A negative correlation between these measures was demonstrated in Alzheimer's disease (Pearson's $r = -0.30$,

$P < 0.0001$, Spearman's $\rho = -0.24$, $P < 0.0001$). This relationship was absent in PSP (Pearson's $r = -0.07$, $P = 0.11$, Spearman's $\rho = -0.00$, $P = 0.98$) and in controls (Pearson's $r = -0.01$, $P = 0.75$, Spearman's $\rho = -0.01$, $P = 0.80$). As well as being present at all examined network densities, the negative correlation between disease-related change in functional connectivity strength and tau burden in Alzheimer's disease was replicated in nodal connectivity strength, the equivalent unthresholded measure ($r = -0.34$, $P < 0.0001$, Supplementary Fig. 4B).

Finally, we assessed whether the functional connectivity change at each node related to the strength of its connections in the healthy control brain (i.e. correlating each patient panel of Fig. 2G with the control panel in Fig. 2H). As would be expected from the propensity of highly connected nodes to accrue tau, a negative relationship was demonstrated in Alzheimer's disease (Pearson's $r = -0.23$, $P < 0.0001$, Spearman's $\rho = -0.24$, $P < 0.0001$). Importantly, however, this relationship explained less variance than AV binding, with which we have demonstrated it to be correlated. In PSP, a positive relationship was demonstrated (Pearson's $r = 0.27$, $P < 0.0001$, Spearman's $\rho = 0.26$, $P < 0.0001$).

In summary, nodes that are constitutionally more strongly connected to a larger volume of cortex are more likely to accrue tau pathology in Alzheimer's disease but not PSP. This relationship is independent of the connectivity network to which a node belongs. Once present, the tau pathology appears to cause local functional connectivity strength to fall. By contrast, in PSP tau selectively accumulates in midbrain and deep nuclei, which has the consequence of increasing the strength of cortico-cortical functional connectivity, especially in those nodes that are constitutionally highly connected.

Reorganization of cortical functional connectivity reflects cortical versus subcortical pathology

We hypothesized that the presence of subcortical pathology in PSP might be causing an increase in weighted degree by necessitating an increase in the relative strength of short-range cortico-cortical connections as longer range connections are disrupted. This view is supported by the observation that a consequence of increasing tau burden in PSP is a marked reduction in participation coefficient (Fig. 4D). This relationship was not observed in Alzheimer's disease, where increasing tau burden caused increasing participation. Moderation analysis confirmed this differential relationship at all network densities from 1% to 10% [$\Delta r^2 = 0.21$, $F(1,30) = 7.6$, $P = 0.002$; after partialling out age (Supplementary Fig. 5B) $\Delta r^2 = 0.17$, $F(1,30) = 8.3$, $P = 0.007$].

We further examined this hypothesis by examining the effect of tau on other measures of graph structure in each individual, dissociated from variation in degree by

binarization after thresholding and normalization against 1000 random graphs with the same number of connections at each node.

The clustering coefficient quantifies how many of a node's neighbours are neighbours of each other. All individuals in all groups displayed clustering to at least $2.8\times$ that of random graphs of the same degree (Fig. 5D), consistent with a small-world connectivity distribution. While in Alzheimer's disease a non-significant trend was observed towards reduced clustering with increasing tau burden, in line with previous reports (Stam *et al.*, 2006; Sanz-Arigita *et al.*, 2010), in PSP the opposite relationship were observed. Moderation analysis trended towards significance at the density of primary interest [$\Delta r^2 = 0.08$, $F(1,30) = 3.8$, $P = 0.06$; after partialling out age (Supplementary Fig. 5C) $\Delta r^2 = 0.07$, $F(1,30) = 2.5$, $P = 0.09$], and was significant from 7% to 10% density. The betweenness centrality of a node is a measure of the number of shortest paths between any other two nodes that pass through it. If the presence of subcortical pathology in PSP means that long-range information transfer must occur through a transcortical route, average betweenness centrality should increase. Conversely, predominantly cortical pathology in Alzheimer's disease might increase reliance on cortico-subcortical connections, reducing average betweenness centrality. This prediction was verified (Supplementary Fig. 6A), with a differential relationship between tau burden and betweenness centrality confirmed by moderation analysis at all network densities from 1–10% [$\Delta r^2 = 0.21$, $F(1,30) = 9.3$, $P = 0.005$; after partialling out age (Supplementary Fig. 5D) $\Delta r^2 = 0.20$, $F(1,30) = 8.9$, $P = 0.006$].

Long-range information transfer by a cortico-cortical route implies an inefficient, indirect process, perhaps accounting for the cognitive slowing characteristic of neurodegenerative disorders with predominant subcortical pathology. We tested for this by examining closeness centrality, which is the inverse of the path length between a node and all other nodes in the graph. As would be predicted by this account, increasing disease burden resulted in a higher average path length (lower closeness centrality) in PSP but a lower average path length in Alzheimer's disease (higher closeness centrality) at network densities from 2% to 10% [Fig. 6A, moderation $\Delta r^2 = 0.20$, $F(1,30) = 9.1$, $P = 0.005$; after partialling out age (Supplementary Fig. 5E) $\Delta r^2 = 0.16$, $F(1,30) = 8.0$, $P = 0.008$]. Averaged across the whole brain, this measure is equivalent to the global efficiency of the graph, and indeed the same statistical results were obtained from a moderation analysis of that metric; increasing disease burden resulted in reduced global efficiency in PSP.

While tau-mediated reorganization of connectivity in PSP results in slower and less efficient long-range information transfer, in Alzheimer's disease one might suppose it to be a beneficial consequence of the loss of overall connection strength as those connections that remain are more globally efficient. However, we hypothesized this would be at the cost of local efficiency, which is a measure of the number of

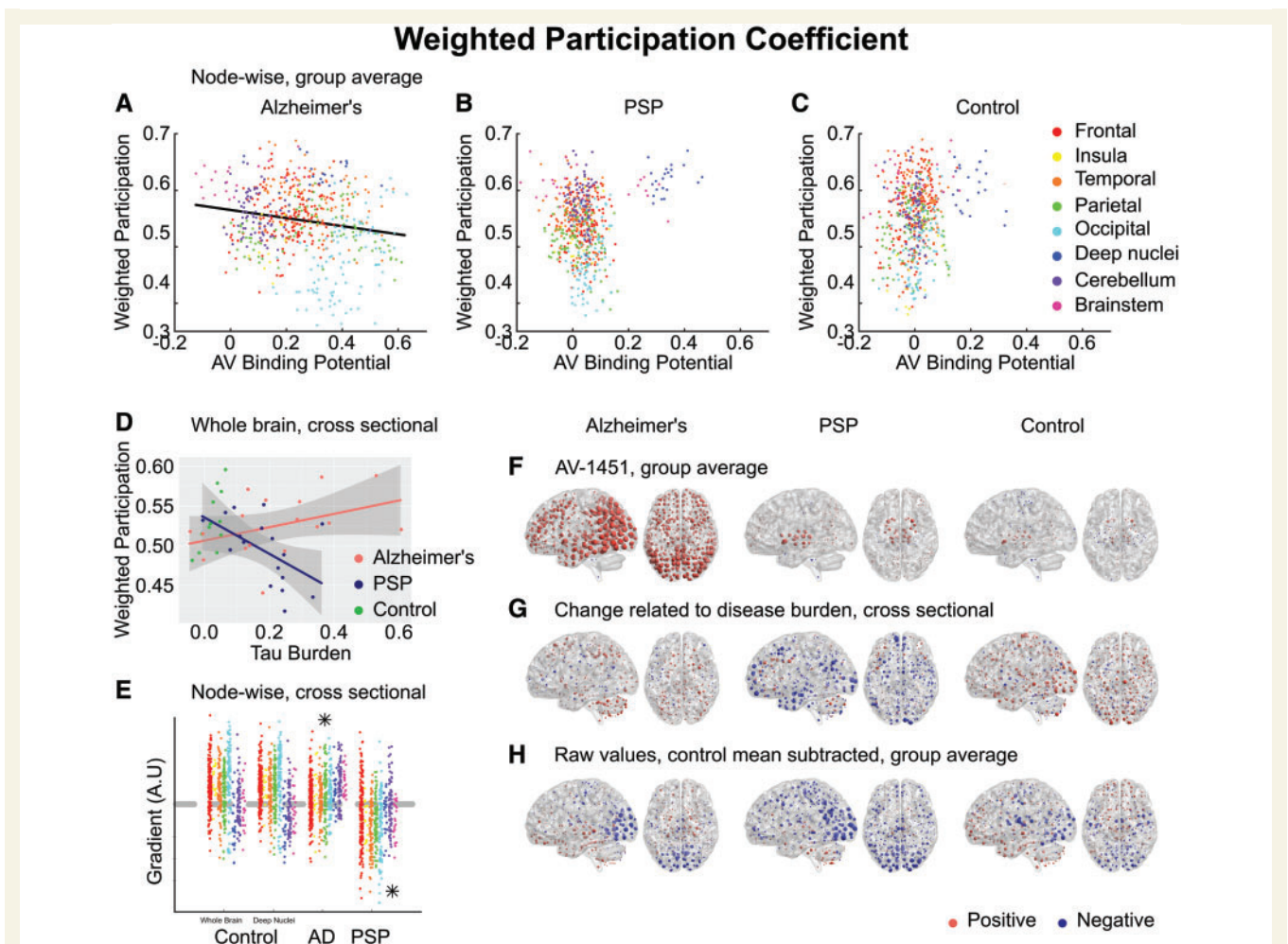


Figure 4 Weighted participation coefficient. (A–C) Group-averaged weighted participation coefficient at each node, plotted against ^{18}F -AV-1451 binding potential at that node. A negative relationship was observed in Alzheimer's disease (AD), in violation of the metabolic demand hypothesis. (D) Between-subjects analysis of the relationship between global tau burden and participation coefficient at a network density of 6%. No significant relationship was found for the control subjects with either method of assessing tau burden. Moderation analysis for a differential relationship between graph metric and tau burden in the two disease groups (Alzheimer's disease and PSP) was statistically significant. (E) The magnitude of disease related change at each node is plotted as a single point, grouped by lobe. Control data are shown for both methods of assessing tau burden. Stars represent statistically significant excesses of positive or negative gradients in the disease groups. (F) Average ^{18}F -AV-1451 binding potential at each node. Red spheres represent increases compared to the cerebellar reference region. Blue spheres represent decreases. The centre of the sphere is placed at the centre of the region of interest. The radius of each sphere is linearly related to the magnitude of binding at that node. All groups are scaled identically. (G) The local tau burden-related change in participation coefficient is plotted for each group at each node. Red spheres represent local increases as a result of greater overall tau burden; blue spheres represent local decreases. The radius of each sphere is linearly related to the magnitude of disease-related change at that node across the whole range of disease burden observed in each group. All groups are scaled identically. Control images are based on the whole-brain method of assessing tau burden. (H) Average raw values for participation coefficient within each group. The control mean for each metric is subtracted at every node. Red spheres represent increases compared to the control mean value. Blue spheres represent decreases. The centre of the sphere is placed at the centre of the region of interest. The radius of each sphere is linearly related to the difference from the control mean at that node. All groups are scaled identically.

strong connections between neighbouring nodes and the robustness of local networks to disruption. Indeed this was found to be the case at network densities from 4% to 10% [Fig. 7A, $\Delta r^2 = 0.15$, $F(1,30) = 6.5$, moderation $P = 0.016$; after partialling out age (Supplementary Fig. 5F) $\Delta r^2 = 0.12$, $F(1,30) = 5.5$, $P = 0.026$].

Finally, we assessed the functional influence of each node on the other nodes in the network by examining the

eigenvector centrality. Again, an opposite effect of disease burden was observed in Alzheimer's disease and PSP at network densities from 3–10% [Supplementary Fig. 7A, $\Delta r^2 = 0.22$, $F(1,30) = 8.5$, $P = 0.007$; after partialling out age (Supplementary Fig. 5G) $\Delta r^2 = 0.20$, $F(1,30) = 8.3$, $P = 0.007$] such that, on average, as PSP progressed each node had less functional influence on every other node in the graph.

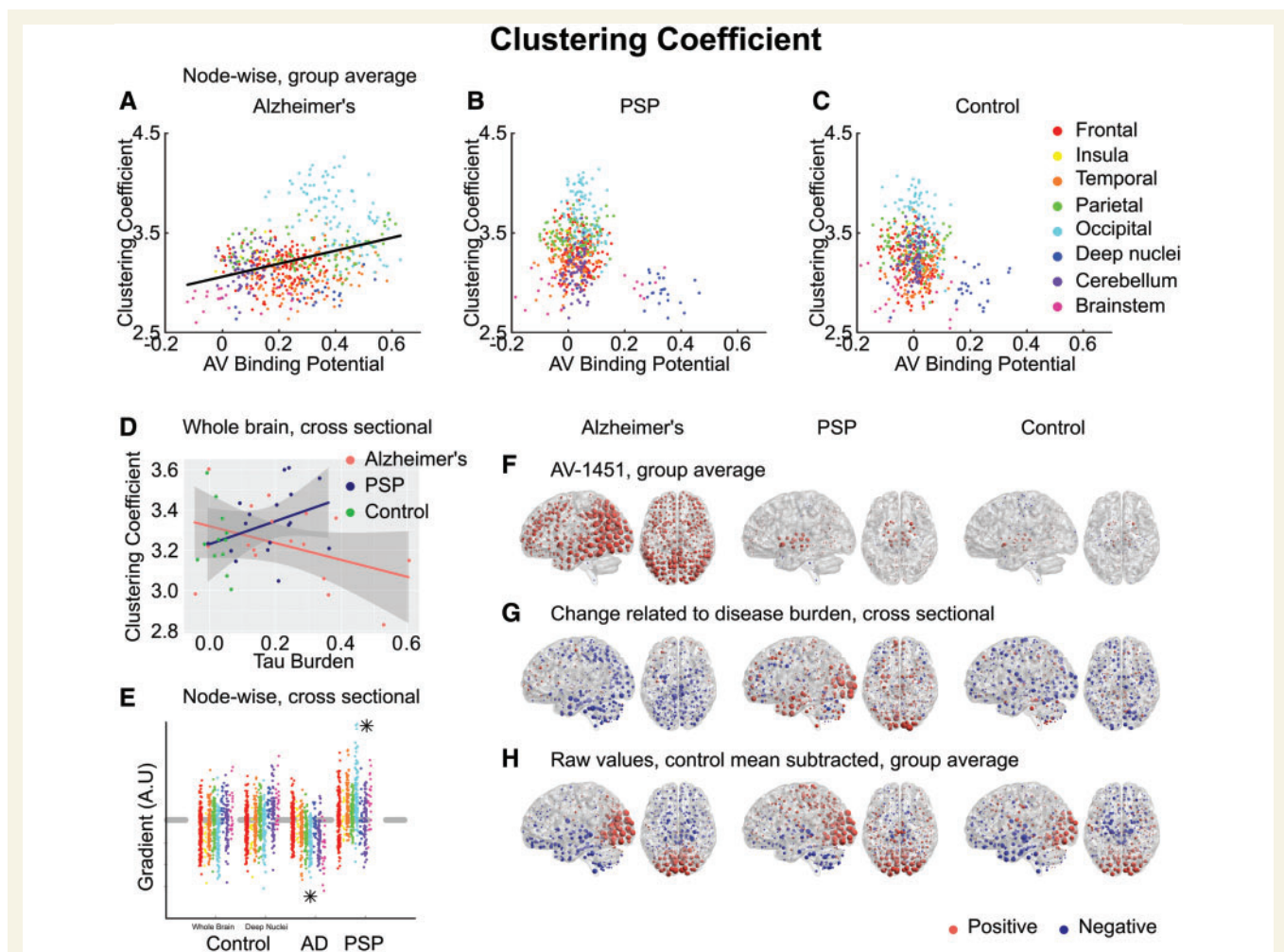


Figure 5 Clustering coefficient. (A–C) Group-averaged clustering coefficient at each node, plotted against ^{18}F -AV-1451 binding potential at that node. A positive relationship was observed in Alzheimer's disease (AD), in violation of the trophic support hypothesis. (D) Between-subjects analysis of the relationship between global tau burden and clustering coefficient at a network density of 6%. No significant relationship was found for the control subjects with either method of assessing tau burden. Moderation analysis for a differential relationship between graph metric and tau burden in the two disease groups (Alzheimer's disease and PSP) was statistically significant. (E) The magnitude of disease related change at each node is plotted as a single point, grouped by lobe. Control data are shown for both methods of assessing tau burden. Stars represent statistically significant excesses of positive or negative gradients in the disease groups. (F) Average ^{18}F -AV-1451 binding potential at each node. Red spheres represent increases compared to the cerebellar reference region. Blue spheres represent decreases. The centre of the sphere is placed at the centre of the region of interest. The radius of each sphere is linearly related to the magnitude of binding at that node. All groups are scaled identically. (G) The local tau burden-related change in clustering coefficient is plotted for each group at each node. Red spheres represent local increases as a result of greater overall tau burden; blue spheres represent local decreases. The radius of each sphere is linearly related to the magnitude of disease-related change at that node across the whole range of disease burden observed in each group. All groups are scaled identically. Control images are based on the whole-brain method of assessing tau burden. (H) Average raw values for clustering coefficient within each group. The control mean for each metric is subtracted at every node. Red spheres represent increases compared to the control mean value. Blue spheres represent decreases. The centre of the sphere is placed at the centre of the region of interest. The radius of each sphere is linearly related to the difference from the control mean at that node. All groups are scaled identically.

Local functional connectivity reorganization is related to tau in Alzheimer's disease

To understand the differential reorganization of functional connectivity in Alzheimer's disease and PSP, we replicated the approach taken for weighted degree; correlating the

gradient of the disease-related change at every individual node with local change in ^{18}F -AV-1451 binding potential. For all metrics, the differential group effects demonstrated by moderation analysis could be replicated by statistical significance of opposite directionality in sign tests performed on the individual gradients at each node (Supplementary Table 2, Figs 4E, 5E, 6B, 7B and

Supplementary Figs 6B and 7B). In all cases, controls showed either no relationship or a weaker effect in the same direction as patients with Alzheimer's disease.

The reorganization of graph metrics followed two distinct patterns. Closeness centrality (Fig. 6D) displayed a global effect, with most nodes increasing in Alzheimer's disease and decreasing in PSP. This was not strongly related to local ^{18}F -AV-1451 binding potential in Alzheimer's disease (Pearson's $r = 0.05$, $P = 0.25$, Spearman's $\rho = 0.06$, $P = 0.18$) or PSP (Pearson's $r = 0.08$, $P = 0.06$, Spearman's $\rho = 0.11$, $P = 0.01$). Similarly, participation coefficient displayed global changes in both diseases (Fig. 4G) (Alzheimer's disease Pearson's $r = 0.09$, Spearman's $\rho = 0.07$, PSP Pearson's $r = 0.08$, Spearman's $\rho = 0.06$).

By contrast, eigenvector centrality (Supplementary Fig. 7D) was more strongly related to local ^{18}F -AV-1451 binding potential in Alzheimer's disease (Pearson's $r = -0.28$, $P < 0.0001$, Spearman's $\rho = -0.25$, $P < 0.0001$). Strikingly, the positive relationship we demonstrated across the whole brain masked opposing regional effects. As global

tau burden increased, the functional influence of frontal regions on all other regions increased, while that of occipital regions decreased. In PSP, no consistent relationship with ^{18}F -AV-1451 was observed (Pearson's $r = -0.10$, $P = 0.02$, Spearman's $\rho = -0.04$, $P = 0.38$), with almost all regions having less functional influence on all other regions as tau burden increased.

Clustering coefficient (Fig. 5G), local efficiency (Fig. 7D) and betweenness centrality (Supplementary Fig. 6D) displayed an intermediate degree of regional specificity, being weakly but significantly correlated with change in ^{18}F -AV-1451 binding potential in Alzheimer's disease (clustering coefficient Pearson's $r = -0.12$, $P < 0.0001$, Spearman's $\rho = -0.14$, $P < 0.0001$, local efficiency Pearson's $r = -0.16$, $P < 0.0001$, Spearman's $\rho = -0.19$, $P < 0.0001$, betweenness centrality Pearson's $r = 0.19$, $P < 0.0001$, Spearman's $\rho = 0.19$, $P < 0.0001$) and PSP (clustering coefficient Pearson's $r = -0.14$, $P < 0.0001$, Spearman's $\rho = -0.12$, $P < 0.0001$, local efficiency Pearson's $r = -0.14$, $P = 0.001$, Spearman's $\rho = -0.11$,

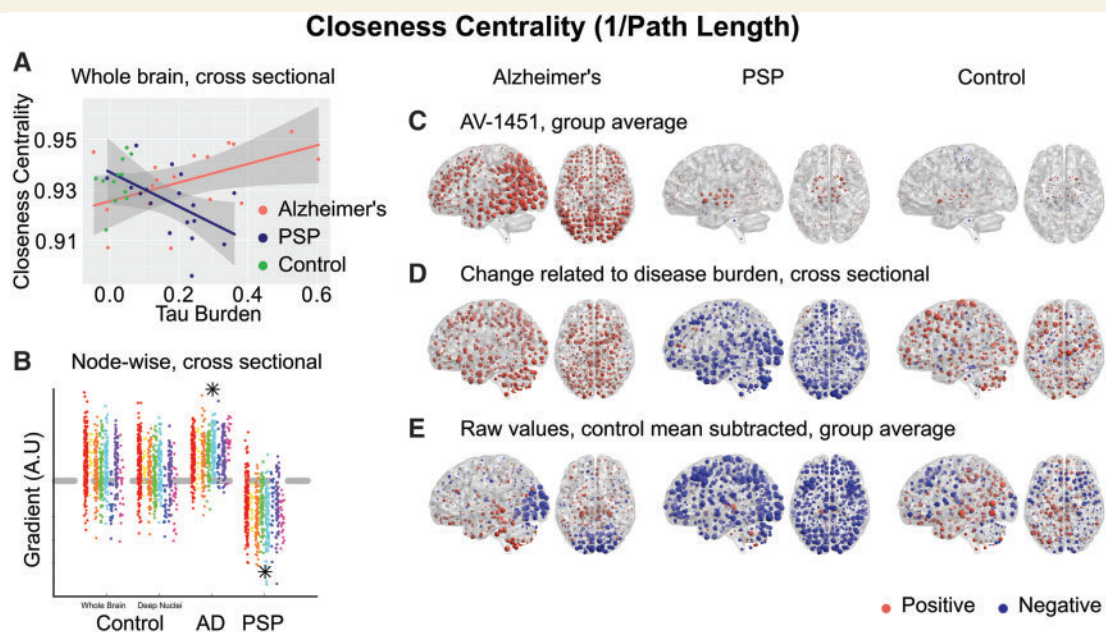


Figure 6 Closeness centrality (1/path length from each node to all other nodes). **(A)** Between-subjects analysis of the relationship between global tau burden and closeness centrality at a network density of 6%. No significant relationship was found for the control subjects with either method of assessing tau burden. Moderation analysis for a differential relationship between graph metric and tau burden in the two disease groups [Alzheimer's disease (AD) and PSP] was statistically significant. **(B)** The magnitude of disease related change at each node is plotted as a single point, grouped by lobe. Control data are shown for both methods of assessing tau burden. Stars represent statistically significant excesses of positive or negative gradients in the disease groups (Supplementary Table 2). **(C)** Average ^{18}F -AV-1451 binding potential at each node. Red spheres represent increases compared to the cerebellar reference region. Blue spheres represent decreases. The centre of the sphere is placed at the centre of the region of interest. The radius of each sphere is linearly related to the magnitude of binding at that node. All groups are scaled identically. **(D)** The local tau burden-related change in closeness centrality is plotted for each group at each node. Red spheres represent local increases as a result of greater overall tau burden; blue spheres represent local decreases. The radius of each sphere is linearly related to the magnitude of disease-related change at that node across the whole range of disease burden observed in each group. All groups are scaled identically. Control images are based on the whole-brain method of assessing tau burden. **(E)** Average raw values for closeness centrality within each group. The control mean for each metric is subtracted at every node. Red spheres represent increases compared to the control mean value. Blue spheres represent decreases. The centre of the sphere is placed at the centre of the region of interest. The radius of each sphere is linearly related to the difference from the control mean at that node. All groups are scaled identically.

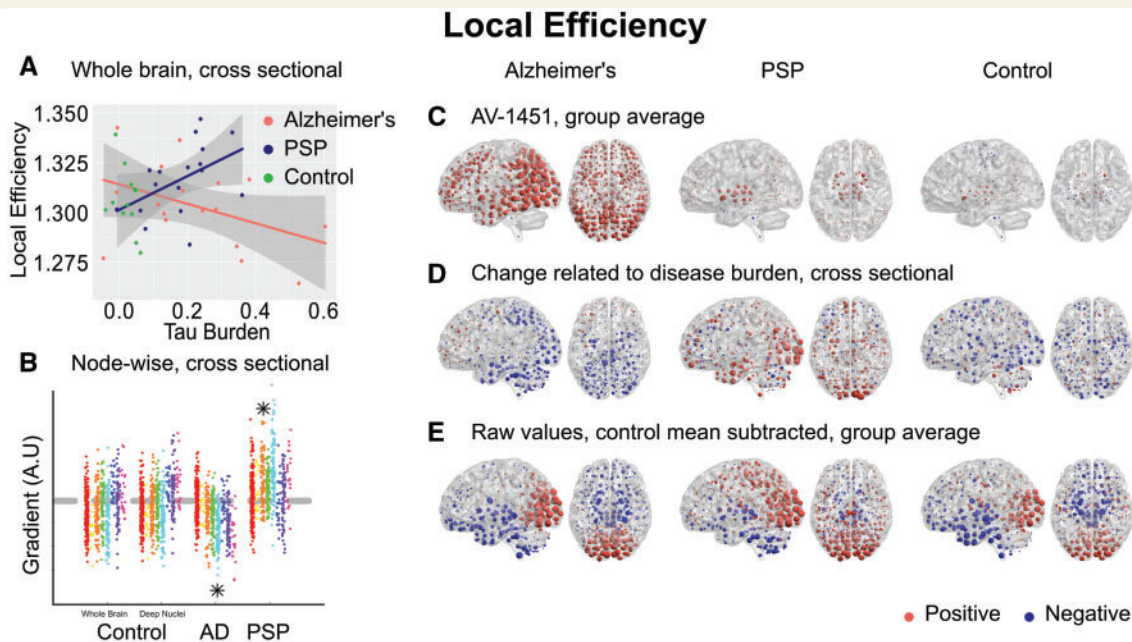


Figure 7 Local efficiency. (A) Between-subjects analysis of the relationship between global tau burden and local efficiency at a network density of 6%. No significant relationship was found for the control subjects with either method of assessing tau burden. Moderation analysis for a differential relationship between graph metric and tau burden in the two disease groups [Alzheimer's disease (AD) and PSP] was statistically significant. (B) The magnitude of disease related change at each node is plotted as a single point, grouped by lobe. Control data are shown for both methods of assessing tau burden. Stars represent statistically significant excesses of positive or negative gradients in the disease groups (Supplementary Table 2). (C) Average ^{18}F -AV-1451 binding potential at each node. Red spheres represent increases compared to the cerebellar reference region. Blue spheres represent decreases. The centre of the sphere is placed at the centre of the region of interest. The radius of each sphere is linearly related to the magnitude of binding at that node. All groups are scaled identically. (D) The local tau burden-related change in local efficiency is plotted for each group at each node. Red spheres represent local increases as a result of greater overall tau burden; blue spheres represent local decreases. The radius of each sphere is linearly related to the magnitude of disease-related change at that node across the whole range of disease burden observed in each group. All groups are scaled identically. Control images are based on the whole-brain method of assessing tau burden. (E) Average raw values for local efficiency within each group. The control mean for each metric is subtracted at every node. Red spheres represent increases compared to the control mean value. Blue spheres represent decreases. The centre of the sphere is placed at the centre of the region of interest. The radius of each sphere is linearly related to the difference from the control mean at that node. All groups are scaled identically.

$P = 0.02$, betweenness centrality Pearson's $r = 0.17$, $P < 0.0001$, Spearman's $\rho = 0.08$, $P = 0.08$).

Discussion

We have demonstrated that in Alzheimer's disease a strong relationship exists between the propensity of a node to display elevated ^{18}F -AV-1451 binding and the volume of cortex to which it is strongly connected (Fig. 2A). Further, we have demonstrated that this effect exists both within and between intrinsic connectivity networks (Fig. 3). This is consistent with the theory of trans-neuronal spread. The predictions of the competing hypotheses that highly active brain regions are vulnerable to tau accumulation due to a positive relationship with metabolic demand (Fig. 4A) or negative relationship with clustering due to a lack of trophic support (Fig. 5A) were not supported by the data.

In contrast, in PSP, we have demonstrated the opposite findings. Those brain regions that accrue most tau display

weak connectivity (Fig. 2B), but are predicted to have high metabolic demand (Fig. 4B) and a lack of trophic support (Fig. 5B).

Further, we have explored the consequences of tau accumulation with cross-sectional analyses at a variety of spatial scales. In Alzheimer's disease, we have demonstrated that with greater levels of tau pathology the strongest internodal connections are weakened (Fig. 2G). This reorganization of the brain network leads to more direct long-range connections passing through fewer nodes (Fig. 6A and Supplementary Fig. 6A), at the cost of lower local efficiency (Fig. 7A)

In PSP, where tau accumulation is predominantly subcortical, we demonstrate the opposite reorganization of the connectivity graph. With greater levels of tau in midbrain and deep nuclei (Fig. 2F), the strongest functional connections are strengthened; these are predominantly cortical (Fig. 2G and H). Information transfer therefore takes a less direct path (Supplementary Fig. 6A), passing through a larger number of cortical nodes *en route* (Fig. 4A), as deep structures can no longer sustain long range

connectivity. This is accompanied by a decrease in participation coefficient (Fig. 4D) and an increase in clustering (Fig. 5D) as connectivity becomes increasingly modular.

Insights into the mechanisms of disease progression in humans

It has been proposed that the pathological mechanisms underlying Alzheimer's disease begin in a single, vulnerable location and spread from cell to cell, rather than occurring independently in a large number of vulnerable cell populations (Guo and Lee, 2014; Goedert, 2015). The primary direct evidence for such propagation of tau comes from rodent studies. For example, the injection of brain extract from transgenic mice expressing mutant tau into mice expressing wild-type human tau caused wild-type tau to form filaments and spread to neighbouring brain regions (Clavaguera *et al.*, 2009). Further, pathological tau from human brains causes disease in wild-type mice, in which the pathological human tau species becomes self-propagating (Clavaguera *et al.*, 2013). This tau propagation is mediated by the presence and strength of synaptic connectivity rather than spatial proximity (Liu *et al.*, 2012; Iba *et al.*, 2013; Ahmed *et al.*, 2014).

Associative studies of the healthy brain have demonstrated that large-scale, functionally connected neural networks strongly resemble the known patterns of atrophy in distinct neurodegenerative syndromes mediated by tau and TDP-43 (Zhou *et al.*, 2012). Further human evidence comes from the observation that patterns of atrophy in the rare disease non-fluent variant primary progressive aphasia (nfvPPA) strongly correspond to structural and functional connectivity in the healthy speech production network (Mandelli *et al.*, 2016). This is an important observation, because clinically and radiologically indistinguishable cases of nfvPPA can be caused either by tau or by the unrelated protein TAR DNA-binding protein 43 (TDP-43), which has been demonstrated to propagate trans-neuronally (Braak *et al.*, 2013).

Here, we go beyond these associative studies to measure tau burden and functional connectivity in the same individuals at both the whole-brain and regional level. Our observation that those brain areas that are more strongly functionally connected have accrued more tau pathology in Alzheimer's disease (Fig. 2A), independent of which connectivity network they belong to (Fig. 3), is consistent with trans-neuronal spread. We demonstrate that the presence of tau is not, in itself, inducing stronger regional connectivity by our cross-sectional analysis of the Alzheimer's disease group, in which we demonstrate that as cortical tau accumulates the overall functional connectivity of cortex falls (Fig. 2D), and this between-subjects effect is strongest in those brain regions with most tau accumulation (Fig. 2F and G). Crucially, we demonstrate that ^{18}F -AV-1451 binding potential at each node is better than the connectivity of that node in the healthy brain at accounting for regional variance in

connectivity change, arguing against the presence of tau being a secondary marker of neurodegeneration in vulnerable hubs. In other words, it is not coincidence that Alzheimer's disease tends to impact large networks; it is a predictable consequence of trans-neuronal spread of a disease-causing protein. Graph theoretic models of transmissible disease epidemics are in agreement that the likelihood of an individual becoming infected (and the dose of the infectious agent received) is directly proportional to its number of infected neighbours and their infectivity (Durrett, 2010). As our nodes represent brain regions of equal volume, the binary portion of degree represents a surrogate measure of the number of neurons to which a brain region is connected, and the weighted portion of degree is a measure of the strength of these connections. By the time Alzheimer's disease is sufficiently advanced to cause the symptoms of MCI, tau is generally already present to some degree throughout the neocortex (Markesbery, 2010), and therefore reaching a disease stage at which the number of neighbours more closely approximates the number of infected neighbours, and the connection strength between infected neighbours (here the weighted portion of degree) becomes a strong driver of infectivity.

Conversely, our analyses do not provide support for models of hub vulnerability due to metabolic demand or lack of trophic support in Alzheimer's disease. It is important to acknowledge that this does not mean that these mechanisms are unimportant, but rather that they are a downstream event of tau accumulation. In other words, while we demonstrate that the propensity of a node to accrue tau is not related to metabolic demand or trophic support, these factors might still contribute to determining the vulnerability of brain regions to the presence of a given amount of tau. This hypothesis could be addressed in future studies by relating the information content of tau ligand binding to other measures of neurodegeneration such as longitudinal changes in grey matter volume.

In PSP, we do find support for models of hub vulnerability due to metabolic demand and lack of trophic support, but not for models of trans-neuronal spread. This is in line with other recent studies, demonstrating that neurodegeneration in PSP is related to local gene expression patterns (Rittman *et al.*, 2016).

Is the difference between Alzheimer's disease and PSP mediated by tau isoform or intrinsic connectivity?

A striking feature of our results is that we demonstrate a strong relationship between ^{18}F -AV-1451 binding potential and the strength of functional connectivity in Alzheimer's disease but not PSP. There are at least two potential (and not mutually exclusive) explanations for this dissociation.

The first possibility is that trans-neuronal tau propagation might occur more slowly in PSP. Cellular models have demonstrated that the propensity of tau to propagate

intracellularly depends on its ability to form aggregates (Falcon *et al.*, 2015). Once present in a new cell, the ability of tau fibrils to induce the aggregation of constitutionally present tau depends on the conformation of the fibril structure (Nonaka *et al.*, 2010; Fitzpatrick *et al.*, 2017). It might be that the straight filaments of predominantly 4R tau that characterize PSP are simply less able to propagate or need to be present in higher concentrations before they can induce a chain reaction of local tau aggregation (Guo *et al.*, 2016). This view is supported by our demonstration that tau is restricted to brainstem and deep nuclei in PSP despite these nodes being highly promiscuous between networks, displaying a high participation coefficient (Fig. 4B) and low clustering (Fig. 5B).

Second, it is possible that tau propagation does occur, but that it is limited in range to a subcortical intrinsic connectivity network (Raj *et al.*, 2012) (perhaps network 5 in Laird *et al.*, 2011). Such a subcortical network may be poorly visualized by multi-echo functional MRI, and is less frequently observed at rest than the DMN (Greicius *et al.*, 2003), which has been implicated in Alzheimer's disease (Greicius *et al.*, 2004). Together, therefore, our findings of weak functional connectivity in deep nuclei and brainstem nodes (Fig. 2B) might mask meaningful functional connectivity within and between these regions, accounting for the restricted and stereotyped pattern of tau accumulation in early PSP (Ellison *et al.*, 2012) and cortical escape in advanced PSP (Schofield *et al.*, 2012).

Cross-sectional data reveals patterns less visible at the group level

Computational modelling of connectivity-dependent cell death predicts a dissociation between changes in functional connectivity in early and late Alzheimer's disease (de Haan *et al.*, 2012). It has been proposed that, in early disease, hubs compensate for declines in structural connectivity by increasing their firing rate, manifesting as stronger functional connectivity (Maestú *et al.*, 2015). As disease progresses, this mechanism breaks down as neural damage prevents the maintenance of this metabolically demanding compensation (Jones *et al.*, 2015). This dissociation is thought to underlie some of the seemingly inconsistent findings in the analysis of graph properties in neurodegenerative disease. By using a cross-sectional approach across a range of disease severity, we demonstrate relationships consistent with this hypothesis. In Alzheimer's disease, weighted degree (Fig. 2D) and betweenness centrality (Supplementary Fig. 6A) consistently fall as tau burden increases. However, in early disease where tau burden is low (our sample includes a range of severity, including PiB-positive MCI), the regression line for these metrics is above the control average. Similarly, examining the regional changes related to disease burden reveals striking patterns that are obscured at the group level. This underlines the more general principal that one should be cautious in interpreting a

main effect of group in the presence of an interaction, or correlation with severity.

Reorganization of brain networks

Our examination of two distinct tau-mediated neurodegenerative pathologies with different distributions of pathology has enabled us to distinguish their consequences. We demonstrate strongly opposing effects in a range of metrics resulting from the presence of predominantly cortical (Alzheimer's disease) or subcortical (PSP) tau. The direction of these effects in Alzheimer's disease is consistent with the previously recognized impact of neurodegeneration, leading to increasingly random cortical connectivity (Sanz-Arigita *et al.*, 2010; Stam, 2014) and a reduction in small-world properties (Stam *et al.*, 2006). Eigenvector centrality showed particularly strong regional effects in Alzheimer's disease, with a negative correlation observed between disease-related changes in this metric and local tau burden at each node—i.e. those brain regions that displayed less tau pathology had greater functional influence on other brain regions.

In contrast, cortico-subcortical functional connectivity is preferentially impaired in PSP-Richardson's syndrome, resulting in cerebral information transfer taking a less direct path through a larger number of cortical nodes, reducing closeness centrality and eigenvector centrality, but increasing cortical degree, betweenness centrality and local efficiency. This results in an excessively modular connectivity arrangement, with decreasing participation coefficient and increasing clustering. These findings tie together classical observations of the 'subcortical dementia' phenotype of PSP (Albert *et al.*, 1974) with more modern observations that behavioural change and cognitive impairment in PSP correlates with frontal cortical hypometabolism (D'Antona *et al.*, 1985; Foster *et al.*, 1988) and atrophy (Cordato *et al.*, 2002, 2005). We propose that increases in cortical functional connectivity can compensate for subcortical tau burden in PSP. Increasingly indirect information transfer accounts for the cognitive slowing that is the hallmark of the 'subcortical dementias', but performance on untimed tests is preserved until cortical regions become atrophic in late disease.

Study limitations

The main limitation of our analysis is that it is cross-sectional, and we use ^{18}F -AV-1451 binding as a surrogate marker of tau burden. By making observations about the relationship between tau burden and functional connectivity in this way, we assume a uniformity of effect within our disease groups. As novel PET ligands such as ^{18}F -AV-1451 gain maturity, longitudinal assessment of tau burden and functional connectivity in the same individuals will be an important and powerful validation of our results. Definite evidence of the causal relationship between tau and connectivity will require the combination of longitudinal assessment and interventional studies targeting tau pathology.

It should also be noted that ^{18}F -AV-1451 binding identifies predominantly aggregated tau in tangles, and does not directly measure oligomeric tau, which may be more toxic to the cell and synaptic plasticity, nor extracellular forms of tau that may mediate spread of pathology. The molecular binding target of ^{18}F -AV-1451 in non-Alzheimer's disease tauopathies is disputed; elevated 'off-target' binding has been demonstrated in the basal ganglia of healthy controls (Johnson *et al.*, 2016), albeit to a lesser degree than that observed in PSP (Fig. 2F) (Passamonti *et al.*, 2017), and in TDP-43 associated disorders without evident tau pathology (Bevan-Jones *et al.*, 2017a). Nonetheless, ^{18}F -AV-1451 is able to recapitulate the distribution of post-mortem neuropathology in these disorders, making it appropriate for use here (Smith *et al.*, 2016).

Our analysis is focused towards cortico-cortical functional connectivity. In particular, multi-echo MRI might have a poor signal-to-noise ratio in deep brain structures, although the main advantage of using this sequence is that it enables robust de-noising of movement-related artefacts pipeline (Kundu *et al.*, 2012, 2013). This is critical in clinical populations, in which functional MRI data may differentially suffer from quality degradation due to head movements.

Finally, by examining proportionately thresholded graphs with 1–10% density, our analysis focusses on the strongest interregional functional connections. However, it is possible that we are missing additional effects of neurodegeneration on weak or medium-strength connections. Tract-tracing studies indicate that there are weak anatomical connections, equivalent to a few axons, between some cortical areas (Ypma and Bullmore, 2016). Such weak links may have functional importance in complex networks (Granovetter, 1983). However, weak connections are difficult to evaluate with functional MRI, as it is not possible to disentangle them from correlation arising from signal noise. Future evaluation of these weaker connections with *in vivo* tractography, neuropathology or novel methods might reveal additional effects not evident in our dataset. In the interim, the thresholding procedure retains several advantages; by retaining only the most strongly correlated edges one is less likely to include false positive correlations and topologically random edges. It also allows the computationally intense process of normalization of metrics against random graphs of equal density. The consistency between the results using thresholded nodal weighted degree and unthresholded nodal connectivity strength provides reassurance in the choice of thresholding of connections.

Conclusion

This study reveals the differential relationship between tau burden and functional connectivity in two distinct human neurodegenerative tauopathies. Our results enable us to disentangle the causes of tau accumulation from their consequences. They have wide-ranging implications, from the validation of models of tau trafficking in humans to

corroborating computational models of hub compensation in Alzheimer's disease, while accounting for the contrasting cognitive phenotype of these two conditions. These insights into the relationship between tau burden and brain connectivity changes will inform translational models and clinical trials of disease-modifying therapies.

Acknowledgements

We would like to thank our volunteers for participating in this study, the radiographers/technologists at the Wolfson Brain Imaging Centre and PET/CT Unit, Addenbrooke's Hospital, for their invaluable support in data acquisition, Young T. Hong and Tim D. Fryer for their assistance in modelling the PET data, Franklin I Aigbirhio for radioligand production, and Edward T. Bullmore for advice on interpretation and control analyses. We thank Avid (Lilly) for supplying the precursor for the manufacturing of ^{18}F -AV-1451 for use in this study.

Funding

The NIMROD study was funded by the National Institute for Health Research (NIHR, RG64473) Cambridge Biomedical Research Centre and Biomedical Research Unit in Dementia, PSP Association, the Wellcome Trust (JBR 103838), the Medical Research Council (MC-A060-5PQ30). T.E.C. is supported by a personal fellowship from the Association of British Neurologists and Patrick Berthoud charitable trust.

Supplementary material

Supplementary material is available at *Brain* online.

References

- Abdelnour F, Voss HU, Raj A. Network diffusion accurately models the relationship between structural and functional brain connectivity networks. *Neuroimage* 2014; 90: 335–47.
- Ahmed Z, Cooper J, Murray TK, Garn K, McNaughton E, Clarke H, et al. A novel *in vivo* model of tau propagation with rapid and progressive neurofibrillary tangle pathology: the pattern of spread is determined by connectivity, not proximity. *Acta Neuropathol* 2014; 127: 667–83.
- Albert ML, Feldman RG, Willis AL. The 'subcortical dementia' of progressive supranuclear palsy. *J Neurol Neurosurg Psychiatry* 1974; 37: 121–30.
- Alexander-Bloch AF, Gogtay N, Meunier D, Birn R, Clasen L, Lalonde F, et al. Disrupted modularity and local connectivity of brain functional networks in childhood-onset schizophrenia. *Front Syst Neurosci* 2010; 4: 147.
- Appel SH. A unifying hypothesis for the cause of amyotrophic lateral sclerosis, parkinsonism, and Alzheimer disease. *Ann Neurol* 1981; 10: 499–505.
- Ashburner J. A fast diffeomorphic image registration algorithm. *Neuroimage* 2007; 38: 95–113.

- Baker H, Ridley R, Duchen L, Crow T, Bruton C. Induction of β (A4)-amyloid in primates by injection of Alzheimer's disease brain homogenate. *Mol Neurobiol* 1994; 8: 25–39.
- Ballatore C, Lee VM, Trojanowski JQ. Tau-mediated neurodegeneration in Alzheimer's disease and related disorders. *Nat Rev Neurosci* 2007; 8: 663–72.
- Bevan-Jones W, Cope T, Jones P, Passamonti L, Hong Y, Fryer T, et al. [18F] AV-1451 binding *in vivo* mirrors the expected distribution of TDP-43 pathology in the semantic variant of primary progressive aphasia. *J Neurol Neurosurg Psychiatry* 2017a, doi: 10.1136/jnnp-2017-316402.
- Bevan-Jones WR, Surendranathan A, Passamonti L, Rodríguez PV, Arnold R, Mak E, et al. Neuroimaging of Inflammation in Memory and Related Other Disorders (NIMROD) study protocol: a deep phenotyping cohort study of the role of brain inflammation in dementia, depression and other neurological illnesses. *BMJ Open* 2017b; 7: e013187.
- Braak H, Braak E. Neuropathological staging of Alzheimer-related changes. *Acta Neuropathol* 1991; 82: 239–59.
- Braak H, Braak E. Staging of Alzheimer's disease-related neurofibrillary changes. *Neurobiol Aging* 1995; 16: 271–8.
- Braak H, Brettschneider J, Ludolph AC, Lee VM, Trojanowski JQ, Del Tredici K. Amyotrophic lateral sclerosis—a model of corticofugal axonal spread. *Nat Rev Neurol* 2013; 9: 708.
- Brier MR, Gordon B, Friedrichsen K, McCarthy J, Stern A, Christensen J, et al. Tau and Abeta imaging, CSF measures, and cognition in Alzheimer's disease. *Sci Transl Med* 2016; 8: 338ra66.
- Buckner RL, Sepulcre J, Talukdar T, Krienen FM, Liu H, Hedden T, et al. Cortical hubs revealed by intrinsic functional connectivity: mapping, assessment of stability, and relation to Alzheimer's disease. *J Neurosci* 2009; 29: 1860–73.
- Chennu S, Annen J, Wannez S, Thibaut A, Chatelle C, Cassol H, et al. Brain networks predict metabolism, diagnosis and prognosis at the bedside in disorders of consciousness. *Brain* 2017; 140: 2120–32.
- Chien DT, Bahri S, Szardenings AK, Walsh JC, Mu F, Su MY, et al. Early clinical PET imaging results with the novel PHF-tau radioligand [F-18]-T807. *J Alzheimers Dis* 2013; 34: 457–68.
- Clavaguera F, Akatsu H, Fraser G, Crowther RA, Frank S, Hench J, et al. Brain homogenates from human tauopathies induce tau inclusions in mouse brain. *Proc Natl Acad Sci USA* 2013; 110: 9535–40.
- Clavaguera F, Bolmont T, Crowther RA, Abramowski D, Frank S, Probst A, et al. Transmission and spreading of tauopathy in transgenic mouse brain. *Nat Cell Biol* 2009; 11: 909–13.
- Cordato N, Duggins A, Halliday G, Morris J, Pantelis C. Clinical deficits correlate with regional cerebral atrophy in progressive supranuclear palsy. *Brain* 2005; 128: 1259–66.
- Cordato N, Pantelis C, Halliday G, Velakoulis D, Wood S, Stuart G, et al. Frontal atrophy correlates with behavioural changes in progressive supranuclear palsy. *Brain* 2002; 125: 789–800.
- Crossley NA, Mechelli A, Scott J, Carletti F, Fox PT, McGuire P, et al. The hubs of the human connectome are generally implicated in the anatomy of brain disorders. *Brain* 2014; 137: 2382–95.
- D'Antona R, Baron JC, Samson Y, Serdaru M, Viader F, Agid Y, et al. Subcortical dementia. Frontal cortex hypometabolism detected by positron tomography in patients with progressive supranuclear palsy. *Brain* 1985; 108 (Pt 3): 785–99.
- Dai Z, Yan C, Li K, Wang Z, Wang J, Cao M, et al. Identifying and mapping connectivity patterns of brain network hubs in Alzheimer's disease. *Cereb Cortex* 2014; bhu246.
- de Haan W, Mott K, van Straaten EC, Scheltens P, Stam CJ. Activity dependent degeneration explains hub vulnerability in Alzheimer's disease. *PLoS Comput Biol* 2012; 8: e1002582.
- Durrett R. Some features of the spread of epidemics and information on a random graph. *Proc Natl Acad Sci USA* 2010; 107: 4491–8.
- Ellison D, Love S, Chimelli LMC, Harding B, Lowe JS, Vinters HV, et al. *Neuropathology: a reference text of CNS pathology*. Elsevier Health Sciences; 2012.
- Falcon B, Cavallini A, Angers R, Glover S, Murray TK, Barnham L, et al. Conformation determines the seeding potencies of native and recombinant Tau aggregates. *J Biol Chem* 2015; 290: 1049–65.
- Fitzpatrick AWP, Falcon B, He S, Murzin AG, Murshudov G, Garringer HJ, et al. Cryo-EM structures of tau filaments from Alzheimer's disease. *Nature* 2017; 547: 185–90.
- Foster NL, Gilman S, Berent S, Morin EM, Brown MB, Koeppe RA. Cerebral hypometabolism in progressive supranuclear palsy studied with positron emission tomography. *Ann Neurol* 1988; 24: 399–406.
- Gardner RC, Boxer AL, Trujillo A, Mirsky JB, Guo CC, Gennatas ED, et al. Intrinsic connectivity network disruption in progressive supranuclear palsy. *Ann Neurol* 2013; 73: 603–16.
- Goedert M. Alzheimer's and Parkinson's diseases: the prion concept in relation to assembled A β , tau, and α -synuclein. *Science* 2015; 349: 1255555.
- Goedert M, Spillantini MG. A century of Alzheimer's disease. *Science* 2006; 314: 777–81.
- Golbe LI, Ohman-Strickland PA. A clinical rating scale for progressive supranuclear palsy. *Brain* 2007; 130: 1552–65.
- Granovetter M. The strength of weak ties: a network theory revisited. *Soc Theory* 1983: 201–33.
- Greicius MD, Krasnow B, Reiss AL, Menon V. Functional connectivity in the resting brain: a network analysis of the default mode hypothesis. *Proc Natl Acad Sci USA* 2003; 100: 253–8.
- Greicius MD, Srivastava G, Reiss AL, Menon V. Default-mode network activity distinguishes Alzheimer's disease from healthy aging: evidence from functional MRI. *Proc Natl Acad Sci USA* 2004; 101: 4637–42.
- Guo JL, Lee VM. Cell-to-cell transmission of pathogenic proteins in neurodegenerative diseases. *Nat Med* 2014; 20: 130–8.
- Guo JL, Narasimhan S, Changolkar L, He Z, Stieber A, Zhang B, et al. Unique pathological tau conformers from Alzheimer's brains transmit tau pathology in nontransgenic mice. *J Exp Med* 2016; 213: 2635–54.
- Höglinger GU, Respondek G, Stamelou M, Kurz C, Josephs KA, Lang AE, et al. Clinical diagnosis of progressive supranuclear palsy: the Movement Disorder Society Criteria. *Mov Disord* 2017; 32: 853–64.
- Iba M, Guo JL, McBride JD, Zhang B, Trojanowski JQ, Lee VM. Synthetic tau fibrils mediate transmission of neurofibrillary tangles in a transgenic mouse model of Alzheimer's-like tauopathy. *J Neurosci* 2013; 33: 1024–37.
- Ittner LM, Götz J. Amyloid- β and tau—a toxic pas de deux in Alzheimer's disease. *Nat Rev Neurosci* 2011; 12: 65–72.
- Johnson KA, Schultz A, Betensky RA, Becker JA, Sepulcre J, Rentz D, et al. Tau positron emission tomographic imaging in aging and early Alzheimer disease. *Ann Neurol* 2016; 79: 110–19.
- Jones DT, Knopman DS, Gunter JL, Graff-Radford J, Vemuri P, Boeve BF, et al. Cascading network failure across the Alzheimer's disease spectrum. *Brain* 2015; 139: 547–62.
- Joyce KE, Laurienti PJ, Burdette JH, Hayasaka S. A new measure of centrality for brain networks. *PLoS One* 2010; 5: e12200.
- Klunk WE, Engler H, Nordberg A, Wang Y, Blomqvist G, Holt DP, et al. Imaging brain amyloid in Alzheimer's disease with Pittsburgh Compound-B. *Ann Neurol* 2004; 55: 306–19.
- Kundu P, Brenowitz ND, Voon V, Worbe Y, Vértes PE, Inati SJ, et al. Integrated strategy for improving functional connectivity mapping using multiecho fMRI. *Proc Natl Acad Sci USA* 2013; 110: 16187–92.
- Kundu P, Inati SJ, Evans JW, Luh WM, Bandettini PA. Differentiating BOLD and non-BOLD signals in fMRI time series using multi-echo EPI. *Neuroimage* 2012; 60: 1759–70.
- Laird AR, Fox PM, Eickhoff SB, Turner JA, Ray KL, McKay DR, et al. Behavioral interpretations of intrinsic connectivity networks. *J Cogn Neurosci* 2011; 23: 4022–37.
- Lehmann M, Ghosh PM, Madison C, Laforce R, Corbetta-Rastelli C, Weiner MW, et al. Diverging patterns of amyloid deposition and hypometabolism in clinical variants of probable Alzheimer's disease. *Brain* 2013; 136: 844–58.

- Litvan I, Agid Y, Calne D, Campbell G, Dubois B, Duvoisin R, et al. Clinical research criteria for the diagnosis of progressive supranuclear palsy (Steele-Richardson-Olszewski syndrome) Report of the NINDS-SPSP International Workshop*. *Neurology* 1996; 47: 1–9.
- Liu L, Drouet V, Wu JW, Witter MP, Small SA, Clelland C, et al. Trans-synaptic spread of tau pathology *in vivo*. *PLoS One* 2012; 7: e31302.
- Liu WK, Le TV, Adamson J, Baker M, Cookson N, Hardy J, et al. Relationship of the extended tau haplotype to tau biochemistry and neuropathology in progressive supranuclear palsy. *Ann Neurol* 2001; 50: 494–502.
- Maestú F, Peña JM, Garcés P, González S, Bajo R, Bagic A, et al. A multicenter study of the early detection of synaptic dysfunction in mild cognitive impairment using magnetoencephalography-derived functional connectivity. *Neuroimage Clin* 2015; 9: 103–9.
- Mandelli ML, Vilaplana E, Brown JA, Hubbard HI, Binney RJ, Attygalle S, et al. Healthy brain connectivity predicts atrophy progression in non-fluent variant of primary progressive aphasia. *Brain* 2016; 139 (Pt 10): 2778–91.
- Markesbery WR. Neuropathologic alterations in mild cognitive impairment: a review. *J Alzheimers Dis* 2010; 19: 221–8.
- McKhann GM, Knopman DS, Chertkow H, Hyman BT, Jack CR, Kawas CH, et al. The diagnosis of dementia due to Alzheimer's disease: recommendations from the National Institute on Aging-Alzheimer's Association workgroups on diagnostic guidelines for Alzheimer's disease. *Alzheimers Dement* 2011; 7: 263–9.
- Myeku N, Clelland CL, Emrani S, Kukushkin NV, Yu WH, Goldberg AL, et al. Tau-driven 26S proteasome impairment and cognitive dysfunction can be prevented early in disease by activating cAMP-PKA signaling. *Nat Med* 2016; 22: 46.
- Nisbet RM, Polanco JC, Ittner LM, Götz J. Tau aggregation and its interplay with amyloid- β . *Acta Neuropathol* 2015; 129: 207–20.
- Nonaka T, Watanabe ST, Iwatsubo T, Hasegawa M. Seeded aggregation and toxicity of α -synuclein and tau: cellular models of neurodegenerative diseases. *J Biol Chem* 2010; 285: 34885–98.
- Okello A, Koivunen J, Edison P, Archer H, Turkheimer F, Nägren K, et al. Conversion of amyloid positive and negative MCI to AD over 3 years An 11C-PIB PET study. *Neurology* 2009; 73: 754–60.
- Ossenkoppele R, Schonhaut DR, Baker SL, O'Neil JP, Janabi M, Ghosh PM, et al. Tau, amyloid, and hypometabolism in a patient with posterior cortical atrophy. *Ann Neurol* 2015; 77: 338–42.
- Ossenkoppele R, Schonhaut DR, Schöll M, Lockhart SN, Ayakta N, Baker SL, et al. Tau PET patterns mirror clinical and neuroanatomical variability in Alzheimer's disease. *Brain* 2016; 139 (Pt 5): 1551–67.
- Passamonti L, Vázquez Rodríguez P, Hong YT, Allinson KS, Williamson D, Borchert RJ, et al. 18F-AV-1451 positron emission tomography in Alzheimer's disease and progressive supranuclear palsy. *Brain* 2017; 140: 781–91.
- Power JD, Barnes KA, Snyder AZ, Schlaggar BL, Petersen SE. Spurious but systematic correlations in functional connectivity MRI networks arise from subject motion. *Neuroimage* 2012; 59: 2142–54.
- Power JD, Schlaggar BL, Lessov-Schlaggar CN, Petersen SE. Evidence for hubs in human functional brain networks. *Neuron* 2013; 79: 798–813.
- Prusiner SB. Some speculations about prions, amyloid, and Alzheimer's disease. *N Engl J Med* 1984; 310: 661–3.
- R Core Team. R: a language and environment for statistical computing. Vienna, Austria: R Foundation for Statistical Computing; 2016.
- Raj A, Kuceyeski A, Weiner M. A network diffusion model of disease progression in dementia. *Neuron* 2012; 73: 1204–15.
- Raj A, LoCastro E, Kuceyeski A, Tosun D, Relkin N, Weiner M, et al. Network diffusion model of progression predicts longitudinal patterns of atrophy and metabolism in Alzheimer's disease. *Cell Rep* 2015; 10: 359–69.
- Rittman T, Rubinov M, Vértes PE, Patel AX, Ginestet CE, Ghosh BC, et al. Regional expression of the MAPT gene is associated with loss of hubs in brain networks and cognitive impairment in Parkinson disease and progressive supranuclear palsy. *Neurobiol Aging* 2016; 48: 153–60.
- Roberson ED, Scarce-Levie K, Palop JJ, Yan F, Cheng IH, Wu T, et al. Reducing endogenous tau ameliorates amyloid β -induced deficits in an Alzheimer's disease mouse model. *Science* 2007; 316: 750–4.
- Sanz-Arigita EJ, Schoonheim MM, Damoiseaux JS, Rombouts SA, Maris E, Barkhof F, et al. Loss of 'small-world' networks in Alzheimer's disease: graph analysis of FMRI resting-state functional connectivity. *PLoS One* 2010; 5: e13788.
- Saxena S, Caroni P. Selective neuronal vulnerability in neurodegenerative diseases: from stressor thresholds to degeneration. *Neuron* 2011; 71: 35–48.
- Schofield EC, Hodges JR, Bak TH, Xuereb JH, Halliday GM. The relationship between clinical and pathological variables in Richardson's syndrome. *J Neurol* 2012; 259: 482–90.
- Schöll M, Lockhart SN, Schonhaut DR, O'Neil JP, Janabi M, Ossenkoppele R, et al. PET imaging of tau deposition in the aging human brain. *Neuron* 2016; 89: 971–82.
- Schöll M, Ossenkoppele R, Strandberg O, Palmqvist S, Jögi J, Ohlsson T, et al. Distinct 18F-AV-1451 tau PET retention patterns in early- and late-onset Alzheimer's disease. *Brain* 2017; 140: 2286–94.
- Schwarz AJ, Yu P, Miller BB, Shcherbinin S, Dickson J, Navitsky M, et al. Regional profiles of the candidate tau PET ligand 18F-AV-1451 recapitulate key features of Braak histopathological stages. *Brain* 2016; 139: 1539–50.
- Sisodia S, Koo E, Beyreuther K, Unterbeck A, Price D. Evidence that beta-amyloid protein in Alzheimer's disease is not derived by normal processing. *Science* 1990; 248: 492–6.
- Smith R, Puschmann A, Schöll M, Ohlsson T, Van Swieten J, Honer M, et al. 18F-AV-1451 tau PET imaging correlates strongly with tau neuropathology in MAPT mutation carriers. *Brain* 2016; 139: 2372–2379.
- Smith SM, Fox PT, Miller KL, Glahn DC, Fox PM, Mackay CE, et al. Correspondence of the brain's functional architecture during activation and rest. *Proc Natl Acad Sci USA* 2009; 106: 13040–5.
- Stam C, Jones B, Nolte G, Breakspear M, Scheltens P. Small-world networks and functional connectivity in Alzheimer's disease. *Cereb Cortex* 2006; 17: 92–9.
- Stam CJ. Modern network science of neurological disorders. *Nat Rev Neurosci* 2014; 15: 683–95.
- Taniguchi-Watanabe S, Arai T, Kametani F, Nonaka T, Masuda-Suzukake M, Tarutani A, et al. Biochemical classification of tauopathies by immunoblot, protein sequence and mass spectrometric analyses of sarkosyl-insoluble and trypsin-resistant tau. *Acta Neuropathol* 2016; 131: 267–80.
- The Mathworks Inc. Matlab and statistics and machine learning toolbox. Release 2015b ed. Natick, MA: The Mathworks Inc; 2015.
- Whitfield-Gabrieli S, Nieto-Castanon A. Conn: a functional connectivity toolbox for correlated and anticorrelated brain networks. *Brain Connect* 2012; 2: 125–41.
- Williams DR, Holton JL, Strand C, Pittman A, de Silva R, Lees AJ, et al. Pathological tau burden and distribution distinguishes progressive supranuclear palsy-parkinsonism from Richardson's syndrome. *Brain* 2007; 130: 1566–76.
- Xia CF, Arteaga J, Chen G, Gangadharmath U, Gomez LF, Kasi D, et al. [18 F] T807, a novel tau positron emission tomography imaging agent for Alzheimer's disease. *Alzheimers Dement* 2013; 9: 666–76.
- Xia C, Dickerson BC. Multimodal PET imaging of amyloid and Tau pathology in Alzheimer disease and non-Alzheimer disease dementias. *PET Clin* 2017; 12: 351–9.
- Ypma RJ, Bullmore ET. Statistical analysis of tract-tracing experiments demonstrates a dense, complex cortical network in the mouse. *PLoS Comput Biol* 2016; 12: e1005104.
- Zhou J, Gennatas ED, Kramer JH, Miller BL, Seeley WW. Predicting regional neurodegeneration from the healthy brain functional connectome. *Neuron* 2012; 73: 1216–27.

ARTICLE

DOI: 10.1038/s41467-017-01958-7

OPEN

Evidence for causal top-down frontal contributions to predictive processes in speech perception

Thomas E. Cope¹, E. Sohoglu², W. Sedley³, K. Patterson^{1,2}, P.S. Jones¹, J. Wiggins¹, C. Dawson¹, M. Grube³, R.P. Carlyon², T.D. Griffiths³, Matthew H. Davis^{1,2} & James B. Rowe^{1,2}

Perception relies on the integration of sensory information and prior expectations. Here we show that selective neurodegeneration of human frontal speech regions results in delayed reconciliation of predictions in temporal cortex. These temporal regions were not atrophic, displayed normal evoked magnetic and electrical power, and preserved neural sensitivity to manipulations of sensory detail. Frontal neurodegeneration does not prevent the perceptual effects of contextual information; instead, prior expectations are applied inflexibly. The precision of predictions correlates with beta power, in line with theoretical models of the neural instantiation of predictive coding. Fronto-temporal interactions are enhanced while participants reconcile prior predictions with degraded sensory signals. Excessively precise predictions can explain several challenging phenomena in frontal aphasias, including agrammatism and subjective difficulties with speech perception. This work demonstrates that higher-level frontal mechanisms for cognitive and behavioural flexibility make a causal functional contribution to the hierarchical generative models underlying speech perception.

¹Department of Clinical Neurosciences, University of Cambridge, Cambridge CB2 0SZ, UK. ²Medical Research Council Cognition and Brain Sciences Unit, University of Cambridge, Cambridge CB2 7EF, UK. ³Institute of Neuroscience, Newcastle University, Newcastle NE1 7RU, UK. Matthew H. Davis and James B. Rowe contributed equally to this work. Correspondence and requests for materials should be addressed to T.E.C. (email: thomascope@gmail.com)

It has long been recognised that perception relies on the integration of sensory input with expectations based on prior knowledge or experience¹. This can be instantiated in hierarchical generative models, which contain both top-down connections for priors or beliefs about sensory evidence, and bottom-up connections for prediction error. The layers of these hierarchical models represent progressively more abstract descriptions of the underlying sensory data^{2, 3}. An influential implementation is known as predictive coding^{4, 5}, in which the top-down generative connections express predictions for expected sensory signals, while bottom-up processes pass forward prediction errors to update the model. This method of information transfer is highly efficient⁶. Neural models of predictive coding are well formalised, and we therefore conceptualise and interpret our study in this framework.

There is empirical evidence for predictive coding in health, for vision^{7, 8}, hearing^{9–11} and the link between perception and action in motor control^{12–14}. Furthermore, dysfunctional predictive coding mechanisms can explain a range of neurological and psychiatric phenomena, in schizophrenia¹⁵, functional movement disorders^{16, 17}, alien limb syndrome¹⁸, tinnitus¹⁹ and hallucinations²⁰. Although these disorders have been explained in terms of aberrant predictive coding, the functional consequences of degradation of the neural architecture responsible for generating top-down predictions are unknown. This is a critical and novel test for hierarchical models of perception, which motivates the following hypothesis: degeneration of top-down prediction mechanisms in frontal lobe should have a substantial impact on lower-level sensory responses in temporal lobe, and should impair

perceptual function when prior knowledge and sensory input must be combined (Fig. 1).

We test this hypothesis in the context of speech perception. Speech is a natural domain in which to study prediction, as humans are able to exploit a wide variety of visual, contextual and semantic cues to improve perception, especially in difficult listening environments^{21, 22}. Indeed, contradictory beliefs established by mismatching visual and auditory speech can lead to false perception^{23, 24}. It is important to note that such multi-modal integration can be modelled in terms of predictive coding regardless of whether or not visual information occurs before auditory information²⁵; what is important is that auditory sensory predictions are set up based on information from prior experience, sentential context or sensory information from another domain. We exploited the importance of written text in supporting perception of degraded speech^{26, 27}. There is evidence for left lateralised top-down information transfer²⁸ from frontal language²⁹ and motor speech^{30, 31} regions to auditory cortex during speech perception; in predictive coding theory this top-down transfer generates prior expectations for speech content and explains how listeners combine prior knowledge and sensory signals during perception and perceptual learning^{32, 33}.

To assess the effects of disrupted predictions we studied patients with early non-fluent primary progressive aphasia (nfvPPA), which is associated with selective neurodegeneration of the frontal lobe language and motor speech areas³⁴, but preservation of temporal lobe auditory regions. Disordered speech output in nfvPPA is characterised by apraxia of speech and/or agrammatism³⁵. In contrast to stroke aphasia the neural damage

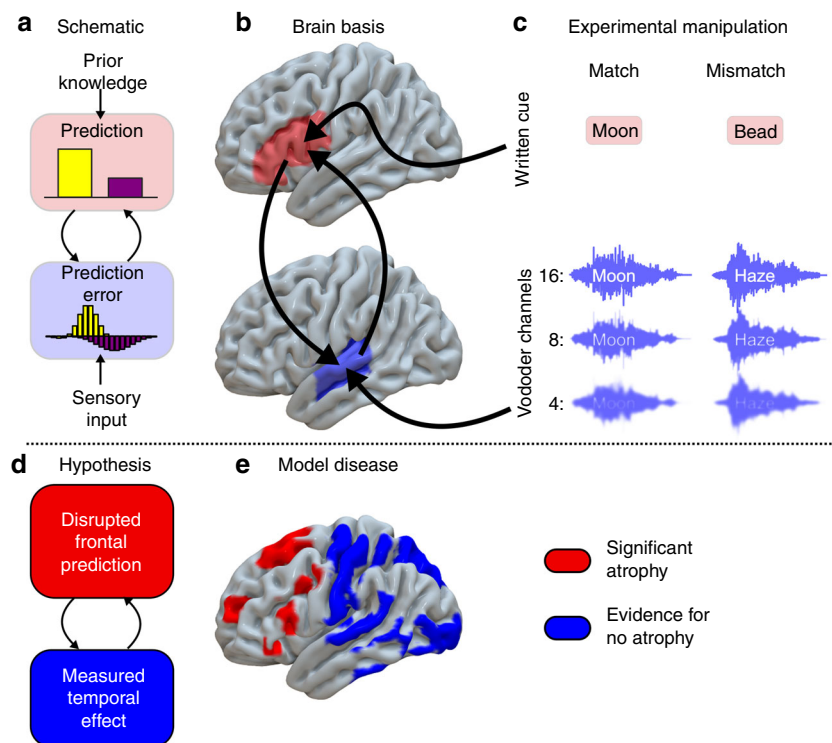


Fig. 1 An illustration of the experimental motivation. **a** A schematic Bayesian framework for predictive coding in speech perception. **b** The putative brain basis of this framework²⁸. Predictions are generated in inferior frontal gyrus and/or frontal motor speech regions (pink), and instantiated in auditory regions of superior temporal lobe (pale blue). **c** The two dimensional experimental manipulation employed here to detect a dissociation between normal temporal lobe responses to sensory detail (number of vocoder channels) and abnormal frontal lobe responses to prior congruency. **d** Our experiment relies on detecting the consequences of degraded predictions in abnormal frontal brain regions by measuring their effects in normal temporal regions. **e** Voxel-based morphometry in our patient group. Regions coloured in red displayed consistent reductions in grey matter volume (FWE $p < 0.05$). Regions coloured blue had strong evidence for normal cortical volume in nfvPPA (Bayesian probability of the null > 0.7 , cluster volume $> 1 \text{ cm}^3$). Uncoloured (grey) areas had no strong evidence for or against atrophy

Table 1 Demographic details of the experimental groups

	Number	Age	Gender	Age leaving education	MMSE	ACE-R	Raven's matrices
nfvPPA	11	72 (9)	8F, 3M	18 (3)	28 (2)	84 (12)	36 (9)
MEG controls	11	72 (8)	7F, 4M	17 (2)	29 (1)	95 (2)	46 (7)
MRI controls	36	73 (7)	17F, 19M	—	—	—	—

Mean (standard deviation). There were no statistically significant differences in age, gender or education between nfvPPA patients and MEG controls. nfvPPA patients scored more poorly than controls on the Addenbrooke's Cognitive Examination (Revised) and Raven's Progressive Matrices, but were still within the population normal range. Most of the difference between nfvPPA and controls on the ACE-R was accounted for by verbal fluency. Audiometric thresholds are available in Supplementary Fig. 1B. One patient was unable to tolerate the MEG scanner environment so, for that case, results contribute only to the behavioural analysis

in frontal regions is partial^{36, 37} enabling us to study a disruption of predictive mechanisms, rather than a system reorganised following their complete absence. Additionally, this patient cohort presents fewer problems for the modelling and interpretation of magnetoencephalography (MEG) or electroencephalography (EEG), as atrophy is subtle in early nfvPPA^{38, 39}.

For patients and matched control participants we recorded behavioural and neural data showing the influence of top-down and bottom-up manipulations on speech perception using an established paradigm involving presentation of written text that matches or mismatches with degraded spoken words^{27, 32, 40}. With this paradigm, we can determine whether and how frontal cortical neurodegeneration impairs speech perception. The presence and function of top-down influences on speech perception is controversial (see refs. ^{41–44}), as is the question of whether frontal cortical regions make a critical contribution to speech perception, through predictive coding or alternative mechanisms. Some authors suggest that these contributions are task-specific and not a core component of speech perception systems⁴⁵. The present study provides causal neural evidence with which to assess both of these claims.

Here we demonstrate distant neural effects of the degeneration of top-down signals from frontal lobes, during speech perception. We provide evidence of a direct relationship between the degree of frontal lobe degeneration and a delay in the neural mechanism for the reconciliation of predictions, which results in their inflexible application. Bayesian perceptual inference simulations demonstrate that this results in aberrantly precise prior expectations, which manifest as increased beta power during the instantiation of predictions, in agreement with theoretical frameworks of predictive coding. Finally, we show task-dependent enhancements in fronto-temporal interaction in nfvPPA, reflecting degraded neural mechanisms working harder to reconcile excessively precise predictions. We explain how inflexible predictions are able to account for several previously poorly understood symptoms and signs in frontal non-fluent aphasias, including difficulties with parsing the structure and content of running speech. Together, our results provide causal evidence for a critical role of frontal regions for the reconciliation of predictions during the perception and comprehension of speech.

Results

Structural consequences of nfvPPA. To confirm the dissociation between frontal atrophy and intact temporal cortex, upon which our experiment relies, we used voxel-based morphometry to compare grey matter volume in nine of our patients with nfvPPA (see Table 1 for participant characteristics) to 36 age-matched healthy individuals using whole brain statistical parametric mapping (SPM) *t*-test and Bayesian null tests. As anticipated, brain regions of interest displayed a localised pattern of atrophy in nfvPPA (Fig. 1e), with grey matter volume loss in left inferior frontal regions (family wise error corrected (FWE) peak $p = 0.001$ at montreal neurological institute (MNI) $[-37, 17, 7]$; Bayes posterior probability of no difference < 0.00001), but not in left

primary auditory cortex (FWE $p = 1$; Bayes posterior probability of no difference 0.75 at MNI $[-59, -24, 9]$) or superior temporal gyrus (FWE $p = 1$; Bayes posterior probability of no difference 0.91 at MNI $[-67, -17, 3]$). Significant atrophy was also observed in right inferior frontal regions (FWE $p = 0.004$; peak MNI $[37, 20, 6]$) but not right primary auditory cortex (FWE $p = 1$ at MNI $[59, -24, 9]$) or superior temporal gyrus (FWE $p = 1$ at MNI $[67 -17 3]$). Significant atrophy in left inferior frontal regions lay within pars triangularis, pars opercularis and anterior insula in the Desikan–Killiany Atlas (Supplementary Table 1).

Subjective speech perception symptoms in nfvPPA. While the core symptoms in nfvPPA relate to apraxia of speech and agrammatism, patients often complain of a feeling of speech deafness. To test for this symptom in our cohort, we asked patients and controls to rate their subjective difficulty with five listening scenarios, by placing a mark on a line from 'very easy' to 'very difficult'. Patients could respond appropriately to such rating scales. Patients and controls displayed very similar subjective difficulty ratings for 'speech in noise', 'localising sounds', 'understanding station announcements' and 'how loud others say their television is' (all $t(20) p > 0.3$, Supplementary Fig. 1A). However, there was a difference in their assessments of difficulty in understanding speech in quiet environments ($t(20) = 2.66, p = 0.015$): controls universally rated this as very easy, while patients rated it to be almost as difficult as understanding speech in noise (interaction $F(1,20) = 8.21, p = 0.010$). Patients and controls had similar, age-appropriate, hearing acuity (Supplementary Fig. 1B).

Evoked neural responses during the reconciliation of predictions. To assess the neural correlates of degraded predictive mechanisms in nfvPPA (Fig. 1d), we recorded simultaneous MEG and EEG during a speech perception task. We manipulated prior expectations using matching or mismatching text cues, before participants heard spoken words that were varied in sensory detail by manipulating the number of vocoder channels (Figs. 1c, 2a)⁴⁶. Overall evoked power was similar for the two groups of participants (Supplementary Fig. 3); frontal neurodegeneration did not lead to any large difference in the magnitude of the neural response evoked by single spoken words that could manifest as spurious group by condition interactions in neural activity.

To confirm that patients have normal responses to manipulations of sensory detail independent of predictions (as expected given preserved cortical volume in auditory cortex and superior temporal gyrus, Fig. 1e), we first assessed the neural effect of the number of vocoder channels (Fig. 3). Across all 21 individuals, SPM *F*-test peak effects were observed in the planar gradiometers at 96 ms (scalp-time FWE $p < 0.001$), in magnetometers at 188 ms (FWE $p < 0.001$) and again at 380 ms (FWE $p < 0.001$), and in EEG at 392 ms (FWE $p < 0.001$). These findings are consistent with previous studies in young individuals⁴⁰. No reliable group by sensory interactions were found at the scalp locations of the peak main effect or at all scalp-time locations. Together, these results

are consistent with the idea that patients and controls produce similar neural responses to manipulations of sensory detail in degraded speech. Crucially for the interpretation of later results, the latency of these responses was also the same in both groups. In magnetometers, where the late effects of vocoder channel number were most clearly seen, control peaks occurred at 196 ms and 340 ms, and patient peaks at 172 ms and 372 ms (Fig. 3).

Having performed these control analyses, we tested our primary hypothesis by examining the neural effect of manipulating whether prior expectations matched sensory input. Across all 21 participants, during the reconciliation of predictions there

were significant SPM *F*-test main effects of cue congruency in all sensor types (Fig. 4a); planar gradiometers at 464 ms (scalp-time peak FWE $p < 0.001$), magnetometers at 400 ms (FWE $p < 0.001$), and EEG at 700 ms (FWE $p < 0.001$). At these scalp locations, significant group by congruency interactions were observed in the planar gradiometers and in the magnetometers (unpaired $t(19)$, $p < 0.05$ sustained over at least eight sequential samples), but not in the EEG electrodes. In the planar gradiometers, between 264 ms and 464 ms controls had a significantly larger effect of congruency than patients (Fig. 4b). The scalp topography averaged across this time window resembled that observed during the peak of the main effect, but with the pattern being stronger in controls (Fig. 4c). In the magnetometers, a cluster with similar timing and scalp topography was observed between 240 and 560 ms (Fig. 4b). Two additional clusters were also observed. In later time windows, from 728 to 808 ms, group by congruency interactions were observed in the opposite direction, with patients showing a significantly greater effect than controls. Again, the scalp topographies in this cluster resembled those during the main effect (Fig. 4c). This indicates that the effect of congruency was present in both groups, but that the effect was significantly delayed in nvfPPA. Finally, an early cluster was observed between 152 ms and 224 ms, with the controls displaying a significantly greater effect of congruency than patients. Intriguingly, the scalp topography in this time window was different to that observed during the conjoint main effect, with dipoles having a much more anterior centre of mass (Fig. 4c). This anterior topography is consistent with a frontal source, expected to appear in this earlier time window as shown in similar previous studies with young healthy listeners^{33, 40}.

To assess the underlying neural sources of these effects, multimodal sensor data were combined⁴⁷ and inverted into source space with sLORETA⁴⁸. For the main effect of vocoder channel number, reconstructions were performed across all individuals combined, because no group difference or group by clarity interaction was demonstrated in sensor space. The main effect of sensory detail shown in MEG sensors and EEG electrodes is explained by increased activity for 16 channel speech in temporal lobe auditory areas in mid-latency time windows (200–280 ms and 290–440 ms; Fig. 5a), replicating previous findings in younger individuals^{33, 40}.

To localise the group by cue congruency interaction, we first display source reconstructions for the main effect of cue congruency in each group (Fig. 5b) for time windows defined by the main data features in overall sensor power averaged over conditions and participants (Supplementary Fig. 3). Given our findings of delayed congruency effects in patients, an additional, late, time window (710–850 ms) was also examined post hoc. We focus on the two principal sources observed in young healthy individuals for this task^{33, 40}, extracting average power in each

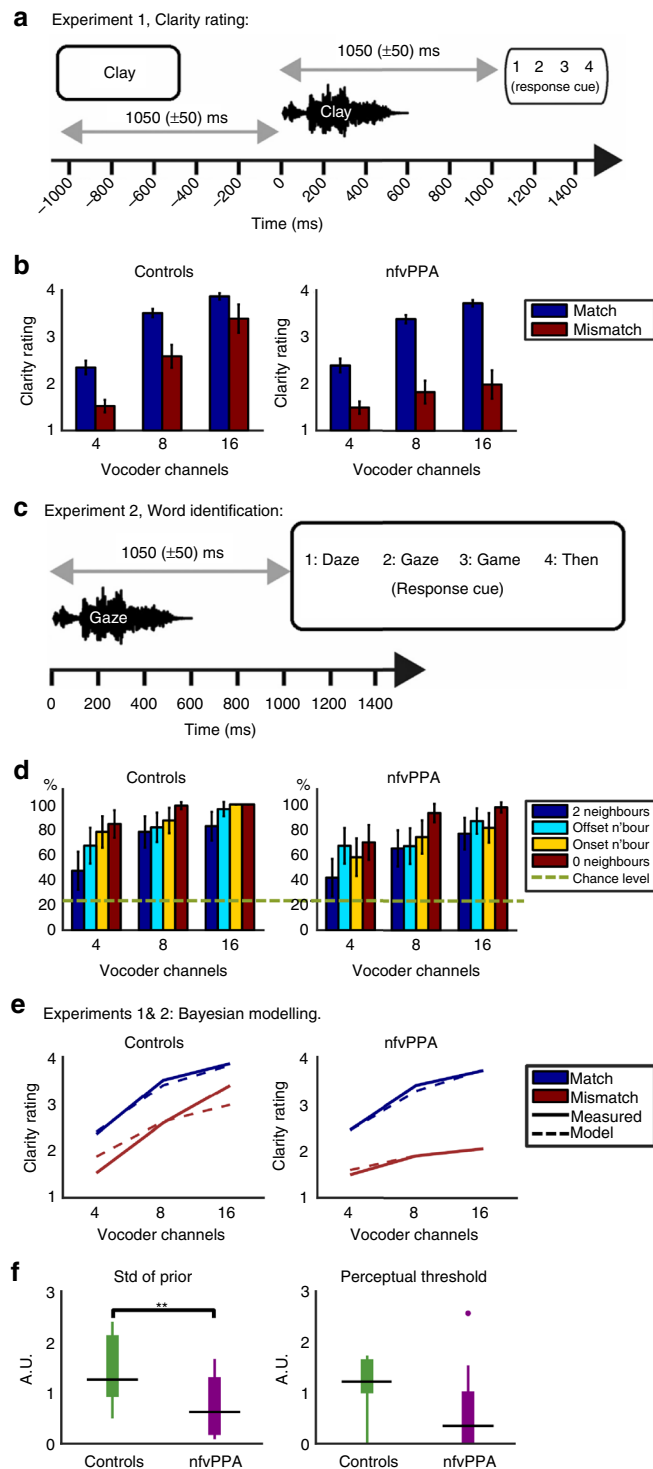


Fig. 2 Behaviour. **a** Experiment 1 design. A Match trial is shown. In a Mismatch trial, the written and vocoded words would share no phonology (for example the written cue ‘clay’ might be paired with the vocoded word ‘sing’). **b** Group-averaged clarity ratings for each condition. Error bars represent standard error across individuals within each group. **c** Four alternative forced choice vocoded word identification task. **d** Group-averaged per cent correct report for each condition. Chance performance at 25%. Error bars represent standard error across individuals within each group. **e** Overall group fits for single subject Bayesian data modelling of the data from **b**. **f** Derived parameters from the Bayesian data modelling. A.U., arbitrary units. Patients with nvfPPA displayed significantly more precise prior expectations than controls (Wilcoxon $U(11,11)$ $p < 0.01$). They also displayed a trend towards a reduction in perceptual thresholds (Wilcoxon $U(11,11)$ $p = 0.075$)

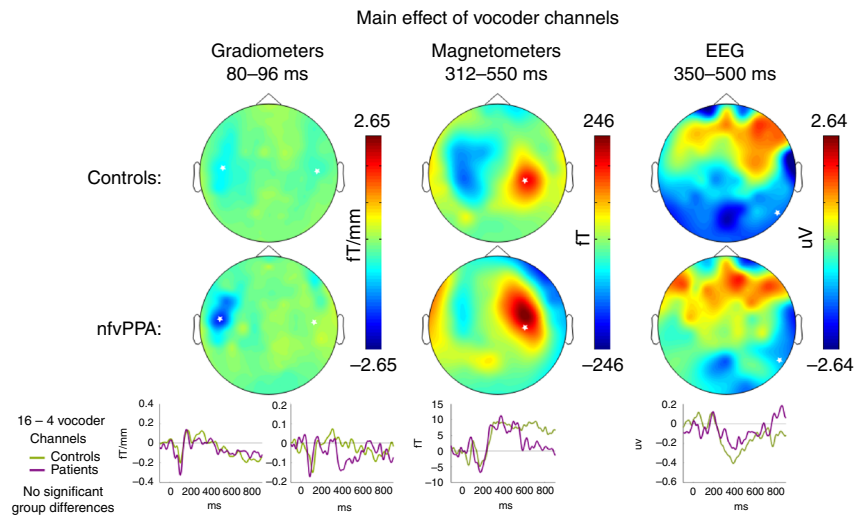


Fig. 3 The effect of vocoder channel number. Illustrative topographic plots are shown of the main effect of vocoder channels across all participants. No group by sensory detail interactions were observed either at the peak locations (marked by white stars) or in a confirmatory SPM analysis

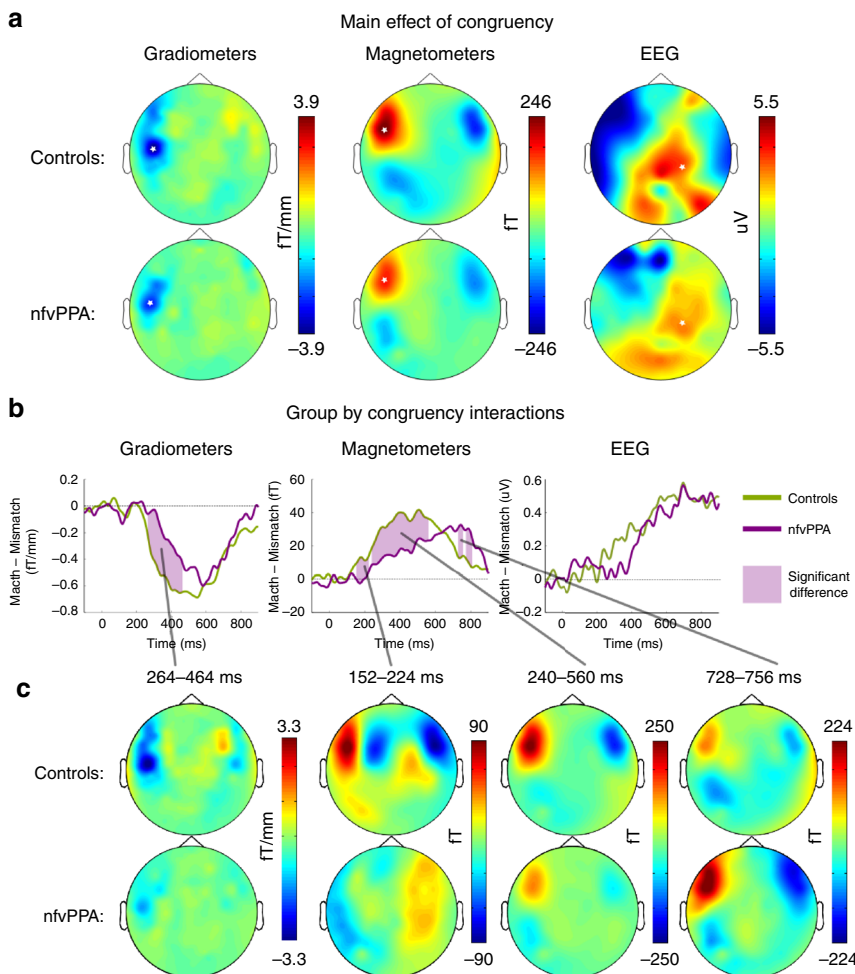


Fig. 4 The effect of prime congruency. **a** Illustrative scalp topographic plots of the main effect of cue congruency for each group from 400 ms to 700 ms, a period of where both groups showed a large statistical effect of congruency with similar topography. White stars indicate the scalp location of the peak congruency effect across both groups between -100 ms and 900 ms (FWE $p < 0.001$ for all sensor types). **b** Significant group by congruency interactions ($p < 0.05$ sustained for more than 25 ms at the scalp locations marked by white stars in the upper panel) were observed in planar gradiometers and magnetometers, and are shaded in lilac. **c** Topographic plots for each group are shown averaged across each significant cluster of group by congruency interaction

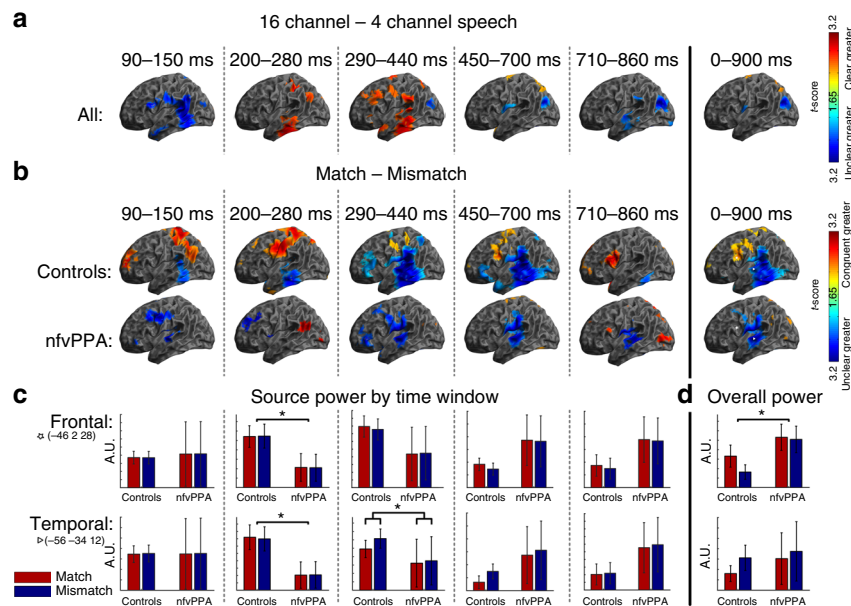


Fig. 5 Evoked source space analysis. **a** Evoked source reconstructions (sLORETA) for the main effect of clarity for all participants combined. **b** Source reconstructions for the main effect of congruency for each group individually. **c** Illustrative bar charts are plotted at the bottom for source power by group and condition in the frontal (IFG) and temporal (STG) regions of interest for each time window. A.U., arbitrary units. Statistically significant differences are marked by asterisks (detail in 'Results' section of text). Error bars represent the between-subject standard error of the mean (not the between condition standard error, which is much lower due to the repeated measures design). **d** Overall power in each source by group and condition across the whole time window of interest

Table 2 Repeated measures ANOVA of behavioural data from experiments 1 (Fig. 1b) and 2 (Fig. 1d)

A: Experiment 1	DF	F	p (Greenhouse-Geisser)
Group	1,40	7.7	0.011
Clarity	2,40	69.3	<0.001
Group * Clarity	2,40	17.1	<0.001
Congruency	1,40	1.2	0.287
Group * Congruency	1,40	13.2	0.002
Clarity * Congruency	2,40	2.3	0.140
Group * Clarity * Congruency	2,40	8.2	0.007
B: Experiment 2			
Group	1,120	10.9	0.003
Vocoder channels	2,120	5.8	0.015
Distractor difficulty	3,120	0.8	0.457
Group * Clarity	2,120	0.2	0.765
Group * Distractor difficulty	3,120	1.1	0.334
Vocoder channels * Distractor difficulty	6,120	4.2	0.004
Group * Vocoder channels * Distractor difficulty	6,120	1.8	0.149

Statistically significant rows at $p < 0.05$ are indicated in bold

condition at frontal and superior temporal voxels of interest defined by the main effect of congruency averaged across the whole epoch (Fig. 5d). No group differences were demonstrated in the earliest (90–150 ms frontal $F(1,18) = 0.06$, $p = 0.81$, temporal $F(1,18) < 0.01$, $p = 0.99$) or later (450–700 ms frontal $F(1,18) = 4.24$, $p = 0.054$, temporal $F(1,18) = 2.84$, $p = 0.11$, 710–860 ms frontal $F(1,18) = 3.10$, $p = 0.10$, temporal $F(1,18) = 2.96$, $p = 0.10$) time windows. Between 200 and 280 ms, there were significant main effects of group in both frontal ($F(1,18) = 6.37$,

$p = 0.02$) and temporal ($F(1,18) = 5.07$, $p = 0.04$) voxels, with greater responses in controls than patients. Between 290 and 440 ms, this main effect had dissipated (frontal $F(1,18) = 2.51$, $p = 0.13$, temporal $F(1,18) = 1.63$, $p = 0.21$), but there was a group by condition interaction, with controls showing a greater effect of cue congruency in the superior temporal ($F(1,18) = 4.46$, $p = 0.049$) but not the frontal ($F(1,18) = 0.76$, $p = 0.39$) voxel.

The analysis across the whole epoch is of particular interest. Across all individuals, a repeated-measures ANOVA (Supplementary Table 2) confirmed the pattern of opposing effects of prior knowledge in frontal and superior temporal regions seen in a previous study⁴⁰ ($F(1,134) = 60.1$, $p < 0.001$). However, there was a group by source by congruency interaction ($F(1,134) = 11.9$, $p = 0.001$), primarily driven by the absence of a significant effect of congruency in frontal regions in nfvPPA (Fig. 5b). When the total power in the frontal region was examined, a main effect of group was observed such that patients had significantly more frontal power than controls, but their modulation of frontal power by congruency was absent (Fig. 5d).

Behavioural experiment 1 vocoded word clarity rating. Given these neural differences, we sought to understand the perceptual correlates of neural delay in the reconciliation of predictions by examining the behavioural consequences of manipulations of prior knowledge in our two groups (Figs. 2a, 1c). All individuals reported that the perceptual clarity of vocoded words was significantly increased by matching text cues (Fig. 2b), but this effect was greater in patients with nfvPPA than in controls. A repeated-measures ANOVA revealed that Group, Number of Vocoder Channels and Cue Congruency were significant either as main effects or as part of two-way or three-way interactions (see Table 2, Experiment 1 for statistical details).

A replication experiment outside the MEG scanner confirmed that the difference between match and mismatch trials was due to a facilitatory effect of matching prior knowledge and not simply increased confusion in the face of mismatching priors: ratings of

perceptual clarity after a mismatching text cue were not statistically different from those after a 'neutral' or uninformative cue (repeated measures ANOVA $F(1,120) = 2.09, p = 0.15$). Furthermore, patients with nfvPPA had a much larger difference in clarity rating between 'neutral' and 'match' trials than controls (Supplementary Fig. 1C). It is important to note that participants were explicitly instructed to rate clarity across their own range of perceptual experience within the experiment, and were given training until they were able to do this. Comparing clarity ratings across groups is not, therefore, a direct measure of comparative listening difficulty as a rating of '1' simply means 'one of the least clear words I heard in the experiment', while a '4' means 'one of the clearest words I heard'. To fully assess the perceptual basis of our findings, we assessed the elements contributing to perceptual clarity with a further experiment and Bayesian modelling. These elements included: (1) patients' and controls' ability to identify degraded spoken words and (2) participants' introspective ability to perform higher-level estimation of the global precision of sensory input.

Behavioural experiment 2 vocoded word identification. To ensure that our finding was not a consequence of impaired word identification in patients leading to a group difference in reliance on prior knowledge⁴⁹, we performed a second experiment in which participants identified noise vocoded words in the absence of prior expectations (Fig. 2c). To reduce response demands for patients with non-fluent speech we used a four-alternative forced-choice identification task. All individuals with nfvPPA were above chance at identifying even the most degraded vocoded speech and, as a group, performed almost as well as controls (Fig. 2d). Both groups were influenced in the same way by the number of noise vocoder channels and the number of close distractor items presented as alternatives in the forced choice. As expected, it was easier for all individuals to identify words with more vocoder channels and if there were fewer close distractor items. This effect was strongest for the most degraded speech, manifesting as an interaction between vocoder channels and distractor difficulty (Table 2, Experiment 2).

Crucially, these data show that a lower-level impairment in perceiving vocoded speech cannot be the sole explanation of our finding of an increased congruency effect in nfvPPA patients. Patients performed better at identifying speech with eight channels than controls did with four channels (repeated measures ANOVA $F(1,63) = 7.1, p = 0.015$). Yet, patients still display a larger congruency effect for 8-channel vocoded words than controls do for 4-channel speech ($t(20) = 2.17, p = 0.04$). Hence, the magnitude of congruency effects in clarity rating is not simply related to objective abilities at word identification, but rather reflects a difference in the mechanisms by which prior knowledge influences lower-level perceptual processing. We investigate the nature of this effect with a Bayesian perceptual model combining word report and clarity rating data.

Bayesian modelling of experiments 1 and 2. To dissociate changes in the precision of predictions from difficulties with higher level estimation of the precision of sensory input, we performed hierarchical Bayesian inference simulations (c.f. ref.³³; Supplementary Fig. 2). Individual differences in word discriminability were accounted for by defining the precision of sensory input for each subject as the percentage above chance for word identification at each vocoder channel number in Experiment 2. This allowed us to individually optimise two free parameters against the clarity ratings measured in Experiment 1. These parameters were the precision of prior expectations (as measured by their standard deviation), and a perceptual threshold below which the observer rated speech as unclear (Supplementary

Fig. 2). The model explained 97.6% of the variance in the group-averaged clarity ratings (Fig. 2e). 99.4% of the variance could be explained by additionally accounting for non-linearities in the effect of the increasing sensory detail on perceptual clarity beyond 16 vocoder channels, but analysis of the Akaike information criterion suggested that this increase in variance explained did not outweigh the loss of parsimony compared to the simpler model (see Supplementary Discussion). The simpler model was therefore retained, but all of the group differences and associations between model outputs and neurophysiology reported in the results that follow remained significant if the complex model were used.

Patients had significantly more precise prior expectations than controls (Wilcoxon rank sum $U(11,11) = 83, p = 0.005$; Fig. 2f). There was a trend towards patients having lower perceptual thresholds ($U(11,11) = 99, p = 0.075$), meaning that patients required less sensory detail to give a clarity rating of 2 or higher, reflecting an appropriate downwards extension of the subjective clarity scale rather than a higher level introspective deficit resulting in patients not being ideal observers of their sensory experience (see 'Discussion'). The model results confirm that the consequence of degraded neural mechanisms for sensory predictions is not that the brain is unable to use prior knowledge (written cues) to modulate perception, but rather that patients with nfvPPA apply their prior knowledge with greater precision and inflexibility.

Induced oscillatory dynamics. To examine the effects of nfvPPA and task manipulations on induced oscillatory activity, we performed a time–frequency analysis of the planar gradiometer data, averaged across sensors (Fig. 6). First, we inspected the neural instantiation of predictions by analysing induced activity during the period following presentation of the written word but before the onset of the auditory stimulus. Based on recent studies in the auditory domain we expected this updating of predictions to manifest as an increase in beta frequency oscillations preceding the onset of the spoken word¹⁹. This was confirmed by SPM analysis across time–frequency space in our cohort, with a significant increase in beta power (10–28 Hz) for both groups of participants beginning around 800 ms after the onset of the written word, i.e. a~250 ms before the onset of the spoken word (cluster FWE $p = 0.001$, Fig. 6). At the time (992 ms) and frequency (24 Hz) of the peak effect for both groups overall, the single subject magnitude of the induced response correlated significantly with their precision of prior expectations as simulated by our behavioural Bayesian model (Pearson's $r(19) = -0.52, p = 0.017$; Spearman's $\rho = -0.54, p = 0.012$). A confirmatory SPM across the whole time window confirmed the group difference implied by this relationship, with patients displaying a single cluster of greater induced beta (20–34 Hz) power from 868 ms (cluster FWE $p = 0.010$). There were no induced effects that were greater in controls than in patients.

Second, we complemented our evoked analysis by assessing oscillatory power during the reconciliation of predictions, i.e. after the onset of the spoken word, averaged across sensors. The results in this section were not altered by subtraction of the condition-averaged evoked waveform subtracted from every trial, confirming that these are true induced responses rather than high-frequency contamination from the evoked responses described previously. Figure 7a illustrates the oscillatory power induced by hearing noise vocoded speech for each group, normalised to the pre-visual stimulus baseline and averaged across the whole brain. Across all conditions, the general pattern was for increased alpha and beta power for the first ~200 ms, followed by a desynchronisation from ~200 ms onwards.

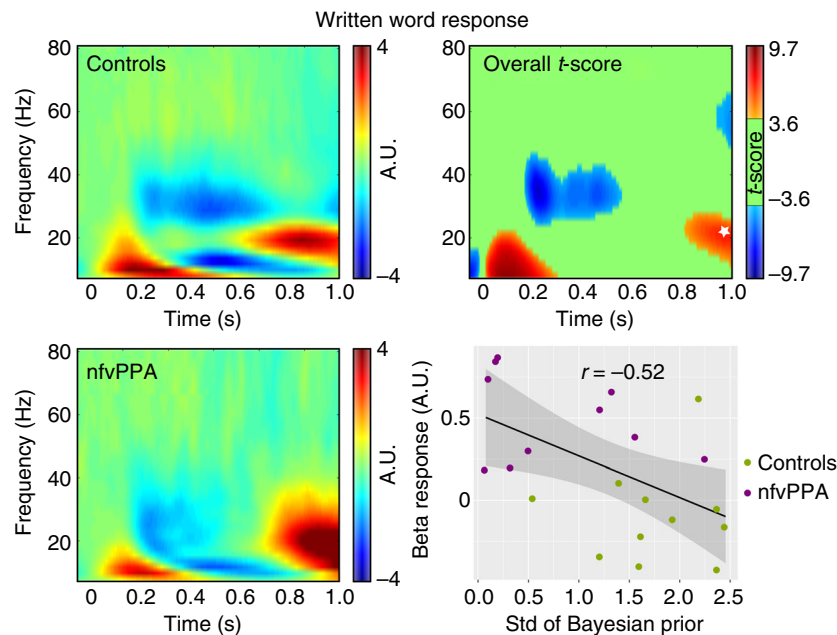


Fig. 6 Analysis of induced responses after the written but before spoken word. Total induced power after written word onset by group, the overall t -score for difference from baseline for both groups combined, and the relationship between single subject response at the late beta peak (indicated by a white star) and precision of their prior expectations in the Bayesian behavioural model. A.U., arbitrary units. The grey shaded area in the bottom right plot indicates the 95% confidence band for the regression line, marked in black

SPM across time–frequency space demonstrated a significant main effect of congruency in both groups separately (Fig. 7a). In controls, this effect peaked at 436 ms at a frequency of 12 Hz (FWE $p < 0.001$), with greater suppression of this response for spoken words that matched prior written text. In patients, a similar effect was observed, also at 12 Hz, but with a later peak at 824 ms (FWE $p < 0.001$).

Across all 21 individuals SPM demonstrated two time–frequency clusters that showed a group by congruency interaction. In the first, extending from 276 to 444 ms between 4 and 24 Hz (peak 300 ms, 16 Hz), controls displayed a greater effect of congruency than patients (cluster FWE $p < 0.001$). In the second, beginning at 680 ms and extending beyond the end of the analysis from 6 to 34 Hz (peak 888 ms, 20 Hz), the interaction was reversed, with patients showing a greater effect of congruency than controls (cluster FWE $p < 0.001$). The scalp distribution and source localisations of this effect are illustrated in Supplementary Fig. 4: effects were restricted to the left hemisphere and localised to areas around superior temporal gyrus. Both interaction clusters remained significant (FWE $p \leq 0.002$) in a confirmatory analysis in which power was normalised to the pre-auditory stimulus baseline. To illustrate the time-course of this oscillatory dissociation, the data from all three sensor types were restricted to 12–24 Hz, encompassing the interactions in both directions, and the total effect of congruency on power in this band across the whole brain was plotted in Fig. 7b.

To investigate this delay in this beta response in individual patients, single subject time–frequency decompositions were performed and the time taken to reach 80% of the peak overall power contrast between matching and mismatching prior knowledge was defined for each subject. The effect latencies for controls were all tightly clustered between 275 and 400 ms (Fig. 7c). Every single patient was delayed compared to every single control, with a range of 412–1048 ms (Fig. 7d). In the patient group neural response latency was negatively correlated with grey matter volume in our left frontal region of interest ($r = -0.68$, $p = 0.042$; Fig. 7e) but not in our left temporal region of

interest ($r = 0.34$, $p = 0.36$; Fig. 7f). There was a trend towards a negative relationship between latency and the standard deviation of prior expectations, though this did not reach significance ($r = -0.37$, $p = 0.1$).

To summarise, all participants show the same congruency-induced reduction in activity in the STG, but nfVPPA patients are delayed in showing this response compared to controls. Thus, the differential response of patients and controls reflects a top-down effect of frontal neurodegeneration on brain responses in posterior regions that remain structurally intact (compare, Figs. 5b and 1e) and that respond normally to bottom-up manipulations of speech clarity (Fig. 3).

Coherence and connectivity during prediction reconciliation.

To determine whether these effects are due to frontal degeneration or fronto-temporal disconnection, we examined coherence and connectivity between the frontal and temporal lobe sources of interest (Fig. 5c) during the 900 ms immediately following the onset of each spoken word. We employed two MEG connectivity analysis methods that give complementary information concerning fronto-temporal dynamics during the reconciliation of predictions: Imaginary Coherence, which is immune to volume conduction effects and source spread⁵⁰ as well as differences in power⁵¹, and Granger causality. These analyses allow us to be confident that relationships we describe are true reflections of the underlying brain dynamics. Both groups had significant fronto-temporal coherence up to around 25 Hz (Fig. 8a). Coherence in the beta band (13–23 Hz) was significantly stronger in patients than controls (Fig. 8b). Therefore an overall reduction of fronto-temporal connectivity cannot explain our observed differences between nfVPPA patients and controls.

Imaginary coherence does not provide robust indices of directionality, because inter-regional interactions potentially occur over more than one oscillatory cycle. We therefore also examined Granger causal relationships between our sources of interest⁵². This metric allows us to look at the directionality of

non-zero-lag fronto-temporal interactions while still being relatively robust to volume conduction. Granger causality tests whether information from the past activity of one region can predict future activity in another better than its own past. Highly significant bi-directional Granger causal relationships were observed between temporal and frontal sources (Fig. 8c). To

compare these, while avoiding confounds due to differences in signal to noise ratio between regions and between individuals (which can alter the magnitude of Granger Causal relationships⁵⁰), we divided the magnitude of each frequency value by the across-frequency mean for each individual and region to create a profile of relative influence for each region at each frequency. This analysis demonstrated significantly stronger temporal to frontal Granger Causal relationships at low frequencies, while frontal to temporal influences were stronger at higher, beta band, frequencies (Fig. 8d). These findings are in agreement with a recent study of MEG connectivity during written language comprehension, which showed that rhythmic information from temporal and parietal lobes was carried at lower frequencies than that from frontal cortex⁵³.

Overall, our finding of increased imaginary coherence in the patient group in a frequency band where frontal to temporal Granger causal influences predominate demonstrates that frontal neurodegeneration increases rather than reduces top-down connectivity from frontal to temporal regions during speech perception.

Discussion

The principal finding of this study is that neurodegeneration of the frontal language network results in the delayed neural resolution of predictions in temporal lobe. Conversely, the temporal lobe neural responses to bottom-up manipulations of sensory detail were not delayed. This proves that the resolution of sensory predictions is causally mediated by frontal regions in humans. Our source-space analysis demonstrates that frontal regions are working harder overall in nfvPPA patients. Our finding that, in the patient group, coherence is increased in a frequency band where frontal to temporal influences predominate, suggests that increased fronto-temporal interaction is required to reconcile excessively precise predictions. This view is supported by recent observations that left inferior frontal imaginary coherence is decreased in nfvPPA during the resting state⁵⁴, confirming that the increased fronto-temporal coherence we observe here reflects the specific engagement of these mechanisms during language perception and not simply a global upregulation. Together, the results of this study resolve a key controversy in speech perception by demonstrating that frontal regions play a core role in reconciling predictions with sensory input during speech perception²⁸⁻³⁰.

This observed impairment of predictive processing has significant perceptual consequences. Most strikingly, frontal neurodegeneration does not reduce the degree to which the brain employs contextual prior knowledge to guide lower-level speech perception. Rather, through Bayesian modelling, we show that prior knowledge of expected speech content is applied in an overly precise or inflexible fashion, thereby producing a larger-than-normal behavioural effect of prior knowledge on nfvPPA patients' ratings of speech clarity. In validation of computational

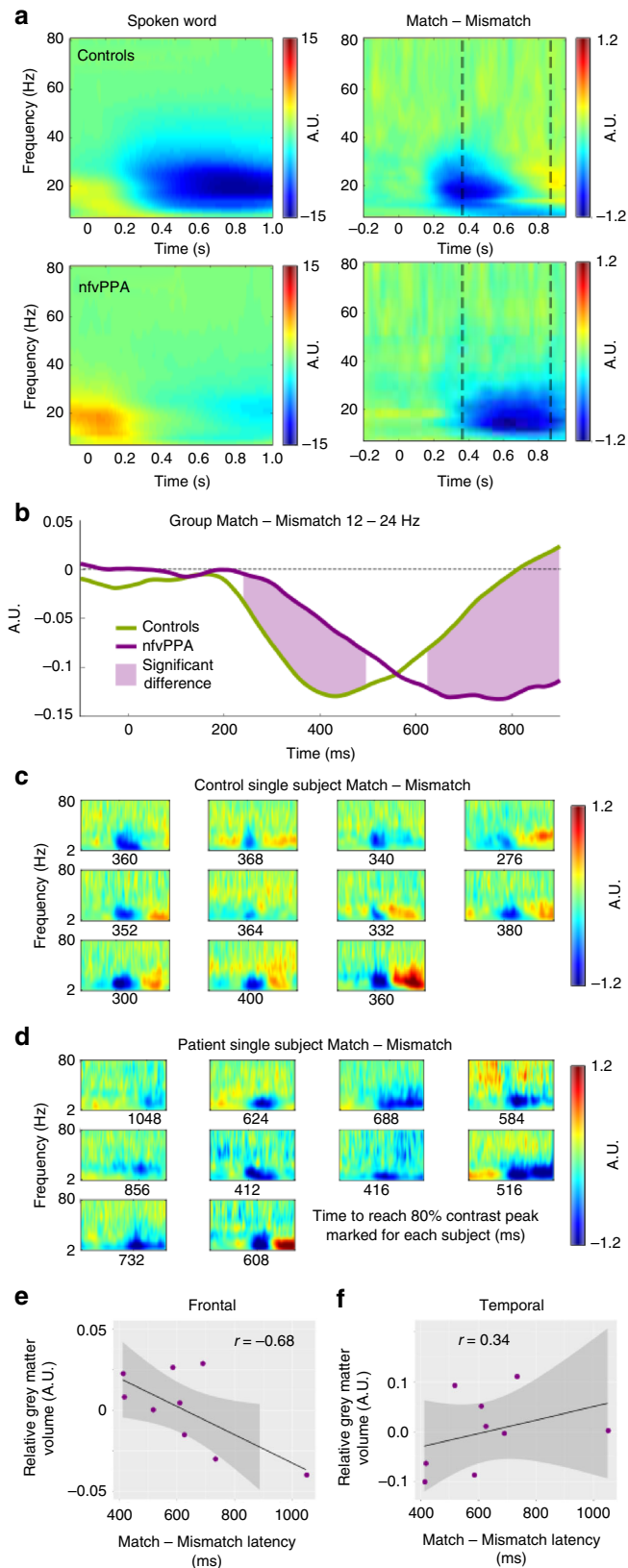


Fig. 7 Analysis of induced responses after the spoken word. **a** Total induced power after spoken word onset and main effect of cue congruency by group. **b** Overall induced power difference between Match and Mismatch conditions in the alpha/beta overlap range. **c** Single subject time-frequency profiles for each control. The time taken to reach 80% of the peak power contrast between Match and Mismatch trials is indicated for each individual by the number below the corresponding abscissa. **d** Single subject time-frequency profiles for each patient. **e** Significant negative correlation between frontal grey matter volume (adjusted for age and total-intracranial volume at the co-ordinates in Fig. 5c) and the time taken to express a congruency contrast (**d**). The grey shaded area indicates the 95% confidence band for the regression line, marked in black. **f** No significant correlation between similarly adjusted superior temporal grey matter volume and effect latency

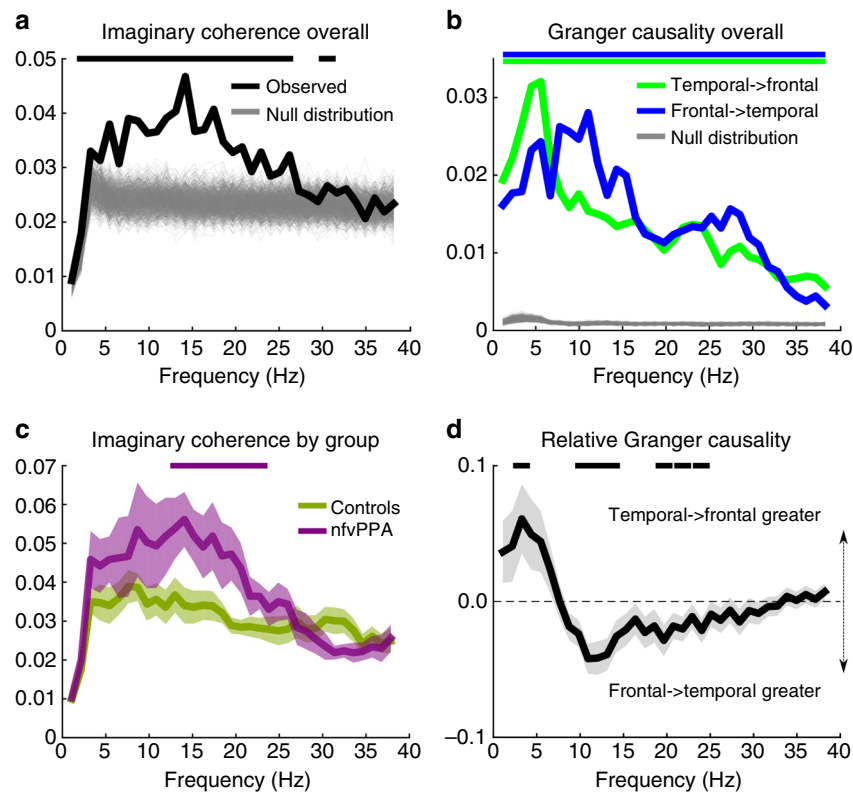


Fig. 8 Coherence and connectivity analysis. For the time series of frontal and temporal sources of interest between 0 and 900 ms after every spoken word onset. The evoked waveform was subtracted from the time series of frontal and temporal source activity between 0 and 900 ms after every spoken word onset before analysis. Horizontal lines at the top of each plot denote frequencies at which the line of matching colour statistically exceeds either the null distribution **a** and **c**, its counterpart condition (**b**) or differs from zero (**d**). **A**: Imaginary coherence. The median of the observed inter-source coherence is shown in black. 1000 randomisations of the null distribution are shown in grey. **b** Imaginary coherence by group. Shading represents standard error of the mean. **c** Granger causality. Median influences from temporal to frontal sources are shown in green and frontal to temporal sources in blue. 1000 randomisations of the null distribution are shown in grey. **d** Relative normalised Granger causal relationships between temporal and frontal sources by frequency. Grey shading represents the standard error of the directionality contrast in a repeated measures general linear model

and theoretical models of predictive coding^{19, 55, 56}, we demonstrate that the precision of participants' predictions correlates with the magnitude of induced beta-frequency oscillations, which have recently been shown to correspond temporally and quantitatively to the updating of predictions¹⁹.

Previous neuro-imaging evidence has suggested that frontally-mediated top-down predictions during speech perception are able to explain MEG response magnitudes^{33, 40} and fMRI pattern information in the superior temporal gyrus³². Here, we go beyond these associations and provide causal evidence for a functional contribution of frontal networks in supporting top-down predictions by demonstrating that disruption of these networks has the remote effect of delaying the reconciliation of predictions in temporal lobe regions that are anatomically intact, with striking behavioural consequences.

Patients with nfvPPA lacked normal modulation of frontal neural activity by cue congruency, were delayed in engaging frontal regions, and showed greater frontal activity and fronto-temporal coherence than control participants. This is analogous to the observation that elderly controls globally upregulate cognitive control networks that are selectively engaged by younger listeners only when speech is degraded, and thus appear to lack difficulty-related modulation of activity⁵⁷.

In contrast to these changes, patients displayed normal power of evoked neural responses for analyses combined over sensors and had normal neural responses to changes in sensory detail. These observations provide reassurance that the lack of atrophy in auditory regions of temporal lobe does not mask a microscopic

abnormality in auditory neural function. Similarly, it is reassuring that in both groups clarity ratings were similar for mismatching and neutral cues, and the response to questionnaires suggests similar ecological perception of speech in most conditions. This excludes trivial explanations for our behavioural results such as patients becoming confused by mismatches or having an altered approach to subjective rating scales. The group difference in uncued identification of vocoded speech was small, and was accounted for in our Bayesian modelling, by using the results of Experiment 2 to individually define the precision of the sensory input for each subject and number of noise vocoder channels. Thus, our observation of abnormal effects of cue congruency in nfvPPA cannot easily be explained by basic auditory processing deficits, or by higher signal detection thresholds.

Most strikingly, patients displayed a significant delay in the effects of cue congruency in temporal lobe in our sensor space, source space and induced analyses. Under the predictive coding framework, these effects arise because the integration of prediction error is an iterative process, whereby predictions are recursively updated in the light of sensory input to minimise error³². For the patients with nfvPPA, the degraded neural architecture and aberrantly precise predictions might mean that this updating requires more iterations and/or that each iteration takes more time. As a consequence more frontal activity and fronto-temporal coherence is observed, and reconciliation of predictions with sensory signals is delayed.

The behavioural data, Bayesian modelling and neurophysiological results all support the proposal that perceptual predictions

operate within an hierarchical generative network, which for speech perceptions spans auditory, superior temporal, and inferior frontal cortices. Predictive coding is one framework to understand such processing, and makes a number of specific claims about the nature of top-down and bottom-up signals, which we evaluate here.

Firstly, the spatial and temporal pattern of neurophysiological responses in elderly control participants replicated those previously demonstrated in young people⁴⁰, which have been successfully modelled in a predictive coding framework³³, and which cannot be effectively modelled by sharpening theories of neural representation³². Current instantiations of predictive coding models state that each stage of the processing hierarchy passes forwards to the next stage only prediction errors and backwards only predictions^{2, 3}. An alternative hypothesis—which might explain some of the present data—is that prior expectations are set up in frontal regions but not fed back to superior temporal regions^{41, 42}. When auditory input is received, a process of sensory analysis begins in temporal lobe, with the output fed forwards to frontal regions in real-time, where a matching process occurs. If frontal regions detect that the auditory information matches expectations, they indicate that further processing is unnecessary by feeding back a stop signal to temporal regions. Such a mechanism could also account for our observation of a delayed reduction in superior temporal activity when the text cue is matching. However, this stop-signal hypothesis is unable to account for an increase in top-down, frontal to temporal, connectivity in the patient group. It is also inconsistent with fMRI evidence demonstrating an interaction of prior knowledge and sensory detail in superior temporal representations of degraded speech³². These fMRI findings can only be simulated by a computational model in which superior temporal regions represent the discrepancy between predicted and heard speech (i.e. prediction error). In the predictive coding model, the delayed neural effects of cue congruency observed here reflect an iterative process whereby predictions are recursively updated to minimise error; this process operates more slowly in our patient group, and is reflected in greater fronto-temporal coherence.

Most models of prediction and perception, including our own Bayesian modelling, make the assumption that perceptual outcomes represent an ideal observation of peripheral sensation. This might not be the case if individuals hold aberrant beliefs about the fidelity of their sensory input based on differences in previous experience. The results of our Bayesian modelling are inconsistent with the view that our patients are not ideal observers of their sensory experience. If patients with nfvPPA had learnt that their auditory input were unreliable, this could only explain the present data by proposing a dissociation between an underestimation of the precision of their sensory input when reporting perceptual clarity (Experiment 1) and an intact ability to discriminate sensory features when distinguishing alternative vocoded words (Experiment 2)⁴¹. This would manifest in our Bayesian modelling as an increase in perceptual threshold, as any given distribution of sensory input would be reported as less clear. In fact, we found that patients did not statistically differ from controls in terms of their perceptual thresholds. Indeed, the trend was towards lower thresholds, which might reflect an appropriate downwards extension of the bottom-end of their perceptual clarity rating scale to reflect the fact that they were slightly less good at identifying vocoded speech than controls (Experiment 2), indicating that they had access to slightly less sensory detail during the experiment. Therefore, our behavioural results cannot be accounted for by patients with nfvPPA not being ideal observers of vocoded speech.

The hypothesis that beta oscillations represent the instantiation of predictions has existed for some time (see ref. ⁵⁶ for review). It

has been supported by evidence including computational simulations⁵⁵, and empirical observations of backward beta connectivity in speech processing⁵⁸. More recently, direct recordings from human auditory cortex have directly linked beta frequency oscillations to the updating of predictions¹⁹, based on correlations between observed brain activity and Bayes-optimal predictions generated from presented stimuli. In our cohort, we not only replicate the finding of beta oscillations as a correlate of prediction instantiation, but go further in demonstrating that, irrespective of disease status, the strength of this beta activity across participants relates to the precision of their predictions, as determined by our Bayesian behavioural modelling.

In clinic, patients with nfvPPA often complain of difficulties in hearing speech that are disproportionate to any measured deficits and resistant to hearing aids. We found a dissociation in subjective assessment between understanding speech in noise (which was rated as equally difficult for both groups), and speech in quiet (which only patients rated as difficult). Greater difficulty in quiet environments may seem counterintuitive at first, but it is consistent with the predictive coding hypothesis. Successful perception and comprehension of speech requires continuous updating of predictions based on sentential context and other cues. In a noisy environment, it is beneficial for listeners to rely heavily on these prior predictions as the patients do, because the sensory signal to noise ratio is poor. In a quiet environment, however, this is a suboptimal strategy as greater reliance can and should be placed on more precise or informative sensory inputs. If patients are unable to flexibly adapt the precision of their predictions to quiet listening environments, speech-in-quiet will remain difficult. It might be that globally strong predictions in nfvPPA are an adaptation to their inflexibility, as dysfunctioning networks are forced to choose one prediction strength for all scenarios. If, instead, predictions were globally weakened, this would be beneficial to the perception of speech-in-quiet but detrimental to speech-in-noise, perhaps having a greater overall cost to intelligibility in a dynamic environment (see ref. ¹⁴ for similar arguments in motor control).

We probed for subjective clarity ratings around 1050 ms after the onset of the spoken word (Fig. 2a). It could be argued that the abnormal precision of prior expectations in patients might be adaptive to the experimental context. Delayed processing might mean that they have less time for predictions to be enacted before a decision must be made, and therefore stronger predictions are required if they are to have meaningful effects. If so, our finding of increased prior precision in patients might be attenuated if clarity ratings were requested after a longer delay. However, predictions on this slower timescale would be of limited real-world consequence for speech perception and comprehension, because content-containing words such as nouns and verbs are separated by similarly short intervals in typical sentences⁵⁹, the temporal range in which human perception is optimal⁶⁰. Visual cues from lip reading also operate over millisecond timescales and are mediated by similar increases in fronto-temporal functional connectivity to those we demonstrate here⁶¹.

As well as explaining subjective difficulties with speech perception in nfvPPA, domain-general inflexibility in predictions could account for two other poorly understood behavioural abnormalities in this group. As shown in Supplementary Fig. 5 and Supplementary Results, we replicate the previous observation that deficits in basic auditory processing are overrepresented in patients with nfvPPA^{62, 63}; in Supplementary Discussion we provide a predictive coding explanation for this in terms of inflexible priors. Secondly, agrammatism is a prominent symptom in both nfvPPA and its vascular analogue Broca-type aphasia. Patients are observed to have particular difficulties understanding complex grammatical structures containing

hierarchical structures or the passive voice^{64, 65}. These structures are infrequent in daily language, and it would be reasonable to hold a prior expectation for more frequent, subject-oriented linear word orders. If patients are less able to flexibly modify this prior on the basis of violations (in this case grammatical cues), it could account for their selective behavioural impairment. This view is consistent with emerging perspectives of linguistic processing as a specialised function of a more general cognitive computational system for complex and flexible thought, based on dynamic functional interactions between inferior frontal and superior temporal cortex⁶⁶. It is empirically supported in our group by recent evidence demonstrating that patients with frontal-lobe aphasias are impaired at detecting violations of ordering relationships in structured auditory sequences, regardless of whether those sequences are constructed of linguistic or non-linguistic stimuli⁶⁷.

Methods

Ethics. All study procedures were approved by the UK National Research Ethics Service. Protocols for MEG and MRI were reviewed by the Suffolk Research Ethics Committee, and for neuropsychological tests outside of the scanner environments by the County Durham & Tees Valley Ethics Committee. All participants had mental capacity and gave informed consent to participation in the study.

Participants. Eleven patients with early nfvPPA were identified according to consensus diagnostic criteria³⁵. The diagnosis of degenerative language disorders is complex, but nfvPPA is characterised by an aphasia with prominent apraxia of speech and/or agrammatism but without problems in single-word comprehension or object knowledge and naming. Particular care was taken to exclude patients with yes/no confusion that would confound behavioural analysis, and to include only those who lacked the lexical difficulties of logopenic and mixed aphasias. This was done in order to select patients most likely to have underlying Tau or TDP-43 related pathology preferentially involving frontal lobes (rather than Alzheimer-type pathology of parietal lobes)^{39, 68–71}. On the short form of the Boston Diagnostic Aphasia Examination all patients scored 10/10 for responsive naming, 12/12 for special categories, at least 15/16 for basic word discrimination and at least 9/10 for following complex commands. One patient was unable to tolerate the MEG scanner environment so, in this specific case, contributed results only to the behavioural analysis.

We obtained standardised volumetric T1 MRI scans on nine of the patients within two months of their MEG session, which were used for co-registration and voxel-based morphometry.

Eleven age-, gender- and education-matched controls were recruited for behavioural and physiological studies (demographic information in Table 1). Thirty-six healthy age-matched control MRI datasets were selected for voxel-based morphometry.

Voxel Based Morphometry. Nine patients with nfvPPA underwent structural MR imaging at the Wolfson Brain Imaging Centre, University of Cambridge, UK using a 3T Siemens Magnetom Tim Trio scanner with a Siemens 32-channel phased-array head coil (Siemens Healthcare, Erlangen, Germany). A T1-weighted magnetisation-prepared rapid gradient-echo (MPRAGE) image was acquired with repetition time (TR) = 2300 ms, echo time (TE) = 2.86 ms, matrix = 192 × 192, in-plane resolution of 1.25 × 1.25 mm, 144 slices of 1.25 mm thickness, inversion time = 900 ms and flip angle = 9°. These images were compared to 36 healthy control scans with identical parameters.

All analysis was performed using SPM12 (<http://www.fil.ion.ucl.ac.uk/spm>). Images were first approximately aligned by coregistration to an average image in MNI space, before segmentation and calculation of total intracranial volume (TIV). After segmentation, a study-specific DARTEL template was created from the patient scans and the nine closest age-matched controls using default parameters. The remaining controls were then warped to this template. The templates were affine aligned to the SPM standard space using 'Normalise to MNI space' and the transformation applied to all individual modulated grey-matter segments together with an 8 mm FWHM Gaussian smoothing kernel. The resulting images were entered into a full factorial general linear model with a single factor having two levels, and age and TIV as covariates of no interest. This model was estimated in two ways. Firstly, a classical estimation based on the restricted maximum likelihood was performed to assess for group difference. Voxels were defined as atrophic if they were statistically significant at the peak FWE $p < 0.05$ level. Secondly, a Bayesian estimation was performed on the same model, and a Bayesian contrast between patients and controls specified. The resulting Bayesian map was subjected to hypothesis testing for the null in SPM12, resulting in a map of the posterior probability of the null at each voxel. For visualisation in Fig. 1e, this map was thresholded for posterior probabilities for the null above 0.7 and cluster volumes of greater than 1 cm³.

To assess for the dissociation between atrophic and preserved cortical regions, both model estimations were assessed at voxels of interest. Atrophic regions were assessed with classical SPM across the whole brain. This identified highly significant peaks centred in left (MNI [-37, 17, 7]) and right (MNI [37, 20, 6]) inferior frontal regions but no peaks in superior temporal regions (Supplementary Table 1). Superior temporal voxels of interest were therefore defined from the Neuromorphometrics atlas, at locations corresponding to left Heschl's gyrus within planum temporale (primary auditory cortex, MNI [-59, -24, 9]) and superior temporal gyrus (MNI [-67, -17, 3]). Frequentist probability of atrophy and Bayesian probability of no atrophy are reported at each of these four locations in results.

To create Fig. 1e, a rendering of the significant regions in each analysis, the DARTEL template images were further warped using the 'Population to ICBM Registration' function with the transformation parameters applied to all thresholded statistical maps.

To extract grey matter volume for correlation with the latency of MEG responses (Fig. 7e, f), a full factorial general linear model was constructed with the nine patients alone, with age and TIV as covariates of no interest. Each subject's age and TIV adjusted grey matter volume was extracted at the voxel closest to the MEG regions of interest (left frontal [-46 2 28]; left temporal [-56 -34 12]). A secondary SPM analysis with neural latency entered as a covariate into the model and small volume correction of 8 mm (to match the FWHM Gaussian smoothing kernel) at each location confirmed the results of the primary analysis—correlations below $p < 0.05$ were observed at the frontal but not the temporal location.

Modifications to the Sohoglu MEG paradigm. Stimuli and experimental procedures during neuroimaging were closely modelled on a task previously performed to evaluate influences of prior knowledge and sensory degradation in young, healthy listeners⁴⁰ (Figs. 1c, 2a). In this task, individuals are presented with a written word, followed 1050 (±50) ms later by a spoken word, which is acoustically degraded using a noise vocoder⁴⁶. After a further delay of 1050 (±50) ms, participants are asked to rate the perceptual clarity of the vocoded word. This allows for a factorial manipulation of two stimulus dimensions that in previous studies have been shown to affect speech perception: (1) the degree of correspondence between the written and spoken words can be modified by presenting text that either matches or mismatches with the speech, (2) the amount of sensory detail can be manipulated by varying the number of channels in the noise vocoder. 108 trials of each condition were presented across six blocks. Each block contained 18 trials of each combination of vocoder channel number and cue congruency in one of two fixed random orders counterbalanced across groups. To avoid predictability, each subject observed 216 words twice in written form and twice in spoken form (once as part of a match pair and once as part of a mismatch pair) and 108 words only once (in either a match or mismatch pair). The following modifications were made to the Sohoglu et al.⁴⁰ paradigm in order to simplify procedures for patients and elderly controls. The number of channels used in the vocoder was doubled to 4/8/16, the range expected to cover the steepest portion of the psychometric response function in older adults⁷². The duration of the visual prime was increased from 200 ms to 500 ms. The resolution of the clarity rating scale was reduced from 1–8 to 1–4, so that a four-button box could be used to indicate responses. Finally, the neutral priming condition was removed to reduce the overall number of trials inside the scanner by a third, while minimising the reduction in the power with which we could test for an effect of prime congruency. 108 trials of each condition were presented across six presentation blocks. A fully crossed 2 × 3 factorial design was employed, with two levels of prime congruency (matching/mismatching) and three levels of sensory detail (4/8/16 vocoder channels). Each spoken word was presented no more than twice to each participant, once with a congruent prime and once with an incongruent prime.

Behavioural data stimuli and procedure. To ensure that we were observing an effect of prediction and that patients were not simply being confused by mismatching written words, experiment 1 was repeated outside the scanner with identical parameters but an additional, neutral, cue condition (Supplementary Fig. 1C), mirroring that of ref.⁴⁰. Eighteen trials of each condition were presented in a single block.

A second experiment was undertaken to assess participants' ability to identify vocoded words. In this task, (Fig. 2c), no prior written text was provided. Participants simply heard a noise vocoded word and, 1050±50 ms after word onset, were presented with four alternatives, from which they selected the word that they had heard. We used this forced choice response format to ensure that performance was not confounded by speech production difficulties. As in Experiment 1, the clarity of the spoken word was varied between 4, 8 and 16 noise vocoder channels. The closeness of the three distractor items to the correct response was also varied by manipulating the number of neighbours between the spoken word and the alternatives. In the example shown in Fig. 2c, the spoken word is 'Gaze'. The alternatives presented to the participant comprised 'Daze' (an offset neighbour), 'Gaze' (the target), 'Game' (an onset neighbour), and 'Then' (not a neighbour). This set of four response alternatives occurred in trials where the spoken word was either: (1) "Gaze" (such that there were two word neighbours, "Daze" and "Game" in the response array), (2) "Daze" (only one onset neighbour, "Gaze"), (3) "Game" (one offset neighbour "Gaze"), or (4) "Then" (no neighbours in the response array). This achieved a factorial experimental design with a 3-level manipulation of

sensory detail fully crossed with a 4-level manipulation of distractor difficulty. There were 90 trials in a single block; at each of the three levels of sensory detail there were ten spoken words in each of cases (1) and (4) above, and five each in (2) and (3). This resulted in 30 sets of four response options each being presented three times and having three of its four members heard during the experiment. Word presentation orders were randomised across participants, but the sensory detail and written neighbour difficulty order was fixed.

Finally, we exactly replicated a subset of the tasks used by Grube et al.⁶² to demonstrate peripheral auditory processing deficits in nfvPPA. We selected a cross section of tasks on which the patients with nfvPPA had displayed particular difficulties, covering a range of processing from simple to complex. These comprised pitch change detection (Grube task P1), 2 Hz and 40 Hz frequency modulation detection (Grube tasks M1 and M2), and dynamic ripple discrimination (Grube task M4)⁶².

Auditory stimuli were presented in a quiet room through Sennheiser HD250 linear 2 headphones, driven by a Behringer UCA 202 external sound card, and visual stimuli were displayed on a laptop computer screen. Participants indicated responses either by pressing a number on a keyboard (clarity rating outside of MEG) or a button on a custom made response box (all other experiments).

Behavioural data modelling. Subjective ratings of clarity were modelled using an hierarchical Bayesian inference approach previously described for data of this type³³ (Supplementary Fig. 2). This model exploits the principles of predictive coding, in which perception arises from a combined representation of sensory input and prior beliefs^{4, 5, 73}. It is able to explain both the perceptual benefit of matching prior information, as the precision of the 'posterior' (or subjective experience) is increased by congruency between the prior and the sensory input, as well as the previously observed dissociated modulations of superior temporal gyrus activity by cue congruency and sensory detail^{33, 40}.

The model is able to predict subjective clarity as a function of the precision of the posterior distribution, which is estimated as the precision of the sensory input multiplied by a weighted function of the precision of the prior. The weighting given to the prior information depends on its congruency. In the case of a mismatching prior, the precision of the posterior simply matches the precision of the sensory input, while for matching priors it increases as a function of the precision of prior expectation. Finally, the precision of the posterior is compared against a perceptual threshold (below which degraded speech is deemed completely unclear and given a rating of 1), and the height above this threshold is mapped to the rest of the rating scale (participants were instructed to use the full range of the rating scale, and undertook practice trials to familiarise themselves with the range of experimental stimuli—all participants were able to do this).

The precision of the sensory input was individually pre-defined for each subject at each level of sensory detail, based on their measured ability to correctly report words with that number of vocoder channels (Fig. 2d). The weighting of matching prior information was defined as 0.5, reflecting the experimental context in which 50% of written words were congruent with (i.e. matched) the degraded spoken words. In open set listening situations like those used in the present experiment, the weighting of prior expectation for the occurrence of any uncued word is the inverse of the number of nouns in the participant's lexicon. We therefore approximated the weighting to zero for both mismatching and neutral prior expectations³². This accounts for the observation that clarity ratings in this and previous experiments were almost identical following mismatching and neutral (uninformative) written words^{27, 40}.

It is possible that the patients might have an inappropriately high weighting for the written cue. In other words, they apply their prior expectations inflexibly, being unable to account for the fact that they will only be correct half the time. As we have a binary situation (the text was either fully matching or fully mismatching) we are unable to assess this possibility directly—in our model allowing the weighting of matching prior information to vary would be mathematically equivalent to allowing the precision of the prior to vary. Accordingly, we use the terms 'excessively precise priors' and 'inflexible priors' interchangeably.

The precision of the prior expectation and the level of the perceptual threshold were then individually optimised to provide the best-fit to each subject's clarity ratings by global minimisation of squared residuals (using the Global Optimisation Toolbox in MATLAB).

Alternative data models. It was observed that model fits were less good for the mismatch condition in some controls, with the model systematically under-predicting slope. The primary driver of this effect seemed to be a washing out of the effect of prior knowledge in the face of very clear speech for some individuals (i.e. there is less perceptual clarity benefit to prior knowledge if the auditory token is itself very clear). This has been previously observed in young healthy individuals^{27, 40} and seems to result from participants nearing the upper end of their psychometric response functions and entering a region of non-linear response. That is, doubling from 8 to vocoder 16 channels results in more benefit in terms of perceptual clarity than doubling from 16 to 32 channels. Indeed, as can be observed from Fig. 2d many controls are reaching ceiling performance at reporting 16 channel vocoded speech in the absence of prior information. While we know that humans are able to detect sensory detail changes even in the face of unimpaired word identification (think, for example, of hi-fi reviews), it is not unreasonable to assume that these changes in

perceptual clarity might result in smaller rating changes than those that meaningfully improve word identification performance.

The model as originally formulated does not account for non-linearities of this type because the relative increase in the precision of the posterior distribution resulting from congruent prior expectations is modelled as being a constant function of sensory detail. In reality, congruent prior expectations are shifting the position on the psychometric response function (see ref. 27). As we do not have experimental data for higher degrees of sensory detail (for example unprimed 24 or 32 channel speech) we cannot account for this directly. If, however, we allow the weighting of prior expectations to vary in the Match case for 16 channel speech this would simulate the effect of entering a flatter portion of the psychometric response function. Doing this did improve the model fits overall by reducing the under-prediction of slope in the controls. Although this resulted in small changes in the optimised values of the other model parameters it did not affect any of the statistical results or relationships reported in the paper (the priors are still more precise in the patients at $p < 0.01$, and their precision still significantly correlates with beta power during the instantiation of predictions with $r = -0.51$).

We compared the performance of the original model and the new model with the Akaike information criterion (corrected for small samples, AICc), which assesses whether additional model parameters sufficiently improve the information provided to account for reductions in parsimony. The simpler (original) model was favoured for 10 of the 11 patients, and 8 of the 11 controls. On average, the simpler model had an AICc 4.02 points lower than the more complex model (lower AICc scores are better).

Therefore, we report the results of the simpler model in the main text. Overall, however, we take reassurance from the fact that both models result in the same statistical relationships between the precision of prior expectations and beta power during the instantiation of predictions.

MEG and EEG data acquisition and analysis. An Elekta Neuromag Vectorview System was used to simultaneously acquire magnetic fields from 102 magnetometers and 204 paired planar gradiometers, and electrical potentials from 70 Ag–AgCl scalp electrodes in an Easycap extended 10–10% system, with additional electrodes providing a nasal reference, a forehead ground, and paired horizontal and vertical electrooculography. All data were digitally sampled at 1 kHz and high-pass filtered above 0.01 Hz. Head shape, EEG electrode locations, and the position of three anatomical fiducial points (nasion, left and right pre-auricular) were measured before scanning with a 3D digitiser (Fastrak Polhemus). The initial impedance of all EEG electrodes was optimised to below 5 k Ω , and if this could not be achieved in a particular channel, or if it appeared noisy to visual inspection, it was excluded from further analysis.

During data acquisition, the 3D position of five evenly distributed head position indicator coils was monitored relative to the MEG sensors (magnetometers and gradiometers). These data were used by Neuromag Maxfilter 2.2, to perform Signal Source Separation⁷⁴ for motion compensation, and environmental noise suppression.

Subsequent pre-processing and analysis was undertaken in SPM12 (Wellcome Trust Centre for Neuroimaging, London, UK), FieldTrip (Donders Institute for Brain, Cognition, and Behavior, Radboud University, Nijmegen, The Netherlands) and EEG lab (Swartz Center for Computational Neuroscience, University of California San Diego), implemented in MATLAB 2013a. Artefact rejection for eye movements and blinks was undertaken by separate independent component analysis decomposition for the three sensor types. For MEG data, components were automatically identified that were both significantly temporally correlated with contemporaneous electrooculography data and spatially correlated with separately acquired template data for blinks and eye movements. For EEG data, components spatially and temporally consistent with eye blinks were automatically identified with ADJUST⁷⁵. These components were then projected out from the dataset with a translation matrix. Due to a technical difficulty during acquisition, one control subject had no signal recorded from two thirds of their EEG sensors, and one patient had seven sensors that failed quality control—these individuals were excluded from the EEG analysis, but included in MEG and behavioural analyses.

For evoked analysis, the data were then sequentially epoched from –500 to 1500 ms relative to speech onset, downsampled to 250 Hz, EEG data referenced to the average of all sensors, baseline corrected to the 100 ms before speech onset, lowpass filtered below 40 Hz, robustly averaged across epochs, refiltered below 40 Hz (to remove any high-frequency components introduced by the robust averaging procedure), planar gradiometer data were root-mean-square combined, all data were smoothed with a 10 mm spatial kernel and 25 ms temporal kernel before conversion to images in a window from –100 to 900 ms for statistical analysis.

For induced analysis, the de-artefacted continuous data were downsampled, re-referenced, baseline corrected as above, lowpass filtered below 100 Hz, notch filtered to exclude line noise between 48 and 52 Hz, then epoched, before being submitted to four separate time frequency decompositions by the Morlet wavelet method: two separate time windows of –500 to 1500 ms relative to written word and speech onsets were examined, with and without pre-subtraction of the condition-averaged waveform from every trial. These were robustly averaged and log rescaled compared to pre-visual baseline power in each frequency band. Morlet decomposition parameters were focused for sensitivity to low-mid frequencies, with seven wavelet cycles in a range from 4 to 80 Hz in steps of 2 Hz.

Sensor-space evoked analysis. For each sensor type separately, a flexible factorial design was specified in SPM12, and interrogated across all participants for main effects of prime congruency and clarity. For all sensor types, a scalp position of peak effect was defined where peak FWE $p < 0.01$. The sensor data at this scalp position was then compared across groups at every time point. A significant group \times condition interaction was defined as at least seven consecutive timepoints of $p < 0.05$, exceeding the temporal smoothing induced by lowpass filtering at 40 Hz. This approach does not represent double dipping as the location of interest was defined by an orthogonal contrast^{76–78}, and in any case for the effect of congruency (where group \times condition interactions were observed with this method), for both the planar gradiometers and the magnetometers the location of peak effect for patients alone was within 2 mm of the conjoint peak effect.

Evoked data source reconstruction. Source inversion methods by the sLORETA algorithm were identical to those employed by Sohoglu et al.⁴⁰, except that they were undertaken in SPM12 rather than SPM8. It was observed that the time windows of interest defined in healthy young controls were slightly earlier than the main data features in our cohort of more elderly controls, who displayed similar overall profiles to patients with nvPPA (Supplementary Fig. 3). The time windows of interest were therefore slightly lengthened and delayed, to ensure that the main data variance was captured.

The aim of the source data analysis was to localise and explore the brain basis of the group by congruency interaction statistically demonstrated in the sensor space data. While localisation of the main effect of clarity was undertaken across all individuals, and is shown in Fig. 5, in the absence of a group by clarity interaction in sensor space, no further analysis was performed on this condition.

From the previous studies in healthy young controls, it was anticipated that significant main effects of congruency would be observed in opposite directions in left frontal regions and left superior temporal gyrus. This was indeed the case, with a small left frontal region being significantly more active across the whole time window with Matching prior information, and a larger region centred on left superior temporal gyrus being significantly more active with Mismatching prior information. These peak locations were defined as voxels of interest, and the source power averaged for each condition at each location within every time window of interest for every individual. Independent, repeated measures ANOVAs were then performed in each time window. Those that demonstrated a statistically significant main effect of group or a group by congruency interaction are illustrated in Fig. 5c (the main effect of congruency was not examined, as this would represent double dipping at these voxels).

Sensor-space induced analysis. The primary analysis of induced data was undertaken in the planar gradiometers because of their superior signal to noise ratio for data of this kind⁷⁹. Other sensor types were examined secondarily to check for consistency of effect, which was confirmed in all cases. Visual inspection of the time \times frequency data at a variety of scalp positions revealed no clear difference in the pattern of effect (although its strength differed, as shown in Supplementary Fig. 4), so data were collapsed across all sensors for statistical comparison. A flexible factorial design was specified in SPM12 for time \times frequency data across a time window of -100 to 1000 ms, and interrogated across all participants for all contrasts of interest (main effects of group, prime congruency and sensory detail, all pairwise and the three-way interaction). A second, confirmatory, analysis was performed with the condition-averaged waveform subtracted from every trial with identical statistical results, demonstrating that the effects were induced rather than evoked (we make no claims as to whether they are dynamic or structural⁸⁰).

Induced data source reconstruction. The significant group by condition interactions observed in alpha and beta frequency bands were localised with the 'Data Analysis in Sensor Space' toolbox in SPM12. sLORETA was not available in this toolbox, so for closest comparability with the evoked reconstructions, the eLOR-ETA algorithm was used. Reconstructions used time frequency data at the frequency of maximum group \times congruency interaction, ± 6 Hz. Data were truncated at 50 principal components, to avoid any problems with beamforming after Signal Source Separation, which reduces the number of independent components in the data to around 70⁷⁴. Lead fields were calculated over a window of interest from 350 ms to 900 ms, and sources reconstructed in three separate time windows of equal duration defined by the sensor space group \times congruency interaction: 300–450 ms, where controls had a greater main effect of congruency; 450–600 ms, where there was no group \times congruency interaction; and 600–750 ms, where patients had a greater main effect of congruency. A flexible factorial design was specified in SPM12, and the group by congruency interaction (already statistically demonstrated across the whole brain) thresholded for visualisation at uncorrected $p < 0.01$.

Coherence and connectivity analyses. The timeseries of the frontal ($[-46, 2, 28]$) and temporal ($[-56, -34, 12]$) sources of interest (Fig. 5b) were extracted between 0 and 912 ms after every spoken word using the function `spm_egg_inv_extract`. The condition-averaged waveform (i.e. the evoked response) in each source was then subtracted from every trial to result in data with zero-mean and approximate stationarity within the time window of interest. The Fourier spectra were then

computed in FieldTrip using multitapers with a ± 4 Hz smoothing box. This decomposition was then subjected to separate FieldTrip connectivity analyses with either imaginary coherence or Granger causality. This same procedure was repeated 1000 times with the trial labels in each region shuffled to create a null distribution. Statistical assessment of the presence of coherence or connectivity at each frequency involved the comparison of the observed data against the null distribution (Fig. 8a, c). Between-group comparisons of imaginary coherence employed unpaired t -tests with unequal variance (the normality assumption was not violated), cluster corrected for multiple comparisons (Fig. 8b). To compare the strength of Granger causal relationships between regions, we first corrected for differences in signal to noise ratio between participants and regions by dividing the magnitude of each frequency value by the across-frequency mean for that individual-region pair. This created a profile of relative influence for each region at each frequency, corrected for overall differences in signal strength. At each frequency, the significance of 'directionality' (i.e. temporal to frontal vs frontal to temporal) was assessed with a repeated measures general linear model, and the output corrected for multiple comparisons (Fig. 8d).

Data availability. The processed data that support the findings of this study are available on request from the corresponding author T.E.C. The raw data are not publicly available due to file size, and because participant consent was not obtained for such data sharing, but anonymised data may also be requested for non-commercial academic research purposes. Code for the Bayesian behavioural modelling is available from https://github.com/thomascope/Bayesian_Model_Code. Code for MEG pre-processing and analysis is available from <https://github.com/thomascope/VESPA/tree/master/SPM12version/Standalone%20preprocessing%20pipeline>.

Received: 23 June 2017 Accepted: 27 October 2017

Published online: 18 December 2017

References

1. von Helmholtz, H. *Helmholtz's Treatise on Physiological Optics*, Wisconsin, Vol. 3 (Optical Society of America, 1925).
2. Hinton, G. E. Learning multiple layers of representation. *Trends Cogn. Sci.* **11**, 428–434 (2007).
3. Friston, K. Hierarchical models in the brain. *PLoS Comput. Biol.* **4**, e1000211 (2008).
4. Rao, R. P. & Ballard, D. H. Predictive coding in the visual cortex: a functional interpretation of some extra-classical receptive-field effects. *Nat. Neurosci.* **2**, 79–87 (1999).
5. Friston, K. A theory of cortical responses. *Philos. Trans. R. Soc. B: Biol. Sci.* **360**, 815–836 (2005).
6. Musmann, H. Predictive image coding. *Image Transm. Tech.* **73**, 112 (1979).
7. Murray, S. O., Kersten, D., Olshausen, B. A., Schrater, P. & Woods, D. L. Shape perception reduces activity in human primary visual cortex. *Proc. Natl Acad. Sci. USA* **99**, 15164–15169 (2002).
8. Alink, A., Schwiedrzik, C. M., Kohler, A., Singer, W. & Muckli, L. Stimulus predictability reduces responses in primary visual cortex. *J. Neurosci.* **30**, 2960–2966 (2010).
9. Arnal, L. H., Morillon, B., Kell, C. A. & Giraud, A.-L. Dual neural routing of visual facilitation in speech processing. *J. Neurosci.* **29**, 13445–13453 (2009).
10. Phillips, H. N. et al. Convergent evidence for hierarchical prediction networks from human electrocorticography and magnetoencephalography. *Cortex* **82**, 192–205 (2016).
11. Grahn, J. A. & Rowe, J. B. Feeling the beat: premotor and striatal interactions in musicians and nonmusicians during beat perception. *J. Neurosci.* **29**, 7540–7548 (2009).
12. Kilner, J. M., Friston, K. J. & Frith, C. D. Predictive coding: an account of the mirror neuron system. *Cogn. Process.* **8**, 159–166 (2007).
13. Shipp, S., Adams, R. A. & Friston, K. J. Reflections on agranular architecture: predictive coding in the motor cortex. *Trends Neurosci.* **36**, 706–716 (2013).
14. Wolpe, N. et al. Ageing increases reliance on sensorimotor prediction through structural and functional differences in frontostriatal circuits. *Nat. Commun.* **7**, 13034 (2016).
15. Brown, H., Adams, R. A., Pareés, I., Edwards, M. & Friston, K. Active inference, sensory attenuation and illusions. *Cogn. Process.* **14**, 411–427 (2013).
16. Pareés, I. et al. Loss of sensory attenuation in patients with functional (psychogenic) movement disorders. *Brain* **137**, 2916–2921 (2014).
17. Edwards, M. J., Adams, R. A., Brown, H., Pareés, I. & Friston, K. J. A Bayesian account of 'hysteria'. *Brain* **135**, 3495–3512 (2012).
18. Wolpe, N. et al. The medial frontal-prefrontal network for altered awareness and control of action in corticobasal syndrome. *Brain* **137**, 208–220 (2014).
19. Sedley, W. et al. Neural signatures of perceptual inference. *eLife* **5**, e11476 (2016).

20. Kumar, S. et al. A brain basis for musical hallucinations. *Cortex* **52**, 86–97 (2014).
21. Sumbly, W. H. & Pollack, I. Visual contribution to speech intelligibility in noise. *J. Acoust. Soc. Am.* **26**, 212–215 (1954).
22. Miller, G. A. & Isard, S. Some perceptual consequences of linguistic rules. *J. Verbal Learn. Verbal Behav.* **2**, 217–228 (1963).
23. Van Wassenhove, V., Grant, K. W. & Poeppel, D. Visual speech speeds up the neural processing of auditory speech. *Proc. Natl Acad. Sci. USA* **102**, 1181–1186 (2005).
24. McGurk, H. & MacDonald, J. Hearing lips and seeing voices. *Nature* **264**, 746–748 (1976).
25. Schwartz, J.-L. & Savariaux, C. No, there is no 150 ms lead of visual speech on auditory speech, but a range of audiovisual asynchronies varying from small audio lead to large audio lag. *PLoS Comput. Biol.* **10**, e1003743 (2014).
26. Remez, R. E., Rubin, P. E., Pisoni, D. B. & Carrell, T. D. Speech perception without traditional speech cues. *Science* **212**, 947–949 (1981).
27. Sohoglu, E., Peelle, J. E., Carlyon, R. P. & Davis, M. H. Top-down influences of written text on perceived clarity of degraded speech. *J. Exp. Psychol. Hum. Percept. Perform.* **40**, 186–199 (2014).
28. Park, H., Ince, R. A., Schyns, P. G., Thut, G. & Gross, J. Frontal top-down signals increase coupling of auditory low-frequency oscillations to continuous speech in human listeners. *Curr. Biol.* **25**, 1649–1653 (2015).
29. Fedorenko, E., Duncan, J. & Kanwisher, N. Language-selective and domain-general regions lie side by side within Broca's area. *Curr. Biol.* **22**, 2059–2062 (2012).
30. Meister, I. G., Wilson, S. M., Deblieck, C., Wu, A. D. & Iacoboni, M. The essential role of premotor cortex in speech perception. *Curr. Biol.* **17**, 1692–1696 (2007).
31. D'Ausilio, A. et al. The motor somatotopy of speech perception. *Curr. Biol.* **19**, 381–385 (2009).
32. Blank, H. & Davis, M. H. Prediction errors but not sharpened signals simulate multivoxel fMRI patterns during speech perception. *PLoS Biol.* **14**, e1002577 (2016).
33. Sohoglu, E. & Davis, M. H. Perceptual learning of degraded speech by minimizing prediction error. *Proc. Natl Acad. Sci.* **113**, E1747–E1756 (2016).
34. Murray, B., Lynch, T. & Farrell, M. Clinicopathological features of the tauopathies. *Biochem. Soc. Trans.* **33**, 595–599 (2005).
35. Gorno-Tempini, M. L. et al. Classification of primary progressive aphasia and its variants. *Neurology* **76**, 1006–1014 (2011).
36. Mohandas, E. & Rajmohan, V. Frontotemporal dementia: an updated overview. *Indian J. Psychiatry* **51**, S65–S69 (2009).
37. Mackenzie, I. R. et al. A harmonized classification system for FTLTD-TDP pathology. *Acta Neuropathol.* **122**, 111–113 (2011).
38. Gorno-Tempini, M. L. et al. Cognition and anatomy in three variants of primary progressive aphasia. *Ann. Neurol.* **55**, 335–346 (2004).
39. Rogalski, E. et al. Anatomy of language impairments in primary progressive aphasia. *J. Neurosci.* **31**, 3344–3350 (2011).
40. Sohoglu, E., Peelle, J. E., Carlyon, R. P. & Davis, M. H. Predictive top-down integration of prior knowledge during speech perception. *J. Neurosci.* **32**, 8443–8453 (2012).
41. Norris, D., McQueen, J. M. & Cutler, A. Prediction, Bayesian inference and feedback in speech recognition. *Lang. Cognit. Neurosci.* **31**, 4–18 (2016).
42. Norris, D., McQueen, J. M. & Cutler, A. Merging information in speech recognition: Feedback is never necessary. *Behav. Brain Sci.* **23**, 299–325 (2000).
43. McQueen, J. M., Norris, D. & Cutler, A. Are there really interactive processes in speech perception? *Trends Cogn. Sci.* **10**, 533–533 (2006).
44. McClelland, J. L., Mirman, D. & Holt, L. L. Are there interactive processes in speech perception? *Trends Cogn. Sci.* **10**, 363–369 (2006).
45. Lotto, A. J., Hickok, G. S. & Holt, L. L. Reflections on mirror neurons and speech perception. *Trends Cogn. Sci.* **13**, 110–114 (2009).
46. Shannon, R. V., Zeng, F. G., Kamath, V., Wygonski, J. & Ekelid, M. Speech recognition with primarily temporal cues. *Science* **270**, 303–304 (1995).
47. Henson, R. N., Mouchlianitis, E. & Friston, K. J. MEG and EEG data fusion: simultaneous localisation of face-evoked responses. *Neuroimage* **47**, 581–589 (2009).
48. Pascual-Marqui, R. D. Standardized low-resolution brain electromagnetic tomography (sLORETA): technical details. *Methods Find. Exp. Clin. Pharmacol.* **24**, 5–12 (2002).
49. Shankweiler, D. et al. Reading differences and brain: cortical integration of speech and print in sentence processing varies with reader skill. *Dev. Neuropsychol.* **33**, 745–775 (2008).
50. Nolte, G. et al. Identifying true brain interaction from EEG data using the imaginary part of coherency. *Clin. Neurophysiol.* **115**, 2292–2307 (2004).
51. Bowyer, S. M. Coherence a measure of the brain networks: past and present. *Neuropsychiatr. Electrophysiol.* **2**, 1 (2016).
52. Gow, D. W., Segawa, J. A., Ahlfors, S. P. & Lin, F.-H. Lexical influences on speech perception: a Granger causality analysis of MEG and EEG source estimates. *Neuroimage* **43**, 614–623 (2008).
53. Schoffelen, J.-M. et al. Frequency-specific directed interactions in the human brain network for language. *Proc. Natl Acad. Sci. USA* **114**, 8083–8088 (2017).
54. Ranasinghe, K. G. et al. Distinct spatiotemporal patterns of neuronal functional connectivity in primary progressive aphasia variants. *Brain* **140**, 2737–2751 (2017).
55. Bastos, A. M. et al. Canonical microcircuits for predictive coding. *Neuron* **76**, 695–711 (2012).
56. Arnal, L. H. & Giraud, A.-L. Cortical oscillations and sensory predictions. *Trends Cogn. Sci.* **16**, 390–398 (2012).
57. Erb, J. & Obleser, J. Upregulation of cognitive control networks in older adults' speech comprehension. *Front. Syst. Neurosci.* **7**, 116 (2013).
58. Fontolan, L., Morillon, B., Liegeois-Chauvel, C. & Giraud, A.-L. The contribution of frequency-specific activity to hierarchical information processing in the human auditory cortex. *Nat. Commun.* **5**, 4694 (2014).
59. Altmann, G. T. & Kamide, Y. Incremental interpretation at verbs: restricting the domain of subsequent reference. *Cognition* **73**, 247–264 (1999).
60. Cope, T. E., Grube, M., Singh, B., Burn, D. J. & Griffiths, T. D. The basal ganglia in perceptual timing: timing performance in Multiple System Atrophy and Huntington's disease. *Neuropsychologia* **52**, 73–81 (2014).
61. Giordano, B. L. et al. Contributions of local speech encoding and functional connectivity to audio-visual speech perception. *eLife* **6**, e24763 (2017).
62. Grube, M. et al. Core auditory processing deficits in primary progressive aphasia. *Brain* **139**, 1817–1829 (2016).
63. Goll, J. C. et al. Non-verbal sound processing in the primary progressive aphasias. *Brain* **133**, 272–285 (2010).
64. Grodzinsky, Y. The neurology of syntax: language use without Broca's area. *Behav. Brain Sci.* **23**, 1–21 (2000).
65. Goodman, E. & Bates, J. C. On the inseparability of grammar and the lexicon: evidence from acquisition, aphasia and real-time processing. *Lang. Cogn. Process.* **12**, 507–584 (1997).
66. Friederici, A. D., Chomsky, N., Berwick, R. C., Moro, A. & Bolhuis, J. J. Language, mind and brain. *Nat. Hum. Behav.* **1**, 713–722 (2017).
67. Cope, T. E. et al. Artificial grammar learning in vascular and progressive non-fluent aphasias. *Neuropsychologia* **104**, 201–213 (2017).
68. Sajjadi, S. A., Patterson, K., Arnold, R. J., Watson, P. C. & Nestor, P. J. Primary progressive aphasia: a tale of two syndromes and the rest. *Neurology* **78**, 1670–1677 (2012).
69. Sajjadi, S. A., Patterson, K. & Nestor, P. J. Logopenic, mixed, or Alzheimer-related aphasia? *Neurology* **82**, 1127–1131 (2014).
70. Rohrer, J. D., Rossor, M. N. & Warren, J. D. Alzheimer's pathology in primary progressive aphasia. *Neurobiol. Aging* **33**, 744–752 (2012).
71. Mandelli, M. L. et al. Healthy brain connectivity predicts atrophy progression in non-fluent variant of primary progressive aphasia. *Brain* **139**, 2778–2791 (2016).
72. Sheldon, S., Pichora-Fuller, M. K. & Schneider, B. A. Priming and sentence context support listening to noise-vocoded speech by younger and older adults. *J. Acoust. Soc. Am.* **123**, 489–499 (2008).
73. Hickok, G. The cortical organization of speech processing: feedback control and predictive coding the context of a dual-stream model. *J. Commun. Disord.* **45**, 393–402 (2012).
74. Taulu, S., Simola, J. & Kajola, M. Applications of the signal space separation method. *IEEE Trans. Signal Process.* **53**, 3359–3372 (2005).
75. Mognon, A., Jovicich, J., Bruzzone, L. & Buiatti, M. ADJUST: an automatic EEG artifact detector based on the joint use of spatial and temporal features. *Psychophysiology* **48**, 229–240 (2011).
76. Friston, K. & Henson, R. Commentary on: divide and conquer; a defence of functional localisers. *Neuroimage* **30**, 1097–1099 (2006).
77. Kriegeskorte, N., Simmons, W. K., Bellgowan, P. S. & Baker, C. I. Circular analysis in systems neuroscience: the dangers of double dipping. *Nat. Neurosci.* **12**, 535–540 (2009).
78. Kilner, J. Bias in a common EEG and MEG statistical analysis and how to avoid it. *Clin. Neurophysiol.* **124**, 2062–2063 (2013).
79. Muthukumaraswamy, S. D. & Singh, K. D. Visual gamma oscillations: the effects of stimulus type, visual field coverage and stimulus motion on MEG and EEG recordings. *Neuroimage* **69**, 223–230 (2013).
80. David, O., Kilner, J. M. & Friston, K. J. Mechanisms of evoked and induced responses in MEG/EEG. *Neuroimage* **31**, 1580–1591 (2006).

Acknowledgements

The authors would like to acknowledge assistance with the optimisation of stimulus presentation and MEG data acquisition from Maarten Van Casteren, statistical advice from Prof. Richard Henson, neuropathological opinion from Dr. Kieren Allinson, and contributions to behavioural interpretations from Dr. Dennis Norris. Most importantly, we would like to thank the patients and their families for giving so generously and freely of their time. This study was supported by the National Institute for Health Research, the Association of British Neurologists and Patrick Berthoud Charitable Trust (TEC fellowship); the Wellcome Trust (JBR Senior Fellowship, 103838); the Evelyn Trust; and the Medical Research Council Cognition and Brain Sciences unit (MC-A060-5PQ30, MC-A060-5PQ80).

Author contributions

The study was conceptualised by M.H.D. and J.B.R., and designed by T.E.C., E.S., K.P., C.D., M.G., R.P.C. and M.H.D. Data were collected by T.E.C. and J.W., and analysed by T.E.C. with assistance from E.S., W.S. and P.S.J. All authors contributed to interpreting the results and writing the paper.

Additional information

Supplementary Information accompanies this paper at [10.1038/s41467-017-01958-7](https://doi.org/10.1038/s41467-017-01958-7).

Competing interests: The authors declare no competing financial interests

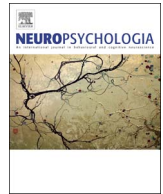
Reprints and permission information is available online at <http://npg.nature.com/reprintsandpermissions/>

Publisher's note: Springer Nature remains neutral with regard to jurisdictional claims in published maps and institutional affiliations.



Open Access This article is licensed under a Creative Commons Attribution 4.0 International License, which permits use, sharing, adaptation, distribution and reproduction in any medium or format, as long as you give appropriate credit to the original author(s) and the source, provide a link to the Creative Commons license, and indicate if changes were made. The images or other third party material in this article are included in the article's Creative Commons license, unless indicated otherwise in a credit line to the material. If material is not included in the article's Creative Commons license and your intended use is not permitted by statutory regulation or exceeds the permitted use, you will need to obtain permission directly from the copyright holder. To view a copy of this license, visit <http://creativecommons.org/licenses/by/4.0/>.

© The Author(s) 2017



Artificial grammar learning in vascular and progressive non-fluent aphasia



Thomas E. Cope^{a,b,*,1}, Benjamin Wilson^{b,1}, Holly Robson^c, Rebecca Drinkall^c, Lauren Dean^b, Manon Grube^b, P. Simon Jones^a, Karalyn Patterson^{a,d}, Timothy D. Griffiths^b, James B. Rowe^{a,d}, Christopher I. Petkov^b

^a Department of Clinical Neurosciences, University of Cambridge, UK

^b Institute of Neuroscience, Newcastle University, UK

^c School of Psychology and Clinical Language Sciences, University of Reading, UK

^d Medical Research Council Cognition and Brain Sciences Unit, Cambridge, UK

ARTICLE INFO

Keywords:

Aphasia
Grammar
Stroke
Frontotemporal dementia
Implicit learning

ABSTRACT

Patients with non-fluent aphasias display impairments of expressive and receptive grammar. This has been attributed to deficits in processing configurational and hierarchical sequencing relationships. This hypothesis had not been formally tested. It was also controversial whether impairments are specific to language, or reflect domain general deficits in processing structured auditory sequences.

Here we used an artificial grammar learning paradigm to compare the abilities of controls to participants with agrammatic aphasia of two different aetiologies: stroke and frontotemporal dementia.

Ten patients with non-fluent variant primary progressive aphasia (nfvPPA), 12 with non-fluent aphasia due to stroke, and 11 controls implicitly learned a novel mixed-complexity artificial grammar designed to assess processing of increasingly complex sequencing relationships. We compared response profiles for otherwise identical sequences of speech tokens (nonsense words) and tone sweeps.

In all three groups the ability to detect grammatical violations varied with sequence complexity, with performance improving over time and being better for adjacent than non-adjacent relationships. Patients performed less well than controls overall, and this was related more strongly to aphasia severity than to aetiology. All groups improved with practice and performed well at a control task of detecting oddball nonwords. Crucially, group differences did not interact with sequence complexity, demonstrating that aphasic patients were not disproportionately impaired on complex structures. Hierarchical cluster analysis revealed that response patterns were very similar across all three groups, but very different between the nonsense word and tone tasks, despite identical artificial grammar structures.

Overall, we demonstrate that agrammatic aphasics of two different aetiologies are not disproportionately impaired on complex sequencing relationships, and that the learning of phonological and non-linguistic sequences occurs independently. The similarity of profiles of discriminatory abilities and rule learning across groups suggests that insights from previous studies of implicit sequence learning in vascular aphasia are likely to prove applicable in nfvPPA.

1. Introduction

Aphasia is an impairment of speech and language that often leaves other cognitive and intellectual capacities preserved. Patients with non-fluent aphasias due to frontal lobe damage exhibit significant impairments in grammar (Caramazza and Zurif, 1976; Caplan et al., 1985; Berndt et al., 1996). The grammatical impairments in comprehension

and production are separable, but tend to be highly correlated (Berndt et al., 1983), suggesting that they stem from disruption of core syntactic processes rather than processes such as memory, executive function or motor function (Wilson et al., 2011). The deficits are phenomenologically similar in patients with damage due to neurodegeneration (non-fluent variant Primary Progressive Aphasia, nfvPPA) and stroke ('Broca's aphasia'), however detailed analysis of speech output has

Abbreviations: nfvPPA, Non-fluent variant Primary Progressive Aphasia; PNFA, Progressive Non-Fluent Aphasia; naPPA, nonfluent/agrammatic Primary Progressive Aphasia; PPA-G, Agrammatic Primary Progressive Aphasia

* Corresponding author at: Department of Clinical Neurosciences, University of Cambridge, UK.

E-mail address: thomascope@gmail.com (T.E. Cope).

¹ Authors contributed equally.

<http://dx.doi.org/10.1016/j.neuropsychologia.2017.08.022>

Received 28 April 2017; Received in revised form 15 August 2017; Accepted 17 August 2017

Available online 24 August 2017

0028-3932/ © 2017 The Authors. Published by Elsevier Ltd. This is an open access article under the CC BY license (<http://creativecommons.org/licenses/by/4.0/>).

revealed somewhat differential impairments (Patterson et al., 2006; Thompson et al., 2013). Impairments of receptive abilities have not been compared in similar detail.

Beyond these linguistic deficits, patients with aphasia also display auditory domain general processing deficits that are not specifically related to language (Caramazza and Zurif, 1976; Dominey et al., 2003; Patel et al., 2008; Christiansen et al., 2010; Goll et al., 2010; Grube et al., 2012; Geranmayeh et al., 2014b; Zimmerer et al., 2014a, 2014b; Zimmerer and Varley, 2015; Grube et al., 2016). Such studies have raised the possibility that deficits in structured sound processing may play a prominent role in language disorders, but the nature and extent of these deficits remains unclear. It also remains unclear whether impairments in aphasia are specific to the speech domain (Conway and Pisoni, 2008), or also apply to non-linguistic auditory sequences (Christiansen et al., 2010). One study identified impairments in implicit musical sequence learning in vascular aphasia (Patel et al., 2008), but direct comparisons outside of a musical framework are lacking. If artificial grammar learning tasks tap into domain general (rather than language specific) processes, one might expect rule acquisition to generalise from sequences of nonsense words to identically structured sequences of other sounds, such as tones.

It has been commonly held that grammatical impairments are specific to complex linguistic constructs such as hierarchical relationships and the passive voice (Goodman and Bates, 1997; Grodzinsky, 2000), but there is limited evidence for such dissociations (Zimmerer et al., 2014a, 2014b). By contrast, some studies suggest that the processing of adjacent relationships may be disproportionately impaired by frontal lesions involving motor association cortex (Opitz and Kotz, 2012). Recent studies examining artificial grammar learning in agrammatic aphasia secondary to stroke have focussed on linear sentential structures with varying transitional probabilities (Schuchard and Thompson, 2017). A key outstanding question, therefore, is whether agrammatic aphasia is characterised specifically by deficits for more complex linguistic structures or rather by a more global impairment in processing structured auditory sequences (Berndt, 2000).

Artificial grammar learning tasks are particularly well suited for delineating competence in structured sequence processing, as they focus on ordering relationships in the absence of other cues (e.g., semantics, phonology or pragmatics). They test learning of the rules governing the order in which stimuli occur in a sequence (Reber, 1967). Participants are typically exposed to sequences of stimuli that follow certain rules, so that the ordering relationships between the sequence elements can be learned implicitly. They are then tested with novel sequences that are either consistent with these rules or that violate them in some way, to assess learning. The implicit nature of these tasks allows the testing of a wide range of participants, including patients with aphasia. Unlike natural language tasks, it is possible to present structurally identical sequences comprised of different tokens, for example nonsense words or non-linguistic tone stimuli, to assess the contribution of phonological processing. Finally, artificial grammars with multiple levels of complexity can be used to quantify how well participants are able to learn increasingly complex rules, which may more closely reflect those in natural language grammars (Romberg and Saffran, 2013; Wilson et al., 2015).

The ability to process auditory sequences, even when stimuli are meaningless, is strongly linked with linguistic proficiency (Gómez and Gerken, 2000; Conway and Pisoni, 2008; Conway et al., 2010; Frost et al., 2015). Neuroimaging studies have demonstrated that artificial grammar processing engages a left-lateralised network of frontal, temporal and parietal brain areas similar to the set of regions involved in syntactic operations during natural language tasks (Friederici et al., 2000; Ni et al., 2000; Friederici and Kotz, 2003; Petersson et al., 2004; Forkstam et al., 2006; Friederici et al., 2006; Hickok and Poeppel, 2007; Bahlmann et al., 2008; Makuuchi et al., 2009; Folia et al., 2011; Friederici, 2011; Fedorenko et al., 2012; Petersson et al., 2012a, 2012b) and is associated with developmental language impairment (Evans

et al., 2009).

The sequence processing ability of patients with non-fluent aphasia has not been systematically compared across aetiologies. Non-fluent variant Primary Progressive Aphasia (nfvPPA), also variously known as Progressive Non-Fluent Aphasia (PNFA), nonfluent/agrammatic Primary Progressive Aphasia (naPPA), and Agrammatic Primary Progressive Aphasia (PPA-G), is an adult onset neurodegenerative aphasia characterised by agrammatism and speech apraxia (Gorno-Tempini et al., 2011). It is in many ways the neurodegenerative equivalent of Broca's aphasia, though some differences do exist in the pattern of speech output impairment (Patterson et al., 2006). The majority of cases are associated with primary tau pathology but a significant minority have TDP-43 related disease (Kertesz et al., 2005; Josephs et al., 2006; Knibb et al., 2006a, 2006b; Mesulam et al., 2014). nfvPPA typically leads to subtle structural neuroimaging changes in left inferior frontal and insular cortex (Gorno-Tempini et al., 2004), which correlate with clinical severity (Rogalski et al., 2011). Chronic non-fluent aphasia due to stroke (Broca's aphasia) results in a similar clinical phenotype of agrammatism and apraxia of speech. The left frontal tissue damage is stable, with partial clinical improvement over time (Kertesz and McCabe, 1977). The extent and pace of this improvement is variable and depends strongly on the integrity of the underlying white matter (Price et al., 2010; Seghier et al., 2016). Better understanding of the abilities of participants with similar symptoms arising from very different aetiologies could provide valuable insights into the neurobiological underpinnings of domain-general and language-related processes, and inform treatment strategies (Brownsett et al., 2014; Geranmayeh et al., 2014a, 2014b).

In the present study, patients with nfvPPA, non-fluent aphasia due to stroke, and matched controls were tested on their implicit learning of a mixed-complexity artificial grammar, combining sequencing relationships of increasing complexity using nonsense words or tones. We aimed to test the following linked hypotheses:

- 1) Rule acquisition differs when structurally identical sequences are comprised of nonsense words rather than non-linguistic tones.
- 2) Artificial grammar learning ability is similar in patients with vascular and neurodegenerative aphasia.
- 3) Grammatical impairments in aphasic patients are disproportionately greater for complex, configurational or hierarchical, sequencing operations.
- 4) Patients with aphasia can improve their ability to detect grammatical disruptions with repeated implicit training.

2. Methods

2.1. Participants

Three groups of participants were recruited. Demographics of the groups are outlined in Table 1. All patients were right handed. One control was left handed. Thirteen patients with mild to moderate nfvPPA were identified from specialist cognitive clinics led by authors JBR and TDG according to consensus diagnostic criteria (Gorno-Tempini et al., 2011). These criteria were strictly applied; particular care was taken to exclude non-fluent patients who had lexical

Table 1
Subject demographics. Mean (s.d., range). Age leaving education is reported as it is a better measure of highest scholastic attainment than number of years in study. No individuals were mature students.

	Control	nfvPPA	Stroke
Number	11	10	12
Age	69 (8, 54–79)	73 (7, 63–82)	60 (11, 33–74)
Age leaving education	18 (2, 15–22)	18 (3, 15–25)	20 (4, 15–26)
Years of musical training	2 (3, 0–10)	1 (1, 0–3)	3 (5, 0–13)

difficulties, in order to select patients most likely to have underlying Tau or TDP-43 related pathology preferentially involving left frontal lobes, rather than Alzheimer-type pathology of parietal lobes (Rogalski et al., 2011; Rohrer et al., 2012; Sajjadi et al., 2012, 2014; Mandelli et al., 2016). Three patients were excluded on the basis of yes/no response confusion (a common early symptom in nvPPA that might otherwise have reduced our power to detect language specific effects), resulting in 10 complete nvPPA datasets. On the short form of the Boston Diagnostic Aphasia Examination (BDAE) (Goodglass et al., 1983) all patients scored 10/10 for responsive naming, 12/12 for special categories, at least 15/16 for basic word discrimination and at least 9/10 for following complex commands. While nvPPA exists on a spectrum, with differing ratios of speech apraxia and agrammatism, all of our patients displayed some degree of impairment of expressive grammar in free speech, and all but two displayed impairment of receptive grammar as measured by the sentence comprehension task on the ‘verb and sentences test’ (VAST) (Bastiaanse et al., 2003) (mean 87.5%, range 70–100%). Similarly, the patients varied in their degree of expressive agrammatism, but none was completely unimpaired. Samples of speech from the participants are available in supplementary materials, and speech profiles are shown in Fig. 1A. BDAE profiles were independently rated by authors TEC, HR and KP. Inter-rater reliability for grammatical form was high, with pairwise Pearson correlations of 0.87, 0.85 and 0.85. Areas of significant grey or white matter loss are shown in Fig. 1B, upper panel.

It is widely recognised that patients with nvPPA report difficulties with understanding speech (Goll et al., 2010; Cope et al., 2014; Grube et al., 2016). We asked the patients in this study to complete visual analogue scales assessing their difficulty with ‘Understanding speech in a quiet room’, ‘Telling the direction a sound is coming from’, ‘Understanding speech in a noisy restaurant’, ‘Hearing announcements at a bus or rail station’ as well as ‘How loud do people tell you your TV is?’ Compared to a matched group of controls, patients differed only in reporting more difficulty with ‘Understanding speech in a quiet room’ ($p = 0.02$). Of the Boston Diagnostic Aphasia Examination (BDAE) subscores, this difficulty was strongly correlated only with ‘Grammatical form’ ($r^2 = 0.778$, $p < 0.001$, Supplementary Figure 1).

Twelve patients with non-fluent aphasia due to left sided stroke were recruited from a volunteer database administered by author HR, supplemented by the identification of incident cases by regional research networks. Recruitment criteria were: a single stroke of at least six months chronicity resulting in at least one month of non-fluent aphasia, with MRI evidence of involvement of either left inferior trigone or operculum. Samples of speech from the participants are available in supplementary materials, and speech profiles (triple marked by authors TEC, HR and KP) are shown in Fig. 1A. On the whole, the stroke group had more severe language impairments than the nvPPA group. All had some degree of impairment of grammatical form in free speech, and all but two had impairment of receptive grammar on the VAST (mean 70%, range 40–100%). Lesion overlap maps are shown in Fig. 1B, lower panel.

Care was taken to recruit an appropriate control group. During development of the artificial grammar, extensive piloting developed structures for which learning was least influenced by years of education or performance on global cognitive tests. Nonetheless, it is important to minimise this potential confound by avoiding the use of biased volunteer panels, which tend to preferentially recruit highly educated individuals with supra-normal motivation in research tasks. Therefore, we recruited 8 neurological controls with either chronic inflammatory demyelinating polyneuropathy or multifocal motor neuropathy with conduction block, and three spouses of patients with nvPPA, resulting in 11 control datasets. These individuals were chosen to represent a cohort of age-matched individuals with healthy brains and similar levels of habitual neurological contact to the patient groups. All scored normally on the Addenbrookes Cognitive Examination – Revised (ACE-R) (mean 96/100, range 92–99) and Raven’s progressive matrices

(mean 47/60, range 37–60).

It was possible to perform pure tone audiometry in all patients with nvPPA, 9 of the 12 patients with stroke aphasia and 8 of the 11 neurological controls. This demonstrated that the groups had well matched and age-appropriate auditory acuity (Supplementary Figure 2).

2.2. Stimuli

The Artificial Grammar (AG) used here generates sequences of stimuli from 8 unique elements (Fig. 2A). These sequences are governed by a number of rules of increasing complexity. Rule 1) if a ‘C’ element occurs it must be immediately followed by a ‘D’ element. This represents a simple, invariant linear relationship between two adjacent sequence elements, and will henceforth be referred to as the ‘linear’ rule. Rule 2) all of the ‘A’ elements in the sequence must occur before all of the ‘B’ elements. This is a more complex rule, requiring the participants to recognise a general property of the sequences, and will henceforth be referred to as the ‘configurational’ rule (Zimmerer and Varley, 2015). Rule 3) each ‘A’ element type must be paired with the appropriate ‘B’ elements in embedded relationships (e.g., $A_1[A_2[A_3B_3]B_2]B_1$). This complex operation requires tracking both the number and the order of the ‘A’ elements and matching these to the subsequent ‘B’ elements, and is referred to as the ‘hierarchical’ rule.

Sequences consistent with the AG are generated by following any path of arrows from start to end in the illustrated state transition graph (Fig. 2A). Ten consistent sequences were used for the exposure phase of the experiment (Table 2). These sequences were of variable length and contained all of the legal transitions possible with the AG. The remaining subset of consistent sequences generated by the AG were kept for the subsequent testing phase, to allow us to present novel, previously unheard sequences (Table 2). During the testing phase, the participants were presented with 4 repetitions each of 6 consistent and 6 violation sequences, in a pseudo-random order. All test sequences were six elements long, meaning that sequence duration could not be used as a cue by participants. The six violation sequences contained two sequences with violations of each of the three AG rules (Table 2). This design allowed us to identify the specific features of the sequences to which the participants were sensitive.

We tested participants with identically structured sequences of both naturally spoken consonant-vowel-consonant (CVC) nonsense words and non-linguistic tone stimuli. The stimuli were designed to provide acoustic cues to highlight the relationships between some of the key sequencing relationships, as follows. In both the CVC and tone experiments, the ‘A’ and ‘B’ elements fell into distinct acoustic categories. In the CVC experiment the ‘A’ elements all took the form “s-vowel-f” (e.g., “sif”) while the ‘B’ elements were “g-vowel-k” (e.g., “gik”). In the tone experiment the ‘A’ elements were all upwards pitch sweeps while the ‘B’ elements were downward sweeps. Furthermore, the A_x-B_x relationships that are critical to Rule 3 were highlighted by the presence of the same vowel sounds in the nonsense word experiment (i.e., A_1 and B_1 both contain the central vowel ‘a’) or the tone height in the tone experiment (i.e., both the A_1 and B_1 pitch sweeps are centred on the same frequency). To ensure that the participants learned aspects of the AG during the exposure phase, rather than simply responding to acoustical properties of the stimuli, we designed the tone stimuli to avoid linear increases or decreases in pitch in the $A_1A_2A_3$ or $B_3B_2B_1$ parts of the sequences. Instead, the centre frequencies of the tone sweeps in such a sequence would be ‘mid-low-high-high-low-mid’. The ‘C’ and ‘D’ elements in the nonsense word experiment were designed to be clearly phonetically distinct from the ‘A’ and ‘B’ stimuli, and in the tone experiments they were continuous pure tones of high or low pitch. Example sequences are available to listen to in the supplementary materials.

The nonsense words were produced by a female speaker, recorded with an Edirol R-09HR (Roland Corp.) sound recorder, and combined into exposure and testing sequences using Matlab (100 ms inter-

A) Boston Diagnostic Aphasia Examination Profiles

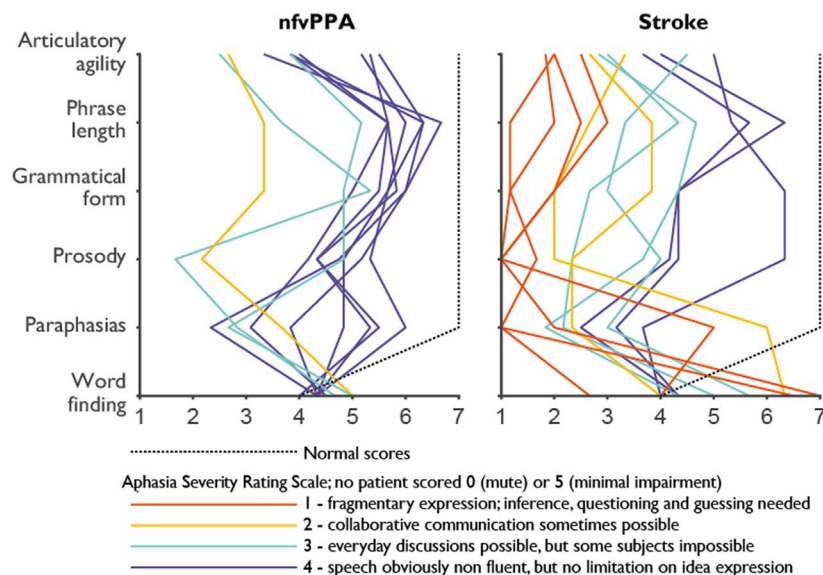
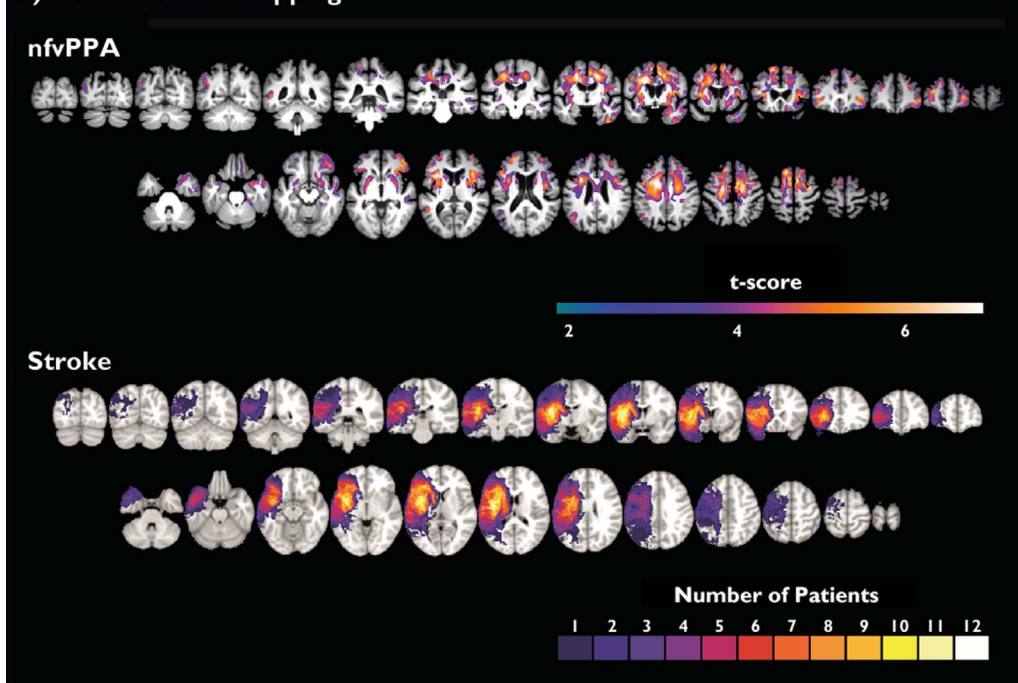


Fig. 1. A) Boston Diagnostic Aphasia Examination Profiles for nfvPPA and stroke groups. Normal values illustrated as broken black line. Colour coding of individual profiles based on Aphasia Severity Rating Scale; 1 = red, 2 = magenta, 3 = yellow, 4 = blue. No patients had an ASRS of 0 (no usable speech or auditory comprehension) or 5 (minimal discernible handicap). B) Upper: Voxel based morphometry of nfvPPA vs age-matched healthy controls. Coloured regions demonstrate cluster-wise significance at FWE < 0.05 with a cluster defining threshold of 0.001 for either grey or white matter volume. Lower: lesion overlap map for the stroke group. (For interpretation of the references to color in this figure legend, the reader is referred to the web version of this article.)

B) Patient Lesion Mapping



stimulus intervals, ISI). The average duration of the nonsense words was 477 ms (standard deviation = 7 ms). The tone stimuli were generated using Matlab. The low tone sweeps were linear sweeps between 100 and 150 Hz (i.e., A₂ began at 100 Hz and increased to 150 Hz, B₂ began at 150 Hz and decreased to 100 Hz). The middle tone sweeps spanned 200 to 300 Hz and the high tone sweeps spanned 400 to 600 Hz. The C and D stimuli were pure tones at 350 and 800 Hz respectively. The duration of all tones was 450 ms, and these were combined into sequences with ISIs of 100 ms. Stimuli were presented through Sennheiser HD250 linear 2 headphones, driven by either an Edirol UA-4X or Behringer UCA 202 external sound card. The amplitudes of all stimuli were root-mean-square (RMS) balanced, and sequences were initially presented to participants at ~75 dB SPL (calibrated with an XL2 sound level meter, NTI Audio). At the start of the exposure phase, participants were asked if this volume was comfortable

and clearly audible and, if not, were allowed to freely adjust the volume to their preference.

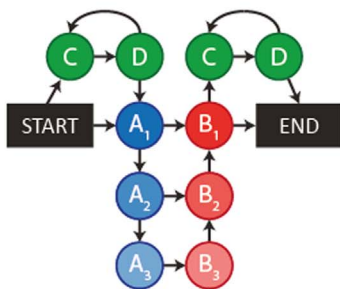
Exposure sequences and test sequences for the CVC and tone languages were presented in exactly the same fixed pseudo-random order. There were no differences between the orders of sequences in the CVC and tone runs; only the sound tokens used to represent each element in the artificial grammar differed.

2.3. Procedure

The experimental procedure and instructions given to participants were tightly constrained, to ensure that explicit learning strategies and the effect of receptive language difficulties were minimised. The exact wording of the instruction is included in supplementary materials.

Participants were exposed to the CVC language for five minutes.

A) Artificial grammar and sequences



Three Tasks

- Task 1: Nonsense word task
- Task 2: Tone sweep task
- Task 3: Oddball deviance detection task

Three levels of Sequence Complexity

- Level 1: **Linear** - C is followed by D
- Level 2: **Configurational** - all A elements occur before B elements
- Level 3: **Hierarchical** - each A element must be paired with the correct B

	Nonsense Words	Tones
A ₁	'saf'	Mid up sweep
A ₂	'sef'	Low up sweep
A ₃	'sif'	High up sweep
B ₁	'gak'	Mid down sweep
B ₂	'gek'	Low down sweep
B ₃	'gik'	High down sweep
C	'pob'	Low tone
D	'jat'	High tone

Example sequences

	Consistent	Violation
Linear	CDCDA ₁ B ₁	CCDDA ₁ B ₁
Configurational	A ₁ A ₂ B ₂ B ₁ CD	A ₁ B ₁ A ₂ B ₂ CD
Hierarchical	A ₁ A ₂ A ₃ B ₃ B ₂ B ₁	A ₁ A ₂ A ₃ B ₂ B ₃ B ₁

Fig. 2. A: Artificial grammar structure and stimuli. B: Cartoon illustrating the distribution of parametric decision variables for an hypothetical experiment with easy, medium and hard to detect rule violations. d' represents the single subject discriminability of each rule violation, while c and β represent different measures of bias (i.e. in our case the tendency to say that a sequence is grammatical if there is no evidence to the contrary). Each rule violation has its own d' measure, reflecting its respective discrimination difficulty, while the bias measures apply to the experimental context as a whole.

B) Distribution of Decision Variables

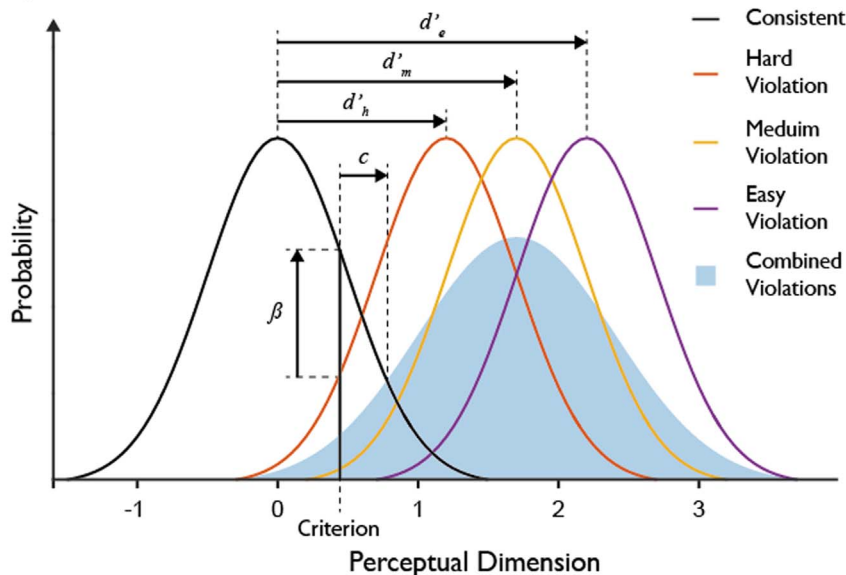


Table 2
Exposure and testing sequences.

Exposure Sequences	Testing Sequences		
A ₁ A ₂ A ₃ B ₃ B ₂ B ₁	A ₁ A ₂ A ₃ B ₃ B ₂ B ₁	Consistent	Familiar
CDA ₁ B ₁ CD	A ₁ B ₁ CD	Consistent	Familiar
A ₁ B ₁ CD	CDA ₁ B ₁ CD	Consistent	Familiar
A ₁ A ₂ B ₂ B ₁	CDA ₁ A ₂ B ₂ B ₁	Consistent	Novel
A ₁ A ₂ B ₂ B ₁	A ₁ A ₂ B ₂ B ₁ CD	Consistent	Novel
CDA ₁ B ₁	CDCDA ₁ B ₁	Consistent	Novel
A ₁ B ₁ CD	CCDDA ₁ B ₁	Violation	Violates Rule 1
CDCDA ₁ B ₁ CD	DCA ₁ B ₁ DC	Violation	Violates Rule 1
CDA ₁ A ₂ A ₃ B ₃ B ₂ B ₁	CDB ₁ A ₁ CD	Violation	Violates Rule 2
A ₁ A ₂ A ₃ B ₃ B ₂ B ₁ CD	A ₁ B ₁ A ₂ B ₂ CD	Violation	Violates Rule 2
A ₁ A ₂ A ₃ B ₃ B ₂ B ₁	A ₁ A ₂ B ₁ B ₂ CD	Violation	Violates Rule 3
	A ₁ A ₂ A ₃ B ₂ B ₃ B ₁	Violation	Violates Rule 3

During this time they were simply instructed to listen to the language and to pay attention to the order of the words (the exact script for the instructions is available as supplementary material). They were then tested by being asked to decide whether 48 individual sequences (Table 2) were correct (i.e. consistent with the artificial grammar) or incorrect (i.e. violated the artificial grammar in some way). Participants were able to express their decision either by pressing a button on a keyboard or custom made response box, or by pointing to yes or no on a piece of paper; whichever they found easiest. At the end of a run, general overall feedback was provided with smiley to sad faces (Wong and Baker, 1988) according to overall percentage correct, along with the performance descriptor 'Great!' (> 60%), 'Well' (55–60%), 'OK' (45–55%), or 'Badly' (< 45%). This exposure-test cycle was then repeated in an identical fashion for the tone language. Again, they were explicitly instructed that the important thing was the order of the sounds.

After a short break, participants were then re-exposed to the CVC

language for three minutes, before being re-tested. Sequences for both exposure and testing were presented in a different fixed pseudo-random order on each repetition. At the end of this run, feedback was provided relative to the previous CVC run with faces paired with the descriptors 'Much Better' (> 110% of previous score), 'Better' (105–110%), 'Same' (90–105%), or 'Worse' (< 90%). This procedure was then repeated for the tone language.

After a longer break, during which tea and biscuits were provided, participants completed a personal details questionnaire, which included questions about musical training and handedness (all patients were right handed). Patients then undertook the short form of the Boston Diagnostic Aphasia Examination (Kaplan, 1983) and the first half of the sentence comprehension section of the Verbs and Sentences Test to assess receptive grammar (Bastiaanse et al., 2003); controls completed an ACE-R and were tested on matrix reasoning (Raven, 1960), similarly demanding tasks of similar duration. Participants then completed another three minute exposure and test session on the CVC and tone languages, for a total of three testing sessions for each language.

Finally, each participant was re-exposed to the CVC language for three minutes, but the testing session that followed was replaced with an 'oddball' task. Participants were told that in this final test the 'incorrect' sequences were wrong in a different way, but were not explicitly instructed that they were listening for novel tokens. Where an ordering violation would first have occurred in an 'incorrect' sequence, the CVC token was replaced by a novel, previously unheard, oddball element ('fen', 'muz', 'rol', 'dut', 'boz' or 'cav'). In this way, we were able to assess whether differential performance on the three grammatical rule types was related to other undesired effects such as stimulus ordering.

All individuals undertook all study procedures on a single day, to ensure that differential patterns of performance consolidation during sleep did not confound our findings. The study procedures took up to four hours, including breaks.

2.4. Stroke lesion mapping

The lesioned area of each brain was manually defined on every slice of each patient's 3T T1-weighted MRI scan in FSL, resulting in a 3D lesion mask. The resulting image was then registered to the standard MNI152 brain using FLIRT (FMRIB's Linear Image Registration Tool (Jenkinson and Smith, 2001); affine transformation model, 12 degrees of freedom). This registration matrix was used to register the patient's lesion mask to the standard space, from which a standardised lesion volume was computed in Matlab. Regions of interest in the left hemisphere (frontal inferior trigone, frontal inferior operculum, rolandic operculum, putamen and caudate) were identified using the aal atlas in SPM12, and the percentage of each sub-region that was lesioned was extracted for analysis (Supplementary Table 1).

2.5. nfvPPA atrophy mapping

Nine of the patients in the nfvPPA group underwent a 3T volumetric T1 MRI scan. From a database of healthy control scans from the same scanner, an age-matched normative sample of 36 individuals was selected by finding the four nearest-neighbours to each patient in terms of age, excluding duplication (mean age of these controls was 73 years). After segmentation, the nine nfvPPA scans and nine nearest-neighbour controls were used to create a DARTEL template. This was then applied to the remaining 27 controls. Resultant images were normalised to MNI space in SPM12 with an 8 mm smoothing kernel, and separate statistical comparisons were performed for grey and white matter, with total intracranial volume and age as covariates (Fig. 1B).

As for the stroke lesion mapping, regions of interest in the nfvPPA patients were then identified using the aal atlas, normalised to MNI space. As distinct from the lesion analysis in the stroke cases, these regions were defined bilaterally. The grey matter volume in each region

was then extracted by applying these regions to each individual's modulated, warped grey matter segmentation and correcting for total intracranial volume.

2.6. Analysis

Performance metrics for analysis were based on signal detection theory (Stanislaw and Todorov, 1999). Standard signal detection measures of discriminability and bias rely on the underlying trial difficulty within a run being constant. In our artificial grammar, it was expected that violations of the linear relationship (complexity level 1) would be easier to detect than configurational violations (complexity level 2), which in turn might be easier to detect than violations of the hierarchical structure (complexity level 3) (see Fig. 2B). To accommodate this, we separately calculated d' and the non-parametric equivalent A' , based on a comparison of performance on each of the three types of violation sequence to all of the consistent sequences. A single value for bias measures was also calculated based on the combined distribution of violation sequences (Fig. 2B). Hit and false alarm rates of 1 were replaced with $(n-0.5)/n$ (where n is the number of trials), and those of 0 with $0.5/n$ (Macmillan and Kaplan, 1985; Stanislaw and Todorov, 1999). The non-parametric analogues of these signal detection metrics, A' for discriminability and β'' for bias, were used for the primary analysis.

All statistical analyses were performed in Matlab R2015b with the Statistics and Machine Learning Toolbox unless otherwise specified. Differences from chance performance in both discriminability measures (A' and d') and measures of bias ($\ln(\beta)$, c and β'') were assessed for each group and condition separately using one-sample Wilcoxon signed rank tests (the non-parametric equivalent of the one sample t -test).

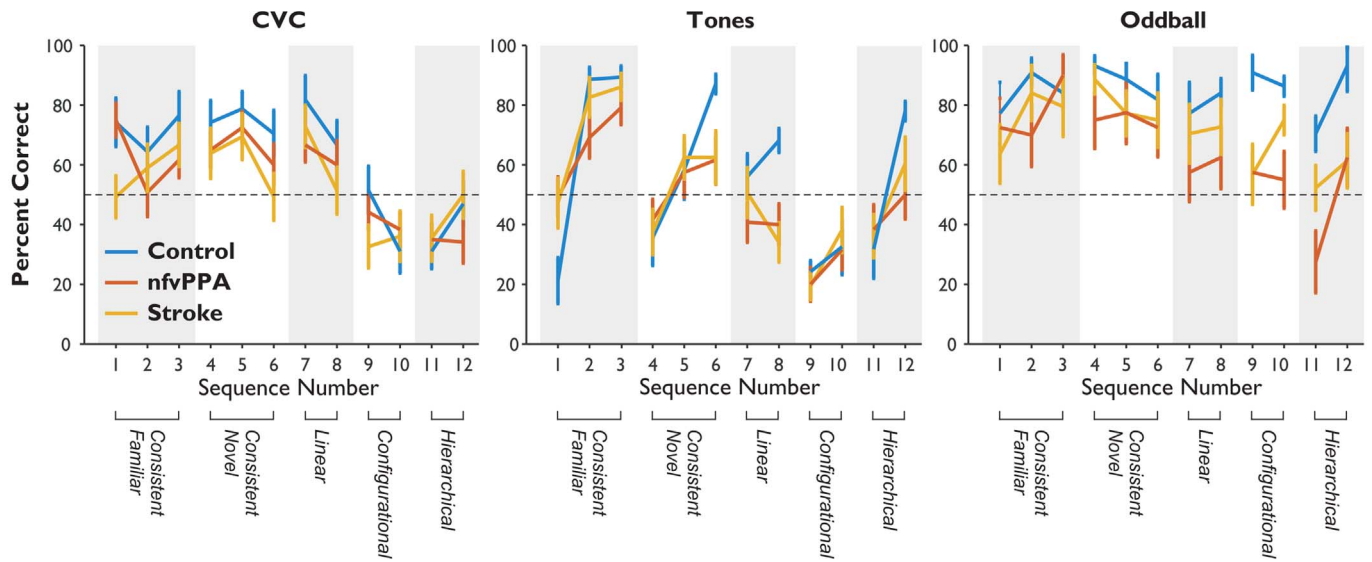
The effects of group and rule complexity on discriminability were assessed with three separate repeated measures ANOVA tests (one for each test type: CVC, tones and oddball), with the factor 'participant number' nested within 'group'. This parametric statistical test was employed because there is no appropriate non-parametric test for repeated measures designs of the kind employed here; the Friedman test does not allow multiple groups to be compared. Significant results were explored with post-hoc comparisons of population marginal means.

The degree of learning across exposure-test pairs was assessed by fitting a general linear model in Minitab 17 for the CVC and tone languages. The response variable was discriminability (A') and the factors were 'participant number' (nested within 'group'), 'rule type', and 'run number'. Significant results were explored with post-hoc Tukey's range tests.

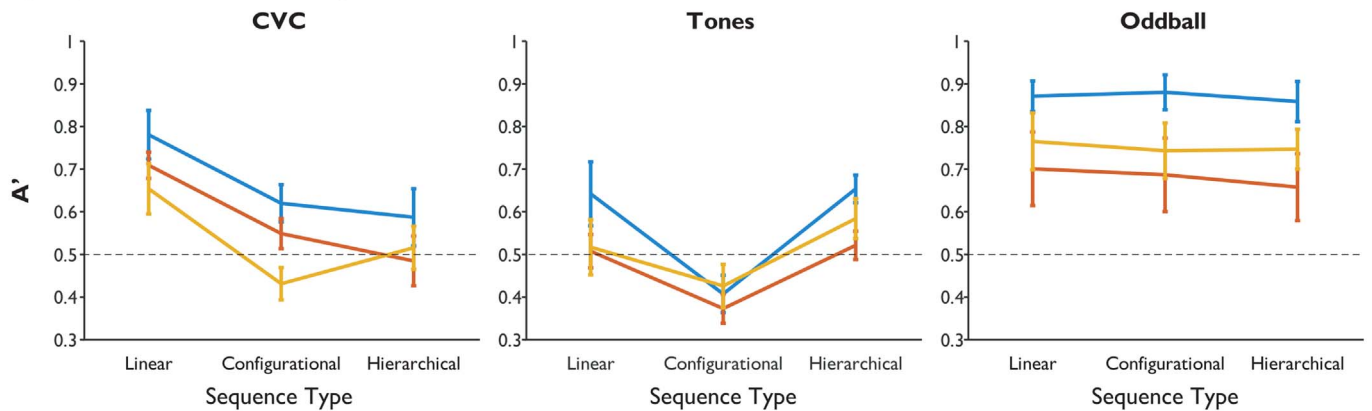
To assess whether the same rules were learned by participants between task types (CVC vs tones vs oddball), and by extension whether learning of the same artificial grammar was transferrable across token types (CVC vs tones), Spearman correlation matrices were constructed based on performance patterns by sequence for each group. From these, hierarchical cluster analysis was performed to construct dendrograms representing the similarity of performance pattern across test and group, using a 'farthest neighbour' linkage method with a data-driven inconsistency coefficient (The Mathworks Inc, 2015).

Exploratory regression analyses were performed in Minitab 17. As there were a large number of variables measured for each subject, stepwise regression was undertaken to determine those variables that best predicted artificial grammar learning. This is an automated process to identify a useful subset of predictors by sequentially adding and removing predictors until an optimal model is obtained. Software default alpha-to-enter and alpha-to-remove values of 0.15 were used, with confirmatory analyses at 0.1/0.15 and 0.1/0.1 yielding identical results. Three separate sets of stepwise regressions were performed; one to explore possible correlations between rule discriminability and neuropsychological and language measures, a second to explore correlations between rule discriminability and stroke lesion site, and a third to explore correlations between rule discriminability and grey

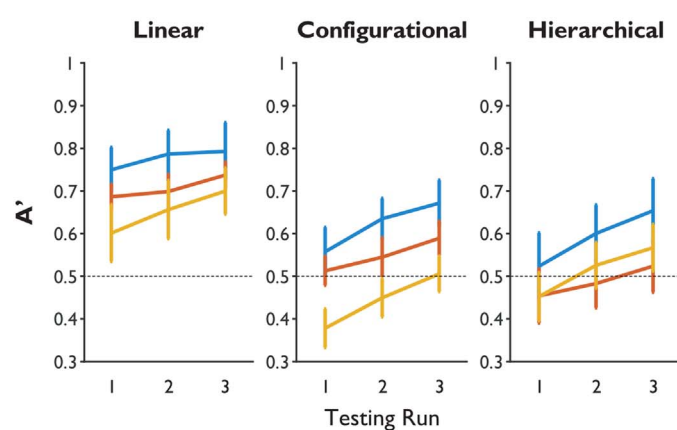
A) Performance on all sequences



B) Signal Detection Analyses



C) Performance over repeated testing - CVC



D) Performance over repeated testing - Tones

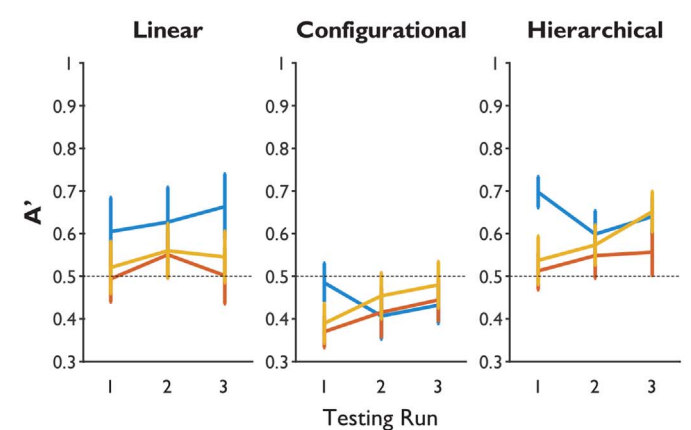


Fig. 3. Group performance on sequence identification. Dashed lines represent chance performance. Error bars represent group-wise standard error of the mean. Controls are in blue, nfvPPA in red and stroke in orange. A) Proportion of correct responses for each testing sequence by group and task. Sequences 1–3 were consistent with the grammar and familiar from the exposure phase, while 4–6 were consistent and novel. Sequences 7–12 contained violations of the types indicated (see Table 2). B) Discriminability of each rule type by group for each language type. C) Overall discriminability by group and run number for the CVC language (improving performance by run represents learning over time). D) Overall discriminability by group and run number for the tone language. (For interpretation of the references to color in this figure legend, the reader is referred to the web version of this article.)

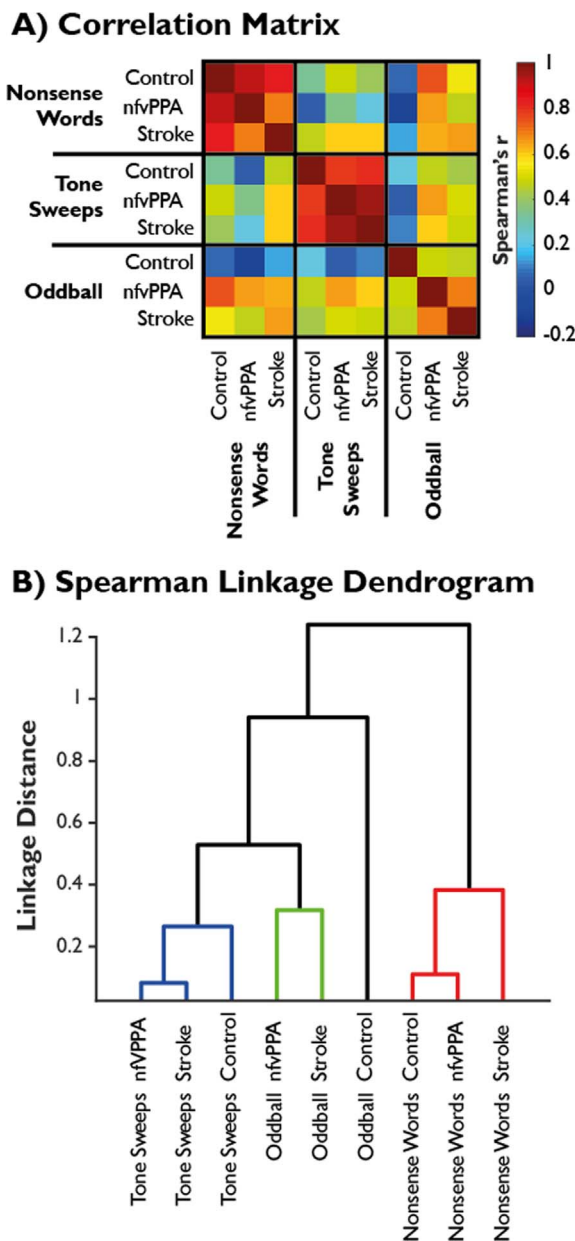


Fig. 4. A) Spearman rank-order correlation matrices. B) Linkage based on hierarchical cluster analysis of Spearman correlations. Three clusters emerge with a linkage distance cutoff of 0.5, and are indicated in colour groupings (blue, green and red). (For interpretation of the references to color in this figure legend, the reader is referred to the web version of this article.)

matter volume in nfvPPA. The potential continuous predictors included in the first model set were Age, Raven's Progressive Matrix score, years of musical training (which we hypothesised might impact tone language difficulty), sentence comprehension (from the Verbs and Sentences Test), and overall aphasia severity (Aphasia Severity Rating Score). For the second set, the potential continuous predictors were age, the proportion of each region of interest lesioned, total lesion volume, and the number of years since stroke. For the third, potential predictors were age, grey matter volume summed across regions of interest in each hemisphere, and corrected whole brain grey matter volume.

3. Results

Raw performance for each individual sequence is shown in Fig. 3A, and the results of the signal detection theory analysis are illustrated in

Fig. 3B. The hierarchical cluster analysis is illustrated in Fig. 4. Performance did not differ between sequences heard during exposure and test phases (Fig. 3A sequences 1–3) and those that were novel during the test phase (Fig. 3A sequences 4–6), so these were collapsed. Results are presented for the non-parametric discrimination measure A' , but the same pattern of findings was present for the parametric equivalent d' (Supplementary Tables 2 and 3).

For the CVC language, discriminability as measured by A' showed significant main effects of rule complexity and group, but no group x rule interaction or consistent inter-individual differences (Fig. 3B, Table 3A). Post-hoc comparison of marginal means indicated that the group difference is driven by the control participants performing significantly better than participants in the stroke group ($p=0.0058$). Participants with nfvPPA performed at an intermediate level, and were not statistically different from either controls ($p=0.14$) or stroke ($p=0.50$). Further, all groups performed better at detecting violations of linear grammatical rules than configurational ($p=0.0001$) or hierarchical ($p=0.0001$), which in turn did not differ ($p=0.99$).

The tone language discriminability measured by A' showed significant main effects of rule complexity and group, but no group x rule interaction or consistent inter-individual differences (Fig. 3B, Table 3A). For this language, post-hoc comparison of marginal means indicated that the group difference is driven by the control participants performing significantly better than participants in the nfvPPA group ($p=0.048$). Participants with stroke performed at an intermediate level, and were not statistically different from either controls ($p=0.31$) or nfvPPA ($p=0.57$). Rather than showing lower performance with increasingly complex rule violations, all groups performed significantly more poorly at detecting violations of the configurational rules than both the linear ($p=0.0009$) and hierarchical ($p=0.0001$), which in turn did not differ ($p=0.73$). Possible reasons for this unexpected pattern are discussed below.

All groups performed well at discriminating the oddball stimuli. For all groups, mean and median discriminability was better than for the CVC or tone languages. Crucially, there was no effect of rule type for the oddball language (Table 3A). This is because violations were no longer based on detection of grammatical rules, but on the detection of novel CVC tokens in various positions within the sequence. This observation reassures us that the effect of rule complexity in the CVC language cannot be explained by the position of the violation within a sequence. There was no significant group difference in performance or group x rule interaction (Table 3A), but there was a strongly significant effect of participant, indicating that individuals within each group differed in their ability to detect the novel non-word tokens. Post-hoc comparison of marginal means was not performed, as there was no rationale from the ANOVA to proceed to this.

From Fig. 3A it can be seen that for some sequences, particularly those which violate the more complex rules, participants in all groups performed at a level below chance (50% correct). This would not be expected if participants were simply guessing for these sequences, but would be expected if the grammatical violation was sufficiently subtle that participants made an active decision that the sequence is not inconsistent with the grammar. In other words, participants would display bias towards stating that a sequence was consistent with the artificial grammar unless they had evidence otherwise, but it was not known whether this tendency would differ between groups (Haendiges et al., 1996; Dickey et al., 2008). A bias towards yes (consistent) was demonstrated, but there was no group difference in bias or group x metric interaction (Table 3B, Supplementary Figure 3).

Participants, including patients, improved with practice. Results of the general linear model analysis including run number are illustrated in Fig. 3C, D, and Table 3C. For the CVC language, there were main effects of rule type, run number and group, but no interactions between run number and either rule complexity or group. This suggests, (a) that all groups were learning across repeated exposure-test cycles, (b) that the amount of learning over time was not different between the three

Table 3

A and B: Repeated measures ANOVAs of group against rule for the non-parametric discriminability measure A' (panel A; corresponding to Fig. 3A) and bias (panel B; corresponding to Fig. 3B), with participant number as a nested factor within group. C: The general linear model assessing learning across runs for the non-parametric discriminability measure A' (corresponding to Fig. 3C (CVC) and 3D (Tones)).

A - Fig. 3A	Rule complexity	Group	Group x complexity	Participant	
CVC	F(2,60) = 14.8 p < 0.0001	F(2,60) = 4.11 p = 0.0264	F(4,60) = 0.70 p = 0.5933	F(30,60) = 1.42 p = 0.1246	
Tones	F(2,60) = 9.05 p = 0.0004	F(2,60) = 7.13 p = 0.0029	F(4,60) = 0.49 p = 0.7421	F(30,60) = 0.32 p = 0.9995	
Oddball	F(2,60) = 0.51 p = 0.6018	F(2,60) = 2.59 p = 0.0916	F(4,60) = 0.16 p = 0.9575	F(30,60) = 11.92 p < 0.0001	
B - Fig. 3B	Bias metric	Group	Group x metric	Participant	
CVC	F(2,60) = 6.69 p = 0.0024	F(2,60) = 2.33 p = 0.1150	F(4,60) = 0.45 p = 0.7721	F(30,60) = 4.03 p < 0.0001	
Tones	F(2,60) = 19.1 p < 0.0001	F(2,60) = 0.06 p = 0.9445	F(4,60) = 0.99 p = 0.4184	F(30,60) = 1.72 p = 0.0371	
Oddball	F(2,60) = 3.61 p = 0.033	F(2,60) = 0.18 p = 0.8344	F(4,60) = 0.62 p = 0.6516	F(30,60) = 8.2 p < 0.0001	
C	Rule	Run	Group	Run x Complexity	Run x Group
CVC	F(2,890) = 141.2 p < 0.001	F(2,890) = 28.46 p < 0.001	F(30,890) = 14.4 p = 0.029	F(4,890) = 0.87 p = 0.626	F(4,890) = 0.65 p = 0.479
Fig. 3C					
Tones	F(2,890) = 73.8 p < 0.001	F(2,890) = 2.91 p = 0.055	F(30,890) = 4.26 p = 0.026	F(4,890) = 0.73 p = 0.572	F(4,890) = 3.34 p = 0.010
Fig. 3D					

rule types, and (c) that the group difference in overall discriminability described above was driven by differences in initial grammatical learning, not by a reduced ability to refine the internal grammatical model through feedback and repeated exposure. Tukey tests confirmed that participants improved on each set of exposure and testing ($p < 0.05$ in all cases). Mean A' across groups for run 1 was 0.55, for run 2 was 0.60, and for run 3 was 0.64 (chance performance is 0.5). Control performance was significantly superior to nfvPPA performance, which was in turn significantly superior to performance in the stroke group.

For the tone language, there were main effects of rule type and group, but only a trend towards a main effect of run number. There was an interaction between run number and group, but not run number and rule complexity. Tukey tests demonstrated that control participants performed significantly better than those with stroke, who in turn performed significantly better than those with nfvPPA. Performance on run 3 was significantly better than on run 1, while run 2 did not differ from either run 1 or 3.

Spearman rank-order correlograms are shown in Fig. 4A, and the resultant hierarchical cluster analysis is visualised in Fig. 4B. Rule acquisition patterns are highly correlated between groups within each task, but not between tasks within each group. This is confirmed by the cluster analysis. Performance on CVC and tone languages represent strongly distinct clusters, while oddball performance profiles are less distinct (as expected if sequence ordering is unimportant for novel token detection). The difference in profiles between CVC and tone languages across group was further assessed by a two-sample *t*-test with unequal variance based on the similarities shown in Fig. 4A. In sample 1 were the six within-language similarities (excluding the diagonal) and in sample 2 were the 9 between-language similarities. This confirmed a highly significant group difference in language similarity; $t(12.5) = 5.2$, $p = 0.0002$. Identical pair-wise tests between groups across language (blinded to overall ability by non-parametric Spearman rank-order correlation) confirmed that performance profiles did not differ between groups (control vs nfvPPA $t(12.3) = -0.12$, $p = 0.90$; control vs stroke $t(10.2) = -0.76$, $p = 0.46$; nfvPPA vs stroke $t(12.2) = -0.01$, $p = 0.99$).

Stepwise regression analysis between overall measures of discriminability and the behavioural measures listed in the methods yielded no statistically significant predictors for CVC or oddball language performance. If performance on CVC linear rules (where performance was highest) is considered in isolation, overall aphasia

severity ($\alpha = 0.002$) was the only significant predictor. The only significant predictor for tone language performance was diagnosis ($\alpha = 0.035$), confirming that patients with nfvPPA performed more poorly than those with stroke, independent of aphasia severity.

Lesion volume and site affected performance in the stroke group. Stepwise regression analysis between overall measures of discriminability for each language and the lesion metrics listed in methods yielded a model for the CVC language including only left putamen ($\alpha = 0.06$); in other words, the ability to detect sequencing violations decreased with more severe putaminal lesions. For the oddball language, total lesion volume ($\alpha = 0.016$) and involvement of the left ventral frontal operculum ($\alpha = 0.076$) were included in the model (overall $p = 0.023$), but in opposite directions: participants with larger lesions were less able to detect oddball CVCs, but this deficit was ameliorated if their lesion had a more anterior distribution. The model yielded no statistically significant predictors for the tones language.

Grey matter volume affected performance in the nfvPPA group. The best model for nfvPPA performance on the CVC language included age ($\alpha = 0.002$) and total grey matter volume in the left frontal lobe regions of interest ($\alpha = 0.016$), but not in their right sided equivalents or total grey matter volume. These acted such that performance improved with higher left frontal grey matter volume, and also with age. While it might initially seem counter intuitive that older patients performed better, this is likely to reflect the natural loss of grey matter with age. The model is therefore improved by accounting for the fact that any given value of grey matter volume is relatively more atrophic in a younger individual. There were no statistically significant predictors with grey matter volume in the nfvPPA group for performance on the tone or oddball languages.

4. Discussion

This study successfully used a mixed-complexity artificial grammar learning task with speech sounds and tone stimuli to test aphasic patients with two different aetiologies. The principal observations were that: 1) both healthy individuals and patients with aphasia apply strongly contrasting strategies to assess structured sequences depending on whether the sequences consist of linguistic or non-linguistic auditory tokens; 2) patients with vascular aphasia and nfvPPA show similar patterns of auditory sequence processing impairment compared to controls; 3) aphasic patients are not disproportionately impaired on

more complex auditory sequencing tasks, instead displaying a general impairment in processing structured auditory input; 4) patients with aphasia are capable of implicit learning of this kind through repeated exposure/test cycles. We discuss these results in turn in the following sections.

4.1. Rule acquisition differs when structurally identical sequences are comprised of linguistic or non-linguistic stimuli

In all groups, performance profiles on the CVC language followed the expected pattern of linear relationships being more discriminable than configurational or hierarchical structures. By contrast, participants' judgments about the tone language did not seem to be based on the abstraction of the intended grammatical rules (Fig. 3A, panel 2). This impression was confirmed by correlation and cluster analyses (Fig. 4). Hierarchical clustering based on non-parametric correlations of single subject performance profiles (Fig. 4B) was clearly able to recover the language learned, but not the group structure. This demonstrates that all groups acquired the same set of rules when making decisions about the CVC language; all that differed between groups was their overall performance. Further, a completely different set of rules were acquired for the tone language, but again this learning profile was almost identical across groups. Therefore, rule acquisition was not transferred between the two languages, and the separation of approach to linguistic and non-linguistic structured sequences was strongly maintained in agrammatic aphasia of either type. This is despite the two languages having an identical structure, and being presented and tested in the same order. This finding cannot be trivially explained by a lower level deficit such as the tone language simply being more difficult, more affected by a reduced fidelity of auditory processing or subject to a higher 'lapse rate', which would affect discriminability but could not produce the complete dissociation of response patterns shown here across all groups.

Despite extensive exposure, all groups performed poorly at classifying tone sequence number 1 as consistent with the artificial grammar, and indeed seemed to actively reject it, with control performance for this sequence well below chance. This sequence was comprised entirely of tone sweeps, embedded within a recursive structure. The participants also correctly classified sequence 12, which has similar properties, as inconsistent with the artificial grammar. In this case, good performance on this tone sequence does not reflect an ability to extract the hierarchical rule, but rather a consistent tendency to reject the embedded pattern of tone sweep sequences. Overall, therefore, it does not seem that the tone sequences were assessed for the specific violations of the grammatical rules inherent in the artificial language. Instead, they were judged on the overall 'feel' of the sequence in a manner very different to the CVC language but entirely consistent across groups.

We therefore infer that, while both patient groups are impaired in their ability to learn and discriminate sequencing rules for both CVC and tone languages, they maintain the same separation of processing of these languages seen in control participants. Taken together, these results imply that domain specific processes exist for linguistic and non-linguistic structured sequence learning, which are preserved even in the presence of acquired grammatical deficits. These processes might therefore engage different brain networks (Geranmayeh et al., 2014a, 2014b). It is possible that this separation is instantiated by an assessment of phonological 'well-formedness' in auditory temporal regions (Obrig et al., 2016).

4.2. Artificial grammar learning in aphasia is similar across aetiologies

A second key observation was that patients with nfvPPA and stroke showed similar patterns of performance for the CVC language. All groups were able to correctly classify the grammatical testing sequences as consistent with the exemplary sequences heard during exposure, and this ability fully generalised from the exposure set to the novel

sequences not heard during exposure (Table 2; Fig. 3A). While there was a group difference, with performance in the stroke group being poorer on the CVC task, this effect disappeared when overall aphasia severity was accounted for. This novel result in agrammatic patients with primary progressive aphasia provides the evidence to suggest that existing findings on stroke patients should prove applicable to the progressive aphasias.

The lack of an effect of rule type for the oddball task confirms that the pattern of performance for the CVC language cannot be explained by stimulus-level differences such as the position of the violation within the sequence. The lack of a statistical group difference in the ability to detect oddball CVCs, a task performed at the end of the testing session, suggests that the patients' impairments in this study are not solely due to generic difficulties with performing psychophysical sequence processing tasks, latent yes/no confusion, difficulties with basic auditory processing or differential effects of fatigue between groups.

The only consistent group difference not accounted for by severity was that patients with nfvPPA performed more poorly than those with stroke on the tone based language. There are a number of possible reasons for this. It might be a consequence of the tone language being more affected by the basic auditory sequence processing deficits previously demonstrated in nfvPPA (Goll et al., 2010; Grube et al., 2016). Alternatively, it might reflect involvement of the right IFC, which was spared in the stroke group (Fig. 1B), and is posited to have a role in prosodic and tonality based judgments. Nonetheless, patients with nfvPPA maintained the same pattern of learning as the other groups (Fig. 4), demonstrating that this deficit is a specific difficulty with processing tonal input rather than a breakdown of the separation of phonological vs tonal structured sequence processing.

4.3. Agrammatic aphasic patients are similarly impaired for both complex and simple sequencing operations

As expected, patients did not perform as well as controls, but the magnitude of this performance deficit did not differ by rule complexity, counter to our initial hypothesis. The results demonstrate that aphasic patients showed a global deficit in sequence processing, rather than a selective impairment on complex sequences. Clinically, patients in both groups make errors in the parsing of more complex syntax, and tend to stick to active, subject-relative structures in their expressive language (Grossman and Moore, 2005). We suggest that this does not reflect a specific deficit in the processing of more complex linguistic structures, but rather that these constructions are simply more difficult and therefore more vulnerable to a global deficit. As well as explaining a clinical symptom, this conclusion is consistent with the functional imaging finding that, in nfvPPA, left inferior frontal cortex activity lacks the normal relationship with syntactic complexity (Wilson et al., 2010); it suggests that the efficiency of IFC is so degraded that even the least complex grammatical structures require maximal neural recruitment. This is analogous to the finding that older adults are no longer able to selectively modulate anterior cingulate cortex in response to increasingly difficult listening environments as they have already fully engaged this region in easy listening conditions (Erb and Obleser, 2013).

It is possible that patients attempt to compensate for this deficit by engaging a wider syntactic processing network involving temporoparietal regions (Schofield et al., 2012; Blank et al., 2016), but that this is insufficient to compensate for lost language function (Wilson et al., 2016). In stroke, where the IFC is lost entirely, the presence of residual ability could be due to complete reliance on this wider network (Thompson et al., 2010), or the involvement of contralateral IFC. Future functional imaging studies of implicit grammar learning will inform this debate. In any case, our findings of a general impact on sequence processing suggest that the grammatical deficits observed in aphasia, and the recovery from these, might reflect higher level, domain general processes (Caramazza and Zurif, 1976; Dominey et al., 2003; Patel

et al., 2008; Brownsett et al., 2014; Geranmayeh et al., 2014a, 2014b, in press).

The lack of group by rule complexity interactions is unlikely to be explained by limitations in sample size, as in no case was there even a trend in this direction (all interactions with complexity in Table 3 have p -values > 0.5). Therefore, these results appear to represent a genuine null effect, rather than sub-threshold effects that might become significant with a greater sample size. Moreover, the lack of interaction is also consistent in the tone and CVC experiments, although the response patterns between the two are vastly different. Nor can the results be trivially explained by floor effects in processing the more complex relationships for the following reasons: 1) the nvPPA group show strikingly parallel behaviour in relation to the control group, consistent with a proportional impairment even on the linear sequencing operation (Fig. 3B, panel 1); 2) the stroke patients may well have reached a floor in performance on the complex sequences in the nonsense word task, but even excluding this group did not cause the group by complexity interaction to approach significance; 3) all groups improved over the three testing runs, and performance improvement was parallel in relation to sequencing complexity (i.e. there was a main effect of run but no run-by-complexity interaction, Figs. 3C); and 4) the tone language showed a very different pattern of results to that for the nonsense words yet, again, there was no evidence of a group-by-complexity interaction.

4.4. Patients with aphasia show improved performance over repeated cycles

All three groups demonstrated the same amount of learning across repeated exposure/test cycles of the CVC language; the only difference was in their initial levels of performance (Fig. 3C; Table 3C). This suggests that patients with aphasia were able to update their internal model of the artificial grammar based on feedback and implicit comparison with short periods of exposure. It also suggests that patients did not suffer greater effects of fatigue than controls. By contrast, learning did not occur to the same degree for the tone language (Fig. 3D; Table 3C). It is therefore clear that learning was not transferrable between the CVC and tone languages, despite them sharing the same underlying artificial grammar structure.

Together, these findings provide a theoretical basis upon which an exposure-based speech therapy for grammar could be built with the aim of improving subjective difficulty with speech comprehension (Supplementary Figure 1). The results imply that there is potential for improvement from an intensive paradigm based on repeated exposure-test cycles. This could in principle be made home-deliverable and patient-led, an approach that has demonstrable efficacy for improving speech production in similar patient groups (Varley et al., 2016); the tasks employed in this study were automated and computer based. The finding that learning did not generalise across modalities implies that such a therapy would need to use linguistic material, as it would be unlikely to be so well learnt with non-linguistic material or to transfer across domains. In contrast, the finding that patients were able to generalise perfectly from sequences heard during exposure (Fig. 3A, sequences 1–3), to those that were novel during the test phase (Fig. 3A, sequences 4–6), to the extent that performance did not differ, suggests that such a therapy might not need to be comprehensive with regards to specific sentence structures. Instead, it is envisaged that a graded programme could be designed, such that training focusses initially on those structures that are having most frequent impact on speech comprehension. Clearly our study does not provide evidence that such a therapy would be more efficacious than existing methods for addressing syntactic deficits after stroke, nor do we have any evidence of how well our strategies would work within an already-learned but now-impaired natural language. Indeed, a recent small study of nine patients who had chronic agrammatic aphasia secondary to stroke suggests that implicit learning alone (on a visuo-motor serial reaction time task) does not necessarily translate into improved real-world performance

(Schuchard et al., 2017). Larger scale trials and assessment with other tasks are clearly required in more acute disease cohorts. As our method relies on exposure-based implicit learning rather than explicit instruction, future therapeutic trials could follow recent trends for patient-led practice in the home environment, increasingly with support from internet-based resources (Rogalski et al., 2016). This has the potential for providing the benefits of an intensive approach (Bhagal et al., 2003; Brady et al., 2016; Breitenstein et al., 2017) without the resource constraints that limit the frequency and therefore efficacy of traditional irregular, face-to-face instruction (Sarno et al., 1970; Lincoln et al., 1984).

4.5. Brain behaviour relationships

Our use of stepwise regression, to assess associations between brain structure and function, should be seen as exploratory, since the study was powered only to detect strong effect sizes. Nonetheless, significant associations between brain structure and behavioural performance within the patient groups were observed. The nvPPA group demonstrated significant grey and white matter loss in frontal regions bilaterally. In keeping with previous studies of expressive grammar (Rogalski et al., 2011), the discriminability of grammatical structure in the CVC language correlated with age-corrected loss of volume only in left frontal regions (but not similar right-sided regions or total corrected grey matter volume). No such association was found for the tone language or the oddball task.

In the stroke group there was catastrophic loss of fronto-temporal regions in the dominant hemisphere, but complete contralateral preservation. For the CVC language, the model included only the putamen. The putamen is known from the functional imaging literature to be important in implicit sequence detection and learning in healthy individuals (Grafton et al., 1995; Rauch et al., 1995; Rauch et al., 1997; Grahn and Rowe, 2009). No such relationships were significant for the tone task. Performance on the oddball sound detection task was predicted by overall lesion volume and a weaker, opposite, effect of the extent of involvement of the most frontal region analysed. This suggests that more anterior lesion locations were less deleterious to CVC oddball detection than those located closer to auditory cortex in temporal lobe.

Similar performance in a relatively bilateral disease (nvPPA) and one so clearly unilateral (stroke) immediately poses the question of which components of a broader language network are recruited to underpin the demonstrated learning over repeated exposure-test cycles (Crinion and Price, 2005). Thus, there is clear scope for a functional imaging study to be conducted in these patient groups, the results of which could complement the development of grammar-based speech therapy.

5. Conclusion

In this paper we reconcile a controversy in the literature regarding the effects of structural complexity on receptive grammar in the frontal aphasias. We demonstrate that, while the patients found complex, non-adjacent structuring relationships more difficult to acquire, this did not represent a disproportionate impairment; aphasia resulted in a similar performance penalty for adjacent relationships. We also provide insights into the language-specificity of artificial grammar learning by demonstrating that humans learn otherwise identical linguistic and non-linguistic structured sequences entirely separately, even if the neural architecture underlying this learning is disrupted. Our direct comparison of two patient groups suggests that previous findings regarding implicit sequence learning in stroke aphasia are likely to prove transferrable to nvPPA. Finally, the ability of both patient groups to learn an artificial grammar as demonstrated here provides a rationale and approach for future trials of implicit, exposure-based approaches to rehabilitation of agrammatism in non-fluent aphasia.

Acknowledgements

The Association of British Neurologists, Patrick Berthoud Charitable trust and National Institute for Health Research support TEC. The Wellcome Trust supports BW (WT110198), TDG (WT106964MA), JBR (WT103838) and CP (WT102961MA). The Stroke Association supports HR (TSA 2012/02). Further study support was received from the National Institute of Health Research's Biomedical Research Centre (Cambridge) and Biomedical Research Units in Dementia (Cambridge, Newcastle).

Appendix A. Supplementary Information

Supplementary data associated with this article can be found in the online version at <http://dx.doi.org/%2010.1016/j.neuropsychologia.2017.08.022>

References

- Bahlmann, J., Schubotz, R.I., Friederici, A.D., 2008. Hierarchical artificial grammar processing engages Broca's area. *Neuroimage* 42 (2), 525–534 (Aug 15).
- Bastiaanse, R., Edwards, S., Mass, E., Rispens, J., 2003. Assessing comprehension and production of verbs and sentences: the Verb and Sentence Test (VAST). *Aphasiology* 17 (1), 49–73 (2003/01/01).
- Berndt, R.S., 2000. Sentence comprehension in Broca's aphasia: a critique of the evidence. *Behav. Brain Sci.* 23 (01), 24–.
- Berndt, R.S., Caramazza, A., Zurif, E., 1983. *Language Functions: Syntax*. Language Functions and Brain Organization, pp. 5.
- Berndt, R.S., Mitchum, C.C., Haendiges, A.N., 1996. Comprehension of reversible sentences in "agrammatism": a meta-analysis. *Cognition* 58 (3), 289–308.
- Bhogal, S.K., Teasell, R.W., Foley, N.C., Speechley, M.R., 2003. Rehabilitation of aphasia: more is better. *Top. Stroke Rehabil.* 10 (2), 66–76 (Summer).
- Blank, I., Balewski, Z., Mahowald, K., Fedorenko, E., 2016. Syntactic processing is distributed across the language system. *Neuroimage* 127, 307–323.
- Brady, M.C., Kelly, H., Godwin, J., Enderby, P., Campbell, P., 2016. Speech and language therapy for aphasia following stroke. *Cochrane Libr.*
- Breitenstein, C., Grewe, T., Flöel, A., Ziegler, W., Springer, L., Martus, P., et al., 2017. Intensive speech and language therapy in patients with chronic aphasia after stroke: a randomised, open-label, blinded-endpoint, controlled trial in a health-care setting. *Lancet* 389 (10078), 1528–1538.
- Brownset, S.L., Warren, J.E., Geranmayeh, F., Woodhead, Z., Leech, R., Wise, R.J., 2014. Cognitive control and its impact on recovery from aphasic stroke. *Brain* 137 (1), 242–254.
- Caplan, D., Baker, C., Dehaut, F., 1985. Syntactic determinants of sentence comprehension in aphasia. *Cognition* 21 (2), 117–175.
- Caramazza, A., Zurif, E.B., 1976. Dissociation of algorithmic and heuristic processes in language comprehension: evidence from aphasia. *Brain Lang.* 3 (4), 572–582.
- Christiansen, M.H., Kelly, M.L., Shillcock, R.C., Greenfield, K., 2010a. Impaired artificial grammar learning in agrammatism. *Cognition* 116 (3), 382–393.
- Conway, C.M., Bauernschmidt, A., Huang, S.S., Pisoni, D.B., 2010. Implicit statistical learning in language processing: word predictability is the key. *Cognition* 114 (3), 356–371.
- Conway, C.M., Pisoni, D.B., 2008. Neurocognitive basis of implicit learning of sequential structure and its relation to language processing. *Ann. N. Y. Acad. Sci.* 1145 (1), 113–131.
- Cope, T.E., Patterson, K., Sohoglu, E., Dawson, K., Grube, M., Davis, M.H., et al., 2014. P67. Predictive mechanisms and speech perception in progressive non-fluent aphasia. *Am. J. Neurodegener. Dis.* 3 (Suppl. 1), 123.
- Crinion, J., Price, C.J., 2005. Right anterior superior temporal activation predicts auditory sentence comprehension following aphasic stroke. *Brain* 128 (Pt 12), 2858–2871.
- Dickey, M.W., Milman, L.H., Thompson, C.K., 2008. Judgment of functional morphology in agrammatic aphasia. *J. Neurolinguist.* 21 (1), 35–65.
- Dominey, P.F., Hoen, M., Blanc, J.-M., Lelekov-Boissard, T., 2003. Neurological basis of language and sequential cognition: evidence from simulation, aphasia, and ERP studies. *Brain Lang.* 86 (2), 207–225.
- Erb, J., Obleser, J., 2013. Upregulation of cognitive control networks in older adults' speech comprehension. *Front Syst. Neurosci.* 7, 116.
- Evans, J.L., Saffran, J.R., Robe-Torres, K., 2009. Statistical learning in children with specific language impairment. *J. Speech Lang. Hear. Res.* 52 (2), 321–335.
- Fedorenko, E., Duncan, J., Kanwisher, N., 2012. Language-selective and domain-general regions lie side by side within Broca's area. *Curr. Biol.* 22 (21), 2059–2062 (Nov 6).
- Folia, V., Forkstam, C., Ingvar, M., Hagoort, P., Petersson, K.M., 2011. Implicit artificial syntax processing: genes, preference, and bounded recursion. *Biolinguistics* 5, 105–132.
- Forkstam, C., Hagoort, P., Fernandez, G., Ingvar, M., Petersson, K.M., 2006. Neural correlates of artificial syntactic structure classification. *Neuroimage* 32 (2), 956–967 (Aug 15).
- Friederici, A.D., 2011. The brain basis of language processing: from structure to function. *Physiol. Rev.* 91 (4), 1357–1392.
- Friederici, A.D., Bahlmann, J., Heim, S., Schubotz, R.I., Anwander, A., 2006. The brain differentiates human and non-human grammars: functional localization and structural connectivity. *Proc. Natl. Acad. Sci. USA* 103 (7), 2458–2463 (Feb 14).
- Friederici, A.D., Kotz, S.A., 2003. The brain basis of syntactic processes: functional imaging and lesion studies. *Neuroimage* 20 (Suppl 1), S8–S17.
- Friederici, A.D., Opitz, B., von Cramon, D.Y., 2000. Segregating semantic and syntactic aspects of processing in the human brain: an fMRI investigation of different word types. *Cereb. Cortex* 10 (7), 698–705.
- Frost, R., Armstrong, B.C., Siegelman, N., Christiansen, M.H., 2015. Domain generality versus modality specificity: the paradox of statistical learning. *Trends Cogn. Sci.* 19 (3), 117–125.
- Geranmayeh, F., Brownset, S.L., Wise, R.J., 2014a. Task-induced brain activity in aphasic stroke patients: what is driving recovery? *Brain* 137 (10), 2632–2648.
- Geranmayeh, F., Chau, T., Wise, R., Leech, R., Hampshire, A., 2017. Domain general sub-regions of the medial prefrontal cortex contribute to recovery of language after stroke. *Brain* 140 (7), 1947–1958.
- Geranmayeh, F., Wise, R.J., Mehta, A., Leech, R., 2014b. Overlapping networks engaged during spoken language production and its cognitive control. *J. Neurosci.* 34 (26), 8728–8740 (Jun 25).
- Goll, J.C., Crutch, S.J., Loo, J.H.Y., Rohrer, J.D., Frost, C., Bamiou, D.E., et al., 2010. Non-verbal sound processing in the primary progressive aphasias. *Brain* 133, 272–285.
- Gómez, R.L., Gerken, L., 2000. Infant artificial language learning and language acquisition. *Trends Cogn. Sci.* 4 (5), 178–186.
- Goodglass, H., Barresi, B., Kaplan, E., 1983. *The Boston Diagnostic Aphasia Examination*. A Wolters Kluwer Company: Lippincott Williams & Wilkins, Philadelphia, Pennsylvania, United States.
- Goodman, E., Bates, J.C., 1997. On the inseparability of grammar and the lexicon: evidence from acquisition, aphasia and real-time processing. *Lang. Cogn. Process.* 12 (5–6), 507–584.
- Gorno-Tempini, M.L., Dronkers, N.F., Rankin, K.P., Ogar, J.M., Phengrasamy, L., Rosen, H.J., et al., 2004. Cognition and anatomy in three variants of primary progressive aphasia. *Ann. Neurol.* 55 (3), 335–346.
- Gorno-Tempini, M.L., Hillis, A.E., Weintraub, S., Kertesz, A., Mendez, M., Cappa, S.F., et al., 2011. Classification of primary progressive aphasia and its variants. *Neurology* 76 (11), 1006–1014 (Mar 15).
- Grafton, S.T., Hazeltine, E., Ivry, R., 1995. Functional mapping of sequence learning in normal humans. *J. Cogn. Neurosci.* 7 (4), 497–510 (Fall).
- Grahn, J.A., Rowe, J.B., 2009. Feeling the beat: premotor and striatal interactions in musicians and nonmusicians during beat perception. *J. Neurosci.* 29 (23), 7540–7548 (June 10, 2009).
- Grodzinsky, Y., 2000. The neurology of syntax: language use without Broca's area. *Behav. Brain Sci.* 23 (01), 1–21.
- Grossman, M., Moore, P., 2005. A longitudinal study of sentence comprehension difficulty in primary progressive aphasia. *J. Neurol. Neurosurg. Psychiatry* 76 (5), 644–649.
- Grube, M., Bruffaerts, R., Schaevebeke, J., Neyens, V., De Weer, A.S., Seghers, A., et al., 2016. Core auditory processing deficits in primary progressive aphasia. *Brain* (Apr 9).
- Grube, M., Kumar, S., Cooper, F.E., Turton, S., Griffiths, T.D., 2012. Auditory sequence analysis and phonological skill. *Proc. Biol. Sci.* 279 (1746), 4496–4504 (Nov 7).
- Haendiges, A.N., Berndt, R.S., Mitchum, C.C., 1996. Assessing the elements contributing to a "mapping" deficit: a targeted treatment study. *Brain Lang.* 52 (1), 276–302.
- Hickok, G., Poeppel, D., 2007. The cortical organization of speech processing. *Nat. Rev. Neurosci.* 8 (5), 393–402.
- Jenkinson, M., Smith, S., 2001. A global optimisation method for robust affine registration of brain images. *Med Image Anal.* 5 (2), 143–156.
- Josephs, K.A., Duffy, J.R., Strand, E.A., Whitwell, J.L., Layton, K.F., Parisi, J.E., et al., 2006. Clinicopathological and imaging correlates of progressive aphasia and apraxia of speech. *Brain* 129 (Pt 6), 1385–1398.
- Kaplan, E., 1983. *The Assessment of Aphasia and Related Disorders*. Lippincott Williams & Wilkins, Philadelphia, Pennsylvania, United States.
- Kertesz, A., McCabe, P., 1977. Recovery patterns and prognosis in aphasia. *Brain* 100 (Pt 1), 1–18.
- Kertesz, A., McMonagle, P., Blair, M., Davidson, W., Munoz, D.G., 2005. The evolution and pathology of frontotemporal dementia. *Brain* 128 (Pt 9), 1996–2005.
- Knibb, J.A., Kipps, C.M., Hodges, J.R., 2006a. Frontotemporal dementia. *Curr. Opin. Neurol.* 19 (6), 565–571.
- Knibb, J.A., Xuereb, J.H., Patterson, K., Hodges, J.R., 2006b. Clinical and pathological characterization of progressive aphasia. *Ann. Neurol.* 59 (1), 156–165.
- Lincoln, N.B., McGuirk, E., Mulley, G.P., Lendrem, W., Jones, A.C., Mitchell, J.R., 1984. Effectiveness of speech therapy for aphasic stroke patients. A randomised controlled trial. *Lancet* 1 (8388), 1197–1200 (Jun 2).
- Macmillan, N.A., Kaplan, H.L., 1985. Detection theory analysis of group data: estimating sensitivity from average hit and false-alarm rates. *Psychol. Bull.* 98 (1), 185.
- Makuuchi, M., Bahlmann, J., Anwander, A., Friederici, A.D., 2009. Segregating the core computational faculty of human language from working memory. *Proc. Natl. Acad. Sci. USA* 106 (20), 8362–8367 (May 19).
- Mandelli, M.L., Vilaplana, E., Brown, J.A., Hubbard, H.I., Binney, R.J., Attygalle, S., et al., 2016. Healthy brain connectivity predicts atrophy progression in non-fluent variant of primary progressive aphasia. *Brain* 139 (10), 2778–2791.
- Mesulam, M.M., Weintraub, S., Rogalski, E.J., Wieneke, C., Geula, C., Bigio, E.H., 2014. Asymmetry and heterogeneity of Alzheimer's and frontotemporal pathology in primary progressive aphasia. *Brain* 137 (4), 1176–1192.
- Ni, W., Constable, R.T., Mencl, W.E., Pugh, K.R., Fulbright, R.K., Shaywitz, S.E., et al., 2000. An event-related neuroimaging study distinguishing form and content in sentence processing. *Cogn. Neurosci.* 12 (1), 120–133.
- Obrig, H., Mentzel, J., Rossi, S., 2016. Universal and language-specific sublexical cues in speech perception: a novel electroencephalography-lesion approach. *Brain* 139 (Pt 6),

- 1800–1816.
- Opitz, B., Kotz, S.A., 2012. Ventral premotor cortex lesions disrupt learning of sequential grammatical structures. *Cortex* 48 (6), 664–673.
- Patel, A.D., Iversen, J.R., Wassenaar, M., Hagoort, P., 2008. Musical syntactic processing in agrammatic Broca's aphasia. *Aphasiology* 22 (7–8), 776–789.
- Patterson, K., Graham, N., Ralph, M.A.L., Hodges, J., 2006. Progressive non-fluent aphasia is not a progressive form of non-fluent (post-stroke) aphasia. *Aphasiology* 20 (9), 1018–1034.
- Petersson, K.-M., Folia, V., Hagoort, P., 2012a. What artificial grammar learning reveals about the neurobiology of syntax. *Brain Lang.* 120 (2), 83–95.
- Petersson, K.M., Folia, V., Hagoort, P., 2012b. What artificial grammar learning reveals about the neurobiology of syntax. *Brain Lang.* 120 (2), 83–95.
- Petersson, K.M., Forkstam, C., Ingvar, M., 2004. Artificial syntactic violations activate Broca's region. *Cogn. Sci.* 28 (3), 383–407 (May–Jun).
- Price, C.J., Seghier, M.L., Leff, A.P., 2010. Predicting language outcome and recovery after stroke: the PLORAS system. *Nat. Rev. Neurol.* 6 (4), 202–210.
- Rauch, S.L., Savage, C.R., Brown, H.D., Curran, T., Alpert, N.M., Kendrick, A., et al., 1995. A PET investigation of implicit and explicit sequence learning. *Hum. Brain Mapp.* 3 (4), 271–286.
- Rauch, S.L., Whalen, P.J., Savage, C.R., Curran, T., Kendrick, A., Brown, H.D., et al., 1997. Striatal recruitment during an implicit sequence learning task as measured by functional magnetic resonance imaging. *Hum. Brain Mapp.* 5 (2), 124–132.
- Raven J.C., 1960. *Guide to the standard progressive matrices: sets A, B, C, D and E: HK Lewis.*
- Reber, A.S., 1967. Implicit learning of artificial grammars. *J. Verbal Learn. Verbal Behav.* 6 (6), 855–863.
- Rogalski, E., Cobia, D., Harrison, T.M., Wieneke, C., Thompson, C.K., Weintraub, S., et al., 2011. Anatomy of language impairments in primary progressive aphasia. *J. Neurosci.* 31 (9), 3344–3350 (Mar 2).
- Rogalski, E.J., Saxon, M., McKenna, H., Wieneke, C., Rademaker, A., Corden, M.E., et al., 2016. Communication bridge: a pilot feasibility study of Internet-based speech–language therapy for individuals with progressive aphasia. *Alzheimer's Dement.: Transl. Res. Clin. Interv.*
- Rohrer, J.D., Rossor, M.N., Warren, J.D., 2012. Alzheimer's pathology in primary progressive aphasia. *Neurobiol. Aging* 33 (4), 744–752.
- Romberg, A.R., Saffran, J.R., 2013. All together now: concurrent learning of multiple structures in an artificial language. *Cogn. Sci.* 37 (7), 1290–1320.
- Sajjadi, S.A., Patterson, K., Arnold, R.J., Watson, P.C., Nestor, P.J., 2012. Primary progressive aphasia: a tale of two syndromes and the rest. *Neurology* 78 (21), 1670–1677 (May 22).
- Sajjadi, S.A., Patterson, K., Nestor, P.J., 2014. Logopenic, mixed, or Alzheimer-related aphasia? *Neurology* 82 (13), 1127–1131.
- Sarno, M.T., Silverman, M., Sands, E., 1970. Speech therapy and language recovery in severe aphasia. *J. Speech Hear Res.* 13 (3), 607–623.
- Schofield, T.M., Penny, W.D., Stephan, K.E., Crinion, J.T., Thompson, A.J., Price, C.J., et al., 2012. Changes in auditory feedback connections determine the severity of speech processing deficits after stroke. *J. Neurosci.* 32 (12), 4260–4270 (Mar 21).
- Schuchard, J., Nerantzi, M., Thompson, C.K., 2017. Implicit learning and implicit treatment outcomes in individuals with aphasia. *Aphasiology* 31 (1), 25–48 (2017/01/02).
- Schuchard, J., Thompson, C.K., 2017. Sequential learning in individuals with agrammatic aphasia: evidence from artificial grammar learning. *J. Cogn. Psychol.* 1–14.
- Seghier, M.L., Patel, E., Prejawa, S., Ramsden, S., Selmer, A., Lim, L., et al., 2016. The PLORAS database: a data repository for predicting language outcome and recovery after stroke. *Neuroimage* 124, 1208–1212.
- Stanislaw, H., Todorov, N., 1999. Calculation of signal detection theory measures. *Behav. Res Methods Instrum. Comput.* 31 (1), 137–149.
- The Mathworks Inc, 2015. *Matlab and Statistics and Machine Learning Toolbox.* Release, 2015b ed. Natick, Massachusetts.
- Thompson, C.K., den Ouden, D.-B., Bonakdarpour, B., Garibaldi, K., Parrish, T.B., 2010. Neural plasticity and treatment-induced recovery of sentence processing in agrammatism. *Neuropsychologia* 48 (11), 3211–3227.
- Thompson, C.K., Meltzer-Asscher, A., Cho, S., Lee, J., Wieneke, C., Weintraub, S., et al., 2013. Syntactic and morphosyntactic processing in stroke-induced and primary progressive aphasia. *Behav. Neurol.* 26 (1, 2), 35–54.
- Varley, R., Cowell, P.E., Dyson, L., Inglis, L., Roper, A., Whiteside, S.P., 2016. Self-administered computer therapy for apraxia of speech. *Stroke* 47 (3), 822–828.
- Wilson, B., Smith, K., Petkov, C.I., 2015. Mixed-complexity artificial grammar learning in humans and macaque monkeys: evaluating learning strategies. *Eur. J. Neurosci.* 41 (5), 568–578 (MAR 2015).
- Wilson, S.M., DeMarco, A.T., Henry, M.L., Gesierich, B., Babiak, M., Miller, B.L., et al., 2016. Variable disruption of a syntactic processing network in primary progressive aphasia. *Brain* (Aug 23).
- Wilson, S.M., Dronkers, N.F., Ogar, J.M., Jang, J., Growdon, M.E., Agosta, F., et al., 2010. Neural correlates of syntactic processing in the nonfluent variant of primary progressive aphasia. *J. Neurosci.* 30 (50), 16845–16854 (Dec 15).
- Wilson, S.M., Galantucci, S., Tartaglia, M.C., Rising, K., Patterson, D.K., Henry, M.L., et al., 2011. Syntactic processing depends on dorsal language tracts. *Neuron* 72 (2), 397–403 (Oct 20).
- Wong, D.L., Baker, C.M., 1988. Pain in children: comparison of assessment scales. *Okla. Nurse* 33 (1), 8.
- Zimmerer, V.C., Cowell, P.E., Varley, R.A., 2014a. Artificial grammar learning in individuals with severe aphasia. *Neuropsychologia* 53, 25–38.
- Zimmerer, V.C., Dąbrowska, E., Romanowski, C.A., Blank, C., Varley, R.A., 2014b. Preservation of passive constructions in a patient with primary progressive aphasia. *Cortex* 50, 7–18.
- Zimmerer, V.C., Varley, R.A., 2015. A case of “order insensitivity”? Natural and artificial language processing in a man with primary progressive aphasia. *Cortex* 69, 212–219.